MOLECULAR MECHANISMS AND TREATMENT OF MYCN-DRIVEN TUMORS

EDITED BY: Yusuke Suenaga, Christer Einvik, Atsushi Takatori and Yuyan Zhu
PUBLISHED IN: Frontiers in Oncology

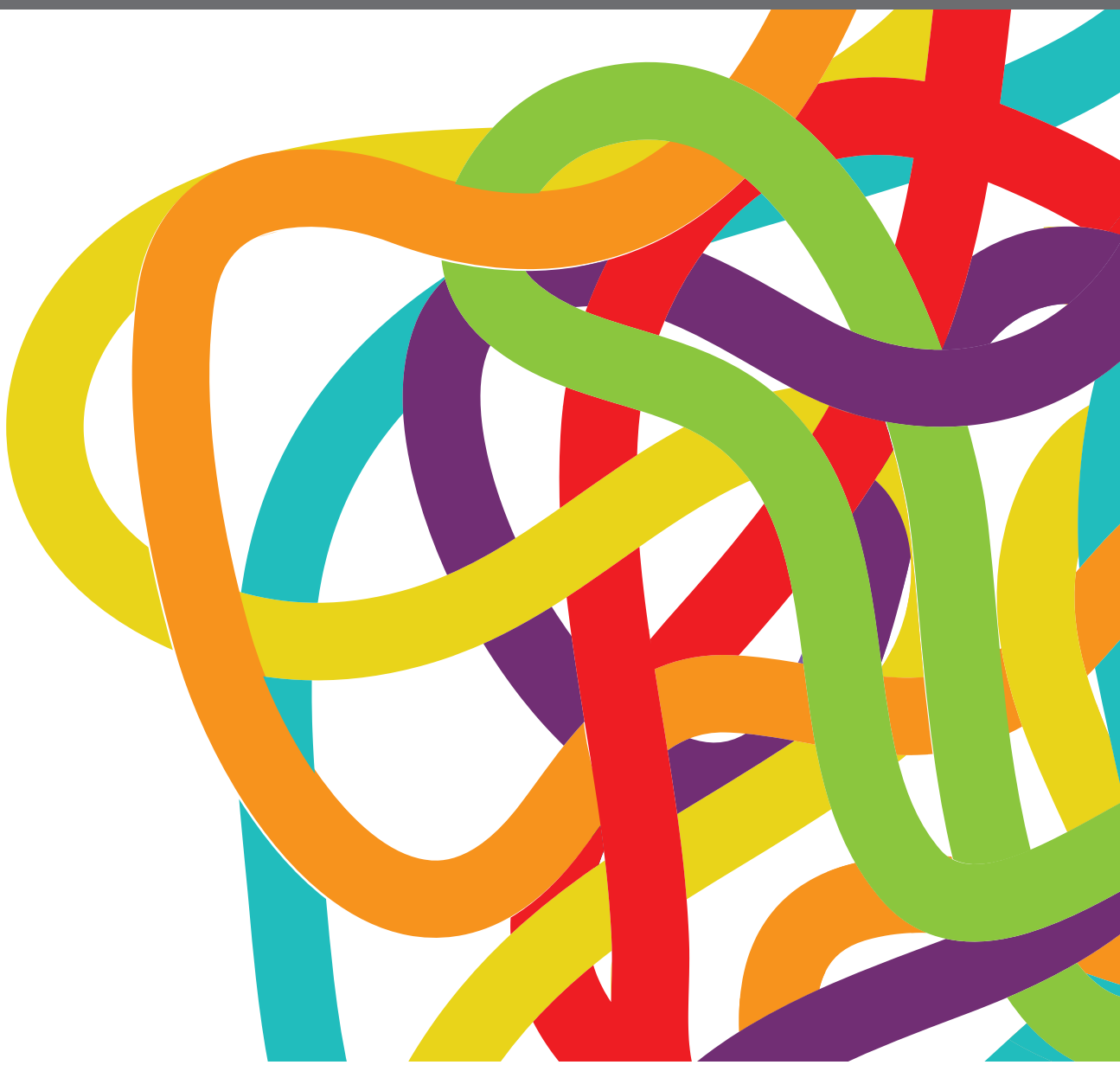

frontiers Research Topics

ISSN 1664-8714
ISBN 978-2-88974-095-6
DOI 10.3389/978-2-88974-095-6

About Frontiers

Frontiers is more than just an open-access publisher of scholarly articles: it is a pioneering approach to the world of academia, radically improving the way scholarly research is managed. The grand vision of Frontiers is a world where all people have an equal opportunity to seek, share and generate knowledge. Frontiers provides immediate and permanent online open access to all its publications, but this alone is not enough to realize our grand goals.

Frontiers Journal Series

The Frontiers Journal Series is a multi-tier and interdisciplinary set of open-access, online journals, promising a paradigm shift from the current review, selection and dissemination processes in academic publishing. All Frontiers journals are driven by researchers for researchers; therefore, they constitute a service to the scholarly community. At the same time, the Frontiers Journal Series operates on a revolutionary invention, the tiered publishing system, initially addressing specific communities of scholars, and gradually climbing up to broader public understanding, thus serving the interests of the lay society, too.

Dedication to Quality

Each Frontiers article is a landmark of the highest quality, thanks to genuinely collaborative interactions between authors and review editors, who include some of the world's best academicians. Research must be certified by peers before entering a stream of knowledge that may eventually reach the public - and shape society; therefore, Frontiers only applies the most rigorous and unbiased reviews.
Frontiers revolutionizes research publishing by freely delivering the most outstanding research, evaluated with no bias from both the academic and social point of view. By applying the most advanced information technologies, Frontiers is catapulting scholarly publishing into a new generation.

What are Frontiers Research Topics?

Frontiers Research Topics are very popular trademarks of the Frontiers Journals Series: they are collections of at least ten articles, all centered on a particular subject. With their unique mix of varied contributions from Original Research to Review Articles, Frontiers Research Topics unify the most influential researchers, the latest key findings and historical advances in a hot research area! Find out more on how to host your own Frontiers Research Topic or contribute to one as an author by contacting the Frontiers Editorial Office: frontiersin.org/about/contact

MOLECULAR MECHANISMS AND TREATMENT OF MYCN-DRIVEN TUMORS

Topic Editors:
Yusuke Suenaga, Chiba Cancer Center, Japan
Christer Einvik, UiT The Arctic University of Norway, Norway
Atsushi Takatori, Chiba Cancer Center Research Institute, Japan
Yuyan Zhu, The First Affiliated Hospital of China Medical University, China

Citation: Suenaga, Y., Einvik, C., Takatori, A., Zhu, Y., eds. (2022). Molecular Mechanisms and Treatment of MYCN-driven Tumors. Lausanne: Frontiers Media SA. doi: 10.3389/978-2-88974-095-6

Table of Contents

frontiers in Oncology

EDITORIAL
published: 30 November 2021
doi: 10.3389/fonc.2021.803443

Editorial: Molecular Mechanisms and Treatment of MYCN-Driven Tumors

Yusuke Suenaga[1]*, *Christer Einvik*[2,3], *Atsushi Takatori*[4] and *Yuyan Zhu*[5,6]

[1] Department of Molecular Carcinogenesis, Chiba Cancer Center Research Institute, Chiba, Japan, [2] Department of Pediatrics, Division of Child and Adolescent Health, UNN - University Hospital of North-Norway, Tromsø, Norway, [3] Pediatric Research Group, Department of Clinical Medicine, Faculty of Health Science, The Arctic University of Norway - UiT, Tromsø, Norway, [4] Division of Innovative Cancer Therapeutics, Chiba Cancer Center Research Institute, Chiba, Japan, [5] Joint Laboratory of Artificial Intelligence and Precision Medicine of China Medical University and Northeastern University, Shenyang, China, [6] Department of Urology, The First Hospital of China Medical University, Shenyang, China

Keywords: MYCN, neuroblastoma, brain tumor, hepatocellular carcinoma, therapeutic targets

Editorial on the Research Topic

Molecular Mechanisms and Treatment of MYCN-Driven Tumors

MYCN encodes a transcription factor that functions as an oncoprotein, similar to other MYC family proteins, c-MYC and L-MYC. Since its discovery as an amplified gene homologous to c-*MYC* in neuroblastoma, *MYCN* has been found to be amplified and overexpressed in various tumors and promotes aggressiveness. In this special issue, we review the current understanding of the oncogenic functions of MYCN and potential therapeutic strategies against MYCN-driven tumors.

OPEN ACCESS

Edited and reviewed by:
Tao Liu,
University of New South Wales, Australia

***Correspondence:**
Yusuke Suenaga
ysuenaga@chiba-cc.jp

Specialty section:
This article was submitted to Molecular and Cellular Oncology, a section of the journal Frontiers in Oncology

Received: *28 October 2021*
Accepted: *12 November 2021*
Published: *30 November 2021*

Citation:
Suenaga Y, Einvik C, Takatori A and Zhu Y (2021) Editorial: Molecular Mechanisms and Treatment of MYCN-Driven Tumors. Front. Oncol. 11:803443. doi: 10.3389/fonc.2021.803443

MECHANISM OF MYCN DYSREGULATION AND DRUGS TARGETING MYCN-DRIVEN TUMORS

The molecular mechanism of MYCN overexpression in tumors has been described in detail by R. Liu et al. Gene amplification, transcription, translation, and protein stability are involved in MYCN upregulation. It is also worth noting that the recently identified point mutation P44L in *MYCN* is an activating mutation that enhances *MYCN* transcription and protein stability.

The review by Z. Liu et al. described the structure and function of MYCN in contrast to c-MYC. It provides a detailed description of the latest findings, including the differences between MYCN and c-MYC in global transcriptional regulation, the ubiquitination and methylation mechanisms that regulate MYCN stability, and the molecular mechanisms leading to synthetic lethality in MYCN-driven tumors, including mutations in ATRX. Inhibitors that target these molecular mechanisms of MYCN expression, downstream gene regulation, or synthetic lethality are discussed in terms of their efficacy in MYCN-driven tumors. *NCYM* is an antisense gene of *MYCN* and is always amplified together with *MYCN*. Its gene product specifically stabilizes MYCN, but not c-MYC. The secondary structure of NCYM identified by Matsuo et al. may be useful for designing NCYM/MYCN-targeting drugs in the future. In addition, Takatori et al. showed that *NLRR1*, a downstream gene of *MYCN*, is also expressed in MYCN-driven tumors, including adult cancers, and that a monoclonal antibody against NLRR1 in combination with EGFR inhibitors may be an effective therapeutic strategy for these tumors. Consistent with this idea, the detailed analysis by Pan et al. of protein-protein interaction networks identified an important

role for EGFR in the MYCN network and pathway, and the combination of drugs targeting MYCN or its downstream genes with EGFR inhibitors may be a promising strategy in the future. Raieli et al. comprehensively investigated the mechanisms of MYCN-induced immunosuppression and showed that the intensity of immunosuppression is associated with poor prognosis in neuroblastoma. Furthermore, they showed that BGA002, an anti-MYCN antigene peptide nucleic acid, enhances NK cell sensitivity in MYCN-amplified neuroblastomas.

MECHANISM OF MYCN-DRIVEN TUMORIGENESIS FROM AN EMBRYOLOGICAL PERSPECTIVE

Otte et al. explained the MYCN-driven tumorigenesis in neuroblastomas. In neuroblastoma, *MYCN* amplification is observed at the time of diagnosis, and non-*MYCN*-amplified tumors do not secondarily acquire *MYCN* amplification. In other words, unlike gene amplification in other tumors, *MYCN* amplification in neuroblastoma is a phenomenon that occurs early in carcinogenesis. Neuroblastoma development is thought to be caused by the inhibition of neural differentiation and promotion of cell proliferation in the sympathoadrenal lineages. However, recent studies revealed that overexpression of MYCN in mouse sympathoadrenal progenitors promotes neuronal differentiation without forming tumors *in vivo* and that MYCN is expressed together with CIP2A in the neural plate destined to form the central nervous system, but is excluded from the neighboring neural crest stem cell domain. Therefore, MYCN may promote neuroblastoma carcinogenesis at an earlier developmental stage than during the migration and differentiation of neural crest cells. Compared to previous models, mouse neuroblastoma developed in recently established models resembles human neuroblastoma, reflecting the gain or loss of copy number of chromosomes; however, these mouse models used Th or Dbh promoters, which overexpress MYCN relatively late in the neural crest differentiation process. To identify the origin of *MYCN*-amplified neuroblastoma, it will be necessary to investigate the effect of MYCN overexpression at an early stage of development. Explaining when and how *MYCN* gene amplification occurs during early development is an important topic that remains to be elucidated in neuroblastoma biology.

Borgenvik et al. discussed how MYCN-targeted drugs can be applied in the treatment of brain tumors, comparing the findings with those of neuroblastoma. In addition, the molecular mechanisms of subtypes, overexpression, and tumor-promoting potential of brain tumors, including the rare tumors in which MYCN is involved, are described in detail. MYCN is expressed in the hindbrain during development and is essential for cerebellar development (Shrestha et al.). Abnormalities in MYCN during cerebellar development cause medulloblastoma, one of the most prevalent causes of brain tumors in children. Consistent with the requirement of MYCN for the promotion of cell proliferation of the cerebellar granule cell precursor by SHH during development, *MYCN* is amplified and overexpressed in the SHH subtype of medulloblastoma and is involved in its aggressiveness. Amplification is also observed in Group 4 medulloblastoma, but the relationship between the physiological roles of MYCN in embryonic development and the oncogenic functions of MYCN in Group 4 medulloblastoma remains to be elucidated.

Metabolic reprogramming is an important mechanism for MYCN-driven tumorigenesis, in addition to promoting cell proliferation and inhibiting cell death. As seen in pluripotent stem cells, a function of MYCN in metabolic reprogramming is providing bio-macromolecules through the activation of the glycolytic system accompanied by upregulated mitochondrial metabolism that leads to high energy production (Otte et al.; Yoshida). By introducing the functions of downstream genes of MYCN (*ASCT2* and *GLDC*) or factors that work in concert with MYCN (ATF4 and MondoA), Yoshida explained the molecular mechanism of this metabolic reprogramming, which cannot be fully explained by the Warburg effect.

Another aspect of the stem cell-like characteristics of *MYCN*-amplified neuroblastoma is its ability to undergo symmetric division *via* inhibition of asymmetric division (Izumi et al.). MYCN promotes symmetric division by mutual regulation of the reprogramming factors OCT4 and LIN28B. In addition, a downstream gene, *HMGA1*, regulates cell fate determinants, such as NUMB, and contributes to MYCN-induced symmetric division. Because all these factors have been reported to be associated with the aggressiveness of neuroblastomas, the maintenance of symmetric division is one of the oncogenic functions of MYCN that could be targeted by drugs in the future.

INDUCTION OF MYCN BY ENVIRONMENTAL FACTORS AND MYCN REGULATION BY MIRNAS

MYCN is highly expressed in hepatocellular carcinomas and correlates with cancer stem cell markers and Wnt/β-catenin signaling (Qin et al.). Indeed, it is expressed in a population of liver cancer stem cells, and high MYCN expression levels are associated with the recurrence of hepatocellular carcinoma. Unlike neuroblastoma, *MYCN* amplification is only approximately 2% in hepatocellular carcinomas, suggesting that the expression of MYCN is induced by mechanisms other than gene amplification. Hepatocellular carcinoma is not only caused by hepatitis B or C virus infection, but also by obesity-induced inflammation. Qin et al. proposed repair signaling and stress adaptation signaling in response to inflammation as the cause of MYCN induction in hepatocellular carcinomas. In addition, disruption of miRNA-mediated repression of MYCN expression, including miR-493, has attracted attention as a molecular mechanism for the high expression of MYCN in hepatocellular carcinoma. Discovery of the feedback mechanism between the miR-17-92 cluster and *MYCN* and its significance in neuroblastoma prognosis by Misiak et al. further emphasizes the importance of post-translational regulation of MYCN as a promising therapeutic target for these tumors.

This special issue focuses on the functions of MYCN and therapeutic strategies for various cancer types. It is our hope that readers will gain knowledge of cancer types outside their area of expertise, which will be useful in the development of new therapies. Elucidation of the physiological functions of MYCN, especially in developmental processes and global transcription, will also contribute to a comprehensive understanding of basic biology, not restricted to molecular oncology.

AUTHOR CONTRIBUTIONS

All authors listed have made a substantial, direct, and intellectual contribution to the work and approved it for publication.

Conflict of Interest: The authors declare that the research was conducted in the absence of any commercial or financial relationships that could be construed as a potential conflict of interest.

frontiers in Oncology

MINI REVIEW
published: 27 May 2020
doi: 10.3389/fonc.2020.00791

Beyond the Warburg Effect: N-Myc Contributes to Metabolic Reprogramming in Cancer Cells

Go J. Yoshida [1,2*†]

[1] Department of Pathology and Oncology, Juntendo University School of Medicine, Tokyo, Japan, [2] Department of Immunological Diagnosis, Juntendo University School of Medicine, Tokyo, Japan

Cancer cells generate large amounts of lactate derived from glucose regardless of the available oxygen level. Cancer cells finely control ATP synthesis by modulating the uptake of substrates and the activity of enzymes involved in aerobic glycolysis (Warburg effect), which enables them to adapt to the tumor microenvironment. However, increasing evidence suggests that mitochondrial metabolism, including the tricarboxylic acid (TCA) cycle, oxidative phosphorylation (OXPHOS), and glutaminolysis, is paradoxically activated in MYCN-amplified malignancies. Unlike non-amplified cells, MYCN-amplified cancer cells significantly promote OXPHOS-dependent ATP synthesis. Furthermore, tumor cells are differentially dependent on fatty acid β-oxidation (FAO) according to N-Myc status. Therefore, upregulation of FAO-associated enzymes is positively correlated with both N-Myc expression level and poor clinical outcome. This review explores therapeutic strategies targeting cancer stem-like cells for the treatment of tumors associated with MYCN amplification.

Keywords: acyclic retinoid, amino acid transporter, cancer stem-like cells, fatty acid β-oxidation, glutaminolysis, mitochondria, N-Myc, TCA cycle

OPEN ACCESS

Edited by:
Yusuke Suenaga,
Chiba Cancer Center, Japan

Reviewed by:
Shunpei Satoh,
Saitama Cancer Center, Japan
Francesco Grignani,
University of Perugia, Italy
Md Shamim Hossain,
Kyushu University, Japan

****Correspondence:***
Go J. Yoshida
medical21go@yahoo.co.jp

†ORCID:
Go J. Yoshida
orcid.org/0000-0002-1472-892X

Specialty section:
This article was submitted to Molecular and Cellular Oncology, a section of the journal Frontiers in Oncology

Received: *12 February 2020*
Accepted: *22 April 2020*
Published: *27 May 2020*

Citation:
Yoshida GJ (2020) Beyond the Warburg Effect: N-Myc Contributes to Metabolic Reprogramming in Cancer Cells. Front. Oncol. 10:791. doi: 10.3389/fonc.2020.00791

INTRODUCTION

N-Myc contains a C-terminal basic region that can bind to DNA and a basic-helix-loop-helix-leucine zipper domain that is responsible for the physical interaction with its counterpart MAX. Myc/MAX heterodimers bind to the DNA sequence 5′-CACGTG-3′, which is termed the consensus E-box (1, 2). N-Myc represses transglutaminase 2 (TG2) transcription in cooperation with specific protein 1 (SP1) and the subsequent recruitment of histone deacetylase 1 (3); however, N-Myc also directly induces the transcription of a specific subset of ATP-binding cassette (ABC) transporter genes. These examples strongly suggest a double-edged sword role for N-Myc in transcriptional regulation according to cell context and tumor microenvironment (4). The Myc family is essential for normal development of the central nervous system (5), and the expression pattern of Myc changes from N-Myc to c-Myc during differentiation to transit-amplifying progenitors (6).

N-Myc is overexpressed in malignant neoplasms of the nervous system, including neuroblastoma, medulloblastoma, glioblastoma multiforme, retinoblastoma, and astrocytoma, as well as in non-neuronal tumors, including hematologic malignancies, small cell lung cancer, neuroendocrine prostate cancer, rhabdomyosarcoma, and Wilms tumors (7). N-Myc is expressed in self-renewing and quiescent hematopoietic stem cells, and expression changes to c-Myc upon differentiation to transit-amplifying progenitors (8). This finding suggests that N-Myc plays a role in the activation of stem cell-like properties characterized by self-renewal potential. Consistently,

enforced expression of N-Myc, but not c-Myc, in murine bone marrow cells causes rapid development of acute myeloid leukemia *in vivo* (9). This is supported by the effect of N-Myc upregulation on driving the formation of a neuroendocrine tumor type that differs from c-Myc-driven prostate cancer in histology and response to androgen receptor (AR) signaling-targeted therapies (10, 11). N-Myc suppresses AR signaling and induces polycomb repressive complex 2 (PRC2) target gene repression irrespective of phosphatase and tensin homolog deleted on chromosome 10 (PTEN) status. N-Myc binds to AR enhancers and forms a complex with AR in a manner dependent on its interaction with enhancer of zeste homolog 2 (EZH2). Furthermore, the catalytic activity of EZH2 promotes N-Myc/AR/EZH2-PRC2 complex formation (10). Thus, N-Myc might play a fundamental role in lineage switching from an epithelial origin to a neuroendocrine prostate carcinoma.

Despite its therapeutic potential, targeting N-Myc directly using small molecules remains challenging. As of this writing, there are very few reports demonstrating the efficacy of any compound targeting the binding between N-Myc and MAX, and effective small molecules capable of interfering with the N-Myc/MAX heterodimer *in vivo* have not been identified (7). Several indirect strategies to target N-Myc-driven malignancy are currently being explored, such as impeding MYCN transcription with inhibitors of bromodomain and extraterminal (BET) proteins such as JQ1; targeting proteins that increase N-Myc stability such as allosteric Aurora-A inhibitors; and exploiting synthetic lethal interactions with agents that deregulate N-Myc such as checkpoint kinase 1 (CHK1) inhibitors (7, 12, 13). CHK1 is involved in DNA repair, which is modulated by c-Myc-induced replicative stress (14). CHK1 transcription is markedly elevated in patients with MYCN-amplified neuroblastomas (13). In addition, the MRN complex is composed of RAD50, meiotic recombination 11 (also referred to as MRE11), and NBS1 (also known as nibrin). MRN plays a critical role in processing, sensing, and repairing the double-strand breaks of DNA (15). Petroni and Giannini reported that N-Myc-dependent proliferation of neuroprogenitor cells is accompanied by DNA replication stress, which is attenuated by the MRN complex, a direct transcriptional target of N-Myc. MRN inhibition via mirin also results in the accumulation of DNA damage response (DDR) markers and replication stress-associated DNA foci in an N-Myc-dependent manner. The functional inactivation of the MRN complex mediated by mirin in N-Myc-expressing neural cells fails to induce CHK1 phosphorylation and S phase arrest, whereas it activates both p53 and ATM to trigger apoptotic cell death (16). CCT244747, which is a highly selective and orally active CHK1 inhibitor, has shown therapeutic effects in an N-Myc-driven transgenic murine model of neuroblastoma (17). Zirath et al. (18) demonstrated that the compound 10058-F4, which is thought to disrupt the interaction between c-MYCN-Myc and MAX, impairs respiratory chain and FAO, resulting in apoptosis. A recent study showed *in vitro* that 10058-F4 is effective against acute promyelocytic leukemia and acute lymphoblastic leukemia with c-Myc overexpression (19).

METABOLIC REPROGRAMMING THROUGH THE REGULATION OF AMINO ACID TRANSPORTERS BY N-MYC

Amino acid transporters contribute to metabolic reprogramming and maintain cancer stem-like phenotypes. xCT (SLC7A11) takes up cystine in exchange for glutamine, which is used for the synthesis of reduced glutathione (GSH) (20, 21), whereas ASCT2 (solute carrier family 1 member 5; SLC1A5) simultaneously takes up glutamine (22, 23). The heterodimer composed of LAT1 (SLC7A5) and CD98 heavy chain (SLC3A2) is broadly and highly expressed in cancer cells and provides essential amino acids characterized by leucine, thereby activating the mammalian target of rapamycin (mTOR) complex1 (24). Oncogenic c-Myc and hypoxia-induced factor 2α (HIF2α) upregulate LAT1 in a coordinated manner, whereas miR-126 suppresses LAT1 expression (25, 26). The leucine influx mediated by LAT1 is associated with another amino acid antiporter, ASCT2 (27). Pharmacological inhibition of ASCT2 suppresses LAT1-mediated leucine uptake, which leads to mTOR signaling inactivation in malignancy (28). Glutamine contributes to the synthesis of α-ketoglutarate (α-KG) via its conversion to glutamate, thereby promoting the tricarboxylic acid (TCA) cycle and the synthesis of nucleotides required for cellular proliferation (27, 29). CD44 variant (CD44v)-positive cancer stem-like cells (CSCs) express high levels of xCT and ASCT2, which promote GSH synthesis from cysteine and α-KG from glutamine, respectively (30). Because c-Myc regulates amino acid transporters such as ASCT2 (23), c-Myc is likely to induce metabolic reprogramming in CD44v-positive CSCs. Collectively, metabolic reprogramming, which is orchestrated by the increased expression and interplay of amino acid transporters, results in glutamine addiction and protects CSCs from redox stress.

Ren et al. (31) reported that MYCN-amplified neuroblastoma cells prominently depend on ASCT2 to maintain sufficient level of glutamine to activate TCA cycle. MYCN amplification is present in ∼30–40% of high-grade neuroblastoma patients and is a poor prognostic factor (32, 33). MYCN-amplified neuroblastoma cells need an efficient machinery to meet the metabolic demands to keep enough amount of glutamine, which is a process which strictly relies on the interaction of specific amino acid transporters. High expression levels of Myc

Abbreviations: ACR, acyclic retinoid; α-KG, α-ketoglutarate; AMPK, AMP-activated protein kinase; AR, androgen receptor; BET, bromodomain and extraterminal; CD44v, CD44 variant; CHK1, checkpoint kinase 1; CPT1C, carnitine palmitoyltransferase 1; CSCs, cancer stem-like cells; EpCAM, epithelial cell adhesion molecule; ER, endoplasmic reticulum; EZH2, zeste homolog 2; FAO, fatty acid β-oxidation; GLDC, glycine decarboxylase; HCC, hepatocellular carcinoma; LDH-A, lactate dehydrogenase A; MCT, monocarboxylate transporter; mTOR, mammalian target of rapamycin; NASH, non-alcoholic steatohepatitis; OXPHOS, oxidative phosphorylation; PRC2, polycomb repressive complex 2; PTEN, phosphatase and tensin homolog deleted on chromosome 10; ROS, reactive oxygen species; SCD1, stearoyl-CoA desaturase-1; TCA, tricarboxylic acid; UFA, unsaturated fatty acid.

are necessary to maintain the glutaminolytic phenotype and addiction to glutamine as a bioenergetic substrate (23, 34–36). Induction of key regulatory genes encoding glutamine transporters, glutaminase, and lactate dehydrogenase A (LDH-A) is important for glutaminolysis correlated with the Myc-induced increase in glutamine uptake and glutaminase flux. Glutamine addiction is associated with the activity of Myc in redirecting glucose carbon utilization away from mitochondria as a result of LDH-A activation (23, 35). Consequently, Myc-transformed cells become dependent on glutamine anapleurosis to maintain mitochondrial integrity and TCA cycle function. Indeed, MYCN-amplified neuroblastoma cells display addiction to glutamine metabolism (36). Ren et al. (31) identified a well-conserved N-Myc binding site in the ASCT2 promoter region. Although N-Myc and ATF4 cooperatively transactivate ASCT2, this amino acid transporter is significantly upregulated in response to glucose and/or glutamine deprivation and endoplasmic reticulum (ER) stress (**Figure 1**).

MITOCHONDRIAL METABOLIC REPROGRAMMING IN N-MYC-DRIVEN CANCER CELLS

Alptekin et al. proposed an alternative therapeutic strategy against MYCN-amplified neuroblastoma. These authors demonstrated that upregulation of genes associated with the serine-glycine-one-carbon (SGOC) metabolic pathway underlies the excessive dependence on glycine decarboxylase (GLDC) (38). N-Myc activates GLDC transcription and is essential for maintaining high levels of GLDC expression in MYCN-amplified neuroblastoma cells, suggesting that GLDC and other SGOC pathway genes are cooperatively upregulated (38). Xia et al. reported that the SGOC pathway is inhibited by N-Myc-dependent metabolic vulnerability (39). Genes encoding SGOC-associated enzymes including PHGDH, PSAT1, PHSH, and SHMT are direct transcriptional targets of ATF4. The SGOC pathway provides potential targets for preventing therapeutic resistance in neuroblastoma (40). Increasing evidence supports the pathophysiological significance of GLDC upregulation (41, 42). Increased expression of GLDC in CSCs from non-small-cell lung cancer is essential for their proliferation and tumorigenic ability by driving glycolysis, pyrimidine biosynthesis, and sarcosine production (41). In addition, GLDC upregulation is essential for the viability and growth of glioblastoma cells expressing high levels of serine hydroxymethyltransferase 2, which changes serine into glycine in mitochondria (42). GLDC contributes to metabolic reprogramming exclusively in MYCN-amplified neuroblastoma cells, as demonstrated by the effect of GLDC knockdown on central carbon metabolism pathways, including glycolysis and the TCA cycle, as well as lipid synthesis. GLDC knockout decreases the levels of glucose-6-phosphate, 3-phosphoglycerate, and lactate (38), suggesting that GLDC drives aerobic glycolysis. In addition, GLDC knockdown inhibits the glutamine-dependent reductive carboxylation pathway (38). Glutaminolysis and the reductive carboxylation pathway contribute to the synthesis of acetyl-CoA for lipid synthesis in tumor cells (27, 43, 44). Consistent with this finding, GLDC knockdown considerably decreases levels of fatty acids (palmate and myristic acid) and sterols (lanosterol and cholesterol) (38).

MYCN-amplified neuroblastoma cells exhibit enhanced expression of genes and proteins involved in aerobic glycolysis (Warburg effect), oxidative phosphorylation (OXPHOS), detoxification of reactive oxygen species (ROS), and FAO (45). In MYCN-amplified tumor cells, glycolytic enzymes including hexokinase isoform 2 are upregulated, and enzymes associated with the TCA cycle and the electron transport chain, such as citrate synthase and isocitrate dehydrogenase isoform 2, are expressed at high levels. Increased expression of N-Myc-induced respiratory subunit genes is correlated with adverse clinical outcome in patients with neuroblastoma (45). A moderate increase in ROS in malignant neoplasms modulates cancer cellular signaling via the oxidation of cysteine. H_2O_2 inactivates PTEN, a widely-known tumor suppressor, by oxidizing cysteine residues in the active site; this results in the formation of a disulfide bond, which prevents PTEN from inactivating the phosphatidylinositol-3-kinase (PI3K) signaling pathway (46). Therefore, cancer cells finely maintain ROS level within a narrow window which stimulates cellular proliferation. Because most mitochondrial proteins are overexpressed in MYCN-amplified neuroblastoma, and OXPHOS results in the production of intracellular ROS in mitochondria (47), the members of the peroxiredoxin ROS scavenger system, such as peroxiredoxin 6, are upregulated (45). Cancer cells tend to produce large amounts of lactate from glucose, regardless of the available oxygen level, and they activate glycolytic metabolism even before exposure to hypoxic conditions (27, 48). However, neoplastic cells highly depend on the TCA cycle and OXPHOS in mitochondria, rather than on aerobic glycolysis in cytoplasm (27, 49). The metabolic symbiosis between tumor cells and cancer-associated fibroblasts (CAFs) needs the expression of different subtypes of monocarboxylate transporter (MCT) by each cell population. Epithelial tumor cells typically express MCT1, which promotes the uptake of lactate generated and provided by MCT4-expressing and caveolin1-negative CAFs (50, 51). Cancer cells synthesize pyruvate from lactate, providing the TCA cycle and subsequent OXPHOS with an intermediate metabolite. Oliynyk et al. (45) demonstrated that MYCN-amplified neuroblastoma cells depend on both aerobic glycolysis and the TCA cycle; however, metabolic reprogramming driven by N-Myc may rely mostly on mitochondrial metabolism. Furthermore, N-Myc overexpression is related to the FAO process. Indeed, acyl-CoA dehydrogenase is involved in regulating the first step of FAO and is negatively correlated with clinical outcome of patients with MYCN-amplified malignancy (45). Accordingly, the FAO inhibitor etomoxir, which inhibits the rate-limiting FAO enzyme carnitine palmitoyltransferase 1 (CPT1C), suppresses the growth of xenograft tumors derived from MYCN-amplified neuroblastoma (45). This finding suggests that neuroblastoma cells are differentially susceptible to FAO inhibition according to N-Myc expression.

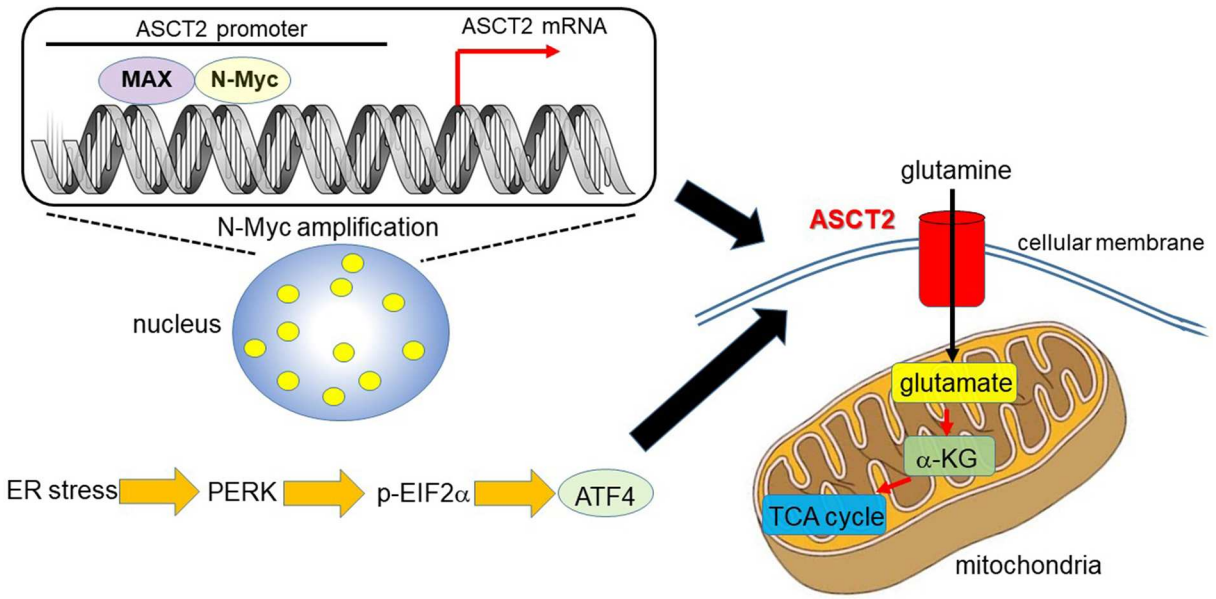

FIGURE 1 | N-Myc and ATF4 act together to upregulate ASCT2, thereby enhancing mitochondrial metabolism. In MYCN-amplified neuroblastoma, the N-Myc/MAX heterodimer binds to the ASCT2 promoter region and aberrantly regulates its transcriptional level (7, 31). Endoplasmic reticulum (ER) stress induces ATF4 via protein kinase-like ER kinase (PERK) and phosphorylated eukaryotic initiation factor 2α (p-EIF2α) (37). ATF4 activates amino acid and glucose metabolism, and promotes protein translation to support increased biosynthetic activities. As such, ATF4 upregulates ASCT2 under ER stress conditions in N-Myc-overexpressing cancer cells. ASCT2 upregulation thus promotes robust uptake of glutamine, which is converted into glutamate and subsequently α-ketoglutarate (α-KG), a substrate of the TCA cycle.

LIPID METABOLIC REPROGRAMMING IN N-MYC-DRIVEN TUMOR CELLS

High expression levels of CPT1C, a brain-specific metabolic enzyme, in N-Myc-positive neuroblastoma cells suggest that increased FAO might be an important metabolic feature in this malignancy (52). While CPT1A and CPT1B exist on the cytosolic surface of mitochondria, CPT1C is localized in endoplasmic reticulum; CPT catalyzes the synthesis of acyl-carnitine from acyl-CoA and promotes lipid conveyance through the membrane of mitochondria (52, 53). The production of acyl-carnitine represents a pivotal regulatory step before FAO because both CPT1A and CPT1C are likely to be inhibited by malonyl-CoA, a final metabolite of the FAO of acyl-CoA molecules. Malonyl-CoA, a fatty acid precursor, simultaneously promotes fatty acid biosynthesis and inhibits fatty acid catabolism, thereby regulating the balance of intracellular fatty acids (18, 54). MYCN-amplified neuroblastoma cells show high levels of CPT1C expression, and inhibition of both CPT1C and peroxisomal β-oxidation leads to lipid accumulation (18). Furthermore, impairment of bromodomain-containing protein 4 (BRD4) due to JQ1 significantly downregulates N-Myc in association with the formation of lipid droplets (18). These findings strongly suggest that N-Myc contributes to lipid metabolic reprogramming, and N-Myc inhibition is responsible for lipid accumulation. Treatment with 10058-F4, which inhibits the c-Myc/MAX complex and the N-Myc/MAX interaction, downregulates several enzymes directly involved in FAO as well as glycolysis and the TCA cycle. High expression levels of FAO-associated enzymes are correlated with robust N-Myc activity and poor clinical outcome in patients with neuroblastoma (18).

Qin et al. (55) reported that signaling networks that regulate ER stress, characterized by the endocannabinoid cancer inhibition pathway, are regulated by stearoyl-CoA desaturase-1 (SCD1) in hepatic tumor-initiating cells with high N-Myc expression. SCD1 is a rate-limiting enzyme which contributes to the synthesis of monounsaturated fatty acids. Deletion of the gene encoding SCD1 increases the rate of FAO mediated by the AMP-activated protein kinase (AMPK) pathway and the upregulation of enzymes necessary for FAO (56). AMPK phosphorylation significantly increases when the function of SCD1 is inhibited, and this inhibition of SCD1 activity has favorable effects for lipid metabolism, such as attenuated lipogenesis and/or increased FAO; these effects are partly attributed to an increase in AMPK activation (57). Changes in AMPK phosphorylation caused by SCD1 up and downregulation affect NAD^+ levels following changes in NAD^+-dependent deacetylase sirtuin-1 activity and epigenetic alterations characterized by histone H3 residue 9 acetylation and methylation status (56).

Deregulated N-Myc requires MondoA for lipid metabolic reprogramming in Myc-driven tumors (58). MondoA is associated with the outer membrane of mitochondria, where it can sense both glycolytic intermediate metabolites characterized by glucose 6-phosphate and mitochondrial metabolites necessary for glutaminolysis (59, 60). Metabolites drive the nuclear localization of MondoA, which activates the transcription

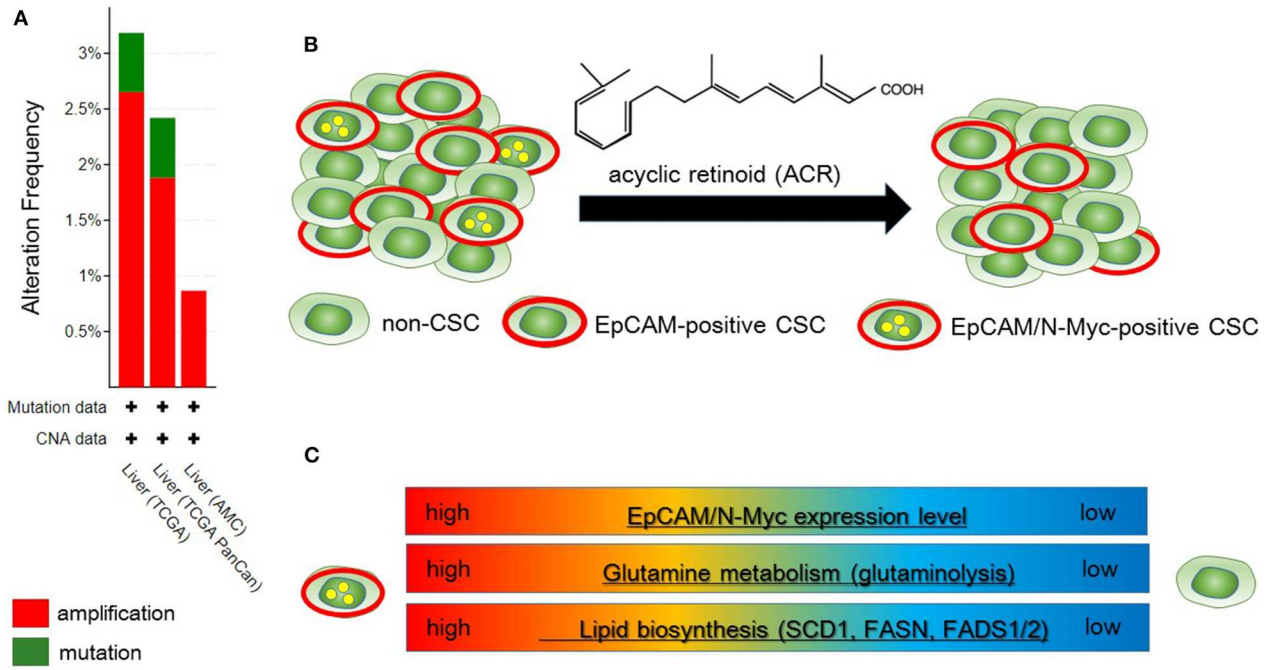

FIGURE 2 | Metabolic reprogramming in N-Myc-positive hepatic cancer stem-like cells (CSCs) is a potential therapeutic target. **(A)** According to the Cancer Genome Atlas data from the cBio Cancer Genomics Portal at Memorial Sloane Kettering Cancer Center (http://www.cbioportal.org/), ~2.5% of hepatocellular carcinoma (HCC) patients have MYCN amplification. **(B)** Primary HCC tissues include both EpCAM-positive and EpCAM/N-Myc double-positive hepatic CSCs (left). Treatment with acyclic retinoid selectively eliminates N-Myc-positive CSCs (right) (64). **(C)** Glutamine metabolism as well as lipid metabolism with SCD1 and fatty acid synthase (FASN) are activated in EpCAM/N-Myc-positive hepatic CSCs (64, 65).

of genes related to glucose metabolism (61). Depletion of MondoA inhibits N-Myc-induced glutamine uptake, glutaminolysis, and glutamine-derived lipid biosynthesis, which is why apoptosis occurs in the absence of MondoA (58). There is a collaboration network between the nutrient-utilizing N-Myc and the nutrient-sensing MondoA, and the orchestrated interaction between N-Myc and MondoA is critical for amino acid transport, lipid metabolism, nucleotide biosynthesis, and mitochondrial biogenesis. MondoA depletion is responsible for the significant downregulation of fatty acid synthase (FASN), stearoyl-CoA desaturase (SCD), and sterol regulatory element- binding protein-1 (SREBP-1). Metabolite set enrichment analysis indicates that N-Myc activation broadly alters the cellular metabolic characteristics, promotes fundamental changes in amino acid metabolism, and results in an increased amount of precursors for *de novo* lipid and purine biosynthesis (58). *De novo* lipogenesis in N-Myc overexpressing cancer cells depends on MondoA, which is required for N-Myc-induced expression of SREBP-1, FASN, and SCD. The observation that oleate (C18:1) can partially rescue the synthetic lethal effect of N-Myc overexpressing cancer cells lacking N-Myc and MondoA strongly suggests the pivotal role of lipogenesis. Inhibitors of fatty acid synthesis are toxic to N-Myc overexpressing tumor cells (58). Taken together, these findings indicate that metabolic pathways downstream of N-Myc and MondoA, particularly SREBP-1-dependent lypogenesis, are crucial for the survival of N-Myc overexpressing carcinoma.

THE NOVEL SIGNIFICANCE OF N-MYC IN HEPATIC CANCER STEM CELLS

Qin et al. identified N-Myc as one of the hepatic CSC markers in parallel with α-fetoprotein (AFP), epithelial cell adhesion molecule (EpCAM), CD90, CD133, delta-like 1 homolog, and glypican 3 (62–64), and N-Myc plays a pathological role in recurrence of *de novo* hepatocellular carcinoma (HCC). N-Myc is highly expressed in hepatic CSCs compared with non-CSCs. Furthermore, MYCN amplification occurs in at most 2.5% of HCC patients (**Figure 2A**). In *de novo* HCC, there is a positive correlation between the expression of N-Myc and that of canonical Wnt signaling target molecules such as EpCAM (64, 66), suggesting that N-Myc contributes to the stemness of HCC in cooperation with Wnt/β-catenin signaling. There is no correlation between the expression levels of c-Myc and N-Myc in *de novo* HCC. Alterations of fatty acid metabolism associated with metabolic reprogramming play a pivotal role in facilitating carcinogenesis in the liver (67). HCC cells import fatty acids and other lipids from the bloodstream; however, HCC cells upregulate enzymes involved in the biosynthesis of fatty acids, including SREBP-1-regulated genes including

ATP citrate lyase (ACLY), acetyl-CoA carboxylase (ACC), FAS, and SCD-1, leading to the *de novo* synthesis of fatty acids (68). Lipid droplets are considered to be intracellular spherical organelles which are surrounded by a phospholipid single layer (69). The generation of lipid droplets is promoted by hypoxia related to HIF1- and HIF2-mediated repression of CPT1A, an essential enzyme involved in mitochondrial FAO (70). In addition, lipid-modifying enzymes that convert saturated fatty acid (SFA) to monounsaturated fatty acids (MUFA) are responsible for carcinogenesis. This is partly because the ratio of long chain n6-polyunsaturated fatty acids to n3-polyunsaturated fatty acids is associated with a higher risk of HCC development in non-alcoholic steatohepatitis (NASH) model mice (71).

Qin et al. investigated the therapeutic effect of acyclic retinoid (ACR), a synthetic retinoid X receptor α-ligand, against hepatic CSCs expressing high levels of N-Myc. Hepatic CSCs with high expression levels of both EpCAM and N-Myc are more susceptible to ACR than non-CSCs negative for N-Myc expression (64). In general, inhibition of retinoid signaling in the liver is associated with the rapid progression of HCC associated with ROS. Thus, retinoids play crucial roles in mediating lipid metabolism in normal hepatic cells, and altered retinoid-inducing signaling is related to the progression of non-alcoholic fatty liver disease/NASH (NAFLD/NASH) (72). Sp1 may promote the transcription of N-Myc in collaboration with E2F, whereas ACR-induced nuclear translocation of transglutaminase 2 inhibits N-Myc expression in association with the inactivation of Sp1 (64, 73). ACR is a promising vitamin A-like compound for the chemoprevention of HCC because it selectively kills N-Myc-overexpressing CSCs (**Figure 2B**). ACR has chemopreventive effects on HCC mediated by the inhibition of the hyper-phosphorylation of retinoid receptors and lipid metabolic reprogramming (74, 75). Indeed, lipid metabolic reprogramming is required for the initiation step of HCC tumorigenesis (64, 75). Because lipid biogenesis as well as glutaminolysis are essential for the proliferation of N-Myc-driven cancer cells (**Figure 2C**), inhibitors of fatty acid synthesis show specific toxicity to malignancy with high expression level of N-Myc (58, 76). The growth-suppressive activity of ACR in HCC cells involves upregulation of pyruvate dehydrogenase kinase 4, which decreases the flux of glycolytic carbon into OXPHOS in mitochondria (75, 77). This response switches the energy source from glucose to fatty acids to maintain the stable ATP production. Although synthetic inhibitors of unsaturated fatty acids (UFAs) such as oleic acid are toxic to N-Myc-overexpressing cells, UFA treatment partially rescues apoptosis induced by knockdown of MondoA, a nutrient-sensing transcription factor (58). Collectively, these findings indicate that disruption of N-Myc-induced lipid metabolic reprogramming may be responsible for the specific toxicity of ACR to hepatic CSCs (64, 65).

CONCLUSIONS AND PERSPECTIVES

N-Myc enables metabolic reprogramming of cancer cells, which cannot be simply explained by constitutive aerobic glycolysis (Warburg effect). However, MYCN-amplified cells depend on the TCA cycle and OXPHOS as well as lipid metabolism, rather than the Warburg effect. N-Myc upregulates ASCT2, the amino acid transporter contributing to glutamine addiction. MondoA, a nutrient-sensing transcription factor associated with Myc signaling, plays an important role in maintaining N-Myc-induced glutaminolysis and glutamine-derived lipid biosynthesis. ACR, a leading compound of vitamin A, was recently shown to specifically kill EpCAM-positive liver CSCs expressing high levels of N-Myc. ACR holds much promise for preventing *de novo* HCC recurrence. Such CSC population is enriched in enzymes necessary for lipid desaturation including FADS1/2 and SCD1. Considering the complexity of mitochondrial metabolism, further investigation is warranted to design novel therapeutic strategies targeting metabolic reprogramming triggered by N-Myc.

AUTHOR CONTRIBUTIONS

GY searched the articles, wrote the manuscript, and submitted the paper to the journal.

FUNDING

This review article was financially supported by the Japan Society for the Promotion of Science (19K23898).

REFERENCES

1. Blackwell TK, Huang J, Ma A, Kretzner L, Alt FW, Eisenman RN, et al. Binding of myc proteins to canonical and noncanonical DNA sequences. *Mol Cell Biol.* (1993) 13:5216–24. doi: 10.1128/MCB.13.9.5216
2. Wenzel A, Schwab M. The MYCN/max protein complex in neuroblastoma. Short review. *Eur J Cancer.* (1995) 31A:516–9. doi: 10.1016/0959-8049(95)00060-V
3. Liu T, Tee AE, Porro A, Smith SA, Dwarte T, Liu PY, et al. Activation of tissue transglutaminase transcription by histone deacetylase inhibition as a therapeutic approach for Myc oncogenesis. *Proc Natl Acad Sci U S A.* (2007) 104:18682–7. doi: 10.1073/pnas.0705524104
4. Henderson MJ, Haber M, Porro A, Munoz MA, Iraci N, Xue C, et al. ABCC multidrug transporters in childhood neuroblastoma: clinical and biological effects independent of cytotoxic drug efflux. *J Natl Cancer Inst.* (2011) 103:1236–51. doi: 10.1093/jnci/djr256
5. Hurlin PJ. Control of vertebrate development by MYC. *Cold Spring Harb Perspect Med.* (2013) 3:a014332. doi: 10.1101/cshperspect.a014332
6. Knoepfler PS, Cheng PF, Eisenman RN. N-myc is essential during neurogenesis for the rapid expansion of progenitor cell populations and the inhibition of neuronal differentiation. *Genes Dev.* (2002) 16:2699–712. doi: 10.1101/gad.1021202
7. Rickman DS, Schulte JH, Eilers M. The expanding world of N-MYC-driven tumors. *Cancer Discov.* (2018) 8:150–63. doi: 10.1158/2159-8290.CD-17-0273
8. King B, Boccalatte F, Moran-Crusio K, Wolf E, Wang J, Kayembe C, et al. The ubiquitin ligase Huwe1 regulates the maintenance and lymphoid commitment of hematopoietic stem cells. *Nat Immunol.* (2016) 17:1312–21. doi: 10.1038/ni.3559

9. Kawagoe H, Kandilci A, Kranenburg TA, Grosveld GC. Overexpression of N-Myc rapidly causes acute myeloid leukemia in mice. *Cancer Res.* (2007) 67:10677–85. doi: 10.1158/0008-5472.CAN-07-1118
10. Dardenne E, Beltran H, Benelli M, Gayvert K, Berger A, Puca L, et al. N-Myc induces an EZH2-mediated transcriptional program driving neuroendocrine prostate cancer. *Cancer Cell.* (2016) 30:563–77. doi: 10.1016/j.ccell.2016.09.005
11. Lee JK, Phillips JW, Smith BA, Park JW, Stoyanova T, McCaffrey EF, et al. N-Myc drives neuroendocrine prostate cancer initiated from human prostate epithelial cells. *Cancer Cell.* (2016) 29:536–47. doi: 10.1016/j.ccell.2016.03.001
12. Barone G, Anderson J, Pearson AD, Petrie K, Chesler L. New strategies in neuroblastoma: therapeutic targeting of MYCN and ALK. *Clin Cancer Res.* (2013) 19:5814–21. doi: 10.1158/1078-0432.CCR-13-0680
13. Cole KA, Huggins J, Laquaglia M, Hulderman CE, Russell MR, Bosse K, et al. RNAi screen of the protein kinome identifies checkpoint kinase 1 (CHK1) as a therapeutic target in neuroblastoma. *Proc Natl Acad Sci U S A.* (2011) 108:3336–41. doi: 10.1073/pnas.1012351108
14. Dominguez-Sola D, Ying CY, Grandori C, Ruggiero L, Chen B, Li M, et al. Non-transcriptional control of DNA replication by c-MYC. *Nature.* (2007) 448:445–51. doi: 10.1038/nature05953
15. Stracker TH, Petrini JH. The MRE11 complex: starting from the ends. *Nat Rev Mol Cell Biol.* (2011) 12:90–103. doi: 10.1038/nrm3047
16. Petroni M, Giannini G. A MYCN-MRN complex axis controls replication stress for the safe expansion of neuroprogenitor cells. *Mol Cell Oncol.* (2016) 3:e1079673. doi: 10.1080/23723556.2015.1079673
17. Walton MI, Eve PD, Hayes A, Valenti MR, De Haven Brandon AK, Box G, et al. CCT244747 is a novel potent and selective CHK1 inhibitor with oral efficacy alone and in combination with genotoxic anticancer drugs. *Clin Cancer Res.* (2012) 18:5650–61. doi: 10.1158/1078-0432.CCR-12-1322
18. Zirath H, Frenzel A, Oliynyk G, Segerstrom L, Westermark UK, Larsson K, et al. MYC inhibition induces metabolic changes leading to accumulation of lipid droplets in tumor cells. *Proc Natl Acad Sci U S A.* (2013) 110:10258–63. doi: 10.1073/pnas.1222404110
19. Bashash D, Sayyadi M, Safaroghli-Azar A, Sheikh-Zeineddini N, Riyahi N, Momeny M. Small molecule inhibitor of c-Myc 10058-F4 inhibits proliferation and induces apoptosis in acute leukemia cells, irrespective of PTEN status. *Int J Biochem Cell Biol.* (2019) 108:7–16. doi: 10.1016/j.biocel.2019.01.005
20. Ishimoto T, Nagano O, Yae T, Tamada M, Motohara T, Oshima H, et al. CD44 variant regulates redox status in cancer cells by stabilizing the xCT subunit of system xc(-) and thereby promotes tumor growth. *Cancer Cell.* (2011) 19:387–400. doi: 10.1016/j.ccr.2011.01.038
21. Yoshida GJ, Saya H. Therapeutic strategies targeting cancer stem cells. *Cancer Sci.* (2016) 107:5–11. doi: 10.1111/cas.12817
22. McGivan JD, Bungard CI. The transport of glutamine into mammalian cells. *Front Biosci.* (2007) 12:874–82. doi: 10.2741/2109
23. Wise DR, DeBerardinis RJ, Mancuso A, Sayed N, Zhang XY, Pfeiffer HK, et al. Myc regulates a transcriptional program that stimulates mitochondrial glutaminolysis and leads to glutamine addiction. *Proc Natl Acad Sci U S A.* (2008) 105:18782–7. doi: 10.1073/pnas.0810199105
24. Scalise M, Pochini L, Galluccio M, Console L, Indiveri C. Glutamine transport and mitochondrial metabolism in cancer cell growth. *Front Oncol.* (2017) 7:306. doi: 10.3389/fonc.2017.00306
25. Elorza A, Soro-Arnaiz I, Melendez-Rodriguez F, Rodriguez-Vaello V, Marsboom G, de Carcer G, et al. HIF2α acts as an mTORC1 activator through the amino acid carrier SLC7A5. *Mol Cell.* (2012) 48:681–91. doi: 10.1016/j.molcel.2012.09.017
26. Miko E, Margitai Z, Czimmerer Z, Varkonyi I, Dezso B, Lanyi A, et al. miR-126 inhibits proliferation of small cell lung cancer cells by targeting SLC7A5. *FEBS Lett.* (2011) 585:1191–6. doi: 10.1016/j.febslet.2011.03.039
27. Yoshida GJ. Metabolic reprogramming: the emerging concept and associated therapeutic strategies. *J Exp Clin Cancer Res.* (2015) 34:111. doi: 10.1186/s13046-015-0221-y
28. Nicklin P, Bergman P, Zhang B, Triantafellow E, Wang H, Nyfeler B, et al. Bidirectional transport of amino acids regulates mTOR and autophagy. *Cell.* (2009) 136:521–34. doi: 10.1016/j.cell.2008.11.044
29. Timmerman LA, Holton T, Yuneva M, Louie RJ, Padro M, Daemen A, et al. Glutamine sensitivity analysis identifies the xCT antiporter as a common triple-negative breast tumor therapeutic target. *Cancer Cell.* (2013) 24:450–65. doi: 10.1016/j.ccr.2013.08.020
30. Okazaki S, Umene K, Yamasaki J, Suina K, Otsuki Y, Yoshikawa M, et al. Glutaminolysis-related genes determine sensitivity to xCT-targeted therapy in head and neck squamous cell carcinoma. *Cancer Sci.* (2019) 110:3453–63. doi: 10.1111/cas.14182
31. Ren P, Yue M, Xiao D, Xiu R, Gan L, Liu H, et al. ATF4 and N-Myc coordinate glutamine metabolism in MYCN-amplified neuroblastoma cells through ASCT2 activation. *J Pathol.* (2015) 235:90–100. doi: 10.1002/path.4429
32. Seeger RC, Brodeur GM, Sather H, Dalton A, Siegel SE, Wong KY, et al. Association of multiple copies of the N-myc oncogene with rapid progression of neuroblastomas. *N Engl J Med.* (1985) 313:1111–6. doi: 10.1056/NEJM198510313131802
33. Brodeur GM, Seeger RC, Schwab M, Varmus HE, Bishop JM. Amplification of N-myc in untreated human neuroblastomas correlates with advanced disease stage. *Science.* (1984) 224:1121–4. doi: 10.1126/science.6719137
34. Goetzman ES, Prochownik EV. The role for Myc in coordinating glycolysis, oxidative phosphorylation, glutaminolysis, and fatty acid metabolism in normal and neoplastic tissues. *Front Endocrinol (Lausanne).* (2018) 9:129. doi: 10.3389/fendo.2018.00129
35. Wise DR, Thompson CB. Glutamine addiction: a new therapeutic target in cancer. *Trends Biochem Sci.* (2010) 35:427–33. doi: 10.1016/j.tibs.2010.05.003
36. Qing G, Li B, Vu A, Skuli N, Walton ZE, Liu X, et al. ATF4 regulates MYC-mediated neuroblastoma cell death upon glutamine deprivation. *Cancer Cell.* (2012) 22:631–44. doi: 10.1016/j.ccr.2012.09.021
37. Rozpedek W, Pytel D, Mucha B, Leszczynska H, Diehl JA, Majsterek I. The role of the PERK/eIF2alpha/ATF4/CHOP signaling pathway in tumor progression during endoplasmic reticulum stress. *Curr Mol Med.* (2016) 16:533–44. doi: 10.2174/1566524016666160523143937
38. Alptekin A, Ye B, Yu Y, Poole CJ, van Riggelen J, Zha Y, et al. Glycine decarboxylase is a transcriptional target of MYCN required for neuroblastoma cell proliferation and tumorigenicity. *Oncogene.* (2019) 38:7504–20. doi: 10.1038/s41388-019-0967-3
39. Xia Y, Ye B, Ding J, Yu Y, Alptekin A, Thangaraju M, et al. Metabolic reprogramming by MYCN confers dependence on the serine-glycine-one-carbon biosynthetic pathway. *Cancer Res.* (2019) 79, 3837–3850. doi: 10.1158/0008-5472.CAN-18-3541
40. Zhao E, Hou J, Cui H. Serine-glycine-one-carbon metabolism: vulnerabilities in MYCN-amplified neuroblastoma. *Oncogenesis.* (2020) 9:14. doi: 10.1038/s41389-020-0200-9
41. Zhang WC, Shyh-Chang N, Yang H, Rai A, Umashankar S, Ma S, et al. Glycine decarboxylase activity drives non-small cell lung cancer tumor-initiating cells and tumorigenesis. *Cell.* (2012) 148:259–72. doi: 10.1016/j.cell.2011.11.050
42. Kim D, Fiske BP, Birsoy K, Freinkman E, Kami K, Possemato RL, et al. SHMT2 drives glioma cell survival in ischaemia but imposes a dependence on glycine clearance. *Nature.* (2015) 520:363–7. doi: 10.1038/nature14363
43. Altman BJ, Stine ZE, Dang CV. From Krebs to clinic: glutamine metabolism to cancer therapy. *Nat Rev Cancer.* (2016) 16:619–34. doi: 10.1038/nrc.2016.71
44. Zhang J, Pavlova NN, Thompson CB. Cancer cell metabolism: the essential role of the nonessential amino acid, glutamine. *EMBO J.* (2017) 36:1302–15. doi: 10.15252/embj.201696151
45. Oliynyk G, Ruiz-Perez MV, Sainero-Alcolado L, Dzieran J, Zirath H, Gallart-Ayala H, et al. MYCN-enhanced oxidative and glycolytic metabolism reveals vulnerabilities for targeting neuroblastoma. *iScience.* (2019) 21:188–204. doi: 10.1016/j.isci.2019.10.020
46. Sullivan LB, Chandel NS. Mitochondrial reactive oxygen species and cancer. *Cancer Metab.* (2014) 2:17. doi: 10.1186/2049-3002-2-17
47. Murphy MP. How mitochondria produce reactive oxygen species. *Biochem J.* (2009) 417:1–13. doi: 10.1042/BJ20081386
48. Warburg O. On the origin of cancer cells. *Science.* (1956) 123:309–14. doi: 10.1126/science.123.3191.309
49. Vyas S, Zaganjor E, Haigis MC. Mitochondria and Cancer. *Cell.* (2016) 166:555–66. doi: 10.1016/j.cell.2016.07.002
50. Pavlides S, Tsirigos A, Vera I, Flomenberg N, Frank PG, Casimiro MC, et al. Loss of stromal caveolin-1 leads to oxidative stress, mimics hypoxia and drives inflammation in the tumor microenvironment, conferring the "reverse

Warburg effect": a transcriptional informatics analysis with validation. *Cell Cycle.* (2010) 9:2201–19. doi: 10.4161/cc.9.11.11848
51. Yoshida GJ, Azuma A, Miura Y, Orimo A. Activated fibroblast program orchestrates tumor initiation and progression; molecular mechanisms and the associated therapeutic strategies. *Int J Mol Sci.* (2019) 20:2256. doi: 10.3390/ijms20092256
52. Reilly PT, Mak TW. Molecular pathways: tumor cells Co-opt the brain-specific metabolism gene CPT1C to promote survival. *Clin Cancer Res.* (2012) 18:5850–5. doi: 10.1158/1078-0432.CCR-11-3281
53. Saggerson D. Malonyl-CoA, a key signaling molecule in mammalian cells. *Annu Rev Nutr.* (2008) 28:253–72. doi: 10.1146/annurev.nutr.28.061807.155434
54. Zaugg K, Yao Y, Reilly PT, Kannan K, Kiarash R, Mason J, et al. Carnitine palmitoyltransferase 1C promotes cell survival and tumor growth under conditions of metabolic stress. *Genes Dev.* (2011) 25:1041–51. doi: 10.1101/gad.1987211
55. Qin XY, Su T, Yu W, Kojima S. Lipid desaturation-associated endoplasmic reticulum stress regulates MYCN gene expression in hepatocellular carcinoma cells. *Cell Death Dis.* (2020) 11:66. doi: 10.1038/s41419-020-2257-y
56. Dziewulska A, Dobosz AM, Dobrzyn A, Smolinska A, Kolczynska K, Ntambi JM, et al. SCD1 regulates the AMPK/SIRT1 pathway and histone acetylation through changes in adenine nucleotide metabolism in skeletal muscle. *J Cell Physiol.* (2020) 235:1129–40. doi: 10.1002/jcp.29026
57. Kim E, Lee JH, Ntambi JM, Hyun CK. Inhibition of stearoyl-CoA desaturase1 activates AMPK and exhibits beneficial lipid metabolic effects in vitro. *Eur J Pharmacol.* (2011) 672:38–44. doi: 10.1016/j.ejphar.2011.09.172
58. Carroll PA, Diolaiti D, McFerrin L, Gu H, Djukovic D, Du J, et al. Deregulated Myc requires MondoA/Mlx for metabolic reprogramming and tumorigenesis. *Cancer Cell.* (2015) 27:271–85. doi: 10.1016/j.ccell.2014.11.024
59. Han KS, Ayer DE. MondoA senses adenine nucleotides: transcriptional induction of thioredoxin-interacting protein. *Biochem J.* (2013) 453:209–18. doi: 10.1042/BJ20121126
60. Kaadige MR, Looper RE, Kamalanaadhan S, Ayer DE. Glutamine-dependent anapleurosis dictates glucose uptake and cell growth by regulating MondoA transcriptional activity. *Proc Natl Acad Sci U S A.* (2009) 106:14878–83. doi: 10.1073/pnas.0901221106
61. O'Shea JM, Ayer DE. Coordination of nutrient availability and utilization by MAX- and MLX-centered transcription networks. *Cold Spring Harb Perspect Med.* (2013) 3:a014258. doi: 10.1101/cshperspect.a014258
62. Sun JH, Luo Q, Liu LL, Song GB. Liver cancer stem cell markers: progression and therapeutic implications. *World J Gastroenterol.* (2016) 22:3547–57. doi: 10.3748/wjg.v22.i13.3547
63. Wang K, Sun D. Cancer stem cells of hepatocellular carcinoma. *Oncotarget.* (2018) 9:23306–14. doi: 10.18632/oncotarget.24623
64. Qin XY, Suzuki H, Honda M, Okada H, Kaneko S, Inoue I, et al. Prevention of hepatocellular carcinoma by targeting MYCN-positive liver cancer stem cells with acyclic retinoid. *Proc Natl Acad Sci U S A.* (2018) 115:4969–74. doi: 10.1073/pnas.1802279115
65. Yoshida GJ. How to eliminate MYCN-positive hepatic cancer stem cells to prevent the recurrence? *Proc Natl Acad Sci U S A.* (2018) 115:E6388–E9. doi: 10.1073/pnas.1808092115
66. Yamashita T, Ji J, Budhu A, Forgues M, Yang W, Wang HY, et al. EpCAM-positive hepatocellular carcinoma cells are tumor-initiating cells with stem/progenitor cell features. *Gastroenterology.* (2009) 136:1012–24. doi: 10.1053/j.gastro.2008.12.004
67. Wang M, Han J, Xing H, Zhang H, Li Z, Liang L, et al. Dysregulated fatty acid metabolism in hepatocellular carcinoma. *Hepat Oncol.* (2016) 3:241–51. doi: 10.2217/hep-2016-0012
68. Currie E, Schulze A, Zechner R, Walther TC, Farese RV Jr. Cellular fatty acid metabolism and cancer. *Cell Metab.* (2013) 18:153–61. doi: 10.1016/j.cmet.2013.05.017
69. Tirinato L, Pagliari F, Limongi T, Marini M, Falqui A, Seco J, et al. An overview of lipid droplets in cancer and cancer stem cells. *Stem Cells Int.* (2017) 2017:1656053. doi: 10.1155/2017/1656053
70. Du W, Zhang L, Brett-Morris A, Aguila B, Kerner J, Hoppel CL, et al. HIF drives lipid deposition and cancer in ccRCC via repression of fatty acid metabolism. *Nat Commun.* (2017) 8:1769. doi: 10.1038/s41467-017-01965-8
71. Muir K, Hazim A, He Y, Peyressatre M, Kim DY, Song X, et al. Proteomic and lipidomic signatures of lipid metabolism in NASH-associated hepatocellular carcinoma. *Cancer Res.* (2013) 73:4722–31. doi: 10.1158/0008-5472.CAN-12-3797
72. Shirakami Y, Sakai H, Shimizu M. Retinoid roles in blocking hepatocellular carcinoma. *Hepatobiliary Surg Nutr.* (2015) 4:222–8. doi: 10.3978/j.issn.2304-3881.2015.05.01
73. Kramps C, Strieder V, Sapetschnig A, Suske G, Lutz W. E2F and Sp1/Sp3 Synergize but are not sufficient to activate the MYCN gene in neuroblastomas. *J Biol Chem.* (2004) 279:5110–7. doi: 10.1074/jbc.M304758200
74. Matsushima-Nishiwaki R, Okuno M, Takano Y, Kojima S, Friedman SL, Moriwaki H. Molecular mechanism for growth suppression of human hepatocellular carcinoma cells by acyclic retinoid. *Carcinogenesis.* (2003) 24:1353–9. doi: 10.1093/carcin/bgg090
75. Qin XY, Tatsukawa H, Hitomi K, Shirakami Y, Ishibashi N, Shimizu M, et al. Metabolome analyses uncovered a novel inhibitory effect of acyclic retinoid on aberrant lipogenesis in a mouse diethylnitrosamine-induced hepatic tumorigenesis model. *Cancer Prev Res (Phila).* (2016) 9:205–14. doi: 10.1158/1940-6207.CAPR-15-0326
76. Yoshida GJ. Emerging roles of Myc in stem cell biology and novel tumor therapies. *J Exp Clin Cancer Res.* (2018) 37:173. doi: 10.1186/s13046-018-0835-y
77. Qin XY, Wei F, Tanokura M, Ishibashi N, Shimizu M, Moriwaki H, et al. The effect of acyclic retinoid on the metabolomic profiles of hepatocytes and hepatocellular carcinoma cells. *PLoS One.* (2013) 8:e82860. doi: 10.1371/journal.pone.0082860

Conflict of Interest: The author declares that the research was conducted in the absence of any commercial or financial relationships that could be construed as a potential conflict of interest.

frontiers in Oncology

MINI REVIEW
published: 21 October 2020
doi: 10.3389/fonc.2020.570815

The Role of MYCN in Symmetric vs. Asymmetric Cell Division of Human Neuroblastoma Cells

Hideki Izumi[1], Yasuhiko Kaneko[2†] and Akira Nakagawara[3†]*

[1] Laboratory of Molecular Medicine, Life Sciences Institute, Saga-Ken Medical Centre Koseikan, Saga, Japan, [2] Research Institute for Clinical Oncology, Saitama Cancer Center, Saitama, Japan, [3] SAGA HIMAT, Tosu, Japan

Asymmetric cell division (ACD) is an important physiological event in the development of various organisms and maintenance of tissue homeostasis. ACD produces two different cells in a single cell division: a stem/progenitor cell and differentiated cell. Although the balance between self-renewal and differentiation is precisely controlled, disruptions to ACD and/or enhancements in the self-renewal division (symmetric cell division: SCD) of stem cells resulted in the formation of tumors in *Drosophila* neuroblasts. ACD is now regarded as one of the characteristics of human cancer stem cells, and is a driving force for cancer cell heterogeneity. We recently reported that MYCN controls the balance between SCD and ACD in human neuroblastoma cells. In this mini-review, we discuss the mechanisms underlying MYCN-mediated cell division fate.

Keywords: MYCN, TRIM32, NCYM, ALDH18A1, asymmetric cell division, neuroblastoma

OPEN ACCESS

Edited by:
Christer Einvik, UiT The Arctic University of Norway, Norway

Reviewed by:
Monica Fedele, Consiglio Nazionale delle Ricerche (CNR), Italy
Sofie Mohlin, Lund University, Sweden

****Correspondence:***
Hideki Izumi
izumi-hideki@koseikan.jp
orcid.org/0000-0003-1484-934X

† These authors have contributed equally to this work

Specialty section:
This article was submitted to Molecular and Cellular Oncology, a section of the journal Frontiers in Oncology

Received: *09 June 2020*
Accepted: *21 September 2020*
Published: *21 October 2020*

Citation:
Izumi H, Kaneko Y and Nakagawara A (2020) The Role of MYCN in Symmetric vs. Asymmetric Cell Division of Human Neuroblastoma Cells. Front. Oncol. 10:570815. doi: 10.3389/fonc.2020.570815

INTRODUCTION

Neuroblastoma is a common cancer in children and exhibits a broad clinical behavior (1–3). Patients are classified into low-, intermediate-, and high-risk groups based on clinical and biological characteristics (1–3). Minimal treatment may be sufficient for the low-risk group, whereas despite intensive treatment, high-risk patients still present with a dismal outcome. The reasons for this heterogeneity remained unclear until molecular, genetic, and biochemical analyses of tumors provided insights into their different clinical behaviors. Among the many genetic and biochemical features of neuroblastoma, amplification of the *MYCN* oncogene correlates with an aggressive phenotype and poor prognosis (1–3). Approximately 20% of neuroblastomas show *MYCN* gene amplification. Recent studies reported that MYCN not only exhibited oncogenic activity, but also played a central role in normal neural stem and progenitor cell self-renewal (4–6).

Neuroblastoma originates from cells of the neural crest, which is a multipotent cell population comprising the embryonic structure (7). The neural crest is composed of migrating cell populations that give rise to diverse cell lineages, including Schwann cells, melanocytes, craniofacial cartilage and bones, smooth muscle, peripheral and intestinal neurons, and glia. Thus, the neural crest acts

Abbreviations: ACD, asymmetric cell division; ALDH18A1, Aldehyde dehydrogenase family 18 member A1; ALK, Anaplastic lymphoma kinase; AURKA, Aurora kinase A; Brat, brain tumor; CDK1, cyclin dependent kinase 1; C-TAD, C-terminal transactivation domain; CTCF, CCCTC-binding factor; Fbxw7, F-box and WD repeat domain-containing 7; GSK3β, glycogen synthase kinase 3β; HMGA1, high mobility group A1; MYCNOS, MYCN opposite strand; N-TAD, N-terminal transactivation domain; NuMA, Nuclear mitotic apparatus; OCT4, Octamer-binding transcription factor 4; PI-3K, Phosphoinositide 3-kinase; PLK1, Polo-like kinase 1; POUHD, POU transcription factor homeodomain; POUs, POU transcription factor-specific domain; SCD, symmetric cell division; TRIM3, tripartite motif-containing 3; TRIM32, tripartite motif-containing 32.

as pluripotent stem cells that differentiate into mature peripheral nerve tissue. The pluripotent neural crest is suspected to be involved in the tumorigenesis of neuroblastoma due to the abnormal expression of *MYCN*. Neuroblastoma cells are derived from the pluripotent neural crest that has cancer stem cell-like properties (8). Therefore, human neuroblastoma cultured cells exhibit both proliferative and differentiating abilities, and possess similar characteristics to cancer stem cells (9, 10).

Cancer stem cells are considered to undergo asymmetric cell division (ACD), a physiological event resulting in tumor cell heterogeneity (11, 12). ACD is a strategy that maintains the correct number of self-renewing stem cells and differentiated cells in a single division. Therefore, ACD balances the stem cell pool with its progenitor pool. Recent studies revealed that the misregulation of this balance between self-renewal and differentiation by ACD led to the emergence of abnormal stem cells, resulting in tumorigenesis in *Drosophila* neuroblast populations (13). Therefore, cancer stem cells may use ACD as a strategy to generate more cancer stem cells in addition to many differentiated cancer cells. We herein investigated the mechanisms underlying ACD using a series of human neuroblastoma cultured cells as a model system (14–16).

MYCN

Asymmetric cell division studies were originally conducted using model organisms, such as nematode embryos (17, 18), *Drosophila* neuroblasts (13), and *Drosophila* germ stem cells (19). The findings of these genetic studies revealed that the mechanism of ACD is highly conserved. Previous studies demonstrated the ACD of stem cells in muscle (20), skin (21), the gut (22), mammary glands (23), the hematopoietic system (24), and the developing mouse brain (25, 26). Comparisons of ACD studies using these organisms and model systems revealed ACD in neuroblastoma cells in an evolutionarily conserved manner (14). The magnitude of *MYCN* gene expression influences the regulation of cell division fate. The overexpression of *MYCN* induces symmetric cell division (SCD) (self-renewal division), and the decreased expression of *MYCN* causes ACD (14). Furthermore, the transcriptional activity of MYCN is important for inducing SCD in human neuroblastoma cells (14). Although the specific transcriptional target(s) of MYCN currently remain unclear, except the high mobility group A1 (HMGA1) oncogene, several key molecular pathways involved in MYCN-mediated cell division fate have been identified (**Figure 1**).

TRIM32

Tripartite motif-containing 32 (TRIM32) was identified as an ACD inducer in human neuroblastoma cells (15). Previous studies established *TRIM32*, an ortholog of *Drosophila melanogaster*, *Brat*, which participates in ACD as a neural determinant and inhibits *Drosophila* MYC (dMYC) function in the neuroblasts of fly (27). In addition, mouse TRIM32 was shown to exhibit ubiquitin ligase activity, and facilitated the degradation of the c-MYC oncoprotein in neurogenesis (28). However, the functions of TRIM32 in human cancers remain largely unknown. We recently reported that TRIM32 promoted the proteasomal degradation of MYCN at spindle poles during cell division, while *TRIM32* overexpression induced ACD in human neuroblastoma cells (**Figures 1**, **2**) (15). *TRIM3*, another ortholog of *D. melanogaster*, *Brat*, is frequently deleted in human glioblastoma (29). Moreover, TRIM3 has been shown to facilitate the degradation of c-MYC and regulate ACD in human glioma cells (29). Thus, TRIM32/TRIM3 may not only induce ACD, but also function as a tumor suppressor in human tumors.

NCYM (MYCNOS)

NCYM (*MYCNOS*) is a *de novo* evolutionary *cis*-antisense gene for *MYCN* that encodes a 109-amino acid small protein and only exists in humans and chimpanzees (30). NCYM induces the expression of not only MYCN, LIN28B, NANOG, and SOX2, but also OCT4, a MYCN-mediated core reprogramming factor (31). MYCN and OCT4 form a positive feedback loop (**Figure 1**) (31). A previous study reported that *NCYM* promoted malignant transformation and metastasis in *NCYM/MYCN* double transgenic mice (30). These findings indicated that MYCN cooperates with NCYM to promote the malignant transformation of neuroblastoma and its stemness. NCYM was shown to suppress the degradative activity of GSK3β against MYCN and facilitated the induction of SCD, while the knockdown of *NCYM* destabilized the MYCN protein and caused ACD (**Figure 1**) (31). On the other hand, *NCYM* also functions as a non-coding RNA and cooperates with CTCF to promote the progression of neuroblastoma by facilitating the expression of *MYCN* (32). Since the NCYM protein has some homology with the OCT4 protein (**Figure 3**), NCYM may function as a transcription factor in addition to non-coding RNA.

ALDH18A1

Aldehyde dehydrogenase family 18 member A1 (ALDH18A1) was originally identified as the key enzyme for the synthesis of proline from glutamate, which catalyzes the coupled phosphorylation and reduction conversion of glutamate to β-pyrroline-5-carboxylate (P5C) and plays a critical role in regulating glutamine metabolism (33). A recent study revealed that ALDH18A1 formed a positive feedback loop with MYCN and was involved in the malignant transformation of neuroblastoma cells (**Figure 1**) (34). These findings demonstrated that the overexpression of *ALDH18A1* decreased the rate of ACD and induced SCD, whereas the knockdown of *ALDH18A1* increased the rate of ACD (34). Furthermore, molecular docking was applied to screen ALDH18A1 inhibitors, and the findings obtained showed that one compound, termed YG1702, from the approximately >200,000 compounds tested specifically inhibited the function of ALDH18A1 (34). Therefore, YG1702 has potential as a therapeutic drug that induces ACD and reduces the malignant transformation of *MYCN*-amplified neuroblastoma cells.

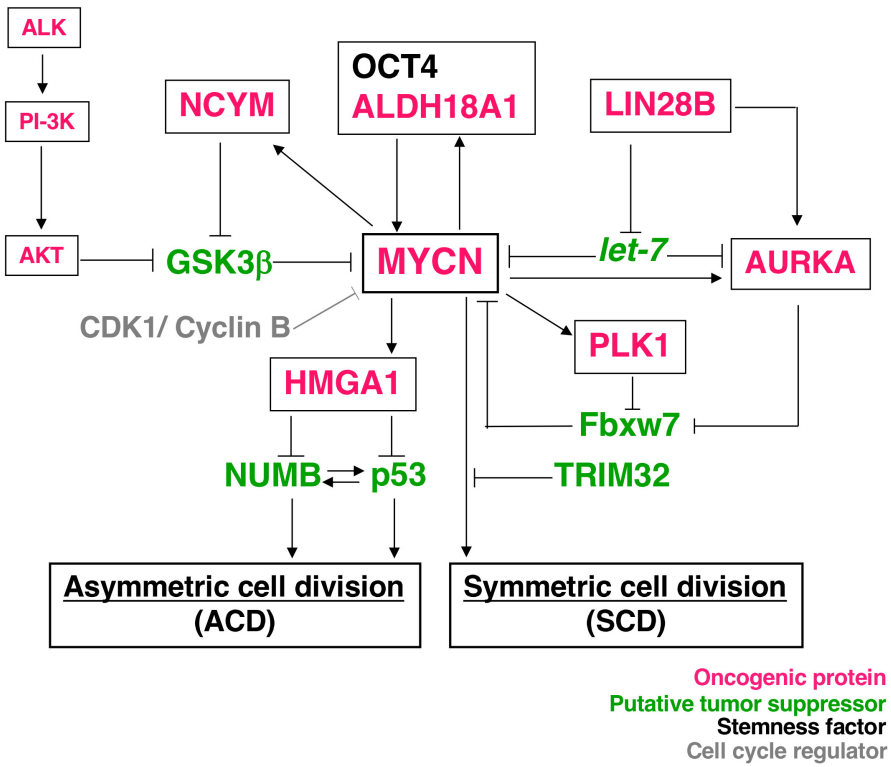

FIGURE 1 | Molecular pathways of MYCN-mediated cell division fate. MYCN protein stability depends on the interaction partners. The receptor type-tyrosine kinase, ALK, activates downstream targets, such as PI-3K, and eventually activates AKT. Activated AKT stabilizes the MYCN protein by inhibiting GSK-3β. NCYM also stabilizes MYCN for inhibition of the GSK3β-MYCN interaction. MYCN induces the expression of NCYM and HMGA1. OCT4 and MYCN or ALDH18A1 and MYCN form a positive feedback loop for their transcriptional expression. HMGA1 inhibits the expression of NUMB and p53. On the other hand, LIN28B inhibits the microRNA, *let-7*, and contributes to the stability of the MYCN and AURKA (Aurora-A) protein. AURKA and PLK1 also stabilize the MYCN protein to inhibit Fbxw7-dependent MYCN ubiquitination. Thus, many oncogenic proteins contribute to the stability of MYCN. As a result, MYCN-dependent tumor cells display symmetric cell division (SCD) and the degradation of MYCN causes asymmetric cell division (ACD).

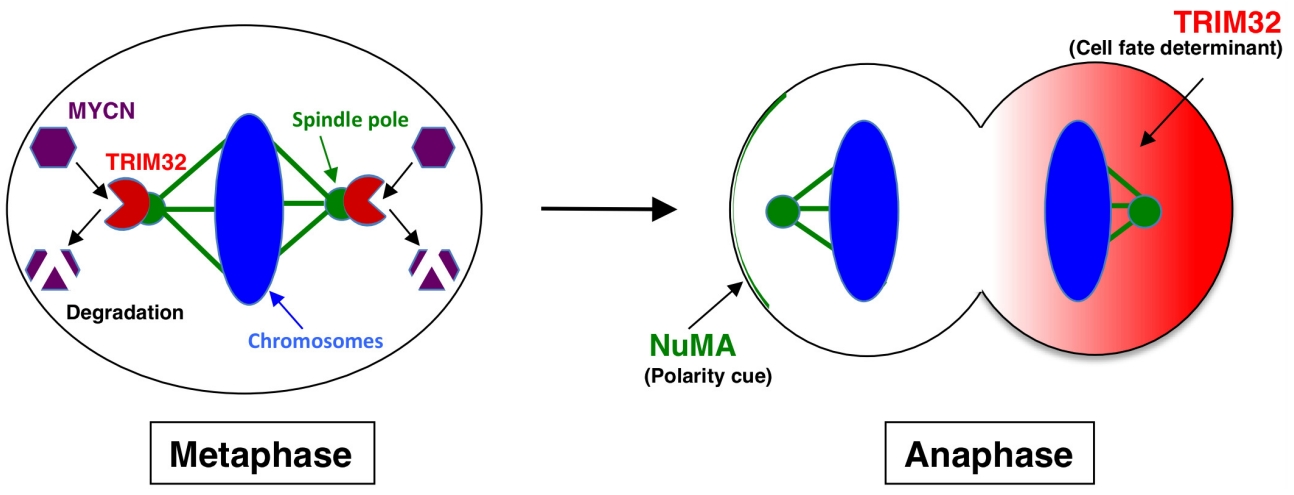

FIGURE 2 | Molecular mechanism underlying TRIM32-mediated asymmetric cell division. During metaphase, TRIM32 is recruited to spindle poles (mitotic centrosomes) by CDK1/cyclin B signaling. In parallel, MYCN accumulates at spindle poles through GSK-3β signaling. Thus, TRIM32 associates with MYCN at spindle poles during metaphase. TRIM32 then facilitates the ubiquitination and degradation of MYCN by a proteasome complex at spindle poles. During anaphase, TRIM32 asymmetrically localizes to the one of the daughter cells without the NuMA crescent.

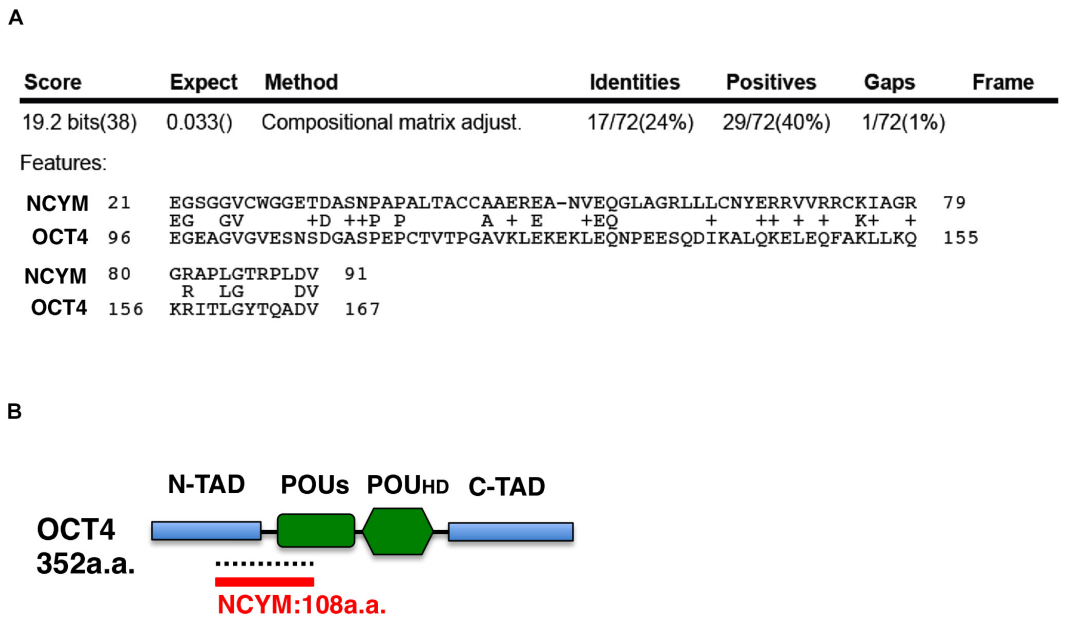

FIGURE 3 | The NCYM protein has weak homology with the OCT4 protein. **(A)** Amino acid comparisons between the NCYM and OCT4 proteins. Identities are 24% and positives are 40%. **(B)** Molecular structure of the OCT4 protein. The OCT4 protein consists of four domains: the N-terminal transactivation domain (N-TAD), C-terminal transactivation domain (C-TAD), POU transcription factor-specific domain (POUs), and POU transcription factor homeodomain (POUHD). OCT4 shares weak homology with NCYM around the N-TAD and POUs domains.

HMGA1, NUMB, AND p53

The important transcriptional target of MYCN in neuroblastoma is the high mobility group A1 (HMGA1) oncogene (35) (**Figure 1**). The HMGA1 protein is an architectural chromatin protein that is abundantly expressed during embryonic development and in most cancer tissues, but is weakly expressed or absent in normal adult tissues. It is important as an additional potential mechanism by which MYCN may induce the SCD of neuroblastoma stem cells. HMGA1 has been shown to induce the SCD of cancer stem cells by negatively regulating the expression of NUMB (36) or p53 (37) (**Figure 1**). NUMB is a cell fate determinant, and its expression is the basis for achieving the ACD of stem cells and its expression is either lost or reduced in many tumors (38). In *Drosophila* neuroblasts, NUMB mutations induce the formation of tumors (13). The NUMB protein contributes to the stabilization of p53 by suppressing the effects of HDM2, which is an E3-ubiquitin ligase (39). The deletion of p53 in mammary stem cells was shown to abolish NUMB asymmetry during cell division (23). These findings indicate that p53 and NUMB work in concert with ACD; however, the underlying mechanisms are not yet known in neuroblastoma cells.

AURKA, PLK1, AND LIN28B

Mitotic kinases, such as Aurora kinase A (AURKA) and Polo-like kinase 1 (PLK1), are reported to stabilize MYCN by inhibiting the Fbxw7-mediated degradation of the MYCN protein (40–42) and may promote SCD in *MYCN*-amplified neuroblastoma cells (**Figure 1**). *AURKA* and *PLK1* are up-regulated by MYCN and are frequently overexpressed in *MYCN*-amplified neuroblastomas (40, 43). On the other hand, *AURKA* and *Polo* (*Drosophila* ortholog of PLK1) were shown to be necessary for asymmetric protein localization during mitosis in model organisms, such as a *Drosophila* external sensory organ (44), and functioned as tumor suppressors in *Drosophila* neuroblasts (45, 46). Therefore, AURKA- and PLK1-mediated cell division fates (ACD or SCD) may be context-dependent.

The *LIN28B* gene encodes a developmentally regulated RNA binding protein and is a key repressor of the *let-7* family of miRNAs, which act as potent tumor suppressors by post-transcriptionally repressing multiple oncogenic targets, including *MYCN* (**Figure 1**) (47). In neuroblastoma cells, LIN28B promotes AURKA expression (48) and increases MYCN expression by repressing *let-7* miRNAs (47). Since LIN28B is involved in SCD in *Drosophila* intestine stem cells (49) and *Caenorhabditis elegans* embryos (50), it may control the cell division fate in neuroblastoma cells in an evolutionarily conserved manner.

CONCLUDING REMARKS

Why do neuroblastoma cultured cells exhibit ACD? As discussed above, many cultured neuroblastoma cells show the unique characteristics of proliferation and differentiation capabilities (9, 10). Previous studies demonstrated that human neuroblastoma cell lines may be classified into three distinct cellular phenotypes with different differentiation potentials: the sympathoadrenal

neuroblast type (N-type), substrate adherent type (S-type), and intermediate type (I-type) (9, 10). Based on its morphological and growth characteristics, the I-type was recognized as a neuroblastoma stem cell by its unique differentiation and malignant potentials (9, 10). In addition, neuroblastoma is a typical childhood cancer that may arise at the fetal development stage when a large number of stem cells exhibit ACD.

In this mini-review, we discussed a group of molecules that are involved in ACD and SCD through the regulation of the MYCN protein. Since the major function of MYCN is as a transcription factor, further studies are needed to clarify whether HMGA1, a target of MYCN, is involved in the cell division fate of human neuroblastoma cells.

Since this mini-review mainly described the intrinsic factors of ACD, further studies are needed on extrinsic factors including the tumor microenvironment. The findings obtained may contribute to direct applications for therapeutic strategies.

Therefore, human neuroblastoma cultured cells have potential as a very useful model system for providing insights into the mechanisms underlying ACD.

AUTHOR CONTRIBUTIONS

HI performed a literature review and submitted the manuscript to the journal. HI, YK, and AN wrote the manuscript. All authors contributed to the article and approved the submitted version.

FUNDING

This article was financially supported by the Japan Society for the Promotion of Science (18K07223), Takeda Research Support, Japan, and Gold Ribbon Network, Japan.

REFERENCES

1. Brodeur GM. Neuroblastoma: biological insights into a clinical enigma. *Nat Rev Cancer.* (2003) 3:203–16. doi: 10.1038/nrc1014
2. Matthay KK, Maris JM, Schleiermacher G, Nakagawara A, Mackall CL, Diller L, et al. Neuroblastoma. *Nat Rev Dis Primers.* (2016) 2:16078.
3. Nakagawara A, Li Y, Izumi H, Muramori K, Inada H, Nishi M. Neuroblastoma. *Jpn J Clin Oncol.* (2018) 48:214–41.
4. Kerosuo L, Neppala P, Hsin J, Mohlin S, Vieceli FM, Torok Z, et al. Enhanced expression of MycN/CIP2A drives neural crest toward a neural stem cell-like fate: implications for priming of neuroblastoma. *Proc Natl Acad Sci USA.* (2018) 115:E7351–60.
5. Zhang JT, Weng ZH, Tsang KS, Tsang LL, Chan HC, Jiang XH. MycN is critical for the maintenance of human embryonic stem cell-derived neural crest stem cells. *PLoS One.* (2016) 11:e0148062. doi: 10.1371/journal.pone.0148062
6. Huang M, Weiss WA. Neuroblastoma and MYCN. *Cold Spring Harb Perspect Med.* (2013) 3:a014415. doi: 10.1101/cshperspect.a014415
7. De Preter K, Vandesompele J, Heimann P, Yigit N, Beckman S, Schramm A, et al. Human fetal neuroblast and neuroblastoma transcriptome analysis confirms neuroblast origin and highlights neuroblastoma candidate genes. *Genome Biol.* (2006) 7:R84. doi: 10.1186/gb-2006-7-9-r84
8. Cotterman R, Knoepfler PS. N-Myc regulates expression of pluripotency genes in neuroblastoma including lif, klf2, klf4, and lin28b. *PLoS One.* (2009) 4:e5799. doi: 10.1371/journal.pone.0005799
9. Ross RA, Spengler BA. Human neuroblastoma stem cells. *Semin Cancer Biol.* (2007) 17:241–7. doi: 10.1016/j.semcancer.2006.04.006
10. Ross RA. *Cellular Heterogeneity. Neuroblastoma*. Berlin: Springer (2005). p. 55–62.
11. Morrison SJ, Kimble J. Asymmetric and symmetric stem-cell divisions in development and cancer. *Nature.* (2006) 441:1068–74. doi: 10.1038/nature04956
12. Meacham CE, Morrison SJ. Tumour heterogeneity and cancer cell plasticity. *Nature.* (2013) 501:328–37. doi: 10.1038/nature12624
13. Caussinus E, Gonzalez C. Induction of tumor growth by altered stem-cell asymmetric division in *Drosophila melanogaster*. *Nat Genet.* (2005) 37:1125–9. doi: 10.1038/ng1632
14. Izumi H, Kaneko Y. Evidence of asymmetric cell division and centrosome inheritance in human neuroblastoma cells. *Proc Natl Acad Sci USA.* (2012) 109:18048–53. doi: 10.1073/pnas.1205525109
15. Izumi H, Kaneko Y. Trim32 facilitates degradation of MYCN on spindle poles and induces asymmetric cell division in human neuroblastoma cells. *Cancer Res.* (2014) 74:5620–30. doi: 10.1158/0008-5472.CAN-14-0169
16. Izumi H, Kaneko Y. Symmetry breaking in human neuroblastoma cells. *Mol Cell Oncol.* (2014) 1:e968510. doi: 10.4161/23723548.2014.968510
17. Gonczy P. Mechanisms of asymmetric cell division: flies and worms pave the way. *Nat Rev Mol Cell Biol.* (2008) 9:355–66. doi: 10.1038/nrm2388
18. Sawa H. Control of cell polarity and asymmetric division in *C. elegans*. *Curr Top Dev Biol.* (2012) 101:55–76. doi: 10.1016/B978-0-12-394592-1.00003-X
19. Yamashita YM, Mahowald AP, Perlin JR, Fuller MT. Asymmetric inheritance of mother versus daughter centrosome in stem cell division. *Science.* (2007) 315:518–21. doi: 10.1126/science.1134910
20. Shinin V, Gayraud-Morel B, Gomes D, Tajbakhsh S. Asymmetric division and cosegregation of template DNA strands in adult muscle satellite cells. *Nat Cell Biol.* (2006) 8:677–87. doi: 10.1038/ncb1425
21. Lechler T, Fuchs E. Asymmetric cell divisions promote stratification and differentiation of mammalian skin. *Nature.* (2005) 437:275–80. doi: 10.1038/nature03922
22. Quyn AJ, Appleton PL, Carey FA, Steele RJ, Barker N, Clevers H, et al. Spindle orientation bias in gut epithelial stem cell compartments is lost in precancerous tissue. *Cell Stem Cell.* (2010) 6:175–81. doi: 10.1016/j.stem.2009.12.007
23. Cicalese A, Bonizzi G, Pasi CE, Faretta M, Ronzoni S, Giulini B, et al. The tumor suppressor p53 regulates polarity of self-renewing divisions in mammary stem cells. *Cell.* (2009) 138:1083–95. doi: 10.1016/j.cell.2009.06.048
24. Wu M, Kwon HY, Rattis F, Blum J, Zhao C, Ashkenazi R, et al. Imaging hematopoietic precursor division in real time. *Cell Stem Cell.* (2007) 1:541–54. doi: 10.1016/j.stem.2007.08.009
25. Wang X, Tsai JW, Imai JH, Lian WN, Vallee RB, Shi SH. Asymmetric centrosome inheritance maintains neural progenitors in the neocortex. *Nature.* (2009) 461:947–55. doi: 10.1038/nature08435
26. Costa MR, Wen G, Lepier A, Schroeder T, Gotz M. Par-complex proteins promote proliferative progenitor divisions in the developing mouse cerebral cortex. *Development.* (2008) 135:11–22. doi: 10.1242/dev.009951
27. Betschinger J, Mechtler K, Knoblich JA. Asymmetric segregation of the tumor suppressor brat regulates self-renewal in Drosophila neural stem cells. *Cell.* (2006) 124:1241–53. doi: 10.1016/j.cell.2006.01.038
28. Schwamborn JC, Berezikov E, Knoblich JA. The TRIM-NHL protein TRIM32 activates microRNAs and prevents self-renewal in mouse neural progenitors. *Cell.* (2009) 136:913–25. doi: 10.1016/j.cell.2008.12.024
29. Chen G, Kong J, Tucker-Burden C, Anand M, Rong Y, Rahman F, et al. Human Brat ortholog TRIM3 is a tumor suppressor that regulates asymmetric cell division in glioblastoma. *Cancer Res.* (2014) 74:4536–48. doi: 10.1158/0008-5472.CAN-13-3703
30. Suenaga Y, Islam SM, Alagu J, Kaneko Y, Kato M, Tanaka Y, et al. NCYM, a Cis-antisense gene of MYCN, encodes a de novo evolved protein that inhibits GSK3beta resulting in the stabilization of MYCN in human neuroblastomas. *PLoS Genet.* (2014) 10:e1003996. doi: 10.1371/journal.pgen.1003996

31. Kaneko Y, Suenaga Y, Islam SM, Matsumoto D, Nakamura Y, Ohira M, et al. Functional interplay between MYCN, NCYM, and OCT4 promotes aggressiveness of human neuroblastomas. *Cancer Sci.* (2015) 106:840–7. doi: 10.1111/cas.12677
32. Zhao X, Li D, Pu J, Mei H, Yang D, Xiang X, et al. CTCF cooperates with noncoding RNA MYCNOS to promote neuroblastoma progression through facilitating MYCN expression. *Oncogene.* (2016) 35:3565–76. doi: 10.1038/onc.2015.422
33. Hu CA, Khalil S, Zhaorigetu S, Liu Z, Tyler M, Wan G, et al. Human Delta1-pyrroline-5-carboxylate synthase: function and regulation. *Amino Acids.* (2008) 35:665–72. doi: 10.1007/s00726-008-0075-0
34. Guo YF, Duan JJ, Wang J, Li L, Wang D, Liu XZ, et al. Inhibition of the ALDH18A1-MYCN positive feedback loop attenuates MYCN-amplified neuroblastoma growth. *Sci Transl Med.* (2020) 12:eaax8694. doi: 10.1126/scitranslmed.aax8694
35. Giannini G, Cerignoli F, Mellone M, Massimi I, Ambrosi C, Rinaldi C, et al. High mobility group A1 is a molecular target for MYCN in human neuroblastoma. *Cancer Res.* (2005) 65:8308–16. doi: 10.1158/0008-5472.CAN-05-0607
36. Puca F, Tosti N, Federico A, Kuzay Y, Pepe A, Morlando S, et al. HMGA1 negatively regulates NUMB expression at transcriptional and post transcriptional level in glioblastoma stem cells. *Cell Cycle.* (2019) 18:1446–57. doi: 10.1080/15384101.2019.1618541
37. Puca F, Colamaio M, Federico A, Gemei M, Tosti N, Bastos AU, et al. HMGA1 silencing restores normal stem cell characteristics in colon cancer stem cells by increasing p53 levels. *Oncotarget.* (2014) 5:3234–45. doi: 10.18632/oncotarget.1914
38. Pece S, Confalonieri S, Romano PR, Di Fiore P. P. NUMB-ing down cancer by more than just a NOTCH. *Biochim Biophys Acta.* (2011) 1815:26–43. doi: 10.1016/j.bbcan.2010.10.001
39. Colaluca IN, Tosoni D, Nuciforo P, Senic-Matuglia F, Galimberti V, Viale G, et al. NUMB controls p53 tumour suppressor activity. *Nature.* (2008) 451:76–80. doi: 10.1038/nature06412
40. Otto T, Horn S, Brockmann M, Eilers U, Schuttrumpf L, Popov N, et al. Stabilization of N-Myc is a critical function of Aurora A in human neuroblastoma. *Cancer Cell.* (2009) 15:67–78. doi: 10.1016/j.ccr.2008.12.005
41. Brockmann M, Poon E, Berry T, Carstensen A, Deubzer HE, Rycak L, et al. Small molecule inhibitors of aurora-a induce proteasomal degradation of N-myc in childhood neuroblastoma. *Cancer Cell.* (2013) 24:75–89. doi: 10.1016/j.ccr.2013.05.005
42. Xiao D, Yue M, Su H, Ren P, Jiang J, Li F, et al. Polo-like Kinase-1 regulates Myc stabilization and activates a feedforward circuit promoting tumor cell survival. *Mol Cell.* (2016) 64:493–506. doi: 10.1016/j.molcel.2016.09.016
43. Ackermann S, Goeser F, Schulte JH, Schramm A, Ehemann V, Hero B, et al. Polo-like kinase 1 is a therapeutic target in high-risk neuroblastoma. *Clin Cancer Res.* (2011) 17:731–41. doi: 10.1158/1078-0432.CCR-10-1129
44. Berdnik D, Knoblich JA. Drosophila Aurora-A is required for centrosome maturation and actin-dependent asymmetric protein localization during mitosis. *Curr Biol.* (2002) 12:640–7. doi: 10.1016/s0960-9822(02)00766-2
45. Wang H, Somers GW, Bashirullah A, Heberlein U, Yu F, Chia W. Aurora-A acts as a tumor suppressor and regulates self-renewal of Drosophila neuroblasts. *Genes Dev.* (2006) 20:3453–63. doi: 10.1101/gad.1487506
46. Wang H, Ouyang Y, Somers WG, Chia W, Lu B. Polo inhibits progenitor self-renewal and regulates Numb asymmetry by phosphorylating Pon. *Nature.* (2007) 449:96–100. doi: 10.1038/nature06056
47. Molenaar JJ, Domingo-Fernandez R, Ebus ME, Lindner S, Koster J, Drabek K, et al. LIN28B induces neuroblastoma and enhances MYCN levels via let-7 suppression. *Nat Genet.* (2012) 44:1199–206. doi: 10.1038/ng.2436
48. Schnepp RW, Khurana P, Attiyeh EF, Raman P, Chodosh SE, Oldridge DA, et al. A LIN28B-RAN-AURKA signaling network promotes neuroblastoma tumorigenesis. *Cancer Cell.* (2015) 28:599–609. doi: 10.1016/j.ccell.2015.09.012
49. Chen CH, Luhur A, Sokol N. Lin-28 promotes symmetric stem cell division and drives adaptive growth in the adult Drosophila intestine. *Development.* (2015) 142:3478–87. doi: 10.1242/dev.127951
50. Harandi OF, Ambros VR. Control of stem cell self-renewal and differentiation by the heterochronic genes and the cellular asymmetry machinery in *Caenorhabditis elegans*. *Proc Natl Acad Sci USA*. (2015) 112:E287–96. doi: 10.1073/pnas.1422852112

Conflict of Interest: The authors declare that the research was conducted in the absence of any commercial or financial relationships that could be construed as a potential conflict of interest.

frontiers in Oncology

REVIEW
published: 27 January 2021
doi: 10.3389/fonc.2020.624079

MYCN Function in Neuroblastoma Development

Jörg Otte, Cecilia Dyberg, Adena Pepich and John Inge Johnsen*

Childhood Cancer Research Unit, Department of Children's and Women's Health, Karolinska Institutet, Stockholm, Sweden

Dysregulated expression of the transcription factor MYCN is frequently detected in nervous system tumors such as childhood neuroblastoma. Here, gene amplification of *MYCN* is a single oncogenic driver inducing neoplastic transformation in neural crest-derived cells. This abnormal *MYCN* expression is one of the strongest predictors of poor prognosis. It is present at diagnosis and is never acquired during later tumorigenesis of *MYCN* non-amplified neuroblastoma. This suggests that increased *MYCN* expression is an early event in these cancers leading to a peculiar dysregulation of cells that results in embryonal or cancer stem-like qualities, such as increased self-renewal, apoptotic resistance, and metabolic flexibility.

Keywords: MYCN, neuroblastoma, childhood cancer, neural crest, cancer stem cell

OPEN ACCESS

Edited by:
Yuyan Zhu,
The First Affiliated Hospital of China Medical University, China

Reviewed by:
Beisi Xu,
St. Jude Children's Research Hospital, United States
Renato Franco,
University of Campania Luigi Vanvitelli, Italy

****Correspondence:***
Jörg Otte
jorg.otte@ki.se

Specialty section:
This article was submitted to Molecular and Cellular Oncology, a section of the journal Frontiers in Oncology

Received: *30 October 2020*
Accepted: *10 December 2020*
Published: *27 January 2021*

Citation:
Otte J, Dyberg C, Pepich A and Johnsen JI (2021) MYCN Function in Neuroblastoma Development. Front. Oncol. 10:624079. doi: 10.3389/fonc.2020.624079

INTRODUCTION

MYCN belongs to a small family of genes, which in addition to *MYCN* (or *N-Myc*) includes two closely related genes, *C-Myc* and *L-Myc*. MYC proteins are master regulators of cell fate and part of a network of interacting transcription factors. Together, these transcription factors regulate the expression of multiple genes involved in cell-proliferation, growth, senescence, metabolism, differentiation, and apoptosis (1). More specifically, MYC proteins bind to active promoters and enhancers altering transcription mediated by all three RNA polymerases and affecting the expression of more than 15% of all genes in a cell (2–4). Dysregulated expression of *MYC* genes are frequently observed in cancers of different origin, implicating that MYC proteins have central functions during carcinogenesis (2–4). Additionally, MYC proteins also affect the tumor microenvironment; MYC protein was shown to regulate the interaction between tumor cells and the host immune cells by controlling the synthesis of cytokines mediating communication between tumor cells and myeloid cells (5–7).

Studies in mice showed that both *Myc* (*C-myc)* and *Mycn* (*N-myc)*, but not *Mycl* (*L-myc*), are fundamental for normal development as targeted deletions of these two genes in mice are embryonic lethal at mid-gestation (8–12). While *C-myc* is expressed throughout the mouse embryo and at all developmental stages analyzed; *N-myc* expression is restricted to hematopoietic stem cells and cells within the developing nervous system (12–16). The restricted expression pattern of *N-myc* during development may be mirrored in human tumors since cancers with a neural cell origin like neuroblastoma, medulloblastoma, retinoblastoma, astrocytoma and glioblastoma, as well as, hematological malignancies frequently overexpress *MYCN*. However, overexpression of *MYCN* has also been reported in Wilms tumors, rhabdomyosarcomas, prostate, pancreatic and lung cancers (17). The mechanisms for *MYCN* overexpression in tumors have several facets, ranging from induced transcriptional activation of *MYCN*, increased MYCN protein stabilization caused by

dysregulated MYCN phosphorylation, and reduced proteasomal degradation to *MYCN* gene amplification (17–19). Pediatric cancers usually develop during a much shorter time-period and with significantly fewer genetic abnormalities compared to adult tumors. Some of these childhood tumors have embryonal characteristics that are most probably initiated by aberrations in genes and/or deregulated expression of genes causing retention of cell immaturity and increased proliferation capacity (18). In mice models, guided ectopic expression of N-myc to the developing nervous system has been shown to be a potent oncogenic driver and results in the development of medulloblastoma and neuroblastoma (20–22).

MYCN IN NEUROBLASTOMA

Neuroblastoma is a cancer of the peripheral nervous system that almost exclusively occurs during early childhood. Although neuroblastoma is a relatively rare disease affecting 1 of 8,000 live births, or 6%–10% of all childhood tumors, the disease still accounts for 12%–15% of all cancer-related deaths in children. 40% of the patients diagnosed with neuroblastoma are younger than 1 year and the median age for diagnosis is 17-18 months whereas less than 5% of the patients are older than 10 years establishing neuroblastoma as the most common and deadly tumor of infancy (23). Clinically, neuroblastoma is characterized with a heterogeneous disease spectrum ranging from patients with widespread tumors that spontaneously regress or differentiate without treatment to treatment-resistant tumors with metastatic spread despite intensive multimodal treatment approaches. This heterogeneity is mirrored in overall patient survival; neuroblastoma patients with low- to intermediate-risk disease have 85-90% survival rates, whereas 50% of patients with high-risk neuroblastoma succumb to the disease.

The risk stratification of low-, intermediate- and high-risk patients usually becomes evident through chromosomal analysis. Low-risk neuroblastoma commonly displays whole chromosomal gains with a hyperdiploid (near triploid or penta/hexaploid) chromosomal landscape, whereas high-risk neuroblastoma contains segmental chromosomal aberrations that affect only a part of a given chromosome. The most common chromosomal aberration related to poor prognosis in neuroblastoma is somatically acquired segmental gain of 17q, hemizygous deletions of 1p and 11q, and *MYCN* gene amplification. In addition, genomic rearrangements at chromosomal region 5p15.33, located proximal of the telomerase reverse transcriptase gene (*TERT*) that results in chromosomal changes, DNA methylation and enhanced TERT expression have also been observed in high-risk neuroblastoma samples. Gene amplification of *MYCN* was one of the earliest genetic markers discovered in neuroblastoma and is still one of the strongest predictors of poor prognosis. The prevalence of *MYCN* amplification in neuroblastoma patients is 20%–30% and the overall survival for these patients remains at less than 50% (23–25). In high-risk neuroblastoma patients, if amplification of *MYCN* occurs it is always present at diagnosis. Patients with low-risk disease lack *MYCN* gene amplification and never progress to high-risk disease nor do they acquire extra copies of the *MYCN* gene (17, 23, 26). This indicates that *MYCN* gene amplification is an early and perhaps initiating event driving the development of a high-risk neuroblastoma subgroup of tumors which is in contrast to most other cancers where gene amplifications are considered to be late events during tumorigenesis (17, 27).

Adult cancer is a multistep process that evolves over many years caused by genomic instabilities giving rise to transformed cells that have the capacity to develop into life-threatening malignant tumor cells. Pediatric cancers, on the other hand, develop during a short time-period and contain much fewer genomic aberrations and mutations compared to adult cancers. This suggests that certain pediatric cancers, including neuroblastoma, arise from cells with embryonal features or from mature prenatal cells that through external factors have acquired embryonal properties favoring proliferation (18). Although *MYCN* gene amplification is detected in approximately 50% of high-risk neuroblastoma cases and an oncogenic driver for neuroblastoma, there exists no current evidence describing when and how the amplification of the *MYCN* gene is initiated. Neither is it known in detail how and in which cell type the expression of *MYCN* is initiated in order to drive neuroblastoma tumorigenesis. Furthermore, it should be noted that the 2p24 chromosomal amplicon observed in high-risk neuroblastoma encodes other genes in addition to *MYCN*, such as the anaplastic lymphoma kinase (*ALK*). *ALK* has also been shown to drive neuroblastoma formation and to potentiate the oncogenic activity of *MYCN* in neuroblastoma (28–30).

NEUROBLASTOMA IS A NEURAL CREST DERIVED MALIGNANCY

Neuroblastoma derives from cells within the neural crest, a transient structure consisting of multipotent progenitor cells present during embryogenesis. The majority of the tumors are located in the abdomen along the sympathetic chain and in the adrenal gland medullary region (23, 27). The neural crest develops between the neural plate and non-neural ectoderm, in an area named the neural plate border, during gastrulation and neurulation (**Figure 1**) (31). Neural crest cells undergo epithelial-to-mesenchymal transition (EMT) during neurulation and migrate extensively from the neuroepithelium to more distant locations in the embryo where the cells differentiate into a wide variety of cell types for specific organ systems including the peripheral and enteric nervous systems, skin pigment, cardiovascular system and craniofacial skeleton (32). Neural crest cell maturation, migration, specification and differentiation are tightly controlled processes guided by gene regulatory networks, consisting of various transcription factors. These transcription factors become sequentially activated by external factors like BMPs, Wnt and FGF (33). The cell of origin for neuroblastoma has yet to be determined, but the combination of timing in disease onset and clinical presentation suggest that neuroblastoma is derived from sympathoadrenal progenitor cells within the neural crest that differentiate to sympathetic ganglion cells and adrenal catecholamine-secreting chromaffin cells.

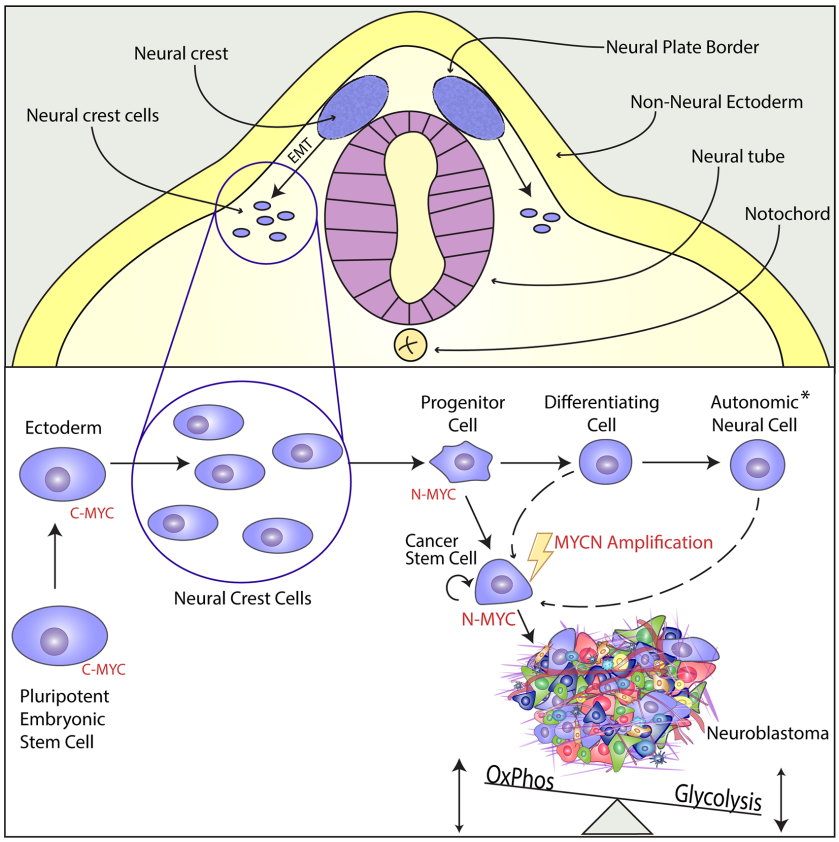

FIGURE 1 | N-MYC acts as a Cancer Stem Cell Factor in the Developing Neural Crest and Promotes Tumorigenesis in Neuroblastoma. Upper Panel: The neural crest is a transient structure located in the neural plate border, an area between the neural plate and the non-neural ectoderm. From the neural crest, multipotent progenitor cells delaminate, migrate through epithelial-to-mesenchymal-transition (EMT), and differentiate into versatile structures within the whole organism. Lower Panel: While C-Myc is the main regulator in pluripotent cells of early embryonal development, MycN is highly expressed in the multipotent cells of the migratory and post-migratory neural crest. During differentiation, MycN expression is downregulated and the sympathoadrenal precursor cells or progenitor cells mature into different cell types of the autonomic neural cell lineage (see asterisk), such as sympathetic ganglion cells, chromaffin cells of the adrenal medulla or cells of the peripheral nervous system. Even though there is strong evidence that *MYCN* gene amplification is an early and maybe initiating event, it has not been proven yet when and how the amplification takes place. The aberrant expression of MYCN induces a unique cancer stem cell-like phenotype by enabling infinite self-renewal, apoptotic resistance, and *via* metabolic reprogramming characterized by increased glycolysis together with an active oxidative phosphorylation. The establishing neuroblastoma consists of heterogeneous cell populations.

Recent reports, based primarily on *in vitro* studies of neuroblastoma cell lines, have demonstrated that neuroblastoma consists of two phenotypically different subpopulations of cells, called adrenergic and mesenchymal. These two subpopulations show distinct networks of super enhancer-associated transcription factors (34, 35). *In vitro*, these cell lineages can interconvert and exhibit differences in sensitivity to chemotherapeutic drugs. Interestingly, the mesenchymal population of cells seems to be more drug resistant which may be important for the development of drug resistance frequently observed in patients with high-risk neuroblastoma (19, 34). The identity of a cell from the adrenergic subtype is defined by key regulatory genes, such as *PHOX2B*, *HAND2*, or *GATA3*, which are interconnected by reciprocal regulation (35). This core regulatory circuitry can be reinforced by MYCN amplification through a mechanism called "enhancer invasion". Enhancer invasion depends on combined enhancer co-occupation of individual gene enhancer/promoter regions by MYCN and TWIST1 (36). Another regulatory loop involving MYCN has recently been identified and depends on ASCL1 which is directly regulated by MYCN together with LMO1. In the same study, it has been shown that *ASCL1* is, itself, a part of the core regulatory circuitry under the adrenergic identity and expression of *ASCL1* can induce differentiation arrest in neuroblastoma cells (37).

Overexpression of *Mycn* in migrating neural crest cells of chicken embryos increases the proportion of neurons at the cost of other cells. Loss of *Mycn* in mouse embryos decreases the size of the entire nervous system, including spinal, peripheral and cranial ganglia and reduces the number of mature neurons in the spinal ganglia (9). In the sympathetic ganglia, expression of *C-myc* is considerably higher compared to *N-myc*. This indicates that *N-myc* expression is induced in the sympathetic ganglia during gestation and then switched off before birth (38). Interestingly, the expression

level of *C-myc* does not change after *N-myc* downregulation. On the other hand, downregulation of *N-myc* strongly upregulates the expression of *Phox2b*, *Mash1, Hand2*, and *Gata3* genes.

MYCN AS AN ONCOGENIC DRIVER IN NEUROBLASTOMA

Despite that several molecular prognostic factors with oncogenic potentials have been described in neuroblastoma, only activating *ALK* mutations and *MYCN* overexpression were shown to be *de novo* oncogenic drivers. This is seen when mutation or overexpression of these molecules give rise to neuroblastoma in genetically engineered animal models.

The *ALK* gene located on chromosome 2p23 encodes a receptor tyrosine kinase that is normally expressed at high levels in the nervous system and was originally identified as a fusion protein in non-Hodgkin's lymphoma. Zhu et al. generated transgenic zebrafish models in which human *MYCN*, human *ALK* or *ALK* harboring the F1174L activating mutation (ALK^{F1174L}) were placed under control of the dopamine β-hydroxylase (*dbh*) promoter (30). F1174L mutation is one of the most frequent activating somatic mutations in human cell lines and neuroblastoma patients (39). Tumor penetrance and the rate of tumor induction were much higher in zebrafish expressing both *MYCN* and *ALK* compared to zebrafish expressing either *MYCN* or *ALK*. Additionally, zebrafish expressing both *MYCN* and ALK^{F1174L} transgenes demonstrated increased tumor penetrance compared to all other transgene combinations. The expression of *alk* increased the effect of *mycn* by blocking apoptosis in *MYCN*-overexpressing sympathoadrenal neuroblasts (30). *ALK* mutations can be detected in all clinical stages while an association with a poorer outcome can only be detected in intermediate- and high-risk neuroblastoma. In 2%–3% of all cases, *ALK* can be further activated by gene amplification leading to protein expression and kinase activity. Interestingly, this is specific to neuroblastoma as it has been described that *ALK* amplification does not result in protein expression in non-small-cell lung cancer and is therefore not involved in its pathogenesis but maybe only a passenger event (40–42).

Targeted expression of *Lin28b* to sympathetic adrenergic lineage cells gives rise to neuroblastoma. One mechanism of induced tumor development indicates a Lin28B-mediated downregulation of Let-7 which results in high MYCN protein expression suggesting that *MYCN* is the actual driver of oncogenesis (43). Others have described let-7-independent pro-tumorigenic effects of LIN28B e.g. *via* protein-protein interaction with the transcription factor ZNF143 recruiting LIN28B to activate promoters of genes involved in neuroblastoma progression (44, 45).

MYCN is highly expressed in the early post-migratory neural crest (**Figure 1**) and regulates ventral migration and growth of cells within the neural crest during normal murine sympathoadrenal development. *MYCN* expression is gradually downregulated in differentiating sympathetic neurons, which suggest that sympathoadrenal maturation is independent of *MYCN* expression. The sympathoadrenal precursor cells maturate into neural or chromaffin cells. Moreover, it has been proposed that the preneoplastic lesions, which can develop into neuroblastoma, arise in sympathoadrenal precursor cells not having received or reacted to signals controlling the neuronal or chromaffin cell fate. Studies in zebrafish demonstrated that ectopic expression of *mycn* in sympathoadrenal precursor cells obstruct the development of chromaffin cells causing the development of neuroblastoma. An excess of precursor cells is produced during the transition to sympathoadrenal cells, which during normal stages of maturation, are submitted to controlled apoptosis caused by deficiency of local neural growth factors. As MYCN is a master transcription factor important for both proper cell proliferation and apoptosis, a persistent expression of MYCN during the maturation stages of sympathoadrenal precursors could result in inhibition of apoptotic signaling and maintained proliferation that ultimately could result in the development of neuroblastoma (17).

In a genetically engineered neuroblastoma mouse model, called Th-MYCN (22), accumulation of small, blue round cell populations in the paravertebral ganglia are observed at embryonic day 14 (46). This population of cells called neuroblasts later develops into neuroblastoma observed in 100% of the Mycn homozygous mice from postnatal week 6. Similar observations were shown in transgenic zebrafish with neural crest cells expressing mycn. Furthermore, overexpression of *MYCN* in primary neural crest cells isolated from an embryonic neural tube explant developed tumors that were highly similar to *MYCN* amplified neuroblastoma when the cells were inoculated in mice (47). However, blocking expression of *Mycn* in neural crest cells was recently shown to induce perinatal lethality in mice which suggests that primary neural crest cells are not the origin of *MYCN* amplified neuroblastoma (48). This is in line with a study showing that *Mycn* is expressed together with the phosphorylating-stabilizing factor, *CIP2A* in regions of the neural plate and that Mycn protein is excluded from the neural crest stem cell domain (49). This indicates that high-risk subgroups of neuroblastoma may be initiated before the emigration of neural crest cells and before sympathoadrenal specification. The importance of *MYC* expression in neuroblastoma is further emphasized by the fact that neuroblastoma without *MYCN* gene amplification frequently expressed high levels of *C-MYC* indicating that *C-MYC* and *N-MYC* are mutually exclusive in neuroblastoma (50).

MYCN AS A STEM CELL FACTOR

The interrelation of neural crest development and neuroblastoma tumorigenesis is one good example of how developmental biology and cancer research fuel each other in their mutual discoveries. In fact, it was the early analysis of teratocarcinomas that led to the discovery of embryonic stem cells (ESC) (51). The theory of cancer stem cells has elucidated the exploitation of embryonic pathways by malignant cells, not only in pediatric tumors, but in most cancers. More recent studies have further demonstrated that malignant as

well as non-malignant tissues can possess unexpected plasticity (52, 53).

The Nobel-prize awarded discovery of induced pluripotency by Yamanaka in 2006 has opened a new chapter in regenerative medicine and demonstrated a paradigm shift in our understanding of cellular plasticity and lineage restriction (54). By reprogramming fibroblasts to become induced pluripotent stem cells (iPS) with activation of merely four transcription factors (*SOX2*, *OCT4*, *KLF4*, and *C-MYC*), Yamanaka showed that no definite cell state is truly irreversible. *KLF4* and *C-MYC* are well known oncogenes, indicating similarities in reprogramming and tumorigenesis. The oncogenic potential of iPS-derived cells is a major concern in today`s regenerative medicine (55) and has led to a deeper analysis of *C-MYC* and its tumorigenic potential during the process of reprogramming. Other protocols for the generation of iPS cells without direct *MYC* activation have been described, although they usually have a lower reprogramming efficiency (56).

One important hallmark of all stem cells is their continuous self-renewal which can be described as proliferation without differentiation. By inhibiting the expression of cell lineage specifiers while simultaneously inducing cell cycle progression, MYC proteins fulfill a major function in establishing self-renewal in ESCs, as well as in cancer stem cells (1, 57, 58).

During early embryogenesis in mice, C-*myc* and N-*myc* are highly redundant and can compensate each other's loss. Single knock-outs have no effect on the self-renewal or pluripotency of mouse ESCs, while N-*myc* can be substituted for C-*myc* during reprogramming (10, 57, 59, 60). However, later during development *Myc* expression becomes tissue specific and single knock-outs of *C-myc* and *N-myc* become lethal during mid-gestation (10, 12, 16, 26). Besides tissue specific expression, Myc proteins are highly conserved in their structure and function which has been proven in murine development by transgenic mice expressing *N-myc* from the *C-myc* gene locus which generated healthy and fertile offspring (61). These along with other studies have shown that C-myc and N-myc fulfill similar functions as stem cell factors, but tissue specific differences have been described within their networks of protein interactions and transcriptional regulation (62). Insights obtained mainly by the analysis of C-myc as a pluripotency factor can, to a certain degree, be transferred to N-myc's role in stem cell research and during oncogenesis.

MYCN AS AN APOPTOSIS REGULATOR

Oncogenic transformation and cellular reprogramming are similar processes that are impeded by cell intrinsic barriers. A critical mechanism is the induction of apoptosis or senescence facilitated by p53, the most commonly mutated gene in the Pan-Cancer cohort of The Cancer Genome Atlas (TCGA) (63). Balance in p53 activity is essential for self-renewal of undifferentiated cells and is tightly regulated at the mRNA-, as well as at the protein-level (64). During reprogramming, p53 acts as a roadblock. Thereby p53 inhibition increases reprogramming efficiency, but at the cost of increased oxidative stress, shortened telomeres and higher risk of DNA damage (65). Results by Olsen et al. have indicated that cultured primary mouse neural crest cells with a heterozygous p53 deletion ($p53^{+/-}$) allow more permissive tumor induction by lentiviral *MYCN* transduction than p53 wild type cells (47). In the vast majority of human neuroblastoma, however, no p53 mutations are detectable at diagnosis and tumor cells express nuclear protein as well as a functional cytochrome c-caspase cascade (66–68). C-myc and N-myc can both bind the p53 promoter and induce its expression without eliciting apoptosis indicating additional anti-apoptotic effects regulated by Myc (69, 70). Many players in this complex network have been studied extensively constituting promising candidates for future targeted therapies (71). The main antagonist of p53 is Mdm2, an E3–ligase contributing to the ubiquitination and the repression of p53. Mdm2 is directly induced by N-myc but also regulates N-myc in a feedback-manner (72, 73). In neuroblastoma, Mdm2 can acts as a tumor promoting factor as seen in Mdm2 haploinsufficient ($Mdm2^{+/-}$) MYCN transgenic mice which show a decreased tumor incidence, latency, and reduced tumor growth (74). The same study described that $Mdm2^{+/-}$ tumors had a decreased level of $p19^{Arf}$ (Cdkn2a), another tumor suppressor that is reciprocally regulated by N-myc. $p19^{Arf}$ in turn can be inhibited by Twist-1 which is also a direct target of N-myc (75). The upregulation of Twist-1 correlates with *MYCN*-amplification in neuroblastoma indicating that apoptosis evading mechanisms are different in *MYCN* amplified compared to non-amplified neuroblastoma (76). A direct targeting of the *MYCN* gene using siRNA, CRISPR/Cas9 crRNA molecules or specific alkylating agents induced apoptosis in *MYCN* amplified cells but not in non-amplified cells (77). These studies indicate that N-myc alone can prevent apoptosis or senescence in neuroblastoma without depending on mutations in additional tumor-promoting genes. N-myc regulates the transcriptional network around p53 to overcome these intrinsic barriers, similar to the artificial activation of the pluripotency program in healthy somatic cells. Why the incidence of initial p53 mutations in neuroblastoma is only around 2% remains an open question, especially if the selection pressure during early tumorigenesis preferentially selects cells with an active p53 signaling (67). In early analysis of heterozygous p53-deficient mice ($tp53^{+/-}$), it was observed that a high proportion of tumors retain the functional copy of p53 while only a minor fraction lost their wild-type allele. The functional copy of p53 prevented chromosomal instability and induced apoptosis after radiation therapy (78).

During the early onset of neuroblastoma, the cell of origin depends on self-renewal to maintain tumor growth as a homeostatic process. It is known from pluripotent cells that increased cellular stress can disturb this homeostasis, inhibit self-renewal and induce differentiation or senescence. P53 can alleviate cellular stress by DNA damage control or by reducing oxidative phosphorylation (65). Downstream effects of MYCN might induce a transient reduction of p53 protein, e.g. during G1 cell cycle checkpoint phase. There is further evidence that micro RNAs such as miR-380-5p contribute to this fine-tuned balance

(79). Chemotherapy, however, disturbs this balanced activity of p53 by inducing massive DNA damage forcing p53 wild-type tumors to regress. Many high-risk neuroblastomas relapse as a therapy-resistant metastatic disease with increased frequency of mutations in P53-MDM2- $p19^{Arf}$ pathway (80).

MYCN CONFERS METABOLIC PLASTICITY

During embryonic development, stem cells undergo rapid cell duplications while passing through different cell states in a continuously changing environment. Their metabolism is challenged to provide a sufficient amount of energy, in the form of ATP, but also to generate molecules for biosynthetic demands such as DNA replication or cell growth. This versatile flexibility is re-acquired by somatic cells during reprogramming and is also shared by cancer cells (81).

Differentiated somatic cells usually generate energy by metabolizing glucose to carbon dioxide. In the initial anaerobic glycolytic step, glucose is oxidized to pyruvate which can be converted into lactate. Alternatively, pyruvate can enter the mitochondrial matrix where it is further catabolized to Acetyl-CoA feeding the tricarboxylic acid (TCA) cycle. The TCA cycle takes part in cellular redox reactions by providing reduced oxidizing agents such as NADH and FADH as electron sources for oxidative phosphorylation (OxPhos), which is the mitochondrial direct ATP synthesis pathway when under an aerobic state. While OxPhos produces vastly more ATP per glucose molecule, ATP generation is faster during anaerobic glycolysis (82, 83). The observation that cancer cells fulfill a glycolytic switch, meaning they depend mostly on anaerobic glycolysis despite a sufficient oxygen supply, is referred to as the Warburg effect or aerobic glycolysis (82).

Otto Warburg stated in his article from1956, "On the Origin of Cancer Cells", that the "irreversible injury of respiration" constitutes the first phase of cancer development (84). A deeper understanding of the cellular metabolism has revealed that cataplerosis, the use of partially oxidized metabolites from the TCA cycle, is an important and eclectic source for versatile anabolic processes (85). Thus, pyruvate and alpha-ketoglutarate, key intermediates in the TCA cycle, are important building blocks for non-essential amino acids and Acetyl-CoA is the precursor molecule of fatty acid synthesis and histone acetylation. Further, direct derivatives of glucose can be incorporated into the pentose phosphate pathway providing ribose for nucleotide synthesis (82, 85). Otto Warburg couldn't be aware that the incomplete oxidation of substrates constitutes an advantage for the anabolic processes in cancer tissue despite a less efficient ATP generation. The investigation of embryonic stem cells and later of induced pluripotent stem cells has shown, however, that dependency on glycolysis in pluripotent stem cells and cancer cells is not a consequence, but a pre-requisite of successful embryonal development and tumorigenesis (81).

ESCs can obtain different states of pluripotency, of which the naïve state better reflects the ground state pluripotency of the inner cell mass from the preimplantation blastocyst than the primed pluripotency state. While MYC proteins are crucial in order to maintain pluripotency in both states, human naïve pluripotent cells show a specific nuclear expression of MYCN associated with a higher glycolytic flux (86). If the glycolytic enzyme hexokinase II is pharmacologically inhibited by the pyruvate analog 3-bromopyruvate, cultured ESCs switch from anaerobic glycolysis to OxPhos and lose their pluripotency, even under pluripotency promoting conditions indicating the functional role of the glycolytic metabolism in pluripotency (87). Likewise, the generation of iPS from somatic cells highly depend on functional glycolysis as its inhibition reduces reprogramming efficiency while it is supported by the stimulation of glycolytic activity (88). Several studies have indicated that the metabolic restructuring during reprogramming precedes the expression of pluripotency factors. The expression of MYC in cancer cells or as a transduced factor during reprogramming supports this switch by inducing hypoxia inducible factor 1a (Hif1A) and its downstream targets pyruvate dehydrogenase kinase and other glycolytic enzymes (88–91). However, a study in MYC inducible cancer cell lines has shown that highly proliferating MYC expressing cells require active OxPhos together with increased glycolysis to drive their fast cell cycle progression (92).

Similar results have been described in neuroblastoma, where *MYCN*-amplified cells display a distinct metabolic structure defined by high energy consumption and production compared to *MYCN* non-amplified neuroblastoma cells (93, 94). In a detailed metabolic analysis of *MYCN*-amplified neuroblastoma cells, Oliynyk et al. showed that *MYCN* induction upregulates glycolytic enzymes such as hexokinase-2 but that the dominant effect was an increase in OxPhos induction (94). Interestingly, *MYCN* activation not only increased the oxygen consumption rate but also OxPhos response provoked by metabolic stress. This indicates increased flexibility for regulating glycolysis or mitochondrial respiration within MYCN expressing cells (94).

Beyond glucose, glutamine and fatty acids are important fuels for mitochondria generating ATP and other macro-molecules. MYCN enables neuroblastoma cells to oxidize fatty acids with a higher capacity than in non-*MYCN* amplified cells. This feature might become of clinical relevance as it has been shown that the inhibition of β-oxidation induces differentiation in MYCN expressing tumor spheroids and leads to a decreased tumor growth in *MYCN* amplified cell lines when injected into nude mice (94). Another metabolic hallmark of many cancers is increase in glutaminolysis. Glutamine is a versatile nutrient and its derivatives are involved in many anabolic processes within the cell. Its carbon atoms can be fed into the TCA cycle or can be utilized to generate amino or fatty acids. Glutamine further provides nitrogen for amino acid production as well as for nucleotide biosynthesis (95). Highly proliferating cancer cells are often addicted to glutamine and studies have shown that MYCN leads to an upregulation of glutaminolytic enzymes, while also selectively inducing apoptosis in glutamine depleted cells (96, 97). Although, a recent *in vitro* study found that MYCN expression can enable tumor cells to synthesize glutamine from glucose-derived alpha-ketoglutarate (94, 98). The ability to adapt

to a low-glutamine environment is highly beneficial for proliferating cancer cells in a poorly vascularized environment. This has therapeutic implications as the glutamine metabolism is currently studied as an anticancer target (95).

The above-mentioned studies have shown that the metabolism of *MYCN* amplified cells is not only driven by the strong proliferative stimulus but remains flexible to provide high amounts of energy as well as bio-macromolecules for anabolic processes. This metabolic structure of a regulated balance between active OxPhos and glycolysis has also been described during the first days of somatic reprogramming as well as in early naïve ESCs being a prerequisite to successfully achieve pluripotency (89, 99–101). Direct comparisons of *MYCN* amplified versus non amplified cells have shown that MYCN is one of the metabolic master regulators equipping cells with a high versatility resembling mechanisms of self-renewing stem cells.

SELF-RENEWAL IN *MYCN* NON-AMPLIFIED HIGH-RISK NEUROBLASTOMA

MYCN amplification drives tumorigenesis in neural crest cells by maintaining or re-establishing embryonic features in these cells. By conferring stem-like qualities such as infinite self-renewal, apoptotic resistance or metabolic flexibility, MYCN contributes to the life-threatening characteristics of high-risk neuroblastoma. Even though, *MYCN* gene amplification accounts for 50% of all high-risk neuroblastoma cases, the malignant *MYCN* non-amplified neuroblastomas never gain secondary gene amplifications during tumor progression or relapse, which is an uncommon feature of oncogenes in adult cancers (17). High-risk, *MYCN* single copy neuroblastomas often express MYC as the oncogenic driver while MYCN is not expressed in these cells (50). Usually, only one of these two MYC proteins can be expressed in a tumor cell at a time, with MYC often dominating over MYCN by repressing *MYCN* expression (50, 102). Coincidentally, higher MYCN expression in *MYCN* non-amplified tumors was reported to be correlated with favorable prognosis (50, 103). It must be mentioned that these tumor cells never reach the MYCN mRNA expression level of *MYCN* amplified tumors. Most MYC target genes are regulated in a dose dependent manner and non-*MYCN*-amplified tumor cells that artificially overexpress MYCN retain their ability of neuronal differentiation (104, 105).

Inducing stemness without direct MYC overexpression has been shown by reprogramming somatic cells without using MYC. Interestingly, similar pathways that are used to avoid MYC transduction in iPS generation are potentially involved in the tumorigenesis of *MYCN* non-amplified neuroblastomas.

Lin28b, as one example, has been a part of the pluripotency factors first used in reprogramming of human somatic cells that did not depend on the enforced overexpression of MYC (106). It has always been suspected, however, that Lin28b expression leads to an indirect activation of endogenous MYC proteins (56).

Another strategy involves the activation of the Wnt pathway, a well described and highly conserved signaling cascade in embryonal development, tissue stem cells and tumorigenesis. Together with MYC proteins and other factors, Wnt signaling is involved in the initial induction of neural crest cells, their maintenance and later cell fate determination (33, 107). High-risk *MYCN* non-amplified neuroblastoma often have an increased Wnt activity which contributes to its high aggressiveness by inducing *c-MYC* expression (108). A reciprocal mechanism has been described for the Wnt-inhibitor *Dickkopf-3* (DKK3) which induces tumor cell maturation and correlates with a favorable prognosis. In *MYCN* amplified tumors, Dkk3 is often downregulated by MYCN leading to an undifferentiated phenotype and higher aggressiveness (109). With the help of strong Wnt signaling, artificial *c-MYC* activation becomes dispensable when self-renewal and pluripotency is re-induced in differentiated somatic cells (110). Of the aforementioned mechanisms, activation of endogenous *MYC* genes is most closely associated with high risk in *MYCN* non-amplified neuroblastoma. Comprehensive transcriptome analyses elucidates the expression of MYC target genes and their embedded pathways, which can be indicative for the clinical outcome, independent of *MYCN* amplification (111). If the expression of MYC downstream factors such as Hif or the Krüppel-like family of transcription factors (Klf) is highly expressed, the oncogenic activity of MYC becomes irrelevant (112).

PRECLINICAL *IN VIVO* MODELS OF NEUROBLASTOMA

Weiss et al. have previously demonstrated that Mycn has the potential to drive neuroblastoma in a transgenic model mouse model, i.e. *Th-MYCN* mice, which carry, in their germline, human *MYCN* cDNA under the control of the rat tyrosine-hydroxylase promoter (22). Neuroblastoma growth in these *Th-MYCN* mice begins with hyperplastic lesions in sympathetic ganglia through the first few weeks after birth (58). Mice containing *MYCN* transgene targeted to the neural crest cells develop neuroblastoma with a phenotype very similar to the human neuroblastoma (46).

Incorrect MycN expression shortly after birth in the paravertebral ganglia caused neuroblast hyperplasia in *Th-MYCN* mice. *N-myc* amplification existed at low levels in perinatal neuroblast hyperplasia from both hemizygote and homozygote mice. The level of N-myc in hyperplasias and tumor tissue was highest at week 1 of age. A stepwise increase of *N-myc* amplification was only seen in tumor formation of hemizygote mice. The neuroblast hyperplasia in the ganglia from *Th-MYCN* did not express differentiation markers, such as beta-III-tubulin or tyrosine hydroxylase, differing from nearby neuronal cells (46).

Althoff et al. generated a transgenic mice, termed *LSL-MYCN;Dbh-iCre*, with Cre-conditional induction of *MYCN* in *Dbh*-expressing cells. These mice form tumors irrespective of strain background with an incident of 75% (113).

In the *Th-MYCN* mouse model, tumor penetrance is only high in a 129 x 1/SvJ strain background. Tumors in *LSL-MYCN;Dbh-iCre* mice arise in superior cervical ganglion, celiac ganglion or the adrenals covering all locations, in which human neuroblastomas arise. They consist of small blue round cells harboring neurosecretory vesicles. The cells express neuroblastoma specific genes such as paired-Phox2b, Dbh, Th, and high levels of N-myc compared to normal tissue. The level of differentiation and tumor location resemble the human neuroblastoma more in the *LSL-MYCN;Dbh-iCRe* than in the Th-MYCN model.

Hierarchical clustering shows that tumors from the *Th-MYCN* mouse model and *LSL-MYCN;Dbh-iCre* mice are very similar, both at miRNA and mRNA level. In tumors from *LSL-MYCN;Dbh-iCre* mice a partial gain of murine chromosome 11 was observed, syntenic to human chromosome 17q. Therefore, this model resembles more closely the genetic aberrations observed in human neuroblastomas better than the *Th-MYCN* model which lack any additional chromosomal aberrations.

Since neural crest cells are the suspected embryonic precursor cell in neuroblastoma, Olsen et al., generated neuroblastoma tumors through forced expression of Mycn in neural crest cells. The tumors were phenotypically and molecularly similar to human *MYCN-amplified* neuroblastoma. The neural crest derived neuroblastomas acquired copy number gains and losses that are similar to those observed in human *MYCN*-amplified neuroblastoma. These copy number gains and losses included 2p gain, 17q gain and loss of 1p36. To form tumors in these experiments, they used p53 compromised neural crest cells from the neural tube demonstrating high expression sox10, p75, scl1, and low expression of Th and Phox2b. The embryonic cells were transduced with *MYCN-IRES-GFP* retrovirus and inoculated subcutaneously in mice. With 100% tumor penetrance this proved to be a good, reliable and more rapid method of making a neuroblastoma mouse model (47).

In another study, Alam et al. examined which cell types drive neuroblastoma growth in the *Th-MYCN* transgenic mice model. They showed that both primary tumors and hyperplasia are comprised predominantly of highly proliferative Phox2B$^+$ neuronal progenitors. N-myc stimulates the growth of these progenitors by both promoting their proliferation and preventing their differentiation. They also identified a small population of undifferentiated Nestin$^+$ cells in both primary tumors and hyperplastic lesions. These cells may serve as precursors of phox2b$^+$ neuronal progenitors. Sympathetic neural crest cells express the pro neural genes *Mash1* and P*hox2B*. Mash1 and Phox2b promote further neuronal differentiation by upregulating, the levels of Hand2, Phox2A, and Gata3. These transcription factors collaborate by inducing the expression of Th and dopamine β-hydroxylase, enzymes essential in the catecholamine biosynthesis. Phox2B$^+$ in hyperplastic cells from *Th-MYCN* sympathetic ganglia exhibited the morphology of undifferentiated, small round cells and expressed no measurable levels of Th. Alam et al. suggests that Phox2b$^+$ hyperplastic cells are halted at the progenitor stage and that Phox2b$^+$ neuronal progenitors are the main cellular target of N-myc in driving neuroblastoma expansion from hyperplasia to tumors. Most of the tumor cells expressed Phox2b, and the majority of the Phox2b$^+$ tumor cells expressed Ki67, but no measurable levels of Th (58).

Taken together N-myc not only blocks neural progenitors' differentiation but also promotes the proliferation of Phox2B$^+$ neuronal progenitors. This leads to marked increases of the progenitor population in sympathetic ganglia and subsequently the formation of hyperplastic lesions. Alam et al. also proposes that nestin$^+$ cells in sympathetic ganglia are possibly the cells of origin for neuroblastoma in *Th-MYCN* mice (58).

The zebrafish model showed that *MYCN* induced neuroblastoma does not develop from the earliest cells populating the superior cervical ganglia. Instead, tumors arise from neuroblasts that migrate into the inter-renal gland later in development, after the kidney has developed. The neuroblasts overexpressing N-myc fail to differentiate, resulting in reduced numbers of chromaffin cells (30).

Neuroblastoma tumors from *Th-MYCN* mice are composed of several cell populations, including Phox2b$^+$Th$^-$, Phox2b$^-$Th$^+$, and Phox2b$^+$Th$^+$ cells. The varying degrees of differentiation in these tumors indicate that the tumors are heterogeneous and may show a molecular resemblance to embryonic stem cells. Sphere forming neuroblastomas were mainly composed of Mycn$^+$ and phox2b$^+$ cells (114).

PERSPECTIVES AND CONCLUSIONS

Here, we have emphasized the role of MYCN as an oncogenic driver in neuroblastoma. This is seen in part through MYCN's ability to initiate stem-like qualities in neural crest-derived cells. A process that is reminiscent of the artificial induction of pluripotency in somatic cells and depends on MYC protein activity. MYCN is significantly involved in the induction of self-renewal by the blockage of differentiation factors as well as by inducing proliferation. While the strong pro-proliferative signal of artificial MYCN overexpression usually leads to apoptosis, the apoptotic machinery in *MYCN* amplified tumors is reorganized in a unique way that allows them to resist apoptotic signals and maybe even benefit from active p53 signaling.

Increased metabolic flexibility by neglecting the Warburg Effect and retaining mitochondrial respiration, as well as, glutamine independence further contributes to the malignancy of *MYCN* amplified tumors and their often observed therapeutic resistance.

The observation that *MYCN* non-amplified tumors never gain extra copies of the *MYCN* gene during their development supports the assumption that a high expression of MYCN in an already established neuroblastoma overloads connected signaling pathways, such as Wnt or HIF signaling.

The extensive and unique restructuring of cellular mechanisms are further reflected by the incompatibility of *MYCN* amplification with other oncogenic events such as genomic rearrangements affecting the *TERT* locus or mutations within the *ATRX* gene. Both might be explained by the fact that the high MYCN expression

already deregulates the affected pathways of telomere lengthening, causing mitochondrial dysfunctions and replicative stress. MYCN's combined effects on DNA damage are incompatible in neuroblastoma (115, 116).

The accumulated data demonstrates that high MYCN expression can act as a single oncogenic driver in neuroblastoma and the mechanisms for how MYCN induces neoplastic transformation has been thoroughly described. However, we still do not know how and at which stage during neural crest development *MYCN* becomes amplified and which cells are affected by sustained high expression of MYCN. The existing animal models are excellent references for studying the mechanisms of induction in tumorigenesis driven by MYCN. Drawbacks of these animal models can be seen however during normal development in which the N-myc expression is controlled by the Dbh or Th promotor. Both are activated relatively late during the maturation of cells within the neural crest and may therefore not fully reflect the initial neoplastic events in humans. Furthermore, for patients with non-amplified *MYCN* neuroblastoma, high expression of MYCN is not correlated with adverse outcomes, in fact the opposite is observed. Instead, a trend correlating high MYCN expression to improved outcomes was evident in these neuroblastoma patients (103). Recent studies indicate that the initial oncogenic event for the development of neuroblastoma must occur early in the neural crest development and no studies to date have identified the precise cell of origin for neuroblastoma. Additionally, which developmental cues or molecular signals and mechanisms are inducing the somatic amplification of the *MYCN* locus at chromosome 2p24.3? Is the gene amplification of *MYCN* the initial genetic aberration in neuroblastoma? Is *MYCN* amplification guided by other earlier genetic aberrations or is the amplification of the chromosome 2p24.3 locus induced by random genomic insults induced by untidy or downregulated DNA repair mechanisms and/or external signals? These are questions that we should address in order to fully understand the biology of *MYCN* amplified neuroblastoma.

AUTHOR CONTRIBUTIONS

Conceptualization: JO, CD, and JJ. Writing: JO, CD, and JJ. General review and correction of the manuscript: AP and JJ. Figure Design: AP. Supervision: JJ. All authors contributed to the article and approved the submitted version.

FUNDING

This work was supported with grants from the Swedish Childhood Cancer Foundation, the Swedish Cancer Foundation, the Swedish Foundation for Strategic Research (www.nnbcr.se), Märta and Gunnar V Philipson Foundation and The Cancer Research Foundations of Radiumhemmet.

REFERENCES

1. Dang CV. MYC on the path to cancer. *Cell* (2012) 149:22–35. doi: 10.1016/j.cell.2012.03.003
2. Meyer N, Penn LZ. Reflecting on 25 years with MYC. *Nat Rev Cancer* (2008) 8:976–90. doi: 10.1038/nrc2231
3. Dang CV. Enigmatic MYC conducts an unfolding systems biology symphony. *Genes Cancer* (2010) 1:526–31. doi: 10.1177/1947601910378742
4. Büchel G, Carstensen A, Mak KY, Roeschert I, Leen E, Sumara O, et al. Association with Aurora-A Controls N-MYC-Dependent Promoter Escape and Pause Release of RNA Polymerase II during the Cell Cycle. *Cell Rep* (2017) 21:3483–97. doi: 10.1016/j.celrep.2017.11.090
5. Casey SC, Baylot V, Felsher DW. MYC: Master Regulator of Immune Privilege. *Trends Immunol* (2017) 38:298–305. doi: 10.1016/j.it.2017.01.002
6. Kortlever RM, Sodir NM, Wilson CH, Burkhart DL, Pellegrinet L, Brown Swigart L, et al. Myc Cooperates with Ras by Programming Inflammation and Immune Suppression. *Cell* (2017) 171:1301–15.e14. doi: 10.1016/j.cell.2017.11.013
7. Topper MJ, Vaz M, Chiappinelli KB, DeStefano Shields CE, Niknafs N, Yen RWC, et al. Epigenetic Therapy Ties MYC Depletion to Reversing Immune Evasion and Treating Lung Cancer. *Cell* (2017) 171:1284–300.e21. doi: 10.1016/j.cell.2017.10.022
8. Hatton BA, Knoepfler PS, Kenney AM, Rowitch DH, Moreno De Alborán I, Olson JM, et al. N-myc is an essential downstream effector of shh signaling during both normal and neoplastic cerebellar growth. *Cancer Res* (2006) 66:8655–61. doi: 10.1158/0008-5472.CAN-06-1621
9. Charron J, Malynn BA, Fisher P, Stewart V, Jeannotte L, Goff SP, et al. Embryonic lethality in mice homozygous for a targeted disruption of the N-myc gene. *Genes Dev* (1992) 6:2248–57. doi: 10.1101/gad.6.12a.2248
10. Davis AC, Wims M, Spotts GD, Hann SR, Bradley A. A null c-myc mutation causes lethality before 10.5 days of gestation in homozygotes and reduced fertility in heterozygous female mice. *Genes Dev* (1993) 7:671–82. doi: 10.1101/gad.7.4.671
11. Sawai S, Shimono A, Wakamatsu Y, Palmes C, Hanaoka K, Kondoh H. Defects of embryonic organogenesis resulting from targeted disruption of the N-myc gene in the mouse. *Development* (1993) 117:1445–55.
12. Stanton BR, Perkins AS, Tessarollo L, Sassoon DA, Parada LF. Loss of N-myc function results in embryonic lethality and failure of the epithelial component of the embryo to develop. *Genes Dev* (1992) 6:2235–47. doi: 10.1101/gad.6.12a.2235
13. Knoepfler PS, Cheng PF, Eisenman RN. N-myc is essential during neurogenesis for the rapid expansion of progenitor cell populations and the inhibition of neuronal differentiation. *Genes Dev* (2002) 16:2699–712. doi: 10.1101/gad.1021202
14. Nagy A, Moens C, Ivanyi E, Pawling J, Gertsenstein M, Hadjantonakis AK, et al. Dissecting the role of N-myc in development using a single targeting vector to generate a series of alleles. *Curr Biol* (1998) 8:661–6. doi: 10.1016/s0960-9822(98)70254-4
15. Trumpp A, Refaell Y, Oskarsson T, Gasser S, Murphy M, Martin GR, et al. C-Myc regulates mammalian body size by controlling cell number but not cell size. *Nature* (2001) 414:768–73. doi: 10.1038/414768a
16. Zimmerman KA, Yancopoulos GD, Collum RG, Smith RK, Kohl NE, Denis KA, et al. Differential expression of myc family genes during murine development. *Nature* (1986) 319:780–3. doi: 10.1038/319780a0
17. Rickman DS, Schulte JH, Eilers M. The expanding world of N-MYC-driven tumors. *Cancer Discov* (2018) 8:150–64. doi: 10.1158/2159-8290.CD-17-0273
18. Marshall GM, Carter DR, Cheung BB, Liu T, Mateos MK, Meyerowitz JG, et al. The prenatal origins of cancer. *Nat Rev Cancer* (2014) 14:277–89. doi: 10.1038/nrc3679
19. Johnsen JI, Dyberg C, Wickström M. Neuroblastoma—A neural crest derived embryonal malignancy. *Front Mol Neurosci* (2019) 12:9. doi: 10.3389/fnmol.2019.00009
20. Swartling FJ, Savov V, Persson AI, Chen J, Hackett CS, Northcott PA, et al. Distinct Neural Stem Cell Populations Give Rise to Disparate Brain Tumors

in Response to N-MYC. *Cancer Cell* (2012) 21:601–13. doi: 10.1016/j.ccr.2012.04.012
21. Swartling FJ, Grimmer MR, Hackett CS, Northcott PA, Fan QW, Goldenberg DD, et al. Pleiotropic role for MYCN in medulloblastoma. *Genes Dev* (2010) 24:1059–72. doi: 10.1101/gad.1907510
22. Weiss WA, Aldape K, Mohapatra G, Feuerstein BG, Bishop JM. Targeted expression of MYCN causes neuroblastoma in transgenic mice. *EMBO J* (1997) 16:2985–95. doi: 10.1093/emboj/16.11.2985
23. Maris JM. Recent advances in neuroblastoma. *N Engl J Med* (2010) 362:2202. doi: 10.1056/nejmra0804577
24. Brodeur GM, Seeger RC, Schwab M, Varmus HE, Michael Bishop J. Amplification of N-myc in untreated human neuroblastomas correlates with advanced disease stage. *Science (80-)* (1984) 224:1121–4. doi: 10.1126/science.6719137
25. Schwab M, Ellison J, Busch M. Enhanced expression of the human gene N-myc consequent to amplification of DNA may contribute to malignant progression of neuroblastoma. *Proc Natl Acad Sci U S A* (1984) 81:4940–4. doi: 10.1073/pnas.81.15.4940
26. Huang M, Weiss WA. Neuroblastoma and MYCN. *Cold Spring Harb Perspect Med* (2013) 3:1–23. doi: 10.1101/cshperspect.a014415
27. Matthay KK, Maris JM, Schleiermacher G, Nakagawara A, Mackall CL, Diller L, et al. Neuroblastoma. *Nat Rev Dis Primers* (2016) 2:1–21. doi: 10.1038/nrdp.2016.78
28. Heukamp LC, Thor T, Schramm A, De Preter K, Kumps C, De Wilde B, et al. Targeted expression of mutated ALK induces neuroblastoma in transgenic mice. *Sci Transl Med* (2012) 4:141ra91. doi: 10.1126/scitranslmed.3003967
29. Berry T, Luther W, Bhatnagar N, Jamin Y, Poon E, Sanda T, et al. The ALKF1174L Mutation Potentiates the Oncogenic Activity of MYCN in Neuroblastoma. *Cancer Cell* (2012) 22:117–30. doi: 10.1016/j.ccr.2012.06.001
30. Zhu S, Lee JS, Guo F, Shin J, Perez-Atayde AR, Kutok JL, et al. Activated ALK Collaborates with MYCN in Neuroblastoma Pathogenesis. *Cancer Cell* (2012) 21:362–73. doi: 10.1016/j.ccr.2012.02.010
31. Groves AK, LaBonne C. Setting appropriate boundaries: Fate, patterning and competence at the neural plate border. *Dev Biol* (2014) 389:2–12. doi: 10.1016/j.ydbio.2013.11.027
32. Coelho-Aguiar JM, Le Douarin NM, Dupin E. Environmental factors unveil dormant developmental capacities in multipotent progenitors of the trunk neural crest. *Dev Biol* (2013) 384:13–25. doi: 10.1016/j.ydbio.2013.09.030
33. Tomolonis JA, Agarwal S, Shohet JM. Neuroblastoma pathogenesis: deregulation of embryonic neural crest development. *Cell Tissue Res* (2018) 372:245–62. doi: 10.1007/s00441-017-2747-0
34. Van Groningen T, Koster J, Valentijn LJ, Zwijnenburg DA, Akogul N, Hasselt NE, et al. Neuroblastoma is composed of two super-enhancer-associated differentiation states. *Nat Genet* (2017) 49:1261–6. doi: 10.1038/ng.3899
35. Boeva V, Louis-Brennetot C, Peltier A, Durand S, Pierre-Eugène C, Raynal V, et al. Heterogeneity of neuroblastoma cell identity defined by transcriptional circuitries. *Nat Genet* (2017) 49:1408–13. doi: 10.1038/ng.3921
36. Zeid R, Lawlor MA, Poon E, Reyes JM, Fulciniti M, Lopez MA, et al. Enhancer invasion shapes MYCN-dependent transcriptional amplification in neuroblastoma. *Nat Genet* (2018) 50:515–23. doi: 10.1038/s41588-018-0044-9
37. Wang L, Tan TK, Durbin AD, Zimmerman MW, Abraham BJ, Tan SH, et al. ASCL1 is a MYCN- and LMO1-dependent member of the adrenergic neuroblastoma core regulatory circuitry. *Nat Commun* (2019) 10:1–15. doi: 10.1038/s41467-019-13515-5
38. Soldatov R, Kaucka M, Kastriti ME, Petersen J, Chontorotzea T, Englmaier L, et al. Spatiotemporal structure of cell fate decisions in murine neural crest. *Science (80-)* (2019) 364:1–13. doi: 10.1126/science.aas9536
39. Hallberg B, Palmer RH. The role of the ALK receptor in cancer biology. *Ann Oncol* (2016) 27:iii4–15. doi: 10.1093/annonc/mdw301
40. Zito Marino F, Rocco G, Morabito A, Mignogna C, Intartaglia M, Liguori G, et al. A new look at the ALK gene in cancer: copy number gain and amplification. *Expert Rev Anticancer Ther* (2016) 16:493–502. doi: 10.1586/14737140.2016.1162098
41. Marino FZ, Botti G, Aquino G, Ferrero S, Gaudioso G, Palleschi A, et al. Unproductive effects of alk gene amplification and copy number gain in non-small-cell lung cancer. Alk gene amplification and copy gain in nsclc. *Int J Mol Sci* (2020) 21:1–12. doi: 10.3390/ijms21144927
42. Trigg RM, Turner SD. ALK in neuroblastoma: Biological and therapeutic implications. *Cancers (Basel)* (2018) 10:1–16. doi: 10.3390/cancers10040113
43. Molenaar JJ, Domingo-Fernández R, Ebus ME, Lindner S, Koster J, Drabek K, et al. LIN28B induces neuroblastoma and enhances MYCN levels via let-7 suppression. *Nat Genet* (2012) 44:1199–206. doi: 10.1038/ng.2436
44. Schnepp RW, Khurana P, Attiyeh EF, Raman P, Chodosh SE, Oldridge DA, et al. A LIN28B-RAN-AURKA Signaling Network Promotes Neuroblastoma Tumorigenesis. *Cancer Cell* (2015) 28:599–609. doi: 10.1016/j.ccell.2015.09.012
45. Tao T, Shi H, Mariani L, Abraham BJ, Durbin AD, Zimmerman MW, et al. LIN28B regulates transcription and potentiates MYCN-induced neuroblastoma through binding to ZNF143 at target gene promotors. *Proc Natl Acad Sci U S A* (2020) 117:16516–26. doi: 10.1073/pnas.1922692117
46. Hansford LM, Thomas WD, Keating JM, Burkhart CA, Peaston AE, Norris MD, et al. Mechanisms of embryonal tumor initiation: Distinct roles for MycN expression and MYCN amplification. *Proc Natl Acad Sci U S A* (2004) 101:12664–9. doi: 10.1073/pnas.0401083101
47. Olsen RR, Otero JH, García-López J, Wallace K, Finkelstein D, Rehg JE, et al. MYCN induces neuroblastoma in primary neural crest cells. *Oncogene* (2017) 36:5075–82. doi: 10.1038/onc.2017.128
48. Yang CL, Serra-Roma A, Gualandi M, Bodmer N, Niggli F, Schulte JH, et al. Lineage-restricted sympathoadrenal progenitors confer neuroblastoma origin and its tumorigenicity. *Oncotarget* (2020) 11:2357–71. doi: 10.18632/oncotarget.27636
49. Kerosuo L, Neppala P, Hsin J, Mohlin S, Vieceli FM, Török Z, et al. Enhanced expression of MycN/CIP2A drives neural crest toward a neural stem cell-like fate: Implications for priming of neuroblastoma. *Proc Natl Acad Sci U S A* (2018) 115:E7351–60. doi: 10.1073/pnas.1800039115
50. Westermann F, Muth D, Benner A, Bauer T, Henrich KO, Oberthuer A, et al. Distinct transcriptional MYCN/c-MYC activities are associated with spontaneous regression or malignant progression in neuroblastomas. *Genome Biol* (2008) 9. doi: 10.1186/gb-2008-9-10-r150
51. Solter D. From teratocarcinomas to embryonic stem cells and beyond: A history of embryonic stem cell research. *Nat Rev Genet* (2006) 7:319–27. doi: 10.1038/nrg1827
52. Clevers H. What is an adult stem cell? *Sci (80-)* (2015) 350:1319–20. doi: 10.1126/science.aad7016
53. Batlle E, Clevers H. Cancer stem cells revisited. *Nat Med* (2017) 23:1124–34. doi: 10.1038/nm.4409
54. Takahashi K, Yamanaka S. Induction of Pluripotent Stem Cells from Mouse Embryonic and Adult Fibroblast Cultures by Defined Factors. *Cell* (2006) 126:663–76. doi: 10.1016/j.cell.2006.07.024
55. Lee AS, Tang C, Rao MS, Weissman IL, Wu JC. Tumorigenicity as a clinical hurdle for pluripotent stem cell therapies. *Nat Med* (2013) 19:998–1004. doi: 10.1038/nm.3267
56. Nakagawa M, Koyanagi M, Tanabe K, Takahashi K, Ichisaka T, Aoi T, et al. Generation of induced pluripotent stem cells without Myc from mouse and human fibroblasts. *Nat Biotechnol* (2008) 26:101–6. doi: 10.1038/nbt1374
57. Varlakhanova NV, Cotterman RF, Wilhelmine N, Morgan J, Rae L, Murray S, et al. myc maintains embryonic stem cell pluripotency and self-renewal. *Differentiation* (2010) 80:9–19. doi: 10.1016/j.diff.2010.05.001
58. Alam G, Cui H, Shi H, Yang L, Ding J, Mao L, et al. MYCN promotes the expansion of Phox2B-positive neuronal progenitors to drive neuroblastoma development. *Am J Pathol* (2009) 175:856–66. doi: 10.2353/ajpath.2009.090019
59. Sawai S, Shimono A, Hanaoka K, Kondoh H. Embryonic lethality resulting from disruption of both N-myc alleles in mouse zygotes. *New Biol* (1991) 3:861–9.
60. Blelloch R, Venere M, Yen J, Ramalho-santos M. Correspondence Generation of Induced Pluripotent Stem Cells in the Absence of Drug Selection. *Cell Stem Cell* (2007) 1:245–7. doi: 10.1016/j.stem.2007.08.008
61. Malynn BA, De Alboran IM, O'Hagan RC, Bronson R, Davidson L, DePinho RA, et al. N-myc can functionally replace c-myc in murine development, cellular growth, and differentiation. *Genes Dev* (2000) 14:1390–9. doi: 10.1101/gad.14.11.1390
62. Baluapuri A, Wolf E, Eilers M. Target gene-independent functions of MYC oncoproteins. *Nat Rev Mol Cell Biol* (2020) 21:255–67. doi: 10.1038/s41580-020-0215-2

63. Kandoth C, McLellan MD, Vandin F, Ye K, Niu B, Lu C, et al. Mutational landscape and significance across 12 major cancer types. *Nature* (2013) 502:333–9. doi: 10.1038/nature12634
64. Jain AK, Barton MC. p53 : emerging roles in stem cells, development and beyond. *Development* (2018) 145. doi: 10.1242/dev.158360
65. Fu X, Wu S, Li B, Xu Y, Liu J. Functions of p53 in pluripotent stem cells. *Protein Cell* (2020) 11:71–8. doi: 10.1007/s13238-019-00665-x
66. Vogan K, Bernstein M, Leclerc JM, Brisson L, Brossard J, Brodeur GM, et al. Absence of p53 Gene Mutations in Primary Neuroblastomas. *Cancer Res* (1993) 53:5269–73.
67. Chen L, Malcolm AJ, Wood KM, Cole M, Variend S, Cullinane C, et al. P53 Is Nuclear and Functional in Both Undifferentiated and Differentiated Neuroblastoma. *Cell Cycle* (2007) 6:2685–96. doi: 10.4161/cc.6.21.4853
68. Kim E, Shohet J. Targeted molecular therapy for neuroblastoma: The ARF/MDM2/p53 Axis. *J Natl Cancer Inst* (2009) 101(22):1527–9. doi: 10.1093/jnci/djp376
69. Chen L, Iraci N, Gherardi S, Gamble LD, Wood KM, Perini G, et al. p53 Is a Direct Transcriptional Target of MYCN in Neuroblastoma. *Cancer Res* (2010) 70:1377–88. doi: 10.1158/0008-5472.CAN-09-2598
70. Reisman D, Elkind NB, Roy B, Beamon J, Rotter V. c-Myc Trans-activates the p53 Promoter through a Required Downstream CACGTG Motif. *Cell Growth Differ* (1993) 4:57–65.
71. Valter K, Zhivotovsky B, Gogvadze V. Cell death-based treatment of neuroblastoma review-Article. *Cell Death Dis* (2018) 9:1–15. doi: 10.1038/s41419-017-0060-1
72. Slack A, Chen Z, Tonelli R, Pule M, Hunt L, Pession A, et al. The p53 regulatory gene MDM2 is a direct transcriptional target of MYCN in neuroblastoma. *Proc Natl Acad Sci U S A* (2005) 102:731–6. doi: 10.1073/pnas.0405495102
73. Gu L, Zhang H, He J, Li J, Huang M, Zhou M. MDM2 regulates MYCN mRNA stabilization and translation in human neuroblastoma cells. *Oncogene* (2012) 31:1342–53. doi: 10.1038/onc.2011.343
74. Chen Z, Lin Y, Barbieri E, Burlingame S, Hicks J, Ludwig A, et al. Mdm2 deficiency suppresses MYCN-driven neuroblastoma tumorigenesis in vivo. *Neoplasia* (2009) 11:753–62. doi: 10.1593/neo.09466
75. Selmi A, de Saint-Jean M, Jallas AC, Garin E, Hogarty MD, Bénard J, et al. TWIST1 is a direct transcriptional target of MYCN and MYC in neuroblastoma. *Cancer Lett* (2015) 357:412–8. doi: 10.1016/j.canlet.2014.11.056
76. Valsesia-Wittmann S, Magdeleine M, Dupasquier S, Garin E, Jallas AC, Combaret V, et al. Oncogenic cooperation between H-Twist and N-Myc overrides failsafe programs in cancer cells. *Cancer Cell* (2004) 6:625–30. doi: 10.1016/j.ccr.2004.09.033
77. Yoda H, Inoue T, Shinozaki Y, Lin J, Watanabe T, Koshikawa N, et al. Direct targeting of MYCN gene amplification by site-specific DNA alkylation in neuroblastoma. *Cancer Res* (2019) 79:830–40. doi: 10.1158/0008-5472.CAN-18-1198
78. Venkatachalam S, Shi YP, Jones SN, Vogel H, Bradley A, Pinkel D, et al. Retention of wild-type p53 in tumors from p53 heterozygous mice: Reduction of p53 dosage can promote cancer formation. *EMBO J* (1998) 17:4657–67. doi: 10.1093/emboj/17.16.4657
79. Swarbrick A, Woods SL, Shaw A, Balakrishnan A, Phua Y, Nguyen A, et al. MiR-380-5p represses p53 to control cellular survival and is associated with poor outcome in MYCN-amplified neuroblastoma. *Nat Med* (2010) 16:1134–40. doi: 10.1038/nm.2227
80. Carr-Wilkinson J, O'Toole K, Wood KM, Challen CC, Baker AG, Board JR, et al. High frequency of p53/MDM2/p14ARF pathway abnormalities in relapsed neuroblastoma. *Clin Cancer Res* (2010) 16:1108–18. doi: 10.1158/1078-0432.CCR-09-1865
81. Nishimura K, Fukuda A, Hisatake K. Mechanisms of the metabolic shift during somatic cell reprogramming. *Int J Mol Sci* (2019) 20. doi: 10.3390/ijms20092254
82. Vander Heiden MG, Cantley LC, Thompson CB. Understanding the warburg effect: The metabolic requirements of cell proliferation. *Science (80-)* (2009) 324:1029–33. doi: 10.1126/science.1160809
83. Pfeiffer T, Schuster S, Bonhoeffer S. Erratum: Cooperation and competition in the evolution of ATP-producing pathways (Science (April 20) (504)). *Science (80-)* (2001) 293:1436. doi: 10.1126/science.293.5534.1436
84. Warburg O. On the origin of cancer cells. *Science (80-)* (1956) 123:309–14. doi: 10.1126/science.123.3191.309
85. Folmes CDL, Dzeja PP, Nelson TJ, Terzic A. Metabolic plasticity in stem cell homeostasis and differentiation. *Cell Stem Cell* (2012) 11:596–606. doi: 10.1016/j.stem.2012.10.002
86. Gu W, Gaeta X, Sahakyan A, Plath K, Lowry WE, Christofk HR, et al. Glycolytic Metabolism Plays a Functional Role in Regulating Human Pluripotent Stem Cell State Article Glycolytic Metabolism Plays a Functional Role in Regulating Human Pluripotent Stem Cell State. *Cell S* (2016) 19:476–90. doi: 10.1016/j.stem.2016.08.008
87. Rodrigues AS, Pereira SL, Correia M, Gomes A, Perestrelo T, Ramalho-Santos J. Differentiate or Die: 3-Bromopyruvate and Pluripotency in Mouse Embryonic Stem Cells. *PLoS ONE* (2015) 10(8):e0135617. doi: 10.1371/journal.pone.0135617
88. Folmes CDL, Nelson TJ, Martinez-Fernandez A, Arrell DK, Lindor JZ, Dzeja PP, et al. Somatic oxidative bioenergetics transitions into pluripotency-dependent glycolysis to facilitate nuclear reprogramming. *Cell Metab* (2011) 14:264–71. doi: 10.1016/j.cmet.2011.06.011
89. Prigione A, Rohwer N, Hoffmann S, Mlody B, Drews K, Bukowiecki R, et al. HIF1α modulates cell fate reprogramming through early glycolytic shift and upregulation of PDK1-3 and PKM2. *Stem Cells* (2014) 32:364–76. doi: 10.1002/stem.1552
90. Cliff TS, Dalton S. Metabolic switching and cell fate decisions: implications for pluripotency, reprogramming and development. *Curr Opin Genet Dev* (2017) 46:44–9. doi: 10.1016/j.gde.2017.06.008
91. Qing G, Skuli N, Mayes PA, Pawel B, Martinez D, Maris JM, et al. Combinatorial regulation of neuroblastoma tumor progression by N-Myc and hypoxia inducible factor HIF-1α. *Cancer Res* (2010) 70:10351–61. doi: 10.1158/0008-5472.CAN-10-0740
92. Morrish F, Neretti N, Sedivy JM, Hockenbery DM. The oncogene c-Myc coordinates regulation of metabolic networks to enable rapid cell cycle entry. *Cell Cycle* (2008) 7:1054–66. doi: 10.4161/cc.7.8.5739
93. Tjaden B, Baum K, Marquardt V, Simon M, Trajkovic-Arsic M, Kouril T, et al. N-Myc-induced metabolic rewiring creates novel therapeutic vulnerabilities in neuroblastoma. *Sci Rep* (2020) 10:1–10. doi: 10.1038/s41598-020-64040-1
94. Oliynyk G, Ruiz-Pérez MV, Sainero-Alcolado L, Dzieran J, Zirath H, Gallart-Ayala H, et al. MYCN-enhanced Oxidative and Glycolytic Metabolism Reveals Vulnerabilities for Targeting Neuroblastoma. *iScience* (2019) 21:188–204. doi: 10.1016/j.isci.2019.10.020
95. Altman BJ, Stine ZE, Dang CV. From Krebs to clinic: Glutamine metabolism to cancer therapy. *Nat Rev Cancer* (2016) 16:619–34. doi: 10.1038/nrc.2016.71
96. Qing G, Li B, Vu A, Skuli N, Walton ZE, Liu X, et al. ATF4 Regulates MYC-Mediated Neuroblastoma Cell Death upon Glutamine Deprivation. *Cancer Cell* (2012) 22:631–44. doi: 10.1016/j.ccr.2012.09.021
97. Wang T, Liu L, Chen X, Shen Y, Lian G, Shah N, et al. MYCN drives glutaminolysis in neuroblastoma and confers sensitivity to an ROS augmenting agent article. *Cell Death Dis* (2018) 9:1–12. doi: 10.1038/s41419-018-0295-5
98. Bott AJ, Peng I, Fan Y, Wu S, Girnun G, Zong W, et al. Oncogenic Myc Induces Expression of Glutamine Synthetase through Promoter Demethylation. *Cell Metab* (2015) 22:1068–77. doi: 10.1016/j.cmet.2015.09.025
99. Kida YS, Kawamura T, Wei Z, Sogo T, Jacinto S, Shigeno A, et al. ERRs mediate a metabolic switch required for somatic cell reprogramming to pluripotency. *Cell Stem Cell* (2015) 16:547–55. doi: 10.1016/j.stem.2015.03.001
100. Zhou W, Choi M, Margineantu D, Margaretha L, Hesson J, Cavanaugh C, et al. HIF1α induced switch from bivalent to exclusively glycolytic metabolism during ESC-to-EpiSC/hESC transition. *EMBO J* (2012) 31:2103–16. doi: 10.1038/emboj.2012.71
101. Folmes CDL, Terzic A. Energy metabolism in the acquisition and maintenance of stemness. *Semin Cell Dev Biol* (2016) 52:68–75. doi: 10.1016/j.semcdb.2016.02.010
102. Breit S, Schwab M. Suppression of MYC by high expression of NMYC in human neuroblastoma cells. *J Neurosci Res* (1989) 24:21–8. doi: 10.1002/jnr.490240105

103. Cohn BSL, London WB, Huang D, Katzenstein HM, Salwen HR, Reinhart T, et al. MYCN Expression Is Not Prognostic of Adverse Outcome in Advanced-Stage Neuroblastoma With Nonamplified MYCN. *J Clin Oncol* (2000) 18:3604–13. doi: 10.1200/JCO.2000.18.21.3604
104. Murphy DJ, Junttila MR, Pouyet L, Karnezis A, Shchors K, Bui DA, et al. Distinct Thresholds Govern Myc's Biological Output In Vivo. *Cancer Cell* (2008) 14:447–57. doi: 10.1016/j.ccr.2008.10.018
105. Edsjö A, Nilsson H, Vandesompele J, Karlsson J, Pattyn F, Culp LA, et al. Neuroblastoma cells with overexpressed MYCN retain their capacity to undergo neuronal differentiation. *Lab Invest* (2004) 84:406–17. doi: 10.1038/labinvest.3700061
106. Yu J, Vodyanik MA, Smuga-otto K, Antosiewicz-bourget J, Frane JL, Tian S, et al. Induced Pluripotent Stem Cell Lines Derived from Human Somatic Cells. *Science (80-)* (2007) 318:1917–20. doi: 10.1126/science.1151526
107. Becker J, Wilting J. WNT signaling, the development of the sympathoadrenal–paraganglionic system and neuroblastoma. *Cell Mol Life Sci* (2018) 75:1057–70. doi: 10.1007/s00018-017-2685-8
108. Liu X, Mazanek P, Dam V, Wang Q, Zhao H, Guo R, et al. Deregulated Wnt/beta-catenin program in high-risk neuroblastomas without MYCN amplification. *Oncogene* (2008) 27:1478–88. doi: 10.1038/sj.onc.1210769
109. Koppen A, Ait-aissa R, Koster J, Øra I, Bras J, Van Sluis PG, et al. Dickkopf-3 expression is a marker for neuroblastic tumor maturation and is down-regulated by MYCN. (2008) 1464:1455–64. doi: 10.1002/ijc.23180
110. Li W, Zhou H, Abujarour R, Zhu S, Young Joo J, Lin T, et al. Generation of human-induced pluripotent stem cells in the absence of exogenous Sox2. *Int J Cancer* (2009) 27:2992–3000. doi: 10.1002/stem.240
111. Fredlund E, Ringne M, Maris JM, Påhlman S. High Myc pathway activity and low stage of neuronal differentiation associate with poor outcome in neuroblastoma. *PNAS* (2008) 105:14094–99. doi: 10.1073/pnas.0804455105
112. Cotterman R, Knoepfler PS. N-Myc regulates expression of pluripotency genes in neuroblastoma including lif, klf2, klf4, and lin28b. *PloS One* (2009) 4. doi: 10.1371/journal.pone.0005799
113. Althoff K, Beckers A, Bell E, Nortmeyer M, Thor T, Sprüssel A, et al. A Cre-conditional MYCN-driven neuroblastoma mouse model as an improved tool for preclinical studies. *Oncogene* (2015) 34:3357–68. doi: 10.1038/onc.2014.269
114. Liu M, Xia Y, Ding J, Ye B, Zhao E, Choi JH, et al. Transcriptional Profiling Reveals a Common Metabolic Program in High-Risk Human Neuroblastoma and Mouse Neuroblastoma Sphere-Forming Cells. *Cell Rep* (2016) 17:609–23. doi: 10.1016/j.celrep.2016.09.021
115. Zeineldin M, Federico S, Chen X, Fan Y, Xu B, Stewart E, et al. MYCN amplification and ATRX mutations are incompatible in neuroblastoma. *Nat Commun* (2020) 11. doi: 10.1038/s41467-020-14682-6
116. Peifer M, Hertwig F, Roels F, Dreidax D, Gartlgruber M, Menon R, et al. Telomerase activation by genomic rearrangements in high-risk neuroblastoma. *Nature* (2015) 526:700–4. doi: 10.1038/nature14980

Conflict of Interest: The authors declare that the research was conducted in the absence of any commercial or financial relationships that could be construed as a potential conflict of interest.

frontiers in Oncology

REVIEW
published: 28 January 2021
doi: 10.3389/fonc.2020.626751

Targeting MYCN in Molecularly Defined Malignant Brain Tumors

Anna Borgenvik[1], *Matko Čančer*[2], *Sonja Hutter*[1] *and Fredrik J. Swartling*[1]*

[1] Department of Immunology, Genetics and Pathology, Science for Life Laboratory, Rudbeck Laboratory, Uppsala University, Uppsala, Sweden, [2] Department of Oncology-Pathology, Karolinska Institutet, Stockholm, Sweden

Misregulation of MYC genes, causing MYC overexpression or protein stabilization, is frequently found in malignant brain tumors highlighting their important roles as oncogenes. Brain tumors in children are the most lethal of all pediatric malignancies and the most common malignant primary adult brain tumor, glioblastoma, is still practically incurable. MYCN is one of three MYC family members and is crucial for normal brain development. It is associated with poor prognosis in many malignant pediatric brain tumor types and is focally amplified in specific adult brain tumors. Targeting MYCN has proved to be challenging due to its undruggable nature as a transcription factor and for its importance in regulating developmental programs also in healthy cells. In this review, we will discuss efforts made to circumvent the difficulty of targeting MYCN specifically by using direct or indirect measures to treat MYCN-driven brain tumors. We will further consider the mechanism of action of these measures and suggest which molecularly defined brain tumor patients that might benefit from MYCN-directed precision therapies.

Keywords: MYCN, brain tumor, targeted therapies, c-MYC, OCT4, medulloblastoma, glioma

OPEN ACCESS

Edited by:
Yusuke Suenaga, Chiba Cancer Center, Japan

Reviewed by:
Eishu Hirata, Kanazawa University, Japan
Sabina Quader, Innovation Centre of NanoMedicine (iCONM), Japan

***Correspondence:**
Fredrik J. Swartling
fredrik.swartling@igp.uu.se

Specialty section:
This article was submitted to Molecular and Cellular Oncology, a section of the journal Frontiers in Oncology

Received: *06 November 2020*
Accepted: *09 December 2020*
Published: *28 January 2021*

Citation:
Borgenvik A, Čančer M, Hutter S and Swartling FJ (2021) Targeting MYCN in Molecularly Defined Malignant Brain Tumors. Front. Oncol. 10:626751. doi: 10.3389/fonc.2020.626751

INTRODUCTION

The development of massive sequencing efforts and molecular profiling of malignant brain cancer biopsies from patients and the strive to characterize them better has transformed the diagnosis of these tumors (1–5). The augmented conception that malignant brain tumors could no longer be defined as a rather small selection of histologically defined entities but in fact comprise over a hundred different molecular subgroups, suggest it is time for a change in how treatment could be more specialized and tailored. The generation of more clinically relevant models recapitulating such subgroups, including MYCN-driven brain cancers have helped improved our understanding how these biologically distinct tumors can be efficiently targeted. Recent single-cell sequencing technologies can help to further recognize the heterogeneity of the brain cancer (6, 7). Altogether, this can improve therapies, risk-stratification schemes and reduce recurrences, which are usually fatal for these types of tumors.

Here, we will describe the prevalence of MYCN alterations in malignant brain cancer in children and adults. We will also portray current treatment regimens and patient outcomes and reflect on how targeted treatments of MYCN would improve future therapies for the most common and aggressive types of brain tumors. In order to develop such targeted strategies, we must first define what we have learned from the biological properties and regulation of MYCN in normal and malignant cells. We will specifically address what molecular information we can use from

appropriate cell systems and animal models of brain cancer in order to develop better MYCN-targeted treatments.

Brain cancer as compared to other tumors outside of the central nervous system (CNS) present an obvious hallmark. They reside in a partially protected compartment that implicates difficulties and complications concerning drug delivery and penetrance over the blood-brain barrier (BBB). The difference in childhood and adult tumors is still evident as well as the fact that treatment can affect normal brain development and can cause severe long-term side effects. The translational transfer of basic molecular findings from the bench into reliable, tailored drugs for these patients to the bed-side is thus not always straight-forward and requires careful selection and testing.

DIAGNOSIS AND MOLECULAR PROFILING OF BRAIN TUMORS WITH MYC FAMILY ACTIVATION

Brain and other CNS tumors are the most common solid tumors in children and the most common cause of pediatric cancer death. Gliomas are the most common brain tumors in children, with the majority being low-grade gliomas (LGGs). The most frequently diagnosed single histological type of tumor is pilocytic astrocytoma, which accounts for 18% of primary brain tumors in children ages 0–14 years (8). These tumors are clinically classified as WHO grade I and are almost always associated with single genetic alterations in the RAS/MAPK pathway (9, 10).

Meningiomas, pituitary tumors, and malignant gliomas are among the most common primary adult brain tumors (11) Primary brain tumor incidence is seven to eight times higher in adults as compared to children in the United States (8). Here, non-malignant brain tumors are overall more than twice as common as malignant brain tumors. This review will focus on the most common types of malignant primary brain tumors in children and on primarily malignant gliomas in adults (**Figure 1**).

High-Grade Gliomas in Children

Pediatric high-grade gliomas (pHGGs) account for approximately 17% of all pediatric CNS tumors (8). pHGGs are a histologically heterogeneous group of tumors with the most frequent types being anaplastic astrocytoma (WHO grade III) and glioblastoma (GBM) (WHO grade IV). The outcome for pHGGs as a whole is poor with 5-year survival rate of 20% (12). In general, HGGs in children are biologically distinct from their adult counterparts. Molecular profiling of large cohorts of pHGG patients resulted in discovery of several genetic and epigenetic subtypes (13). Important molecular features of pHGGs include recurrent mutations in genes encoding the histone variants H3.3 and H3.1 with the mutations K27M or G34R/V defining distinct epigenetic subgroups. The last update (2016) of the WHO classification of CNS tumors recognizes established molecular variants of HGG including IDH-wildtype and -mutant GBM, as well as H3.3/H3.1 K27-mutant diffuse midline glioma, which were formerly known as diffuse intrinsic pontine glioma (DIPG). The latter group is associated with the most

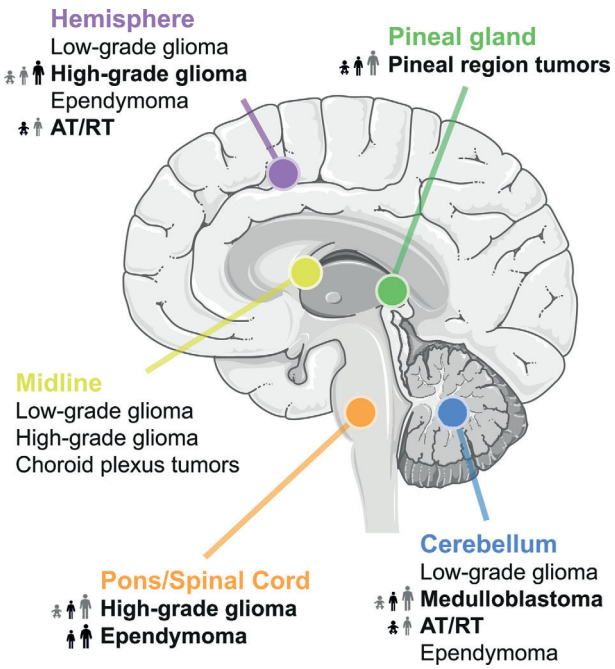

FIGURE 1 | Location of common brain tumors. Tumor entities with known MYC involvement are highlighted in bold and their frequency across all age groups is indicated.

dismal outcome with less than 10% of patients surviving beyond 2 years (14). The H3.3 G34 subtype pHGGs typically occur in the cerebral hemisphere and upregulated MYCN expression has been observed in this subgroup (15). Mutations in IDH1, which are frequent in adult gliomas, are only found in a small proportion of pHGGs (16). Among the remaining approximately 50% of tumors that lack histone H3 and IDH1 mutations (H3/IDH1-WT) several subgroups are emerging. One biologically very aggressive subtype is characterized by enrichment of MYCN amplifications, whereas other subgroups are enriched for amplification in receptor tyrosine kinase genes PDGFRA or EGFR (17). Finally, a specific malignant type of spinal ependymoma in older children and adults with poor prognosis and a propensitiy to metastasize, has recently been shown to contain MYCN amplifications (18).

High-Grade Gliomas in Adults

Due to its critical role in regulating cell cycle and metabolism, MYC has been found overexpressed in GBM, with a tendency towards correlation of astrocytic GBM grade with the level of both nuclear and cytoplasmic MYC (19–21). In addition to increased immunostaining, authors also demonstrated positive correlation of astrocytoma grade with the number of MYC copies. MYCN overexpression and amplification have also been frequently associated with GBM (in about 40% of tumor samples) (22, 23).

IDH1 mutation is a known predictor of response to temozolomide (24) and conveys sensitivity to metabolites of alkylating agents. In a subset of IDH1 mutant GBM, Odia et al. found a correlation with MYC expression (25), indicating

MYC status as an adverse prognostic factor for IDH-mutant GBM.

In malignant glioma with primitive neuroectodermal components (MG-PNET), a rare type of brain tumor that most likely develops from already existing glioma, about half of the patients demonstrate mutually exclusive MYC or MYCN amplifications (26).

MYCN was early found to form extrachromosomal double minutes in neuroblastoma (NB) (27). Recent sequencing efforts show that both MYC and MYCN frequently form extrachromosomal amplifications in GBM (28, 29). Accumulation of such extrachromosomal DNA is essentially connected to tumor evolution and is associated with overall poor prognosis in cancer (30).

Embryonal Tumors in Children

CNS embryonal tumors, including medulloblastoma (MB) and atypical teratoid/rhabdoid tumors (ATRT), account for 13.1% of primary CNS tumors in children (8). Nearly two-thirds of embryonal tumors are diagnosed as MB, which is the most frequent malignant brain tumor of childhood. Integrative genomic studies have shown that MB is not a single entity, but rather a heterogeneous group with distinct clinical and biologic features (6). Molecular subgrouping of MB into WNT, SHH, Group 3 and Group 4 tumors, was integrated in the most recent WHO classification and is currently used for risk stratification replacing diagnosis and treatment of these entities by histopathology. MYC amplifications are the most frequently observed driver events in Group 3, whereas MYCN is overexpressed or amplified in SHH subtype and some Group 4 MBs (3, 31). ATRTs are a variant of embryonal brain tumors occurring predominantly in very young children. Despite sharing the common genetic hallmark of mutations in SMARCB1, recent studies have revealed three distinct subgroups (TYR, SHH, MYC) based on methylation and gene expression data (32). MYC overexpression is the marker of the ATRT-MYC subtype, which is comprised of mostly supratentorial tumors.

Pineal Brain Tumors in Children and Adults

Additionally, a MYC-subgroup has recently been identified in pineoblastoma, a rare but quite frequently metastatic, pediatric brain tumor of the pineal gland with modest overall survival despite intensive therapy (33). Interestingly, while pineoblastoma usually present with molecular profiles distinct from medulloblastoma some embryonal tumors identified as pineoblastoma in the pineal region were recently identified as WNT-driven medulloblastomas using methylation profiling (34).

CURRENT TREATMENT OF BRAIN TUMORS

There is no current international consensus on the treatment of neither pediatric nor adult brain tumors. However, most patients see surgical tumor resection, radiotherapy, and chemotherapy. Factors such as diagnosis, grade, location, tumor dissemination, and age impact how each of these parts are implemented in the treatment plan. Surgical removal of the tumor mass is always included when it is possible to do so. Successful surgery depends on how much of the tumor can be safely resected and is the biggest prognostic factor for overall survival and deciding subsequent radiotherapy and chemotherapeutic regimens.

Radiation therapy is often given as a high dose fractioned over several occasions and directed at the primary tumor site. Patients with spinal metastases receive radiation therapy to the entire cranio-spinal axis. For adult brain tumors, radiotherapy is a major part of standard treatment. In children, MB patients have great benefits on survival from irradiation (35) and evidence points to that conclusion also for ATRT tumors (36). Despite the detrimental side effects radiation therapy has on young patients it is rarely omitted from treatment unless the patient is younger than 3–4 years. MB can be further stratified to identify high-risk MYC/MYCN overexpressed tumors (37). Those patients that would commonly receive a higher dose of radiotherapy (38).

The youngest patients with high-grade brain tumors that are not eligible for radiation and/or surgery are especially negatively affected by the lack of efficient and safe chemotherapeutics. Tumor treating fields is a low toxicity, non-invasive, non-pharmacological treatment of both newly diagnosed and recurrent GBM, used in combination with standard therapy. It is electromagnetic fields administered through the skin of the scalp and its arrangement is individualized to optimize effect at the tumor site. As it is suggested to target primarily dividing cells during mitosis and causes DNA damage in cycling cells, normal cells in the brain should be spared (39). Data also suggest that tumor treating fields is both safe and feasible in pediatric patients (40).

Many chemotherapeutics have been used empirically for decades despite showing substantial effects on prolonging survival of brain tumor patients. On the other hand, targeted therapies for primary brain tumors have of yet not lived up to the expectations and some of these lead to treatment resistance in recurrent tumors. Due to the inability of current treatment options to cure or even extensively prolong survival of patients, both adult and pediatric patients are often enrolled in multinational clinical trials. Careful stratification of patients into correct molecular subgroups and repeated biopsying (41) could help improving the success rate of targeted therapies.

Immunotherapies in brain cancer is a rapidly emerging field. Checkpoint inhibitors have been intensively tested but unfortunately shown limited efficacy in glioblastoma patients (42). It is evident that immunological responses need to be increased in these patients in order to show better effects. MYC is known to suppress checkpoint proteins PD-1 and CD47 (43) and MYC inhibition is found to re-express these proteins making these immunotherapies effective again (44). Recent animal studies further suggest that p53 depletion is suppressing major histocompatibility complex (MHC) class 1 presentation, which mediates T cell immune escape in MYC-driven medulloblastoma (45).

Chimeric antigen receptor (CAR) T cell transfer is an interesting option in pediatric brain tumor patients (46) as

long as severe side effects of cytokine release can be carefully managed and avoided. It is further known that delivery of CAR T cell therapies into the cerebrospinal fluid compartment could provide a better chance for this treatment to reach the tumors. Such an approach has shown promising results when tested in animals using PDX models of medulloblastoma (47) and many clinical trials for children with brain tumors are currently ongoing and under evaluation.

Finally, dendritic cells are important antigen-presenting cells that express both MHC class 1 and 2 molecules and can stimulate antitumor immune responses. Dendritic cell vaccines (48) are currently tested in clinical trials for GBMs and has shown rather promising results as they may increase survival for these patients (49).

MYCN BIOLOGY AND REGULATION IN NORMAL CELLS

The family of MYC proteins (c-MYC, MYCN, and MYCL) are basic helix-loop-helix-zipper (bHLHZ) transcription factors, tightly regulated by extracellular growth stimulatory signals and an intricate intrinsic mechanism behind expression, activation, and degradation of MYC proteins (**Figure 2**). The MYC family of transcription factors binds Enhancer BOX (E-BOX) sequences to promote or repress transcription of its targets. This is enabled and coordinated when the MYC protein heterodimerizes with MYC Associated Factor X (MAX) and together bind to the E-BOX (50). Around 20,000 E-BOX sequences are found in the human genome why MYC is often referred to as a transcriptional master regulator.

MYC and MYCN siblings are similar in structure, and can often substitute each other's functions (51). MYC proteins are often redundant in cancer and showing mutually exclusive expression patterns of MYC and MYCN in patient samples (52, 53). Repression of target genes by MYC proteins involves another co-factor, MYC interacting zinc finger 1 (MIZ1) that tethers MYC-MAX into a ternary complex to promoter regions of negative cell cycle regulators like CDKN1A or CDKN2B (54, 55). Still, there are important differences in how MYC members interact with certain co-factors including MIZ1 (56) and regulate signaling pathways, revealing an increased complexity in how to target these factors using direct or indirect therapies. It is also recognized that MYC proteins interact with chromatin modifying co-factors in order to remodel chromatin structure close to their binding sites (57).

The transcriptional output signature of MYC is highly dependent on the cellular context. The different MYC family members are very similar but MYCL and MYCN are distinctly expressed in specific tissues (lung and neuronal tissue, respectively) unlike c-MYC which is found expressed in most tissues. MYCN is crucial for normal brain development (58, 59).

A proliferating cell would allow stabilization of the MYC proteins while a quiescent cell quickly degrades the proteins through the ubiquitin degradation pathway, dependent on the E3 ubiquitin ligase FBW7. Two phosphorylation sites play major roles in the life cycle of MYC. These are serine 62 (S62) and threonine 58 (T58) (60). Consecutive phosphorylation and dephosphorylation at these sites govern the activity, stability, and degradation of the protein (61). Several proteins related to mitogenic signaling are associated with or directly phosphorylates MYCN at serine 62 to stabilize the protein. Among those are mitogen-activated protein kinases (ERKs) and cyclin-dependent kinases (CDKs), both important for cell growth and proliferation (60, 61). Phosphorylation of this residue causes a conformational change from *cis* to *trans* which increases the affinity for DNA binding and subsequent transcriptional activity of MYC. On the other hand, it also makes it recognizable by glycogen synthase kinase 3 beta (GSK3β), a kinase that will phosphorylate MYC at T58 (60). Mutations at this site will lead to MYC protein stability and can also cause MYCN-driven MB emphasizing the importance of this key event in MYC regulation (62). This is the start of the MYC degradation process and is followed by dephosphorylation of S62 by protein phosphatase 2 (PP2A) that only binds MYC when both sites are phosphorylated (63). The E3 ubiquitin ligase F-box and WD repeat domain-containing 7 (FBW7) recognizes phosphorylated T58 and sentence MYC to proteasomal degradation (64). In normal cells this is a well-functioning machinery tightly controlled at all levels to avoid neoplastic development. The last resort of safety checks is MYC's ability to promote apoptosis when expressed at high levels (65, 66). In cancer, however, it is often overcome by mutations in proapoptotic pathways including p53. This will allow uncontrolled effects of MYC overexpression and activation leading to rapid proliferation and tumor formation.

DIRECT OR INDIRECT TARGETING OF MYCN IN BRAIN TUMORS

Genetically Engineered Proof-of-Concept Inhibition Models of MYCN

MYC proteins play an important role in oncogenesis and progression of tumors and many reports have shown that suppression of MYC or MYCN by genetic means results in growth arrest, induction of apoptosis or senescence leading to tumor regression. Knockdown of MYC even results in regression of brain tumors driven by Trp53 and Pten loss in astrocytic cells (67).

In an attempt to attenuate MYCN expression in NB, Galderisi et al. (68) utilized antisense MYCN oligonucleotides, where they demonstrated three-fold decrease in mRNA levels. Subsequently, the reduction on MYCN led to either differentiation or apoptosis, depending on the NB cell type. In another study, von Bueren et al. (69) demonstrated reduced proliferation and clonogenicity, and induced G1 arrest following siRNA-mediated MYC downregulation in DAOY MB cells. Although this may support the idea of tumor cells being addicted to MYC/MYCN signaling, such strategy should be taken with caution, as the authors (69) showed increased resistance to apoptosis and ionizing radiation upon MYC suppression.

Inducible transgenic brain tumor models, where for example *tet*-inducible promoter regulates a transgene, can be utilized to turn on and off cancer genes. We have previously utilized this

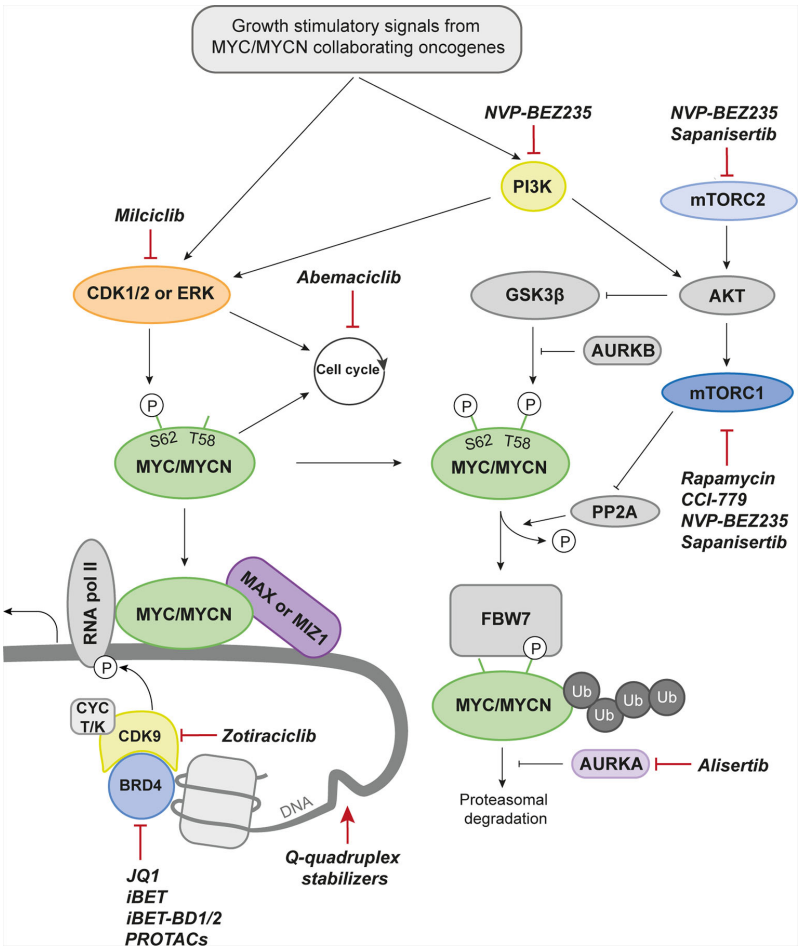

FIGURE 2 | Drug Targets in MYCN Biology. Proteins that can be targeted pharmacologically and discussed in the current review are marked in color. Drugs with preclinical data are denominated with group affiliation. A selected set of drugs that have reached the clinical stage (either approved or in clinical trials for the indicated target) are named. CDK1/2, Cyclin dependent kinase 1/2; MAX, MYC-associated factor X; MIZ1, MYC-interacting zinc-finger protein 1; RNA pol II, RNA polymerase II; BRD4, Bromodomain-containing protein 4; CYC T/K, Cyclin T/K; PROTACs, Proteolysis targeting chimeras; PI3K, Phosphoinositide 3-kinase; AURKB, Aurora kinase B; FBW7, F-box and WD repeat domain-containing 7; Ub, Ubiquitin; AURKA, Aurora kinase A; mTORC2, Mammalian target of rapamycin complex 2; mTORC1, Mammalian target of rapamycin complex 1; AKT, Protein kinase B; PP2A, Protein phosphatase 2; P, phosphorylation.

strategy to first demonstrate the role of MYCN in Group 3 MB development and subsequently showed that long-term withdrawal of MYCN results in tumor regression and life-long remission (70). These tumors likely show robust oncogene addiction as short-term withdrawal of MYCN further showed good efficacy regardless of additional p53 mutations (71).

Direct MYC/MYCN Inhibitors

A MYC dominant negative gene product, called Omomyc, has a capacity to promote MYC-induced apoptosis (72). In ATRT, Omomyc-mediated MYC suppression led to decreased cell proliferation *in vitro* and *in vivo*, while at the same time significantly prolonging animal survival (73). Similarly, expression of Omomyc in well-established mouse model of glioma (74) prevented tumor formation *in vivo*, reduced proliferative and self-renewal capacity of glioma initiating cells, and lead to mitotic crisis in tumor cells (75). A purified peptide of Omomyc shows further promise *in vivo*. This mini-protein shows sufficient biodistribution to suppress tumor growth in lung cancer models while avoiding toxicity in treated animals (76). As described above, the MYC-MAX protein-protein interaction is required for MYC binding to DNA and poses as a great potential target in MYC and MYCN-driven cancers (77). Recently a MYC-MAX complex inhibitor, MYCMI-6, was described by Castell et al. (78) that not only decreases proliferation and induces apoptosis, but it spares cells with normal levels of MYC. MYCMI-6 is also described to target MYCN-MAX interactions and shows great promise *in vivo* (78). Another example of MYC-MAX inhibition is MYCi975, found in a drug screen with rapid *in vivo* testing for drug efficacy in prostate cancer (44). This drug affects both MYC-MAX protein interaction as well as MYC protein stability and was successfully

used in combination with anti-PD1 therapy. MYCi975 is yet to be tested in brain tumor models but decreased MYCN protein levels in a neuroblastoma cell line (44).

The bottleneck for successful treatment of a brain tumor is to be able to deliver a therapy that can circumvent various barriers and efficiently reach the tumor cells in the brain (79, 80). Apart from the normal BBB the brain tumor itself also creates a barrier referred to as the blood-tumor barrier (BTB) that portrays features of non-uniform permeability and active efflux of molecules/drugs that are pumped out (81). It is not clear how well many direct MYC inhibitors or MYC-MAX interaction inhibitors penetrate the BBB/BTB and if they will provide efficacy in malignant brain tumors. Different approaches allowing for more efficient brain tumor delivery of such drugs exist (82). First, direct local delivery of the drug by intrathecal or intraventricular delivery means could be useful were osmotic pumps could provide long-term delivery of drugs. Second, and especially if tumors are considered inoperable (like e.g. DIPGs), convection enhanced delivery can be an option where drugs are directly infused into the parenchyma to promote a forced bulk convective flow into the tumors. Third, focused ultrasound pulses that transiently open up the BBB/BTB could precede delivery of a MYC/MYCN inhibitor. Here, low intensity ultrasound is often combined with circulating microbubbles (made up by lipids, albumin, or polymers) that vibrate in response to the sound to create increased vessel permeability.

MYCN Transcriptional Machinery

MYC-MAX bind E-BOX sequences in promoters and enhancers as discussed above and recruits the protein complexes needed for transcription and proximal promoter pause release to start elongation (83). In more detail, the acetylated lysine residues on histone tails of open chromatin are bound by bromodomain containing proteins (BRDs) and coactivators of the BET family. The BET family of epigenetic readers consists of BRD2, BRD3, BRD4, and BRDT of which BRD4 is the most studied and understood (84). BRD4 binding recruits the P-TEFb complex made up of CDK9 and binding partner cyclin T that phosphorylates RNA Pol II to engage elongation by pause release (85). Bromodomain and BET inhibitors are so called epigenetic drugs and the BET inhibitors JQ1, described a decade ago by Filippakopoulos et al. (86) and iBET by Nicodeme et al. (87), were proof-of-principle drugs of MYC transcriptional inhibition. JQ1 shows good efficacy in multiple MYC cancers as well as MYCN overexpressed CNS tumors such as MBs (88, 89) and NBs (90). JQ1 and iBET are pan-BRD inhibitors but as BRD4 is often the most dominant BRD in cells these drugs preferentially inhibit BRD4 and sequentially blocks MYC and MYCN dependent transcription. BET inhibitors regularly but not always inhibit the transcription of the MYC/N oncogene itself (91) by competitive binding to the acetyl binding domains of the BET proteins. Though widely used in a laboratory setting, JQ1 was found unfit for clinical applications due to the very short half-life of the drug and numerous efforts have been made to find improved alternative inhibitors of BET that are currently investigated in several clinical trials (92, 93). BET inhibitor resistance is another problem and as for many targeted therapies intracellular re-routing and compensatory mechanisms are likely causes. Finding the mechanisms will help to choose the appropriate drug combination to block any likely escape path for the cancer cells. Targeted nanoparticle delivery of combined JQ1 and temozolomide across the BBB to GBM cells *in vivo* prolonged survival and lowered the systemic drug toxicity in mice (94). However, as the authors discuss, the efficiency of delivery is dependent on the specific surface markers on cancer cells and it requires careful thought and investigation of the individual tumor to design these ligand-targeted nanoparticles (94).

A new generation of BET inhibitors recently emerged, specifically targeting only one of two bromodomains (BDs) on the BRDs (95, 96) in contrast to pan-BRD inhibitors that have equal affinity for both. iBET-BD1, and not iBET-BD2, was found to have similar antiproliferative effects on cancer cell lines as a pan-BRD inhibitor. Also, iBET-BD1 was enough to displace BRDs from chromatin, even at MYC super enhancers in cancer cells (95). By contrast, novel iBET-BD2 compounds still showed good efficacy in MYC-driven pediatric tumors (96). These separate findings need to be further investigated to understand how these inhibitors could be used against MYCN-driven brain tumors.

Targeting the transcriptional machinery is not limited to BET inhibition but there are more traditional strategies using kinase inhibitors that would offer small molecule drugs able to penetrate the BBB. Zotiraciclib is an inhibitor with effects against CDKs, both cell cycle and transcriptional kinases (97) and was recently given orphan drug status in combination with temozolomide for treatment of GBM. Its effect is mainly through inhibition of CDK9, the kinase domain of P-TEFb binding to BRD4 and phosphorylating RNA polymerase II (98) making it principally similar to the successful strategy of targeting MYCN through BET inhibition.

Three-dimensional DNA structures called G-quadruplexes can form in guanine rich regions and do so also in the MYC promoter region. They are two or more secondary structures between tetrads of guanine molecules bound by hydrogen bonds (99). In the c-MYC promoter, stabilization of G-quadruplexes using small molecule inhibitors decreases MYC gene transcription (99–101). Several c-MYC G-quadruplex stabilizers have emerged (102–107), but it is so far unknown if these also target MYCN. However, similar to c-MYC, G-quadruplex structures have been identified near the MYCN promoter region (108). Enniatin B has been found to specifically target MYCN G-quadruplexes (109), which is both promising and discouraging as the more developed drugs targeting c-MYC might be c-MYC specific. This would indicate that MYCN-driven brain cancers have a long way to go in this promising field.

A new strategy deployed for targeting proteins are Proteolysis Targeted Chimeras (PROTACs). PROTACs are bifunctional three-parted drugs with one of the units binding to the protein of interest and one binding to the VHL domain of ubiquitin ligase protein E3. These two units are tethered by a linker to put the E3 ligase in close proximity to the targeted protein for ubiquitylation and subsequent proteasomal degradation (110). The PROTAC compound MZ1 selectively targets BRD4 and fine tuning of this principle lead another group to developed A1874, which is able to degrade

BRD4 and at the same time stabilize p53 by binding specifically to the E3 ligase MDM2 (111, 112). To the best of our knowledge, the ability of PROTACs to cross the BBB is not yet known.

Ribosome Biosynthesis

As MYCN plays an important role in protein synthesis, there has been a growing number of discussions whether the biosynthesis of ribosomes and thus protein synthesis can be exploited in targeting MYC/MYCN dysregulated tumors. Two inhibitors, originally identified as RNA pol I inhibitors, quarfloxin (113) and CX-5461 (114), blocked ribosome synthesis in human MYCN-amplified NB cells, leading to reduction of MYCN protein levels (114). Authors furthermore demonstrated the antitumor effect of CX-5461 *in vivo* opening a new therapeutic avenue for MYCN-amplified tumors. To our knowledge, indirect targeting of MYCN *via* RNA pol I inhibition has not been evaluated, but given its promising efficacy in NB (115), it is worth considering in the future.

Cell Cycle and MYCN Stability

Tumor cells proliferate rapidly and hijack cell cycle regulation through mutation or deregulation of inherent vital cell cycle promoting and/or safety mechanisms. MYC's strong correlation to cell proliferation is well known (116–118) and blocking the cell cycle of rapidly dividing cancer cells is a reasonable strategy deployed for treatment of cancer. CDK inhibitors such as Palbociclib, targeting CDK4/6, have shown great success in hormone receptor positive, HER2-negative metastatic breast cancer and have reignited a previous interest in cell cycle inhibition (119, 120). CDK4/6 inhibition can also be used against MYCN-driven tumors to cause a G1 arrest and its effect has been proven in both MB (88) and NB (121, 122). The ability of CDK4/6 inhibitors to penetrate the BBB has been under investigation. Of the three clinically approved CDK4/6 inhibitors palbociclib, ribociclib, and abemaciclib, it is abemaciclib that shows most promise (33). Abemaciclib is now in clinical trials for high-grade and recurrent brain tumors in both children and adults (NCT02644460, NCT03220646).

Three decades ago, CDK2 was in the spotlight for promising drug targets. The interest was dampened when it was shown that CDK2 inhibition was not sufficient to stop proliferation of cancer cells and none of the interphase CDKs are necessary for cell cycle progression as CDK1 was enough to do their job (123, 124). As inhibitor specificity has improved and more is known about CDK2 biology the interest in targeting this kinase has sprouted anew. In addition to CDK2s role in cell cycle commitment it is also one of several kinases that phosphorylates MYC proteins on S62 (125). A few CDK2 inhibitors are currently in clinical trials, however none of these are CDK2 specific. Hence, other CDKs or even classes of proteins could also be involved in their effects. Milciclib is a highly selective CDK2 inhibitor that also has affinity for CDK7/4/5 and tropomyosin receptor kinase A (TrKA) (126). It has been quite successful in clinical trials and is now on Phase II for thymic carcinoma (NCT01011439). The dual role of CDK2 in MYCN-driven brain tumors was shown to successfully target MYCN-driven MB in 2018. Combining milciclib with JQ1 did indeed prolong survival of MYCN-driven MB bearing mice (88). CDK2 was not found to be amplified or overexpressed in the MYCN-driven MB model GTML emphasizing the potential of inhibiting MYCN driven brain tumors with this strategy even at normal levels of CDK2. Also, the aforementioned CDK9 inhibitor zotiraciclib has affinity and inhibitory effects on CDK2. Both milciclib and zotiraciclib penetrates the BBB making them highly interesting to study further in MYCN-driven brain tumors, perhaps even in combination.

Aurora Kinases

A family of serine/threonine kinases, named Aurora, plays an important role in regulation of key steps in cell division. They are involved in organization of centrosomes, condensation of chromatin, chromosome attachment to microtubules, and establishment of metaphase plate (127). Aurora kinase A (encoded by AURKA) is aberrantly expressed in many cancers (128), including GBM (129–132), making it a plausible candidate for a targeted GBM therapy. Expression of both AURKA and AURKB (Aurora kinase B) is tightly regulated by MYC transcription factor (133). Moreover, Aurora kinases A and B directly phosphorylate MYC to promote its stabilization and increase its transcriptional activity (134, 135). In pediatric NB and MB, transcription factor MYCN binds Aurora kinase A, thus attenuating G2/M arrest and stabilizing MYCN protein (136), and conversely inhibition of Aurora kinase A promotes MYCN degradation and cell death (71, 137, 138). These findings highlight the importance of Aurora kinases as druggable targets, particularly in tumors which are driven by aberrant MYC/MYCN signaling. In this section of the review, we will further explore therapeutic potential of Aurora kinase inhibitors in brain tumor therapy.

Alisertib is a second generation, ATP competitive Aurora kinase A inhibitor, which inhibits autophosphorylation at T288. Combined Alisertib and BRD4 inhibition results in synergistic decrease of viability in high-risk, MYCN amplified NB cells (139). Alisertib shows also an advantage in pediatric GBM, where *in vitro* effects were observed in a number of patient-derived cells and *in vivo*, by prolonging mouse survival (140). However, emergence of AURKA negative and CD133 positive cells results in relapse *in vivo*, which suggests a need of dual inhibition to overcome resistance. We have previously showed that AURKA inhibition together with BRD4 inhibition successfully inhibits a number of patient-derived GBM cells (141). Interestingly, GBM cells that were most sensitive to AURKA inhibition were those with high level of MYCN expression, although we must emphasize that the combined AURKA and BRD4 inhibition shows strong synergistic antitumor activity in all evaluated GBM cells, irrespective of MYCN levels (141).

Alisertib inhibition in a MYCN-driven model of group 3 MB (70) disrupts AURKA-MYCN complex and inhibits cell viability both *in vitro* and *in vivo* (71, 142). The inhibition of tumor growth was exercised through nearly completed reduction of MYCN protein expression, cell cycle arrest in G2/M phase, but not apoptosis, which is indicative of AURKA inhibition.

Aurora kinase A, among other functions, regulates MYC/MYCN protein stability. Unlike many inhibitors that target

Aurora A activity, Gustafson et al. (138) developed a conformation-specific compound CD532 that binds to Aurora A, destabilizes MYC/MYCN and targets them for proteasomal degradation. Although developed in MYCN-amplified neuroblastoma models, this compound shows promising effects on cell cycle and MYC/MYCN stability.

Upstream Regulation of MYCN *via* PI3K and mTOR

Phosphoinositide 3-kinases (PI3K) regulates MYCN stability through AKT and GSK3β in cerebellar neuron precursors (143, 144), which suggests that MYCN effects can be counteracted by inhibiting upstream MYCN signaling. Indeed, authors (143) demonstrated a substantial loss of wild-type MYCN upon PI3K inhibitor wortmannin, while mutant $MYCN^{T50A}$ and $MYCN^{S54A}$ levels remained unchanged. Similarly, in MYCN-driven models of NB, Cage et al. (145) showed ablation of MYCN following the treatments with two different PI3K inhibitors PIK-75 and PW-12. Furthermore, in mouse allografts of SHH MB authors (145) demonstrated uniform absence of MYCN, reduced proliferation and vascularity, as well as increase of apoptosis following *in vivo* treatment with PW-12, altogether resulting in a significant, more than five-fold decrease in tumor volume.

MYCN is indirectly regulated by upstream signaling mediated through e.g. mammalian target of rapamycin complexes (mTORC), which regulates cell growth and protein synthesis (as reviewed in (146). Over the past decade several mTOR inhibitors have been developed and proven successful in many different cancer models [as reviewed in (147)]. First generation mTOR inhibitors rapamycin and its ester analogue CCI-779 (Temsirolimus) not only inhibited growth and induced cell death in several MYCN-amplified NB cells, but also significantly reduced MYCN protein levels (148). Similarly, another group identified dual PI3K/mTOR inhibitor, NVP-BEZ235 (Dactolisib), to specifically destabilize MYCN proteins in MYCN-dependent tumors (149). More recently, our group has proved that many of such second generation mTOR inhibitors are indeed successful in inhibiting MYCN-amplified SHH MB tumor models both *in vitro* and *in vivo* (52). RapaLink-1, a bivalent third generation mTOR inhibitor, which combines rapamycin with INK128 (Sapanisertib) by an inert chemical linker, has also shown great efficacy in MYCN-driven brain tumor models (150). Several mTOR inhibitors have already been approved or are currently undergoing clinical trials (151), making mTOR inhibition a very promising therapeutic avenue for MYCN-deregulated brain tumors. Especially for SHH-dependent medulloblastoma where more direct SHH pathway drugs, including SMO inhibitors, are shown to induce severe side effects in young children or infants (152). For instance, mTOR inhibitors, such as everolimus, are well tolerated in children

TABLE 1 | Drugs and compounds for targeting of MYCN signaling.

Inhibitor	Tumor type	Target	Phase	Reference
Direct MYC/MYCN inhibitors				
Omomyc	Glioma, ATRT	MYC proteins	Preclinical	(1–5)
MYCMI-6	Various cancers, NB	MYC proteins	Preclinical	(6)
Inhibitors of MYCN transcriptional machinery				
JQ1	Various cancers, MB, and NB	BRD4	Preclinical	(7–10)
I-BET				(11)
Zotiraciclib	GBM	CDK9	Clinical orphan drug	(12)
Enniatin B	N/A	MYCN	Biochemical	(13)
MZ1	N/A	BRD4	Biochemical	(14)
A1874	Colon cancer, lung cancer, osteosarcoma	BRD4	Preclinical	(15)
Cell cycle related inhibitors targeting MYCN				
Palbociclib	MB, NB	CDK4/6	Preclinical	(9, 16, 17)
Abemaciclib	DIPG, brain tumor (NOS), NB, ATRT	CDK4/6	Clinical trial	(19), NCT02644460, NCT03220646
Milciclib	MB	CDK2	Preclinical	(9)
	Thymic carcinoma		Clinical trial	NCT01011439
Alisertib	GBM, MB, NB	Aurora A	Preclinical	(20–23)
	High-risk AML		Clinical trial	NCT02560025
PI3K/AKT/mTOR inhibitors targeting MYCN				
PIK-75, PW-12	MB	PI3K	Preclinical	(24)
Rapamycin	NB	mTORC1	Preclinical	(25)
Temsirolimus	NB	mTORC1	Preclinical	(25)
	CNS tumors		Clinical trial	NCT00003712
NVP-BEZ235	MYCN-dependent tumors	mTORC1/2, PI3K	Preclinical	(26)
	Breast cancer		Clinical trial	NCT00620594
Everolimus	Breast cancer	mTORC1	Clinical trial	NCT01783444
	Pediatric epilepsy		Approved	(27)
Sapanisertib	MB	mTORC1/2, PI3K	Preclinical	(28)
Ribosome biosynthesis inhibitors targeting MYCN				
Quarfloxin, CX-5461	MYCN-driven NB	RNA Polymerase I	Preclinical	(29)

A list of a selection of drugs or compounds identified as potential direct or indirect targets of MYC/MYCN-driven CNS/PNS tumors. Compounds in the clinical development for another tumor type (and not for brain tumors/CNS tumors) are mentioned in cases where they showed promising results in preclinical CNS tumor models.

treated for epilepsy (153), which is in line with findings of Wu et al., where young mice treated with the BBB penetrable mTOR inhibitor, Sapanisertib showed no toxicity against cerebellar development (154). In **Table 1**, we present a list of selected potential drugs for MYC/MYCN targeted therapy discussed in this paper where the progress of these in preclinical and clinical research is summarized.

The OCT4/mTOR Malignancy Axis

mTOR is known to promote octamer-binding transcription factor 4 (OCT4) levels in embryonic stem cells (155). In MYCN-driven human brain tumor models generated from primary embryonic or induced pluripotent stem cell (iPSC)-derived neural stem cells we could show a significant correlation of mTOR pathway activation and OCT4 levels (52). When we overexpressed OCT4 we further found increased mRNA levels of 4EBP1 gene (EIF4EBP1) as well as elevated phosphorylation of 4EBP1 that marks mTOR pathway activity downstream of mTORC1. The OCT4/mTOR axis correlated with poor prognosis in SHH MB patients and OCT4-overexpression increased the malignancy of these pediatric brain tumors (**Figure 3**).

OCT4 has previously been shown to increase metastasis and malignancy in MB cell lines (156) and malignancy in GBM where AKT is activating OCT4 (157). OCT4 phosphorylation at T235 by AKT is increasing OCT4 stability and correlate with apoptotic resistance and tumor malignancy (158).

OCT4 has an important regulatory role in MYCN-amplified tumors (**Figure 3**). In MYCN-driven NB OCT4 was found to induce increased levels of MYCN by increasing the levels of its cis-antisense gene NCYM (159). Subsequently, NCYM is stabilizing MYCN by inhibiting GSK3β to protect MYCN from proteasomal degradation (160). In this auto-regulatory loop MYCN can again induce OCT4 and other stem-cell related genes. NCYM correlates with OCT4 levels and with poor prognosis in MYCN-amplified tumors. Various inhibitors of mTOR and/or PI3K/AKT can suppress the OCT4/mTOR axis in malignant brain tumors (52).

At another dimension which might be of importance for treatment resistance in MYCN-driven cancer, involves OCT4 phosphorylation at S111 *via* MAPKAP2 that can promote MYC expression (**Figure 3**). This might help identifying a therapy-resistance mechanism in MYCN-driven NB, providing an escape route driven by OCT4-activated MYC (161) in recurrent tumors.

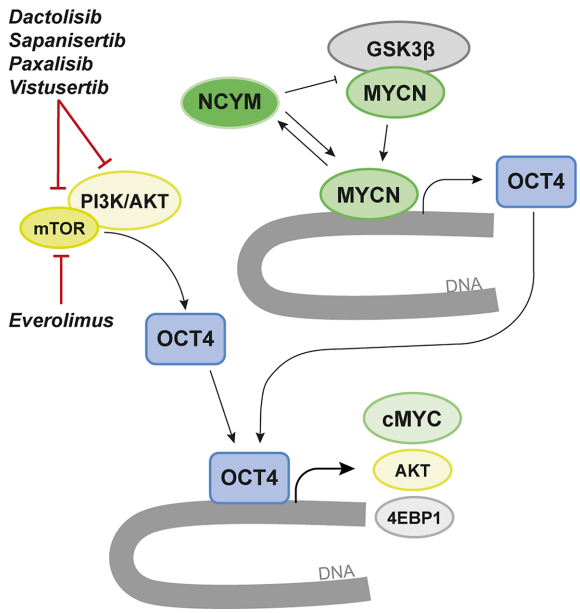

FIGURE 3 | Targeting of MYCN-dependency *via* the OCT4/mTOR Axis. MYCN transcriptionally regulates OCT4 and promotes increased OCT4 levels that correlate with poor prognosis in various brain tumor entities. OCT4 has been found to form a positive regulatory loop that induces increased protein stability of MYCN by increasing the levels of its cis-antisense gene NCYM. In parallel, mTOR/PI3K/AKT promotes OCT4 levels in both normal and malignant cells. Here AKT is known to activate OCT4 by phosphorylation leading to OCT4-dependent upregulation of 4EBP1 and cMYC but also to a positive loop that again promotes AKT expression. We propose a strategy where targeting of OCT4 using various mTOR/PI3K inhibitors could regulate MYCN and suppress MYCN-dependent brain cancer. A few selected inhibitors tested in the brain tumor papers discussed in the review are highlighted.

SUMMARY AND DISCUSSION

MYC family members are found overexpressed in more than half of all cancers highlighting its role as one of the most important oncogenes. MYC proteins are involved in brain tumor initiation, maintenance and progression in both children and adults. MYCN has an important role also in normal brain development. It is known that misregulation of its expression occurs during early development in childhood neoplasms and that MYCN is likely activated during progression in adult brain tumors. While several ways of targeting MYCN is approaching and show promise, there are still many obstacles regarding delivery of direct and indirect ways to target this transcription factor. Better ways and tools to deliver MYCN-targeting drugs that penetrates the BBB is needed using e.g. chemical modifications of substances, nano-particles as drug carriers, or ultrasound technology for temporal opening of the BBB to mediate efficiently high concentrations of the MYCN drug at the tumor site.

While many drugs target cMYC it is important to investigate if they are also relevant for MYCN-driven tumors or if they can be modified to target MYCN specifically to avoid unnecessary side effects. Therefore, it is of utter importance that published data on cMYC targeting also get tested in relevant MYCN-driven cancer cell and mouse models. Appropriate animal brain tumor models should not only be used to test and determine efficacy of novel drugs but will also be valuable in observing tolerability and evident toxicities of the tested compound in the preclinical evaluation. These animal models are useful tools for early detection of side effects from drugs on the normal growth of animals and on their proper brain development or consideration of future use in infant and pediatric brain tumor patients.

As many before have suggested, combination treatments are most likely the best way to circumvent acquired drug resistance. Understanding the mechanisms behind both the drug effect and future resistance will help deciding efficient drug combinations. On this topic, one should also consider that we could shorten the bench to bedside time frame by including relevant standard treatments in preclinical testing of potential MYCN drugs. *In vivo* testing of MYCN drugs for brain tumors should include irradiation and chemotherapy similar to what is used in the clinic to get solid data with a better chance to succeed in affected patients. By simply getting a drug into clinical trials it could benefit specific patients. We stay optimistic and believe that any of these measures will help providing better responses and hopefully even a cure for these devastating malignancies.

AUTHOR CONTRIBUTIONS

AB and FS wrote the majority of the review with extensive contributions from MC and SH. AB, SH, and FS made the figures with input from MC. MC made the table. All authors contributed to the article and approved the submitted version.

ACKNOWLEDGMENTS

We acknowledge support from the Swedish Childhood Cancer Fund, the Swedish Cancer Society, the European Research Council, the Swedish Brain Foundation, the Swedish Research Council, the Ragnar Söderberg Foundation, and SciLifeLab, Sweden.

REFERENCES

1. Brennan CW, Verhaak RG, McKenna A, Campos B, Noushmehr H, Salama SR, et al. The somatic genomic landscape of glioblastoma. *Cell* (2013) 155 (2):462–77. doi: 10.1016/j.cell.2013.09.034
2. Capper D, Jones DTW, Sill M, Hovestadt V, Schrimpf D, Sturm D, et al. DNA methylation-based classification of central nervous system tumours. *Nature* (2018) 555(7697):469–74. doi: 10.1038/nature26000
3. Cavalli FMG, Remke M, Rampasek L, Peacock J, Shih DJH, Luu B, et al. Intertumoral Heterogeneity within Medulloblastoma Subgroups. *Cancer Cell* (2017) 31(6):737–54.e6. doi: 10.1016/j.ccell.2017.05.005
4. Clarke M, Mackay A, Ismer B, Pickles JC, Tatevossian RG, Newman S, et al. Infant High-Grade Gliomas Comprise Multiple Subgroups Characterized by Novel Targetable Gene Fusions and Favorable Outcomes. *Cancer Discovery* (2020) 10(7):942–63. doi: 10.1158/2159-8290.CD-19-1030
5. Verhaak RGW, Bafna V, Mischel PS. Extrachromosomal oncogene amplification in tumour pathogenesis and evolution. *Nat Rev Cancer* (2019) 19(5):283–8. doi: 10.1038/s41568-019-0128-6
6. Hovestadt V, Ayrault O, Swartling FJ, Robinson GW, Pfister SM, Northcott PA. Medulloblastomics revisited: biological and clinical insights from thousands of patients. *Nat Rev Cancer* (2020) 20(1):42–56. doi: 10.1038/s41568-019-0223-8
7. Neftel C, Laffy J, Filbin MG, Hara T, Shore ME, Rahme GJ, et al. Integrative Model of Cellular States, Plasticity, and Genetics for Glioblastoma. *An Cell* (2019) 178(4):835–49.e21. doi: 10.1016/j.cell.2019.06.024
8. Ostrom QT, Cioffi G, Gittleman H, Patil N, Waite K, Kruchko C, et al. CBTRUS Statistical Report: Primary Brain and Other Central Nervous System Tumors Diagnosed in the United States in 2012-2016. *Neuro Oncol* (2019) 21(Suppl 5):v1–v100. doi: 10.1093/neuonc/noz150
9. Jones DT, Hutter B, Jäger N, Korshunov A, Kool M, Warnatz HJ, et al. Recurrent somatic alterations of FGFR1 and NTRK2 in pilocytic astrocytoma. *Nat Genet* (2013) 45(8):927–32. doi: 10.1038/ng.2682
10. Zhang J, Wu G, Miller CP, Tatevossian RG, Dalton JD, Tang B, et al. Whole-genome sequencing identifies genetic alterations in pediatric low-grade gliomas. *Nat Genet* (2013) 45(6):602–12. doi: 10.1038/ng.2611
11. McNeill KA. Epidemiology of Brain Tumors. *Neurol Clin* (2016) 34(4):981–98. doi: 10.1016/j.ncl.2016.06.014
12. Jones C, Perryman L, Hargrave D. Paediatric and adult malignant glioma: close relatives or distant cousins? *Nat Rev Clin Oncol* (2012) 9(7):400–13. doi: 10.1038/nrclinonc.2012.87
13. Gajjar A, Bowers DC, Karajannis MA, Leary S, Witt H, Gottardo NG. Pediatric Brain Tumors: Innovative Genomic Information Is Transforming the Diagnostic and Clinical Landscape. *J Clin Oncol* (2015) 33(27):2986–98. doi: 10.1200/JCO.2014.59.9217
14. Hoffman LM, Veldhuijzen van Zanten SEM, Colditz N, Baugh J, Chaney B, Hoffmann M, et al. Clinical, Radiologic, Pathologic, and Molecular Characteristics of Long-Term Survivors of Diffuse Intrinsic Pontine Glioma (DIPG): A Collaborative Report From the International and European Society for Pediatric Oncology DIPG Registries. *J Clin Oncol* (2018) 36(19):1963–72. doi: 10.1200/jco.2017.75.9308
15. Bjerke L, Mackay A, Nandhabalan M, Burford A, Jury A, Popov S, et al. Histone H3.3. mutations drive pediatric glioblastoma through upregulation of MYCN. *Cancer Discovery* (2013) 3(5):512–9. doi: 10.1158/2159-8290.CD-12-0426
16. Mackay A, Burford A, Carvalho D, Izquierdo E, Fazal-Salom J, Taylor KR, et al. Integrated Molecular Meta-Analysis of 1,000 Pediatric High-Grade and Diffuse Intrinsic Pontine Glioma. *Cancer Cell* (2017) 32(4):520–37.e5. doi: 10.1016/j.ccell.2017.08.017
17. Korshunov A, Schrimpf D, Ryzhova M, Sturm D, Chavez L, Hovestadt V, et al. H3-/IDH-wild type pediatric glioblastoma is comprised of molecularly and prognostically distinct subtypes with associated oncogenic drivers. *Acta Neuropathol* (2017) 134(3):507–16. doi: 10.1007/s00401-017-1710-1
18. Ghasemi DR, Sill M, Okonechnikov K, Korshunov A, Yip S, Schutz PW, et al. MYCN amplification drives an aggressive form of spinal ependymoma. *Acta Neuropathol* (2019) 138:1075–89. doi: 10.1007/s00401-019-02056-2
19. Faria MH, Khayat AS, Burbano RR, Rabenhorst SH. c -MYC amplification and expression in astrocytic tumors. *Acta Neuropathol* (2008) 116(1):87–95. doi: 10.1007/s00401-008-0368-0
20. Orian JM, Vasilopoulos K, Yoshida S, Kaye AH, Chow CW, Gonzales MF. Overexpression of multiple oncogenes related to histological grade of astrocytic glioma. *Br J Cancer* (1992) 66(1):106–12. doi: 10.1038/bjc.1992.225
21. Herms JW, von Loewenich FD, Behnke J, Markakis E, Kretzschmar HA. c-myc oncogene family expression in glioblastoma and survival. *Surg Neurol* (1999) 51(5):536–42. doi: 10.1016/S0090-3019(98)00028-7
22. Hui AB, Lo KW, Yin XL, Poon WS, Ng HK. Detection of multiple gene amplifications in glioblastoma multiforme using array-based comparative genomic hybridization. *Lab Invest* (2001) 81(5):717–23. doi: 10.1038/labinvest.3780280
23. Hodgson JG, Yeh R-F, Ray A, Wang NJ, Smirnov I, Yu M, et al. Comparative analyses of gene copy number and mRNA expression in glioblastoma multiforme tumors and xenografts. *Neuro-Oncology* (2009) 11(5):477–87. doi: 10.1215/15228517-2008-113
24. Wang P, Wu J, Ma S, Zhang L, Yao J, Hoadley Katherine A, et al. Oncometabolite D-2-Hydroxyglutarate Inhibits ALKBH DNA Repair Enzymes and Sensitizes IDH Mutant Cells to Alkylating Agents. *Cell Rep* (2015) 13(11):2353–61. doi: 10.1016/j.celrep.2015.11.029
25. Odia Y, Orr BA, Bell WR, Eberhart CG, Rodriguez FJ. cMYC expression in infiltrating gliomas: associations with IDH1 mutations, clinicopathologic features and outcome. *J Neurooncol* (2013) 115(2):249–59. doi: 10.1007/s11060-013-1221-4
26. Perry A, Miller CR, Gujrati M, Scheithauer BW, Zambrano SC, Jost SC, et al. Malignant Gliomas with Primitive Neuroectodermal Tumor-like Components: A Clinicopathologic and Genetic Study of 53 Cases. *Brain Pathol* (2009) 19(1):81–90. doi: 10.1111/j.1750-3639.2008.00167.x
27. Kohl NE, Kanda N, Schreck RR, Bruns G, Latt SA, Gilbert F, et al. Transposition and amplification of oncogene-related sequences in human

neuroblastomas. *Cell* (1983) 35(2 Pt 1):359–67. doi: 10.1016/0092-8674(83)90169-1
28. Turner KM, Deshpande V, Beyter D, Koga T, Rusert J, Lee C, et al. Extrachromosomal oncogene amplification drives tumour evolution and genetic heterogeneity. *Nature* (2017) 543(7643):122–5. doi: 10.1038/nature21356
29. deCarvalho AC, Kim H, Poisson LM, Winn ME, Mueller C, Cherba D, et al. Discordant inheritance of chromosomal and extrachromosomal DNA elements contributes to dynamic disease evolution in glioblastoma. *Nat Genet* (2018) 50(5):708–17. doi: 10.1038/s41588-018-0105-0
30. Kim H, Nguyen NP, Turner K, Wu S, Gujar AD, Luebeck J, et al. Extrachromosomal DNA is associated with oncogene amplification and poor outcome across multiple cancers. *Nat Genet* (2020) 52(9):891–7. doi: 10.1038/s41588-020-0678-2
31. Northcott PA, Buchhalter I, Morrissy AS, Hovestadt V, Weischenfeldt J, Ehrenberger T, et al. The whole-genome landscape of medulloblastoma subtypes. *Nature* (2017) 547(7663):311–7. doi: 10.1038/nature23095
32. Johann PD, Erkek S, Zapatka M, Kerl K, Buchhalter I, Hovestadt V, et al. Atypical Teratoid/Rhabdoid Tumors Are Comprised of Three Epigenetic Subgroups with Distinct Enhancer Landscapes. *Cancer Cell* (2016) 29(3):379–93. doi: 10.1016/j.ccell.2016.02.001
33. Li BK, Vasiljevic A, Dufour C, Yao F, Ho BLB, Lu M, et al. Pineoblastoma segregates into molecular sub-groups with distinct clinico-pathologic features: a Rare Brain Tumor Consortium registry study. *Acta Neuropathol* (2020) 139(2):223–41. doi: 10.1007/s00401-019-02111-y
34. Liu APY, Priesterbach-Ackley LP, Orr BA, Li BK, Gudenas B, Reddingius RE, et al. WNT-activated embryonal tumors of the pineal region: ectopic medulloblastomas or a novel pineoblastoma subgroup? *Acta Neuropathol* (2020) 140(4):595–7. doi: 10.1007/s00401-020-02208-9
35. Frič R, Due-Tønnessen BJ, Lundar T, Egge A, Kronen Krossnes B, Due-Tønnessen P, et al. Long-term outcome of posterior fossa medulloblastoma in patients surviving more than 20 years following primary treatment in childhood. *Sci Rep* (2020) 10(1):9371. doi: 10.1038/s41598-020-66328-8
36. Bartelheim K, Nemes K, Seeringer A, Kerl K, Buechner J, Boos J, et al. Improved 6-year overall survival in AT/RT - results of the registry study Rhabdoid 2007. *Cancer Med* (2016) 5(8):1765–75. doi: 10.1002/cam4.741
37. Shih DJ, Northcott PA, Remke M, Korshunov A, Ramaswamy V, Kool M, et al. Cytogenetic prognostication within medulloblastoma subgroups. *J Clin Oncol* (2014) 32(9):886–96. doi: 10.1200/jco.2013.50.9539
38. Northcott PA, Robinson GW, Kratz CP, Mabbott DJ, Pomeroy SL, Clifford SC, et al. Medulloblastoma. *Nat Rev Dis Primers* (2019) 5(1):11. doi: 10.1038/s41572-019-0063-6
39. Ghiaseddin AP, Shin D, Melnick K, Tran DD. Tumor Treating Fields in the Management of Patients with Malignant Gliomas. *Curr Treat Options Oncol* (2020) 21(9):76. doi: 10.1007/s11864-020-00773-5
40. Goldman S, Hwang E, Lai J-S, Kocak M, Lulla R, Dhall G, et al. PDCT-07. FEASIBILITY TRIAL OF TTFIELDS (TUMOR TREATING FIELDS) FOR CHILDREN WITH RECURRENT OR PROGRESSIVE SUPRATENTORIAL HIGH-GRADE GLIOMA (HGG) AND EPENDYMOMA: A PEDIATRIC BRAIN TUMOR CONSORTIUM STUDY: PBTC-048. *Neuro Oncol* (2018) 20(Suppl 6):vi201–vi2. doi: 10.1093/neuonc/noy148.837
41. Morrissy AS, Cavalli FMG, Remke M, Ramaswamy V, Shih DJH, Holgado BL, et al. Spatial heterogeneity in medulloblastoma. *Nat Genet* (2017) 49(5):780–8. doi: 10.1038/ng.3838
42. Brahm CG, van Linde ME, Enting RH, Schuur M, Otten RHJ, Heymans MW, et al. The Current Status of Immune Checkpoint Inhibitors in Neuro-Oncology: A Systematic Review. *Cancers* (2020) 12(3). doi: 10.3390/cancers12030586
43. Casey SC, Tong L, Li Y, Do R, Walz S, Fitzgerald KN, et al. MYC regulates the antitumor immune response through CD47 and PD-L1. *Science* (2016) 352(6282):227–31. doi: 10.1126/science.aac9935
44. Han H, Jain AD, Truica MI, Izquierdo-Ferrer J, Anker JF, Lysy B, et al. Small-Molecule MYC Inhibitors Suppress Tumor Growth and Enhance Immunotherapy. *Cancer Cell* (2019) 36(5):483–97.e15. doi: 10.1016/j.ccell.2019.10.001
45. Garancher A, Suzuki H, Haricharan S, Chau LQ, Masihi MB, Rusert JM, et al. Tumor necrosis factor overcomes immune evasion in p53-mutant medulloblastoma. *Nat Neurosci* (2020) 23(7):842–53. doi: 10.1038/s41593-020-0628-4
46. Patterson JD, Henson JC, Breese RO, Bielamowicz KJ, Rodriguez A. CAR T Cell Therapy for Pediatric Brain Tumors. *Front Oncol* (2020) 10:1582. doi: 10.3389/fonc.2020.01582
47. Donovan LK, Delaidelli A, Joseph SK, Bielamowicz K, Fousek K, Holgado BL, et al. Locoregional delivery of CAR T cells to the cerebrospinal fluid for treatment of metastatic medulloblastoma and ependymoma. *Nat Med* (2020) 26(5):720–31. doi: 10.1038/s41591-020-0827-2
48. Eagles ME, Nassiri F, Badhiwala JH, Suppiah S, Almenawer SA, Zadeh G, et al. Dendritic cell vaccines for high-grade gliomas. *Ther Clin Risk Manag* (2018) 14:1299–313. doi: 10.2147/TCRM.S135865
49. Liau LM, Ashkan K, Tran DD, Campian JL, Trusheim JE, Cobbs CS, et al. First results on survival from a large Phase 3 clinical trial of an autologous dendritic cell vaccine in newly diagnosed glioblastoma. *J Transl Med* (2018) 16(1):142. doi: 10.1186/s12967-018-1507-6
50. Blackwood EM, Eisenman RN. Max: a helix-loop-helix zipper protein that forms a sequence-specific DNA-binding complex with Myc. *Science* (1991) 251(4998):1211–7. doi: 10.1126/science.2006410
51. Malynn BA, de Alboran IM, O'Hagan RC, Bronson R, Davidson L, DePinho RA, et al. N-myc can functionally replace c-myc in murine development, cellular growth, and differentiation. *Genes Dev* (2000) 14(11):1390–9. doi: 10.1101/gad.14.11.1390
52. Čančer M, Hutter S, Holmberg KO, Rosén G, Sundström A, Tailor J, et al. Humanized Stem Cell Models of Pediatric Medulloblastoma Reveal an Oct4/mTOR Axis that Promotes Malignancy. *Cell Stem Cell* (2019) 25(6):855–70.e11. doi: 10.1016/j.stem.2019.10.005
53. Westermann F, Muth D, Benner A, Bauer T, Henrich KO, Oberthuer A, et al. Distinct transcriptional MYCN/c-MYC activities are associated with spontaneous regression or malignant progression in neuroblastomas. *Genome Biol* (2008) 9(10):R150. doi: 10.1186/gb-2008-9-10-r150
54. Seoane J, Pouponnot C, Staller P, Schader M, Eilers M, Massagué J. TGFbeta influences Myc, Miz-1 and Smad to control the CDK inhibitor p15INK4b. *Nat Cell Biol* (2001) 3(4):400–8. doi: 10.1038/35070086
55. Staller P, Peukert K, Kiermaier A, Seoane J, Lukas J, Karsunky H, et al. Repression of p15INK4b expression by Myc through association with Miz-1. *Nat Cell Biol* (2001) 3(4):392–9. doi: 10.1038/35070076
56. Vo BT, Wolf E, Kawauchi D, Gebhardt A, Rehg JE, Finkelstein D, et al. The Interaction of Myc with Miz1 Defines Medulloblastoma Subgroup Identity. *Cancer Cell* (2016) 29(1):5–16. doi: 10.1016/j.ccell.2015.12.003
57. Kress TR, Sabò A, Amati B. MYC: connecting selective transcriptional control to global RNA production. *Nat Rev Cancer* (2015) 15(10):593–607. doi: 10.1038/nrc3984
58. Stanton BR, Perkins AS, Tessarollo L, Sassoon DA, Parada LF. Loss of N-myc function results in embryonic lethality and failure of the epithelial component of the embryo to develop. *Genes Dev* (1992) 6(12a):2235–47. doi: 10.1101/gad.6.12a.2235
59. Knoepfler PS, Cheng PF, Eisenman RN. N-myc is essential during neurogenesis for the rapid expansion of progenitor cell populations and the inhibition of neuronal differentiation. *Genes Dev* (2002) 16(20):2699–712. doi: 10.1101/gad.1021202
60. Sears R, Nuckolls F, Haura E, Taya Y, Tamai K, Nevins JR. Multiple Ras-dependent phosphorylation pathways regulate Myc protein stability. *Genes Dev* (2000) 14(19):2501–14. doi: 10.1101/gad.836800
61. Sjostrom SK, Finn G, Hahn WC, Rowitch DH, Kenney AM. The Cdk1 complex plays a prime role in regulating N-myc phosphorylation and turnover in neural precursors. *Dev Cell* (2005) 9(3):327–38. doi: 10.1016/j.devcel.2005.07.014
62. Swartling FJ, Savov V, Persson AI, Chen J, Hackett CS, Northcott PA, et al. Distinct neural stem cell populations give rise to disparate brain tumors in response to N-MYC. *Cancer Cell* (2012) 21(5):601–13. doi: 10.1016/j.ccr.2012.04.012
63. Arnold HK, Sears RC. Protein phosphatase 2A regulatory subunit B56alpha associates with c-myc and negatively regulates c-myc accumulation. *Mol Cell Biol* (2006) 26(7):2832–44. doi: 10.1128/MCB.26.7.2832-2844.2006
64. Yada M, Hatakeyama S, Kamura T, Nishiyama M, Tsunematsu R, Imaki H, et al. Phosphorylation-dependent degradation of c-Myc is mediated by the

F-box protein Fbw7. *EMBO J* (2004) 23(10):2116–25. doi: 10.1038/sj.emboj.7600217
65. Evan GI, Wyllie AH, Gilbert CS, Littlewood TD, Land H, Brooks M, et al. Induction of apoptosis in fibroblasts by c-myc protein. *Cell* (1992) 69 (1):119–28. doi: 10.1016/0092-8674(92)90123-T
66. Nesbit CE, Grove LE, Yin X, Prochownik EV. Differential apoptotic behaviors of c-myc, N-myc, and L-myc oncoproteins. *Cell Growth Differ* (1998) 9(9):731–41.
67. Zheng H, Ying H, Yan H, Kimmelman AC, Hiller DJ, Chen AJ, et al. Pten and p53 converge on c-Myc to control differentiation, self-renewal, and transformation of normal and neoplastic stem cells in glioblastoma. *Cold Spring Harb Symp Quant Biol* (2008) 73:427–37. doi: 10.1101/sqb.2008.73.047
68. Galderisi U, Di Bernardo G, Cipollaro M, Peluso G, Cascino A, Cotrufo R, et al. Differentiation and apoptosis of neuroblastoma cells: role of N-myc gene product. *J Cell Biochem* (1999) 73(1):97–105. doi: 10.1002/(SICI)1097-4644(19990401)73:1<97::AID-JCB11>3.0.CO;2-M
69. von Bueren AO, Shalaby T, Oehler-Jänne C, Arnold L, Stearns D, Eberhart CG, et al. RNA interference-mediated c-MYC inhibition prevents cell growth and decreases sensitivity to radio- and chemotherapy in childhood medulloblastoma cells. *BMC Cancer* (2009) 9:10. doi: 10.1186/1471-2407-9-10
70. Swartling FJ, Grimmer MR, Hackett CS, Northcott PA, Fan QW, Goldenberg DD, et al. Pleiotropic role for MYCN in medulloblastoma. *Genes Dev* (2010) 24(10):1059–72. doi: 10.1101/gad.1907510
71. Hill RM, Kuijper S, Lindsey JC, Petrie K, Schwalbe EC, Barker K, et al. and P53 Defects Emerge at Medulloblastoma Relapse and Define Rapidly Progressive, Therapeutically Targetable Disease. *Cancer Cell* (2015) 27 (1):72–84. doi: 10.1016/j.ccell.2014.11.002
72. Soucek L, Jucker R, Panacchia L, Ricordy R, Tatò F, Nasi S. Omomyc, a potential Myc dominant negative, enhances Myc-induced apoptosis. *Cancer Res* (2002) 62(12):3507–10.
73. Alimova I, Pierce A, Danis E, Donson A, Birks DK, Griesinger A, et al. Inhibition of MYC attenuates tumor cell self-renewal and promotes senescence in SMARCB1-deficient Group 2 atypical teratoid rhabdoid tumors to suppress tumor growth in vivo. *Int J Cancer* (2019) 144 (8):1983–95. doi: 10.1002/ijc.31873
74. Ding H, Roncari L, Shannon P, Wu X, Lau N, Karaskova J, et al. Astrocyte-specific expression of activated p21-ras results in malignant astrocytoma formation in a transgenic mouse model of human gliomas. *Cancer Res* (2001) 61(9):3826–36.
75. Annibali D, Whitfield JR, Favuzzi E, Jauset T, Serrano E, Cuartas I, et al. Myc inhibition is effective against glioma and reveals a role for Myc in proficient mitosis. *Nat Commun* (2014) 5:4632. doi: 10.1038/ncomms5632
76. Beaulieu ME, Jauset T, Massó-Vallés D, Martínez-Martín S, Rahl P, Maltais L, et al. Intrinsic cell-penetrating activity propels Omomyc from proof of concept to viable anti-MYC therapy. *Sci Trans Med* (2019) 11(484). doi: 10.1126/scitranslmed.aar5012
77. Whitfield JR, Beaulieu ME, Soucek L. Strategies to Inhibit Myc and Their Clinical Applicability. *Front Cell Dev Biol* (2017) 5:10. doi: 10.3389/fcell.2017.00010
78. Castell A, Yan Q, Fawkner K, Hydbring P, Zhang F, Verschut V, et al. A selective high affinity MYC-binding compound inhibits MYC:MAX interaction and MYC-dependent tumor cell proliferation. *Sci Rep* (2018) 8 (1):10064. doi: 10.1038/s41598-018-28107-4
79. Dong X. Current Strategies for Brain Drug Delivery. *Theranostics* (2018) 8 (6):1481–93. doi: 10.7150/thno.21254
80. Pardridge WM. Blood-Brain Barrier and Delivery of Protein and Gene Therapeutics to Brain. *Front Aging Neurosci* (2019) 11:373. doi: 10.3389/fnagi.2019.00373
81. Arvanitis CD, Ferraro GB, Jain RK. The blood-brain barrier and blood-tumour barrier in brain tumours and metastases. *Nat Rev Cancer* (2020) 20 (1):26–41. doi: 10.1038/s41568-019-0205-x
82. Aldape K, Brindle KM, Chesler L, Chopra R, Gajjar A, Gilbert MR, et al. Challenges to curing primary brain tumours. *Nat Rev Clin Oncol* (2019) 16 (8):509–20. doi: 10.1038/s41571-019-0177-5
83. Rahl PB, Lin CY, Seila AC, Flynn RA, McCuine S, Burge CB, et al. c-Myc regulates transcriptional pause release. *Cell* (2010) 141(3):432–45. doi: 10.1016/j.cell.2010.03.030
84. Filippakopoulos P, Picaud S, Mangos M, Keates T, Lambert JP, Barsyte-Lovejoy D, et al. Histone recognition and large-scale structural analysis of the human bromodomain family. *Cell* (2012) 149(1):214–31. doi: 10.1016/j.cell.2012.02.013
85. Patel MC, Debrosse M, Smith M, Dey A, Huynh W, Sarai N, et al. BRD4 coordinates recruitment of pause release factor P-TEFb and the pausing complex NELF/DSIF to regulate transcription elongation of interferon-stimulated genes. *Mol Cell Biol* (2013) 33(12):2497–507. doi: 10.1128/MCB.01180-12
86. Filippakopoulos P, Qi J, Picaud S, Shen Y, Smith WB, Fedorov O, et al. Selective inhibition of BET bromodomains. *Nature* (2010) 468(7327):1067–73. doi: 10.1038/nature09504
87. Nicodeme E, Jeffrey KL, Schaefer U, Beinke S, Dewell S, Chung CW, et al. Suppression of inflammation by a synthetic histone mimic. *Nature* (2010) 468(7327):1119–23. doi: 10.1038/nature09589
88. Bolin S, Borgenvik A, Persson CU, Sundström A, Qi J, Bradner JE, et al. Combined BET bromodomain and CDK2 inhibition in MYC-driven medulloblastoma. *Oncogene* (2018) 37(21):2850–62. doi: 10.1038/s41388-018-0135-1
89. Bandopadhayay P, Bergthold G, Nguyen B, Schubert S, Gholamin S, Tang Y, et al. BET bromodomain inhibition of MYC-amplified medulloblastoma. *Clin Cancer Res* (2014) 20(4):912–25. doi: 10.1158/1078-0432.CCR-13-2281
90. Puissant A, Frumm SM, Alexe G, Bassil CF, Qi J, Chanthery YH, et al. Targeting MYCN in neuroblastoma by BET bromodomain inhibition. *Cancer Discovery* (2013) 3(3):308–23. doi: 10.1158/2159-8290.CD-12-0418
91. Delmore JE, Issa GC, Lemieux ME, Rahl PB, Shi J, Jacobs HM, et al. BET bromodomain inhibition as a therapeutic strategy to target c-Myc. *Cell* (2011) 146(6):904–17. doi: 10.1016/j.cell.2011.08.017
92. Alqahtani A, Choucair K, Ashraf M, Hammouda DM, Alloghbi A, Khan T, et al. Bromodomain and extra-terminal motif inhibitors: a review of preclinical and clinical advances in cancer therapy. *Future Sci OA* (2019) 5 (3):Fso372. doi: 10.4155/fsoa-2018-0115
93. Xu Y, Vakoc CR. Targeting Cancer Cells with BET Bromodomain Inhibitors. *Cold Spring Harb Perspect Med* (2017) 7(7). doi: 10.1101/cshperspect.a026674
94. Lam FC, Morton SW, Wyckoff J, Vu Han TL, Hwang MK, Maffa A, et al. Enhanced efficacy of combined temozolomide and bromodomain inhibitor therapy for gliomas using targeted nanoparticles. *Nat Commun* (2018) 9 (1):1991. doi: 10.1038/s41467-018-04315-4
95. Gilan O, Rioja I, Knezevic K, Bell MJ, Yeung MM, Harker NR, et al. Selective targeting of BD1 and BD2 of the BET proteins in cancer and immunoinflammation. *Science* (2020) 368(6489):387–94. doi: 10.1126/science.aaz8455
96. Slavish PJ, Chi L, Yun MK, Tsurkan L, Martinez NE, Jonchere B, et al. Bromodomain-Selective BET Inhibitors Are Potent Antitumor Agents against MYC-Driven Pediatric Cancer. *Cancer Res* (2020) 80(17):3507–18. doi: 10.1158/0008-5472.CAN-19-3934
97. Goh KC, Novotny-Diermayr V, Hart S, Ong LC, Loh YK, Cheong A, et al. TG02, a novel oral multi-kinase inhibitor of CDKs, JAK2 and FLT3 with potent anti-leukemic properties. *Leukemia* (2012) 26(2):236–43. doi: 10.1038/leu.2011.218
98. Su YT, Chen R, Wang H, Song H, Zhang Q, Chen LY, et al. Novel Targeting of Transcription and Metabolism in Glioblastoma. *Clin Cancer Res* (2018) 24 (5):1124–37. doi: 10.1158/1078-0432.CCR-17-2032
99. Burge S, Parkinson GN, Hazel P, Todd AK, Neidle S. Quadruplex DNA: sequence, topology and structure. *Nucleic Acids Res* (2006) 34(19):5402–15. doi: 10.1093/nar/gkl655
100. Liu JN, Deng R, Guo JF, Zhou JM, Feng GK, Huang ZS, et al. Inhibition of myc promoter and telomerase activity and induction of delayed apoptosis by SYUIQ-5, a novel G-quadruplex interactive agent in leukemia cells. *Leukemia* (2007) 21(6):1300–2. doi: 10.1038/sj.leu.2404652
101. Nasiri HR, Bell NM, McLuckie KI, Husby J, Abell C, Neidle S, et al. Targeting a c-MYC G-quadruplex DNA with a fragment library. *Chem Commun (Camb)* (2014) 50(14):1704–7. doi: 10.1039/C3CC48390H
102. Brown RV, Danford FL, Gokhale V, Hurley LH, Brooks TA. Demonstration that drug-targeted down-regulation of MYC in non-Hodgkins lymphoma is directly mediated through the promoter G-quadruplex. *J Biol Chem* (2011) 286(47):41018–27. doi: 10.1074/jbc.M111.274720

103. Calabrese DR, Chen X, Leon EC, Gaikwad SM, Phyo Z, Hewitt WM, et al. Chemical and structural studies provide a mechanistic basis for recognition of the MYC G-quadruplex. *Nat Commun* (2018) 9(1):4229. doi: 10.1038/s41467-018-06315-w
104. Das T, Panda D, Saha P, Dash J. Small Molecule Driven Stabilization of Promoter G-Quadruplexes and Transcriptional Regulation of c-MYC. *Bioconjug Chem* (2018) 29(8):2636–45. doi: 10.1021/acs.bioconjchem.8b00338
105. González V, Hurley LH. The C-terminus of nucleolin promotes the formation of the c-MYC G-quadruplex and inhibits c-MYC promoter activity. *Biochemistry* (2010) 49(45):9706–14. doi: 10.1021/bi100509s
106. Mathad RI, Hatzakis E, Dai J, Yang D. c-MYC promoter G-quadruplex formed at the 5'-end of NHE III1 element: insights into biological relevance and parallel-stranded G-quadruplex stability. *Nucleic Acids Res* (2011) 39(20):9023–33. doi: 10.1093/nar/gkr612
107. Hu MH, Wang YQ, Yu ZY, Hu LN, Ou TM, Chen SB, et al. Discovery of a New Four-Leaf Clover-Like Ligand as a Potent c-MYC Transcription Inhibitor Specifically Targeting the Promoter G-Quadruplex. *J Med Chem* (2018) 61(6):2447–59. doi: 10.1021/acs.jmedchem.7b01697
108. Benabou S, Ferreira R, Aviñó A, González C, Lyonnais S, Solà M, et al. Solution equilibria of cytosine- and guanine-rich sequences near the promoter region of the n-myc gene that contain stable hairpins within lateral loops. *Biochim Biophys Acta* (2014) 1840(1):41–52. doi: 10.1016/j.bbagen.2013.08.028
109. Li F, Chen H, Zhou J, Yuan G. Exploration of the selective recognition of the G-quadruplex in the N-myc oncogene by electrospray ionization mass spectrometry. *Rapid Commun Mass Spectrom* (2015) 29(3):247–52. doi: 10.1002/rcm.7101
110. Toure M, Crews CM. Small-Molecule PROTACS: New Approaches to Protein Degradation. *Angew Chem Int Ed Engl* (2016) 55(6):1966–73. doi: 10.1002/anie.201507978
111. Hines J, Lartigue S, Dong H, Qian Y, Crews CM. MDM2-Recruiting PROTAC Offers Superior, Synergistic Antiproliferative Activity via Simultaneous Degradation of BRD4 and Stabilization of p53. *Cancer Res* (2019) 79(1):251–62. doi: 10.1158/0008-5472.CAN-18-2918
112. Zengerle M, Chan KH, Ciulli A. Selective Small Molecule Induced Degradation of the BET Bromodomain Protein BRD4. *ACS Chem Biol* (2015) 10(8):1770–7. doi: 10.1021/acschembio.5b00216
113. Drygin D, Siddiqui-Jain A, O'Brien S, Schwaebe M, Lin A, Bliesath J, et al. Anticancer activity of CX-3543: a direct inhibitor of rRNA biogenesis. *Cancer Res* (2009) 69(19):7653–61. doi: 10.1158/0008-5472.CAN-09-1304
114. Bywater MJ, Poortinga G, Sanij E, Hein N, Peck A, Cullinane C, et al. Inhibition of RNA polymerase I as a therapeutic strategy to promote cancer-specific activation of p53. *Cancer Cell* (2012) 22(1):51–65. doi: 10.1016/j.ccr.2012.05.019
115. Hald ØH, Olsen L, Gallo-Oller G, Elfman LHM, Løkke C, Kogner P, et al. Inhibitors of ribosome biogenesis repress the growth of MYCN-amplified neuroblastoma. *Oncogene* (2019) 38(15):2800–13. doi: 10.1038/s41388-018-0611-7
116. Dean M, Levine RA, Ran W, Kindy MS, Sonenshein GE, Campisi J. Regulation of c-myc transcription and mRNA abundance by serum growth factors and cell contact. *J Biol Chem* (1986) 261(20):9161–6.
117. Kelly K, Cochran BH, Stiles CD, Leder P. Cell-specific regulation of the c-myc gene by lymphocyte mitogens and platelet-derived growth factor. *Cell* (1983) 35(3 Pt 2):603–10. doi: 10.1016/0092-8674(83)90092-2
118. Reed JC, Alpers JD, Nowell PC, Hoover RG. Sequential expression of protooncogenes during lectin-stimulated mitogenesis of normal human lymphocytes. *Proc Natl Acad Sci USA* (1986) 83(11):3982–6. doi: 10.1073/pnas.83.11.3982
119. Finn RS, Crown JP, Lang I, Boer K, Bondarenko IM, Kulyk SO, et al. The cyclin-dependent kinase 4/6 inhibitor palbociclib in combination with letrozole versus letrozole alone as first-line treatment of oestrogen receptor-positive, HER2-negative, advanced breast cancer (PALOMA-1/TRIO-18): a randomised phase 2 study. *Lancet Oncol* (2015) 16(1):25–35. doi: 10.1016/s1470-2045(14)71159-3
120. Turner NC, Ro J, André F, Loi S, Verma S, Iwata H, et al. Palbociclib in Hormone-Receptor-Positive Advanced Breast Cancer. *N Engl J Med* (2015) 373(3):209–19. doi: 10.1056/NEJMoa1505270
121. Hart LS, Rader J, Raman P, Batra V, Russell MR, Tsang M, et al. Preclinical Therapeutic Synergy of MEK1/2 and CDK4/6 Inhibition in Neuroblastoma. *Clin Cancer Res* (2017) 23(7):1785–96. doi: 10.1158/1078-0432.CCR-16-1131
122. Rader J, Russell MR, Hart LS, Nakazawa MS, Belcastro LT, Martinez D, et al. Dual CDK4/CDK6 inhibition induces cell-cycle arrest and senescence in neuroblastoma. *Clin Cancer Res* (2013) 19(22):6173–82. doi: 10.1158/1078-0432.CCR-13-1675
123. Santamaría D, Barrière C, Cerqueira A, Hunt S, Tardy C, Newton K, et al. Cdk1 is sufficient to drive the mammalian cell cycle. *Nature* (2007) 448(7155):811–5. doi: 10.1038/nature06046
124. Tetsu O, McCormick F. Proliferation of cancer cells despite CDK2 inhibition. *Cancer Cell* (2003) 3(3):233–45. doi: 10.1016/S1535-6108(03)00053-9
125. Hydbring P, Bahram F, Su Y, Tronnersjö S, Högstrand K, von der Lehr N, et al. Phosphorylation by Cdk2 is required for Myc to repress Ras-induced senescence in cotransformation. *Proc Natl Acad Sci USA* (2010) 107(1):58–63. doi: 10.1073/pnas.0900121106
126. Brasca MG, Amboldi N, Ballinari D, Cameron A, Casale E, Cervi G, et al. Identification of N,1,4,4-tetramethyl-8-{[4-(4-methylpiperazin-1-yl)phenyl]amino}-4,5-dihydro-1H-pyrazolo[4,3-h]quinazoline-3-carboxamide (PHA-848125), a potent, orally available cyclin dependent kinase inhibitor. *J Med Chem* (2009) 52(16):5152–63. doi: 10.1021/jm9006559
127. Carmena M, Earnshaw WC. The cellular geography of aurora kinases. *Nat Rev Mol Cell Biol* (2003) 4(11):842–54. doi: 10.1038/nrm1245
128. Bischoff JR, Anderson L, Zhu Y, Mossie K, Ng L, Souza B, et al. A homologue of Drosophila aurora kinase is oncogenic and amplified in human colorectal cancers. *EMBO J* (1998) 17(11):3052–65. doi: 10.1093/emboj/17.11.3052
129. Lehman NL, O'Donnell JP, Whiteley LJ, Stapp RT, Lehman TD, Roszka KM, et al. Aurora A is differentially expressed in gliomas, is associated with patient survival in glioblastoma and is a potential chemotherapeutic target in gliomas. *Cell Cycle* (2012) 11(3):489–502. doi: 10.4161/cc.11.3.18996
130. Loh J-K, Lieu A-S, Chou C-H, Lin F-Y, Wu C-H, Howng S-L, et al. Differential expression of centrosomal proteins at different stages of human glioma. *BMC Cancer* (2010) 10:268–. doi: 10.1186/1471-2407-10-268
131. Samaras V, Stamatelli A, Samaras E, Arnaoutoglou C, Arnaoutoglou M, Stergiou I, et al. Comparative immunohistochemical analysis of aurora-A and aurora-B expression in human glioblastomas. Associations with proliferative activity and clinicopathological features. *Pathol Res Pract* (2009) 205(11):765–73. doi: 10.1016/j.prp.2009.06.011
132. Barton VN, Foreman NK, Donson AM, Birks DK, Handler MH, Vibhakar R. Aurora kinase A as a rational target for therapy in glioblastoma. *J Neurosurg Pediatr* (2010) 6(1):98. doi: 10.3171/2010.3.PEDS10120
133. den Hollander J, Rimpi S, Doherty JR, Rudelius M, Buck A, Hoellein A, et al. Aurora kinases A and B are up-regulated by Myc and are essential for maintenance of the malignant state. *Blood* (2010) 116(9):1498–505. doi: 10.1182/blood-2009-11-251074
134. Dauch D, Rudalska R, Cossa G, Nault J-C, Kang T-W, Wuestefeld T, et al. A MYC–aurora kinase A protein complex represents an actionable drug target in p53-altered liver cancer. *Nat Med* (2016) 22(7):744–53. doi: 10.1038/nm.4107
135. Jiang J, Wang J, Yue M, Cai X, Wang T, Wu C, et al. Direct Phosphorylation and Stabilization of MYC by Aurora B Kinase Promote T-cell Leukemogenesis. *Cancer Cell* (2020) 37(2):200–15.e5. doi: 10.1016/j.ccell.2020.01.001
136. Otto T, Horn S, Brockmann M, Eilers U, Schuttrumpf L, Popov N, et al. Stabilization of N-Myc is a critical function of Aurora A in human neuroblastoma. *Cancer Cell* (2009) 15(1):67–78. doi: 10.1016/j.ccr.2008.12.005
137. Brockmann M, Poon E, Berry T, Carstensen A, Deubzer HE, Rycak L, et al. Small molecule inhibitors of aurora-a induce proteasomal degradation of N-myc in childhood neuroblastoma. *Cancer Cell* (2013) 24(1):75–89. doi: 10.1016/j.ccr.2013.05.005
138. Gustafson WC, Meyerowitz JG, Nekritz EA, Chen J, Benes C, Charron E, et al. Drugging MYCN through an allosteric transition in Aurora kinase A. *Cancer Cell* (2014) 26(3):414–27. doi: 10.1016/j.ccr.2014.07.015
139. Felgenhauer J, Tomino L, Selich-Anderson J, Bopp E, Shah N. Dual BRD4 and AURKA Inhibition Is Synergistic against MYCN-Amplified and Nonamplified Neuroblastoma. *Neoplasia* (2018) 20(10):965–74. doi: 10.1016/j.neo.2018.08.002

140. Kogiso M, Qi L, Braun FK, Injac SG, Zhang L, Du Y, et al. Concurrent Inhibition of Neurosphere and Monolayer Cells of Pediatric Glioblastoma by Aurora A Inhibitor MLN8237 Predicted Survival Extension in PDOX Models. *Clin Cancer Res* (2018) 24(9):2159–70. doi: 10.1158/1078-0432.CCR-17-2256
141. Čančer M, Drews LF, Bengtsson J, Bolin S, Rosén G, Westermark B, et al. BET and Aurora Kinase A inhibitors synergize against MYCN-positive human glioblastoma cells. *Cell Death Dis* (2019) 10(12):881. doi: 10.1038/s41419-019-2120-1
142. Ahmad Z, Jasnos L, Gil V, Howell L, Hallsworth A, Petrie K, et al. Molecular and in vivo characterization of cancer-propagating cells derived from MYCN-dependent medulloblastoma. *PloS One* (2015) 10(3):e0119834. doi: 10.1371/journal.pone.0119834
143. Kenney AM, Widlund HR, Rowitch DH. Hedgehog and PI-3 kinase signaling converge on Nmyc1 to promote cell cycle progression in cerebellar neuronal precursors. *Development* (2004) 131(1):217–28. doi: 10.1242/dev.00891
144. Manning BD, Toker A. AKT/PKB Signaling: Navigating the Network. *Cell* (2017) 169(3):381–405. doi: 10.1016/j.cell.2017.04.001
145. Cage TA, Chanthery Y, Chesler L, Grimmer M, Knight Z, Shokat K, et al. Downregulation of MYCN through PI3K Inhibition in Mouse Models of Pediatric Neural Cancer. *Front Oncol* (2015) 5:111. doi: 10.3389/fonc.2015.00111
146. Gustafson WC, Weiss WA. Myc proteins as therapeutic targets. *Oncogene* (2010) 29(9):1249–59. doi: 10.1038/onc.2009.512
147. Zheng Y, Jiang Y. mTOR Inhibitors at a Glance. *Mol Cell Pharmacol* (2015) 7 (2):15–20. doi: 10.4255/mcpharmacol.15.02
148. Johnsen JI, Segerström L, Orrego A, Elfman L, Henriksson M, Kågedal B, et al. Inhibitors of mammalian target of rapamycin downregulate MYCN protein expression and inhibit neuroblastoma growth in vitro and in vivo. *Oncogene* (2008) 27(20):2910–22. doi: 10.1038/sj.onc.1210938
149. Vaughan L, Clarke PA, Barker K, Chanthery Y, Gustafson CW, Tucker E, et al. Inhibition of mTOR-kinase destabilizes MYCN and is a potential therapy for MYCN-dependent tumors. *Oncotarget* (2016) 7(36):57525–44. doi: 10.18632/oncotarget.10544
150. Fan Q, Aksoy O, Wong RA, Ilkhanizadeh S, Novotny CJ, Gustafson WC, et al. A Kinase Inhibitor Targeted to mTORC1 Drives Regression in Glioblastoma. *Cancer Cell* (2017) 31:424–35. doi: 10.1016/j.ccell.2017.01.014
151. Hua H, Kong Q, Zhang H, Wang J, Luo T, Jiang Y. Targeting mTOR for cancer therapy. *J Hematol Oncol* (2019) 12(1):71. doi: 10.1186/s13045-019-0754-1
152. Robinson GW, Kaste SC, Chemaitilly W, Bowers DC, Laughton S, Smith A, et al. Irreversible growth plate fusions in children with medulloblastoma treated with a targeted hedgehog pathway inhibitor. *Oncotarget* (2017) 8 (41):69295–302. doi: 10.18632/oncotarget.20619
153. Kotulska K, Chmielewski D, Borkowska J, Jurkiewicz E, Kuczyński D, Kmieć T, et al. Long-term effect of everolimus on epilepsy and growth in children under 3 years of age treated for subependymal giant cell astrocytoma associated with tuberous sclerosis complex. *Eur J Paediatr Neurol* (2013) 17(5):479–85. doi: 10.1016/j.ejpn.2013.03.002
154. Wu CC, Hou S, Orr BA, Kuo BR, Youn YH, Ong T, et al. mTORC1-Mediated Inhibition of 4EBP1 Is Essential for Hedgehog Signaling-Driven Translation and Medulloblastoma. *Dev Cell* (2017) 43(6):673–88.e5. doi: 10.1016/j.devcel.2017.10.011
155. Zhou J, Su P, Wang L, Chen J, Zimmermann M, Genbacev O, et al. mTOR supports long-term self-renewal and suppresses mesoderm and endoderm activities of human embryonic stem cells. *Proc Natl Acad Sci U.S.A.* (2009) 106(19):7840–5. doi: 10.1073/pnas.0901854106
156. da Silva PBG, Teixeira Dos Santos MC, Rodini CO, Kaid C, Pereira MCL, Furukawa G, et al. High OCT4A levels drive tumorigenicity and metastatic potential of medulloblastoma cells. *Oncotarget* (2017) 8(12):19192–204. doi: 10.18632/oncotarget.15163
157. Zhao QW, Zhou YW, Li WX, Kang B, Zhang XQ, Yang Y, et al. Akt–mediated phosphorylation of Oct4 is associated with the proliferation of stem–like cancer cells. *Oncol Rep* (2015) 33(4):1621–9. doi: 10.3892/or.2015.3752
158. Lin Y, Yang Y, Li W, Chen Q, Li J, Pan X, et al. Reciprocal regulation of Akt and Oct4 promotes the self-renewal and survival of embryonal carcinoma cells. *Mol Cell* (2012) 48(4):627–40. doi: 10.1016/j.molcel.2012.08.030
159. Kaneko Y, Suenaga Y, Islam SM, Matsumoto D, Nakamura Y, Ohira M, et al. Functional interplay between MYCN, NCYM, and OCT4 promotes aggressiveness of human neuroblastomas. *Cancer Sci* (2015) 106(7):840–7. doi: 10.1111/cas.12677
160. Suenaga Y, Islam SM, Alagu J, Kaneko Y, Kato M, Tanaka Y, et al. NCYM, a Cis-antisense gene of MYCN, encodes a de novo evolved protein that inhibits GSK3β resulting in the stabilization of MYCN in human neuroblastomas. *PloS Genet* (2014) 10(1):e1003996. doi: 10.1371/journal.pgen.1003996
161. Wei SJ, Nguyen TH, Yang IH, Mook DG, Makena MR, Verlekar D, et al. MYC transcription activation mediated by OCT4 as a mechanism of resistance to 13-cisRA-mediated differentiation in neuroblastoma. *Cell Death Dis* (2020) 11(5):368. doi: 10.1038/s41419-020-2563-4

Conflict of Interest: The authors declare that the research was conducted in the absence of any commercial or financial relationships that could be construed as a potential conflict of interest.

frontiers in Oncology

MINI REVIEW
published: 03 February 2021
doi: 10.3389/fonc.2020.625332

Molecular Mechanisms of *MYCN* Dysregulation in Cancers

Ruochen Liu[1,2,3], *Pengfei Shi*[1,2,3], *Zhongze Wang*[1,2], *Chaoyu Yuan*[1,2] *and Hongjuan Cui*[1,2,3]*

[1] State Key Laboratory of Silkworm Genome Biology, College of Sericulture, Textile and Biomass Sciences, Southwest University, Chongqing, China, [2] Cancer Center, Reproductive Medicine Center, Medical Research Institute, Southwest University, Chongqing, China, [3] NHC Key Laboratory of Birth Defects and Reproductive Health (Chongqing Key Laboratory of Birth Defects and Reproductive Health, Chongqing Population and Family Planning Science and Technology Research Institute), Chongqing, China

MYCN, a member of *MYC* proto-oncogene family, encodes a basic helix-loop-helix transcription factor N-MYC. Abnormal expression of N-MYC is correlated with high-risk cancers and poor prognosis. Initially identified as an amplified oncogene in neuroblastoma in 1983, the oncogenic effect of N-MYC is expanded to multiple neuronal and nonneuronal tumors. Direct targeting N-MYC remains challenge due to its "undruggable" features. Therefore, alternative therapeutic approaches for targeting *MYCN*-driven tumors have been focused on the disruption of transcription, translation, protein stability as well as synthetic lethality of *MYCN*. In this review, we summarize the latest advances in understanding the molecular mechanisms of *MYCN* dysregulation in cancers.

Keywords: MYCN, cancer, gene amplification, G-quadruplex, NCYM, super enhancer, synthetic lethality

OPEN ACCESS

Edited by:
Atsushi Takatori, Chiba Cancer Center, Japan

Reviewed by:
Enrique Hernandez-Lemus, Instituto Nacional de Medicina Genómica (INMEGEN), Mexico
Heike Laman, University of Cambridge, United Kingdom
Shunpei Satoh, Saitama Cancer Center, Japan

***Correspondence:**
Hongjuan Cui
hcui@swu.edu.cn

Specialty section:
This article was submitted to Molecular and Cellular Oncology, a section of the journal Frontiers in Oncology

Received: *02 November 2020*
Accepted: *18 December 2020*
Published: *03 February 2021*

Citation:
Liu R, Shi P, Wang Z, Yuan C and Cui H (2021) Molecular Mechanisms of MYCN Dysregulation in Cancers. Front. Oncol. 10:625332. doi: 10.3389/fonc.2020.625332

INTRODUCTION

N-MYC is a transcription factor of the MYC oncogene family. This gene family of humans consists of three members, namely, *MYCC*, *MYCN*, *MYCL*, which encodes C-MYC, N-MYC, and L-MYC protein respectively ("MYC" was used to indicate all three genes in this review). The first identified *MYC* gene was *MYCC* as a homolog of an avian retroviral gene *v-myc*, then *MYCN* in neuroblastoma and *MYCL* in lung cancer (1–3). These proteins show similar structure with the highest homology in five short stretches called MYC boxes 1 to 4 at the N terminus and in the basic helix-loop-helix-leucine-zipper (bHLH-LZ) domain at the C terminus (**Figure 1A**) (6–9). The former enables MYC to interact with different effector proteins including TRRAP and P400 which mediate chromatin remodeling and modification (10, 11), the latter allows MYC to form a heterodimer with partner proteins that also contain a bHLH-LZ domain, such as MAX. MYC/MAX heterodimer bind to the target motif called E-box with the consensus sequence of CAC(G/A)TG to regulate the expression of targeted genes (**Figure 1B**). In addition, MYC can also bind to targeted sequences that show deviation from or no similarity to the E-box, suggesting the association of MYC to chromatin can be instructed by other factors (12, 13). For example, MYC can invade promoter regions of active genes and cause global transcriptional amplification (**Figure 1C**) (4, 14, 15). The two different action modes of MYC seem conflicting, *i.e.*, gene-specific regulation model versus global gene activation model. The third model, gene-specific affinity model, in which the affinity of promoters for MYC is different and relies on the MYC levels and the interaction of MYC with core promoter-binding factors, such as WDR5 (**Figure 1D**), has been

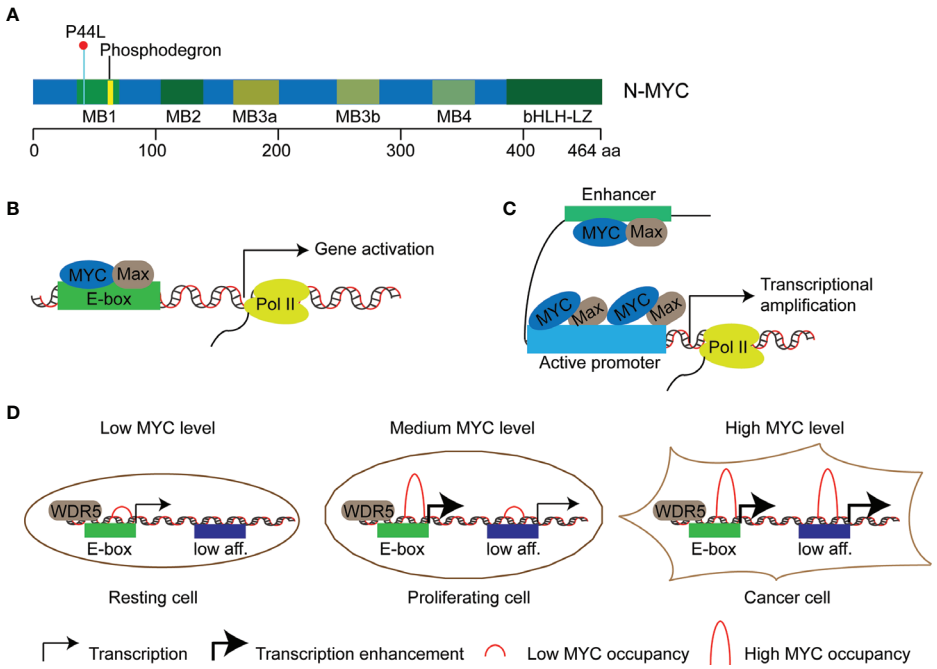

FIGURE 1 | Models of transcriptional regulation of target genes by MYC proteins. **(A)** Schematic diagram of N-MYC protein structure. Five highly conserved stretched called MYC boxes 1 to 4 (MB) and the basic helix-loop-helix-leucine-zipper (bHLH-LZ) domain at the C terminus are shown. The recurrent somatic mutation P44L and the putative N-MYC phosphodegron are shown in cyanine and yellow respectively. **(B)** Gene-specific regulation model: MYC/Max dimer binds and regulates a subset of genes with E-boxes in their promoters. **(C)** Global gene activation model: MYC accumulates in the promoter regions of active genes independent of E-box and leads to transcriptional amplification in cancer cells with high level of MYC proteins (4). **(D)** Gene-specific affinity model: high-affinity binding sites, such as those with E-boxes and WDR5 (WD-repeat protein 5) binding, are already fully occupied by MYC at physiological MYC protein level (medium level) in proliferating cells; low-affinity (low aff.) binding sites can be occupied by MYC at oncogenic MYC protein level (high level) in cancer cells (5).

proposed to reconcile the action modes of MYC (5, 16). MYC proteins affect transcription of a large number of genes and thus regulate fundamental cellular processes, including proliferation, metabolism, apoptosis, differentiation, and immune surveillance (17–21).

With evolutionarily conserved domains, the three MYC proteins share certain extent of functional redundancy. For instance, when N-MYC is expressed from the *MYCC* locus, it can rescue development, cellular growth, and differentiation in *MYCC* deficient mice (22). On the other hand, C-MYC, N-MYC, and L-MYC have their own unique features. Enhanced expression of different MYC paralogs induces tumors with different biological characteristics in medulloblastoma (23, 24), prostate cancer (25), and lung cancer (26). Furthermore, the amplification of *MYC* genes is mutually exclusive, and the switch of gene expression among the members is associated with cell lineage shift, tumor progression, and treatment resistance (27, 28). Different collaborative proteins of MYC paralogs help to demarcate a unique subset of responsive genes, which could partially explain the distinct biological functions among MYC members. For example, N-MYC interacts with TWIST1 at enhancers to activate developmental genes important to neuroblastoma tumorigenesis, while TCF3 (E2A) is selectively required for progression of C-MYC driven myeloma (15). In this mini-review, we focus on N-MYC-driven tumors. Since discovered in 1983 in neuroblastoma (1, 3), the oncogenic effect of N-MYC has been demonstrated both in various neuronal [*e.g.*, glioblastoma (29), medulloblastoma (30), astrocytoma (31)], and nonneuronal [*e.g.*, prostate cancers (32), breast cancers (33), hematologic malignancies (34), pancreatic tumors (35), Wilms tumors (36), hepatocellular carcinoma (37), rhabdomyosarcoma (38), ovarian cancers (39)] tumors. Specifically, this mini-review summarizes the latest advances in the regulation network of N-MYC expression (**Figure 2**) and the related therapeutic targets for *MYCN*-driven tumors.

MOLECULAR MECHANISMS OF *MYCN* DYSREGULATION AND THE THERAPEUTIC TARGETS

The tissue specificity and strength of *MYC* gene expression are under tight control in normal circumstances. Studies of mice show that the expression of *MYCN* is high during early developmental stages and in specific tissues including forebrain, hindbrain, and kidney of newborn mice, while *MYCC* is broadly expressed throughout the tissues and the developmental stages analyzed. Clinical observation of *MYCN*

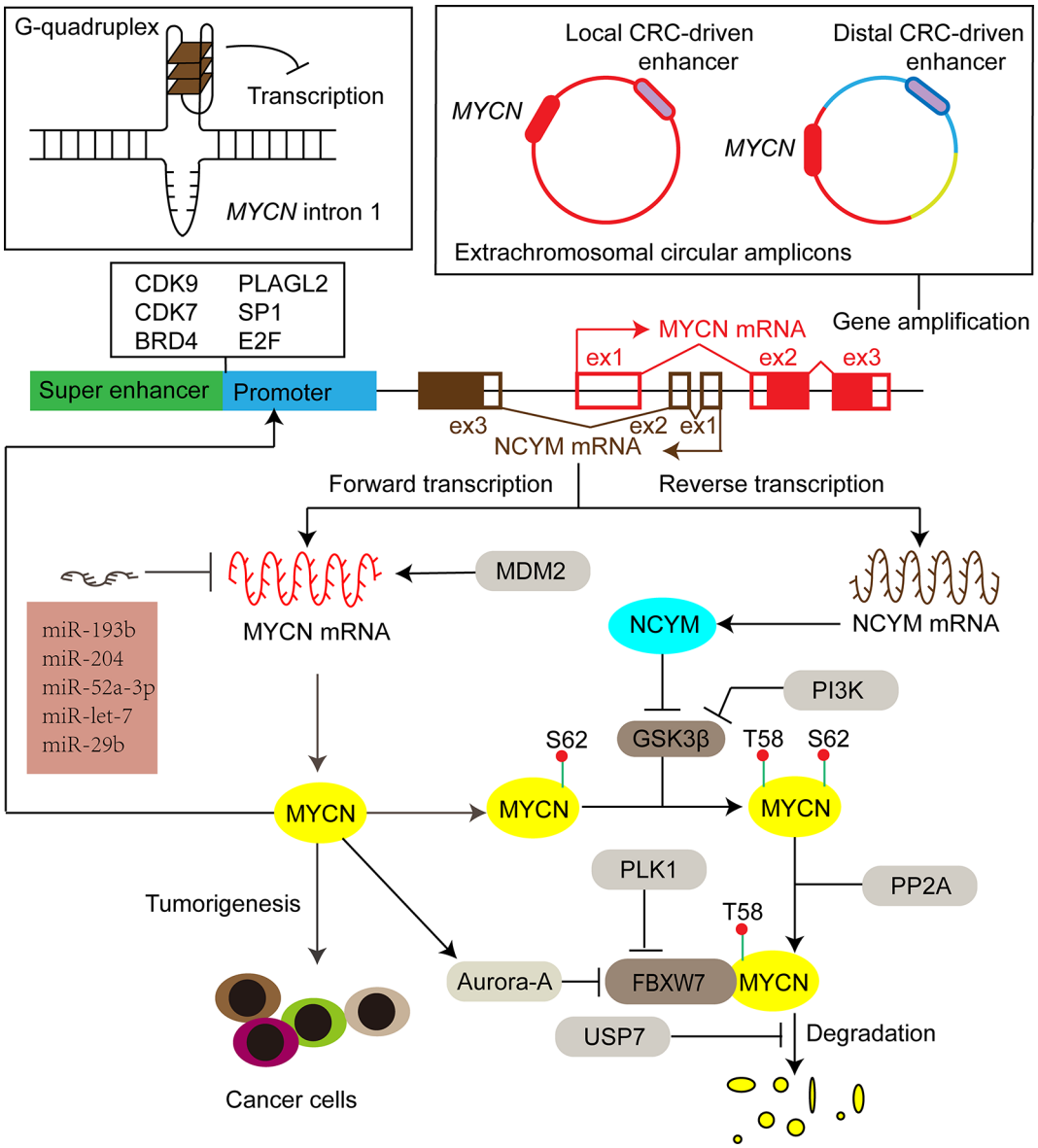

FIGURE 2 | The expression of *MYCN* is activated or repressed at DNA, mRNA and protein levels by different factors, including secondary DNA structure, enhancers, transcription factors, miRNAs, ubiquitination-dependent proteasome degradation machinery and its cis-antisense gene *NCYM*. Filled red and brown boxes indicate translated regions of MYCN and NCYM respectively, while the blank counterparts represent untranslated regions. CRC core regulatory circuitry, CDK9 cyclin-dependent kinase 9, CDK7 cyclin-dependent kinase 7, BRD4 bromodomain-containing 4, PLAGL2 pleiomorphic adenoma gene-like 2, SP1 specific protein 1, GSK3β glycogen synthase kinase 3β, PI3K phosphoinositide 3-kinase, FBXW7 F-box and WD repeat domain-containing 7, PP2A protein phosphatase 2A, PLK1 polo-like kinase 1, USP7 ubiquitin-specific protease 7, MDM2 murine double minute 2.

amplification in human neuroblastoma firstly pointed out the potential association between *MYCN* gene and tumorigenesis (1, 3). Although amplified DNAs encompassing *MYCN* are more than 100 kb and can include adjacent co-amplified genes, *MYCN* has emerged as the only consistently amplified gene (40). Using transgenic animal models, multiple studies establish that N-MYC overexpression is a driver of cancers. For example, targeted expression of human N-MYC causes neuroblastoma in transgenic mice and zebrafish (41, 42). Neuroblastomas with enhanced expression of N-MYC without *MYCN* amplification are known to be similarly high-risk and poor prognosis (43). Recent studies show that high N-MYC protein and RNA levels could be better biomarkers than *MYCN* gene amplification in predicting the prognosis of neuroblastoma patients (44, 45), underscoring the importance of aberrant expression of N-MYC in tumor progression. Here, we discuss mechanisms of *MYCN* dysregulation at DNA, mRNA and protein levels, and corresponding therapeutic targets.

GENE AMPLIFICATION OF *MYCN*

Gene amplification is a frequent mechanism that can cause proto-oncogene overexpression. It is a process that involves unscheduled DNA replication, recombination and/or formation of extrachromosomal DNA, leading to a selective increase of gene copy number up to several hundred (40). The occurrence of proto-oncogene amplification can be detected by the presence of "double minutes" or "homogeneously staining chromosomal regions". *MYCN* was the first discovered paradigm of proto-oncogene amplification and is an important bio-marker to stratify clinical risk. It was initially detected in about 20% to 25% of neuroblastoma, then at a much lower incidence in small cell lung cancer, retinoblastoma, hepatocellular carcinoma, malignant gliomas, and peripheral neuroectodermal tumors (46, 47). Amplification of *MYCN* has been recognized as a consequence of genomic instability and occurs sporadically (48). Overexpression of N-MYC initiates tumorigenesis by preventing the normal physiological process of neural crest cell death in *TH-MYCN* transgenic mice in which human *MYCN* is under the control of a tyrosine hydroxylase (TH) promoter, and the formation of neuroblastoma involves further changes of the persisting embryonal neural crest cells, including *MYCN* amplification (49). In addition, *MYCN* amplification is associated with advanced neuroblastomas, suggesting that the amplification is a late event during the tumorigenesis (49–51)

Although multiple replication-based mechanisms, such as double rolling-circle replication, have been proposed to explain gene amplification, the important factors that induce and regulate *MYCN* amplification remain to be completely investigated (52–55). Proto-oncoprotein c-MYB transcription factor is implicated in the regulation of cell growth and proliferation of neuroblastoma (56). The functional ortholog of *Drosophila melanogaster*, Dm-Myb, is directly implicated in the site-specific DNA replication, leading to amplification of the chromosomal loci with the chorion gene cluster (57). Aygun and Altungoz showed that c-MYB is involved in the control of *MYCN* amplification in *MYCN*-amplified neuroblastoma cell lines (58). Specifically, the *MYCN* gene dosage is increased upon knockdown of c-MYB expression, which may be associated with the elevated expression of geminin protein that causes a shift from genomic DNA replication to *MYCN* amplification (58–60). Recent sequencing studies indicate that the structure of extrachromosomal *MYCN* amplicons are shaped by enhancer sequences (61, 62). Specifically, Helmsauer et al. reported two distinct classes of extrachromosomal circular *MYCN* amplicons: the first class co-amplifies a local core regulatory circuitry (CRC)-driven enhancer; the second class shows a complex chimeric structure with a distal CRC-driven enhancer instead of the local enhancer (**Figure 2**) (61). Long inverted repeats and microhomology are significantly associated with boundary regions of the *MYCN* amplicon units, and thus might also be involved in the initiation or regulation of *MYCN* amplification (55, 58). Elucidating the mechanisms of *MYCN* amplification may bring about new therapeutic strategies targeting *MYCN* amplification to treat *MYCN*-driven tumors.

Although the amplified genes tend to overexpress, gene amplification not necessarily leads to high level of gene expression. In fact, there is inconsistency between *MYCN* gene dosage, mRNA and protein levels, and clinical outcomes (44, 63). For example, low DNA dosage but high RNA level is detected in some neuroblastoma samples, while high DNA dosage but low RNA level in some other samples (45). Additional *MYCN* gene copies may also suppress their own expression (58). Genome-wide analysis in humans and some model organisms revealed that genes in copy number variation regions are expressed at lower and more variable levels than genes mapped elsewhere (64). Alternatively, as in plants, repeated genes may suffer from homology-dependent gene silencing that involves DNA methylation or histone modification (65, 66). Consistently, only a weak positive correlation of *MYCN* expression with copy number is detected in Wilms tumor, while a strong negative correlation of *MYCN* expression with DNA methylation level at specific loci is observed (67). Importantly, transcriptional and posttranscriptional regulation determines the final level of N-MYC protein in both *MYCN* amplified and non-amplified tumors. For instance, enhancer hijacking that repositions a super enhancer close to the affected genes through chromosomal translocation accounts for the high level of C-MYC or N-MYC expression in some neuroblastoma cells without *MYCC* amplification or without a high *MYCN* copy number, respectively (68, 69).

REGULATION OF *MYCN* TRANSCRIPTION

Super Enhancer and Transcription Factors

A general feature of *MYC* genes is their transcriptional regulation by upstream super enhancers (SEs) (70). SE regions are occupied by abundant transcription factors, cofactors, and chromatin regulators, thereby promoting transcription of *MYC* genes (71). Specifically, H3K27 acetylation (H3K27ac), a marker of active enhancers and promoters, is enriched in the SE regions and recognized by BRD4 of bromodomain and extra-terminal domain (BET) protein family that recruits positive transcription elongation factor b (P-TEFb) to the promoters to phosphorylate RNA polymerase II, and thus facilitates transcriptional initiation, pause release and elongation (72–74). BET inhibitors, such as JQ1 and OTX015, can displace the BRD4 oncoprotein from chromatin (75), which potently represses *MYCN* transcription in neuroblastoma cell lines and effectively reduces neuroblastoma cell viability *in vitro* and *in vivo* (76, 77). It has been reported that the toxic effects of BET inhibitors depend on p53 (78). The combination of MDM2 (an E3-ubiquitin ligase involved in proteasomal degradation of p53) inhibitor (CGM097) and OTX015 results in p53 activation and decreased expression of MYC proteins, which synergistically promotes neuroblastoma cell death (79). A recent study shows that triple-negative breast cancer (TNBC) cells with high expression of *MYCN* are also sensitive to BET inhibitors (80). Furthermore, combined BET and MEK inhibition synergistically represses the growth of *MYCN*-expressing patient-derived xenograft TNBC tumors (80).

Besides BET proteins, transcriptional cyclin-dependent kinases (CDKs) are recruited to SEs, especially CDK7, a catalytic subunit of the transcription factor IIH complex (TFIIH), and CDK9, a kinase subunit of P-TEFb (81, 82). These CDKs regulate the transcriptional cycle of RNA polymerase II *via* phosphorylating the C-terminal domain of the polymerase, which enhances expression of SE-associated oncogenes, such as *MYCN* (83–85). A covalent inhibitor of CDK7, THZ1, selectively targets *MYCN*-amplified neuroblastoma cells, leading to global suppression of *MYCN*-dependent transcriptional amplification and sustained growth inhibition of tumors in a mouse model of neuroblastoma (85). CYC065 (fadraciclib), a clinical inhibitor of CDK9 and CDK2 (a major regulator of apoptotic cell death), selectively targets *MYCN*-amplified neuroblastoma through a loss of *MYCN* transcription and growth arrest, followed by sensitizing cells for apoptosis as a result of CDK2 inhibition (86). Furthermore, the combined use of CYC065 with temozolomide (a reference therapy for relapsed neuroblastoma), leads to long-term repression of neuroblastoma growth *in vivo* (86).

Recent studies reveal that several super-enhancer harboring transcription factors including HAND2, ISL1, PHOX2B, GATA3, and TBX2 constitute a CRC that is essential for the *MYCN* expression and the survival of *MYCN*-amplified neuroblastoma cells (61, 87). BRD4 and CDK7 inhibitors synergistically repress the expression of all the CRC transcription factors and N-MYC, which inhibits neuroblastoma cell growth (87). Knockdown of each CRC transcription factors also suppresses the expression of *MYCN* (87). Interestingly, the CRC-driven enhancers (local or distal) are associated with extrachromosomal circular *MYCN* amplicons (**Figure 2**) (61), underscoring the role of the CRC transcription factors in the regulation of *MYCN* expression.

Other transcription factors, such as specific protein 1 (SP1) (88), E2F (89), and pleiomorphic adenoma gene-like 2 (PLAGL2) (90), participate in the regulation of *MYCN* expression. The three transcription factors directly bind to the cognate binding sites in the *MYCN* promoter, contributing to *MYCN* activation. Moreover, N-MYC regulates *PLAGL2* transcription through five N-MYC-binding E-boxes in the *PLAGL2* promoter region, forming a positively regulatory loop between the two transcription factors, which is crucial for expression of each other in neuroblastoma tumors (90). Lipid desaturation-associated endoplasmic reticulum (ER) stress inhibits *MYCN* expression *via* upregulating the transcriptional repressor ATF3 in hepatocellular carcinoma cells (91). Since these transcription factors including SP1, E2F2, and PLAGL2 are involved in the regulation of *MYCN* expression, they mediate the effects of metabolic change and pharmacological treatment on *MYCN* expression and *MYCN*-driven tumors (92). Aldehyde dehydrogenase family 18 member A1 (ALDH18A1) is a key enzyme for the synthesis of proline from glutamate and plays important role in the proliferation, self-renewal, and tumorigenicity of neuroblastoma cells (93). ALDH18A1 promotes the transcription of *MYCN via* the *miR-29b*/SP1 regulatory loop. ALDH18A1-specific inhibitor, YG1702, inhibits *MYCN* expression and attenuates the growth of human neuroblastoma (93). All-trans retinoic acids have been used for neuroblastoma therapy for decades by inhibiting the expression of *MYCN* and inducing the neuronal differentiation of neuroblastoma cells (94–96). Loss of E2F binding or suppression of PLAGL2 expression mediates the negative regulation of *MYCN* expression by retinoic acid (89, 90). Acyclic retinoid dampens *MYCN* gene expression and suppresses cell proliferation of *MYCN*-overexpressed hepatocellular carcinoma cells, at least in part by ER stress-induced ATF3 signaling pathway (91).

G-Quadruplex

Another feature of *MYC* genes is their transcriptional regulation by non-B DNA structures including single-stranded bubbles, Z-DNA, and G-quadruplexes (97). G-quadruplexes are four-stranded DNA secondary structures and consist of stacked G-quartets that formed by the assembly of four Hoogsteen hydrogen-bonded guanines in guanine-rich regions of DNA. A G-quadruplex forming sequence lies in the promoter of *MYCC* gene (98) and in intron 1 of *MYCN* gene (99) respectively. This sequence exists in equilibrium between transcriptionally active forms (double helical and single stranded) and a silenced form (G-quadruplex), which controls up to 90% of *MYCC* transcription (100). Thus, targeting *MYC* expression through G-quadruplex stabilization becomes an attractive candidate for the treatment of *MYC*-driven tumors. Cationic porphyrin TMPyP4 is a small molecule able to stabilize G-quadruplex structure and efficiently repress *MYCC* transcription, which establishes the principle that MYC transcription can be controlled by ligand-mediated G-quadruplex stabilization (98). A cell penetrating thiazole peptide, TH3, shows improved targeting specificity to *MYCC* G-quadruplex over other tested G-quadruplexes (100). This peptide down-regulates *MYCC* expression in cancer cells and reduces proliferative activities by inducing S phase cell cycle arrest and apoptosis (100). Nucleolin is a protein involved in the folding the G-quadruplex (101). Quarfloxin (CX-3543), a fluoroquinolone-based antitumor agent, can inhibit *MYCC* expression by redistribution of nucleolin from the nucleolus to the nucleoplasm to bind to *MYCC* G-quadruplex (102). Treating neuroblastoma cells with quarfloxin represses N-MYC expression and causes G2-cell cycle arrest and apoptosis (103). The most profound anti-tumor effects of quarfloxin are associated with *MYCN* amplification (103), implying the above drugs that target *MYCC* G-quadruplex can also be used to target *MYCN* G-quadruplex for treatment of *MYCN*-driven tumors.

POSTTRANSCRIPTIONAL REGULATION OF *MYCN* MRNA

Along with transcription factors, noncoding RNAs including long noncoding RNA (lncRNAs) and microRNAs (miRNAs) are involved in the regulatory network of *MYCN* expression. miR-506-3p is a potent differentiation inducer and a strong repressor of *MYCN* expression in neuroblastoma cells by targeting PLAGL2 transcription factor (90, 104). miR-204 directly binds *MYCN* mRNA, represses *MYCN* expression, and inhibits a subnetwork of oncogenes that strongly correlate with *MYCN*-amplified

neuroblastoma and poor patient outcome (105). miR-193b targets several important oncogenes including *MYCN* and is expressed at low levels in neuroblastoma cell lines (106). *MYCN* mRNA is a direct target of miR-520c-3p in cholangiocarcinoma, and transcription factor SP1-induced lncRNA HOXD-AS1 enhances *MYCN* expression through competitively binding to miR-520c-3p, which associates with lymph node invasion, advanced TNM stage and poor prognosis (107). A miRNA network, consisting of miR-29b, miR-29a, and miR-193b, mediates posttranscriptional regulation of the *MYCN* expression by ALDH18A1 (93, 108). miRNA let-7 is a strong negative regulator of *MYCN* expression and can inhibit proliferation and clonogenic growth of *MYCN*-amplified neuroblastoma cells (108). LIN28B, an RNA-binding protein and a suppressor of microRNA biogenesis, selectively blocks the biogenesis of let-7 miRNA, consequently leading to increased *MYCN* expression in neuroblastoma cells (109). These results indicate that *MYCN* is targeted by several miRNAs. Increased expression of these miRNAs inhibits cell proliferation and tumorigenesis (105). Furthermore, miR-506-3p has been reported to mediate the antitumor effect of retinoic acid in neuroblastoma cells (90). These results underscore the potential of miRNA-based anticancer therapy. Interestingly, the E3-ubiquitin ligase MDM2 increases the *MYCN* mRNA stability and translation by binding to AU-rich elements of the 3′ UTR of *MYCN* mRNA through its C-terminal RING domain (110). RNAi-mediated knockdown of MDM2 leads to remarkable suppression of neuroblastoma cell growth and induction of cell death through a p53-independent pathway (110).

REGULATION OF *MYCN* TRANSLATION

Efficient translation guarantees the oncogenic level of N-MYC protein. N-MYC has been shown to promote the expression of many genes involved in ribosome biogenesis and protein synthesis (111), suggesting N-MYC contributes to its own overexpression by enhancing the capacity of translation. The N-MYC protein level is decreased as a result of ribosome biogenesis inhibition (103). Mammalian target of rapamycin (mTOR) is a serine/threonine protein kinase that controls initiation of protein translation (112). mTOR directly phosphorylates and inactivates eukaryotic translation initiation factor 4E (eIF4E)-binding protein 1 (4E-BP1), which leads to activation of eIF4E and thus promotes cap-dependent translation of mRNAs including MYC family (112). Pharmacological inhibition of the AKT/mTOR pathway reduces N-MYC level and exhibits therapeutic efficacy in *MYCN*-amplified neuroblastoma (113, 114).

REGULATION OF N-MYC STABILITY

After translation, the stability and activity of *N-MYC* protein are tightly controlled by ubiquitination-dependent proteasome degradation that is a brake in the *MYCN*-driven cancers. The degradation of the N-MYC proto-oncoprotein in neural stem/progenitor cells is required for the arrest of proliferation and the start of differentiation. Two E3 ubiquitin ligases FBXW7 and HUWE1 ubiquitinate N-MYC through Lys 48-mediated linkages and target it for destruction by the proteasome (115, 116). The recognition of N-MYC by FBXW7 involves several sequential reactions, *i.e.*, phosphorylation on Ser62 by CDK1 (117), phosphorylation on Thr58 by glycogen synthase kinase 3β (GSK3β), dephosphorylation of Ser62 by protein phosphatase 2A (PP2A) (118), which facilitates the Thr58 phosphorylated N-MYC binding with FBXW7 (116).

Dysregulation of the degradation process will cause the accumulation of N-MYC protein to the oncogenic level. Aurora-A, a member of the Aurora kinase family, is identified in an shRNA screen of genes that are highly expressed in *MYCN*-amplified neuroblastoma cells and contributes to the stabilization of N-MYC (119). Mechanistically, the catalytic domain of Aurora-A interacts directly with N-MYC through binding sites that flank either side of MYC box 1 which contains the phosphodegron (Thr58) recognized by FBXW7, thereby preventing the binding of FBXW7 with N-MYC substrate (120). Furthermore, the expression of Aurora-A is increased in the *MYCN*-amplified neuroblastoma, suggesting a potential feed-forward loop that improves the stability of both proteins (121). Two Aurora-A kinase activity inhibitors, MLN8054 and MLN8237, disrupt the Aurora-A/N-MYC complex and promote FBXW7-mediated degradation of N-MYC, which correlates with tumor regression and prolonged survival in a mouse model of *MYCN*-driven neuroblastoma (122, 123). MLN8237 destabilizes N-MYC and synergizes with BCL2/BCLxL inhibitor (venetoclax or navitoclax) to kill *MYCN*-amplified tumor cells including neuroblastoma and rhabdomyosarcoma (124, 125). Since the degradation of N-MYC is regulated in part by a kinase-independent function of Aurora-A, CD532, a conformation-disrupting inhibitor of Aurora-A, acts as a more potent N-MYC inhibitor than the kinase activity inhibitor MLN8237 in neuroblastoma (126).

Polo-like kinase 1 (PLK1), a serine/threonine kinase that promotes G2/M-phase transformation, has an elevated expression level in high-risk neuroblastoma and is associated with poor prognosis of patients (127). PLK1 interacts with and phosphorylates FBXW7, promoting auto polyubiquitination and proteasomal degradation of FBXW7, which counteracts FBXW7-mediated degradation of N-MYC (128). In turn, stabilized N-MYC directly enhances the transcription of *PLK1*, forming a positive feedforward regulatory loop that reinforces the progress of *MYCN*-driven cancers. Inhibitors of *PLK1*, such as BI6727 and BI2356, preferentially trigger apoptosis of *MYCN*-amplified neuroblastoma and small cell lung cancer, and this therapeutic efficacy is synergistically enhanced by combined use with antagonists of anti-apoptotic B cell lymphoma 2 (BCL2) (128). UME103 and 9b, two novel dual PLK1 and BRD4 inhibitors, show better antitumor activity by inhibiting the transcription of *MYCN* gene and promoting the degradation of N-MYC protein (129, 130).

Ubiquitin-specific protease 7 (USP7) regulates the stability and activity of N-MYC in neuroblastoma (131). USP7 directly binds to N-MYC, deubiquitinates it, which preventing

degradation of N-MYC by the 26S proteasome. The expression of USP7 is enhanced in patients of neuroblastoma with poorer prognosis. A small molecular inhibitor of USP's deubiquitinase activity, P22077, destabilizes N-MYC, thereby markedly repressing the growth of *MYCN*-amplified human neuroblastoma cell lines in xenograft mouse models (131). Novel, selective inhibitors of USP7, USP7-055, and USP7-797, have been developed recently for tumor therapy including *MYCN*-amplified neuroblastoma (132).

NCYM, A CIS-ANTISENSE GENE OF *MYCN*

An interesting feature of *MYCN* gene is its cis-antisense transcript called *NCYM*. NCYM was initially recognized as a large non-coding RNA (133, 134), while recent studies indicate it encodes a *de novo* evolved protein that promotes tumor progression (135). The transcription of *NCYM* begins from intron 1 of the *MYCN* gene in the opposite direction to that of the *MYCN*, ultimately generating NCYM protein with 109 amino acids (**Figure 2**) (135). As a cis-antisense gene of *MYCN*, *NCYM* is always co-amplified with *MYCN* (136). Both coding and noncoding transcripts of *NCYM* contribute to higher N-MYC expression. NCYM stabilizes N-MYC protein by inhibiting the activity of GSK3β, thereby preventing phosphodegron-mediated N-MYC degradation (135). Noncoding transcript variants of *NCYM* may reinforce *MYCN* translation *via* expelling exon 1b through alternative splicing or promoter shift (136). MYCN stimulates transcription of both *NCYM* and *MYCN*, forming a positive regulatory loop and leading to high expression of both genes (137).

NVP-BEZ235, a dual inhibitor of both phosphoinositide 3-kinase (PI3K) and mTOR, promotes the degradation of N-MYC by GSK3β activation and effectively decreases tumor burden in the *MYCN* transgenic mouse. In contrast, NVP-BEZ235 cannot prolong the survival of the *MYCN*/*NCYM* double transgenic mice (135). This might be related to the N-MYC-independent functions of NCYM, *e.g.*, NCYM-mediated inhibition of GSK3β also lead to the stabilization of β-catenin, which promotes bladder cancer progression (138); NCYM promotes generation of MYC-nicks, cytoplasmic cleavage products of N-MYC and C-MYC, which inhibits apoptosis and enhances cancer cell migration (139). TAp63, an isoform of *p63* protein and a *p53* family protein, suppresses *MYCN*/*NCYM* bidirectional transcription, repressing neuroblastoma growth (140). Thus, the implication of *NCYM* gene in *MYCN*-driven tumors increases complexity and contributes to treatment resistance.

SOMATIC MUTATION OF *MYCN*

In addition to deregulated expression of N-MYC due to gene amplification or dysregulation at mRNA and protein levels, a recurrent somatic mutation, proline 44 to leucine (P44L) (**Figure 1A**), is identified in various tumors (141), including, glioma (142), neoplastic cysts of the pancreas (143), medulloblastoma (144), neuroblastoma (145), Wilms tumor (67), skin basal cell carcinoma (146), T-lineage acute lymphoblastic leukemia (147), NUT midline carcinoma (148), Ovarian mesonephric-like adenocarcinoma (149). Notably, P44L mutation of N-MYC has occurred in 1.7% of high-risk neuroblastoma without *MYCN* amplification (145). Since the frequent occurrence of P44L switch in different cancers, this mutation has long been assumed as an activating one, but it has not been functionally or biochemically characterized until recently (28). KE Mengwasser compared the function of P44L mutant with the wild type N-MYC in terms of promoting proliferation, and they found that P44L N-MYC mutant displayed 2- and 4.5-fold higher log2-fold-change in pancreas cells and breast cells, respectively (150). Similarly, Liu et al. observed a modest but significantly shorter latency for the induction of highly penetrant T-lineage leukemia in P44L N-MYC expressing cells than that of wild-type N-MYC expressing cells (147). These evidences solidly confirm that P44L N-MYC is indeed an activating mutation.

Mechanistically, as P44L mutation site locates adjacent to the conserved phosphor-degron sites recognized by E3 ubiquitin ligases FBXW7 and HUWE1 (**Figure 1A**), a hypothesis was proposed in which P44L mutation could perturb the interaction between these ligases and N-MYC substrate, therefore, prevented N-MYC degradation and enhanced oncogenicity (147). Consistently, Liu et al. show that the degradation of the N-MYC protein is significantly delayed in the P44L mutated type than that of the wild type after the cells are treated with cycloheximide to block protein translation (147). However, Bonilla et al. display that the interacting with FBXW7 is not affected by the P44L mutation, instead, the autoubiquitination of FBXW7 is increased in the presence of P44L mutation, suggesting a different mechanism for the enhanced stability of P44L N-MYC (146). Furthermore, the P44L mutation is associated with increased mRNA levels of *MYCN* in neuroblastoma (145). A previous study shows that MYCN can be directly recruited to the intron1 region of its own gene which contains two putative E-box sites and thus promotes its own transcription in neuroblastoma cells (151). Considering this positive auto-regulatory loop, it is possible that P44L mutation enhances *MYCN* mRNA level through the auto-activating mechanism with the more stable form of N-MYC protein.

SYNTHETIC LETHAL INTERACTION WITH DEREGULATED *MYCN*

The concept of synthetic lethality means targeting specific targets including proteins and metabolites that are essential for the viability of tumor cells with specific physiology, such as N-MYC overexpression. This strategy can kill cancer cells only while spares normal counterpart. For instance, checkpoint kinase 1 (CHK1) is a key player in the DNA damage checkpoint control, and inhibition of CHK1 sensitizes cells to additional genomic instability (152). Overexpression of N-MYC causes replication stress and DNA damage by the ectopic replication-fork firing, which results in remarkably higher sensitivity of N-MYC overexpressing tumors to CHK1 inhibition, and thereby CKH1

inhibition is synthetic lethal with N-MYC overexpression (153, 154). Similarly, we demonstrate that N-MYC sensitizes neuroblastoma cells to apoptosis induced by various death ligand or DNA-damaging drugs (155, 156). These results indicate targeting DNA repair system or drugs causing DNA damage could be synthetic lethal in *MYCN*-driven tumors. Recent studies reveal various strategies based on N-MYC-mediated synthetic lethality, including glutaminase inhibition or glutamine deprivation (157), BCL2 inhibition (125), eliminating SKP2 complexes (158), kinesin spindle protein (KSP) inhibition (159), G9a inhibition (160), poly (ADP-ribose) polymerase (PARP) inhibition (161, 162).

CONCLUSION AND PERSPECTIVES

Here we describe the regulatory network of *MYCN* expression (**Figure 2**). Multiple mechanisms can cause abnormal level of N-MYC, including gene amplification, enhanced transcription, translation and protein stability. Various therapeutic targets have been found to address N-MYC overexpression based on knowledge of these regulatory mechanisms. However, strategies that globally inhibiting gene expression (such as inhibiting CDK7 and BDR4) has not yet convincingly demonstrated that these inhibitors specifically target tumors with high N-MYC level, nor have these inhibitors reached advanced stages in clinical trials (16). Although directly and specifically targeting N-MYC has not yet been available, promise remains in developing new approaches to effectively treat *MYCN*-driven tumors. For examples, short interfering RNA (siRNA)-mediated silence of *MYCN* induces neurogenesis and inhibits proliferation in neuroblastoma models resistant to retinoic acid (163). Clinical applications of siRNA are developing and the first siRNA-based drug Patisiran (Onpattro) was approved for clinical use to treat transthyretin amyloidosis by the U.S. Food and Drug Administration (FDA) in 2018 (164). In addition, Yoda et al. identify a pyrrole-imidazole polyamide, MYCN-A3, able to directly target *MYCN* amplicons, which specifically reduces copy number and suppresses gene expression of *MYCN* (165).

AUTHOR CONTRIBUTIONS

RL wrote the manuscript. PS drew the cartoon figures. ZW and CY collected the articles. HC provided the idea and revised the manuscript. All authors contributed to the article and approved the submitted version.

FUNDING

This research was supported by the National Key Research and Development Program of China (2016YFC1302204, 2017YFC1308601), the National Natural Science Foundation of China (81872071, 81672502), the Natural Science Foundation of Chongqing (cstc2019jcyj-zdxmX0033), and Chongqing University Innovation Team Building Program funded projects (CXTDX201601010).

REFERENCES

1. Kohl NE, Kanda N, Schreck RR, Bruns G, Latt SA, Gilbert F, et al. Transposition and amplification of oncogene-related sequences in human neuroblastomas. *Cell* (1983) 35:359–67. doi: 10.1016/0092-8674(83)90169-1
2. Nau MM, Brooks BJ, Battey J, Sausville E, Gazdar AF, Kirsch IR, et al. L-myc, a new myc-related gene amplified and expressed in human small cell lung cancer. *Nature* (1985) 318:69–73. doi: 10.1038/318069a0
3. Schwab M, Alitalo K, Klempnauer K-H, Varmus HE, Bishop JM, Gilbert F, et al. Amplified DNA with limited homology to myc cellular oncogene is shared by human neuroblastoma cell lines and a neuroblastoma tumour. *Nature* (1983) 305:245–8. doi: 10.1038/305245a0
4. Lin CY, Lovén J, Rahl PB, Paranal RM, Burge CB, Bradner JE, et al. Transcriptional amplification in tumor cells with elevated c-Myc. *Cell* (2012) 151:56–67. doi: 10.1016/j.cell.2012.08.026
5. Lorenzin F, Benary U, Baluapuri A, Walz S, Jung LA, von Eyss B, et al. Different promoter affinities account for specificity in MYC-dependent gene regulation. *eLife* (2016) 5:e15161. doi: 10.7554/eLife.15161
6. Kohl NE, Legouy E, DePinho RA, Nisen PD, Smith RK, Gee CE, et al. Human N-myc is closely related in organization and nucleotide sequence to c-myc. *Nature* (1986) 319:73–7. doi: 10.1038/319073a0
7. Legouy E, DePinho R, Zimmerman K, Collum R, Yancopoulos G, Mitsock L, et al. Structure and expression of the murine L-myc gene. *EMBO J* (1987) 6:3359–66. doi: 10.1002/j.1460-2075.1987.tb02657.x
8. Sarid J, Halazonetis TD, Murphy W, Leder P. Evolutionarily conserved regions of the human c-myc protein can be uncoupled from transforming activity. *Proc Natl Acad Sci* (1987) 84:170–3. doi: 10.1073/pnas.84.1.170
9. Stanton LW, Schwab M, Bishop JM. Nucleotide sequence of the human N-myc gene. *Proc Natl Acad Sci* (1986) 83:1772–6. doi: 10.1073/pnas.83.6.1772
10. McMahon SB, Van Buskirk HA, Dugan KA, Copeland TD, Cole MD. The novel ATM-related protein TRRAP is an essential cofactor for the c-Myc and E2F oncoproteins. *Cell* (1998) 94:363–74. doi: 10.1016/S0092-8674(00)81479-8
11. Fuchs M, Gerber J, Drapkin R, Sif S, Ikura T, Ogryzko V, et al. The p400 complex is an essential E1A transformation target. *Cell* (2001) 106:297–307. doi: 10.1016/S0092-8674(01)00450-0
12. Blackwell TK, Huang J, Ma A, Kretzner L, Alt FW, Eisenman RN, et al. Binding of myc proteins to canonical and noncanonical DNA sequences. *Mol Cell Biol* (1993) 13:5216–24. doi: 10.1128/MCB.13.9.5216
13. Guo J, Li T, Schipper J, Nilson KA, Fordjour FK, Cooper JJ, et al. Sequence specificity incompletely defines the genome-wide occupancy of Myc. *Genome Biol* (2014) 15:482. doi: 10.1186/s13059-014-0482-3
14. Nie Z, Hu G, Wei G, Cui K, Yamane A, Resch W, et al. c-Myc is a universal amplifier of expressed genes in lymphocytes and embryonic stem cells. *Cell* (2012) 151:68–79. doi: 10.1016/j.cell.2012.08.033
15. Zeid R, Lawlor MA, Poon E, Reyes JM, Fulciniti M, Lopez MA, et al. Enhancer invasion shapes MYCN-dependent transcriptional amplification in neuroblastoma. *Nat Genet* (2018) 50:515–23. doi: 10.1038/s41588-018-0044-9
16. Baluapuri A, Wolf E, Eilers M. Target gene-independent functions of MYC oncoproteins. *Nat Rev Mol Cell Biol* (2020) 21:255–67. doi: 10.1038/s41580-020-0215-2
17. Meyer N, Penn LZ. Reflecting on 25 years with MYC. *Nat Rev Cancer* (2008) 8:976–90. doi: 10.1038/nrc2231
18. Dang CV. MYC on the path to cancer. *Cell* (2012) 149:22–35. doi: 10.1016/j.cell.2012.03.003
19. Yoshida GJ. Emerging roles of Myc in stem cell biology and novel tumor therapies. *J Exp Clin Cancer Res* (2018) 37:173. doi: 10.1186/s13046-018-0964-3

20. Yang L, Shi P, Zhao G, Xu J, Peng W, Zhang J, et al. Targeting cancer stem cell pathways for cancer therapy. *Signal Transduct Target Ther* (2020) 5:8. doi: 10.1038/s41392-020-0110-5
21. Izumi H, Kaneko Y, Nakagawara A. The role of MYCN in symmetric vs. asymmetric cell division of human neuroblastoma cells. *Front Oncol* (2020) 10:570815. doi: 10.3389/fonc.2020.570815
22. Malynn BA, de Alboran IM, O'Hagan RC, Bronson R, Davidson L, DePinho RA, et al. N-myc can functionally replace c-myc in murine development, cellular growth, and differentiation. *Genes Dev* (2000) 14:1390–9. doi: 10.1101/gad.14.11.1390
23. Kawauchi D, Robinson G, Uziel T, Gibson P, Rehg J, Gao C, et al. A mouse model of the most aggressive subgroup of human medulloblastoma. *Cancer Cell* (2012) 21:168–80. doi: 10.1016/j.ccr.2011.12.023
24. Vo BT, Wolf E, Kawauchi D, Gebhardt A, Rehg JE, Finkelstein D, et al. The interaction of Myc with Miz1 defines medulloblastoma subgroup identity. *Cancer Cell* (2016) 29:5–16. doi: 10.1016/j.ccell.2015.12.003
25. Beltran H, Prandi D, Mosquera JM, Benelli M, Puca L, Cyrta J, et al. Divergent clonal evolution of castration-resistant neuroendocrine prostate cancer. *Nat Med* (2016) 22:298–305. doi: 10.1038/nm.4045
26. Dammert MA, Brägelmann J, Olsen RR, Böhm S, Monhasery N, Whitney CP, et al. MYC paralog-dependent apoptotic priming orchestrates a spectrum of vulnerabilities in small cell lung cancer. *Nat Commun* (2019) 10:3485. doi: 10.1038/s41467-019-11371-x
27. Massó-Vallés D, Beaulieu M-E, Soucek L. MYC, MYCL, and MYCN as therapeutic targets in lung cancer. *Expert Opin Ther Targets* (2020) 24:101–14. doi: 10.1080/14728222.2020.1723548
28. Rickman DS, Schulte JH, Eilers M. The expanding world of N-MYC–driven tumors. *Cancer Discov* (2018) 8:150–63. doi: 10.1158/2159-8290.CD-17-0273
29. Bjerke L, Mackay A, Nandhabalan M, Burford A, Jury A, Popov S, et al. Histone H3.3 mutations drive pediatric glioblastoma through upregulation of MYCN. *Cancer Discov* (2013) 3:512–9. doi: 10.1158/2159-8290.CD-12-0426
30. Pfister S, Remke M, Benner A, Mendrzyk F, Toedt G, Felsberg J, et al. Outcome prediction in pediatric medulloblastoma based on DNA copy-number aberrations of chromosomes 6q and 17q and the MYC and MYCN loci. *J Clin Oncol* (2009) 27:1627–36. doi: 10.1200/JCO.2008.17.9432
31. Garson JA, McIntyre PG, Kemshead JT. N-MYC amplification in malignant astrocytoma. *Lancet* (1985) 326:718–9. doi: 10.1016/S0140-6736(85)92950-2
32. Berger A, Brady NJ, Bareja R, Robinson B, Conteduca V, Augello MA, et al. N-Myc–mediated epigenetic reprogramming drives lineage plasticity in advanced prostate cancer. *J Clin Invest* (2019) 129:3924–40. doi: 10.1172/JCI127961
33. Mizukami Y, Nonomura A, Takizawa T, Noguchi M, Michigishi T, Nakamura S, et al. N-myc protein expression in human breast carcinoma: prognostic implications. *Anticancer Res* (1995) 15:2899–905. doi: 10.1007/BF02307090
34. Hirvonen H, Hukkanen V, Salmi TT, Pelliniemi T-T, Alitalo R. L-myc and N-myc in hematopoietic malignancies. *Leuk Lymphoma* (1993) 11:197–205. doi: 10.3109/10428199309086996
35. Yang HW, Kutok JL, Lee NH, Piao HY, Fletcher CDM, Kanki JP, et al. Targeted expression of human *MYCN* selectively causes pancreatic neuroendocrine tumors in transgenic zebrafish. *Cancer Res* (2004) 64:7256–62. doi: 10.1158/0008-5472.CAN-04-0931
36. Williams RD, Al-Saadi R, Natrajan R, Mackay A, Chagtai T, Little S, et al. Molecular profiling reveals frequent gain of MYCN and anaplasia-specific loss of 4q and 14q in Wilms tumor. *Genes Chromosomes Cancer* (2011) 50:982–95. doi: 10.1002/gcc.20907
37. Qin X-Y, Suzuki H, Honda M, Okada H, Kaneko S, Inoue I, et al. Prevention of hepatocellular carcinoma by targeting MYCN-positive liver cancer stem cells with acyclic retinoid. *Proc Natl Acad Sci* (2018) 115:4969–74. doi: 10.1073/pnas.1802279115
38. Driman D, Thorner PS, Greenberg ML, Chilton-MacNeill S, Squire J. *MYCN* gene amplification in rhabdomyosarcoma. *Cancer* (1994) 73:2231–7. doi: 10.1002/1097-0142(19940415)73:8<2231::AID-CNCR2820730832>3.0.CO;2-E
39. Baratta MG, Schinzel AC, Zwang Y, Bandopadhayay P, Bowman-Colin C, Kutt J, et al. An in-tumor genetic screen reveals that the BET bromodomain protein, BRD4, is a potential therapeutic target in ovarian carcinoma. *Proc Natl Acad Sci* (2015) 112:232–7. doi: 10.1073/pnas.1422165112
40. Schwab M. *MYCN* in neuronal tumours. *Cancer Lett* (2004) 204:179–87. doi: 10.1016/S0304-3835(03)00454-3
41. Weiss WA, Aldape K, Mohapatra G, Feuerstein BG, Bishop JM. Targeted expression of *MYCN* causes neuroblastoma in transgenic mice. *EMBO J* (1997) 16:2985–95. doi: 10.1093/emboj/16.11.2985
42. Zhu S, Lee J-S, Guo F, Shin J, Perez-Atayde AR, Kutok JL, et al. Activated ALK collaborates with *MYCN* in neuroblastoma pathogenesis. *Cancer Cell* (2012) 21:362–73. doi: 10.1016/j.ccr.2012.02.010
43. Valentijn LJ, Koster J, Haneveld F, Aissa RA, van Sluis P, Broekmans MEC, et al. Functional MYCN signature predicts outcome of neuroblastoma irrespective of *MYCN* amplification. *Proc Natl Acad Sci* (2012) 109:19190–5. doi: 10.1073/pnas.1208215109
44. Chang H-H, Tseng Y-F, Lu M-Y, Yang Y-L, Chou S-W, Lin D-T, et al. MYCN RNA levels determined by quantitative in situ hybridization is better than MYCN gene dosages in predicting the prognosis of neuroblastoma patients. *Mod Pathol* (2020) 33:531–40. doi: 10.1038/s41379-019-0410-x
45. Yang Yi, Zhao J, Zhang Y, Yv Bo, Wang J, Feng H, et al. MYCN Fish combined with immunohistochemistry is a more prognostic factor for neuroblastoma. *Res Square* (2020). doi: 10.21203/rs.3.rs-62365/v1
46. Yoshida GJ. Beyond the Warburg effect: N-Myc contributes to metabolic reprogramming in cancer cells. *Front Oncol* (2020) 10:791. doi: 10.3389/fonc.2020.00791
47. Schwab M. Oncogene amplification in solid tumors. *Semin Cancer Biol* (1999) 9:319–25. doi: 10.1006/scbi.1999.0126
48. Schwab M, Corvi R, Amler LC. N-MYC oncogene amplification: a consequence of genomic instability in human neuroblastoma. *Neuroscientist* (1995) 1:277–85. doi: 10.1177/107385849500100505
49. Hansford LM, Thomas WD, Keating JM, Burkhart CA, Peaston AE, Norris MD, et al. Mechanisms of embryonal tumor initiation: distinct roles for MycN expression and *MYCN* amplification. *Proc Natl Acad Sci U S A* (2004) 101:12664–9. doi: 10.1073/pnas.0401083101
50. Brodeur G, Seeger R, Schwab M, Varmus H, Bishop J. Amplification of N-myc in untreated human neuroblastomas correlates with advanced disease stage. *Science* (1984) 224:1121–4. doi: 10.1126/science.6719137
51. Kohl N, Gee C, Alt F. Activated expression of the N-myc gene in human neuroblastomas and related tumors. *Science* (1984) 226:1335–7. doi: 10.1126/science.6505694
52. Tower J. Developmental gene amplification and origin regulation. *Annu Rev Genet* (2004) 38:273–304. doi: 10.1146/annurev.genet.37.110801.143851
53. Watanabe T, Tanabe H, Horiuchi T. Gene amplification system based on double rolling-circle replication as a model for oncogene-type amplification. *Nucleic Acids Res* (2011) 39:e106–6. doi: 10.1093/nar/gkr442
54. Amler LC, Schwab M. Amplified N-myc in human neuroblastoma cells is often arranged as clustered tandem repeats of differently recombined DNA. *Mol Cell Biol* (1989) 9:4903–13. doi: 10.1128/MCB.9.11.4903
55. Nevim A. Biological and genetic features of neuroblastoma and their clinical importance. *Curr Pediatr Rev* (2018) 14:73–90. doi: 10.2174/1573396314666180129101627
56. Raschellà G, Negroni A, Skorski T, Pucci S, Nieborowska-Skorska M, Romeo A, et al. Inhibition of proliferation by c-myb antisense RNA and oligodeoxynucleotides in transformed neuroectodermal cell lines. *Cancer Res* (1992) 52:4221–6. doi: 10.1097/00002820-199215040-00008
57. Beall EL, Manak JR, Zhou S, Bell M, Lipsick JS, Botchan MR. Role for a Drosophila Myb-containing protein complex in site-specific DNA replication. *Nature* (2002) 420:833–7. doi: 10.1038/nature01228
58. Aygun N, Altungoz O. *MYCN* is amplified during S phase, and c–myb is involved in controlling MYCN expression and amplification in *MYCN* –amplified neuroblastoma cell lines. *Mol Med Rep* (2019) 19:345–61. doi: 10.3892/mmr.2018.9686
59. McGarry TJ, Kirschner MW. Geminin, an inhibitor of DNA replication, is degraded during mitosis. *Cell* (1998) 93:1043–53. doi: 10.1016/S0092-8674(00)81209-X
60. Albertson DG. Gene amplification in cancer. *Trends Genet* (2006) 22:447–55. doi: 10.1016/j.tig.2006.06.007
61. Helmsauer K, Valieva ME, Ali S, Chamorro González R, Schöpflin R, Röefzaad C, et al. Enhancer hijacking determines extrachromosomal circular MYCN amplicon architecture in neuroblastoma. *Nat Commun* (2020) 11:5823. doi: 10.1038/s41467-020-19452-y
62. Morton AR, Dogan-Artun N, Faber ZJ, MacLeod G, Bartels CF, Piazza MS, et al. Functional enhancers shape extrachromosomal oncogene amplifications. *Cell* (2019) 179:1330–41.e13. doi: 10.1016/j.cell.2019.10.039

63. Cohn SL, London WB, Huang D, Katzenstein HM, Salwen HR, Reinhart T, et al. MYCN expression is not prognostic of adverse outcome in advanced-stage neuroblastoma with nonamplified MYCN. *J Clin Oncol* (2000) 18:3604–13. doi: 10.1200/JCO.2000.18.21.3604
64. Henrichsen CN, Chaignat E, Reymond A. Copy number variants, diseases and gene expression. *Hum Mol Genet* (2009) 18:R1–8. doi: 10.1093/hmg/ddp011
65. Law JA, Jacobsen SE. Establishing, maintaining and modifying DNA methylation patterns in plants and animals. *Nat Rev Genet* (2010) 11:204–20. doi: 10.1038/nrg2719
66. Birchler JA, Pal Bhadra M, Bhadra U. Making noise about silence: repression of repeated genes in animals. *Curr Opin Genet Dev* (2000) 10:211–6. doi: 10.1016/S0959-437X(00)00065-4
67. Williams RD, Chagtai T, Alcaide-German M, Apps J, Wegert J, Popov S, et al. Multiple mechanisms of MYCN dysregulation in Wilms tumour. *Oncotarget* (2015) 6:7232–43. doi: 10.18632/oncotarget.3377
68. Zimmerman MW, Durbin AD, He S, Oppel F, Shi H, Tao T, et al. Retinoic acid rewires the adrenergic core regulatory circuitry of neuroblastoma but can be subverted by enhancer hijacking of *MYC* or *MYCN*. *bioRxiv* (2020), 2020.07.23.218834. doi: 10.1101/2020.07.23.218834
69. Zimmerman MW, Liu Y, He S, Durbin AD, Abraham BJ, Easton J, et al. *c-MYC* drives a subset of high-risk pediatric neuroblastomas and is activated through mechanisms including enhancer hijacking and focal enhancer amplification. *Cancer Discov* (2018) 8:320–35. doi: 10.1158/2159-8290.CD-17-0993
70. Lovén J, Hoke HA, Lin CY, Lau A, Orlando DA, Vakoc CR, et al. Selective inhibition of tumor oncogenes by disruption of super-enhancers. *Cell* (2013) 153:320–34. doi: 10.1016/j.cell.2013.03.036
71. Hnisz D, Abraham BJ, Lee TII, Lau A, Saint-André V, Sigova AA, et al. Super-enhancers in the control of cell identity and disease. *Cell* (2013) 155:934–47. doi: 10.1016/j.cell.2013.09.053
72. Kouskouti A, Talianidis I. Histone modifications defining active genes persist after transcriptional and mitotic inactivation. *EMBO J* (2005) 24:347–57. doi: 10.1038/sj.emboj.7600516
73. Sims RJ, Belotserkovskaya R, Reinberg D. Elongation by RNA polymerase II: the short and long of it. *Genes Dev* (2004) 18:2437–68. doi: 10.1101/gad.1235904
74. Yang Z, He N, Zhou Q. Brd4 recruits P-TEFb to chromosomes at late mitosis to promote G1 gene expression and cell cycle progression. *Mol Cell Biol* (2008) 28:967–76. doi: 10.1128/MCB.01020-07
75. Filippakopoulos P, Qi J, Picaud S, Shen Y, Smith WB, Fedorov O, et al. Selective inhibition of BET bromodomains. *Nature* (2010) 468:1067–73. doi: 10.1038/nature09504
76. Henssen A, Althoff K, Odersky A, Beckers A, Koche R, Speleman F, et al. Targeting MYCN-driven transcription by BET-bromodomain inhibition. *Clin Cancer Res* (2016) 22:2470–81. doi: 10.1158/1078-0432.CCR-15-1449
77. Puissant A, Frumm SM, Alexe G, Bassil CF, Qi J, Chanthery YH, et al. Targeting MYCN in neuroblastoma by BET bromodomain inhibition. *Cancer Discov* (2013) 3:308–23. doi: 10.1158/2159-8290.CD-12-0418
78. Mazar J, Gordon C, Naga V, Westmoreland TJ. The killing of human neuroblastoma cells by the small molecule JQ1 occurs in a p53-dependent manner. *Anti-Cancer Agents Med Chem* (2020) 20:1613–25. doi: 10.2174/1871520620666200424123834
79. Maser T, Zagorski J, Kelly S, Ostrander A, Goodyke A, Nagulapally A, et al. The MDM2 inhibitor CGM097 combined with the BET inhibitor OTX015 induces cell death and inhibits tumor growth in models of neuroblastoma. *Cancer Med* (2020) 9:8144–58. doi: 10.1002/cam4.3407
80. Schafer JM, Lehmann BD, Gonzalez-Ericsson PI, Marshall CB, Beeler JS, Redman LN, et al. Targeting MYCN-expressing triple-negative breast cancer with BET and MEK inhibitors. *Sci Transl Med* (2020) 12:eaaw8275. doi: 10.1126/scitranslmed.aaw8275
81. Shiekhattar R, Mermelstein F, Fisher RP, Drapkin R, Dynlacht B, Wessling HC, et al. Cdk-activating kinase complex is a component of human transcription factor TFIIH. *Nature* (1995) 374:283–7. doi: 10.1038/374283a0
82. Peng J, Marshall NF, Price DH. Identification of a cyclin subunit required for the function of Drosophila P-TEFb. *J Biol Chem* (1998) 273:13855–60. doi: 10.1074/jbc.273.22.13855
83. Fisher RP. Secrets of a double agent: CDK7 in cell-cycle control and transcription. *J Cell Sci* (2005) 118:5171–80. doi: 10.1242/jcs.02718
84. Larochelle S, Amat R, Glover-Cutter K, Sansó M, Zhang C, Allen JJ, et al. Cyclin-dependent kinase control of the initiation-to-elongation switch of RNA polymerase II. *Nat Struct Mol Biol* (2012) 19:1108–15. doi: 10.1038/nsmb.2399
85. Chipumuro E, Marco E, Christensen CL, Kwiatkowski N, Zhang T, Hatheway CM, et al. CDK7 inhibition suppresses super-enhancer-linked oncogenic transcription in MYCN-driven cancer. *Cell* (2014) 159:1126–39. doi: 10.1016/j.cell.2014.10.024
86. Poon E, Liang T, Jamin Y, Walz S, Kwok C, Hakkert A, et al. Orally bioavailable CDK9/2 inhibitor shows mechanism-based therapeutic potential in MYCN-driven neuroblastoma. *J Clin Invest* (2020) 130:5875–92. doi: 10.1172/JCI134132
87. Durbin AD, Zimmerman MW, Dharia NV, Abraham BJ, Iniguez AB, Weichert-Leahey N, et al. Selective gene dependencies in MYCN-amplified neuroblastoma include the core transcriptional regulatory circuitry. *Nat Genet* (2018) 50:1240–6. doi: 10.1038/s41588-018-0191-z
88. Tuthill MC, Wada RK, Arimoto JM, Sugino CN, Kanemaru KK, Takeuchi KK, et al. N-myc oncogene expression in neuroblastoma is driven by Sp1 and Sp3. *Mol Genet Metab* (2003) 80:272–80. doi: 10.1016/S1096-7192(03)00133-1
89. Strieder V, Lutz W. E2F proteins regulate MYCN expression in neuroblastomas. *J Biol Chem* (2003) 278:2983–9. doi: 10.1074/jbc.M207596200
90. Zhao Z, Shelton SD, Oviedo A, Baker AL, Bryant CP, Omidvarnia S, et al. The PLAGL2/MYCN/miR-506-3p interplay regulates neuroblastoma cell fate and associates with neuroblastoma progression. *J Exp Clin Cancer Res* (2020) 39:41. doi: 10.1186/s13046-020-1531-2
91. Qin X-Y, Su T, Yu W, Kojima S. Lipid desaturation-associated endoplasmic reticulum stress regulates MYCN gene expression in hepatocellular carcinoma cells. *Cell Death Dis* (2020) 11:66. doi: 10.1038/s41419-020-2257-y
92. Zhao E, Hou J, Cui H. Serine–glycine-one-carbon metabolism: vulnerabilities in MYCN-amplified neuroblastoma. *Oncogenesis* (2020) 9:14. doi: 10.1038/s41389-020-0200-9
93. Guo Y-F, Duan J-J, Wang J, Li L, Wang D, Liu X-Z, et al. Inhibition of the ALDH18A1-MYCN positive feedback loop attenuates *MYCN*-amplified neuroblastoma growth. *Sci Transl Med* (2020) 12:eaax8694. doi: 10.1126/scitranslmed.aax8694
94. Thiele CJ, Reynolds CP, Israel MA. Decreased expression of N-myc precedes retinoic acid-induced morphological differentiation of human neuroblastoma. *Nature* (1985) 313:404–6. doi: 10.1038/313404a0
95. Matthay KK, Reynolds CP, Seeger RC, Shimada H, Adkins ES, Haas-Kogan D, et al. Long-term results for children with high-risk neuroblastoma treated on a randomized trial of myeloablative therapy followed by 13-cis-retinoic acid: a children's oncology group study. *J Clin Oncol* (2009) 27:1007–13. doi: 10.1200/JCO.2007.13.8925
96. Veal GJ, Errington J, Rowbotham SE, Illingworth NA, Malik G, Cole M, et al. Adaptive dosing approaches to the individualization of 13-*Cis*-retinoic acid (Isotretinoin) treatment for children with high-risk neuroblastoma. *Clin Cancer Res* (2013) 19:469–79. doi: 10.1158/1078-0432.CCR-12-2225
97. Levens D. "You don't muck with MYC". *Genes Cancer* (2010) 1:547–54. doi: 10.1177/1947601910377492
98. Siddiqui-Jain A, Grand CL, Bearss DJ, Hurley LH. Direct evidence for a G-quadruplex in a promoter region and its targeting with a small molecule to repress c-MYC transcription. *Proc Natl Acad Sci* (2002) 99:11593–8. doi: 10.1073/pnas.182256799
99. Trajkovski M, Webba da Silva M, Plavec J. Unique structural features of interconverting monomeric and dimeric G-quadruplexes adopted by a sequence from the intron of the N-myc gene. *J Am Chem Soc* (2012) 134:4132–41. doi: 10.1021/ja208483v
100. Dutta D, Debnath M, Müller D, Paul R, Das T, Bessi I, et al. Cell penetrating thiazole peptides inhibit c-MYC expression via site-specific targeting of c-MYC q-quadruplex. *Nucleic Acids Res* (2018) 46:5355–65. doi: 10.1093/nar/gky385
101. González V, Guo K, Hurley L, Sun D. Identification and characterization of nucleolin as a c-myc G-quadruplex-binding protein. *J Biol Chem* (2009) 284:23622–35. doi: 10.1074/jbc.M109.018028
102. Brooks TA, Hurley LH. Targeting MYC expression through G-quadruplexes. *Genes Cancer* (2010) 1:641–9. doi: 10.1177/1947601910377493

103. Hald Ø.H., Olsen L, Gallo-Oller G, Elfman LHM, Løkke C, Kogner P, et al. Inhibitors of ribosome biogenesis repress the growth of MYCN-amplified neuroblastoma. *Oncogene* (2019) 38:2800–13. doi: 10.1038/s41388-018-0611-7
104. Zhao Z, Ma X, Shelton SD, Sung DC, Li M, Hernandez D, et al. A combined gene expression and functional study reveals the crosstalk between N-Myc and differentiation-inducing microRNAs in neuroblastoma cells. *Oncotarget* (2016) 7:79372–87. doi: 10.18632/oncotarget.12676
105. Ooi CY, Carter DR, Liu B, Mayoh C, Beckers A, Lalwani A, et al. Network modeling of microRNA–mRNA interactions in neuroblastoma tumorigenesis identifies miR-204 as a direct inhibitor of MYCN. *Cancer Res* (2018) 78:3122–34. doi: 10.1158/0008-5472.CAN-17-3034
106. Roth SA, Hald Ø.H., Fuchs S, Løkke C, Mikkola I, Flægstad T, et al. MicroRNA-193b-3p represses neuroblastoma cell growth via downregulation of Cyclin D1, MCL-1 and MYCN. *Oncotarget* (2018) 9:18160–79. doi: 10.18632/oncotarget.24793
107. Li J, Jiang X, Li Z, Huang L, Ji D, Yu L, et al. SP1-induced HOXD-AS1 promotes malignant progression of cholangiocarcinoma by regulating miR-520c-3p/MYCN. *Aging (Albany NY)* (2020) 12:16304–25. doi: 10.18632/aging.103660
108. Buechner J, Tømte E, Haug BH, Henriksen JR, Løkke C, Flægstad T, et al. Tumour-suppressor microRNAs let-7 and mir-101 target the proto-oncogene MYCN and inhibit cell proliferation in MYCN-amplified neuroblastoma. *Br J Cancer* (2011) 105:296–303. doi: 10.1038/bjc.2011.220
109. Molenaar JJ, Domingo-Fernández R, Ebus ME, Lindner S, Koster J, Drabek K, et al. LIN28B induces neuroblastoma and enhances MYCN levels via let-7 suppression. *Nat Genet* (2012) 44:1199–206. doi: 10.1038/ng.2436
110. Gu L, Zhang H, He J, Li J, Huang M, Zhou M. MDM2 regulates MYCN mRNA stabilization and translation in human neuroblastoma cells. *Oncogene* (2012) 31:1342–53. doi: 10.1038/onc.2011.343
111. Boon K, Caron HN, van Asperen R, Valentijn L, Hermus M-C, van Sluis P, et al. N-myc enhances the expression of a large set of genes functioning in ribosome biogenesis and protein synthesis. *EMBO J* (2001) 20:1383–93. doi: 10.1093/emboj/20.6.1383
112. Bjornsti M-A, Houghton PJ. The TOR pathway: a target for cancer therapy. *Nat Rev Cancer* (2004) 4:335–48. doi: 10.1038/nrc1362
113. Chen H, Liu H, Qing G. Targeting oncogenic Myc as a strategy for cancer treatment. *Signal Transduct Target Ther* (2018) 3:5. doi: 10.1038/s41392-018-0008-7
114. Dong Y, Gong W, Hua Z, Chen B, Zhao G, Liu Z, et al. Combination of rapamycin and MK-2206 induced cell death via autophagy and necroptosis in MYCN-amplified neuroblastoma cell lines. *Front Pharmacol* (2020) 11:31–1. doi: 10.3389/fphar.2020.00031
115. Zhao X, Heng JI-T, Guardavaccaro D, Jiang R, Pagano M, Guillemot F, et al. The HECT-domain ubiquitin ligase Huwe1 controls neural differentiation and proliferation by destabilizing the N-Myc oncoprotein. *Nat Cell Biol* (2008) 10:643–53. doi: 10.1038/ncb1727
116. Welcker M, Orian A, Jin J, Grim JA, Harper JW, Eisenman RN, et al. The Fbw7 tumor suppressor regulates glycogen synthase kinase 3 phosphorylation-dependent c-Myc protein degradation. *Proc Natl Acad Sci* (2004) 101:9085–90. doi: 10.1073/pnas.0402770101
117. Sjostrom SK, Finn G, Hahn WC, Rowitch DH, Kenney AM. The Cdk1 complex plays a prime role in regulating N-Myc phosphorylation and turnover in neural precursors. *Dev Cell* (2005) 9:327–38. doi: 10.1016/j.devcel.2005.07.014
118. Yeh E, Cunningham M, Arnold H, Chasse D, Monteith T, Ivaldi G, et al. A signalling pathway controlling c-Myc degradation that impacts oncogenic transformation of human cells. *Nat Cell Biol* (2004) 6:308–18. doi: 10.1038/ncb1110
119. Otto T, Horn S, Brockmann M, Eilers U, Schüttrumpf L, Popov N, et al. Stabilization of N-Myc is a critical function of Aurora A in human neuroblastoma. *Cancer Cell* (2009) 15:67–78. doi: 10.1016/j.ccr.2008.12.005
120. Richards MW, Burgess SG, Poon E, Carstensen A, Eilers M, Chesler L, et al. Structural basis of N-Myc binding by Aurora-A and its destabilization by kinase inhibitors. *Proc Natl Acad Sci* (2016) 113:13726–31. doi: 10.1073/pnas.1610626113
121. Shang X, Burlingame SM, Okcu MF, Ge N, Russell HV, Egler RA, et al. *Aurora A* is a negative prognostic factor and a new therapeutic target in human neuroblastoma. *Mol Cancer Ther* (2009) 8:2461–9. doi: 10.1158/1535-7163.MCT-08-0857
122. Brockmann M, Poon E, Berry T, Carstensen A, Deubzer HE, Rycak L, et al. Small molecule inhibitors of Aurora-A induce proteasomal degradation of N-Myc in childhood neuroblastoma. *Cancer Cell* (2013) 24:75–89. doi: 10.1016/j.ccr.2013.05.005
123. Manfredi MG, Ecsedy JA, Meetze KA, Balani SK, Burenkova O, Chen W, et al. Antitumor activity of MLN8054, an orally active small-molecule inhibitor of Aurora A kinase. *Proc Natl Acad Sci* (2007) 104:4106–11. doi: 10.1073/pnas.0608798104
124. Ommer J, Selfe JL, Wachtel M, O'Brien EM, Laubscher D, Roemmele M, et al. Aurora A kinase inhibition destabilizes PAX3-FOXO1 and MYCN and synergizes with navitoclax to induce rhabdomyosarcoma cell death. *Cancer Res* (2020) 80:832–42. doi: 10.1158/0008-5472.CAN-19-1479
125. Ham J, Costa C, Sano R, Lochmann TL, Sennott EM, Patel NU, et al. Exploitation of the apoptosis-primed state of MYCN-amplified neuroblastoma to develop a potent and specific targeted therapy combination. *Cancer Cell* (2016) 29:159–72. doi: 10.1016/j.ccell.2016.01.002
126. Gustafson WC, Meyerowitz JG, Nekritz EA, Chen J, Benes C, Charron E, et al. Drugging MYCN through an allosteric transition in Aurora kinase A. *Cancer Cell* (2014) 26:414–27. doi: 10.1016/j.ccr.2014.07.015
127. Pajtler KW, Sadowski N, Ackermann S, Althoff K, Schoenbeck K, Batzke K, et al. The GSK461364 PLK1 inhibitor exhibits strong antitumoral activity in preclinical neuroblastoma models. *Oncotarget* (2017) 8:6730–41. doi: 10.18632/oncotarget.14268
128. Xiao D, Yue M, Su H, Ren P, Jiang J, Li F, et al. Polo-like kinase-1 regulates Myc stabilization and activates a feedforward circuit promoting tumor cell survival. *Mol Cell* (2016) 64:493–506. doi: 10.1016/j.molcel.2016.09.016
129. Timme N, Han Y, Liu S, Yosief HO, Garcia HD, Bei Y, et al. Small-molecule dual PLK1 and BRD4 inhibitors are active against preclinical models of pediatric solid tumors. *Trans Oncol* (2020) 13:221–32. doi: 10.1016/j.tranon.2019.09.013
130. Wang N-Y, Xu Y, Xiao K-J, Zuo W-Q, Zhu Y-X, Hu R, et al. Design, synthesis, and biological evaluation of 4,5-dihydro-1,2,4 triazolo 4,3-f pteridine derivatives as novel dual-PLK1/BRD4 inhibitors. *Eur J Med Chem* (2020) 191:112152. doi: 10.1016/j.ejmech.2020.112152
131. Tavana O, Li D, Dai C, Lopez G, Banerjee D, Kon N, et al. HAUSP deubiquitinates and stabilizes N-Myc in neuroblastoma. *Nat Med* (2016) 22:1180–6. doi: 10.1038/nm.4180
132. Ohol YM, Sun MT, Cutler G, Leger PR, Hu DX, Biannic B, et al. Novel, selective inhibitors of USP7 uncover multiple mechanisms of antitumor activity *in vitro* and *in vivo*. *Mol Cancer Ther* (2020) 19:1970–80. doi: 10.1158/1535-7163.MCT-20-0184
133. Armstrong B, Krystal G. Isolation and characterization of complementary DNA for N-cym, a gene encoded by the DNA strand opposite to N-myc. *Cell Growth Differ* (1992) 3:385–90. doi: 10.1103/PhysRevE.73.031911
134. Krystal GW, Armstrong BC, Battey JF. N-myc mRNA forms an RNA-RNA duplex with endogenous antisense transcripts. *Mol Cell Biol* (1990) 10:4180–91. doi: 10.1128/MCB.10.8.4180
135. Suenaga Y, Islam SMR, Alagu J, Kaneko Y, Kato M, Tanaka Y, et al. NCYM, a cis-antisense gene of MYCN, encodes a de novo evolved protein that inhibits GSK3β resulting in the stabilization of MYCN in human neuroblastomas. *PloS Genet* (2014) 10:e1003996. doi: 10.1371/journal.pgen.1003996
136. Suenaga Y, Nakatani K, Nakagawara A. De novo evolved gene product NCYM in the pathogenesis and clinical outcome of human neuroblastomas and other cancers. *Jpn J Clin Oncol* (2020) 50:839–46. doi: 10.1093/jjco/hyaa097
137. Kaneko Y, Suenaga Y, Islam SMR, Matsumoto D, Nakamura Y, Ohira M, et al. Functional interplay between MYCN, NCYM, and OCT4 promotes aggressiveness of human neuroblastomas. *Cancer Sci* (2015) 106:840–7. doi: 10.1111/cas.12677
138. Zhu X, Li Y, Zhao S, Zhao S. LSINCT5 activates Wnt/β-catenin signaling by interacting with NCYM to promote bladder cancer progression. *Biochem Biophys Res Commun* (2018) 502:299–306. doi: 10.1016/j.bbrc.2018.05.076
139. Shoji W, Suenaga Y, Kaneko Y, Islam SMR, Alagu J, Yokoi S, et al. NCYM promotes calpain-mediated Myc-nick production in human MYCN-amplified neuroblastoma cells. *Biochem Biophys Res Commun* (2015) 461:501–6. doi: 10.1016/j.bbrc.2015.04.050

140. Suenaga Y, Yamamoto M, Sakuma T, Sasada M, Fukai F, Ohira M, et al. TAp63 represses transcription of MYCN/NCYM gene and its high levels of expression are associated with favorable outcome in neuroblastoma. *Biochem Biophys Res Commun* (2019) 518:311–8. doi: 10.1016/j.bbrc.2019.08.052
141. Forbes SA, Bindal N, Bamford S, Cole C, Kok CY, Beare D, et al. COSMIC: mining complete cancer genomes in the Catalogue of Somatic Mutations in Cancer. *Nucleic Acids Res* (2010) 39:D945–50. doi: 10.1093/nar/gkq929
142. McLendon R, Friedman A, Bigner D, Van Meir EG, Brat DJ, Mastrogianakis GM, et al. Comprehensive genomic characterization defines human glioblastoma genes and core pathways. *Nature* (2008) 455:1061–8. doi: 10.1038/nature07385
143. Wu J, Jiao Y, Dal Molin M, Maitra A, de Wilde RF, Wood LD, et al. Whole-exome sequencing of neoplastic cysts of the pancreas reveals recurrent mutations in components of ubiquitin-dependent pathways. *Proc Natl Acad Sci* (2011) 108:21188–93. doi: 10.1073/pnas.1118046108
144. Jones DTW, Jäger N, Kool M, Zichner T, Hutter B, Sultan M, et al. Dissecting the genomic complexity underlying medulloblastoma. *Nature* (2012) 488:100–5. doi: 10.1038/nature11284
145. Pugh TJ, Morozova O, Attiyeh EF, Asgharzadeh S, Wei JS, Auclair D, et al. The genetic landscape of high-risk neuroblastoma. *Nat Genet* (2013) 45:279–84. doi: 10.1038/ng.2529
146. Bonilla X, Parmentier L, King B, Bezrukov F, Kaya G, Zoete V, et al. Genomic analysis identifies new drivers and progression pathways in skin basal cell carcinoma. *Nat Genet* (2016) 48:398–406. doi: 10.1038/ng.3525
147. Liu Y, Easton J, Shao Y, Maciaszek J, Wang Z, Wilkinson MR, et al. The genomic landscape of pediatric and young adult T-lineage acute lymphoblastic leukemia. *Nat Genet* (2017) 49:1211–8. doi: 10.1038/ng.3909
148. Liao S, Maertens O, Cichowski K, Elledge SJ. Genetic modifiers of the BRD4-NUT dependency of NUT midline carcinoma uncovers a synergism between BETis and CDK4/6is. *Genes Dev* (2018) 32:1188–200. doi: 10.1101/gad.315648.118
149. Dundr P, Gregová M, Němejcová K, Bártů M, Hájková N, Hojný J, et al. Ovarian mesonephric-like adenocarcinoma arising in serous borderline tumor: a case report with complex morphological and molecular analysis. *Diagn Pathol* (2020) 15:91. doi: 10.1186/s13000-020-01012-z
150. Mengwasser KE. *Genetic screening approaches to cancer driver characterization and synthetic lethal target discovery*. Graduate School of Arts & Sciences, Harvard University (2018).
151. Suenaga Y, Kaneko Y, Matsumoto D, Hossain MS, Ozaki T, Nakagawara A. Positive auto-regulation of MYCN in human neuroblastoma. *Biochem Biophys Res Commun* (2009) 390:21–6. doi: 10.1016/j.bbrc.2009.09.044
152. Furnari B, Rhind N, Russell P. Cdc25 mitotic inducer targeted by Chk1 DNA damage checkpoint kinase. *Science* (1997) 277:1495–7. doi: 10.1126/science.277.5331.1495
153. Cole KA, Huggins J, Laquaglia M, Hulderman CE, Russell MR, Bosse K, et al. RNAi screen of the protein kinome identifies checkpoint kinase 1 (CHK1) as a therapeutic target in neuroblastoma. *Proc Natl Acad Sci* (2011) 108:3336–41. doi: 10.1073/pnas.1012351108
154. Höglund A, Nilsson LM, Muralidharan SV, Hasvold LA, Merta P, Rudelius M, et al. Therapeutic implications for the induced levels of Chk1 in Myc-expressing cancer cells. *Clin Cancer Res* (2011) 17:7067–79. doi: 10.1158/1078-0432.CCR-11-1198
155. Li T, Wang L, Ke X-X, Gong X-Y, Wan J-H, Hao X-W, et al. DNA-damaging drug-induced apoptosis sensitized by N-myc in neuroblastoma cells. *Cell Biol Int* (2012) 36:331–7. doi: 10.1042/CBI20110231
156. Cui H, Li T, Ding H-F. Linking of N-Myc to death receptor machinery in neuroblastoma cells. *J Biol Chem* (2005) 280:9474–81. doi: 10.1074/jbc.M410450200
157. Qing G, Li B, Vu A, Skuli N, ZandraW, Liu X, et al. ATF4 regulates MYC-mediated neuroblastoma cell death upon glutamine deprivation. *Cancer Cell* (2012) 22:631–44. doi: 10.1016/j.ccr.2012.09.021
158. Aubry A, Yu T, Bremner R. Preclinical studies reveal MLN4924 is a promising new retinoblastoma therapy. *Cell Death Discovery* (2020) 6:2. doi: 10.1038/s41420-020-0237-8
159. Hansson K, Radke K, Aaltonen K, Saarela J, Manas A, Sjolund J, et al. Therapeutic targeting of KSP in preclinical models of high-risk neuroblastoma. *Sci Trans Med* (2020) 12:eaba4434. doi: 10.1126/scitranslmed.aba4434
160. Bellamy J, Szemes M, Melegh Z, Dallosso A, Kollareddy M, Catchpoole D, et al. Increased efficacy of histone methyltransferase G9a inhibitors against MYCN-amplified neuroblastoma. *Front Oncol* (2020) 10:14. doi: 10.3389/fonc.2020.00818
161. King D, Li XD, Almeida GS, Kwok C, Gravells P, Harrison D, et al. MYCN expression induces replication stress and sensitivity to PARP inhibition in neuroblastoma. *Oncotarget* (2020) 11:2020. 2141–2159. doi: 10.18632/oncotarget.27329
162. Southgate HED, Chen L, Tweddle DA, Curtin NJ. ATR inhibition potentiates PARP inhibitor cytotoxicity in high risk neuroblastoma cell lines by multiple mechanisms. *Cancers* (2020) 12:1095. doi: 10.3390/cancers12051095
163. Maeshima R, Moulding D, Stoker AW, Hart SL. MYCN silencing by RNAi induces neurogenesis and suppresses proliferation in models of neuroblastoma with resistance to retinoic acid. *Nucleic Acid Ther* (2020) 30:237–48. doi: 10.1089/nat.2019.0831
164. Adams D, Gonzalez-Duarte A, O'Riordan WD, Yang C-C, Ueda M, Kristen AV, et al. Patisiran, an RNAi therapeutic, for hereditary transthyretin amyloidosis. *N Engl J Med* (2018) 379:11–21. doi: 10.1056/NEJMoa1716153
165. Yoda H, Inoue T, Shinozaki Y, Lin J, Watanabe T, Koshikawa N, et al. Direct targeting of *MYCN* gene amplification by site-specific DNA alkylation in neuroblastoma. *Cancer Res* (2019) 79:830–40. doi: 10.1158/0008-5472.CAN-18-1198

Conflict of Interest: The authors declare that the research was conducted in the absence of any commercial or financial relationships that could be construed as a potential conflict of interest.

frontiers in Oncology

REVIEW
published: 08 February 2021
doi: 10.3389/fonc.2020.623679

Targeting *MYCN* in Pediatric and Adult Cancers

Zhihui Liu[1]*, *Samuel S. Chen*[1], *Saki Clarke*[1], *Veronica Veschi*[2] and *Carol J. Thiele*[1]*

[1] Pediatric Oncology Branch, Center for Cancer Research, National Cancer Institute, Bethesda, MD, United States,
[2] Department of Surgical, Oncological and Stomatological Sciences, University of Palermo, Palermo, Italy

The deregulation of the *MYC* family of oncogenes, including *c-MYC*, *MYCN* and *MYCL* occurs in many types of cancers, and is frequently associated with a poor prognosis. The majority of functional studies have focused on *c-MYC* due to its broad expression profile in human cancers. The existence of highly conserved functional domains between *MYCN* and *c-MYC* suggests that *MYCN* participates in similar activities. *MYC* encodes a basic helix-loop-helix-leucine zipper (bHLH-LZ) transcription factor (TF) whose central oncogenic role in many human cancers makes it a highly desirable therapeutic target. Historically, as a TF, MYC has been regarded as "undruggable". Thus, recent efforts focus on investigating methods to indirectly target MYC to achieve anti-tumor effects. This review will primarily summarize the recent progress in understanding the function of *MYCN*. It will explore efforts at targeting *MYCN*, including strategies aimed at suppression of *MYCN* transcription, destabilization of MYCN protein, inhibition of *MYCN* transcriptional activity, repression of MYCN targets and utilization of *MYCN* overexpression dependent synthetic lethality.

Keywords: MYCN, Super-enhancer (SE), cofactor, cancer, pediatric cancer, MYC, transcription factor

OPEN ACCESS

Edited by:
Yusuke Suenaga,
Chiba Cancer Center, Japan

Reviewed by:
Robert Eisenman,
Fred Hutchinson Cancer Research Center, United States
Laura Soucek,
Vall d'Hebron Institute of Oncology (VHIO), Spain
Jonathan R. Whitfield,
Vall d'Hebron Institute of Oncology (VHIO), Spain,
in collaboration with reviewer LS

***Correspondence:**
Zhihui Liu
liuzhihu@mail.nih.gov
Carol J. Thiele
thielec@mail.nih.gov

Specialty section:
This article was submitted to Molecular and Cellular Oncology, a section of the journal Frontiers in Oncology

Received: *30 October 2020*
Accepted: *14 December 2020*
Published: *08 February 2021*

Citation:
Liu Z, Chen SS, Clarke S, Veschi V and Thiele CJ (2021) Targeting MYCN in Pediatric and Adult Cancers. Front. Oncol. 10:623679. doi: 10.3389/fonc.2020.623679

INTRODUCTION

MYCN is a member of the *MYC* family of oncogenes, which also includes *c-MYC* and *MYCL* (1). *MYCN* was first reported in 1983 as an amplified gene homologous to v-*myc* in human neuroblastoma (2, 3). Like *c-MYC*, the *MYCN* gene encodes a basic helix-loop-helix-leucine zipper (bHLH-LZ) protein named N-Myc or MYCN. MYCN and c-MYC exhibit high-structural homology, including highly conserved Myc boxes (MB) and a BR-HLH-LZ motif (1, 4, 5). Both MYCN and c-MYC heterodimerize with MAX to bind to an enhancer-box (E-box) sequence with a consensus CAC(C/A)TG motif to regulate gene transcription (1, 4–6). *MYCN* and *c-MYC* differ in their expression patterns and regulation. While *c-MYC* is ubiquitously and highly expressed in most rapidly proliferating cells throughout development and in adult tissues, *MYCN* is preferentially expressed in neural tissues including the forebrain and hindbrain, as well as pre-B cells, cells in the intestine, heart and kidney during embryogenesis (5, 7). Tissue-specific conditional deletions demonstrated that *c-MYC* is necessary for the development and growth of specific hematopoietic cell lineages, crypt progenitor cells in the intestine and many other types of cells where *c-MYC* is expressed (8). *MYCN* but not *c-MYC* is essential during neurogenesis for the rapid expansion of progenitor cells and the inhibition of neuronal differentiation (9). Importantly, investigations at a

gross level indicate that *Mycn* can substitute for *c-Myc* in murine development (10). For example, transgenic expression of *Mycn* from the *c-Myc* locus (*c-Myc*$^{N/N}$) rescues the embryonic lethality associated with the loss of *c-Myc*. Unlike *c-Myc* gene that is expressed throughout lymphocyte development, *Mycn* is only expressed in the precursor stage lymphocyte of development (10, 11), but *Mycn* can replace all *c-Myc* functions required for lymphocyte development in the *c-Myc*$^{N/N}$ mice (10). However, subtle differences between *c-Myc*$^{N/N}$ and normal mice were observed, such as the observation of periodic skeletal muscle dystrophy in some newborn *c-Myc*$^{N/N}$ mice (10). This indicates a general functional similarity between these TFs in regulating certain lineages of murine cell growth and differentiation during embryogenesis and late development.

As TFs, both MYCN and c-MYC directly regulate transcription of genes that are involved in the control of cell growth, the cell cycle, proliferation, survival, apoptosis, pluripotency, self-renewal, DNA replication, RNA biology, metabolism, metastasis, angiogenesis and immune surveillance to play an oncogenic role (5, 12). Most studies indicate that MYC regulates differential gene transcription in the majority of cell types and model systems (4, 12–14). However, instead of regulating differential gene transcription, it has been shown that in B cells, the high levels of c-MYC expression results in a global increase in mRNA levels during the mitogenic stimulation of early B cells (15). Similarly, the expression of high levels of c-MYC in tumor cells leads to an increase in total levels of transcripts in each cell (16). These studies conclude that high levels of c-MYC amplify transcriptional output (15, 16). Further studies and analyses of existing data reveal that MYC dependent changes in global RNA levels may occur only when the cells are cultured under special conditions and/or after prolonged MYC activation. It is possible that a feedback effect from MYC-induced physiological and metabolic changes contributes to a global RNA amplification (4, 12, 13). MYCN interacts with Transcription Factor IIIC complex (TFIIIC), DNA topoisomerase II alpha (TOP2A) and the cohesion complex component RAD21, but in S phase, Aurora-A kinase displaces these interactors from MYCN to block MYCN-dependent promoter release of RNA polymerase II to suppress MYCN-dependent gene transcription (17). MYCN recruits BRCA1 to promoter-proximal regions, stabilizing mRNA de-capping complexes. This enables MYCN to suppress R-loop formation in promoter-proximal regions and prevent MYCN-dependent accumulation of stalled RNAPII, thus, enhancing MYCN transcriptional activation (18). The discovery of this non-canonical transcriptional function of MYCN may explain the discrepancy between universal binding and the small effects on relative and/or absolute mRNA levels of most genes that are bound by the MYC proteins (4, 18).

This review discusses *MYCN* genetic alterations in different types of cancers, the structure and transcriptional function of MYCN and the strategies used to target *MYCN* indirectly.

MYCN Is an Oncogenic Driver in Many Types of Cancers

Deregulation of *MYCN* occurs in both pediatric cancers and adult cancers. *MYCN* amplification has been found in pediatric cancers including neuroblastoma, rhabdomyosarcoma, medulloblastoma, Wilms tumor and retinoblastoma. Amplification of the *MYCN* oncogene is present in 18–20% of all neuroblastomas (40% of high-risk neuroblastomas) and is an adverse prognostic factor (19–23). In alveolar rhabdomyosarcoma, amplification of *MYCN* is present in 25% of cases and overexpression of *MYCN* occurs in 55% of cases (24, 25). Amplification of *MYCN* is observed in 5–10% of medulloblastomas and is associated with poor prognosis (26–28). Copy number gains that include the *MYCN* locus are detected in 12.7% of Wilms tumors and 30.4% of diffuse anaplastic Wilms tumors, and *MYCN* gain is associated with poorer relapse-free and overall survival (29). In retinoblastomas, *MYCN* amplification is present in <5% of patients, and *MYCN* gain is associated with poor prognosis (30, 31). In adult cancers, amplification of *MYCN* is present in 40% of neuroendocrine prostate cancers and 5% of prostate adenocarcinomas (32), 15%-20% of small-cell lung cancers (33, 34) and 17.5% of basal cell carcinomas (35). Overexpression of *MYCN* is present in a subset of T-cell acute lymphoblastic leukemias (36), glioblastoma multiforme (37, 38) and breast cancer (39). Importantly, the amplification or overexpression of *MYCN* in the majority of these adult cancers is found to be associated with a poor prognosis.

To investigate whether *MYCN* functions as an oncogenic driver, genetically engineered mouse models (GEMM) have been generated to express *MYCN* in specific cell lineages. The transgenic expression of *MYCN* in the neural crest lineage of mice or zebrafish alone, or in combination with *LMO1* or activated *ALK* gives rise to neuroblastomas (40–44). The transgenic expression of *MYCN* in murine luminal prostate epithelial cells in combination with *Pten* knockout results in a GEMM model with neuroendocrine prostate cancer formation (45). Mice transplanted with bone marrow expressing *MYCN* developed clonal and transplantable acute myeloid leukemias (46). When neural stem cells (NSCs) from different brain regions are transduced with a protein stabilizing MYCN(T58A) mutation and transplanted into their homotypic regions they give rise to distinct tumors. The transplantation of forbrain MYCN(T58A) NSCs gives rise to gliomas (47), while cerebellum and brain stem MYCN(T58A) NSCs transplants give rise to medulloblastoma and primitive neuroectodermal tumors (47). The enforced expression of *MYCN* in primary cerebellar granule neuron precursors isolated from *Ink4c*(-/-), *p53*(-/-) mice also results in medulloblastomas when transplanted into the brains of immunocompromised mice (48). These studies demonstrate that *MYCN* functions as an oncogene and is capable of driving tumor formation in cells with different lineage specific genetic programs to give rise to distinct tumor types. Thus, the inhibition of *MYCN* will be an important anti-tumor therapeutic strategy in many different human cancers with aberrantly over-expressed *MYCN*.

MYCN Structure: Critical Regions That Mediate Protein-Protein Interaction and Transcriptional Activity

MYCN is composed of 464 amino acids (AA) with several functional domains (**Figure 1**) derived from sequence homology to known c-MYC protein functional domains (NCBI reference number of MYCN, NP_001280157.1 verse c-MYC, CAA25015.2) and mutagenesis analyses (1, 6). The N-terminal transcriptional

regulation domain contains two highly conserved regions known as Myc Homology Box (MB), MBI and MBII. The central region contains 3 more MBs with a nuclear localization signal that overlaps MBIV. The C-terminal basic region (BR) is involved in DNA binding while the HLH-LZ heterodimerizes with Max (1). Many critical proteins regulating various biological processes do not have unique structures, but contain intrinsically disordered regions (IDRs), making this structural region extremely dynamic (49, 50). IDRs are involved in modulation of the specificity or affinity of protein binding interactions (49, 50). The IDRs in a protein can undergo characteristic disorder-to-order transitions upon interactions with specific binding partners and/or through post-translational modifications (49). Using a protein intrinsic disorder region prediction tool PONDR (http://www.pondr.com/) (51) to analyze MYCN, we find that the majority of MYCN residues tend to form broad disordered regions (**Figure 1**), which indicates that MYCN has the potential to bind to many different partners. Moreover, the intrinsically disordered character of MYCN suggests that using it as a direct drug target would be challenging due to its structural flexibility.

Critical regions within MYC/MYCN proteins have been implicated in regulating protein stability. Residues Ser62 (S62) and Thr58 (T58) within MBI are critical phosphorylation sites for MYC/MYCN protein stability during cell cycle progression. As growth factors stimulate cell progression through the cell cycle, protein stability is tightly regulated. Phosphorylation at S62 of MYCN protein is mediated *via* CDK1, which stabilizes MYCN and primes T58 for phosphorylation by GSK3β. GSK3β is repressed by phosphatidylinositol 3-kinase (PI3K) and AKT kinase signaling (52–57). Dephosphorylation of MYC-S62 *via* protein phosphatase 2A (PP2A) enables E3 ligase FBXW7 binding to phosphorylated MYC-T58, targeting it for ubiquitination and subsequent degradation by the proteasome (58, 59). The regulation of MYCN protein stability is cell-cycle dependent. In normal neuronal progenitors, CDK1 phosphorylates MYCN protein at S62 in G1-phase. As cells enter M-phase, signaling by growth factors declines leading to activation of GSK3β enabling phosphorylation of MYCN (T58) which leads to its degradation (52). Two additional ubiquitin ligases, TRIM32 and HUWE1, are involved in regulation of MYCN degradation. During late M-phase, the ubiquitin ligase TRIM32 is bound to the mitotic spindle pole apparatus in conjunction with MYCN, contributing to its ubiquitination and degradation (60). HUWE1, a HECT-domain E3 ubiquitin ligase, binds to MYCN and primes it for MYCN-K48-linked polyubiquitination and proteasomal-mediated degradation (61, 62).

MYCN protein degradation is antagonized through interactions with different proteins at distinct MYCN regions (**Figure 1**). Aurora A kinase (AURKA) associates with the mitotic spindle poles and

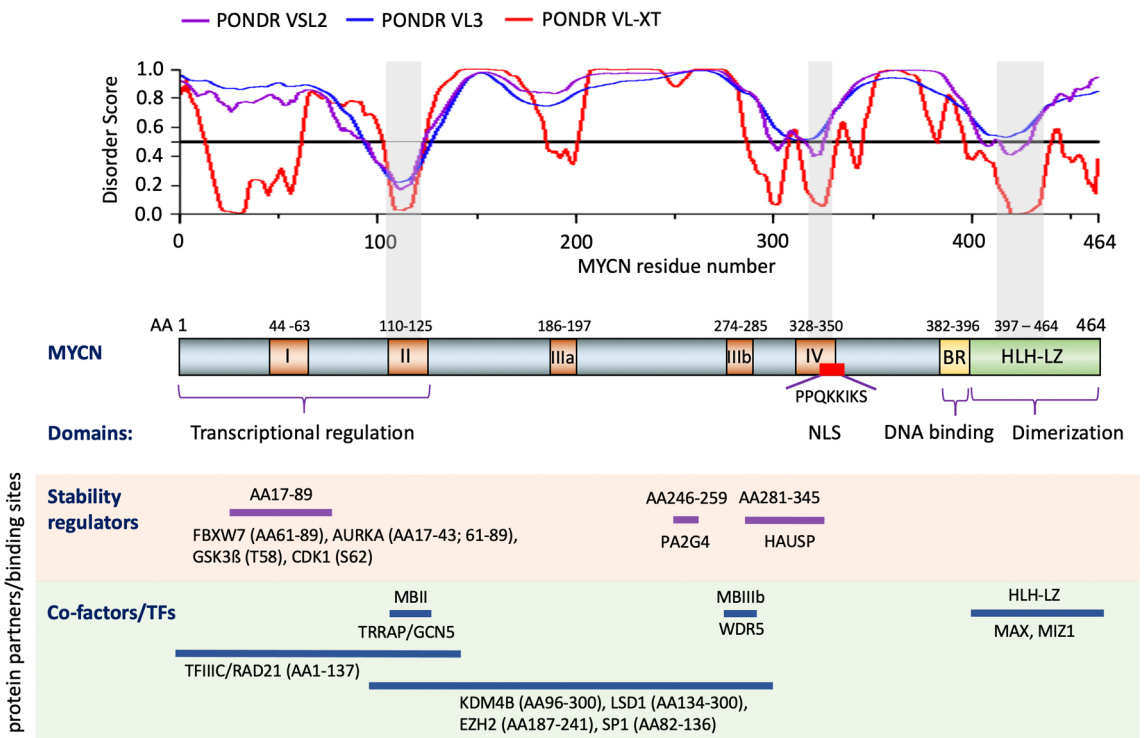

FIGURE 1 | Structure and functional domains of MYCN. Three predictors of the intrinsically disordered region prediction tool PONDR are used to identify intrinsically disordered regions of MYCN (top section). Functional domains of MYCN defined by comparing c-MYC and mutagenesis assay (middle section). Examples of known MYCN protein partners and the regions of MYCN that contributed to the interaction (bottom section). Notes: Color boxes on the MYCN protein diagram: brown box, Myc homology Box (MB) I-IV; yellow box, Basic Region (BR); green box, Helix-Loop-Helix-Leucine Zipper (HLH-LZ); red box, nuclear localization signal (NLS). Gray shade box on the disorder score graph and MYCN protein diagram, regions of MYCN with relatively low disorder score. AA: amino acid.

interacts with the N-terminus of MYCN in cells over-expressing MYCN and in this way interferes with FBXW7-mediated degradation leading to MYCN stabilization (17, 56, 63). The ubiquitin-specific protease HAUSP binds to a partially overlapping region of MBIII and MBIV in MYCN, but not c-MYC (**Figure 1**), to specifically deubiquitinate MYCN, which results in MYCN protein stabilization (64). The proliferation-associated 2AG4 protein (PA2G4) directly binds to and stabilizes MYCN by protecting it from ubiquitin-mediated proteasomal degradation (65). Co-immunoprecipitation results show that a MYCN deletion mutant (AA82–254) binds strongly to PA2G4, and further studies show that a 14 AA MYCN oligopeptide (AA246–259) sequence contributes to this protein-protein interaction (65). Additionally, MYCN has been found to be methylated at R160, R238 and R242; protein arginine methyltransferase 5 (PRMT5) physically interacts with MYCN and increases MYCN protein stability, possibly by methylating MYCN at R242 (66). The identification of different signaling pathways and proteins regulating MYCN protein stability provides additional modes for indirect targeting of MYCN.

TFs, co-repressors and co-activators interact with different regions of MYCN (**Figure 1**), enabling MYCN to activate or repress gene transcription. MYC family proteins directly interact with MAX through HLH-LZ to form a heterodimer and activate transcription by binding to E-box elements (1, 6). Activation involves the recruitment of multiple coactivators and protein complexes to E-box elements. The TIP60 acetyltransferase complex and the histone acetyltransferase GCN5 are bound to MYC indirectly through the TRRAP adaptor protein that interacts with MBII of the MYC protein (67–70). Two other proteins, TIP48 and TIP49, found in the TIP60 complex, are involved in chromatin remodeling and bind to the N-terminus of MYCN (67). Recent studies show that target gene recognition by c-MYC and MYCN depends on its interaction with the histone H3-K4-methyl-associated protein WDR5 and their interaction is mediated through the MBIIIb region of c-MYC (71, 72). MYCN interacts with the H3K9me3/me2 demethylase KDM4B through the region between AA96-300 and when overexpressed MYCN recruits KDM4B to E-box regions to decrease H3K9me3 levels (73). Thus, MYCN may also activate gene transcription by relieving transcriptional repression. Moreover, MYCN AA1-137 also interacts with TFIIIC and RAD21 to regulate the pause release of RNA Polymerase II (17). BRCA1 interacts with MYCN and enables MYCN to suppress R-loop formation in promoter-proximal regions, thus enhancing transcription (18). When MYCN functions as a transcriptional repressor, it interacts with SP1 and MIZ1 to repress gene transcription (74–77). The region between MYCN AA82-136 that includes the MBII domain specifically interacts with SP1 in pull down experiments, whereas MYCN AA400-464 that includes the HLH-LZ domain interacts with MIZ1 (74). These MYCN/SP1/MIZ1 interactions repress gene transcription by recruiting HDAC1 (74). MYCN, *via* MBIII, associates with EZH2, a methyltransferase and member of the polycomb repressor complex 2, to suppress gene transcription (78). Similarly, MYCN physically binds lysine-specific histone demethylase 1A (KDM1A/LSD1) through MBIII to repress gene transcription (79). The above studies show how MYCN interacts with the epigenome to regulate gene transcription.

Targeting *MYCN* Transcription

Many mechanisms have been identified to be involved in the transcriptional regulation of *MYCN* (**Figure 2**). Soon after the discovery of the *MYCN* gene, it was found that retinoic acid (RA) treatment of NB cells resulted in a down-regulation of *MYCN* expression at the mRNA level, and this preceded cell cycle arrest and implementation of a differentiation program (80). This indicated that *MYCN* down-regulation, at least partially, contributes to the biological effect of RA on NB cells. A classic RA response element (RARE) was not implicated in RA regulation of *MYCN* transcription, as studies showed that RA exerts its effects across multiple regulatory regions within the *MYCN* promoter, distally or even on different chromosomes (81). Retinoid repression of MYCN transcription was a major motivation for the inclusion of 13 cis-retinoic acid during the consolidation phase of treatment for high-risk neuroblastomas (82). Retinoid regulation of *MYCN* represents one of the first strategies developed to target *MYCN* gene transcription and provides an example of indirect targeting of *MYCN*.

Gene transcription is mediated by cis-regulatory elements such as enhancers and promoters. Enhancers are distal regulatory elements in the genome that play an important role in driving cell-type-specific gene expression and are frequently mis-regulated in cancer (83, 84). Super-enhancers (SEs) are composed of a cluster of enhancers that are central to the maintenance of cell identity in normal development and disease (85). SEs were found to be associated with various oncogenic molecules including both *c-MYC* and *MYCN*; this makes them putative therapeutic targets for cancer therapy (86–89). Histone deacetylases (HDACs) have an important function in regulating both DNA packaging in chromatin and gene transcription. Treatment of NB cells with HDAC inhibitors such as MS-275, BL1521 or SAHA resulted in a decrease in *MYCN* mRNA levels accompanied by cell apoptosis (90–92). Although not directly demonstrated, recent studies have shown that HDAC inhibition results in enhancer remodeling and suppression of oncogenic SEs possibly through disruption of normal chromatin-looping and TFs depletion on the SEs (93, 94). This may be involved in the HDAC inhibitor mediated repression of *MYCN* transcription (**Figure 2**).

MYC-driven tumors are especially sensitive to inhibition of BET bromodomain containing proteins (BRD1–4) (95). BRD4 belongs to family of proteins that contain variable numbers of bromodomains and a central ET domain and function as chromatin "readers" by binding to acetylated lysine residues (**Figure 2**). BRD4 has also been implicated in regulating RNA-PolII transcriptional activity (96). BET inhibitors downregulate *c-MYC* transcription, suppress *MYC*-dependent target genes and inhibit myeloma cell proliferation (95). An unbiased screen of 673 genetically characterized tumor-derived cell lines shows that neuroblastoma cell lines with *MYCN* amplification are more sensitive to JQ1 treatment compared to *MYCN*-wild-type tumors. BRD4 knock-down phenocopied these effects, indicating that BRD4

functions as a transcriptional regulator of *MYCN*. Importantly, BET bromodomain-mediated inhibition of *MYCN* suppresses neuroblastoma growth both *in vitro* and *in vivo* (97). Similarly, OTX015 (Oncoethix), a small molecule that prevents BRD2/3/4 from binding to acetylated histones, also represses *MYCN* transcription. This study showed that BRD4 binds to super-enhancers (SEs) and *MYCN* target genes, while OTX015 treatment disrupts BRD4 binding and transcription of *MYCN* as well as its target genes (98), which is consistent with the finding that bromodomain inhibitor treatment selectively inhibits oncogenes by disrupting their SEs (99). Importantly, bromodomain and extra-terminal domain inhibitor (BETi), GSK525762, is under phase I clinical trial for solid tumors including NB (100). In addition to *MYC*, many tumor-associated genes such as *RUNX1, FOSL2, BCL3* and *ID2* are driven by SEs in diverse tumor types (99). However, SEs drive many cell identity genes essential for normal cell development, such as Oct4, Sox2 and Nanog in embryonic stem cells (101), so as with many cytotoxic agents a therapeutic window is needed when using BETi for the treatment of cancer patients to minimize side effects. Recent studies showed that the combination of a

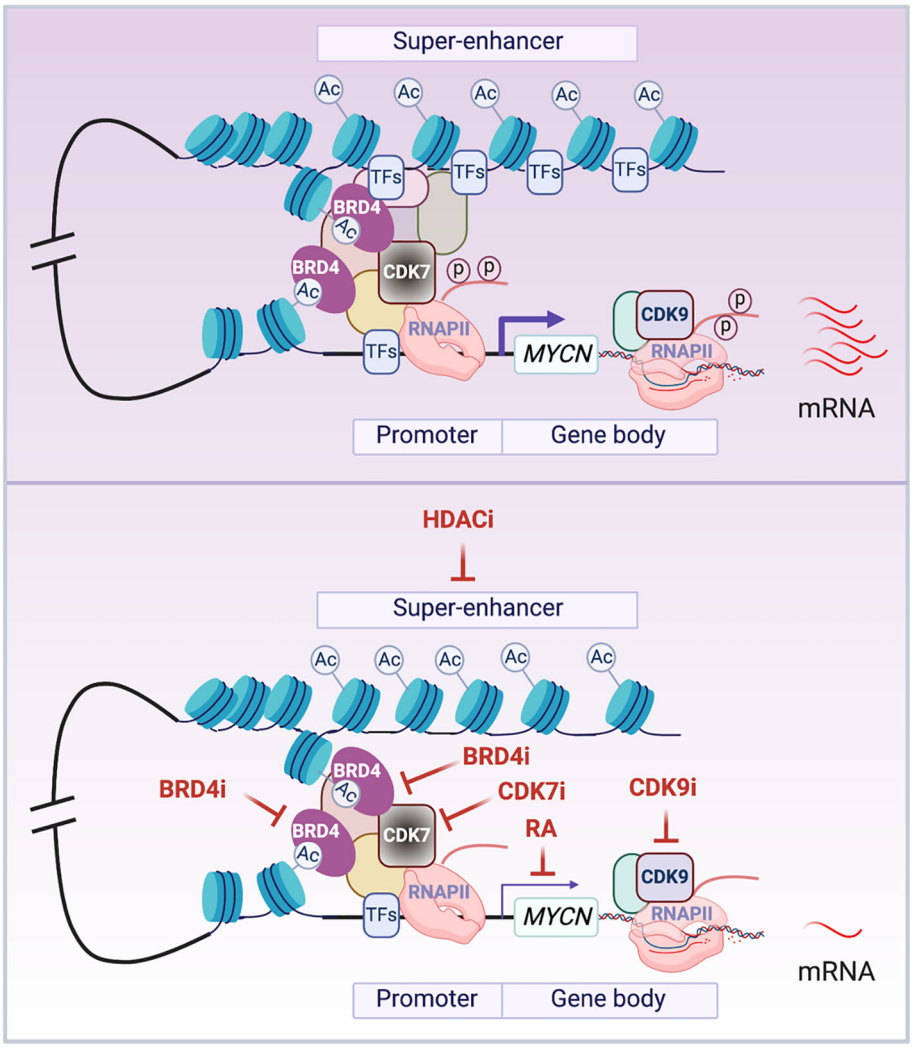

FIGURE 2 | Transcriptional regulation of *MYCN*. The schematic illustrates the presumed looping between the super-enhancer (SE) and the promoter of *MYCN* gene. In cancer cells, MYCN is driven by SEs that are marked by stretches of acetylated lysine 27 of histone 3 (H3K27Ac). BRD4 is a chromatin 'reader' that binds to acetylated lysine residues (AcK) and activates *MYCN* transcription. CDK7 is a TFIIH subunit that phosphorylates the carboxy-terminal domain of RNA Pol II (RNAPII) to initiate *MYCN* gene transcription. CDK9 is a pTEFb subunit that phosphorylates the carboxy-terminal domain of RNAPII to regulate *MYCN* transcriptional elongation. The enrichment or activation of these components of the transcriptional machinery in cancer cells results in aberrantly elevated transcription of *MYCN* (top panel). The treatment of cells with HDAC inhibitors (HDACi) inactivates *MYCN* SEs possibly through disrupting normal looping and depleting transcription factors (TFs) that bind to the SEs; BRD4 inhibitors (BRD4i) impact the 'reader' function of BRD4 to inactivate *MYCN* gene transcription; CDK7 inhibitors (CDK7i) and CDK9 inhibitors (CDK9i) treatment impedes the phosphorylation of RNAPII to inhibit *MYCN* gene transcription initiation and elongation; RA treatment inactivates *MYCN* transcription in a RA response element independent manner (bottom panel). Notes: circled 'Ac' represents H3K27Ac; circled 'p' represents phosphate at the RNAPII tail.

bromodomain inhibitor with a CDK7 inhibitor, an AURKA inhibitor or an HDAC inhibitor is significantly more effective in suppressing *MYCN*-driven NB tumor growth than either drug alone (88, 102, 103). This highlights the importance of combinatorial therapeutic approaches for cancer treatment.

To regulate gene transcription, the RNA polymerase II (RNAPII) transcription initiation apparatus needs to be recruited to promoters by specific DNA binding transcription factors. Promoter-proximal pausing of RNAPII is a post-initiation regulatory event, and c-Myc plays a key role in release of Pol II at many actively transcribed genes in ES cells (104). Cyclin-dependent kinases (CDKs) are important in regulating the transcription cycle of RNAPII. The TFIIH subunit CDK7 and the pTEFb subunit CDK9 phosphorylate the carboxy-terminal domain of RNAPII, facilitating efficient transcriptional initiation, pause release and elongation. This suggests that the inhibition of these CDKs would be expected to block *MYC*-driven transcriptional amplification. Indeed, THZ1, a covalent inhibitor of CDK7, was found to selectively target *MYCN*-amplified NB cells, leading to global repression of *MYCN*-dependent transcriptional amplification and reductions in expression of SE-associated oncogenic drivers including *MYCN* itself and suppression of NB tumor xenograft growth (87). CYC065, an inhibitor of CDK9 and CDK2, was found to selectively target MYCN-amplified NB cells by leading to a selective loss of nascent MYCN transcription (105). These studies indicate that the inhibition of CDK7 or CDK9 can be exploited to disrupt aberrant *MYCN*-driven transcription and to repress *MYCN* gene transcription as a therapeutic for *MYCN*-driven cancers (**Figure 2**).

DNA G-quadruplexes (G4s) are noncanonical DNA structures that are formed by guanine-rich DNA sequences. They often occur in the promoter regions of oncogenes and regulate their expression (106–108). An early study identified a specific G4 structure formed in the *c-MYC* promoter region. Although a cationic porphyrin TmPyP4, which binds non-selectively to G4s *in vitro* was able to inhibit the transcription of c-*MYC* (108), a recent study identified a small molecule DC-34 that more specifically binds to the c-MYC G4 *in vitro*. In a G4-dependent mechanism, DC-34 plays a more potent and selective role in downregulating *MYC* gene transcription compared to other G4 containing oncogenes in leukemia cells. Moreover, the treatment of cancer cells with DC-34 results in a G0-G1 arrest and a reduction of cell viability (106). Although not yet reported, the identification and targeting of G4s within the *MYCN* promoter and regulatory regions would be another approach to inhibit *MYCN* gene transcription.

Many TFs have been validated as oncogenes in human cancers and their dysregulated transcriptional programs result in a high dependency of cancer cells on these gene expression regulators (109). Importantly, RA, inhibitors of HDACs, BET bromodomain containing proteins, CDK7, CDK9 and small molecules that bind to G4s have been demonstrated to be effective for the treatment of many types of cancers by targeting their dysregulated transcriptional programs (109, 110). Thus, targeting *MYCN* at branch points involved in its oncogenic regulation of transcription (**Figure 2**) is an important therapeutic approach for *MYCN*-driven cancers.

Targeting MYCN Protein Stability

MYCN is a short-lived protein whose stability is tightly regulated by different signaling pathways that target it for ubiquitin-mediated degradation by the proteasome (52, 55, 111) (**Figure 3**). A major signaling pathway affecting MYCN protein stability occurs upon activation of PI3K. PI3K activates Akt which phosphorylates GSK3ß, suppressing GSK3ß kinase activity. This results in decreased phosphorylation of MYCN-T58 which is critical for targeted degradation by the proteasome (55) (**Figure 3**). As expected, inhibitors of PI3K destabilize the MYCN protein and suppress tumor growth in the TH-MYCN GEMM NB model (53, 112). In NB cells, AURKA interacts with MYCN by interfering with the FBXW7 subunit of the ubiquitin protein ligase complex to impede MYCN ubiquitination and subsequent degradation (56) (**Figure 3**). Treatment with AURKA inhibitors decreases MYCN protein levels resulting in suppression of NB tumor growth, making AURKA a suitable target for *MYCN*-driven cancers (32, 113–117). Due to the promising preclinical results, the oral AURKA inhibitor MLN8237 is under clinical evaluation for multiple cancers including relapsed NB (118). PLK1 is a serine/threonine kinase formally known as the polo-like kinase. The PLK1 inhibitor BI 2356 exhibits strong antitumor activity in NB cells *in vitro* and *in vivo* (119). PLK1 does not directly bind to the MYCN protein. Rather, it increases MYCN protein stability by destabilizing the FBXW7 ubiquitin ligase complex to counteract FBXW7-mediated degradation of MYCN (120) (**Figure 3**). Importantly, *MYCN*-amplified tumor cells in neuroblastoma and small cell lung cancer are more sensitive to treatment with PLK1 inhibitors than tumors with normal MYCN copy number, indicating that PLK1 inhibitors are potential therapeutics for *MYCN*-overexpressing cancers (120).

Components of the proteasome targeting and degrading system contribute to MYCN protein regulation. The ubiquitin-specific peptidase HAUSP (also known as USP7) binds to and deubiquitinates MYCN leading to its stabilization (64) (**Figure 3**). HAUSP is highly expressed in tumors from NB patients with poor prognoses. Silencing of HAUSP expression in NB cells destabilizes MYCN and results in an inhibition of MYCN mediated functions. Importantly, the HAUSP inhibitor P22077 markedly suppresses the growth of MYCN-amplified human neuroblastoma cell lines in xenograft mouse models (64).

Although first identified as an RNA binding protein, the proliferation associated 2G4 protein, PA2G4, directly binds and stabilizes MYCN by protecting MYCN from proteasomal degradation (65). When PA2G4 is silenced in NB cells using siRNAs or a small molecule inhibitor WS6, MYCN protein levels are markedly reduced (65). WS6 treatment of NB cell lines completely blocked PA2G4-MYCN protein binding, and this competitive chemical inhibition results in a delay of tumorigenesis in the TH-*MYCN* NB mouse model (65).

Protein methylation is a post-translational modification recently identified to regulate protein stability. The protein arginine methyltransferase 5 (PRMT5) interacts with both MYC and MYCN proteins (66, 121). Silencing of PRMT5 in *MYCN*-overexpressing NB cells or *MYC*-driven medulloblastoma cells

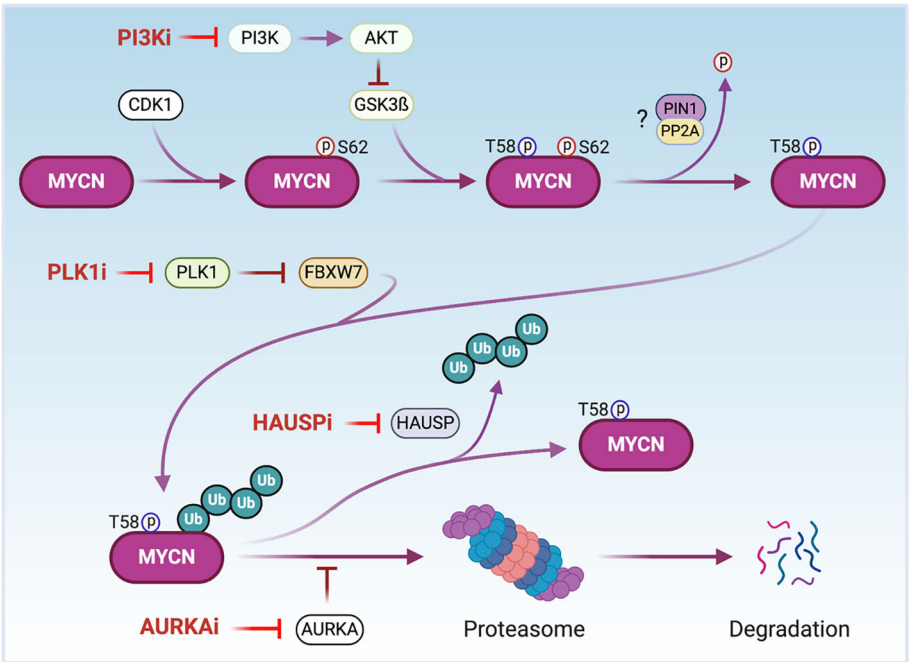

FIGURE 3 | The regulation of MYCN protein stability. CDK1 phosphorylates MYCN at serine 62 (S62) to stabilize MYCN and prime threonine 58 (T58) for phosphorylation *via* GSK3β. AKT phosphorylates GSK3ß inactivating its kinase. After dephosphorylation of S62 possibly through PIN1/PP2A, MYCN is poly-ubiquitinated by the ubiquitin ligase FBXW7 and undergoes proteolytic degradation *via* the proteasome. AURKA binds to and stabilizes phosphorylated and poly-ubiquitinated MYCN to protect MYCN from degradation. PLK1 destabilizes FBXW7 to counteract FBXW7-mediated degradation of MYCN. The ubiquitin-specific protease HAUSP deubiquitinates MYCN to stabilize it. Thus, the treatment of cells with PI3K, AURKA, PLK1 or HAUSP inhibitors (PI3Ki, AURKAi, PLKi or HAUSPi) leads MYCN proteasomal degradation. Notes: circled 'p' represents phosphate; circled 'Ub' represents ubiquitin.

leads to a decrease in MYCN and MYC protein levels and cell growth inhibition (66, 121). Tandem mass spectrometry analysis of immunoprecipitated MYCN protein in NB cells reveals several potential sites of arginine dimethylation on MYCN protein, suggesting that MYCN may be methylated by PRMT5 as a protection from proteasomal degradation (66). Treatment with the PRMT5 inhibitor EPZ015666 results in a decrease of MYC protein levels and medulloblastoma cell growth, which suggests that PRMT5 inhibitors are potential therapeutics for *MYC*- and *MYCN*-driven cancers.

Targeting MYCN Cofactors/Coregulators

We have described critical regions that are needed for MYCN interactions with its cofactors/coregulators in the previous section and in **Figure 1**. As a TF, MYCN cooperates with other TFs to bind to DNA and recruit cofactors/coregulators to activate or repress gene transcription, making these protein partners potential targets to disrupt the transcriptional activity of MYCN (**Figure 4**). The enzymatic activity of many co-regulators makes them attractive drug targets.

The first identified mechanism through which MYCN functions as a TF is *via* heterodimerization with MAX. MYC-MAX complexes recognize E-box DNA sequences, and binding of the heterodimer to gene promoters activates transcription of downstream *MYCN*-related genes. Small-molecule inhibitors of MYC-MAX dimerization illustrate the importance of dimerization to MYC function (**Figure 4**). For instance, the peptidomimetic compound IIA4B20 exerts a strong inhibitory effect on MYC-MAX dimerization and DNA binding to functionally inhibit MYC-induced fibroblast transformation (122). The compound 10058-F4 binds to AA402-409 of MYC, which disrupts MYC-MAX dimerization of either c-MYC or MYCN. The treatment of *MYCN*-amplified NB cells with 10058-F4 leads to neural differentiation (123–125). Another known inhibitor of MYC-MAX dimerization is OmoMYC, a c-MYC derived mutant bHLH-LZ domain protein generated by substituting four amino acids within the c-MYC leucine zipper. When overexpressed, OmoMYC competes with MAX for binding to either c-MYC or MYCN and prevents MYC/MYCN proteins from binding to E-boxes and activating transcription (126, 127). The recently discovered MYC inhibitor 361 (MYCi361) binds to the HLH region of the MYC protein (AA366-378), disrupts MYC/MAX heterodimerization, enhances degradation of both MYC and MYCN, and suppresses MYC-dependent tumor cell growth *in vitro* and *in vivo* (128). The asymmetric polycyclic lactam, KI-MS2-008 stabilizes MAX homodimers, resulting in decreased MYC protein levels (129). Treatment of cancer cells with KI-MS2-008 suppresses *MYC*-dependent tumor growth *in vivo*. This is another example whereby altering the ability of MAX

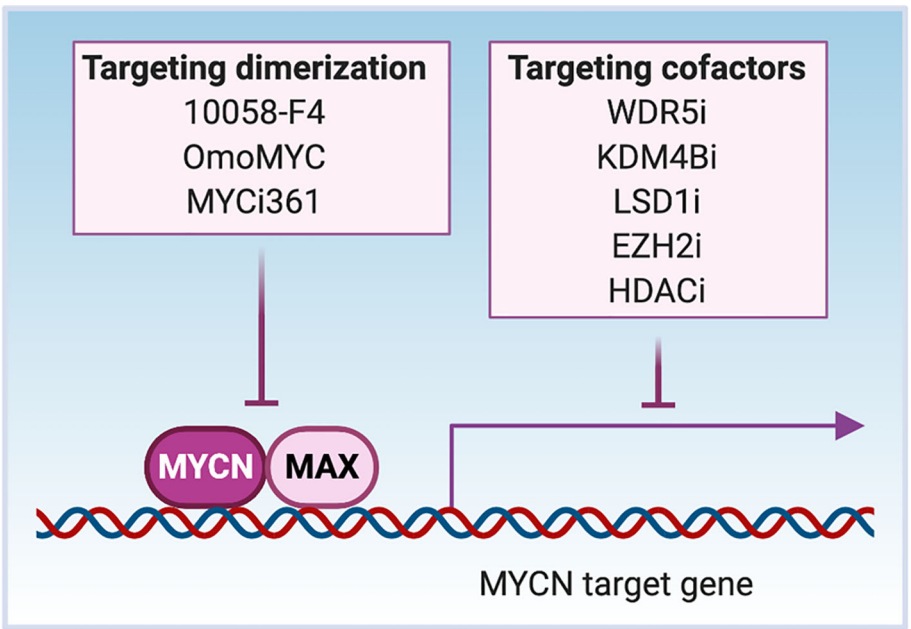

FIGURE 4 | Targeting MYCN transcriptional activity. MYCN heterodimerizes with MAX to bind to the cis-genomic elements in DNA. MYCN interacts with cofactors WDR5 and KDM4B to activate gene transcription, while interacts with LSD1, EZH2 and HADCs to repress gene transcription through affecting chromatin status. Inhibitors such as 10058-F4, OmoMYC and MYCi361 disrupt the dimerization between MYCN and MAX to inhibit the DNA binding of MYCN. The treatment of cells with MYCN cofactor inhibitors (WDR5i, KDM4Bi, LSD1i, EZH2i or HDACi) inactivates MYCN transcriptional activity through regional epigenetic modification and/or opening or closing chromatin.

to dimerize with MYC functionally targets *MYC* (129). It will be interesting to evaluate whether either of these approaches affects MAX/MYCN interactions to inhibit the growth of *MYCN*-driven cancers.

MYCN has been shown to recruit several druggable cofactors with methylase and demethylase activity to regulate gene transcription, and cofactor inhibition provides a way to indirectly target MYCN (**Figure 4**). The histone H3K4 methyltransferase complex subunit WDR5 forms a protein complex with MYCN at the *MDM2* promoter that results in histone H3K4 trimethylation and activation of *MDM2* transcription (72). Treatment of NB cells with the WDR5 antagonist OICR9429 reduces MYCN/WDR5 complex formation and the expression of *MYCN* target genes, resulting in the inhibition of cell growth (72). When MYCN is overexpressed, it interacts with the H3K9me3/me2 demethylase KDM4B and recruits KDM4B to E-box containing regions to decrease H3K9me3 levels (73). Functional studies demonstrate that KDM4B acts as a MYCN co-activator to regulate MYCN signature genes. Knockdown of KDM4B decreases NB cell proliferation *in vitro* and NB xenograft growth *in vivo*, which provides proof-of-concept for the potential therapeutic efficacy of inhibiting KDM4B to target oncogenic MYCN signaling in cancers (73). MYCN has also been found to recruit co-repressors to suppress gene transcription. MYCN associates with EZH2, a methyltransferase and a member of the polycomb repressor complex 2 (PRC2) to repress the NB tumor suppressor gene CLU through a bivalent modification of the chromatin at the CLU promoter (78). The prevalence of this activity has not been evaluated. In *MYCN*-amplified tumors, MYCN increases levels of EZH2 and components of the PRC2 complex leading to increased activity of PRC2-mediated transcriptional repression primarily of differentiation associated genes. Genomic or pharmacologic inhibition of EZH2 suppresses NB growth *in vitro* and *in vivo* (130–132). MYCN also binds the lysine-specific histone demethylase 1A (KDM1A/LSD1) to repress gene transcription. LSD1 co-localizes with MYCN on promoter regions of CLU and CDKN1A, and the treatment with an LSD1 inhibitor restores the expression of these genes and suppresses NB cell growth (79). c-MYC interacts with histone methyltransferase EHMT2 to repress gene transcription, and knockdown of EHMT2 results in decreased tumor volume (133). EHMT2 is essential in NB cells and inhibition of EHMT2 using BIX-01294 decreased proliferation of NB cells and induced apoptosis (132, 134).

Acetylation and deacetylation of histones are key regulatory features of gene transcription and are potential targets that regulate MYCN transcriptional activity. MYCN recruits many HDACs (HDAC1, HDAC2 and HDAC5) to repress gene transcription (74, 135, 136). The histone acetyltransferase, GCN5, binds to MYC and MYCN proteins (67–69). *In vitro* luciferase assays show that MYC recruits GCN5 to activate gene transcription (70); however, few GCN5 specific inhibitors are available and have limited testing in NB cells (137).

Targeting *MYCN* Downstream Targets

As a TF, MYCN regulates many target genes but the critical ones that mediate MYCN tumor initiating functions are not clear. One of the *MYCN* downstream targets that is under clinical evaluation is ornithine decarboxylase 1 (*ODC1*), the rate-limiting enzyme involved in polyamine synthesis (138, 139). In neuroblastoma, the expression levels of *MYCN* are strongly correlated with those of *ODC1*, and high levels of *ODC1* driven by *MYCN* amplification and overexpression are strongly associated with poor clinical outcome in NB patients (138). Treatment of TH-MYCN transgenic mice with the ODC inhibitor α-difluoromethylornithine (DFMO) prevents oncogenesis in hemizygous mice, while delaying tumor development in homozygous mice. Transient *Odc* ablation in hemizygous TH-*MYCN* mice permanently prevented tumor onset. This work indicates that *ODC* mediates an oncogenic function of *MYCN* that is important in tumor initiation and demonstrates the therapeutic potential of polyamine depletion strategies in NB (138, 139). A recent Phase II study of single agent DFMO as maintenance therapy in NB showed increased survival compared to historical controls for high-risk NB patients (140, 141).

The FACT (facilitates chromatin transcription) complex is another potential *MYCN* downstream target that is druggable. FACT facilitates transcriptional elongation on chromatin templates by binding and displacing the H2A/H2B dimer from nucleosomes, a process that is believed to be required for RNA polymerase II to pass through a nucleosomal barrier (142). MYC is confirmed to interact with a component of the FACT complex, the transcription elongation factor SSRP1 (4). SiRNA knockdown experiments demonstrate that expression of *FACT* and *MYCN* is controlled in a forward feedback loop, which drives *MYCN* transcription and protein stability (143). Inhibition of FACT using the small molecule curaxin compound CBL0137 results in a decrease of *MYCN* and *SSRP1* expression, as well as a markedly reduced NB tumor initiation and progression in the TH-MYCN mice especially when combined with standard chemotherapy (143).

Targeting *MYCN* Synthetic Lethal Approach

Synthetic dosage lethality (SDL) is a genetic interaction in which the alteration of one gene, combined with the reduction in function of a second gene, results in lethality (144). SDL is an attractive therapy for cancer because inhibition of such a gene will only induce cell death in cells carrying the specific gene alteration. *MYCN* activates both proliferative and apoptotic cellular responses. Whether it promotes a net proliferative response is dependent on cooperating apoptotic factors such as the antiapoptotic protein BCL2 (145, 146). It has been demonstrated that *MYCN*-amplified neuroblastoma cells are highly sensitive to BCL2 inhibitors ABT-263 (navitoclax) and ABT-199 (venetoclax) (147). When screening for enhancers of ABT-199 sensitivity in *MYCN*-amplified NB, researchers found that the Aurora Kinase A inhibitor (alisertib) cooperates with ABT-199 to induce widespread apoptosis. This drug combination was more effective in killing *MYCN*-amplified NB cells *in vitro* and *in vivo* than either compound alone (147). Moreover, in *MYCN*-amplified NB, Polo-Like Kinase 1 (PLK1) and MYCN create a positive, feedforward activation loop essential for maintaining their high levels of expression (120). BCL2 antagonists have been shown to synergize with inhibitors of PLK1, such as BI6727 or BI2356 and may be an effective drug combination for NB over-expressing *MYCN* (120).

One of the mechanisms through which *MYCN* exerts its tumorigenic effect in NB is to activate transcription of genes involved in proliferation, including checkpoint kinase 1 (*CHK1*), an important regulator of the G1/S and G_2/M checkpoints. This mechanism may contribute to the ability of *MYCN*-amplified NB tumors to become refractory to standard chemotherapy (148). Conversely, tumor cells lacking DNA damage checkpoints during tumorigenesis or during cytotoxic therapy are highly sensitive to additional genomic instability (149). *MYCN* induces replication stresses and DNA damage through excessive replication-fork firing. *MYCN*-overexpressing tumors are more sensitive to CHK1 inhibition (150, 151). Another cell cycle related synthetic lethality protein identified in *MYCN*-amplified NB is cyclin-dependent kinase 2 (CDK2) (152). Knockdown of CDK2 or treatment with the CDK2 inhibitor roscovitine induces apoptosis in *MYCN*-amplified neuroblastoma cell lines but not in those with *MYCN* single copy. Thus, inhibition of CDK2 is synthetically lethal to NB cells with overexpressed *MYCN* (152).

NB arising in adolescents and young adults is frequently associated with loss of function mutations in the alpha thalassemia X-linked (*ATRX*) gene (153, 154). Interestingly, *ATRX* mutations and *MYCN* amplification have never been observed in the same NB tumor, suggesting a potential synthetic lethal condition (153, 154). Doxycycline-induced overexpression of *MYCN* in *ATRX*-mutant NB cell lines showed a marked loss of tumor cells. Moreover, in the LSL-MYCN GEM of NB tumors failed to develop when LSL-MYCN : Dbh-iCre NB mice were crossed with $ATRX^{flox}$ mice demonstrating synthetic lethality between mutant *ATRX* and high levels of *MYCN* (154). This is an example of rare synthetic lethality between an inactivated tumor suppressor and an activated oncogene. *MYCN* has been shown to play an apoptotic role in cancer cells under certain circumstances (155). Thus, it is possible that under the stress of DNA replication, when *ATRX* is inactivated, high levels of *MYCN* induce an apoptotic cellular response. Therefore, ATRX targeting may be a therapeutic approach in *MYCN*-amplified NB tumors. Alternative strategies that increase MYCN protein levels may lead to an SDL situation in *ATRX*-mutant NB cells. Increasing MYCN levels may be achieved by interfering with critical components in the MYCN protein degradation pathway, such as HUWE1. HUWE1 ubiquitinates and directs MYCN degradation to the proteasome (61). Knockdown of the *HUWE1* gene impedes MYCN degradation and increases MYCN protein levels in NB cells (61). HUWE1 inhibitors such as BI8622 and BI8626 have been generated, but not tested in this situation.

Complementing experimental approaches to the identification of SDL in tumor cells, a recent computational approach utilized accumulating tumor genomic data to identify candidate SDL networks in various cancers (156). Synthetic lethality or 'oncogene addiction' offers an attractive therapeutic strategy for *MYCN*-driven cancers. Both bioinformatic analysis and high throughput drug screening can be used to identify novel-druggable synthetic lethal genes to which MYCN expressing cells are 'addicted'.

Prospect of Directly Targeting MYCN

Once considered undruggable, recent advances in chemistry and chemical genomics have begun to directly target transcription factors. Covalent reaction with their protein targets through cysteine residues is a known mechanism for many covalent drugs (157). A recent *in vitro* study that screened a library of cysteine-reactive covalent ligands, consisting of acrylamides and chloroacetamides, identified EN4. EN4 directly and covalently modifies the pure full-length c-MYC protein at cystine 171 (C171) of its intrinsically disordered region (158). In cells EN4 targets MYC interfering with MYC transcriptional activity. This reactive C171 on c-MYC is not conserved in MYCN. However, a similar screening approach could be used to identify small molecules that target cysteine residues in MYCN.

Proteolysis targeting chimeras (PROTACs) induced protein degradation is a recently developed therapeutic strategy, especially for undruggable targets (159). PROTACs are composed of three chemical elements: 1) a ligand binding to a target protein, 2) a ligand binding to E3 ubiquitin ligase, and 3) a linker for conjugating these two ligands (159). The small molecules 10058-F4, 7954-0035-G5, 10074-G5, JKY-2-169, MYCi361 and MYCi975 have been shown to bind to the HLH domain of MYC protein with some binding to MYCN protein as well (125, 128, 160). It may be possible to use these small molecules to develop PROTACs reagents to directly target and degrade the MYC/MYCN proteins (**Figure 5**). Intrinsically disordered region analysis of MYCN indicates that the MB II domain of MYCN is the most ordered region of MYCN having less flexibility and interacts with TRRAP (**Figure 1**). A small molecule or peptide screen to identify binders to the MBII region of MYCN would be another strategy to identify components needed to construct a MYCN PROTAC.

MiRNA are small RNA molecules that regulate their target gene expression at the post-transcriptional level and *via* their effects on the epigenetic machinery. Many miRNAs such as miR-34a, miR-375, miR-393-5p and let-7 are found to inhibit *MYCN* mRNA translation or target MYCN mRNA for degradation to suppress tumor cell growth (161–164). With more and more effective drug delivery systems for small interference RNA (siRNA) and miRNA being developed (165), directly targeting MYCN mRNA using miRNAs or siRNAs is a another approach for the treatment of *MYCN*-driven tumors. Indeed, the recent clinical findings which showed the systemic administration of a next generation antisense targeting the STAT3 TF decreased nuclear STAT3 levels in tumors are proof of principle that direct mRNA targeting of a transcription factor is feasible (166).

Targeting DNA amplification is another possible way to directly target *MYCN*. The genome-editing tool CRISPR-Cas9 is able to cut DNA at a targeted location and lead to cancer cell death if the targeted regions contain copy number gains. Whether this is clinically translatable is unknown. Pyrrole-imidazole (PI) polyamides when conjugated with DNA-alkylating agents could induce sequence-specific DNA alkylation to suppress target gene expression. A recent study showed that a *MYCN*-targeting PI- polyamide, MYCN-A3, binds to and alkylates DNA within the *MYCN* transcript, resulting in a decrease in *MYCN* copy number, downregulation of MYCN expression and suppression of NB growth *in vitro* and in xenografts (167). This indicates that the direct targeting of amplified *MYCN* at a genomic level is feasible. However, the feasibility of developing targeting approaches in pre-clinical models is only the first and sometimes the easiest step in the drug development pipeline.

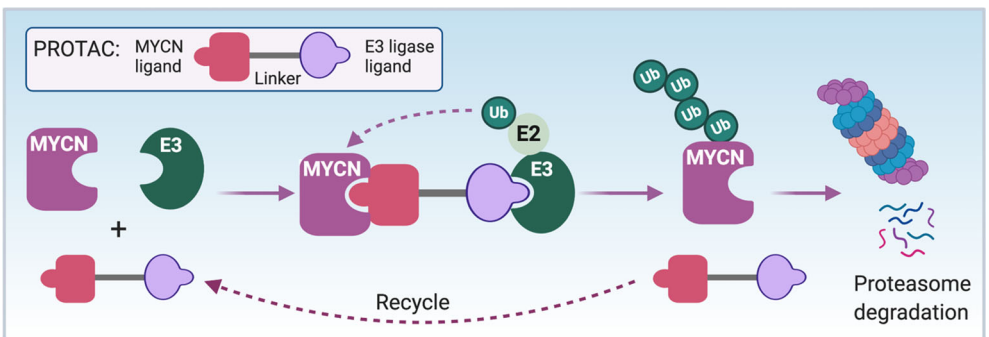

FIGURE 5 | PROTAC strategy to directly target MYCN. The schematic illustrates the mode of action of a proteolysis targeting chimera (PROTAC) targeting MYCN. First of all, a bio-conjugatable analog of a MYCN binding ligand (such as modified 10058-F4 or MYCi361) will be conjugated to E3 ubiquitin ligase binding ligand through a linker to synthesize a MYCN PROTAC. The formation of MYCN-PROTAC-E3 ubiquitin ligase complex will result in a transfer of ubiquitin (Ub) to the lysine residues of MYCN by E2 ubiquitin-conjugating enzyme. Afterwards, the PROTAC will be released and reutilized, and the poly-ubiquitinated MYCN will undergo proteasome degradation. Notes: circled 'Ub' represents ubiquitin.

CONCLUSION

The oncogenic amplification and/or overexpression of *MYC* family genes occur in most human cancers, making MYC family oncogenes one of the most sought-after therapeutic targets. Here we specifically reviewed multiple pharmacological approaches to target *MYCN* by interfering with pathways that MYCN uses to drive oncogenesis. Indirect inhibitors of *MYCN*, such as the BET bromodomain inhibitor, the CDK7 inhibitor, the AURKA inhibitor, the HAUSP inhibitor and the ODC inhibitor have clearly shown benefit in suppressing *MYCN*-amplified tumor growth in the preclinical studies, and a few of these inhibitors including bromodomain inhibitor GSK525762, AURKA inhibitor MLN8237 and ODC inhibitor DFMO are being evaluated in the clinic for *MYCN*-driven cancers. Once again it is possible that combinatorial strategies that integrate these new approaches with standard chemo- and immunotherapy will lead to improved tumor control with less toxicity for patients.

AUTHOR CONTRIBUTIONS

ZL and CT conceptualized and wrote the manuscript while SSC, SC, and VV wrote sections of the manuscript. All authors contributed to the article and approved the submitted version.

ACKNOWLEDGMENTS

We apologize to our respected colleagues whose work we were unable to cite due to space constraints. We thank Tiffany Prout, our administrative assistant for her support. LZ, SSC, SC and CJT acknowledge support from the Center for Cancer Research, the Intramural Research Program of the National Cancer Institute. VV is a research fellow funded by European Union FESR FSE, PON Ricerca e Innovazione 2014–2020. Some of the figures were created with BioRender.com.

REFERENCES

1. Meyer N, Penn LZ. Reflecting on 25 years with MYC. *Nat Rev Cancer* (2008) 8(12):976–90. doi: 10.1038/nrc2231
2. Kohl NE, Kanda N, Schreck RR, Bruns G, Latt SA, Gilbert F, et al. Transposition and amplification of oncogene-related sequences in human neuroblastomas. *Cell* (1983) 35(2 Pt 1):359–67. doi: 10.1016/0092-8674(83)90169-1
3. Schwab M, Alitalo K, Klempnauer KH, Varmus HE, Bishop JM, Gilbert F, et al. Amplified DNA with limited homology to myc cellular oncogene is shared by human neuroblastoma cell lines and a neuroblastoma tumour. *Nature* (1983) 305(5931):245–8. doi: 10.1038/305245a0
4. Baluapuri A, Wolf E, Eilers M. Target gene-independent functions of MYC oncoproteins. *Nat Rev Mol Cell Biol* (2020) 21(5):255–67. doi: 10.1038/s41580-020-0215-2
5. Huang M, Weiss WA. Neuroblastoma and MYCN. *Cold Spring Harb Perspect Med* (2013) 3(10):a014415. doi: 10.1101/cshperspect.a014415
6. Wenzel A, Schwab M. The mycN/max protein complex in neuroblastoma. Short review. *Eur J Cancer* (1995) 31A(4):516–9. doi: 10.1016/0959-8049(95)00060-V
7. Beltran H. The N-myc Oncogene: Maximizing its Targets, Regulation, and Therapeutic Potential. *Mol Cancer Res* (2014) 12(6):815–22. doi: 10.1158/1541-7786.MCR-13-0536
8. Muncan V, Sansom OJ, Tertoolen L, Phesse TJ, Begthel H, Sancho E, et al. Rapid loss of intestinal crypts upon conditional deletion of the Wnt/Tcf-4 target gene c-Myc. *Mol Cell Biol* (2006) 26(22):8418–26. doi: 10.1128/MCB.00821-06
9. Knoepfler PS, Cheng PF, Eisenman RN. N-myc is essential during neurogenesis for the rapid expansion of progenitor cell populations and the inhibition of neuronal differentiation. *Genes Dev* (2002) 16(20):2699–712. doi: 10.1101/gad.1021202
10. Malynn BA, de Alboran IM, O'Hagan RC, Bronson R, Davidson L, DePinho RA, et al. N-myc can functionally replace c-myc in murine development, cellular growth, and differentiation. *Genes Dev* (2000) 14(11):1390–9.
11. Smith RK, Zimmerman K, Yancopoulos GD, Ma A, Alt FW, et al. Transcriptional down-regulation of N-myc expression during B-cell development. *Mol Cell Biol* (1992) 12(4):1578–84. doi: 10.1128/MCB.12.4.1578
12. Kress TR, Sabo A, Amati B. MYC: connecting selective transcriptional control to global RNA production. *Nat Rev Cancer* (2015) 15(10):593–607. doi: 10.1038/nrc3984
13. Sabo A, Kress TR, Pelizzola M, de Pretis S, Gorski MM, Tesi A, et al. Selective transcriptional regulation by Myc in cellular growth control and lymphomagenesis. *Nature* (2014) 511(7510):488–92. doi: 10.1038/nature13537
14. Walz S, Lorenzin F, Morton J, Wiese KE, von Eyss B, Herold S, et al. Activation and repression by oncogenic MYC shape tumour-specific gene expression profiles. *Nature* (2014) 511(7510):483–7. doi: 10.1038/nature13473
15. Nie Z, Hu G, Wei G, Cui K, Yamane A, Resch W, et al. c-Myc is a universal amplifier of expressed genes in lymphocytes and embryonic stem cells. *Cell* (2012) 151(1):68–79. doi: 10.1016/j.cell.2012.08.033
16. Lin CY, Loven J, Rahl PB, Paranal RM, Burge CB, Bradner JE, et al. Transcriptional amplification in tumor cells with elevated c-Myc. *Cell* (2012) 151(1):56–67. doi: 10.1016/j.cell.2012.08.026
17. Buchel G, Carstensen A, Mak KY, Roeschert I, Leen E, Sumara O, et al. Association with Aurora-A Controls N-MYC-Dependent Promoter Escape and Pause Release of RNA Polymerase II during the Cell Cycle. *Cell Rep* (2017) 21(12):3483–97. doi: 10.1016/j.celrep.2017.11.090
18. Herold S, Kalb J, Buchel G, Ade CP, Baluapuri A, Xu J, et al. Recruitment of BRCA1 limits MYCN-driven accumulation of stalled RNA polymerase. *Nature* (2019) 567(7749):545–9. doi: 10.1038/s41586-019-1030-9
19. Seeger RC, Brodeur GM, Sather H, Dalton A, Siegel SE, Wong KY, et al. Association of multiple copies of the N-myc oncogene with rapid progression of neuroblastomas. *N Engl J Med* (1985) 313(18):1111–6. doi: 10.1056/NEJM198510313131802
20. Brodeur GM, Seeger RC, Schwab M, Varmus HE, Bishop JM. Amplification of N-myc in untreated human neuroblastomas correlates with advanced disease stage. *Science* (1984) 224(4653):1121–4. doi: 10.1126/science.6719137
21. Schwab M, Varmus HE, Bishop JM, Grzeschik KH, Naylor SL, Sakaguchi AY, et al. Chromosome localization in normal human cells and neuroblastomas of a gene related to c-myc. *Nature* (1984) 308(5956):288–91. doi: 10.1038/308288a0
22. Campbell K, Naranjo A, Hibbitts E, Gastier-Foster JM, Bagatell R, Irwin MS, et al. Association of heterogeneous MYCN amplification with clinical features, biological characteristics and outcomes in neuroblastoma: A report from the Children's Oncology Group. *Eur J Cancer* (2020) 133:112–9. doi: 10.1016/j.ejca.2020.04.007
23. Campbell K, Gastier-Foster JM, Mann M, Naranjo AH, Van Ryn C, Bagatell R, et al. Association of MYCN copy number with clinical features, tumor biology, and outcomes in neuroblastoma: A report from the Children's Oncology Group. *Cancer* (2017) 123(21):4224–35. doi: 10.1002/cncr.30873
24. Tonelli R, McIntyre A, Camerin C, Walters ZS, Di Leo K, Selfe J, et al. Antitumor activity of sustained N-myc reduction in rhabdomyosarcomas and transcriptional block by antigene therapy. *Clin Cancer Res* (2012) 18(3):796–807. doi: 10.1158/1078-0432.CCR-11-1981
25. Williamson D, Lu YJ, Gordon T, Sciot R, Kelsey A, Fisher C, et al. Relationship between MYCN copy number and expression in rhabdomyosarcomas and

correlation with adverse prognosis in the alveolar subtype. *J Clin Oncol* (2005) 23(4):880–8. doi: 10.1200/JCO.2005.11.078
26. Swartling FJ, Grimmer MR, Hackett CS, Northcott PA, Fan QW, Goldenberg DD, et al. Pleiotropic role for MYCN in medulloblastoma. *Genes Dev* (2010) 24(10):1059–72. doi: 10.1101/gad.1907510
27. Aldosari N, Bigner SH, Burger PC, Becker L, Kepner JL, Friedman HS, et al. MYCC and MYCN oncogene amplification in medulloblastoma. A fluorescence in situ hybridization study on paraffin sections from the Children's Oncology Group. *Arch Pathol Lab Med* (2002) 126(5):540–4. doi: 10.1043/0003-9985(2002)126<0540:MAMOAI>2.0.CO;2
28. Gessi M, von Bueren A, Treszl A, zur Muhlen A, Hartmann W, Warmuth-Metz M, et al. MYCN amplification predicts poor outcome for patients with supratentorial primitive neuroectodermal tumors of the central nervous system. *Neuro Oncol* (2014) 16(7):924–32. doi: 10.1093/neuonc/not302
29. Williams RD, Chagtai T, Alcaide-German M, Apps J, Wegert J, Popov S, et al. Multiple mechanisms of MYCN dysregulation in Wilms tumour. *Oncotarget* (2015) 6(9):7232–43. doi: 10.18632/oncotarget.3377
30. Lee WH, Murphree AL, Benedict WF. Expression and amplification of the N-myc gene in primary retinoblastoma. *Nature* (1984) 309(5967):458–60. doi: 10.1038/309458a0
31. Rushlow DE, Mol BM, Kennett JY, Yee S, Pajovic S, Theriault BL, et al. Characterisation of retinoblastomas without RB1 mutations: genomic, gene expression, and clinical studies. *Lancet Oncol* (2013) 14(4):327–34. doi: 10.1016/S1470-2045(13)70045-7
32. Beltran H, Rickman DS, Park K, Chae SS, Sboner A, MacDonald TY, et al. Molecular characterization of neuroendocrine prostate cancer and identification of new drug targets. *Cancer Discovery* (2011) 1(6):487–95. doi: 10.1158/2159-8290.CD-11-0130
33. Nau MM, Brooks BJ Jr, Carney DN, Gazdar AF, Battey JF, Sausville EA, et al. Human small-cell lung cancers show amplification and expression of the N-myc gene. *Proc Natl Acad Sci USA* (1986) 83(4):1092–6. doi: 10.1073/pnas.83.4.1092
34. Funa K, Steinholtz L, Nou E, Bergh J. Increased expression of N-myc in human small cell lung cancer biopsies predicts lack of response to chemotherapy and poor prognosis. *Am J Clin Pathol* (1987) 88(2):216–20. doi: 10.1093/ajcp/88.2.216
35. Freier K, Flechtenmacher C, Devens F, Hartschuh W, Hofele C, Lichter P, et al. Recurrent NMYC copy number gain and high protein expression in basal cell carcinoma. *Oncol Rep* (2006) 15(5):1141–5. doi: 10.3892/or.15.5.1141
36. Astolfi A, Vendemini F, Urbini M, Melchionda F, Masetti R, Franzoni M, et al. MYCN is a novel oncogenic target in pediatric T-cell acute lymphoblastic leukemia. *Oncotarget* (2014) 5(1):120–30. doi: 10.18632/oncotarget.1337
37. Bjerke L, Mackay A, Nandhabalan M, Burford A, Jury A, Popov S, et al. Histone H3.3. mutations drive pediatric glioblastoma through upregulation of MYCN. *Cancer Discovery* (2013) 3(5):512–9. doi: 10.1158/2159-8290.CD-12-0426
38. Hodgson JG, Yeh RF, Ray A, Wang NJ, Smirnov I, Yu M, et al. Comparative analyses of gene copy number and mRNA expression in glioblastoma multiforme tumors and xenografts. *Neuro Oncol* (2009) 11(5):477–87. doi: 10.1215/15228517-2008-113
39. Mizukami Y, Nonomura A, Takizawa T, Noguchi M, Michigishi T, Nakamura S, et al. N-myc protein expression in human breast carcinoma: prognostic implications. *Anticancer Res* (1995) 15(6B):2899–905.
40. Weiss WA, Aldape K, Mohapatra G, Feuerstein BG, Bishop JM. Targeted expression of MYCN causes neuroblastoma in transgenic mice. *EMBO J* (1997) 16(11):2985–95. doi: 10.1093/emboj/16.11.2985
41. Althoff K, Beckers A, Bell E, Nortmeyer M, Thor T, Sprussel A, et al. A Cre-conditional MYCN-driven neuroblastoma mouse model as an improved tool for preclinical studies. *Oncogene* (2015) 34(26):3357–68. doi: 10.1038/onc.2014.269
42. Zhu S, Lee JS, Guo F, Shin J, Perez-Atayde AR, Kutok JL, et al. Activated ALK collaborates with MYCN in neuroblastoma pathogenesis. *Cancer Cell* (2012) 21(3):362–73. doi: 10.1016/j.ccr.2012.02.010
43. Zhu S, Zhang X, Weichert-Leahey N, Dong Z, Zhang C, Lopez G, et al. LMO1 Synergizes with MYCN to Promote Neuroblastoma Initiation and Metastasis. *Cancer Cell* (2017) 32(3):310–23.e5. doi: 10.1016/j.ccell.2017.08.002
44. Heukamp LC, Thor T, Schramm A, De Preter K, Kumps C, De Wilde B, et al. Targeted expression of mutated ALK induces neuroblastoma in transgenic mice. *Sci Transl Med* (2012) 4(141):141ra91. doi: 10.1126/scitranslmed.3003967
45. Dardenne E, Beltran H, Benelli M, Gayvert K, Berger A, Puca L, et al. N-Myc Induces an EZH2-Mediated Transcriptional Program Driving Neuroendocrine Prostate Cancer. *Cancer Cell* (2016) 30(4):563–77. doi: 10.1016/j.ccell.2016.09.005
46. Kawagoe H, Kandilci A, Kranenburg TA, Grosveld GC. Overexpression of N-Myc rapidly causes acute myeloid leukemia in mice. *Cancer Res* (2007) 67(22):10677–85. doi: 10.1158/0008-5472.CAN-07-1118
47. Swartling FJ, Savov V, Persson AI, Chen J, Hackett CS, Northcott PA, et al. Distinct neural stem cell populations give rise to disparate brain tumors in response to N-MYC. *Cancer Cell* (2012) 21(5):601–13. doi: 10.1016/j.ccr.2012.04.012
48. Zindy F, Uziel T, Ayrault O, Calabrese C, Valentine M, Rehg JE, et al. Genetic alterations in mouse medulloblastomas and generation of tumors de novo from primary cerebellar granule neuron precursors. *Cancer Res* (2007) 67(6):2676–84. doi: 10.1158/0008-5472.CAN-06-3418
49. Wright PE, Dyson HJ. Intrinsically disordered proteins in cellular signalling and regulation. *Nat Rev Mol Cell Biol* (2015) 16(1):18–29. doi: 10.1038/nrm3920
50. Oldfield CJ, Dunker AK. Intrinsically disordered proteins and intrinsically disordered protein regions. *Annu Rev Biochem* (2014) 83:553–84. doi: 10.1146/annurev-biochem-072711-164947
51. Obradovic Z, Peng K, Vucetic S, Radivojac P, Brown CJ, Dunker AK. Predicting intrinsic disorder from amino acid sequence. *Proteins* (2003) 53 Suppl 6:566–72. doi: 10.1002/prot.10532
52. Sjostrom SK, Finn G, Hahn WC, Rowitch DH, Kenney AM. The Cdk1 complex plays a prime role in regulating N-myc phosphorylation and turnover in neural precursors. *Dev Cell* (2005) 9(3):327–38. doi: 10.1016/j.devcel.2005.07.014
53. Chesler L, Schlieve C, Goldenberg DD, Kenney A, Kim G, McMillan A, et al. Inhibition of phosphatidylinositol 3-kinase destabilizes Mycn protein and blocks malignant progression in neuroblastoma. *Cancer Res* (2006) 66(16):8139–46. doi: 10.1158/0008-5472.CAN-05-2769
54. Pulverer BJ, Fisher C, Vousden K, Littlewood T, Evan G, Woodgett JR. Site-specific modulation of c-Myc cotransformation by residues phosphorylated in vivo. *Oncogene* (1994) 9(1):59–70.
55. Kenney AM, Widlund HR, Rowitch DH. Hedgehog and PI-3 kinase signaling converge on Nmyc1 to promote cell cycle progression in cerebellar neuronal precursors. *Development* (2004) 131(1):217–28. doi: 10.1242/dev.00891
56. Otto T, Horn S, Brockmann M, Eilers U, Schuttrumpf L, Popov N, et al. Stabilization of N-Myc is a critical function of Aurora A in human neuroblastoma. *Cancer Cell* (2009) 15(1):67–78. doi: 10.1016/j.ccr.2008.12.005
57. Sears R, Nuckolls F, Haura E, Taya Y, Tamai K, Nevins JR, et al. Multiple Ras-dependent phosphorylation pathways regulate Myc protein stability. *Genes Dev* (2000) 14(19):2501–14. doi: 10.1101/gad.836800
58. Welcker M, Orian A, Jin J, Grim JE, Harper JW, Eisenman RN, et al. The Fbw7 tumor suppressor regulates glycogen synthase kinase 3 phosphorylation-dependent c-Myc protein degradation. *Proc Natl Acad Sci USA* (2004) 101(24):9085–90. doi: 10.1073/pnas.0402770101
59. Yada M, Hatakeyama S, Kamura T, Nishiyama M, Tsunematsu R, Imaki H, et al. Phosphorylation-dependent degradation of c-Myc is mediated by the F-box protein Fbw7. *EMBO J* (2004) 23(10):2116–25. doi: 10.1038/sj.emboj.7600217
60. Izumi H, Kaneko Y. Trim32 facilitates degradation of MYCN on spindle poles and induces asymmetric cell division in human neuroblastoma cells. *Cancer Res* (2014) 74(19):5620–30. doi: 10.1158/0008-5472.CAN-14-0169
61. Zhao X, Heng JI, Guardavaccaro D, Jiang R, Pagano M, Guillemot F, et al. The HECT-domain ubiquitin ligase Huwe1 controls neural differentiation and proliferation by destabilizing the N-Myc oncoprotein. *Nat Cell Biol* (2008) 10(6):643–53. doi: 10.1038/ncb1727
62. King B, Boccalatte F, Moran-Crusio K, Wolf E, Wang J, Kayembe C, et al. The ubiquitin ligase Huwe1 regulates the maintenance and lymphoid commitment of hematopoietic stem cells. *Nat Immunol* (2016) 17(11):1312–21. doi: 10.1038/ni.3559

63. Richards MW, Burgess SG, Poon E, Carstensen A, Eilers M, Chesler L, et al. Structural basis of N-Myc binding by Aurora-A and its destabilization by kinase inhibitors. *Proc Natl Acad Sci USA* (2016) 113(48):13726–31. doi: 10.1073/pnas.1610626113
64. Tavana O, Li D, Dai C, Lopez G, Banerjee D, Kon N, et al. HAUSP deubiquitinates and stabilizes N-Myc in neuroblastoma. *Nat Med* (2016) 22(10):1180–6. doi: 10.1038/nm.4180
65. Koach J, Holien JK, Massudi H, Carter DR, Ciampa OC, Herath M, et al. Drugging MYCN Oncogenic Signaling through the MYCN-PA2G4 Binding Interface. *Cancer Res* (2019) 79(21):5652–67. doi: 10.1158/0008-5472.CAN-19-1112
66. Park JH, Szemes M, Vieira GC, Melegh Z, Malik S, Heesom KJ, et al. Protein arginine methyltransferase 5 is a key regulator of the MYCN oncoprotein in neuroblastoma cells. *Mol Oncol* (2015) 9(3):617–27. doi: 10.1016/j.molonc.2014.10.015
67. Wood MA, McMahon SB, Cole MD. An ATPase/helicase complex is an essential cofactor for oncogenic transformation by c-Myc. *Mol Cell* (2000) 5 (2):321–30. doi: 10.1016/S1097-2765(00)80427-X
68. McMahon SB, Wood MA, Cole MD. The essential cofactor TRRAP recruits the histone acetyltransferase hGCN5 to c-Myc. *Mol Cell Biol* (2000) 20 (2):556–62. doi: 10.1128/MCB.20.2.556-562.2000
69. Park J, Kunjibettu S, McMahon SB, Cole MD. The ATM-related domain of TRRAP is required for histone acetyltransferase recruitment and Myc-dependent oncogenesis. *Genes Dev* (2001) 15(13):1619–24. doi: 10.1101/gad.900101
70. Liu X, Tesfai J, Evrard YA, Dent SY, Martinez E. c-Myc transformation domain recruits the human STAGA complex and requires TRRAP and GCN5 acetylase activity for transcription activation. *J Biol Chem* (2003) 278 (22):20405–12. doi: 10.1074/jbc.M211795200
71. Thomas LR, Wang Q, Grieb BC, Phan J, Foshage AM, Sun Q, et al. Interaction with WDR5 promotes target gene recognition and tumorigenesis by MYC. *Mol Cell* (2015) 58(3):440–52. doi: 10.1016/j.molcel.2015.02.028
72. Sun Y, Bell JL, Carter D, Gherardi S, Poulos RC, Milazzo G, et al. WDR5 Supports an N-Myc Transcriptional Complex That Drives a Protumorigenic Gene Expression Signature in Neuroblastoma. *Cancer Res* (2015) 75 (23):5143–54. doi: 10.1158/0008-5472.CAN-15-0423
73. Yang J, AlTahan AM, Hu D, Wang Y, Cheng PH, Morton CL, et al. The role of histone demethylase KDM4B in Myc signaling in neuroblastoma. *J Natl Cancer Inst* (2015) 107(6):djv080. doi: 10.1093/jnci/djv080
74. Iraci N, Diolaiti D, Papa A, Porro A, Valli E, Gherardi S, et al. A SP1/MIZ1/MYCN repression complex recruits HDAC1 at the TRKA and p75NTR promoters and affects neuroblastoma malignancy by inhibiting the cell response to NGF. *Cancer Res* (2011) 71(2):404–12. doi: 10.1158/0008-5472.CAN-10-2627
75. Gartel AL, Ye X, Goufman E, Shianov P, Hay N, Najmabadi F, et al. Myc represses the p21(WAF1/CIP1) promoter and interacts with Sp1/Sp3. *Proc Natl Acad Sci USA* (2001) 98(8):4510–5. doi: 10.1073/pnas.081074898
76. Staller P, Peukert K, Kiermaier A, Seoane J, Lukas J, Karsunky H, et al. Repression of p15INK4b expression by Myc through association with Miz-1. *Nat Cell Biol* (2001) 3(4):392–9. doi: 10.1038/35070076
77. Liu T, Tee AE, Porro A, Smith SA, Dwarte T, Liu PY, et al. Activation of tissue transglutaminase transcription by histone deacetylase inhibition as a therapeutic approach for Myc oncogenesis. *Proc Natl Acad Sci USA* (2007) 104(47):18682–7. doi: 10.1073/pnas.0705524104
78. Corvetta D, Chayka O, Gherardi S, D'Acunto CW, Cantilena S, Valli E, et al. Physical interaction between MYCN oncogene and polycomb repressive complex 2 (PRC2) in neuroblastoma: functional and therapeutic implications. *J Biol Chem* (2013) 288(12):8332–41. doi: 10.1074/jbc.M113.454280
79. Amente S, Milazzo G, Sorrentino MC, Ambrosio S, Di Palo G, Lania L, et al. Lysine-specific demethylase (LSD1/KDM1A) and MYCN cooperatively repress tumor suppressor genes in neuroblastoma. *Oncotarget* (2015) 6 (16):14572–83. doi: 10.18632/oncotarget.3990
80. Thiele CJ, Reynolds CP, Israel MA. Decreased expression of N-myc precedes retinoic acid-induced morphological differentiation of human neuroblastoma. *Nature* (1985) 313(6001):404–6. doi: 10.1038/313404a0
81. Kanemaru KK, Tuthill MC, Takeuchi KK, Sidell N, Wada RK. Retinoic acid induced downregulation of MYCN is not mediated through changes in Sp1/Sp3. *Pediatr Blood Cancer* (2008) 50(4):806–11. doi: 10.1002/pbc.21273
82. Reynolds CP, Matthay KK, Villablanca JG, Maurer BJ. Retinoid therapy of high-risk neuroblastoma. *Cancer Lett* (2003) 197(1-2):185–92. doi: 10.1016/S0304-3835(03)00108-3
83. Calo E, Wysocka J. Modification of enhancer chromatin: what, how, and why? *Mol Cell* (2013) 49(5):825–37. doi: 10.1016/j.molcel.2013.01.038
84. Hamdan FH, Johnsen SA. Perturbing Enhancer Activity in Cancer Therapy. *Cancers (Basel)* (2019) 11(5). doi: 10.3390/cancers11050634
85. Sengupta S, George RE. Super-Enhancer-Driven Transcriptional Dependencies in Cancer. *Trends Cancer* (2017) 3(4):269–81. doi: 10.1016/j.trecan.2017.03.006
86. Shin HY. Targeting Super-Enhancers for Disease Treatment and Diagnosis. *Mol Cells* (2018) 41(6):506–14. doi: 10.14348/molcells.2018.2297
87. Chipumuro E, Marco E, Christensen CL, Kwiatkowski N, Zhang T, Hatheway CM, et al. CDK7 inhibition suppresses super-enhancer-linked oncogenic transcription in MYCN-driven cancer. *Cell* (2014) 159(5):1126–39. doi: 10.1016/j.cell.2014.10.024
88. Durbin AD, Zimmerman MW, Dharia NV, Abraham BJ, Iniguez AB, Weichert-Leahey N, et al. Selective gene dependencies in MYCN-amplified neuroblastoma include the core transcriptional regulatory circuitry. *Nat Genet* (2018) 50(9):1240–6. doi: 10.1038/s41588-018-0191-z
89. Zimmerman MW, Liu Y, He S, Durbin AD, Abraham BJ, Easton J, et al. MYC Drives a Subset of High-Risk Pediatric Neuroblastomas and Is Activated through Mechanisms Including Enhancer Hijacking and Focal Enhancer Amplification. *Cancer Discovery* (2018) 8(3):320–35. doi: 10.1158/2159-8290.CD-17-0993
90. de Ruijter AJ, Kemp S, Kramer G, Meinsma RJ, Kaufmann JO, Caron HN, et al. The novel histone deacetylase inhibitor BL1521 inhibits proliferation and induces apoptosis in neuroblastoma cells. *Biochem Pharmacol* (2004) 68 (7):1279–88. doi: 10.1016/j.bcp.2004.05.010
91. Cortes C, Kozma SC, Tauler A, Ambrosio S. MYCN concurrence with SAHA-induced cell death in human neuroblastoma cells. *Cell Oncol (Dordr)* (2015) 38(5):341–52. doi: 10.1007/s13402-015-0233-9
92. Jaboin J, Wild J, Hamidi H, Khanna C, Kim CJ, Robey R, et al. MS-27-275, an inhibitor of histone deacetylase, has marked in vitro and in vivo antitumor activity against pediatric solid tumors. *Cancer Res* (2002) 62 (21):6108–15.
93. Sanchez GJ, Richmond PA, Bunker EN, Karman SS, Azofeifa J, Garnett AT, et al. Genome-wide dose-dependent inhibition of histone deacetylases studies reveal their roles in enhancer remodeling and suppression of oncogenic super-enhancers. *Nucleic Acids Res* (2018) 46(4):1756–76. doi: 10.1093/nar/gkx1225
94. Gryder BE, Pomella S, Sayers C, Wu XS, Song Y, Chiarella AM, et al. Histone hyperacetylation disrupts core gene regulatory architecture in rhabdomyosarcoma. *Nat Genet* (2019) 51(12):1714–22. doi: 10.1038/s41588-019-0534-4
95. Delmore JE, Issa GC, Lemieux ME, Rahl PB, Shi J, Jacobs HM, et al. BET bromodomain inhibition as a therapeutic strategy to target c-Myc. *Cell* (2011) 146(6):904–17. doi: 10.1016/j.cell.2011.08.017
96. Donati B, Lorenzini E, Ciarrocchi A. BRD4 and Cancer: going beyond transcriptional regulation. *Mol Cancer* (2018) 17(1):164. doi: 10.1186/s12943-018-0915-9
97. Puissant A, Frumm SM, Alexe G, Bassil CF, Qi J, Chanthery YH, et al. Targeting MYCN in neuroblastoma by BET bromodomain inhibition. *Cancer Discovery* (2013) 3(3):308–23. doi: 10.1158/2159-8290.CD-12-0418
98. Henssen A, Althoff K, Odersky A, Beckers A, Koche R, Speleman F, et al. Targeting MYCN-Driven Transcription By BET-Bromodomain Inhibition. *Clin Cancer Res* (2016) 22(10):2470–81. doi: 10.1158/1078-0432.CCR-15-1449
99. Loven J, Hoke HA, Lin CY, Lau A, Orlando DA, Vakoc CR, et al. Selective inhibition of tumor oncogenes by disruption of super-enhancers. *Cell* (2013) 153(2):320–34. doi: 10.1016/j.cell.2013.03.036
100. Piha-Paul SA, Hann CL, French CA, Cousin S, Brana I, Cassier PA, et al. Phase 1 Study of Molibresib (GSK525762), a Bromodomain and Extra-Terminal Domain Protein Inhibitor, in NUT Carcinoma and Other Solid Tumors. *JNCI Cancer Spectr* (2020) 4(2):pkz093. doi: 10.1093/jncics/pkz093
101. Whyte WA, Orlando DA, Hnisz D, Abraham BJ, Lin CY, Kagey MH, et al. Master transcription factors and mediator establish super-enhancers at key cell identity genes. *Cell* (2013) 153(2):307–19. doi: 10.1016/j.cell.2013.03.035

102. Felgenhauer J, Tomino L, Selich-Anderson J, Bopp E, Shah N. Dual BRD4 and AURKA Inhibition Is Synergistic against MYCN-Amplified and Nonamplified Neuroblastoma. *Neoplasia* (2018) 20(10):965–74. doi: 10.1016/j.neo.2018.08.002
103. Shahbazi J, Liu PY, Atmadibrata B, Bradner JE, Marshall GM, Lock RB, et al. The Bromodomain Inhibitor JQ1 and the Histone Deacetylase Inhibitor Panobinostat Synergistically Reduce N-Myc Expression and Induce Anticancer Effects. *Clin Cancer Res* (2016) 22(10):2534–44. doi: 10.1158/1078-0432.CCR-15-1666
104. Rahl PB, Lin CY, Seila AC, Flynn RA, McCuine S, Burge CB, et al. c-Myc regulates transcriptional pause release. *Cell* (2010) 141(3):432–45. doi: 10.1016/j.cell.2010.03.030
105. Poon E, Liang T, Jamin Y, Walz S, Kwok C, Hakkert A, et al. Orally bioavailable CDK9/2 inhibitor shows mechanism-based therapeutic potential in MYCN-driven neuroblastoma. *J Clin Invest* (2020). doi: 10.1172/JCI134132
106. Calabrese DR, Chen X, Leon EC, Gaikwad SM, Phyo Z, Hewitt WM, et al. Chemical and structural studies provide a mechanistic basis for recognition of the MYC G-quadruplex. *Nat Commun* (2018) 9(1):4229. doi: 10.1038/s41467-018-06315-w
107. Spiegel J, Adhikari S, Balasubramanian S. The Structure and Function of DNA G-Quadruplexes. *Trends Chem* (2020) 2(2):123–36. doi: 10.1016/j.trechm.2019.07.002
108. Siddiqui-Jain A, Grand CL, Bearss DJ, Hurley LH. Direct evidence for a G-quadruplex in a promoter region and its targeting with a small molecule to repress c-MYC transcription. *Proc Natl Acad Sci USA* (2002) 99(18):11593–8. doi: 10.1073/pnas.182256799
109. Bradner JE, Hnisz D, Young RA. Transcriptional Addiction in Cancer. *Cell* (2017) 168(4):629–43. doi: 10.1016/j.cell.2016.12.013
110. Bushweller JH. Targeting transcription factors in cancer - from undruggable to reality. *Nat Rev Cancer* (2019) 19(11):611–24. doi: 10.1038/s41568-019-0196-7
111. Bonvini P, Nguyen P, Trepel J, Neckers LM. In vivo degradation of N-myc in neuroblastoma cells is mediated by the 26S proteasome. *Oncogene* (1998) 16 (9):1131–9. doi: 10.1038/sj.onc.1201625
112. Cage TA, Chanthery Y, Chesler L, Grimmer M, Knight Z, Shokat K, et al. Downregulation of MYCN through PI3K Inhibition in Mouse Models of Pediatric Neural Cancer. *Front Oncol* (2015) 5:111. doi: 10.3389/fonc.2015.00111
113. Yang Y, Ding L, Zhou Q, Fen L, Cao Y, Sun J, et al. Silencing of AURKA augments the antitumor efficacy of the AURKA inhibitor MLN8237 on neuroblastoma cells. *Cancer Cell Int* (2020) 20:9. doi: 10.1186/s12935-019-1072-y
114. Brockmann M, Poon E, Berry T, Carstensen A, Deubzer HE, Rycak L, et al. Small molecule inhibitors of aurora-a induce proteasomal degradation of N-myc in childhood neuroblastoma. *Cancer Cell* (2013) 24(1):75–89. doi: 10.1016/j.ccr.2013.05.005
115. Zormpas-Petridis K, Poon E, Clarke M, Jerome NP, Boult JKR, Blackledge MD, et al. Noninvasive MRI Native T1 Mapping Detects Response to MYCN-targeted Therapies in the Th-MYCN Model of Neuroblastoma. *Cancer Res* (2020) 80(16):3424–35. doi: 10.1158/0008-5472.CAN-20-0133
116. Ommer J, Selfe JL, Wachtel M, O'Brien EM, Laubscher D, Roemmele M, et al. Aurora A Kinase Inhibition Destabilizes PAX3-FOXO1 and MYCN and Synergizes with Navitoclax to Induce Rhabdomyosarcoma Cell Death. *Cancer Res* (2020) 80(4):832–42. doi: 10.1158/0008-5472.CAN-19-1479
117. Gustafson WC, Meyerowitz JG, Nekritz EA, Chen J, Benes C, Charron E, et al. Drugging MYCN through an allosteric transition in Aurora kinase A. *Cancer Cell* (2014) 26(3):414–27. doi: 10.1016/j.ccr.2014.07.015
118. DuBois SG, Marachelian A, Fox E, Kudgus RA, Reid JM, Groshen S, et al. Phase I Study of the Aurora A Kinase Inhibitor Alisertib in Combination With Irinotecan and Temozolomide for Patients With Relapsed or Refractory Neuroblastoma: A NANT (New Approaches to Neuroblastoma Therapy) Trial. *J Clin Oncol* (2016) 34(12):1368–75. doi: 10.1200/JCO.2015.65.4889
119. Ackermann S, Goeser F, Schulte JH, Schramm A, Ehemann V, Hero B, et al. Polo-like kinase 1 is a therapeutic target in high-risk neuroblastoma. *Clin Cancer Res* (2011) 17(4):731–41. doi: 10.1158/1078-0432.CCR-10-1129
120. Xiao D, Yue M, Su H, Ren P, Jiang J, Li F, et al. Polo-like Kinase-1 Regulates Myc Stabilization and Activates a Feedforward Circuit Promoting Tumor Cell Survival. *Mol Cell* (2016) 64(3):493–506. doi: 10.1016/j.molcel.2016.09.016
121. Chaturvedi NK, Mahapatra S, Kesherwani V, Kling MJ, Shukla M, Ray S, et al. Role of protein arginine methyltransferase 5 in group 3 (MYC-driven) Medulloblastoma. *BMC Cancer* (2019) 19(1):1056. doi: 10.1186/s12885-019-6291-z
122. Berg T, Cohen SB, Desharnais J, Sonderegger C, Maslyar DJ, Goldberg J, et al. Small-molecule antagonists of Myc/Max dimerization inhibit Myc-induced transformation of chicken embryo fibroblasts. *Proc Natl Acad Sci USA* (2002) 99(6):3830–5. doi: 10.1073/pnas.062036999
123. Wang H, Hammoudeh DI, Follis AV, Reese BE, Lazo JS, Metallo SJ, et al. Improved low molecular weight Myc-Max inhibitors. *Mol Cancer Ther* (2007) 6(9):2399–408. doi: 10.1158/1535-7163.MCT-07-0005
124. Muller I, Larsson K, Frenzel A, Oliynyk G, Zirath H, Prochownik EV, et al. Targeting of the MYCN protein with small molecule c-MYC inhibitors. *PloS One* (2014) 9(5):e97285. doi: 10.1371/journal.pone.0097285
125. Follis AV, Hammoudeh DI, Wang H, Prochownik EV, Metallo SJ. Structural rationale for the coupled binding and unfolding of the c-Myc oncoprotein by small molecules. *Chem Biol* (2008) 15(11):1149–55. doi: 10.1016/j.chembiol.2008.09.011
126. Soucek L, Helmer-Citterich M, Sacco A, Jucker R, Cesareni G, Nasi S. Design and properties of a Myc derivative that efficiently homodimerizes. *Oncogene* (1998) 17(19):2463–72. doi: 10.1038/sj.onc.1202199
127. Savino M, Annibali D, Carucci N, Favuzzi E, Cole MD, Evan GI, et al. The action mechanism of the Myc inhibitor termed Omomyc may give clues on how to target Myc for cancer therapy. *PloS One* (2011) 6(7):e22284. doi: 10.1371/journal.pone.0022284
128. Han H, Jain AD, Truica MI, Izquierdo-Ferrer J, Anker JF, Lysy B, et al. Small-Molecule MYC Inhibitors Suppress Tumor Growth and Enhance Immunotherapy. *Cancer Cell* (2019) 36(5):483–497 e15. doi: 10.1016/j.ccell.2019.10.001
129. Struntz NB, Chen A, Deutzmann A, Wilson RM, Stefan E, Evans HL, et al. Stabilization of the Max Homodimer with a Small Molecule Attenuates Myc-Driven Transcription. *Cell Chem Biol* (2019) 26(5):711–723 e14. doi: 10.1016/j.chembiol.2019.02.009
130. Wang C, Liu Z, Woo CW, Li Z, Wang L, Wei JS, et al. EZH2 Mediates epigenetic silencing of neuroblastoma suppressor genes CASZ1, CLU, RUNX3, and NGFR. *Cancer Res* (2012) 72(1):315–24. doi: 10.1158/0008-5472.CAN-11-0961
131. Chen L, Alexe G, Dharia NV, Ross L, Iniguez AB, Conway AS, et al. CRISPR-Cas9 screen reveals a MYCN-amplified neuroblastoma dependency on EZH2. *J Clin Invest* (2018) 128(1):446–62. doi: 10.1172/JCI90793
132. Veschi V, Liu Z, Voss TC, Ozbun L, Gryder B, Yan C, et al. Epigenetic siRNA and Chemical Screens Identify SETD8 Inhibition as a Therapeutic Strategy for p53 Activation in High-Risk Neuroblastoma. *Cancer Cell* (2017) 31 (1):50–63. doi: 10.1016/j.ccell.2016.12.002
133. Tu WB, Shiah YJ, Lourenco C, Mullen PJ, Dingar D, Redel C, et al. MYC Interacts with the G9a Histone Methyltransferase to Drive Transcriptional Repression and Tumorigenesis. *Cancer Cell* (2018) 34(4):579–95.e8. doi: 10.1016/j.ccell.2018.09.001
134. Lu Z, Tian Y, Salwen HR, Chlenski A, Godley LA, Raj JU, et al. Histone-lysine methyltransferase EHMT2 is involved in proliferation, apoptosis, cell invasion, and DNA methylation of human neuroblastoma cells. *Anticancer Drugs* (2013) 24(5):484–93. doi: 10.1097/CAD.0b013e32835ffdbb
135. Lodrini M, Oehme I, Schroeder C, Milde T, Schier MC, Kopp-Schneider A, et al. MYCN and HDAC2 cooperate to repress miR-183 signaling in neuroblastoma. *Nucleic Acids Res* (2013) 41(12):6018–33. doi: 10.1093/nar/gkt346
136. Sun Y, Liu PY, Scarlett CJ, Malyukova A, Liu B, Marshall GM, et al. Histone deacetylase 5 blocks neuroblastoma cell differentiation by interacting with N-Myc. *Oncogene* (2014) 33(23):2987–94. doi: 10.1038/onc.2013.253
137. Secci D, Carradori S, Bizzarri B, Bolasco A, Ballario P, Patramani Z, et al. Synthesis of a novel series of thiazole-based histone acetyltransferase inhibitors. *Bioorg Med Chem* (2014) 22(5):1680–9. doi: 10.1016/j.bmc.2014.01.022
138. Hogarty MD, Norris MD, Davis K, Liu X, Evageliou NF, Hayes CS, et al. ODC1 is a critical determinant of MYCN oncogenesis and a therapeutic

target in neuroblastoma. *Cancer Res* (2008) 68(23):9735–45. doi: 10.1158/0008-5472.CAN-07-6866
139. Gamble LD, Hogarty MD, Liu X, Ziegler DS, Marshall G, Norris MD, et al. Polyamine pathway inhibition as a novel therapeutic approach to treating neuroblastoma. *Front Oncol* (2012) 2:162. doi: 10.3389/fonc.2012.00162
140. Sholler GLS, Ferguson W, Bergendahl G, Bond JP, Neville K, Eslin D, et al. Maintenance DFMO Increases Survival in High Risk Neuroblastoma. *Sci Rep* (2018) 8(1):14445. doi: 10.1038/s41598-018-32659-w
141. Lewis EC, Kraveka JM, Ferguson W, Eslin D, Brown VI, Bergendahl G, et al. A subset analysis of a phase II trial evaluating the use of DFMO as maintenance therapy for high-risk neuroblastoma. *Int J Cancer* (2020) 147 (11):3152–9. doi: 10.1002/ijc.33044
142. Belotserkovskaya R, Oh S, Bondarenko VA, Orphanides G, Studitsky VM, Reinberg D. FACT facilitates transcription-dependent nucleosome alteration. *Science* (2003) 301(5636):1090–3. doi: 10.1126/science.1085703
143. Carter DR, Murray J, Cheung BB, Gamble L, Koach J, Tsang J, et al. Therapeutic targeting of the MYC signal by inhibition of histone chaperone FACT in neuroblastoma. *Sci Transl Med* (2015) 7 (312):312ra176. doi: 10.1126/scitranslmed.aab1803
144. O'Neil NJ, Bailey ML, Hieter P. Synthetic lethality and cancer. *Nat Rev Genet* (2017) 18(10):613–23. doi: 10.1038/nrg.2017.47
145. Fulda S, Lutz W, Schwab M, Debatin KM. MycN sensitizes neuroblastoma cells for drug-induced apoptosis. *Oncogene* (1999) 18(7):1479–86. doi: 10.1038/sj.onc.1202435
146. Strasser A, Harris AW, Bath ML, Cory S. Novel primitive lymphoid tumours induced in transgenic mice by cooperation between myc and bcl-2. *Nature* (1990) 348(6299):331–3. doi: 10.1038/348331a0
147. Ham J, Costa C, Sano R, Lochmann TL, Sennott EM, Patel NU, et al. Exploitation of the Apoptosis-Primed State of MYCN-Amplified Neuroblastoma to Develop a Potent and Specific Targeted Therapy Combination. *Cancer Cell* (2016) 29(2):159–72. doi: 10.1016/j.ccell.2016.01.002
148. Cole KA, Huggins J, Laquaglia M, Hulderman CE, Russell MR, Bosse K, et al. RNAi screen of the protein kinome identifies checkpoint kinase 1 (CHK1) as a therapeutic target in neuroblastoma. *Proc Natl Acad Sci USA* (2011) 108 (8):3336–41. doi: 10.1073/pnas.1012351108
149. Hoglund A, Nilsson LM, Muralidharan SV, Hasvold LA, Merta P, Rudelius M, et al. Therapeutic implications for the induced levels of Chk1 in Myc-expressing cancer cells. *Clin Cancer Res* (2011) 17(22):7067–79. doi: 10.1158/1078-0432.CCR-11-1198
150. Chen H, Liu H, Qing G. Targeting oncogenic Myc as a strategy for cancer treatment. *Signal Transduct Target Ther* (2018) 3:5. doi: 10.1038/s41392-018-0008-7
151. Dominguez-Sola D, Ying CY, Grandori C, Ruggiero L, Chen B, Li M, et al. Non-transcriptional control of DNA replication by c-Myc. *Nature* (2007) 448(7152):445–51. doi: 10.1038/nature05953
152. Molenaar JJ, Ebus ME, Geerts D, Koster J, Lamers F, Valentijn LJ, et al. Inactivation of CDK2 is synthetically lethal to MYCN over-expressing cancer cells. *Proc Natl Acad Sci USA* (2009) 106(31):12968–73. doi: 10.1073/pnas.0901418106
153. Cheung NK, Zhang J, Lu C, Parker M, Bahrami A, Tickoo SK, et al. Association of age at diagnosis and genetic mutations in patients with neuroblastoma. *JAMA* (2012) 307(10):1062–71. doi: 10.1001/jama.2012.228
154. Zeineldin M, Federico S, Chen X, Fan Y, Xu B, Stewart E, et al. MYCN amplification and ATRX mutations are incompatible in neuroblastoma. *Nat Commun* (2020) 11(1):913.
155. Petroni M, Veschi V, Gulino A, Giannini G. Molecular mechanisms of MYCN-dependent apoptosis and the MDM2-p53 pathway: an Achille's heel to be exploited for the therapy of MYCN-amplified neuroblastoma. *Front Oncol* (2012) 2:141. doi: 10.3389/fonc.2012.00141
156. Jerby-Arnon L, Pfetzer N, Waldman YY, McGarry L, James D, Shanks E, et al. Predicting cancer-specific vulnerability via data-driven detection of synthetic lethality. *Cell* (2014) 158(5):1199–209. doi: 10.1016/j.cell.2014.07.027
157. Lanning BR, Whitby LR, Dix MM, Douhan J, Gilbert AM, Hett EC, et al. A road map to evaluate the proteome-wide selectivity of covalent kinase inhibitors. *Nat Chem Biol* (2014) 10(9):760–7. doi: 10.1038/nchembio.1582
158. Boike L, Cioffi AG, Majewski FC, Co J, Henning NJ, Jones MD, et al. Discovery of a Functional Covalent Ligand Targeting an Intrinsically Disordered Cysteine within MYC. *Cell Chem Biol* (2020). doi: 10.1016/j.chembiol.2020.09.001
159. Gao H, Sun X, Rao Y. PROTAC Technology: Opportunities and Challenges. *ACS Med Chem Lett* (2020) 11(3):237–40. doi: 10.1021/acsmedchemlett.9b00597
160. Jung KY, Wang H, Teriete P, Yap JL, Chen L, Lanning ME, et al. Perturbation of the c-Myc-Max protein-protein interaction via synthetic alpha-helix mimetics. *J Med Chem* (2015) 58(7):3002–24. doi: 10.1021/jm501440q
161. Wei JS, Song YK, Durinck S, Chen QR, Cheuk AT, Tsang P, et al. The MYCN oncogene is a direct target of miR-34a. *Oncogene* (2008) 27(39):5204–13. doi: 10.1038/onc.2008.154
162. Yasukawa K, Liew LC, Hagiwara K, Hironaka-Mitsuhashi A, Qin XY, Furutani Y, et al. MicroRNA-493-5p-mediated repression of the MYCN oncogene inhibits hepatic cancer cell growth and invasion. *Cancer Sci* (2020) 111(3):869–80. doi: 10.1111/cas.14292
163. Zhang H, Liu T, Yi S, Gu L, Zhou M. Targeting MYCN IRES in MYCN-amplified neuroblastoma with miR-375 inhibits tumor growth and sensitizes tumor cells to radiation. *Mol Oncol* (2015) 9(7):1301–11. doi: 10.1016/j.molonc.2015.03.005
164. Molenaar JJ, Domingo-Fernandez R, Ebus ME, Lindner S, Koster J, Drabek K, et al. LIN28B induces neuroblastoma and enhances MYCN levels via let-7 suppression. *Nat Genet* (2012) 44(11):1199–206. doi: 10.1038/ng.2436
165. Singh A, Trivedi P, Jain NK. Advances in siRNA delivery in cancer therapy. *Artif Cells Nanomed Biotechnol* (2018) 46(2):274–83. doi: 10.1080/21691401.2017.1307210
166. Lau YK, Ramaiyer M, Johnson DE, Grandis JR. Targeting STAT3 in Cancer with Nucleotide Therapeutics. *Cancers (Basel)* (2019) 11(11). doi: 10.3390/cancers11111681
167. Yoda H, Inoue T, Shinozaki Y, Lin J, Watanabe T, Koshikawa N, et al. Direct Targeting of MYCN Gene Amplification by Site-Specific DNA Alkylation in Neuroblastoma. *Cancer Res* (2019) 79(4):830–40. doi: 10.1158/0008-5472.CAN-18-1198

Conflict of Interest: The authors declare that the research was conducted in the absence of any commercial or financial relationships that could be construed as a potential conflict of interest.

frontiers in Oncology

ORIGINAL RESEARCH
published: 25 February 2021
doi: 10.3389/fonc.2021.625207

MYCN Drives a Tumor Immunosuppressive Environment Which Impacts Survival in Neuroblastoma

Salvatore Raieli[1], *Daniele Di Renzo*[2], *Silvia Lampis*[1], *Camilla Amadesi*[1], *Luca Montemurro*[3], *Andrea Pession*[3], *Patrizia Hrelia*[2], *Matthias Fischer*[4,5] *and Roberto Tonelli*[2*]

[1] R&D Department, BIOGENERA SpA, Bologna, Italy, [2] Department of Pharmacy and Biotechnologies, University of Bologna, Bologna, Italy, [3] Pediatric Unit, IRCCS Azienda Ospedaliero-Universitaria di Bologna, Bologna, Italy, [4] Department of Experimental Pediatric Oncology, Medical Faculty, University Children's Hospital of Cologne, Cologne, Germany, [5] Center for Molecular Medicine Cologne (CMMC), University of Cologne, Cologne, Germany

OPEN ACCESS

Edited by:
Christer Einvik,
Arctic University of Norway, Norway

Reviewed by:
Prashant Trikha,
Nationwide Children's Hospital, United States
Maria Francesca Baietti,
KU Leuven, Belgium

***Correspondence:**
Roberto Tonelli
roberto.tonelli@unibo.it

Specialty section:
This article was submitted to Molecular and Cellular Oncology, a section of the journal Frontiers in Oncology

Received: 10 November 2020
Accepted: 04 January 2021
Published: 25 February 2021

Citation:
Raieli S, Di Renzo D, Lampis S, Amadesi C, Montemurro L, Pession A, Hrelia P, Fischer M and Tonelli R (2021) MYCN Drives a Tumor Immunosuppressive Environment Which Impacts Survival in Neuroblastoma. Front. Oncol. 11:625207. doi: 10.3389/fonc.2021.625207

A wide range of malignancies presents *MYCN* amplification (MNA) or dysregulation. *MYCN* is associated with poor prognosis and its over-expression leads to several dysregulations including metabolic reprogramming, mitochondria alteration, and cancer stem cell phenotype. Some hints suggest that *MYCN* overexpression leads to cancer immune-escape. However, this relationship presents various open questions. Our work investigated in details the relationship of *MYCN* with the immune system, finding a correlated immune-suppressive phenotype in neuroblastoma (NB) and different cancers where *MYCN* is up-regulated. We found a downregulated Th1-lymphocytes/M1-Macrophages axis and upregulated Th2-lymphocytes/M2-macrophages in MNA NB patients. Moreover, we unveiled a complex immune network orchestrated by N-Myc and we identified 16 genes modules associated to MNA NB. We also identified a *MYCN*-associated immune signature that has a prognostic value in NB and recapitulates clinical features. Our signature also discriminates patients with poor survival in non-MNA NB patients where *MYCN* expression is not discriminative. Finally, we showed that targeted inhibition of *MYCN* by BGA002 (anti-*MYCN* antigene PNA) is able to restore NK sensibility in *MYCN*-expressing NB cells. Overall, our study unveils a *MYCN*-driven immune network in NB and shows a therapeutic option to restore sensibility to immune cells.

Keywords: *MYCN*, immune system, neuroblastoma, immune signature, immune network, anti-*MYCN* antigene PNA, *MYCN* blocking

INTRODUCTION

MYCN is a transcription factor member of the *MYC* proto-oncogene family involved in nervous system development during embryogenesis (1). *MYCN* regulates different fundamental cellular processes including cell cycle, apoptosis, mitochondria dysfunction, and metabolism (2, 3). Indeed, *MYCN* expression deregulation is linked to a wide range of human tumors (4). *MYCN*

overexpression is generally associated to poor prognosis, driving the cancer cells to a stem cell like phenotype, promoting growth, angiogenesis, and metastasis (5, 6).

Considering the *MYCN* restricted expression in embryogenesis and it is impact in cancer (7), N-Myc is a promising target. However, small molecule approaches to specifically target the N-Myc protein resulted inconsistent. Thus, different other approaches have been developed to downregulate N-Myc or its associated pathways (8). Among these strategies, anti-*MYCN* antigene oligonucleotide PNA showed the ability to specifically block *MYCN* expression in a sustained way (3, 9, 10), resulting in an anti-cancer effect.

MYCN amplification (MNA) is established as a major driver of Neuroblastoma (NB) (characterizing 50% of the high-risk group) (11–13). NB is currently the most common and deadly pediatric solid cancer (representing 6–8% of solid tumors in childhood) (14). Current therapy includes chemotherapy, radiotherapy, surgery, and stem cell transplantation, besides the severe side effects still many patients undergo relapse and progression (15–17).

Immune evasion plays a fundamental role in the development and progression of cancers and is driven by the tumor microenvironment remodeling by cancer cells (18). Different studies showed that NB presents the capacity to evade and to harness the immune system to favor metastasis and progression. In this view, tumor infiltrating lymphocytes (CD4+ and CD8+ T-cells) and natural killers (NKs) are favorable associated with the outcome while T regulatory cells and macrophages are associated with poor prognosis (19–21). NB cells can express checkpoint inhibitors or other molecules capable to interact with the immune system such as PD-L1, MIF, chemokines, release of microRNAs to microenvironment cells, suggesting the potential impact of checkpoint inhibitors and immune-therapy also in this tumor (22–25).

However, while anti-GD2 therapy and chimeric antigen receptor (CAR) T cells showed some promising results in non-MNA NB patients, the checkpoint inhibitors have not shown the same success in improving the survival in NB, as in other solid tumors. These poor results can be linked to different factors as low MHC-I expression, low presence of neoantigens, immunosuppressive environment (15, 26–28). Moreover, N-Myc could play a role in the development of this immunosuppressive microenvironment, as MNA is associated to down-regulation of MHC-I expression in NB and to inhibition of the interferon pathway and to PD-L1 expression (29–32). Indeed, MNA-NB still shows a poor outcome and need a missing specific therapy.

In this context, the tremendous amount of interactions between NB cells and the tumor microenvironment leads to a high complexity, leaving different open questions on how NB harness the immune system to sustain its growth and which factors have a dominant role or have context dependent functions. No studies systematically analyzed immune cell infiltration and their molecular interactions or broadly investigate *MYCN* impact on the immune system. Indeed, the NB immunity and the role of *MYCN* in the immunosuppression are still a field of investigation (33).

MATERIALS AND METHODS

Patient Gene Expression Profiles

The NB dataset (accession: E-MTAB-1781) and the small cell lung cancer (SCLC) (accession: E-MTAB-1999) datasets were downloaded from ArrayExpress, (http://www.ebi.ac.uk/arrayexpress) and processed using the quantile algorithm in *limma*. Another NB dataset and Wilms' dataset were downloaded from TARGET data portal (https://ocg.cancer.gov/programs/target; data freely accessible). From NCBI GEO DataSets (https://www.ncbi.nlm.nih.gov/gds) were downloaded the following datasets: retinoblastoma (accession: GSE59983), rhabdomyosarcoma (accession: GSE114621), T acute lymphoblastic leukemia (T-ALL), and acute myeloid leukemia (AML) dataset (accession: GSE13159, as defined in the dataset meta-data) and for the T-helper lymphocyte (Th) profiles (accession: GSE107011). Another SCLC dataset was retrieved from the supplementary of the article (PMID: 26168399) (34). In the article the different cohorts are referred as following: NB1: E-MTAB-1781, NB2: TARGET NB, Wilms: TARGET Wilms, SCLC1: E-MTAB-1999, SCLC2: PMID 26168399, RB: GSE59983, rhabdomyosarcoma (RMS): GSE114621, T-ALL: GSE13159, AML: GSE13159. The replicate probes within the array were replaced by their average before being scaled. Pearson correlation between *MYCN*, *MYC*, and other genes was calculated with R software. The differential expressed genes between *MYCN*-amplified (MNA) patients and non-MNA patients in the NB datasets (E-MTAB-1781, TARGET dataset) were obtained using the *limma* package algorithm (clinical information was retrieved from the dataset meta-data, patient with an unknown MNA status were removed).

Pathway Analysis

Correlated genes with *MYCN* or *MYC* in each dataset were used as ranked gene list to identify enriched pathway through Gene Set Enrichment Analysis (GSEA) (35). We used Gene Ontology (biological process, cellular component, molecular function, C5 from Molecular Signatures Database v7.0), and GSEA software (V. 4.02). We used the differential expressed genes to conduct the pathway enrichment as described above. Graphic representation was performed with R software. Additional data can be found in **Supplementary Tables 1–3**.

Immune Cell Fraction Estimation Analysis

We used CIBERSOFT tool (Cell type Identification By Estimating Relative Subsets Of known RNA Transcripts) as described in the developer instruction (36). NB expression datasets (E-MTAB-1781, TARGET dataset) were used as mixture file input and were performed 1,000 permutations. We used the LM22 gene signature matrix, an available validated signature for 22 human hematopoietic cell phenotypes. Additionally, we derived from GSE107011 the signature for the Th profile and to generate a Th gene signature matrix (we considered Th1, Th2, Th17, T-regulatory, T follicular helper subsets). The Th signature was input in CIBERSOFT and performed 1,000 permutations. Graphic representation and statistical analysis were performed with R software.

Immune Interaction Network

Protein interactions were retrieved from String database, we selected interactions with a score higher than 400. Protein localization was downloaded from Human Protein Atlas (37). We considered as cell surface proteins only proteins which the approved and supported locations included one of the following terms: cell junctions, focal adhesion sites, plasma membrane. Immune population protein expression were obtained from data supplementary (38). We considered as expressed for each immune subpopulation only proteins with a normalized score higher than 1.5 and only if present in the cell surface. The immune network in MNA and non-MNA patients were established filtering the immune surface proteins present in the differential expressed genes (in order to capture weak interactions, we considered log fold change of 0.5 to assign to MNA or non-MNA). The protein-protein interactions were used to build the circular plots. *MYCN* knock out genes were downloaded by KnockTF (39), we considered log fold change of 1 to assign a gene to the *MYCN* positive or negative regulated list. The previous lists were filtered for the subcellular position. The obtained genes were paired with their possible interactors on the immune population to build the circular plots.

WGCNA Module Analysis and Transcriptional Regulator

Immune population protein expression was retrieved as described above. Patient gene expression profiles (GEP) from E-MTAB-1781 were filtered for this list. WGCNA (40) was performed using the WGCNA package (41) and changing the standard parameters: power of 8, signed network, and a minimum module size of 20. The algorithm assigned the 6,641 filtered genes to 16 modules (2,472 were not assigned to any module, the full list is present in **Supplementary Table 4**). Module similarity was conducted calculating Pearson correlation between module eigengenes. Cell populations were grouped in (CD4+ T-cells, CD8+ T-cells, antigen processing cells, B-cells, NK cells) and calculated the number of proteins present in each module. Graph network was building using the iGraph package. For the heatmap, we calculated the number of proteins present in each module for each immune population and then normalized (z-score). We also calculated the average of the module eigengenes for MNA and non-MNA patient groups and then we normalized (z-score). Pathway enrichment was conducted for each module using anRichment package, the results are present in **Supplementary Table 5**. Gene modules were used to infer transcriptional regulators, we then clustered the obtained regulators in three clusters. Patient expression profiles were also clustered according to the cluster regulators. This procedure is also described in details in **Supplementary Methods** and **Supplementary Tables 6**-**8**.

MYCN Immune Score

Immune genes retrieved from Gene Ontology (GO) and literature. Patient gene expression profiles (GEP) from E-MTAB-1781 and TARGET were filtered for this list (gene list is present in **Supplementary Table 9**). We build a logistic regression model to identify which immune genes where associated to MNA *versus* not MNA patients. The model was cross-validated 50-fold using E-MTAB-1781 as training set (80% of observation at each run) and using TARGET dataset as test set. We used L1 penalization (C = 0.1) and SAGE solver. We selected the weights for each gene and averaged (we filtered all zero weights). We selected two different vector weights associated with MYCN, positive weight vector (associated with MNA) and negative weight vector (associated with non-MNA). The two vectors were normalized subtracting the minimum and dividing by the range:

$$\hat{W}_i^{PM} = \frac{W_i^{PM} - \min\left(W^{PM}\right)}{\max\left(W^{PM}\right) - \min\left(W^{PM}\right)}$$

$$\hat{W}_i^{NM} = \frac{W_i^{NM} - \min\left(W^{NM}\right)}{\max\left(W^{NM}\right) - \min\left(W^{NM}\right)}$$

Through univariate cox regression we selected genes significantly associated to the prognosis (we used the same gene list used for the logistic regression model). The obtained p-value was correct with the Bonferroni correction (list of significant genes obtained through univariate cox regression is present in **Supplementary Table 10**). We then used multivariate Cox regression analysis on the obtained genes, we used a Lasso penalization to select genes associated to the prognosis [we used Penalized R package (42) and selecting lambda1 parameter equal to 0.25]. We selected two different vector weights associated with the survival, positive weight vector (associated with hazard) and negative weight vector (associated with reduction in hazard). The two vectors were normalized subtracting the minimum and dividing by the range:

$$\hat{W}_i^{PC} = \frac{W_i^{PC} - \min\left(W^{PC}\right)}{\max\left(W^{PC}\right) - \min\left(W^{PC}\right)}$$

$$\hat{W}_i^{NC} = \frac{W_i^{NC} - \min\left(W^{NC}\right)}{\max\left(W^{NC}\right) - \min\left(W^{NC}\right)}$$

We selected the genes in common between the two vectors and normalized weight were calculated as the sum of the normalized vector for *MYCN* and Cox model. We then build a positive and a negative immune score for each dataset (-MTAB-1781 and TARGET) multiplying each gene x (log2 expression) for each normalized weight (weights are listed in **Supplementary Table 11**).

$$imm^P = \frac{1}{n}\sum_{i=1}^{n} x_i\left(\hat{W}_i^{PM} + \hat{W}_i^{PM}\right)$$

$$imm^N = \frac{1}{n}\sum_{i=1}^{n} x_i\left(\hat{W}_i^{NM} + \hat{W}_i^{NC}\right)$$

We defined the *MYCN* immune score as the ratio between imm^p and imm^n for each patient GEP. We download Neuroblastoma (last 10 years) and *MYCN* abstracts querying PubMed (details are present in the **Supplementary Methods**) to identify genes of the signature present in literature. Patient were

stratified according their positive or negative normalized *MYCN* immune score (low enriched was defined as z score lower than −0.5, medium enriched comprised between −0.5 and 1, high enriched z score higher than 1). Clinical information was retrieved within the dataset (**Supplementary Tables 12** and **13**). Uniform Manifold Approximation and Projection (UMAP) was computed with a minimum distance of 0.5, considering 30 local neighbors and selecting the Euclidean distance as metric (43).

Statistical Analysis and Software

Analysis were conducted in R (RStudio) and Python (Anaconda release). The following libraries from Python (version 3.7) were used: Scikit-learn, Matplotlib, matplotlib.pyplot, Pandas, UMAP, numpy. The following libraries from R (version 3.5) were used for analysis and graphs: ggplot2, dplyr, data.table, tydr, survival, survminer, wordcloud, WGCNA, circlize, iGraph, anRichment, stringr.

Cell Lines and Treatment

The cell lines used in this study were obtained in 2020 and kept in culture for 30 days and seven passages at maximum. Mycoplasma detection was conducted with LookOut Mycoplasma PCR Detection Kit (Sigma-Aldrich). Additional details about the cell line used in this study can be found in **Supplementary Table 14**. Cell lines treatment with BGA002 and quantitative real-time PCR were conducted as described in (3). List of the primers used in this study can be found in **Supplementary Table 15**. Results have been analyzed in Prism software version 6 (GraphPad).

Neuroblastoma Cell Lines and Natural Killers Co-Culture

Kelly-luc cell-line (Kelly NB cell line transfected with luciferase gene) was generated as described in (3). Kelly-luc has been treated with 2.5 μM of BGA002 for 12 h in Opti-MEM. PBMC from healthy donors has been isolated through Ficoll protocol and resuspended in Opti-MEM. NK cells have been isolated using Human NK Cell Enrichment Set–DM (cat no. 557987, BD Bioscience). NB-NK co-culture has been performed in Opti-MEM for 4 h After adding D-luciferine and lysis buffer we measured luminescence Infinite F200 Tecan. Results have been analyzed in Prism software version 6 (GraphPad).

RESULTS

MYCN Is Associated With Immune Repression and a Th2-Lymphocytes/M2-Macrophages Axis Upregulation

In order to investigate which immune system pathways are associated with *MYCN* in NB, we performed GSEA analysis in NB patient datasets. Interestingly, *MYCN* negative correlated genes are significantly enriched of different immune system pathways in both NB cohort 1 (E-MTAB-1781) and NB cohort 2 (TARGET) (**Figure 1A**). Moreover, we performed differential expressed gene analysis, and found that non-MNA patients are enriched of immune pathways (**Figure S1A**). Furthermore, immune pathways represent a consistent part of the enriched pathways in the MNA patients and in the *MYCN* anti-correlated genes (**Figures S1B, C**). Collectively, these data suggest that *MYCN* is negatively associated with the immune system (especially associated to interferon gamma and phagocytosis) in MNA NB. Since, *MYCN* overexpression is present in a large group of tumors (4, 9, 44–48), we investigated if *MYCN* was also associated to immune suppression in different *MYCN*-expressing cancers (SCLC, RMS, RB, Wilms, AML, T-ALL). We observed that different pathways associated to Th1 are negatively correlated to *MYCN* in different cancer types (**Figures 1B**, **S2A, B**). Remarkably, despite *MYC* and *MYCN* are orthologs we did not find the same anti-correlation for *MYC* in these malignancies (**Figure 1B**). In this view, we investigated which T-helper subsets were enriched in NB. The results confirmed a significantly high abundance of Th1 in non-MNA patients, while Th2 and Th17 were enriched in MNA patients (**Figure 1C**). Furthermore, patients enriched for Th1 are not enriched for Th2/Th17 (**Figure S3**). As described before, Th1 cells are polarizing macrophages toward M1 phenotype, while Th2 direct macrophages polarization toward M2 (49). Thus, we investigated macrophage phenotype enrichment in NB, and found that M1 are significantly enriched in non-MNA patients while M2 are more abundant in MNA patients (**Figure 1D**).

MYCN Exerts a Key Role in the Wide Neuroblastoma Immune Network

As *MYCN* overexpression deeply reprograms NB cells, we investigated the difference in immune network between MNA and non-MNA patients. We firstly identified differential expressed immune genes on the MNA and non-MNA which are present in the cell surface, and we mapped the protein-protein interaction between immune population. We found that non-MNA patients present a much more complex network than MNA patients and a more diverse population scenario (**Figures 2A, B**). Moreover, we identified differential expressed genes after *MYCN* silencing which sub-cellular locations is on the surface. Furthermore, we mapped their potential interactors on the immune population, showing that *MYCN* regulates a wide network of interactions in immune cells in the NB context (**Figures S4A, B**). We used an unbiased clustering approach to group genes in NB belonging to immune system with correlating expression patterns, and we annotated their functional properties through GO enrichment analysis. This analysis revealed 16 different modules that are differentially enriched in MNA and non-MNA patients (**Figures 2C–D**, and **S5A, B**). Interestingly, modules 1 and 2 that are enriched in MNA patients are functional annotated with chromosome organization, cell cycle, RNA processing. Modules containing immune activation genes are instead enriched in non-MNA (**Figure 2D**). Moreover, non-MNA are enriched in modules associated to extracellular vesicles, cytokine production and cell communication (**Figure 2D**). We also inferred the putative regulons in order to identify transcription factor dysregulated between MNA and non-MNA.

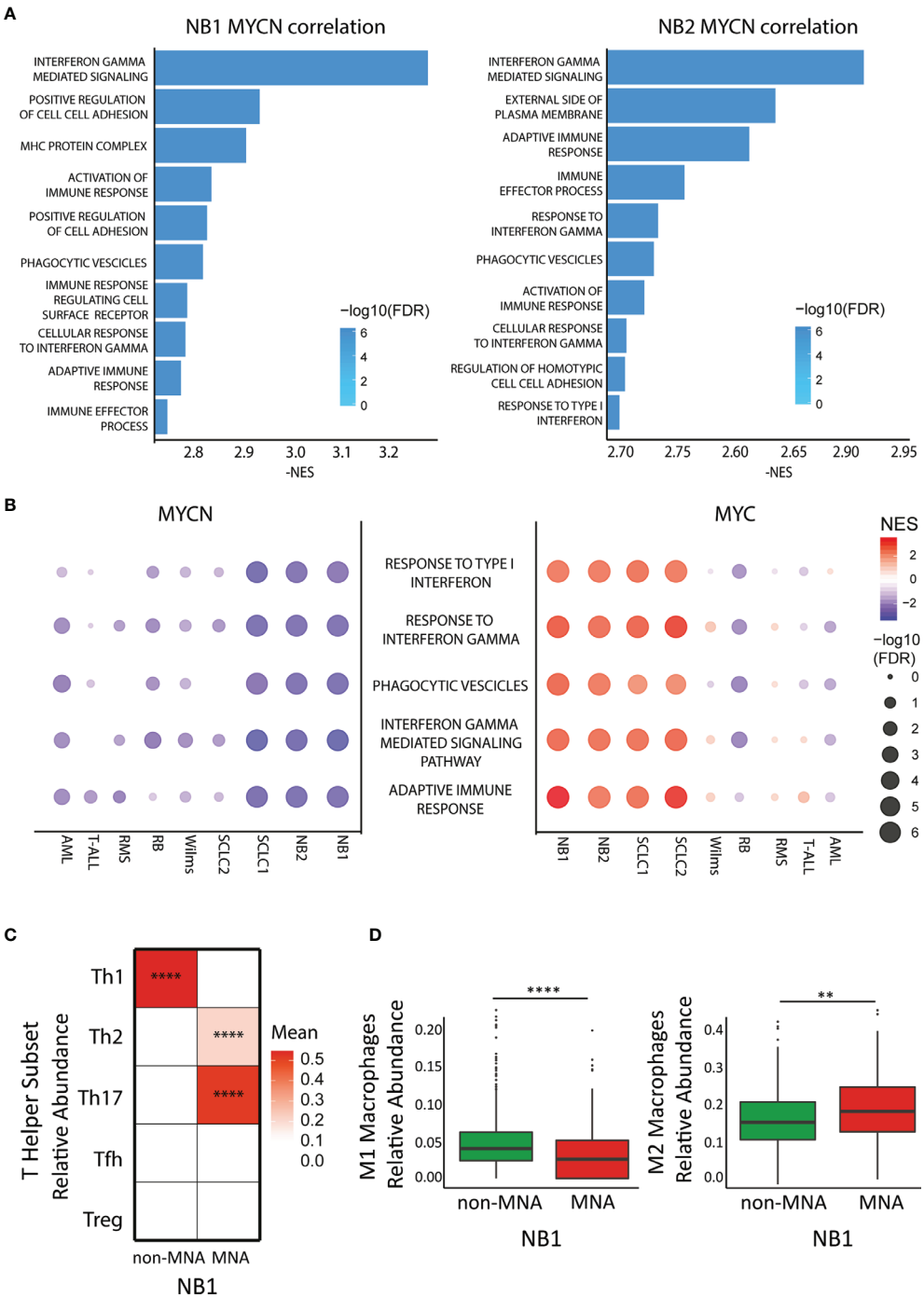

FIGURE 1 | *MYCN* but not *MYC* anticorrelates with immune pathways in cancers. **(A)** Bar plot represents Gene Ontology enriched terms in the *MYCN* negative correlated genes in two neuroblastoma (NB) datasets (left panel: E-MTAB-1781, right panel: TARGET). Bar length represents NES absolute value while color intensity represents -log10 FDR. **(B)** Pathway enrichment for five select immune pathways (GO terms) in different cancer datasets. Symbol size and color intensity indicate—log10 FDR and NES. GO terms enriched in *MYCN* (left panel) and *MYC* (right panel) correlated genes. **(C)** Color intensity indicated the mean of T-helper subset relative abundance in *MYCN* amplified (MNA) and non-MNA patient expression profiles plotted as heatmap. **(D)** Macrophage relative abundance (left panel: M1 population, right panel: M2 population) in MNA and non-MNA patient gene expression profiles. Each symbol represents an individual patient (MNA = 122, non-MNA = 580), the middle line represents the median, the first and third quartiles are indicated as box limits, whiskers represents 1.5 box lengths, extreme values are indicated as single dots. Wilcoxon matched pair test; **P < 0.01; ****P < 0.0001.

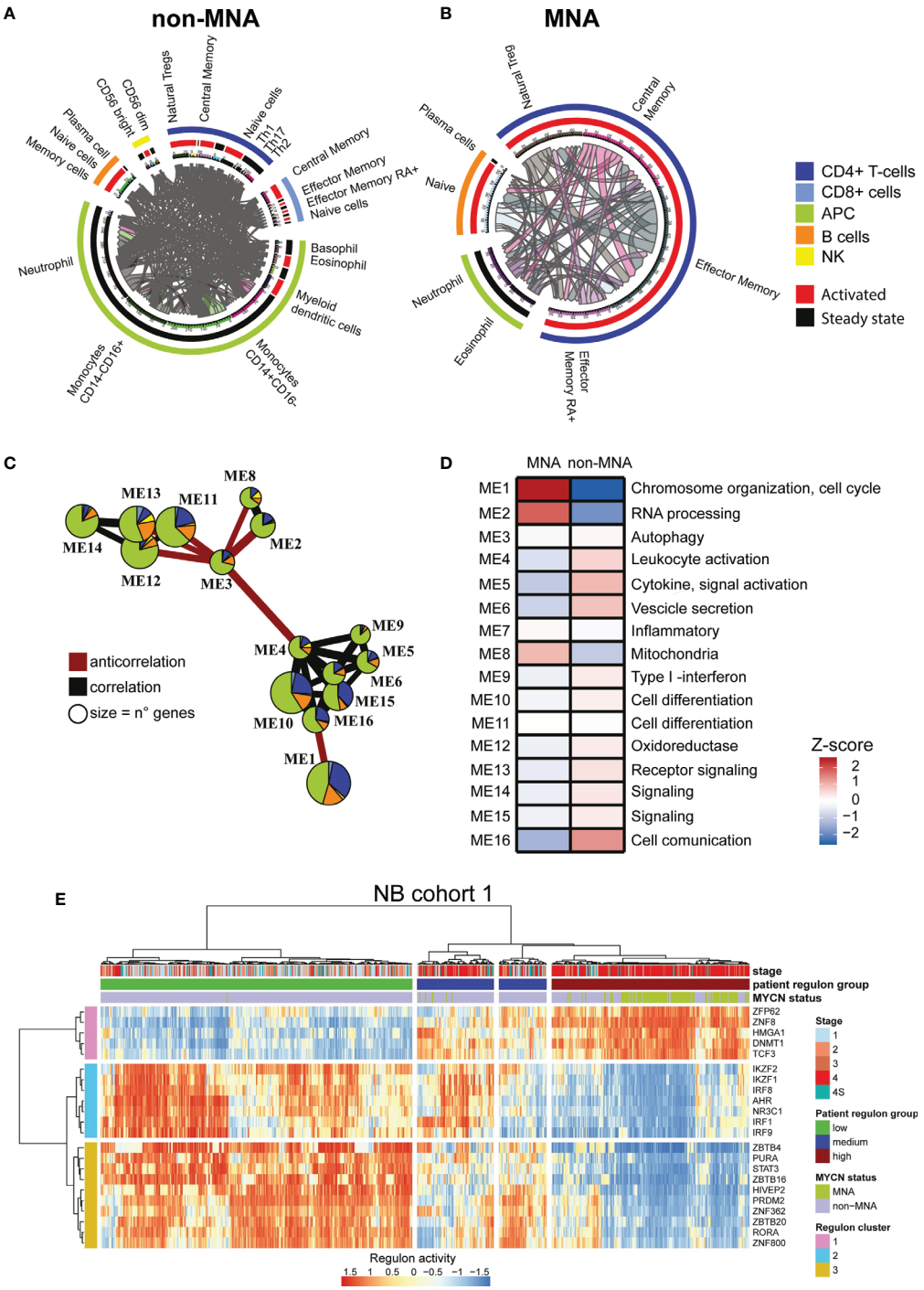

FIGURE 2 | *MYCN* up-regulation impacts a wide immune interaction network. **(A, B)** Circular plots. Immune subpopulations are specified outside the circle, outer circle represents cell types, inner circle represents activation status. Connecting lines indicate connection between two subpopulations and are proportional to the number of connections. **(A)** Immune network in non-(*MYCN* amplification) MNA patients. **(B)** Immune network in MNA patients. **(C)** Immune system gene module network in neuroblastoma (NB). Edges size is proportional to Pearson correlation coefficients, correlation is indicated in gray and negative correlation in red. Modules with no connections are not shown, module size is proportional to the number of genes within. Pie chart colors correspond to immune cell types, the size of the slices corresponds to the number of the genes. **(D)** Heatmap of MNA and non-MNA patient gene expression profiles (MNA = 122, non-MNA = 580) in NB1 cohort (E-MTAB-1781). Color intensity is proportional to z-score of the average eigengenes for each gene module. Main pathway enrichment for each module is listed on the left, full list is present in the Supplementary Tables. **(E)** heatmap representing the normalize relative abundance of regulons in NB1 cohort (E-MTAB-1781). Hierarchical clustering is conducted on the row and the columns using the Euclidean distance. Clinical data are on top.

We identified 22 regulons that are common between the two NB cohorts (**Figures 2E** and **S6A–D**), showing a similar enrichment pattern in MNA and non-MNA patients (**Figures 2E** and **S7A**) and interestingly these transcription factors are also connected through direct protein-protein interactions (**Figure S7B**). Therefore, we apply hierarchical clustering defining three regulon groups with transcriptional factors with similar activity (**Figures 2E** and **S7C**). These three-regulon clusters are differentially enriched of immune modules: regulon cluster one is enriched with genes related to cell-cycle while the other clusters group genes related to immunity (**Figures S7D, E**). Lastly, ChIP-seq public data analysis reveals that the regulon transcription factors are directly regulated by N-Myc (**Figures S8A, B**).

MYCN Effect on Immune System Is an Independent Prognostic Indicator in Neuroblastoma

The identified regulon clusters showed a prognostic impact in both NB cohorts (**Figures S9A–D**). Therefore, we investigated the prognostic impact of *MYCN* regulation of the immune system using a logistic regression and penalized Cox regression, to identify which genes involved in the immune system are associated with the *MYCN* status and the prognosis (AUC = 0.97, **Figures S10A–C**). We built a *MYCN* immune score using the model weight to stratify the NB patients (**Figure 3A**). We identified 430 genes positively associated with MNA and 218 negatively associated. Moreover, we mined PubMed to check which genes in the signature were already identified in literature: 127 were already associated to NB and 60 to *MYCN* (**Figure S10D**). Interestingly, cluster 2-3 transcription factor (TF) regulons were found to negatively regulates *MYCN* positive associated immune signature and positively regulates the negatively associated genes (**Figure S10E**). The *MYCN* immune score was significantly enriched in MNA patients (**Figure 3B**) and according to the score we stratified the patients in three clusters (low, medium, and high *MYCN* immune dysregulation). Remarkably, the high *MYCN* immune dysregulation group was associated with poor prognosis while the low group with a favorable prognosis in NB (**Figure 3C**). Furthermore, the *MYCN* immune score was associated with stage 4 (**Figure 3D**) and high proliferation (**Figure 3E**). We confirmed in an additional NB cohort that the *MYCN* immune score was associated with *MYCN*-status, poor survival, stage, high proliferation and unfavorable histology (**Figures S11A–F**). We also confirmed with a different algorithm (50) that *MYCN* immune score is associated with low immune infiltration and high tumor purity (**Figures S12A, B**). Moreover, the *MYCN* immune score correlated with negative immune checkpoints and anti-correlated with positive immune checkpoints in both cohorts (**Figure S12C**). Interestingly, *MYCN* immune score correlated with Th2 cytokines while negatively associated with Th1 cytokines (**Figure S12D**). As aforementioned, MHC genes are poorly expressed in NB, we investigated whether *MYCN* immune score was associated to MHC genes. Indeed, we noticed that *MYCN* immune score anti-correlated with MHC genes (**Figure S12E**). We also found that *MYCN* immune score is also negatively associated to Toll Like Receptors, as a confirmation that immune receptors are negatively associated to *MYCN* (**Figure S12F**). Moreover, *MYCN* immune score was predictive of the survival in *MYCN* in non-MNA patients in both NB cohorts, while the *MYCN* expression did not (**Figures S13A–D**). Lastly, Cox multivariate analysis showed that *MYCN* immune score is an independent prognostic factor and significantly associated at overall and event free survival in both NB cohorts and also in non-MNA patients (**Figures S14A–H**).

Anti-*MYCN* BGA002 Inhibits CD276 Expression and Restores Natural Killer Susceptibility in Neuroblastoma

We found that NK related pathways are downregulated in MNA-NB patients in the two cohorts used in this study (**Figure 4A**). Indeed, we also found that MHC associated pathway are enriched in genes that are anti-correlating with MYCN (**Figure S15A**). MNA patient GEP showing a reduced expression of NK receptors (NKG2D and Nkp46) and a reduced expression of the cognate ligands (ULBP1, ULBP2, ULPB3, MICA, MICB) known as Self-induced antigen (**Figure S15A**). As reported in literature NK are dysregulated in NB and CD276 has been identified as one of the most relevant factors leading NK inhibition in NB (51–55). Moreover, we found CD276 expression higher in MNA *versus* non-MNA NB patients (**Figures S15B, C**). Thus, we investigated if *MYCN* blocking through the anti-*MYCN* antigene PNA oligonucleotide BGA002 could downregulates its expression in different NB cell lines (comprising MNA, p53 mutated, and non-MNA). Anti-*MYCN* BGA002 potently reduced *MYCN* expression and led to a significant CD276 down-regulation after the treatment in *MYCN*-expressing MNA and non-MNA NB cell lines (**Figure 4B**).

PD-L1 (also named CD274) expression has been reported in NB, but PD-L1 blockade immunotherapy has not reported to be effective in NB (56). We did not find association between neither the survival nor the *MYCN* immune score and PD-L1, while we found that its expression is higher in non-MNA NB patients in both NB cohorts (**Figure S15A**). Moreover, basal expression of CD274 was low (**Figure S15B**). In line with these finding, *MYCN* blocking by BGA002 did not lead to CD274 down-regulation (**Figure 4B**).

HMGA1 has been described as N-Myc transcriptional target (57) and linked to resistance to apoptosis, proliferation induction, and angiogenesis, while it is implicated in the mechanism of resistance to retinoic acid in NB (58–60). We found in the previous section that HMGA1 is a regulon in the cluster 1 associated with poor prognosis in both the NB cohorts, regulated different genes in the *MYCN* immune signature and highly expressed in MNA NB patients (**Figure S15A**). Therefore, we tested if *MYCN* inhibition by anti-*MYCN* BGA002 led to its down-regulation, and indeed we observed a dramatic HMGA1 reduction of expression (**Figure 4B**).

The analysis in the previous section showed that PVR is present in the *MYCN* immune score and negatively associated with the survival (**Supplementary Tables 10** and **11**) and its expression is higher in MNA patients (**Figure S15A**). However, the role of PVR in NB is debated, it has been reported to positively activate NK cells while it has been noticed the

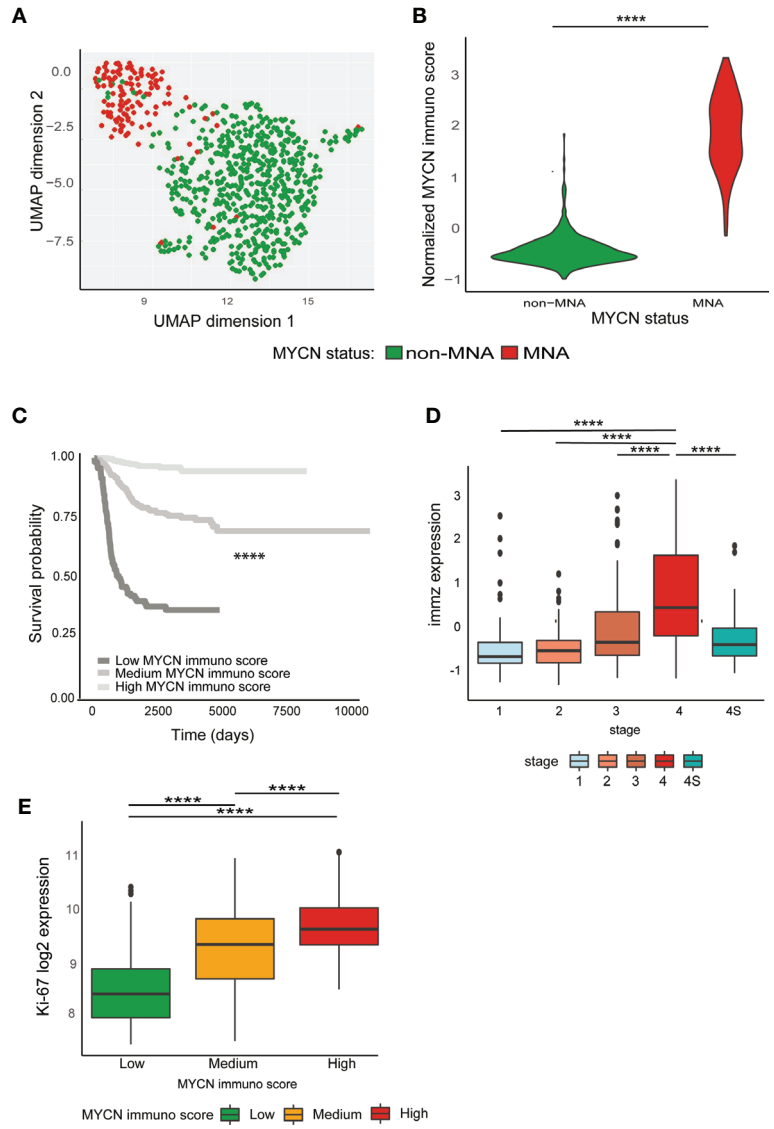

FIGURE 3 | *MYCN* effect on immune system has a prognostic impact. **(A–E)** Analyses conducted on E-MTAB-1781 dataset. **(A)** Uniform Manifold Approximation and Projection (UMAP) projection of *MYCN* amplification (MNA) and non-MNA patient gene expression profiles (PGEP). **(B)** Violin plots represent normalized *MYCN* immune score in MNA and non-MNA PGEP. **(C)** Kaplan–Meier plots for the probability of overall survival over time for patients associated with *MYCN* immune score (high enriched, n = 114; medium enriched, n = 311; low enriched, n = 277). Associated P value is shown in the middle of the plot (log-rank test). **(D)** Normalized *MYCN* immune score in different International Neuroblastoma Staging System Committee (INSS) classification stages. **(E)** Ki-67 log2 expression in patients associated with *MYCN* immune. Wilcoxon matched pair test; ****P < 0.0001.

contrary in other malignancies where is also associated with poor outcome (61, 62). However, *MYCN* blocking by BGA002 led to PVR down-regulation in a small extent (**Figure 4B**).

Considering we found downregulated the NK pathways in MNA-NB patients in the two cohorts used in this study (**Figure 4A**) and because we also found CD276 down-regulation after *MYCN* inhibition by BGA002 (**Figure 4B**), we evaluated the potential effect of *MYCN* inhibition by BGA002 of the reactivation capacity on NK lysis of MNA NB cells (we used Kelly-luc, MNA cell-line transfected with luciferase). We did not notice viability decrease adding the NK-cells alone in co-culture with MNA-NB cells (**Figure 4C**). Indeed, we found that treatment with BGA002 in co-culture with NK in the MNA NB cells significantly impacted on cell viability (**Figure 4C**).

DISCUSSION

MYCN is known to influence diverse aspects of the cancer cells, dysregulating a large network of intracellular pathways (2). Despite previous indication that immune system in NB is altered, the role of *MYCN* in the immune response is not fully

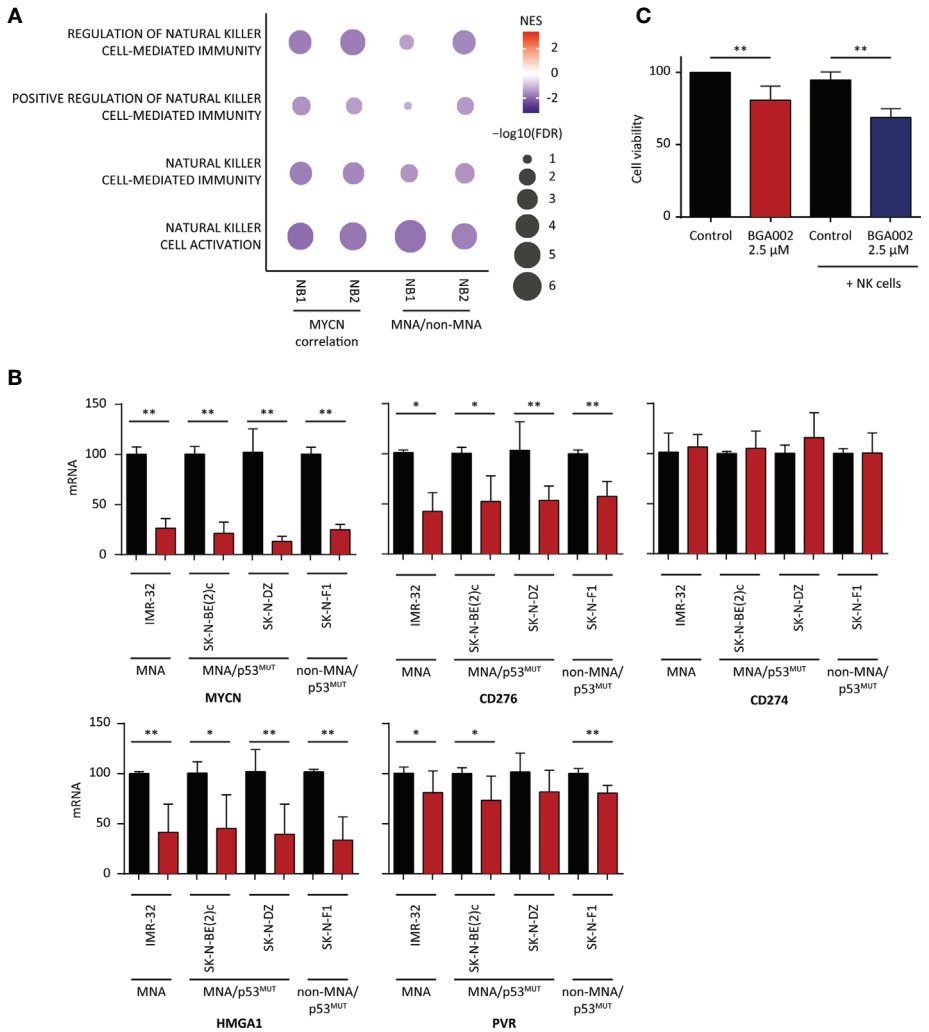

FIGURE 4 | BGA002 blocks CD276 and restores neuroblastoma (NB) susceptibility to natural killer (NK) cells. **(A)** Pathway enrichment for four select immune pathways [Gene Ontology (GO) terms] associated to NK cells. (NB1: E-MTAB-1781, NB2: TARGET NB). Symbol size and color intensity indicate—log10 FDR and NES. GO terms enriched in *MYCN* (left) anti-correlated genes and GO terms enriched in non-*MYCN* amplification (MNA) (right) patients. **(B)** mRNA expression inhibition of different genes (MYCN, CD276, CD274, HMGA1, PVR) in NB cell lines measured through real-time PCR after 12 h of treatment with BGA002 2.5 μM (black is the control, red the treatment, n = 4 biological replicates for each cell line). Wilcoxon matched pair test; *P < 0.05, **P < 0.01, where not shown is not significant (P > 0.05). **(C)** Kelly-luc cell line (MNA NB cell line transfected with luciferase) viability after treatment with BGA002 2.5 μM and NK co-culture (five independent experiments). Wilcoxon matched pair test; **P < 0.01.

understood (19, 33). Since the high complexity showed by the immune system and the intricate relationship between itself and the cancer cells, proper system biology studies are required to map this complex network (63). Our results show that *MYCN* has a great role in dysregulating the immune network in NB, as we showed that different immune pathways are enriched in *MYCN* correlated genes and in MNA *versus* non-MNA differential expressed genes. Moreover, we confirmed in independent cancer mRNA expression patient cohorts that *MYCN* immune anti-correlation is not restricted to NB, but it is a feature also of other malignancies (small cell lung cancer, rhabdomyosarcoma, Wilms' tumor, retinoblastoma, acute myeloid leukemia, and T-acute lymphoid leukemia) (4). Interestingly, we did not find the same anti-correlation pathway with *MYC*, suggesting a different behavior between the two oncogenes of the same family. We found that *MYCN* anti-correlated with Th1 immunity while correlated with Th2, and these subsets are mutually exclusive enriched in NB. As expected by that, *MYCN* correlated with M2 macrophages and inversely correlated with M1 subset. In line with previous literature, Th1 and M1 subsets are associated to anti-tumor immunity while Th2/Th17 and M2 are hijacked by the cancer cells to sustain their growth (64). Indeed, our results evidence a complex regulation in MNA *versus* non-MNA NB, where *MYCN* is a key player in remodeling the immunological micro-environment toward a suppressive phenotype.

We showed that mapping the possible protein-protein interactions between immune cell types in non-MNA NB patients revealed a complex immune network that is lost in MNA patients. Moreover, we found that *MYCN* expression regulated different genes involved in direct interactions with immune cell types playing as a driver of this poor immune environment. We identified 16 immune gene modules that are differently enriched in MNA and non-MNA NB patients, where modules related to immune receptors, signaling, and cytokines are enriched in the latter group. Therefore, all these results confirm a deeply dysregulated immune tumor micro-environment in NB. We also inferred the putative TFs that regulate the immune genes and differed between MNA and non-MNA NB, founding three regulon clusters (22 regulons in total) who are in common between NB1 and NB2 cohorts. Our results show that these regulon clusters are differentially enriched in MNA and non-MNA patients and they regulate the immune landscape in NB. We found that there are direct interactions between these TFs, as well as N-Myc also directly regulates the expression of these regulons as mechanistic explanation of the immune response dysregulation in NB.

Furthermore, we found a link between *MYCN* immune dysregulation and prognostic impact in NB. Generating a *MYCN* immune signature we stratified the NB cohorts in three groups (low, medium and high *MYCN* immune dysregulation) which showed a marked difference in the prognosis. Moreover, the *MYCN* immune score was also associated with other different NB characteristics as stage, proliferation, and histology and we confirmed these associations in an independent NB cohort. As a confirmation, the *MYCN* immune score correlated with immune checkpoints, Th cytokines, MHC genes, and TLRs capturing the immune landscape of the NB. Moreover, apart from MNA, there are other cancer events that can lead to dysregulated N-Myc higher activity (mRNA and protein stabilization, mi-RNA alteration, and so on) making difficult to infer the *MYCN* relevance in these cases (65, 66). Indeed, our score is able to capture this activity in non-MNA patients where *MYCN* mRNA expression level is not able to stratify the patients.

MNA and refractory NB patients are lacking viable therapeutic options (67, 68). Since the broad role of *MYCN* in the pathology, its restricted profile of expression during the embryonal stage, it is a promising target of intervention (69). Despite different attempts, it has been proven to be challenging to specifically target N-Myc with small molecules. We previously reported the specific *MYCN* inhibition through an anti-*MYCN* antigene oligonucleotide PNA (BGA002), showing *MYCN* inhibition and a therapeutic effect *in vitro* and *in vivo* (3, 10). Thus, we investigated if this specific inhibition exerted an effect on the immune suppression guided by *MYCN*. Our results showed that *MYCN* inhibition by BGA002 resulted in a cascade to downregulation of negative immune checkpoints (CD276) and regulons implied (HMGA1) in the immune-suppression phenotype. Indeed, we noticed that anti-*MYCN* treatment also led to NK lysis of MNA NB cells.

Collectively, the data here presented provide demonstrations of the broad role of *MYCN* in suppressing the immune landscape, which play a role in the poor prognosis associated to this oncogene. These data also suggest that *MYCN* blocking can ameliorate the immune suppression characterizing MNA NB patients. Indeed, while specific *MYCN* inhibition by anti-*MYCN* BGA002 can be proposed as a single treatment for MNA NB patients, our results also show that its activity can restore the responsiveness of the immune system against NB, opening the way to use anti-*MYCN* inhibition in combination with immune-therapy.

DATA AVAILABILITY STATEMENT

The datasets presented in this study can be found in online repositories. The names of the repository/repositories and accession number(s) can be found in the article/**Supplementary Material**.

ETHICS STATEMENT

The studies involving human participants were reviewed and approved by the Scientific Ethical Committee of Bologna University. Written informed consent for participation was not required for this study in accordance with the national legislation and the institutional requirements.

AUTHOR CONTRIBUTIONS

SR performed the bioinformatic analysis. CA, SL, and LM performed the experiments and acquired and analyzed the biological data. MF provided dataset for the analysis. SR, DR, and RT wrote the manuscript. AP, PH, and MF revised the manuscript. AP, PH, MF, and RT acquired funds. SR and RT designed and supervised the study. All authors contributed to the article and approved the submitted version.

FUNDING

RT, AP, and PH are funded by the University of Bologna. LM is funded by AGEOP. SR, CA, and SL are funded by BIOGENERA SpA; the funder was not involved in the study design, collection, analysis, interpretation of data, the writing of this article or the decision to submit it for publication.

ACKNOWLEDGMENTS

We would like to thanks Giammario Nieddu, Lucia Cerisoli and Wissem Eljeder in the Biogenera's chemical department for BGA002 supply. We want to also thanks Damiano Bartolucci for suggestions and comments.

SUPPLEMENTARY MATERIAL

The Supplementary Material for this article can be found online at: https://www.frontiersin.org/articles/10.3389/fonc.2021.625207/full#supplementary-material

REFERENCES

1. Mathsyaraja H, Eisenman RN. Parsing Myc Paralogs in Oncogenesis. *Cancer Cell* (2016) 29:1–2. doi: 10.1016/j.ccell.2015.12.009
2. Ruiz-Pérez MV, Henley AB, Arsenian-Henriksson M. The MYCN Protein in Health and Disease. *Genes (Basel)* (2017) 8:113. doi: 10.3390/genes8040113
3. Montemurro L, Raieli S, Angelucci S, Bartolucci D, Amadesi C, Lampis S, et al. A Novel MYCN-Specific Antigene Oligonucleotide Deregulates Mitochondria and Inhibits Tumor Growth in MYCN-Amplified Neuroblastoma. *Cancer Res* (2019) 79:6166–77. doi: 10.1158/0008-5472.CAN-19-0008
4. Rickman DS, Schulte JH, Eilers M. The Expanding World of N-MYC–Driven Tumors. *Cancer Discov* (2018) 8:150–63. doi: 10.1158/2159-8290.CD-17-0273
5. Huang M, Weiss WA. Neuroblastoma and MYCN. *Cold Spring Harb Perspect Med* (2013) 3:22. doi: 10.1101/cshperspect.a014415
6. Matthay KK, Maris JM, Schleiermacher G, Nakagawara A, Mackall CL, Diller L, et al. Neuroblastoma. *Nat Rev Dis Primers* (2016) 2:16078. doi: 10.1038/nrdp.2016.78
7. Zimmerman KA, Yancopoulos GD, Collum RG, Smith RK, Kohl NE, Denis KA, et al. Differential expression of myc family genes during murine development. *Nature* (1986) 319:780–3. doi: 10.1038/319780a0
8. Fletcher JI, Ziegler DS, Trahair TN, Marshall GM, Haber M, Norris MD. Too many targets, not enough patients: rethinking neuroblastoma clinical trials. *Nat Rev Cancer* (2018) 18:389–400. doi: 10.1038/s41568-018-0003-x
9. Tonelli R, McIntyre A, Camerin C, Walters ZS, Leo KD, Selfe J, et al. Antitumor Activity of Sustained N-Myc Reduction in Rhabdomyosarcomas and Transcriptional Block by Antigene Therapy. *Clin Cancer Res* (2012) 18:796–807. doi: 10.1158/1078-0432.CCR-11-1981
10. Tonelli R, Purgato S, Camerin C, Fronza R, Bologna F, Alboresi S, et al. Anti-gene peptide nucleic acid specifically inhibits MYCN expression in human neuroblastoma cells leading to cell growth inhibition and apoptosis. *Mol Cancer Ther* (2005) 4:779–86. doi: 10.1158/1535-7163.MCT-04-0213
11. Campbell K, Gastier-Foster JM, Mann M, Naranjo AH, Van Ryn C, Bagatell R, et al. Association of MYCN copy number with clinical features, tumor biology, and outcomes in neuroblastoma: A report from the Children's Oncology Group. *Cancer* (2017) 123:4224–35. doi: 10.1002/cncr.30873
12. Seeger RC, Brodeur GM, Sather H, Dalton A, Siegel SE, Wong KY, et al. Association of multiple copies of the N-myc oncogene with rapid progression of neuroblastomas. *N Engl J Med* (1985) 313:1111–6. doi: 10.1056/NEJM198510313131802
13. Brodeur GM, Seeger RC, Schwab M, Varmus HE, Bishop JM. Amplification of N-myc in untreated human neuroblastomas correlates with advanced disease stage. *Science* (1984) 224:1121–4. doi: 10.1126/science.6719137
14. Brodeur GM. Neuroblastoma: biological insights into a clinical enigma. *Nat Rev Cancer* (2003) 3:203–16. doi: 10.1038/nrc1014
15. Nallasamy P, Chava S, Verma SS, Mishra S, Gorantla S, Coulter DW, et al. PD-L1, Inflammation, non-coding RNAs, and Neuroblastoma: Immuno-oncology Perspective. *Semin Cancer Biol* (2018) 52:53–65. doi: 10.1016/j.semcancer.2017.11.009
16. Maris JM, Matthay KK. Molecular biology of neuroblastoma. *J Clin Oncol* (1999) 17:2264–79. doi: 10.1200/JCO.1999.17.7.2264
17. Ward E, DeSantis C, Robbins A, Kohler B, Jemal A. Childhood and adolescent cancer statistics, 2014. *CA Cancer J Clin* (2014) 64:83–103. doi: 10.3322/caac.21219
18. Hanahan D, Weinberg RA. Hallmarks of cancer: the next generation. *Cell* (2011) 144:646–74. doi: 10.1016/j.cell.2011.02.013
19. Mina M, Boldrini R, Citti A, Romania P, D'Alicandro V, De Ioris M, et al. Tumor-infiltrating T lymphocytes improve clinical outcome of therapy-resistant neuroblastoma. *Oncoimmunology* (2015) 4:e1019981. doi: 10.1080/2162402X.2015.1019981
20. Shang B, Liu Y, Jiang S, Liu Y. Prognostic value of tumor-infiltrating FoxP3+ regulatory T cells in cancers: a systematic review and meta-analysis. *Sci Rep* (2015) 5:15179. doi: 10.1038/srep15179
21. Vanichapol T, Chutipongtanate S, Anurathapan U, Hongeng S. Immune Escape Mechanisms and Future Prospects for Immunotherapy in Neuroblastoma. *BioMed Res Int* (2018) 2018:e1812535. doi: 10.1155/2018/1812535
22. Challagundla KB, Wise PM, Neviani P, Chava H, Murtadha M, Xu T, et al. Exosome-mediated transfer of microRNAs within the tumor microenvironment and neuroblastoma resistance to chemotherapy. *J Natl Cancer Inst* (2015) 107. doi: 10.1093/jnci/djv135
23. Russell HV, Hicks J, Okcu MF, Nuchtern JG. CXCR4 expression in neuroblastoma primary tumors is associated with clinical presentation of bone and bone marrow metastases. *J Pediatr Surg* (2004) 39:1506–11. doi: 10.1016/j.jpedsurg.2004.06.019
24. Majzner RG, Simon JS, Grosso JF, Martinez D, Pawel BR, Santi M, et al. Assessment of programmed death-ligand 1 expression and tumor-associated immune cells in pediatric cancer tissues. *Cancer* (2017) 123:3807–15. doi: 10.1002/cncr.30724
25. Bach J-P, Rinn B, Meyer B, Dodel R, Bacher M. Role of MIF in inflammation and tumorigenesis. *Oncology* (2008) 75:127–33. doi: 10.1159/000155223
26. Merchant MS, Wright M, Baird K, Wexler LH, Rodriguez-Galindo C, Bernstein D, et al. Phase I Clinical Trial of Ipilimumab in Pediatric Patients with Advanced Solid Tumors. *Clin Cancer Res* (2016) 22:1364–70. doi: 10.1158/1078-0432.CCR-15-0491
27. Burr ML, Sparbier CE, Chan KL, Chan Y-C, Kersbergen A, Lam EYN, et al. An Evolutionarily Conserved Function of Polycomb Silences the MHC Class I Antigen Presentation Pathway and Enables Immune Evasion in Cancer. *Cancer Cell* (2019) 36:385–401.e8. doi: 10.1016/j.ccell.2019.08.008
28. Richards RM, Sotillo E, Majzner RG. CAR T Cell Therapy for Neuroblastoma. *Front Immunol* (2018) 9:2380. doi: 10.3389/fimmu.2018.02380
29. Bernards R, Dessain SK, Weinberg RA. N-myc amplification causes down-modulation of MHC class I antigen expression in neuroblastoma. *Cell* (1986) 47:667–74. doi: 10.1016/0092-8674(86)90509-x
30. Layer JP, Kronmüller MT, Quast T, van den Boorn-Konijnenberg D, Effern M, Hinze D, et al. Amplification of N-Myc is associated with a T-cell-poor microenvironment in metastatic neuroblastoma restraining interferon pathway activity and chemokine expression. *OncoImmunology* (2017) 6:e1320626. doi: 10.1080/2162402X.2017.1320626
31. Brandetti E, Veneziani I, Melaiu O, Pezzolo A, Castellano A, Boldrini R, et al. MYCN is an immunosuppressive oncogene dampening the expression of ligands for NK-cell-activating receptors in human high-risk neuroblastoma. *Oncoimmunology* (2017) 6:e1316439. doi: 10.1080/2162402X.2017.1316439
32. Melaiu O, Mina M, Chierici M, Boldrini R, Jurman G, Romania P, et al. PD-L1 Is a Therapeutic Target of the Bromodomain Inhibitor JQ1 and, Combined with HLA Class I, a Promising Prognostic Biomarker in Neuroblastoma. *Clin Cancer Res* (2017) 23:4462–72. doi: 10.1158/1078-0432.CCR-16-2601
33. Borriello L, Seeger RC, Asgharzadeh S, DeClerck YA. More than the genes, the tumor microenvironment in neuroblastoma. *Cancer Lett* (2016) 380:304–14. doi: 10.1016/j.canlet.2015.11.017
34. George J, Lim JS, Jang SJ, Cun Y, Ozretić L, Kong G, et al. Comprehensive genomic profiles of small cell lung cancer. *Nature* (2015) 524:47–53. doi: 10.1038/nature14664
35. Subramanian A, Tamayo P, Mootha VK, Mukherjee S, Ebert BL, Gillette MA, et al. A knowledge-based approach for interpreting genome-wide expression profiles. *PNAS* (2005) 102:15545–50. doi: 10.1073/pnas.0506580102
36. Newman AM, Steen CB, Liu CL, Gentles AJ, Chaudhuri AA, Scherer F, et al. Determining cell type abundance and expression from bulk tissues with digital cytometry. *Nat Biotechnol* (2019) 37:773–82. doi: 10.1038/s41587-019-0114-2
37. Thul PJ, Åkesson L, Wiking M, Mahdessian D, Geladaki A, Ait Blal H, et al. A subcellular map of the human proteome. *Science* (2017) 356(6340):eaal3321. doi: 10.1126/science.aal3321
38. Rieckmann JC, Geiger R, Hornburg D, Wolf T, Kveler K, Jarrossay D, et al. Social network architecture of human immune cells unveiled by quantitative proteomics. *Nat Immunol* (2017) 18:583–93. doi: 10.1038/ni.3693
39. Feng C, Song C, Liu Y, Qian F, Gao Y, Ning Z, et al. KnockTF: a comprehensive human gene expression profile database with knockdown/knockout of transcription factors. *Nucleic Acids Res* (2020) 48:D93–D100. doi: 10.1093/nar/gkz881
40. Zhang B, Horvath S. A general framework for weighted gene co-expression network analysis. *Stat Appl Genet Mol Biol* (2005) 4(1):17. doi: 10.2202/1544-6115.1128. Article17.
41. Langfelder P, Horvath S. WGCNA: an R package for weighted correlation network analysis. *BMC Bioinformatics* (2008) 9:559. doi: 10.1186/1471-2105-9-559

42. Goeman JJ. L1 penalized estimation in the Cox proportional hazards model. *Biom J* (2010) 52:70–84. doi: 10.1002/bimj.200900028
43. Becht E, McInnes L, Healy J, Dutertre C-A, Kwok IWH, Ng LG, et al. Dimensionality reduction for visualizing single-cell data using UMAP. *Nat Biotechnol* (2019) 37:38–44. doi: 10.1038/nbt.4314
44. Brägelmann J, Böhm S, Guthrie MR, Mollaoglu G, Oliver TG, Sos ML. Family matters: How MYC family oncogenes impact small cell lung cancer. *Cell Cycle* (2017) 16:1489–98. doi: 10.1080/15384101.2017.1339849
45. Lee WH, Murphree AL, Benedict WF. Expression and amplification of the N-myc gene in primary retinoblastoma. *Nature* (1984) 309:458–60. doi: 10.1038/309458a0
46. Hirvonen H, Hukkanen V, Salmi TT, Pelliniemi TT, Alitalo R. L-myc and N-myc in hematopoietic malignancies. *Leuk Lymphoma* (1993) 11:197–205. doi: 10.3109/10428199309086996
47. van Lohuizen M, Breuer M, Berns A. N-myc is frequently activated by proviral insertion in MuLV-induced T cell lymphomas. *EMBO J* (1989) 8:133–6. doi: 10.1002/j.1460-2075.1989.tb03357.x
48. Williams RD, Al-Saadi R, Chagtai T, Popov S, Messahel B, Sebire N, et al. Subtype-specific FBXW7 mutation and MYCN copy number gain in Wilms' tumor. *Clin Cancer Res* (2010) 16:2036–45. doi: 10.1158/1078-0432.CCR-09-2890
49. Orecchioni M, Ghosheh Y, Pramod AB, Ley K. Macrophage Polarization: Different Gene Signatures in M1(LPS+) vs. Classically and M2(LPS-) vs. Alternatively Activated Macrophages. *Front Immunol* (2019) 10:1084. doi: 10.3389/fimmu.2019.01084
50. Yoshihara K, Shahmoradgoli M, Martínez E, Vegesna R, Kim H, Torres-Garcia W, et al. Inferring tumour purity and stromal and immune cell admixture from expression data. *Nat Commun* (2013) 4:2612. doi: 10.1038/ncomms3612
51. Castellanos JR, Purvis IJ, Labak CM, Guda MR, Tsung AJ, Velpula KK, et al. B7-H3 role in the immune landscape of cancer. *Am J Clin Exp Immunol* (2017) 6:66–75.
52. Castriconi R, Dondero A, Augugliaro R, Cantoni C, Carnemolla B, Sementa AR, et al. Identification of 4Ig-B7-H3 as a neuroblastoma-associated molecule that exerts a protective role from an NK cell-mediated lysis. *Proc Natl Acad Sci USA* (2004) 101:12640–5. doi: 10.1073/pnas.0405025101
53. Khan M, Arooj S, Wang H. NK Cell-Based Immune Checkpoint Inhibition. *Front Immunol* (2020) 11:167. doi: 10.3389/fimmu.2020.00167
54. Lee Y-H, Martin-Orozco N, Zheng P, Li J, Zhang P, Tan H, et al. Inhibition of the B7-H3 immune checkpoint limits tumor growth by enhancing cytotoxic lymphocyte function. *Cell Res* (2017) 27:1034–45. doi: 10.1038/cr.2017.90
55. Pistoia V, Morandi F, Bianchi G, Pezzolo A, Prigione I, Raffaghello L. Immunosuppressive microenvironment in neuroblastoma. *Front Oncol* (2013) 3:167. doi: 10.3389/fonc.2013.00167
56. Jabbari P, Hanaei S, Rezaei N. State of the art in immunotherapy of neuroblastoma. *Immunotherapy* (2019) 11:831–50. doi: 10.2217/imt-2019-0018
57. Giannini G, Cerignoli F, Mellone M, Massimi I, Ambrosi C, Rinaldi C, et al. High mobility group A1 is a molecular target for MYCN in human neuroblastoma. *Cancer Res* (2005) 65:8308–16. doi: 10.1158/0008-5472.CAN-05-0607
58. Petroni M, Veschi V, Gulino A, Giannini G. Molecular mechanisms of MYCN-dependent apoptosis and the MDM2-p53 pathway: an Achille's heel to be exploited for the therapy of MYCN-amplified neuroblastoma. *Front Oncol* (2012) 2:141. doi: 10.3389/fonc.2012.00141
59. Zaatiti H, Abdallah J, Nasr Z, Khazen G, Sandler A, Abou-Antoun TJ. Tumorigenic proteins upregulated in the MYCN-amplified IMR-32 human neuroblastoma cells promote proliferation and migration. *Int J Oncol* (2018) 52:787–803. doi: 10.3892/ijo.2018.4236
60. Dobrotkova V, Chlapek P, Jezova M, Adamkova K, Mazanek P, Sterba J, et al. Prediction of neuroblastoma cell response to treatment with natural or synthetic retinoids using selected protein biomarkers. *PloS One* (2019) 14: e0218269. doi: 10.1371/journal.pone.0218269
61. Stamm H, Klingler F, Grossjohann E-M, Muschhammer J, Vettorazzi E, Heuser M, et al. Immune checkpoints PVR and PVRL2 are prognostic markers in AML and their blockade represents a new therapeutic option. *Oncogene* (2018) 37:5269–80. doi: 10.1038/s41388-018-0288-y
62. Zhou X, Du J, Wang H, Chen C, Jiao L, Cheng X, et al. Repositioning liothyronine for cancer immunotherapy by blocking the interaction of immune checkpoint TIGIT/PVR. *Cell Commun Signal* (2020) 18:142. doi: 10.1186/s12964-020-00638-2
63. Yang Y. Cancer immunotherapy: harnessing the immune system to battle cancer. *J Clin Invest* (2015) 125:3335–7. doi: 10.1172/JCI83871
64. Tay RE, Richardson EK, Toh HC. Revisiting the role of CD4 + T cells in cancer immunotherapy—new insights into old paradigms. *Cancer Gene Ther* (2020), 1–13. doi: 10.1038/s41417-020-0183-x
65. Otto T, Horn S, Brockmann M, Eilers U, Schüttrumpf L, Popov N, et al. Stabilization of N-Myc Is a Critical Function of Aurora A in Human Neuroblastoma. *Cancer Cell* (2009) 15:67–78. doi: 10.1016/j.ccr.2008.12.005
66. Powers JT, Tsanov KM, Pearson DS, Roels F, Spina CS, Ebright R, et al. Multiple mechanisms disrupt the let-7 microRNA family in neuroblastoma. *Nature* (2016) 535:246–51. doi: 10.1038/nature18632
67. Mallepalli S, Gupta MK, Vadde R. Neuroblastoma: An Updated Review on Biology and Treatment. *Curr Drug Metab* (2019) 20:1014–22. doi: 10.2174/1389200221666191226102231
68. Pastor ER, Mousa SA. Current management of neuroblastoma and future direction. *Crit Rev Oncol Hematol* (2019) 138:38–43. doi: 10.1016/j.critrevonc.2019.03.013
69. Dikic I, Elazar Z. Mechanism and medical implications of mammalian autophagy. *Nat Rev Mol Cell Biol* (2018) 19:349–64. doi: 10.1038/s41580-018-0003-4

Conflict of Interest: RT and AP are co-founders and shareholders of Biogenera. Authors SR, SL and CA are employed by Biogenera.

The remaining authors declare that the research was conducted in the absence of any commercial or financial relationships that could be construed as a potential conflict of interest.

frontiers in Oncology

MINI REVIEW
published: 16 April 2021
doi: 10.3389/fonc.2020.618515

Non-Genomic Control of Dynamic *MYCN* Gene Expression in Liver Cancer

Xian-Yang Qin * *and Luc Gailhouste* *

Liver Cancer Prevention Research Unit, RIKEN Cluster for Pioneering Research, Wako, Japan

Upregulated *MYCN* gene expression is restricted to specialized cell populations such as EpCAM$^+$ cancer stem cells in liver cancer, regardless of DNA amplification and mutation. Here, we reviewed the role of *MYCN* gene expression in liver homeostasis, regeneration, and tumorigenesis, and discussed the potential non-genomic mechanisms involved in controlling *MYCN* gene expression in liver cancer, with a focus on inflammation-mediated signal transduction and microRNA-associated post-transcriptional regulation. We concluded that dynamic *MYCN* gene expression is an integrated consequence of multiple signals in the tumor microenvironment, including tumor growth-promoting signals, lipid desaturation-mediated endoplasmic reticulum stress adaptation signals, and tumor suppressive miRNAs, making it a potential predictive biomarker of tumor stemness and plasticity. Therefore, understanding and tracing the dynamic changes and functions of *MYCN* gene expression will shed light on the origin of liver tumorigenesis at the cellular level and the development of novel therapeutic and diagnostic strategies for liver cancer treatment.

Keywords: MYCN, liver cancer, microenvironment, inflammation, plasticity, lipid desaturation, endoplasmic reticulum stress, miRNA

OPEN ACCESS

Edited by:
Yusuke Suenaga,
Chiba Cancer Center, Japan

Reviewed by:
Shoma Tsubota,
Nagoya University, Japan
Alexander Schramm,
Essen University Hospital, Germany

***Correspondence:**
Xian-Yang Qin
xyqin@riken.jp
Luc Gailhouste
luc.gailhouste@riken.jp

Specialty section:
This article was submitted to Molecular and Cellular Oncology, a section of the journal Frontiers in Oncology

Received: *17 October 2020*
Accepted: *23 December 2020*
Published: *16 April 2021*

Citation:
Qin X-Y and Gailhouste L (2021) Non-Genomic Control of Dynamic MYCN Gene Expression in Liver Cancer. Front. Oncol. 10:618515. doi: 10.3389/fonc.2020.618515

INTRODUCTION

Liver cancer, mostly hepatocellular carcinoma (HCC), is a highly lethal cancer (>600,000 deaths per year worldwide) in which approximately 10% of patients survive the first 5 years after diagnosis (1). Liver cancer is recognized as an inflammation-related cancer, since more than 90% of HCC cases arise in the context of chronic liver injury and unresolved inflammatory microenvironment due to viral infection, alcohol consumption, or high-fat diet (HFD) hypernutrition (2–4). Advances in antiviral therapy have reduced the risk of developing hepatitis B virus- and hepatitis C virus-related HCC (5, 6). In contrast, non-alcoholic steatohepatitis (NASH) which is characterized by obesity-associated inflammation has attracted much attention, and is believed that it will soon be the leading etiology of HCC (7). Notably, mice fed with HFD alone did not develop liver injury and tumorigenesis. However, hyperresponsivity to lipopolysaccharide and endoplasmic reticulum (ER) stress were observed in fatty liver that contributed to the progression of NASH and HCC (8, 9). This suggested that a non-genomic mechanism was involved in the control of cellular responses such as adaptation to inflammatory stresses during hepatic tumorigenesis. In this line, whereas tumor initiation depends on somatic mutations, the mechanisms underlying tumor

promotion are likely to involve epigenetic factors and environmental factors extrinsic to the cancer cell (10).

MYCN is a canonical proto-oncogene basic helix-loop-helix transcription factor that is mainly restricted to the migrating neural crest (11) and governs cell growth and differentiation during embryonic stages (12). Amplification of the *MYCN* locus was first observed in human neuroblastoma (13). *MYCN* amplification is observed in about 20% of neuroblastoma and represents one of the strongest clinical predictors of poor prognosis (14). *MYCN* amplicons are either organized as extrachromosomal double minutes or as homogeneously stained regions in addition to the single copy of *MYCN* on the short arm of chromosome 2, retained at 2p24, in neuroblastoma cells and other solid tumor cells (15). Notably, the *MYCN* gene is located in a non-fragile region of 2.8 Mbp between two common fragile sites, FRA2Ctel and FRA2Ccen, located at 2p24.3 and 2p24.4, respectively (16). A study by Blumrich and colleagues suggested that *MYCN* amplicons might arise from extra rounds of replication of unbroken DNA secondary structures that accumulate at FRA2C (16). Recent clinical studies have reported increased gene expression of *MYCN* in liver tumor tissues (17, 18). However, according to The Cancer Genome Atlas (TCGA) database, nine of the 371 HCC patients (2.4%) with upregulated *MYCN* mRNA expression but not the seven patients (1.9%) with *MYCN* amplification had a dramatically worse prognosis (**Figure S1A**). Data mining using the Cancer Cell Line Encyclopedia (CCLE) database identified a total of 65 *MYCN* mutations, but none of them was detected in HCC cell lines irrespective of their corresponding mRNA abundance (**Table S1**). This highlights the existence of non-genomic mechanisms potentially responsible for *MYCN* overexpression in liver cancer. Notably, data mining in TCGA showed that the expression of *MYCN* in human HCC was not correlated with that of *c-MYC*, another MYC family membranes known to be crucial for liver cancer maintenance (19) and oncogenic reprogramming of terminally differentiated hepatocytes into liver cancer stem cells (CSCs) (20) (**Figure S1B**). In addition, *MYCN* gene expression but not *c-MYC* gene expression was significantly correlated with the liver CSC marker *EpCAM* gene expression (**Figure S1B**). These data highlight the possibility that *MYCN* gene expression is restricted in CSC-like cells and serves as a more sensitive biomarker than *c-MYC* gene expression for the detection of tumor stemness during liver tumorigenesis. Here, we reviewed the role of dynamic *MYCN* gene expression in liver homeostasis, regeneration, and tumorigenesis, and discussed the potential non-genomic mechanisms involved in controlling *MYCN* gene expression in liver cancer, focusing on inflammation-mediated signal transduction and microRNA-associated (miRNA)-post-transcriptional regulation.

MYCN GENE EXPRESSION IN LIVER HOMEOSTASIS, REGENERATION, AND TUMORIGENESIS

Single-cell RNA sequencing provided a comprehensive view of *MYCN* gene expression in both human and mouse livers (21, 22). Under steady-state conditions, the expression of *MYCN* gene is low in hepatocytes (**Figure S1C**) (21). *MYCN* gene expression in the liver is significantly zonated, which is predominantly induced in the pericentral cells and progressively decreases along the liver lobule towards periportal cells (**Figure S1D**) (22). Metabolic liver zonation requires a Wnt/β-catenin signaling gradient (23). In the uninjured liver, diffusible Wnt ligands produced by the pericentral endothelial cells activate β-catenin signaling-induced target genes such as *Axin2* and maintain a population of proliferating and self-renewing cells, surrounding the central vein, that contribute to homeostatic hepatocyte renewal (24). Wnt/β-catenin signaling is critical for organ development, homeostasis, and regeneration through governing stem cell pluripotency (25). During neocortical development, *MYCN* is a direct downstream target of the Wnt/β-catenin pathway and promotes neuronal fate commitment (26). Therefore, the basal expression of *MYCN* gene in the liver is a likely consequence of the activation of Wnt/β-catenin signaling during liver homeostasis.

Cap Analysis of Gene Expression(CAGE)-based transcriptional profiling of isolated primary mouse hepatocytes revealed that low level of *MYCN* gene expression was detected at 2 h and peaked at 48 h after 70% partial hepatectomy (**Figure S1E**) (27). Liver regeneration is a coordinated multistep process that is largely dependent on the re-entry of differentiated adult hepatocytes into the cell cycle and proliferation (28). In response to loss of hepatic tissue, hepatocyte DNA synthesis peaks at around 24 h, accompanied by the induction of gene expression of growth-regulated and cell-cycle-regulated genes at around 48 h (29). It is possible that the induction of *MYCN* gene expression is a mitogenic response of hepatocytes during liver regeneration. Indeed, a major direct mitogen of hepatocytes, the epidermal growth factor (EGF), stimulated *MYCN* gene expression in neuroblastoma cells *via* the recruitment of the transcription factor Sp1 to the *MYCN* promoter region (30).

Transcriptome profiling of frozen human liver tissues using microarray showed that *MYCN* gene expression was low in healthy livers, cirrhotic livers, and adjacent non-tumorous liver tissue, while it was dramatically increased in tumor tissues (17). Project HOPE (High-tech Omics-based Patient Evaluation), a clinical study aiming to provide multi-omics data of cancer patients, showed the upregulation of *MYCN* gene expression in tumor tissues compared to normal tissues in 22% of recruited HCC patients (18). Our previous cohort studies in Japan (n = 102) and Europe (n = 50) confirmed an increase in *MYCN* gene expression in HCC tumor regions as compared to non-tumor regions (17). Importantly, in a long-term (>10 years) follow-up study, *MYCN* gene expression in HCC tumors was significantly higher in patients with recurrence than in those without recurrence and was positively correlated with the *de novo* recurrence of HCC with a single tumor but not with multiple tumors (17). HCC recurrence at approximately 1–2 years after resection was considered to be mainly due to *de novo* carcinogenesis of liver CSCs or tumor-initiating cells (31). *MYCN* gene expression in HCC was positively correlated with the expression of liver CSC markers and Wnt/β-catenin

signaling markers, suggesting that MYCN expression is restricted to CSC-like HCC (17). Consistently, MYCN expression marked an $EpCAM^+$ CSC-like subpopulation, which was selectively depleted by acyclic retinoid (ACR), a promising chemopreventive agent against the recurrence of HCC after curative treatment (17, 32). EpCAM is a well-characterized liver CSC marker and is a direct transcriptional target of Wnt/β-catenin signaling (33). Similar to liver homeostasis, the restricted MYCN expression in liver CSCs is probably related to the activation of Wnt/β-catenin signaling. Furthermore, four out of six liver biopsies of HCC patients (66.7%) who had received 8 weeks of high-dose ACR treatment (600 mg/day), but not low-dose ACR treatment (300 mg/day), after definitive treatment showed decreased *MYCN* gene expression (< 0.5-fold) (17). In line with this, clinical studies showed that administration of ACR at 600 mg/day, but not 300 mg/day, reduced HCC recurrence after curative treatment (34). Collectively, MYCN expression marked CSC-like subpopulations in heterogeneous HCC and served as a potential therapeutic target and prognostic marker for HCC.

REGULATION OF MYCN GENE EXPRESSION BY TISSUE REPAIR SIGNALS IN THE INFLAMMATORY MICROENVIRONMENT OF LIVER CANCER

Activation of inflammatory signal transduction in the tumor microenvironment is strongly linked to tumor initiation and progression based on two mechanisms: tissue repair and stress adaptation. Obesity-associated production of inflammatory cytokines, such as interleukin-6 (IL-6) and tumor necrosis factor-α (TNFα), induce repeated liver injury and compensatory proliferation, which might lead to aberrant stabilization and activation of "repair signals" such as signal transducer and activator of transcription 3 (STAT3)-dependent oncogenic signaling pathways and initiation and progression of HCC (35–37). The involvement of hyperactivated IL-6-STAT3 signaling axis as a driver oncogenic mechanism in promoting cell proliferation and suppressing antitumor immune response in the background of tumor microenvironment has been reported in several cancers (38). STAT3 directly mediates the initiation of *MYCN* transcription in neuroblastoma cells (39). Inhibition of STAT3 with antisense oligonucleotide or pharmacological inhibitors reduced *MYCN* gene expression and decreased neuroblastoma tumorigenicity in preclinical mouse models (39, 40). During early hepatocarcinogenesis, STAT3 activated by paracrine IL-6 produced by inflammatory cells, might directly bind to the promoter and upregulate the gene and protein expression of CD133, a well-defined liver CSC marker representing a specialized subpopulation of highly tumorigenic cells with high MYCN expression (17, 41, 42). Inhibition of STAT3 with sorafenib, the first-line recommended therapy for patients with advanced HCC, decreased CD133 levels and suppressed *in vivo* tumorigenicity by eradicating the liver tumor microenvironment (41). Of note, a recent proteomics-based pathway analysis showed that sorafenib inactivated downstream signaling of MYCN in HCC cells (43). In addition, growth factors such as EGF induced by inflammatory cytokines contribute to the upregulation of *MYCN* gene expression in an inflammatory microenvironment (30). Nerve growth factor (NGF) is expressed by hepatocytes during fibrotic liver injury (44). In *MYCN*-amplified neuroblastoma cells, NGF suppressed *MYCN* gene expression through mitogen-activated protein kinase signaling pathways (45). In contrast, a global transcriptome analysis showed reduced *MYCN* gene expression in NGF-deprived sympathetic neurons (46). It is unclear whether NGF directly regulates *MYCN* gene expression in normal livers and HCC cells.

REGULATION OF MYCN GENE EXPRESSION BY LIPID DESATURATION-MEDIATED STRESS ADAPTATION SIGNALS IN THE INFLAMMATORY MICROENVIRONMENT OF LIVER CANCER

The cell membrane serves as the barrier between life and death for individual cells and the first line of defense in response to environmental stress. In addition to their function as energy storage sources or as building blocks of membranes, membrane lipids have attracted much attention as biologically active molecules. They regulate the formation of membrane assembly of signal complexes by either binding to cognate receptors or recruiting proteins from the cytosol and coordinating signal transduction (47). Membrane lipids are highly diverse in chemical structures, varying in the desaturation and chain elongation of fatty acyl chains, backbones (such as glycerol, sphingoid base, and cholesterol), and head group substituents. Changes in membrane lipid composition affect membrane physical properties, as observed in mammalian cells in response to environmental stimuli (47). For example, macrophages rapidly reprogram their lipid metabolism, especially *de novo* cholesterol biosynthesis (48, 49) and desaturated fatty acid biosynthesis (50), for appropriate inflammatory and host defense functions in response to diverse inflammatory signals. Under inflammatory conditions, the fatty acid synthetic enzyme fatty acid synthase, reshapes macrophage lipid homeostasis for the assembly of cholesterol-dependent inflammatory signals such as Rho GTPase at the plasma membrane (51). In contrast, lipid desaturases such as stearoyl-CoA desaturase (SCD1) and fatty acid desaturase (FADS) were induced to inhibit the inflammatory responses through the production of anti-inflammatory omega-3 polyunsaturated fatty acids or disruption of membrane signaling complexes associated with lipid rafts, also known as membrane microdomains, which are enriched with saturated sphingolipids and cholesterol (52). Importantly, lipid reprograming, especially the upregulation of unsaturated fatty acids, has recently been recognized as a critical feature of stem cell maintenance under both physiological and abnormal conditions (53, 54). Our previous proteome and metabolome analyses demonstrated that high MYCN

expression in liver CSCs was characterized by increased expression of lipid desaturases such as SCD1 and FADS and elevated levels of monounsaturated fatty acids such as palmitoleic acid and oleic acid in comparison to non-CSC HCC cells (55, 56). In addition to the upstream regulatory role of MYCN in lipid metabolism reprograming of cancer cells [reviewed in (57)], inhibition of lipid desaturation using both genetic and pharmacological approaches against SCD1 reduced *MYCN* gene expression and selectively suppressed the proliferation of high *MYCN*-expressing HCC cells, suggesting a direct regulatory role of lipid desaturation on *MYCN* transcription (56). Genome-wide transcriptome analysis using RNA-seq showed that ER stress-related signaling pathways were regulated upon siRNA knock-down of *SCD1* but not *MYCN* in high MYCN-expressing HCC cells (56). Further, mechanistic studies showed that inhibition of lipid desaturation resulted in activation of ER stress signaling pathways, such as the expression of the transcription suppressor, cyclic AMP-dependent transcription factor 3 (ATF3), which reversibly regulates *MYCN* gene expression in high MYCN-expressing CSC-like HCC cells, CSC-rich spheroids, and in clinical HCC tissues (56).

ER stress response, also known as unfolded protein response (UPR), is activated as a cell-defensive mechanism triggered by multiple stress factors and plays a critical role in the switch between cell survival and cell death. Evading ER stress-induced apoptosis and differentiation is critical for the maintenance of long-living and self-renewing stem cells under both normal and malignant conditions (58–60). Therefore, modulation of ER stress-induced loss of stemness represents a potential therapeutic strategy for cancers and chronic inflammatory diseases (61, 62). In line with this, pharmacological targeting of SCD1 achieved remarkable therapeutic outcomes in glioblastoma and liver cancer by triggering ER stress-mediated apoptosis and differentiation of CSCs (63, 64). Mechanistically, enhanced levels of unsaturated fatty acids in CSCs could suppress ER stress by preventing saturated fatty acid-induced calcium accumulation, oxidative stress, or detrimental stiffening of the ER and plasma membrane (65–68). Collectively, under lipid-rich inflammatory conditions, both repair signals and stress adaptation signals contribute to the upregulation of *MYCN* gene expression (**Figure 1**). Inflammatory cytokine-induced chronic injury leads to the activation of repair signals, which triggers downstream *MYCN* gene expression and compensatory proliferation. In contrast, lipid desaturation-mediated membrane reprogramming reduces or counteracts the formation of membrane assembly of stress signal complexes and enables CSCs to survive and evade ER stress-induced apoptosis/differentiation. We propose that the stress adaption mechanism in long-living CSC-like cells contributes to tumorigenesis such as through accumulation of mutations in the survived cells, which is accompanied by the increase of *MYCN* gene expression.

POST-TRANSCRIPTIONAL CONTROL OF MYCN GENE EXPRESSION BY MIRNAS IN LIVER CANCER

miRNAs are evolutionarily conserved small non-coding RNAs of approximately 22 nucleotides in length that modulate gene expression by complementary base pairing with the 3'-untranslated regions (3'-UTRs) of messenger RNAs [reviewed in (69)]. An essential feature of miRNA-based gene regulation is that a single miRNA can recognize numerous mRNAs and, conversely, a target mRNA can be recognized by several miRNAs. A large number of studies have reported the key role of these posttranscriptional regulators in the control of various cellular processes and human diseases (70). In cancer, aberrant

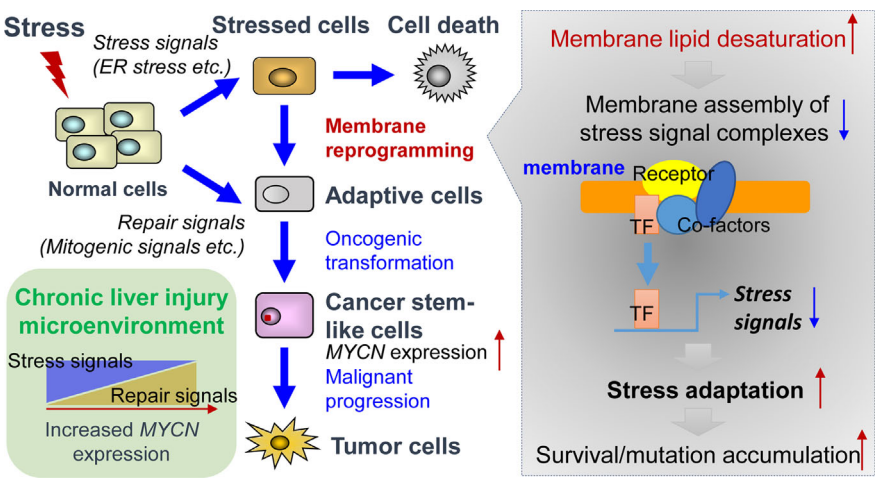

FIGURE 1 | Tissue repair and stress adaptation signal-based control of *MYCN* gene expression in the inflammatory microenvironment of liver cancer. Under lipid-rich inflammatory conditions, inflammatory cytokines-induced chronic injury leads to the activation of repair signals such as mitogenic signals resulting in compensatory proliferation, thereby triggering downstream *MYCN* gene expression. In contrast, lipid desaturation-mediated membrane reprogramming reduces or counteracts the formation of membrane assembly of stress signal complexes and enables the CSCs to survive and evade ER stress-induced apoptosis/differentiation, which leads to the rescue of *MYCN* gene expression and initiates tumorigenesis by accumulation of mutations in long-living CSCs.

expression of miRNAs has been well described and is associated with the deregulation of critical genes involved in tumor progression (71). Indeed, cancer-related miRNAs can act as oncogenes (called oncomirs) or tumor-suppressors, depending on their targets, and promote or negatively influence tumor growth, invasion, and/or drug resistance, respectively (72). Specific miRNA profiles have been identified in neuroblastoma, which reflect different subtypes of tumors and correlate with the advancement of the disease or its prognosis [reviewed in (73)]. In this malignancy, numerous *MYCN*-targeting miRNAs have been identified. Loss of miR-34a at chromosome band 1p36, a region frequently deleted due to loss of heterozygosity in neuroblastoma cells (74), is associated with *MYCN* amplification and promotion of tumor aggressiveness (75). Thus far, several additional miRNA/MYCN regulatory axes have been characterized. In a model of *MYCN*-amplified neuroblastoma cells, experimental overexpression of miR-101 and let-7e induced a decrease in MYCN protein levels and inhibited cell growth *via* the direct regulation of MYCN (76, 77). In another interesting study by Neviani and colleagues, the tumor-suppressor miR-186 was detected in natural killer cell-derived exosomes, which exhibited cytotoxicity against neuroblastoma cells with high *MYCN* levels (78). The authors showed that *MYCN* expression was directly inhibited by miR-186. In addition, the targeted delivery of miR-186 to *MYCN*-amplified neuroblastoma cells or natural killer cells resulted in significant tumor growth inhibition. A recent study based on the modeling of miRNA-mRNA interactions identified a regulatory loop between *MYCN*

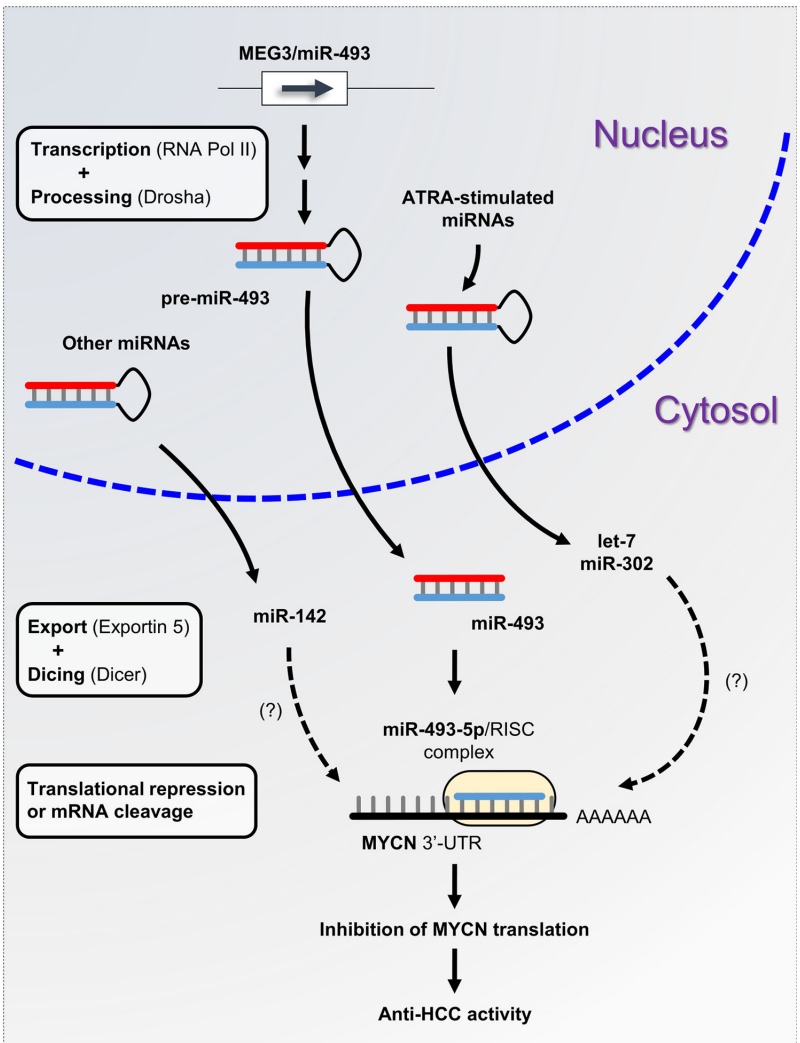

FIGURE 2 | miRNA-based control of *MYCN* gene expression in liver cancer. miRNA biogenesis is a multistep process. Following transcription by RNA polymerase II, primary precursor miRNAs (pri-miRNAs) are cleaved into precursor miRNAs (pre-miRNAs) by the RNase III enzyme Drosha and exported out of the nucleus to produce mature miRNAs. Subsequently, mature miRNAs are loaded onto the RNA-induced silencing complex (RISC) and directed to the 3'-UTR of target mRNAs. Here, we propose the miRNA/MYCN regulatory network model, in which the tumor-suppressor miR-493-5p and the ATRA-stimulated miRNAs modulate *MYCN* expression and impede HCC progression.

and miR-204 in neuroblastoma cells (79). The authors showed that miR-204 directly targeted *MYCN* mRNA and decreased its protein levels. In contrast, MYCN was able to bind to the promoter of miR-204 and inhibit the expression of the miRNA. Remarkably, the capability of MYCN to activate the expression of critical oncomirs, such as miR-221, miR-9, or the miR-17-92 cluster, has also been observed in neuroblastoma cells and other types of solid tumor cells (80).

A plethora of studies have described the functional interconnection between miRNAs and MYCN in neuroblastoma. However, little is known about the miRNAs involved in the posttranscriptional regulation of *MYCN* in liver cancer. The aberrant expression of miRNAs is a typical hallmark of hepatocarcinogenesis and tumor progression (81). We previously demonstrated that maternally expressed 3 (MEG3)-derived miR-493-5p tumor-suppressor was epigenetically silenced by CpG hypermethylation in HCC cells and tumor tissues from patients (82). Experimental overexpression of miR-493-5p promoted an anti-cancer response by inhibiting HCC cell growth and invasion, in part, through the negative regulation of insulin-like growth factor 2 (IGF2) and the IGF2-derived intronic oncomir miR-483-3p. More recently, our group highlighted *MYCN* as another major target of miR-493-5p using global gene expression analysis of liver cancer cells with restored expression of miR-493-5p (83). More precisely, real-time qPCR data showed an inverse and significant correlation between miR-493-5p and *MYCN* expression levels in the tumors of patients with advanced HCC. A dual-luciferase reporter activity assay validated miR-493-5p-mediated inhibition of *MYCN via* the targeting of two distinct regions in the *MYCN* 3'-UTR (**Figure 2**). To the best of our knowledge, no additional miRNA interacting directly with *MYCN* mRNA has been described in liver cancer thus far. However, in a study based on big data mining and connectivity map analysis, Xiong et al. uncovered the existence of a potential hsa_circRNA_104515/hsa-miR-142-5p/MYCN regulatory axis in HCC (84). In agreement with this finding, we found that TargetScanHuman predicted an exact consequential pairing of the *MYCN* 3'-UTR with positions 2-8 (7mer-m8) of mature miR-142-5p (**Figure S1F**). Interestingly, two reports described downregulation of miR-142-5p in liver cancer cells and showed that forced expression of miR-142-5p inhibited HCC cell growth and invasion (85, 86). Taken together, these data strongly suggest the tumor-suppressive role of miR-142-5p through post-transcriptional control of *MYCN* and its therapeutic potential in liver cancer. Finally, recent studies showed that all-*trans* retinoic acid (ATRA), which is an isomer of retinoic acid, was able to modulate the expression of more than 300 miRNAs and inhibit the growth of various types of tumor cells (87). Among the miRNAs upregulated after ATRA treatment, miR-34a-5p, miR-103a-3p, miR-200b/c-3p, miR-302-3p, and members of the let-7 family appeared appealing given their potential ability to target the *MYCN* 3'-UTR as predicted by TargetScanHuman 7.2 (**Figure S1F**). While the tumor-suppressor feature of the let-7 family members has been well-documented, further investigations will be required to evaluate the beneficial role of ATRA-stimulated miRNAs in HCC, since some of these miRNAs may also exhibit oncogenic activity.

CONCLUSIONS

Mature hepatocytes exhibit remarkable plasticity by direct dedifferentiation into an undifferentiated state in the tumor microenvironment, which are believed to represent the cells of origin for liver cancer (88). Since any cell has the potential to become a CSC, the stemness of liver CSCs could be considered as a dynamic state that can be acquired rather than a cell intrinsic property of specialized existing cells [reviewed in (89)]. *MYCN* gene is overexpressed in restricted cell populations such as $EpCAM^+$ CSCs in liver cancer, regardless of DNA amplification and mutation. Dynamic *MYCN* gene expression is an integrated consequence of multiple signals in the tumor microenvironment, including tumor stemness/growth-promoting signals such as Wnt/β-catenin and IL-6-STAT3 signaling, lipid desaturation-mediated ER stress adaptation signals, and tumor suppressive miRNAs. We propose that *MYCN* gene expression might represent a potential predictive biomarker of tumor stemness and plasticity. Hence, understanding and tracing the dynamic changes and functions of *MYCN* gene expression during hepatic tumorigenesis will shed light on the origin of liver tumorigenesis at the cellular level and the development of novel therapeutic and diagnostic strategies for HCC treatment.

AUTHOR CONTRIBUTIONS

X-YQ and LG performed the literature search and wrote the manuscript. All authors contributed to the article and approved the submitted version.

FUNDING

This work was supported by grants from the Ministry of Education, Culture, Sports, Science and Technology of Japan's Grant-in-Aid for Scientific Research (C), JP20K07349 (to X-YQ), and JP20K07604 (to LG) and RIKEN Incentive Research Projects (to X-YQ and LG).

ACKNOWLEDGMENTS

This manuscript is dedicated to the memory of Soichi Kojima (1961–2019).

SUPPLEMENTARY MATERIAL

The Supplementary Material for this article can be found online at: https://www.frontiersin.org/articles/10.3389/fonc.2020.618515/full#supplementary-material

Supplementary Figure 1 | Supporting data of *MYCN* gene expression in the liver. **(A)** Overall survival Kaplan-Meier estimate of HCC patients with *MYCN* overexpression (left) or amplification (right) according to TCGA database (TCGA, PanCancer Atlas). **(B)** Correlation between *MYCN* gene expression and *c-MYC* gene expression (left), *MYCN* gene expression and *EpCAM* gene expression

(middle), and *c-MYC* gene expression and *EpCAM* gene expression (right) in human HCC according to TCGA database (TCGA, PanCancer Atlas). **(C)** *MYCN* gene expression pattern in human liver visualized using a web interface (http://human-liver-cell-atlas.ie-freiburg.mpg.de/), which is based on the single cell RNA-seq data published in (21). **(D)** *Mycn* gene expression in mouse liver zonation according to the single cell RNA-seq data (GSE84498) published in (22). **(E)** *Mycn* gene expression in mouse primary hepatocyte isolated at 2, 30, 48 h or 1 w after partial hepatectomy and at 2 h from sham control during liver regeneration. The data was obtained from the CAGE-based transcriptome data published in **Table S1** in (27). **(F)** Prediction of miR-142-5p, miR-34a-5p, miR-103a-3p, miR-200b/c-3p, miR-302-3p, and members of the let-7 family targeting MYCN 3'-UTR according to TargetScanHuman (http://www.targetscan.org, release 7.2).

REFERENCES

1. Llovet JM, Villanueva A, Lachenmayer A, Finn RS. Advances in targeted therapies for hepatocellular carcinoma in the genomic era. *Nat Rev Clin Oncol* (2015) 12:408–24. doi: 10.1038/nrclinonc.2015.103
2. Bishayee A. The role of inflammation and liver cancer. *Adv Exp Med Biol* (2014) 816:401–35. doi: 10.1007/978-3-0348-0837-8_16
3. Perz JF, Armstrong GL, Farrington LA, Hutin YJ, Bell BP. The contributions of hepatitis B virus and hepatitis C virus infections to cirrhosis and primary liver cancer worldwide. *J Hepatol* (2006) 45:529–38. doi: 10.1016/j.jhep.2006.05.013
4. Calvisi DF, Wang C, Ho C, Ladu S, Lee SA, Mattu S, et al. Increased lipogenesis, induced by AKT-mTORC1-RPS6 signaling, promotes development of human hepatocellular carcinoma. *Gastroenterology* (2011) 140:1071–83. doi: 10.1053/j.gastro.2010.12.006
5. Hosaka T, Suzuki F, Kobayashi M, Seko Y, Kawamura Y, Sezaki H, et al. Long-term entecavir treatment reduces hepatocellular carcinoma incidence in patients with hepatitis B virus infection. *Hepatology* (2013) 58:98–107. doi: 10.1002/hep.26180
6. Ioannou GN, Green PK, Berry K. HCV eradication induced by direct-acting antiviral agents reduces the risk of hepatocellular carcinoma. *J Hepatol* (2017) 68:25–32. doi: 10.1016/j.jhep.2017.08.030
7. Starley BQ, Calcagno CJ, Harrison SA. Nonalcoholic fatty liver disease and hepatocellular carcinoma: a weighty connection. *Hepatology* (2010) 51:1820–32. doi: 10.1002/hep.23594
8. Imajo K, Fujita K, Yoneda M, Nozaki Y, Ogawa Y, Shinohara Y, et al. Hyperresponsivity to low-dose endotoxin during progression to nonalcoholic steatohepatitis is regulated by leptin-mediated signaling. *Cell Metab* (2012) 16:44–54. doi: 10.1016/j.cmet.2012.05.012
9. Nakagawa H, Umemura A, Taniguchi K, Font-Burgada J, Dhar D, Ogata H, et al. ER stress cooperates with hypernutrition to trigger TNF-dependent spontaneous HCC development. *Cancer Cell* (2014) 26:331–43. doi: 10.1016/j.ccr.2014.07.001
10. Maeda S, Kamata H, Luo J-L, Leffert H, Karin M. IKKβ Couples Hepatocyte Death to Cytokine-Driven Compensatory Proliferation that Promotes Chemical Hepatocarcinogenesis. *Cell* (2005) 121:977–90. doi: 10.1016/j.cell.2005.04.014
11. Wakamatsu Y, Watanabe Y, Nakamura H, Kondoh H. Regulation of the neural crest cell fate by N-myc: promotion of ventral migration and neuronal differentiation. *Development* (1997) 124:1953–62.
12. Knoepfler PS. N-myc is essential during neurogenesis for the rapid expansion of progenitor cell populations and the inhibition of neuronal differentiation. *Genes Dev* (2002) 16:2699–712. doi: 10.1101/gad.1021202
13. Schwab M, Varmus HE, Bishop JM, Grzeschik K-H, Naylor SL, Sakaguchi AY, et al. Chromosome localization in normal human cells and neuroblastomas of a gene related to c-myc. *Nature* (1984) 308:288–91. doi: 10.1038/308288a0
14. Maris JM, Hogarty MD, Bagatell R, Cohn SL. Neuroblastoma. *Lancet* (2007) 369:2106–20. doi: 10.1016/S0140-6736(07)60983-0
15. Storlazzi CT, Lonoce A, Guastadisegni MC, Trombetta D, D'Addabbo P, Daniele G, et al. Gene amplification as double minutes or homogeneously staining regions in solid tumors: Origin and structure. *Genome Res* (2010) 20:1198–206. doi: 10.1101/gr.106252.110
16. Blumrich A, Zapatka M, Brueckner LM, Zheglo D, Schwab M, Savelyeva L. The FRA2C common fragile site maps to the borders of MYCN amplicons in neuroblastoma and is associated with gross chromosomal rearrangements in different cancers. *Hum Mol Genet* (2011) 20:1488–501. doi: 10.1093/hmg/ddr027
17. Qin XY, Suzuki H, Honda M, Okada H, Kaneko S, Inoue I, et al. Prevention of hepatocellular carcinoma by targeting MYCN-positive liver cancer stem cells with acyclic retinoid. *Proc Natl Acad Sci USA*. (2018) 115:4969–74. doi: 10.1073/pnas.1802279115
18. Okamura Y, Uesaka K, Sugiura T, Ito T, Yamamoto Y, Ashida R, et al. The Outcomes and Next Landscapes of Project HOPE (High-Tech Omics-Based Patient Evaluation) for Hepatocellular Carcinoma. *Am J Gastroenterol* (2015) 110:S851. doi: 10.14309/00000434-201510001-02018
19. Shachaf CM, Kopelman AM, Arvanitis C, Karlsson Å, Beer S, Mandl S, et al. MYC inactivation uncovers pluripotent differentiation and tumour dormancy in hepatocellular cancer. *Nature* (2004) 431:1112–7. doi: 10.1038/nature03043
20. Holczbauer Á, Factor VM, Andersen JB, Marquardt JU, Kleiner DE, Raggi C, et al. Modeling Pathogenesis of Primary Liver Cancer in Lineage-Specific Mouse Cell Types. *Gastroenterology* (2013) 145:221–31. doi: 10.1053/j.gastro.2013.03.013
21. Aizarani N, Saviano A, Sagar, Mailly L, Durand S, Herman JS, et al. A human liver cell atlas reveals heterogeneity and epithelial progenitors. *Nature* (2019) 572:199–204. doi: 10.1038/s41586-019-1373-2
22. Halpern KB, Shenhav R, Matcovitch-Natan O, Toth B, Lemze D, Golan M, et al. Single-cell spatial reconstruction reveals global division of labour in the mammalian liver. *Nature* (2017) 542:352–6. doi: 10.1038/nature21065
23. Planas-Paz L, Orsini V, Boulter L, Calabrese D, Pikiolek M, Nigsch F, et al. The RSPO-LGR4/5-ZNRF3/RNF43 module controls liver zonation and size. *Nat Cell Biol* (2016) 18:467–79. doi: 10.1038/ncb3337
24. Wang B, Zhao L, Fish M, Logan CY, Nusse R. Self-renewing diploid Axin2+ cells fuel homeostatic renewal of the liver. *Nature* (2015) 524:180–5. doi: 10.1038/nature14863
25. Steinhart Z, Angers S. Wnt signaling in development and tissue homeostasis. *Development* (2018) 145:dev146589. doi: 10.1242/dev.146589
26. Kuwahara A, Hirabayashi Y, Knoepfler PS, Taketo MM, Sakai J, Kodama T, et al. Wnt signaling and its downstream target N-myc regulate basal progenitors in the developing neocortex. *Development* (2010) 137:1035–44. doi: 10.1242/dev.046417
27. Qin XY, Hara M, Arner E, Kawaguchi Y, Inoue I, Tatsukawa H, et al. Transcriptome Analysis Uncovers a Growth-Promoting Activity of Orosomucoid-1 on Hepatocytes. *EBioMedicine* (2017) 24:257–66. doi: 10.1016/j.ebiom.2017.09.008
28. Yanger K, Knigin D, Zong Y, Maggs L, Gu G, Akiyama H, et al. Adult hepatocytes are generated by self-duplication rather than stem cell differentiation. *Cell Stem Cell* (2014) 15:340–9. doi: 10.1016/j.stem.2014.06.003
29. Michalopoulos GK, DeFrances MC. Liver regeneration. *Science* (1997) 276:60–6. doi: 10.1126/science.276.5309.60
30. Hossain S, Takatori A, Nakamura Y, Suenaga Y, Kamijo T, Nakagawara A. NLRR1 enhances EGF-mediated MYCN induction in neuroblastoma and accelerates tumor growth in vivo. *Cancer Res* (2012) 72:4587–96. doi: 10.1158/0008-5472.CAN-12-0943
31. Mishra L, Banker T, Murray J, Byers S, Thenappan A, He AR, et al. Liver stem cells and hepatocellular carcinoma. *Hepatology* (2009) 49:318–29. doi: 10.1002/hep.22704
32. Muto Y, Moriwaki H, Ninomiya M, Adachi S, Saito A, Takasaki KT, et al. Prevention of Second Primary Tumors by an Acyclic Retinoid, Polyprenoic Acid, in Patients with Hepatocellular Carcinoma. *New Engl J Med* (1996) 334:1561–8. doi: 10.1056/NEJM199606133342402
33. Yamashita T, Ji J, Budhu A, Forgues M, Yang W, Wang HY, et al. EpCAM-Positive Hepatocellular Carcinoma Cells Are Tumor-Initiating Cells With Stem/Progenitor Cell Features. *Gastroenterology* (2009) 136:1012–1024.e4. doi: 10.1053/j.gastro.2008.12.004
34. Okita K, Izumi N, Ikeda K, Osaki Y, Numata K, Ikeda M, et al. Survey of survival among patients with hepatitis C virus-related hepatocellular carcinoma treated with peretinoin, an acyclic retinoid, after the completion

of a randomized, placebo-controlled trial. *J Gastroenterol* (2014) 50:667–74. doi: 10.1007/s00535-014-0996-1
35. Park EJ, Lee JH, Yu GY, He G, Ali SR, Holzer RG, et al. Dietary and genetic obesity promote liver inflammation and tumorigenesis by enhancing IL-6 and TNF expression. *Cell* (2010) 140:197–208. doi: 10.1016/j.cell.2009.12.052
36. Umemura A, Park EJ, Taniguchi K, Lee JH, Shalapour S, Valasek MA, et al. Liver damage, inflammation, and enhanced tumorigenesis after persistent mTORC1 inhibition. *Cell Metab* (2014) 20:133–44. doi: 10.1016/j.cmet.2014.05.001
37. Grohmann M, Wiede F, Dodd GT, Gurzov EN, Ooi GJ, Butt T, et al. Obesity Drives STAT-1-Dependent NASH and STAT-3-Dependent HCC. *Cell* (2018) 175:1289–1306 e20. doi: 10.1016/j.cell.2018.09.053
38. Johnson DE, O'Keefe RA, Grandis JR. Targeting the IL-6/JAK/STAT3 signalling axis in cancer. *Nat Rev Clin Oncol* (2018) 15:234–48. doi: 10.1038/nrclinonc.2018.8
39. Sattu K, Hochgrafe F, Wu J, Umapathy G, Schonherr C, Ruuth K, et al. Phosphoproteomic analysis of anaplastic lymphoma kinase (ALK) downstream signaling pathways identifies signal transducer and activator of transcription 3 as a functional target of activated ALK in neuroblastoma cells. *FEBS J* (2013) 280:5269–82. doi: 10.1111/febs.12453
40. Odate S, Veschi V, Yan S, Lam N, Woessner R, Thiele CJ. Inhibition of STAT3 with the Generation 2.5 Antisense Oligonucleotide, AZD9150, Decreases Neuroblastoma Tumorigenicity and Increases Chemosensitivity. *Clin Cancer Res* (2017) 23:1771–84. doi: 10.1158/1078-0432.CCR-16-1317
41. Won C, Kim BH, Yi EH, Choi KJ, Kim EK, Jeong JM, et al. Signal transducer and activator of transcription 3-mediated CD133 up-regulation contributes to promotion of hepatocellular carcinoma. *Hepatology* (2015) 62:1160–73. doi: 10.1002/hep.27968
42. He G, Dhar D, Nakagawa H, Font-Burgada J, Ogata H, Jiang Y, et al. Identification of Liver Cancer Progenitors Whose Malignant Progression Depends on Autocrine IL-6 Signaling. *Cell* (2013) 155:384–96. doi: 10.1016/j.cell.2013.09.031
43. López-Grueso MJ, González R, Muntané J, Bárcena JA, Padilla CA. Thioredoxin Downregulation Enhances Sorafenib Effects in Hepatocarcinoma Cells. *Antioxidants* (2019) 8:501. doi: 10.3390/antiox8100501
44. Oakley F, Trim N, Constandinou CM, Ye W, Gray AM, Frantz G, et al. Hepatocytes Express Nerve Growth Factor during Liver Injury. *Am J Pathol* (2003) 163:1849–58. doi: 10.1016/S0002-9440(10)63544-4
45. Woo CW, Lucarelli E, Thiele CJ. NGF activation of TrkA decreases N-myc expression via MAPK path leading to a decrease in neuroblastoma cell number. *Oncogene* (2004) 23:1522–30. doi: 10.1038/sj.onc.1207267
46. Kristiansen M, Menghi F, Hughes R, Hubank M, Ham J. Global analysis of gene expression in NGF-deprived sympathetic neurons identifies molecular pathways associated with cell death. *BMC Genomics* (2011) 12:551. doi: 10.1186/1471-2164-12-551
47. Ibarguren M, López DJ, Escribá PV. The effect of natural and synthetic fatty acids on membrane structure, microdomain organization, cellular functions and human health. *Biochim Biophys Acta (BBA) - Biomembr* (2014) 1838:1518–28. doi: 10.1016/j.bbamem.2013.12.021
48. Autumn G. York, Williams KJ, Argus JP, Zhou QD, Brar G, Vergnes L, et al. Limiting Cholesterol Biosynthetic Flux Spontaneously Engages Type I IFN Signaling. *Cell* (2015) 163:1716–29. doi: 10.1016/j.cell.2015.11.045
49. Carroll RG, Zasłona Z, Galván-Peña S, Koppe EL, Sévin DC, Angiari S, et al. An unexpected link between fatty acid synthase and cholesterol synthesis in proinflammatory macrophage activation. *J Biol Chem* (2018) 293:5509–21. doi: 10.1074/jbc.RA118.001921
50. Hsieh WY, Zhou QD, York AG, Williams KJ, Scumpia PO, Kronenberger EB, et al. Toll-Like Receptors Induce Signal-Specific Reprogramming of the Macrophage Lipidome. *Cell Metab* (2020) 32:128–43 e5. doi: 10.1016/j.cmet.2020.05.003
51. Wei X, Song H, Yin L, Rizzo MG, Sidhu R, Covey DF, et al. Fatty acid synthesis configures the plasma membrane for inflammation in diabetes. *Nature* (2016) 539:294–8. doi: 10.1038/nature20117
52. Oishi Y, Spann NJ, Link VM, Muse ED, Strid T, Edillor C, et al. SREBP1 Contributes to Resolution of Pro-inflammatory TLR4 Signaling by Reprogramming Fatty Acid Metabolism. *Cell Metab* (2017) 25:412–27. doi: 10.1016/j.cmet.2016.11.009
53. Ben-David U, Gan Q-F, Golan-Lev T, Arora P, Yanuka O, Oren YS, et al. Selective Elimination of Human Pluripotent Stem Cells by an Oleate Synthesis Inhibitor Discovered in a High-Throughput Screen. *Cell Stem Cell* (2013) 12:167–79. doi: 10.1016/j.stem.2012.11.015
54. Li J, Condello S, Thomes-Pepin J, Ma X, Xia Y, Hurley TD, et al. Lipid Desaturation Is a Metabolic Marker and Therapeutic Target of Ovarian Cancer Stem Cells. *Cell Stem Cell* (2017) 20:303–14.e5. doi: 10.1016/j.stem.2016.11.004
55. Qin X-Y, Dohmae N, Kojima S. Reply to Yoshida: Liver cancer stem cells: Identification and lipid metabolic reprogramming. *Proc Natl Acad Sci* (2018) 115:E6390–1. doi: 10.1073/pnas.1808740115
56. Qin X-Y, Su T, Yu W, Kojima S. Lipid desaturation-associated endoplasmic reticulum stress regulates MYCN gene expression in hepatocellular carcinoma cells. *Cell Death Dis* (2020) 11:66. doi: 10.1038/s41419-020-2257-y
57. Yoshida GJ. Beyond the Warburg Effect: N-Myc Contributes to Metabolic Reprogramming in Cancer Cells. *Front Oncol* (2020) 10:791. doi: 10.3389/fonc.2020.00791
58. Rouault-Pierre K, Lopez-Onieva L, Foster K, Anjos-Afonso F, Lamrissi-Garcia I, Serrano-Sanchez M, et al. HIF-2α Protects Human Hematopoietic Stem/Progenitors and Acute Myeloid Leukemic Cells from Apoptosis Induced by Endoplasmic Reticulum Stress. *Cell Stem Cell* (2013) 13:549–63. doi: 10.1016/j.stem.2013.08.011
59. Miharada K, Sigurdsson V, Karlsson S. Dppa5 Improves Hematopoietic Stem Cell Activity by Reducing Endoplasmic Reticulum Stress. *Cell Rep* (2014) 7:1381–92. doi: 10.1016/j.celrep.2014.04.056
60. Heijmans J, van Lidth de Jeude JF, Koo B-K, Rosekrans SL, Wielenga MCB, van de Wetering M, et al. ER Stress Causes Rapid Loss of Intestinal Epithelial Stemness through Activation of the Unfolded Protein Response. *Cell Rep* (2013) 3:1128–39. doi: 10.1016/j.celrep.2013.02.031
61. Wielenga MCB, Colak S, Heijmans J, van Lidth de Jeude JF, Rodermond HM, Paton JC, et al. ER-Stress-Induced Differentiation Sensitizes Colon Cancer Stem Cells to Chemotherapy. *Cell Rep* (2015) 13:489–94. doi: 10.1016/j.celrep.2015.09.016
62. Liu R, Li X, Huang Z, Zhao D, Ganesh BS, Lai G, et al. C/EBP homologous protein-induced loss of intestinal epithelial stemness contributes to bile duct ligation-induced cholestatic liver injury in mice. *Hepatology* (2018) 67:1441–57. doi: 10.1002/hep.29540
63. Ma MKF, Lau EYT, Leung DHW, Lo J, Ho NPY, Cheng LKW, et al. Stearoyl-CoA desaturase regulates sorafenib resistance via modulation of ER stress-induced differentiation. *J Hepatol* (2017) 67:979–90. doi: 10.1016/j.jhep.2017.06.015
64. Pinkham K, Park DJ, Hashemiaghdam A, Kirov AB, Adam I, Rosiak K, et al. Stearoyl CoA Desaturase Is Essential for Regulation of Endoplasmic Reticulum Homeostasis and Tumor Growth in Glioblastoma Cancer Stem Cells. *Stem Cell Rep* (2019) 12:712–27. doi: 10.1016/j.stemcr.2019.02.012
65. Wei Y, Wang D, Topczewski F, Pagliassotti MJ. Saturated fatty acids induce endoplasmic reticulum stress and apoptosis independently of ceramide in liver cells. *Am J Physiol-Endocrinol Metab* (2006) 291:E275–81. doi: 10.1152/ajpendo.00644.2005
66. Borradaile NM, Han X, Harp JD, Gale SE, Ory DS, Schaffer JE. Disruption of endoplasmic reticulum structure and integrity in lipotoxic cell death. *J Lipid Res* (2006) 47:2726–37. doi: 10.1194/jlr.M600299-JLR200
67. Wei Y, Wang D, Gentile CL, Pagliassotti MJ. Reduced endoplasmic reticulum luminal calcium links saturated fatty acid-mediated endoplasmic reticulum stress and cell death in liver cells. *Mol Cell Biochem* (2009) 331:31–40. doi: 10.1007/s11010-009-0142-1
68. Ariyama H, Kono N, Matsuda S, Inoue T, Arai H. Decrease in Membrane Phospholipid Unsaturation Induces Unfolded Protein Response. *J Biol Chem* (2010) 285:22027–35. doi: 10.1074/jbc.M110.126870
69. Gebert LFR, MacRae IJ. Regulation of microRNA function in animals. *Nat Rev Mol Cell Biol* (2019) 20:21–37. doi: 10.1038/s41580-018-0045-7
70. Mendell JT, Olson EN. MicroRNAs in stress signaling and human disease. *Cell* (2012) 148:1172–87. doi: 10.1016/j.cell.2012.02.005
71. Lujambio A, Lowe SW. The microcosmos of cancer. *Nature* (2012) 482:347–55. doi: 10.1038/nature10888
72. Gailhouste L, Ochiya T. Cancer-related microRNAs and their role as tumor suppressors and oncogenes in hepatocellular carcinoma. *Histol Histopathol* (2013) 28:437–51. doi: 10.14670/HH-28.437

73. Domingo-Fernandez R, Watters K, Piskareva O, Stallings RL, Bray I. The role of genetic and epigenetic alterations in neuroblastoma disease pathogenesis. *Pediatr Surg Int* (2013) 29:101–19. doi: 10.1007/s00383-012-3239-7
74. Attiyeh EF, London WB, Mosse YP, Wang Q, Winter C, Khazi D, et al. Chromosome 1p and 11q deletions and outcome in neuroblastoma. *N Engl J Med* (2005) 353:2243–53. doi: 10.1056/NEJMoa052399
75. Wei JS, Song YK, Durinck S, Chen QR, Cheuk AT, Tsang P, et al. The MYCN oncogene is a direct target of miR-34a. *Oncogene* (2008) 27:5204–13. doi: 10.1038/onc.2008.154
76. Molenaar JJ, Domingo-Fernandez R, Ebus ME, Lindner S, Koster J, Drabek K, et al. LIN28B induces neuroblastoma and enhances MYCN levels via let-7 suppression. *Nat Genet* (2012) 44:1199–206. doi: 10.1038/ng.2436
77. Buechner J, Tomte E, Haug BH, Henriksen JR, Lokke C, Flaegstad T, et al. Tumour-suppressor microRNAs let-7 and mir-101 target the proto-oncogene MYCN and inhibit cell proliferation in MYCN-amplified neuroblastoma. *Br J Cancer* (2011) 105:296–303. doi: 10.1038/bjc.2011.220
78. Neviani P, Wise PM, Murtadha M, Liu CW, Wu CH, Jong AY, et al. Natural Killer-Derived Exosomal miR-186 Inhibits Neuroblastoma Growth and Immune Escape Mechanisms. *Cancer Res* (2018) 79:1151–64. doi: 10.1158/0008-5472.CAN-18-0779
79. Ooi CY, Carter DR, Liu B, Mayoh C, Beckers A, Lalwani A, et al. Network Modeling of microRNA-mRNA Interactions in Neuroblastoma Tumorigenesis Identifies miR-204 as a Direct Inhibitor of MYCN. *Cancer Res* (2018) 78:3122–34. doi: 10.1158/0008-5472.CAN-17-3034
80. Ma L, Young J, Prabhala H, Pan E, Mestdagh P, Muth D, et al. miR-9, a MYC/MYCN-activated microRNA, regulates E-cadherin and cancer metastasis. *Nat Cell Biol* (2010) 12:247–56. doi: 10.1038/ncb2024
81. Gailhouste L, Gomez-Santos L, Ochiya T. Potential applications of miRNAs as diagnostic and prognostic markers in liver cancer. *Front Biosci (Landmark Ed)* (2013) 18:199–223. doi: 10.2741/4096
82. Gailhouste L, Liew LC, Yasukawa K, Hatada I, Tanaka Y, Kato T, et al. MEG3-derived miR-493-5p overcomes the oncogenic feature of IGF2-miR-483 loss of imprinting in hepatic cancer cells. *Cell Death Dis* (2019) 10:553. doi: 10.1038/s41419-019-1788-6
83. Yasukawa K, Liew LC, Hagiwara K, Hironaka-Mitsuhashi A, Qin XY, Furutani Y, et al. MicroRNA-493-5p-mediated repression of the MYCN oncogene inhibits hepatic cancer cell growth and invasion. *Cancer Sci* (2020) 111:869–80. doi: 10.1111/cas.14292
84. Xiong DD, Dang YW, Lin P, Wen DY, He RQ, Luo DZ, et al. A circRNA-miRNA-mRNA network identification for exploring underlying pathogenesis and therapy strategy of hepatocellular carcinoma. *J Transl Med* (2018) 16:220. doi: 10.1186/s12967-018-1593-5
85. Lou K, Chen N, Li Z, Zhang B, Wang X, Chen Y, et al. MicroRNA-142-5p Overexpression Inhibits Cell Growth and Induces Apoptosis by Regulating FOXO in Hepatocellular Carcinoma Cells. *Oncol Res* (2017) 25:65–73. doi: 10.3727/096504016X14719078133366
86. Tsang FH, Au SL, Wei L, Fan DN, Lee JM, Wong CC, et al. MicroRNA-142-3p and microRNA-142-5p are downregulated in hepatocellular carcinoma and exhibit synergistic effects on cell motility. *Front Med* (2015) 9:331–43. doi: 10.1007/s11684-015-0409-8
87. Lima L, de Melo TCT, Marques D, de Araujo JNG, Leite ISF, Alves CX, et al. Modulation of all-trans retinoic acid-induced MiRNA expression in neoplastic cell lines: a systematic review. *BMC Cancer* (2019) 19:866. doi: 10.1186/s12885-019-6081-7
88. Mu X, Español-Suñer R, Mederacke I, Affò S, Manco R, Sempoux C, et al. Hepatocellular carcinoma originates from hepatocytes and not from the progenitor/biliary compartment. *J Clin Invest* (2015) 125:3891–903. doi: 10.1172/JCI77995
89. Varga J, Greten FR. Cell plasticity in epithelial homeostasis and tumorigenesis. *Nat Cell Biol* (2017) 19:1133–41. doi: 10.1038/ncb3611

Conflict of Interest: The authors declare that the research was conducted in the absence of any commercial or financial relationships that could be construed as a potential conflict of interest.

frontiers in Oncology

ORIGINAL RESEARCH
published: 21 April 2021
doi: 10.3389/fonc.2021.633579

Control Analysis of Protein-Protein Interaction Network Reveals Potential Regulatory Targets for MYCN

Chunyu Pan[1,2,3†], Yuyan Zhu[2,4†], Meng Yu[5], Yongkang Zhao[6], Changsheng Zhang[1], Xizhe Zhang[2,3,7*] and Yang Yao[8*]*

[1] Northeastern University, Shenyang, China, [2] Joint Laboratory of Artificial Intelligence and Precision Medicine of China Medical University and Northeastern University, Shenyang, China, [3] Early Intervention Unit, Department of Psychiatry, Affiliated Nanjing Brain Hospital, Nanjing Medical University, Nanjing, China, [4] Department of Urology, The First Hospital of China Medical University, Shenyang, China, [5] Department of Reproductive Biology and Transgenic Animal, China Medical University, Shenyang, China, [6] National Institute of Health and Medical Big Data, China Medical University, Shenyang, China, [7] School of Biomedical Engineering and Informatics, Nanjing Medical University, Nanjing, China, [8] Department of Physiology, Shenyang Medical College, Shenyang, China

OPEN ACCESS

Edited by:
Shilpa S. Dhar, University of Texas MD Anderson Cancer Center, United States

Reviewed by:
Amriti Rajender Lulla, University of Texas MD Anderson Cancer Center, United States
Goutham Narla, University of Michigan, United States

***Correspondence:**
Yang Yao
yaoyang1972@gmail.com
Xizhe Zhang
Zhangxizhe@njmu.edu.cn
Changsheng Zhang
zhangchangsheng@mail.neu.edu.cn

[†]These authors contributed equally to this article

Specialty section:
This article was submitted to Molecular and Cellular Oncology, a section of the journal Frontiers in Oncology

Received: *25 November 2020*
Accepted: *04 March 2021*
Published: *21 April 2021*

Citation:
Pan C, Zhu Y, Yu M, Zhao Y, Zhang C, Zhang X and Yao Y (2021) Control Analysis of Protein-Protein Interaction Network Reveals Potential Regulatory Targets for MYCN. Front. Oncol. 11:633579. doi: 10.3389/fonc.2021.633579

Background: MYCN is an oncogenic transcription factor of the MYC family and plays an important role in the formation of tissues and organs during development before birth. Due to the difficulty in drugging MYCN directly, revealing the molecules in MYCN regulatory networks will help to identify effective therapeutic targets.

Methods: We utilized network controllability theory, a recent developed powerful tool, to identify the potential drug target around MYCN based on Protein-Protein interaction network of MYCN. First, we constructed a Protein-Protein interaction network of MYCN based on public databases. Second, network control analysis was applied on network to identify driver genes and indispensable genes of the MYCN regulatory network. Finally, we developed a novel integrated approach to identify potential drug targets for regulating the function of the MYCN regulatory network.

Results: We constructed an MYCN regulatory network that has 79 genes and 129 interactions. Based on network controllability theory, we analyzed driver genes which capable to fully control the network. We found 10 indispensable genes whose alternation will significantly change the regulatory pathways of the MYCN network. We evaluated the stability and correlation analysis of these genes and found EGFR may be the potential drug target which closely associated with MYCN.

Conclusion: Together, our findings indicate that EGFR plays an important role in the regulatory network and pathways of MYCN and therefore may represent an attractive therapeutic target for cancer treatment.

Keywords: PPI network, MYCN, potential targets, network controllability, EGFR

INTRODUCTION

The MYC proto-oncogene family consists of three paralogs: c-MYC, MYCN, and MYCL (1, 2). Abnormal MYC regulation can lead to increased cell proliferation and growth, MYC family members are the dysregulation of MYC family is common in cancer (2). The MYCN cancer gene in the MYC family is a structurally and functionally similar fragment of MYC discovered by *Schwab* (3) in 1983. It acts to promote cell proliferation, and inhibit cell differentiation, apoptosis, or programmed cell death (4–6). Existing researches suggest that MYCN plays a key role in cell proliferation and cell growth during embryonic development (7) and it is associated with a number of childhood-onset tumors, including neuroblastoma, medulloblastoma, rhabdomyosarcoma, glioblastoma multiform, retinoblastoma, astrocytoma, hematologic malignancies, and small-cell lung cancer (8, 9), as well as some adult cancers such as prostate and lung cancer (10, 11). Despite the proven importance of MYCN, which has very promising therapeutic potential, how to directly target MYCN remains an open question. There is no better method to target MYCN directly in existing research (9), but we can still target MYCN indirectly by targeting molecules that interact directly with MYCN to control MYCN activity (9, 12–19). Thus, the problem of targeting MYCN can be translated into the study of the MYCN regulatory network of its interactions.

Recently, network controllability theory has made remarkable achievements in analyzing biological networks, such as Protein-Protein Interaction (PPI) network (20–24), brain network (25, 26) and disease-related networks (27, 28). *Ryouji* (20) applied network controllability theory on breast cancer gene expression networks, and designed a novel method to identify a set of critical control proteins that uniquely and structurally control the entire proteome. *Wu* (29) determined minimum dominating sets of proteins (MDSets) in human and yeast protein interaction networks and found that MDSet proteins were enriched with essential, cancer-related, and virus-targeted genes. *Guo* (30) developed an algorithm for identifying steering nodes to a gene regulatory network related to type 1 diabetes and they found that FASLG and CD80 are steering nodes for controlling the target nodes related to type 1 diabetes and supported by wet experiments.

In the view of control theory, drug targets in a biological network can be interpreted as a steering node. By applying an extra signal to this set of guide nodes, the network is expected to be steered to the desired state. In other words, for a biological system with an abnormal state, if some biomolecules affect other biomolecules by extra perturbations and steer the system towards a healthy state, these perturbed biomolecules can be considered potential drug targets. Thus, the problem of identifying drug targets can be mapped to the problem of finding a set of steering nodes in a network system. By applying a control signal to these nodes, the states of the network are expected to transition between the healthy state and the disease state.

Here, we utilized network controllability theory (31–36) to analyze the protein-protein interaction (PPI) network of MYCN. We identified possible potential drug targets of the MYCN regulatory network and evaluated the importance of these potential targets with several existing databases. The results showed that network controllability theory may provide new ideas to reveal the function of MYCN and target MCYN, which is of great importance and application prospect.

METHODS

Network Controllability

Consider a linear time-invariant networked system, the dynamics of the process can be described as follows:

$$\frac{dx(t)}{dt} = Ax(t) + Bu(t) \tag{1}$$

Where vector $x(t) = (x_1(t),\ldots,x_N(t))^T$ represents the system state vector of N nodes at time t; matrix A is a state parameter describing the components of the system; matrix B of N*M(M≥ N) is the input matrix from which the controlled node is identified by the external controller. Vector $u(t)=(u_1(t),\ldots,u_M(t))^T$ represents the input vector of M nodes at the time t and the controller uses the input vector $u(t)$ to control the entire system and a single control signal $u_i(t)$ can typically drive multiple nodes.

According to the *Kalman* rank condition (31, 37):

$$C = \left(B, AB, A^2B, \ldots, A^{N-1}B\right)$$
$$\text{rank}(C) = N$$

The system is controllable if and only if the N*NM matrix C= (B,AB,A^2B,…,A^{N-1}B) is full rank, and the system can drive any initial state to any final state in a finite time. Based on this theory, *Lin* (33) proposed the theory of structural controllability, in which the state matrix A and the control matrix B can be regarded as a structured matrix, and if there are matrices A and B with non-zero weights that make the *Kalman* criterion hold, then for the way of combining different weights in matrices A and B, the system is almost always controllable except for the all-zero state and some special cases. On this basis, researchers in the field of network control (32, 34) have transformed the problem of least external input to a directed network into a problem of calculating the maximum matching for that network, as shown in **Figure 1**. For a directed network, a maximum matching is a set of maximal edges that do not share the starting and ending node, while nodes that do not have matching edges pointing to them are driver nodes. In contrast, the driver nodes computed by maximum matching is called minimum set of driver nodes (MDS). Since the maximum matching is often not unique for the same network, it is often possible to obtain multiple different MDS for the same network (38–41). In this case, we can analyze the nodes in different MDS and thus assess the importance of the nodes.

Node Classification Based on Network Controllability

This method measures the nodes in different MDS and considers the importance of the nodes in the whole network. For a network, MDS can be obtained by using the maximum

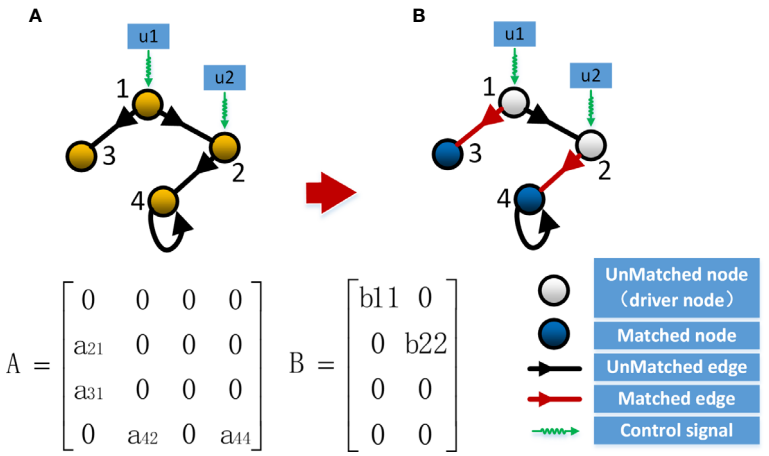

FIGURE 1 | Control of the network system. **(A)** Controllability of a network through the controllability matrix; **(B)** Controllability of a network through the maximum matching.

matching method (34) and the type of node can be determined by the size of MDS after this node removing from the network. A node is indispensable if the size of MDS decreases after removing the node from the network. A node is dispensable if the size of MDS increases after removing the node from the network. A node is neutral if the size of MDS do not change after removing the node from the network. The simple network (**Figure 2A**) has two different maximum matching (**Figure 2B**), and the size of original MDS is 2. The size of the MDS will change when the nodes in this network are removed and the size of MDS after different nodes removed are shown in **Figures 2C–F**.

In this simple network, the removal of node 1 does not change the MDS size of the network, as defined in the classification that node 1 is a neutral node. While the removal of node 2 increases the MDS size, and node 2 is an indispensable node. Similarly, node 3 and node 4 are dispensable nodes. The classification result of MYCN regulatory network is shown in **Figure 3B**.

Source of Data Sets

The Cancer Genome atlas (TCGA, https://tcga-data.nci.nih.gov/tcga), a project initiated jointly by the National Cancer Institute (NCI) and the National Genome Research Institute (NHGRI). Utilize large scale sequencing based genomic analysis techniques to finalize a complete set of mapping associated with all cancer genomic alterations. To date, TCGA has been tested in over 10,000 human samples with whole cancers. We selected PanCancer Atlas Studies as our data set from TCGA for validating the results of the method, which included 32 different cancers with 10,967 samples. Survival analysis is provided by Cbioportal (www.cbioportal.org), it supports the use of custom data and provides researchers with an interactive interface to discover associations between genetic alterations and the clinic, and the data source for Cbioportal is TCGA. Co-expression and pathway analysis is also provided by Cbioportal, whose pathway data are provided by TCGA research and the TCGA PanCanAtlas project (42–50). These pathways have been rigorously extrapolated and validated and are published, which is of great biological significance and very important for the analysis of disease or gene interaction mechanisms.

Data sets of drug targets provided by *Behan* et al.'s work (51), they used genome-scale CRISPR–Cas9 screens in 324 human cancer cell lines from 30 cancer types and developed a data-driven framework to prioritize candidates for cancer therapeutics.

RESULTS

Control Analysis of Human Protein-Protein Interaction Network

Consider a Protein-Protein interactions (PPI) network, a node of the network represents a protein and the interactions between proteins are the edges of the network. We used human binary protein interactions (HuRI) (52), a Protein interaction database which is the largest human protein interactome data to date. The protein-protein interaction in the network is of paramount importance both for understanding the underlying biological processes and for understanding disease occurrence. In addition, we have combined the protein-protein interactions provided by other databases (53–57) to form a more comprehensive network. The specific data sources are shown in **Figure 2A**.

The result of the PPI network consists of 11,584 proteins and 76,434 interactions. The average degree of the network is 13.2 and the diameter of the network is 24. To analyze the control properties of the PPI network, we used the maximum matching method to compute the Minimum Driver nodes Set (MDS) in the network. Although the MDSs are not unique for the PPI network, but the size of all MDSs is same and determined by the network topology. In the PPI network, there are 5436 (46.93%) driver proteins which composed of the MDS of the PPI network. It means that to fully control the PPI network, we need to control nearly half of the proteins in the network. Therefore, the MDS did not provide much information for identifying potential drug target of the network.

Furthermore, We used a control classification method (21) to divide the proteins into three types: indispensable, dispensable,

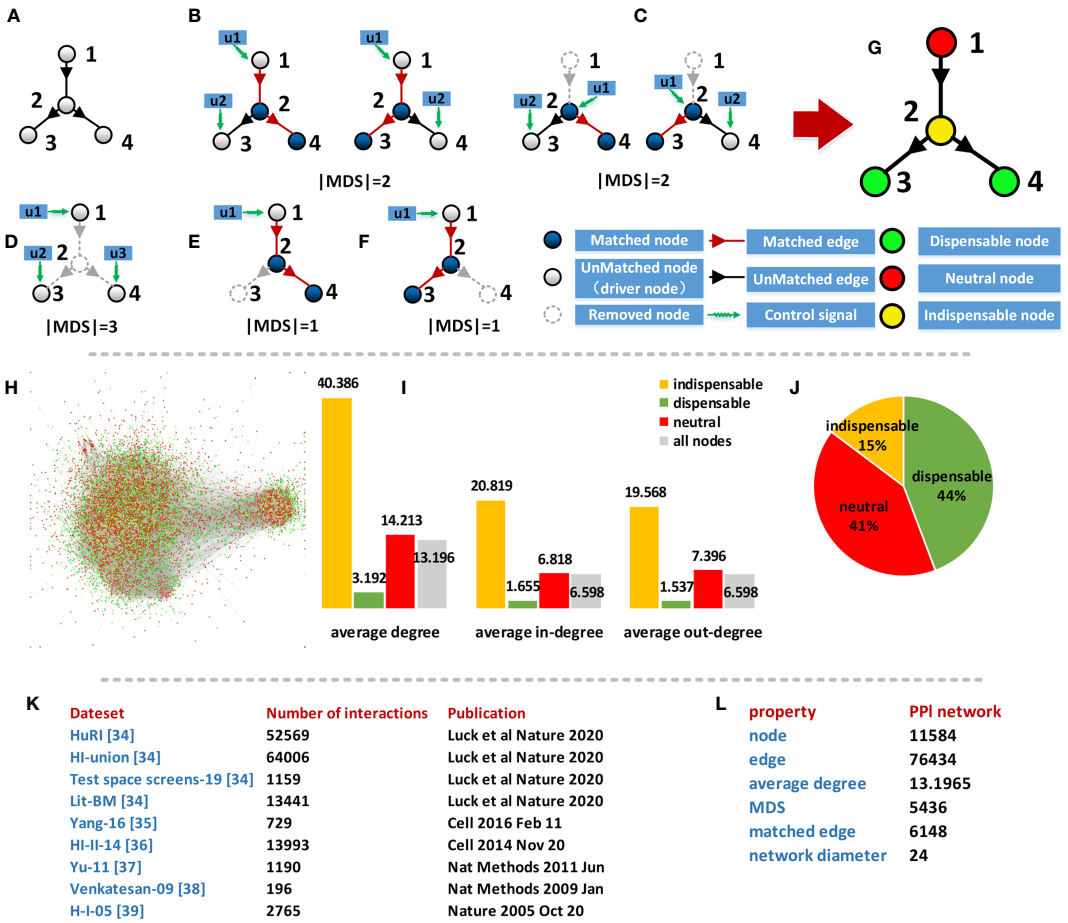

K

Dateset	Number of interactions	Publication
HuRI [34]	52569	Luck et al Nature 2020
HI-union [34]	64006	Luck et al Nature 2020
Test space screens-19 [34]	1159	Luck et al Nature 2020
Lit-BM [34]	13441	Luck et al Nature 2020
Yang-16 [35]	729	Cell 2016 Feb 11
HI-II-14 [36]	13993	Cell 2014 Nov 20
Yu-11 [37]	1190	Nat Methods 2011 Jun
Venkatesan-09 [38]	196	Nat Methods 2009 Jan
H-I-05 [39]	2765	Nature 2005 Oct 20

L

property	PPI network
node	11584
edge	76434
average degree	13.1965
MDS	5436
matched edge	6148
network diameter	24

FIGURE 2 | Characterizing of the PPI network. **(A)** A simple network; **(B)** Two different maximum matching of **(A)**; **(C–F)** The size of MDS after different node removed; **(G)** Classification results of **(A)**; **(H)** Classification results of PPI network; **(I)** Average degree of different type nodes in PPI network; **(J)** Percentages of different types in PPI network; **(K)** Data source of PPI network; **(L)** Basic property of PPI network.

and neutral proteins. This node classification is based on the size changes of MDS after removing the node from the network. A node is indispensable if the size of MDS decreases after removing the node from the network. A node is dispensable if the size of MDS increases after removing the node from the network. A node is neutral if the size of MDS do not change after removing the node from the network. An example network is shown in **Figure 2**. For the PPI network, a total of 1710 (15%) proteins are indispensable, 5218 (44%) proteins are dispensable nodes and 4749 (41%) proteins are neutral. We found the average degree of the indispensable nodes is much higher than the other class nodes, which means the selected indispensable proteins have more interactions and are more closely related to other molecules than the other proteins in the network.

Control Analysis of MYCN Sub-Network

To find potential drug target of MYCN, we extracted the second-order egocentric network of MYCN from the PPI network. The MYCN-egocentric network includes the neighbor nodes that interact directly with MYCN and the neighbor nodes that interact with the neighbors of MYCN. We used the second-order egocentric network to analyze the MYCN network because the goal of our analysis is to find molecules that can be targeted among the direct or indirect interactions of MYCN, and the nodes we selected should not be too far away from MYCN. **Figure 3** shows the result of control analysis of MYCN network. The network consists of 79 nodes and 129 edges and the size of MDS of MYCN network is 49 (62.03%). The number of matching edges is 30 (23.26%) and the network diameter is 4.

By using the node classification method (21) based on controllability analysis, we computed the control types of the proteins in the MYCN network. As the same as the PPI network, the average degree of the indispensable nodes is much higher than the other type nodes in MYCN regulation network (**Figure 3C**). However, the value of average degree is not involved in the processing of the classification and the phenomenon is not accidental or biased. For all the nodes in the MYCN regulatory network, we found 10 (13%) nodes are indispensable, 21 (26%) nodes are neutral nodes and 48 (61%) nodes are dispensable.

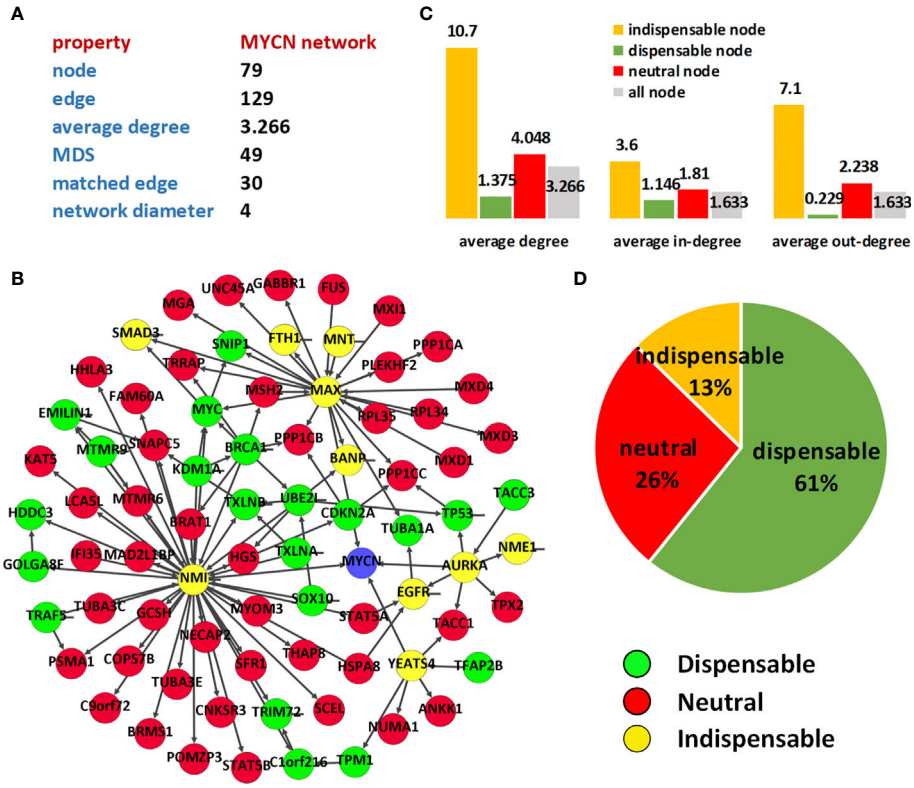

FIGURE 3 | Characterizing of MYCN regulatory network. **(A)** Topological statistics of MYCN regulatory network; **(B)** Node classification of MYCN network; **(C)** Average degree of different type of nodes; **(D)** Percentages of different types in MYCN network.

Table 1 showed the indispensable proteins and their topological properties and associated diseases. Meanwhile, among these 10 indispensable nodes, MAX, AURKA, YEATS4, and NMI are the nodes directly associated with MYCN, these proteins are present in the first-order egocentric network of MYCN and have close interactions with MYCN.

Functional Analysis of Indispensable Proteins

To further investigate the biological significance of indispensable genes in the MYCN network, we perform survival analysis of indispensable genes base on the clinical data of The Cancer Genome Atlas (TCGA) (69) included 32 different cancers with 10,967 samples. Here we used overall survival without disease-specific for a gene, it can eliminate the survival differences in certain diseases. By plotting the relationship between survival months and surviving percentage, can obtain the differences in survival for altered group and unaltered group. **Figure 4** showed the clinical survival of 10 indispensable genes. Among the ten indispensable genes, EGFR and YEATS4 had a significant difference between the altered group and the unaltered group, which suggested that the mutation of these two genes will significantly change the survival of patients. Clinical samples and median survival Months are shown in **Table 2**. Considering the differences in disease grade and treatment strategy, we also divided the sample into multiple groups for statistical analysis (**Supplement 2**).

Furthermore, we performed pathway analysis for the indispensable genes (42–50) based on Cbioportal (70). We found that EGFR, MAX, MNT and SMAD3 are associations with MYCN or MYC family in several pathways, as shown in **Figure 5**. EGFR was indirectly associated with MYC activity in ESAD-2017-RTK-RAS-PI(3)K-pathway and HNSC-2015-RTK-RAS-PI(3)K-pathway by PIK3CA. MAX and MNT are correlated with MYCN in the MYC-pathway, where MAX and MYCN form the MYC/MAX complex, and MNT associated with the MAX/MGA complex. The pathway analysis shows that the indispensable genes computed by the network controllability theory are precise and are directly or indirectly associated with MYCN in different pathways.

Finally, we analyzed the indispensable node that are targeted by the drugs. Based on the database of drug targets in 324 human cancer cell lines from 30 cancer types (51), we found that EGFR is an anti-cancer target in Squamous Cell Lung Carcinoma, Lung Adenocarcinoma, Oral Cavity Carcinoma, Ovarian Carcinoma, Head and Neck Carcinoma and Esophagus. It has a high priority and has a class B biomarker, making it a more desirable target. EGFR has at least one drug that has been developed for the cancer type in which the target was identified as a priority. In relation to our research of the MYCN regulatory network, EGFR

TABLE 1 | Indispensable genes in MYCN regulatory network.

symbol	Full name	Indegree	Outdegree	Diseases associated
AURKA (58)	Aurora Kinase A	1	6	Colorectal Cancer/Colorectal Adenocarcinoma.
BANP (59)	BTG3 Associated Nuclear Protein	3	1	Keratoconus/Brittle Cornea Syndrome 2
EGFR (60)	Epidermal Growth Factor Receptor	4	2	Inflammatory Skin/Bowel Disease, Neonatal, 2/Lung Cancer
FTH1 (61)	Ferritin Heavy Chain 1	2	1	Hemochromatosis/Type 5 and Superficial Siderosis Of The Central Nervous System
MAX (62)	MYC Associated Factor X	8	18	Pheochromocytoma/Hereditary Paraganglioma-Pheochromocytoma Syndromes
MNT (63)	MAX Network Transcriptional Repressor	1	2	Tetanus Neonatorum/Mixed Type Thymoma
NME1 (64)	NME/NM23 Nucleoside Diphosphate Kinase 1	2	1	Anal Canal Carcinoma/Larynx Cancer
NMI (65, 66)	N-Myc And STAT Interactor	11	34	–
SMAD3 (67)	SMAD Family Member 3	3	1	Loeys-Dietz Syndrome 3/Familial Thoracic Aortic Aneurysm And Aortic Dissection
YEATS4 (68)	YEATS Domain Containing 4	1	5	Cellular Myxoid Liposarcoma/Pleomorphic Liposarcoma

may be the potential drug target which closely associated with MYCN.

Overall, based on the survival analysis, cancer pathway and drug targets analysis of indispensable genes, it is clear that the indispensable genes have a significant role in the MYCN regulatory network. The indispensable genes are directly associated with cancers, especially EGFR, MAX, MNT, SMAD3. EGFR is also a drug target that has already been developed and is considered to be the most promising potential target in the MYCN regulatory network.

Indispensable Proteins in Brain Lower Grade Glioma

To further validate the biological significance of indispensable genes, in this section, we verified the effectiveness of our results with the specific-diseases. For the choice of specific-diseases, we should select a disease that is associated with MYCN, to analyze the survival of indispensable genes and the co-expression relationship with MYCN. Due to MYCN plays a key role in cell proliferation and cell growth during embryonic development (7) and it is often associated with a number of childhood-onset tumors, here we combined Brain Lower Grade Glioma to show the results of analysis. The survival curves for indispensable genes for Brain Lower Grade Glioma are shown in **Figure 6**. And the co-expression correlation between indispensable genes and MYCN of Brain Lower Grade Glioma are shown in **Table 3**. We found that BANP, NME1, YEATS4, and EGFR, have relatively significant Spearman's Correlation with MYCN. Among them, YEATS4 has been shown in existing studies to have a direct interaction with MYCN (53–57). Although there are no direct association between three other genes and MYCN in existing studies, from the co-expression of Brain Lower Grade Glioma, it is possible that had correlation between them.

DISCUSSION

MYCN plays an important role in many diseases and cancers (2, 7–11), in-depth understanding of the role of MYCN has a great significance and application prospect. However, MYCN is difficult to directly target and design therapeutic strategies in existing research (9). Therefore, we hope to find potential targets around the MYCN regulatory network and regulate MYCN indirectly by controlling the potential targets. By using network controllability method (21), we found ten indispensable genes in the MYCN regulatory network. Through the pathway, survival, drug target analysis, we found that the indispensable genes, especially EGFR, play an important role in MYCN regulatory networks.

To validate the biological significance of indispensable genes, especially EGFR, we calculated the correlation between the 10 indispensable genes and MYCN using the TCGA dataset (**Supplement 1**). For the 33 cancers proposed by TCGA, we analyzed spearman's correlation, p-value (2-sided t-test), and q-value (Benjamini-Hochberg FDR correction) of MYCN with indispensable genes in expression in different diseases sequentially. Our core target EGFR had significant positive correlation results in Thymoma, Kidney Chromophobe, Diffuse Large B-Cell Lymphoma, Brain Lower Grade Glioma, and Skin Cutaneous Melanoma. All other indispensable genes also had a significant co-expression results with MYCN in specific diseases, this is concur with the results of existing studies. For the ten potential targets we obtained, MAX, AURKA, YEATS4 and NMI are directly associated with MYCN. MAX and AURKA in particular have been rigorously argued to be tightly associated with MYCN activity (71). For the other 6 potential targets, they are indirectly connected to MYCN. Although current research of these genes hasn't a direct interaction with MYCN, in the theory of network control when this type of node changes, it can alter the features of network and affect the state of MYCN result in indirectly target MYCN. Among them, EGFR, MNT, and SMAD3 are all directly or indirectly associated with the MYCN or MYC families in different pathway. EGFR, in particular, is not only significantly different between the altered and unaltered groups in clinical survival data, but also a molecule that can already be drug-targeted (51).

As the driving gene of many kinds of tumors, EGFR plays an important role in promoting the malignant progression of tumors (60). Its role in non-small cell lung cancer, glioblastoma and basal-like breast cancers has spurred many research and drug development efforts. Tyrosine kinase inhibitors have shown

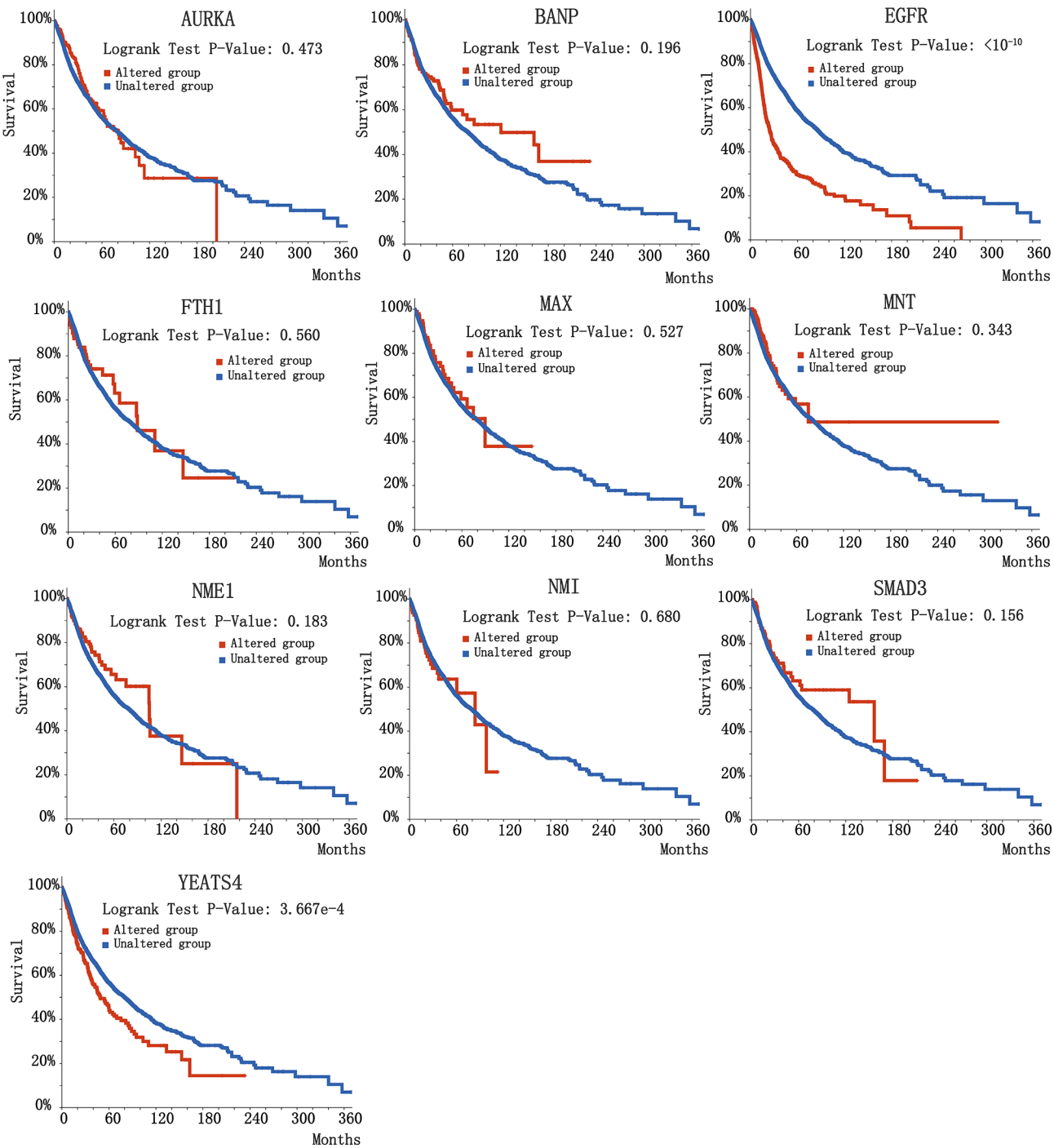

FIGURE 4 | Survival curve of 10 indispensable genes. 10 plots correspond to different indispensable genes, here we chose overall survival data rather than disease-specific survival data.

efficacy in EGFR amplified tumors, most notably gefitinib and erlotinib. But the mutations in EGFR have been shown to confer resistance to these drugs, particularly the variant T790M, which has been functionally characterized as a resistance marker for both of these drugs. The later generation TKI's have seen some success in treating these resistant cases, and targeted sequencing of the EGFR locus has become a common practice in treatment of non-small cell lung cancer (72–74). Therefore, we consider EGFR to be the most promising potential target among these indispensable genes (**Supplement 2**).

TABLE 2 | Clinical samples of indispensable genes.

Id	Name	Type	Number of Cases, Total	Number of Cases, Deceased	Median Months Overall
1	AURKA	Altered group	233	77	80.74
		Unaltered group	10569	3437	78.97
2	BANP	Altered group	237	69	120.62
		Unaltered group	10565	3445	78.67
3	EGFR	Altered group	812	460	24.3
		Unaltered group	9990	3054	85.08
4	FTH1	Altered group	87	27	88.11
		Unaltered group	10715	3487	78.9
5	MAX	Altered group	99	32	89.72
		Unaltered group	10703	3482	78.97
6	MNT	Altered group	147	41	74.93
		Unaltered group	10655	3473	78.97
7	NME1	Altered group	153	42	105.04
		Unaltered group	10649	3472	78.67
8	NMI	Altered group	102	30	83.57
		Unaltered group	10700	3484	78.97
9	SMAD3	Altered group	175	48	156.49
		Unaltered group	10627	3466	78.67
10	YEATS4	Altered group	318	141	49.05
		Unaltered group	10483	3373	80.48

Meanwhile, referring to the biological properties of MYCN (7, 75) (**Supplement 2**), we selected Brain Lower Grade Glioma to validating indispensable genes. Among them, BANP, NME1, YEATS4, and EGFR, have relatively significant Spearman's Correlation with MYCN. It is worth noting that NMI has a high negative correlation with MYCN. Due to the algorithm views the biological network as an abstract network structure in isolation from the specific biological constraints, this algorithm without specific biological constraints is able to filter out genes with high correlation (positive and negative), not just positive correlation. And NMI as an interactor of MYCN, has a high absolute value of correlation with MYCN in the network, which is consistent with the algorithm results. For EGFR, which we considered the most potentially target, there were more significant results in Brain Lower Grade Glioma, both in the co-expression and survival.

TABLE 3 | Co-expression correlation between indispensable genes and MYCN of Brain Lower Grade Glioma.

Name	Spearman's Correlation	p_value	q_value
EGFR	0.274	2.83E-10	1.29E-09
AURKA	0.137	1.913E-3	3.532E-3
BANP	0.26	2.25E-09	9.14E-09
FTH1	-0.282	7.77E-11	3.78E-10
MAX	0.085	0.054	0.0775
MNT	0.161	2.418E-4	5.084E-4
NME1	0.29	1.96E-11	1.02E-10
NMI	-0.3	3.72E-12	2.11E-11
SMAD3	0.0736	0.0954	0.13
YEATS4	0.361	3.02E-17	3.14E-16

Each cancer is extremely complex and different networks will come with different results. In this study, we chose pan-cancer data to construct a more comprehensive network to predict potential targets for MYCN in terms of overall relationships, and

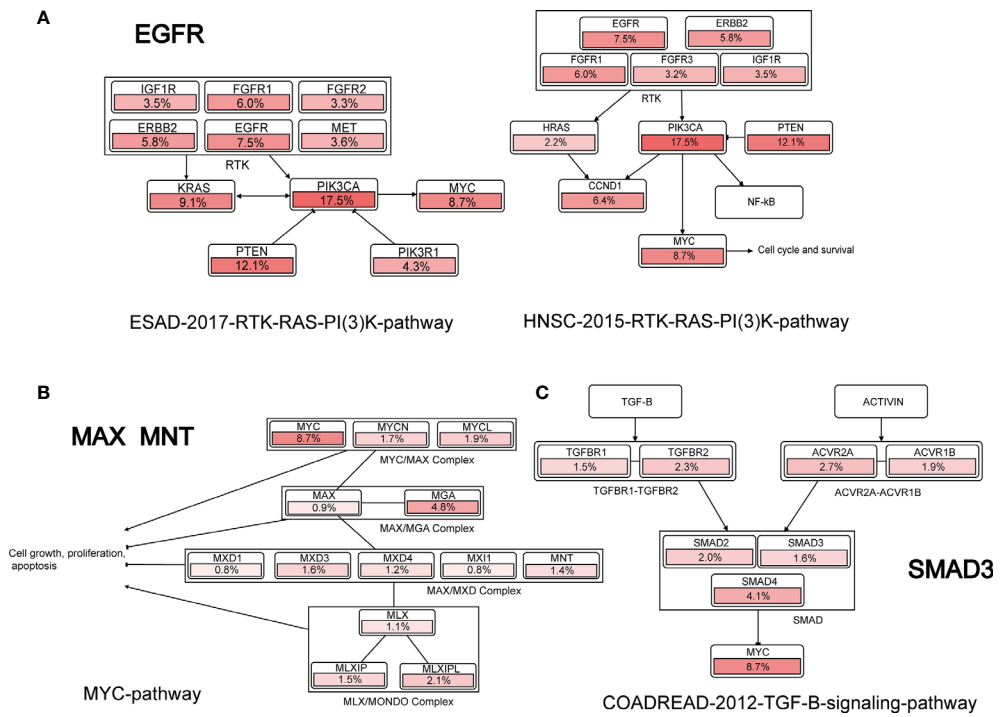

FIGURE 5 | Cancer pathway of indispensable genes. **(A–C)** are the pathways that EGFR, MAX, MNT, SMAD3 associated with MYCN or MYC, respectively.

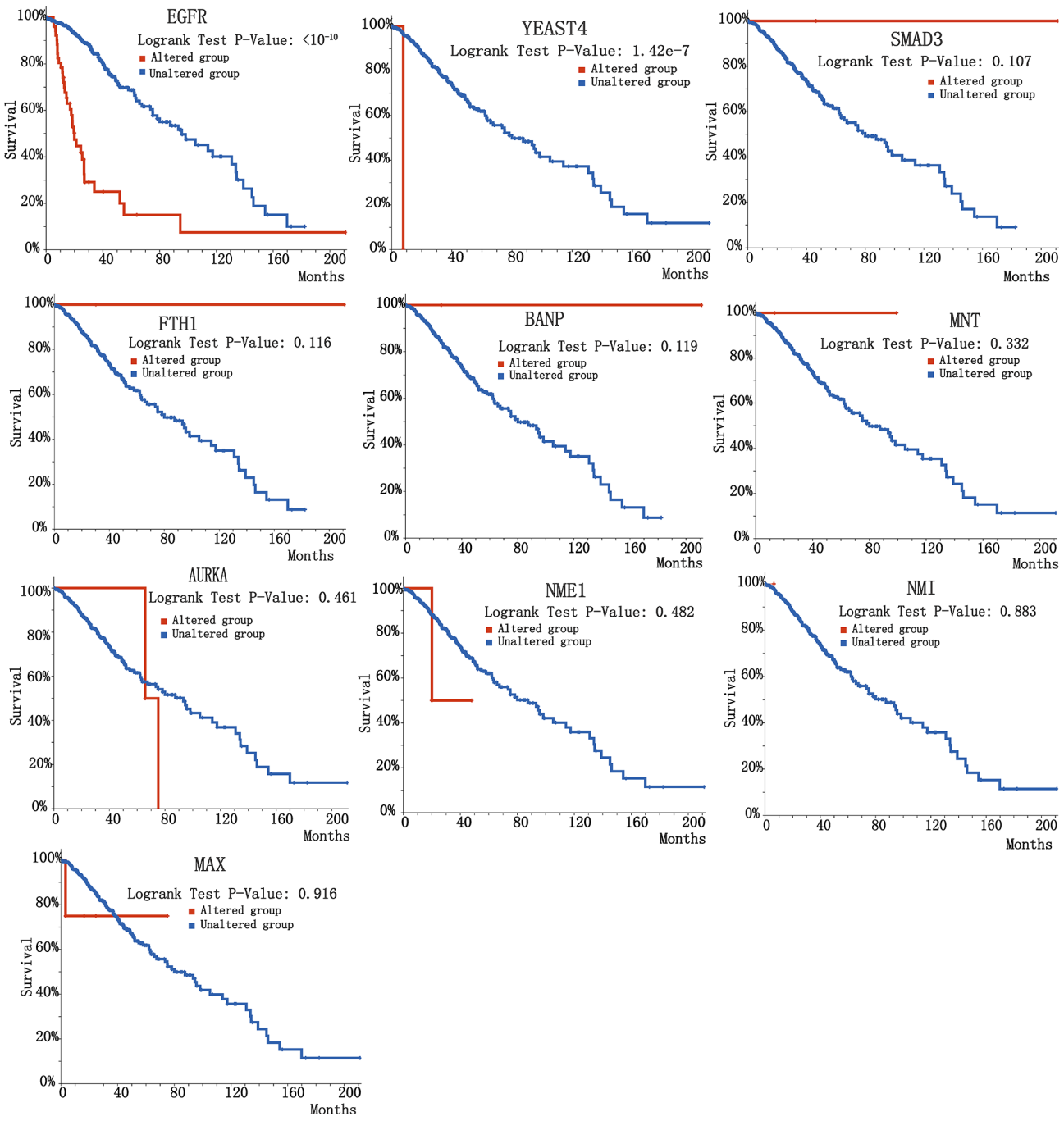

FIGURE 6 | Survival curve of 10 indispensable genes of Brain Lower Grade Glioma. 10 plots are the survival curves of different indispensable genes and Brain Lower Grade Glioma respectively.

finally verified the effect of indispensable genes combined with specific-diseases. The theory of network controllability bring a new view and theoretical framework to the analysis of regulatory networks. However, the composition of nodes and edges will impact the accuracy of the results. Therefore, it is still a challenge to accurate construction of the initial network and find the exact target network from a large amount of data and specific-diseases. This is a new methodological trying to identify potential targets, and after the network control framework analysis, how to design wet experiments to further verify the analysis results is also one of our subsequent concerns.

Overall, the method of network controllability in this paper is able to screen potential targets against MYCN and our findings indicate that EGFR plays an important role in the MYCN

regulatory network. In the future, experimental evidence to support the above regulatory relationship will be further provided through *in vitro* and *in vivo* experimental systems, so as to promote the identification and discovery of potential new regulatory targets.

DATA AVAILABILITY STATEMENT

The original contributions presented in the study are included in the article/**Supplementary Material**. Further inquiries can be directed to the corresponding authors.

ETHICS STATEMENT

The studies involving human participants were reviewed and approved by TCGA Ethics & Policies and were originally published by the National Cancer Institute. The patients/participants provided their written informed consent to participate in this study. Written informed consent was obtained from the individual(s) for the publication of any potentially identifiable images or data included in this article.

AUTHOR CONTRIBUTIONS

XZZ is the lead author. XZZ, YYZ, YKZ and YY conceived the study and revised the manuscript. CYP and CSZ performed data analysis and interpretation and drafted the manuscript. MY searched the databases and acquired the data. All authors contributed substantially to the preparation of the manuscript.

FUNDING

This work was supported by the Fundamental Research Funds for the Central Universities (N2017013, N2017014), National Natural Science Foundation of China (U1908212, 81672523, 81472404, 81472403, 81272834 and 31000572), 2018 Support Plan for innovative talents in Colleges and Universities of Liaoning Province, 2018 "million talents Project" funded Project of Liaoning Province, 2019 Key R & D Projects of Shenyang.

ACKNOWLEDGMENTS

The authors thank the members of participants for taking part in the study.

SUPPLEMENTARY MATERIAL

The Supplementary Material for this article can be found online at: https://www.frontiersin.org/articles/10.3389/fonc.2021.633579/full#supplementary-material

REFERENCES

1. Mathsyaraja H, Eisenman R. Parsing Myc Paralogs in Oncogenesis. *Cancer Cell* (2016) 29(1):1–2. doi: 10.1016/j.ccell.2015.12.009
2. Wilde B, Ayer D. Interactions between Myc and MondoA transcription factors in metabolism and tumourigenesis. *Br J Cancer* (2015) 113(11):1529–33. doi: 10.1038/bjc.2015.360
3. Schwab M, Alitalo K, Klempnauer K-H, Varmus HE, Bishop JM, Gilbert F, et al. Amplified DNA with limited homology to myc cellular oncogene is shared by human neuroblastoma cell lines and a neuroblastoma tumour. *Nature* (1983) 305(5931):245–8. doi: 10.1038/305245a0
4. Chen L, Iraci N, Gherardi S, Gamble L, Wood K, Perini G, et al. p53 is a direct transcriptional target of MYCN in neuroblastoma. *Cancer Res* (2010) 70 (4):1377–88. doi: 10.1158/0008-5472.CAN-09-2598
5. Ly JD, Grubb DR, Lawen A. The mitochondrial membrane potential (Δψm) in apoptosis; an update. *Apoptosis* (2003) 8:115–28:2. doi: 10.1023/A:1022945107762
6. Czabotar P, Lessene G, Strasser A, Adams J. Control of apoptosis by the BCL-2 protein family: Implications for physiology and therapy. *Nat Rev Mol Cell Biol* (2013) 15:49–63. doi: 10.1038/nrm3722
7. Eilers M, Eisenman RN. Myc's broad reach. *Genes Dev* (2008) 22(20):2755–66. doi: 10.1101/gad.1712408
8. Molenaar JJ, Koster J, Ebus ME, van Sluis P, Westerhout EM, de Preter K, et al. Copy number defects of G1-Cell cycle genes in neuroblastoma are frequent and correlate with high expression of E2F target genes and a poor prognosis. *Genes Chrom Cancer* (2011) 51(1):10–9. doi: 10.1002/gcc.20926
9. Rickman DS, Schulte JH, Eilers M. The expanding world of N-MYC-driven tumors. *Cancer Dis* (2018) 2159–8290. CD-2117-0273v2151.
10. Wenzel A, Cziepluch C, Hamann U, Schürmann J, Schwab M. The N-Myc oncoprotein is associated in vivo with the phosphoprotein Max(p20/22) in human neuroblastoma cells. *EMBO J* (1991) 10(12):3703–12. doi: 10.1002/j.1460-2075.1991.tb04938.x
11. Ruiz-Pérez M, Henley A, Arsenian-Henriksson M. The MYCN Protein in Health and Disease. *Genes (Basel)* (2017) 8(4). doi: 10.3390/genes8040113
12. Barone G, Anderson J, Pearson A, Petrie K, Chesler L. New strategies in neuroblastoma: Therapeutic targeting of MYCN and ALK. *Clin Cancer Res* (2013) 19(21):5814–21. doi: 10.1158/1078-0432.CCR-13-0680
13. Cole KA, Huggins J, Laquaglia M, Hulderman CE, Russell MR, Bosse K, et al. RNAi screen of the protein kinome identifies checkpoint kinase 1 (CHK1) as a therapeutic target in neuroblastoma. *Proc Natl Acad Sci USA* (2011) 108 (8):3336–41. doi: 10.1073/pnas.1012351108
14. Dominguez-Sola D, Ying C, Grandori C, Ruggiero L, Chen B, Li M, et al. Non-transcriptional control of DNA replication by c-Myc. *Nature* (2007) 448 (7152):445–51. doi: 10.1038/nature05953
15. Stracker T, Petrini JJ. The MRE11 complex: starting from the ends. *Nat Rev Mol Cell Biol* (2011) 12(2):90–103. doi: 10.1038/nrm3047
16. Petroni M, Giannini G. A MYCN-MRN complex axis controls replication stress for the safe expansion of neuroprogenitor cells. *Mol Cell Oncol* (2016) 3: (2):e1079673. doi: 10.1080/23723556.2015.1079673
17. Walton M, Eve P, Hayes A, Valenti M, De Haven Brandon A, Box G, et al. CCT244747 is a novel potent and selective CHK1 inhibitor with oral efficacy alone and in combination with genotoxic anticancer drugs. *Clin Cancer Res* (2012) 18(20):5650–61. doi: 10.1158/1078-0432.CCR-12-1322
18. Zirath H, Frenzel A, Oliynyk G, Segerström L, Westermark U, Larsson K, et al. MYC inhibition induces metabolic changes leading to accumulation of lipid droplets in tumor cells. *Proc Natl Acad Sci U S A* (2013) 110(25):10258–63. doi: 10.1073/pnas.1222404110
19. Bashash D, Sayyadi M, Safaroghli-Azar A, Sheikh-Zeineddini N, Riyahi N, et al. Small molecule inhibitor of c-Myc 10058-F4 inhibits proliferation and induces apoptosis in acute leukemia cells, irrespective of PTEN status. *Intl J Biochem Cell Biol* (2019) 108:7–16. doi: 10.1016/j.biocel.2019.01.005
20. Ryouji W, Masayuki I, Toshihiko K, Tomoshiro O, Nacher JC, Petter H. Identification of genes and critical control proteins associated with

inflammatory breast cancer using network controllability. *PLoS ONE* (2017) 12(11):e0186353. doi: 10.1371/journal.pone.0186353
21. Vinayagam A, Gibson TE, Lee HJ, Yilmazel B, Roesel C, Hu YH, et al. Controllability analysis of the directed human protein interaction network identifies disease genes and drug targets. *Proc Natl Acad Sci U S A* (2016) 113 (18):4976–81.
22. Wu L, Tang L, Li M, Wang J, Wu F. Biomolecular Network Controllability With Drug Binding Information. *IEEE Trans Nanobioscience* (2017) 16(5):326–32.
23. Wuchty S. Controllability in protein interaction networks. *Proc Natl Acad Sci U S A* (2014) 111(19):7156–60. doi: 10.1073/pnas.1311231111
24. Zhang X. Altering indispensable proteins in controlling directed human protein interaction network. *IEEE-Acm Trans Comput Biol Bioinform* (2018) 15(6):2074–8.
25. Gu S, Pasqualetti F, Cieslak M, Telesford QK, Yu AB, Kahn AE, et al. Controllability of structural brain networks. *Nat Commun* (2015) 6:8414. doi: 10.1038/ncomms9414
26. Muldoon SF, Pasqualetti F, Gu S, Cieslak M, Grafton ST, Vettel JM, et al. Stimulation-Based Control of Dynamic Brain Networks. *PloS Comput Biol* (2016) 12(9):e1005076. doi: 10.1371/journal.pcbi.1005076
27. AL B, Gulbahce N, Loscalzo J. Network medicine: a network-based approach to human disease. *Nat Rev Gen* (2011) 12(1):56–68. doi: 10.1038/nrg2918
28. Wu L, Li M, Wang J-X, Wu F-X. Controllability and Its Applications to Biological Networks. *J Comput Sci Technol* (2019) 34(1):16–34. doi: 10.1007/s11390-019-1896-x
29. Wu L, Li M, Wang J, Wu F. Minimum steering node set of complex networks and its applications to biomolecular networks. *IET Syst Biol* (2016) 10(3):116–23. doi: 10.1049/iet-syb.2015.0077
30. Guo W-F, Zhang S-W, Wei Z-G, Zeng T, Liu F, Zhang J, et al. Constrained target controllability of complex networks. *J Stat Mech: Theory Exp* (2017) 6:063402. doi: 10.1088/1742-5468/aa6de6
31. Kalman R,E. A. Mathematical Description of Linear Dynamical Systems. *J Soc Ind Appl Math Series A Control* (1963) 1(2):152–92. doi: 10.1137/0301010
32. Liu Y-Y, Slotine J-J, Barabási A-L. Controllability of complex networks. *Nature* (2011) 473(7346):167–73. doi: 10.1038/nature10011
33. Lin CT. Structural controllability. *IEEE Trans Autom Contr* (1974) 19(3):201–8. doi: 10.1109/TAC.1974.1100557
34. Murota K. Matrices and matroids for systems analysis. *Algorithms Combin* (2008) 20(1):6–10. doi: 10.1007/978-3-642-03994-2_1
35. Zhang X, Zhu Y, Zhao Y. Altering control modes of complex networks by reversing edges. *Physica A Stat Mech Appl* (2021) 561(C):125249. doi: 10.1016/j.physa.2020.125249
36. Zhang X, Li Q. Altering control modes of complex networks based on edge removal. *Physica a-Statistical Mechanics and Its Applications* (2019) 516:185–93. doi: 10.1016/j.physa.2018.09.146
37. Luenberger DG. *Introduction to dynamic systems: Theory, models and applications*. John Wiley & Sons (1979).
38. Zhang X, Lv T, Pu YJR. Input graph: the hidden geometry in controlling complex networks. *Rep* (2016) 6(1):38209. doi: 10.1038/srep38209
39. Jia T, Liu YY, Csóka E, Pósfai M, Slotine JJ, Barabási AL. Emergence of bimodality in controlling complex networks. *Nat Commun* (2013) 4:2002. doi: 10.1038/ncomms3002
40. Zhang XZ, Wang HZ, Lv TY. Efficient target control of complex networks based on preferential matching. *PloS One* (2017) 12(4):10. doi: 10.1371/journal.pone.0175375
41. Zhang X, Han J, Zhang W. An efficient algorithm for finding all possible input nodes for controlling complex networks. *Sci Rep* (2017) 7(1):10677. doi: 10.1038/s41598-017-10744-w
42. Cancer Genome Atlas Research, N. Comprehensive genomic characterization defines human glioblastoma genes and core pathways. *Nature* (2008) 455 (7216):1061–8. doi: 10.1038/nature07385
43. Cancer Genome Atlas Research, N. Integrated genomic analyses of ovarian carcinoma. *Nature* (2011) 474(7353):609–15. doi: 10.1038/nature10166
44. Muzny DM, Bainbridge MN, Chang K, Dinh HH, Drummond JA, Drummond JA, et al. Comprehensive molecular characterization of human colon and rectal cancer. *Nature* (2012) 487(7407):330–7. doi: 10.1038/nature11252
45. Hammerman PS, Lawrence MS, Voet D, Jing R, Cibulskis K, Sivachenko A, et al. Comprehensive genomic characterization of squamous cell lung cancers. *Nature* (2012) 489(7417):519–25. doi: 10.1038/nature11404
46. Levine DA, Getz G, Gabriel SB, Cibulskis K, Lander E, Sivachenko A, et al. Integrated genomic characterization of endometrial carcinoma. *Nature* (2013) 497(7447):67–73. doi: 10.1038/nature12113
47. Collisson EA, Campbell JD, Brooks AN, Berger AH, Lee W, Chmielecki J, et al. Comprehensive molecular profiling of lung adenocarcinoma. *Nature* (2014) 511(7511):543–50. doi: 10.1038/nature13385
48. Cancer Genome Atlas Research N. Integrated genomic characterization of papillary thyroid carcinoma. *Cell* (2014) 159(3):676–90.
49. Cancer Genome Atlas N. Comprehensive genomic characterization of head and neck squamous cell carcinomas. *Nature* (2015) 517(7536):576–82. doi: 10.1038/nature14129
50. Kim J, Bowlby R, Mungall A, Robertson G, Odze R, Cherniack AD, et al. Integrated genomic characterization of oesophageal carcinoma. *Nature* (2017) 541(7636):169–75. doi: 10.1038/nature20805
51. Behan F, Iorio F, Picco G, Gonçalves E, Beaver C, Migliardi G, et al. Prioritization of cancer therapeutic targets using CRISPR-Cas9 screens. *Nature* (2019) 568(7753):511–6. doi: 10.1038/s41586-019-1103-9
52. Luck K, Kim D, Lambourne L, Spirohn K, Begg B, Bian W, et al. A reference map of the human binary protein interactome. *Nature* (2020) 580(7803):402–8.
53. Yang X, Coulombe-Huntington J, Kang S, Sheynkman GM, Hao T, Richardson A, et al. Widespread Expansion of Protein Interaction Capabilities by Alternative Splicing. *Cell* (2016) 164(4):805–17. doi: 10.1016/j.cell.2016.01.029
54. Rolland T, Taşan M, Charloteaux B, Pevzner SJ, Zhong Q, Sahni N, et al. A proteome-scale map of the human interactome network. *Cell* (2014) 159 (5):1212–26. doi: 10.1016/j.cell.2014.10.050
55. Yu H, Tardivo L, Tam S, Weiner E, Gebreab F, Fan C, et al. Next-generation sequencing to generate interactome datasets. *Nat Methods* (2011) 8(6):478–80. doi: 10.1038/nmeth.1597
56. Venkatesan K, Rual JF, Vazquez A, Stelzl U, Lemmens I, Hirozane-Kishikawa T, et al. An empirical framework for binary interactome mapping. *Nat Methods* (2009) 6(1):83–90. doi: 10.1038/nmeth.1280
57. Rual JF, Venkatesan K, Hao T, Hirozane-Kishikawa T, Dricot A, Li N, et al. Towards a proteome-scale map of the human protein-protein interaction network. *Nature* (2005) 437(7062):1173–8. doi: 10.1038/nature04209
58. Furukawa T, Kanai N, Shiwaku H, Soga N, Uehara A, Horii A. AURKA is one of the downstream targets of MAPK1/ERK2 in pancreatic cancer. *Oncogene* (2006) 25(35):4831–9. doi: 10.1038/sj.onc.1209494
59. Jalota-Badhwar A, Kaul-Ghanekar R, Mogare D, Boppana R, Paknikar K, Chattopadhyay S, et al. SMAR1-derived P44 peptide retains its tumor suppressor function through modulation of p53. *J Biol Chem* (2007) 282 (13):9902–13. doi: 10.1074/jbc.M608434200
60. Rodríguez P, Rodríguez G, González G, Lage A. Clinical development and perspectives of CIMAvax EGF, Cuban vaccine for non-small-cell lung cancer therapy. *MEDICC Rev* (2010) 12(1):17–23. doi: 10.37757/MR2010.V12.N1.4
61. Singh A, Severance S, Kaur N, Wiltsie W, Kosman DJ. Assembly, activation, and trafficking of the Fet3p.Ftr1p high affinity iron permease complex in Saccharomyces cerevisiae. *J Biol Chem* (2006) 281(19):13355–64. doi: 10.1074/jbc.M512042200
62. Ayer D, Lawrence Q, Eisenman R. Mad-Max transcriptional repression is mediated by ternary complex formation with mammalian homologs of yeast repressor Sin3. *Cell* (1995) 80(5):767–76. doi: 10.1016/0092-8674(95)90355-0
63. Hofer B, Ruge M, Dreiseikelmann B. The superinfection exclusion gene (sieA) of bacteriophage P22: identification and overexpression of the gene and localization of the gene product. *J Bacteriol* (1995) 177(11):3080–6. doi: 10.1128/JB.177.11.3080-3086.1995
64. Okabe-Kado J, Kasukabe T, Honma Y, Hanada R, Nakagawara A, Kaneko Y. Clinical significance of serum NM23-H1 protein in neuroblastoma. *Cancer Sci* (2005) 96(10):653–60. doi: 10.1111/j.1349-7006.2005.00091.x
65. Shannon JG, Howe DH, et al. Virulent Coxiella burnetii does not activate human dendritic cells: Role of lipopolysaccharide as a shielding molecule. *Proc Natl Acad Sci U S A* (2005) 102(24):8722–7. doi: 10.1073/pnas.0501863102
66. Philimonenko V, Zhao J, Iben S, Dingová H, Kyselá K, Kahle M, et al. Nuclear actin and myosin I are required for RNA polymerase I transcription. *Nat Cell Biol* (2004) 6(12):1165–72. doi: 10.1038/ncb1190
67. Ross K, Corey D, Dunn J, Kelley TJ. SMAD3 expression is regulated by mitogen-activated protein kinase kinase-1 in epithelial and smooth muscle cells. *Cell Signal* (2007) 19:(5):923–31. doi: 10.1016/j.cellsig.2006.11.008

68. Park JH, Roeder RG. GAS41 is required for repression of the p53 tumor suppressor pathway during normal cellular proliferation. *Mol Cell Biol* (2006) 26(11):4006–16. doi: 10.1128/MCB.02185-05
69. Hoadley K, Yau C, Hinoue T, Wolf D, Lazar A, Drill E, et al. Cell-of-Origin Patterns Dominate the Molecular Classification of 10,000 Tumors from 33 Types of Cancer. *Cell* (2018) 173(2):291–304.e296.
70. Bahceci I, Dogrusoz U, La KC, Babur Ö., Gao J, Schultz N. PathwayMapper: a collaborative visual web editor for cancer pathways and genomic data. *Bioinformatics* (2017) 33(14):2238–40. doi: 10.1093/bioinformatics/btx149
71. Chen H, Liu H, Qing G. Targeting oncogenic Myc as a strategy for cancer treatment. *Signal Transduct Target Ther* (2018) 3:5. doi: 10.1038/s41392-018-0008-7
72. Yewale C, Baradia D, Vhora I, Patil S, Misra A. Epidermal growth factor receptor targeting in cancer: a review of trends and strategies. *Biomaterials* (2013) 34(34):8690–707. doi: 10.1016/j.biomaterials.2013.07.100
73. Charpidou A, Blatza D, Anagnostou V, Syrigos KN. Review. EGFR mutations in non-small cell lung cancer–clinical implications. *In Vivo (Athens Greece)* (2008) 22(4):529–36.
74. Arteaga CL, Engelman JA. ERBB receptors: from oncogene discovery to basic science to mechanism-based cancer therapeutics. *Cancer Cell* (2014) 25 (3):282–303. doi: 10.1016/j.ccr.2014.02.025
75. Vo BT, Wolf E, Kawauchi D, Gebhardt A, Rehg JE, Finkelstein D, et al. The Interaction of Myc with Miz1 Defines Medulloblastoma Subgroup Identity. *Cancer Cell* (2016) 29(1):5–16.1. doi: 10.1016/j.ccell.2015.12.003

Conflict of Interest: The authors declare that the research was conducted in the absence of any commercial or financial relationships that could be construed as a potential conflict of interest.

frontiers in Oncology

ORIGINAL RESEARCH
published: 07 May 2021
doi: 10.3389/fonc.2021.647737

The MicroRNA Landscape of MYCN-Amplified Neuroblastoma

Danny Misiak[1†], Sven Hagemann[1†], Jessica L. Bell[1], Bianca Busch[1], Marcell Lederer[1], Nadine Bley[1], Johannes H. Schulte[2,3] and Stefan Hüttelmaier[1]*

[1] Institute of Molecular Medicine, Martin Luther University Halle-Wittenberg, Halle, Germany, [2] Department of Pediatric Oncology and Hematology, Charité-Universitätsmedizin Berlin, Berlin, Germany, [3] German Consortium for Translational Cancer Research (DKTK), Partner Site Charité Berlin, Berlin, Germany

MYCN gene amplification and upregulated expression are major hallmarks in the progression of high-risk neuroblastoma. MYCN expression and function in modulating gene synthesis in neuroblastoma is controlled at virtually every level, including poorly understood regulation at the post-transcriptional level. MYCN modulates the expression of various microRNAs including the miR-17-92 cluster. MYCN mRNA expression itself is subjected to the control by miRNAs, most prominently the miR-17-92 cluster that balances MYCN expression by feed-back regulation. This homeostasis seems disturbed in neuroblastoma where *MYCN* upregulation coincides with severely increased expression of the miR-17-92 cluster. In the presented study, we applied high-throughput next generation sequencing to unravel the miRNome in a cohort of 97 neuroblastomas, representing all clinical stages. Aiming to reveal the *MYCN*-dependent miRNome, we evaluate miRNA expression in *MYCN*-amplified as well as none amplified tumor samples. In correlation with survival data analysis of differentially expressed miRNAs, we present various putative oncogenic as well as tumor suppressive miRNAs in neuroblastoma. Using microRNA trapping by RNA affinity purification, we provide a comprehensive view of MYCN-regulatory miRNAs in neuroblastoma-derived cells, confirming a pivotal role of the miR-17-92 cluster and moderate association by the let-7 miRNA family. Attempting to decipher how *MYCN* expression escapes elevated expression of inhibitory miRNAs, we present evidence that RNA-binding proteins like the IGF2 mRNA binding protein 1 reduce miRNA-directed downregulation of MYCN in neuroblastoma. Our findings emphasize the potency of post-transcriptional regulation of *MYCN* in neuroblastoma and unravel new avenues to pursue inhibition of this potent oncogene.

Keywords: microRNAs, MYCN, IGF2BP1, mir-17-92 cluster, diagnostic marker, neuroblastoma, pediatric cancer

OPEN ACCESS

Edited by:
Atsushi Takatori, Chiba Cancer Center Research Institute, Japan

Reviewed by:
Cecilia Mannironi, National Research Council (CNR), Italy
Shunpei Satoh, Saitama Cancer Center, Japan

****Correspondence:***
Stefan Hüttelmaier
stefan.huettelmaier@medizin.uni-halle.de

[†]These authors have contributed equally to this work and share first authorship

Specialty section:
This article was submitted to Molecular and Cellular Oncology, a section of the journal Frontiers in Oncology

Received: *30 December 2020*
Accepted: *15 April 2021*
Published: *07 May 2021*

Citation:
Misiak D, Hagemann S, Bell JL, Busch B, Lederer M, Bley N, Schulte JH and Hüttelmaier S (2021) The MicroRNA Landscape of MYCN-Amplified Neuroblastoma. Front. Oncol. 11:647737. doi: 10.3389/fonc.2021.647737

INTRODUCTION

Neuroblastoma, the most common extracranial solid childhood tumor, originates from precursors of the sympathetic nervous system and account for approximately 15% of all cancer-related death in infants (1). The clinical presentation of neuroblastoma is remarkably heterogeneous in pathological, genetic and biological characteristics, ranging from spontaneous regression or differentiation of the tumor to a high-risk aggressive disease. Neuroblastoma is thought to arise from sympathoadrenal

lineage precursor cells, derived from the neural crest. Most frequently tumor initiation emanates from one of the adrenal glands, but is also observed in the neck, chest, abdomen or along the spine (2). Risk classification depends on several clinical and biological factors, such as age at diagnosis, stage, histology and genetic aberrations (2). Favorable neuroblastoma, in particular clinical stage 4S neuroblastoma often undergo remission without any therapy. In contrast, the clinical outcome of patients with high-risk neuroblastoma stagnates despite many therapeutic approaches like surgery, radiation, chemotherapy, stem cell transplantation or immunotherapy (2). The 5-year survival rate of high-risk patients is still under 50% and the treatment remains challenging (3).

The *MYCN* oncogene is frequently amplified in high-risk neuroblastoma and a known biomarker for disease stratification (4). Amplification or severe upregulation results in a lower survival probability and a more aggressive disease. Regulation of MYCN mRNA is not fully understood, but post-transcriptional regulation by microRNAs (miRNAs) seems to be important (5, 6). Some MYCN-targeting miRNAs are downregulated in neuroblastoma like for instance members of the let-7 family. This, at least partially, is due to the increased expression of LIN28B, which impairs let-7 biogenesis and promotes neuroblastoma formation (7–9). Hence, it was assumed that upregulated expression of MYCN protein is supported by the overall downregulation of MYCN-inhibitory miRNAs in neuroblastoma (10). However, various miRNAs impairing MYCN expression, in particular members of the miR-17-92 cluster are substantially transcriptionally activated by MYC/MYCN protein and consequently co-upregulated with *MYC/MYCN* in various malignancies. This suggests that this negative feed-back regulation is at least partially uncoupled in *MYCN*-amplified (MNA) neuroblastoma, either due to a miRNA decoy function of the MYCN-3'UTR, proposed for the let-7a miRNA (11), or by trans-acting factors like RNA-binding proteins (RBPs). In respect of the latter, ELAVL4 (Embryonic lethal, Abnormal Vision, Drosophila-Like 4) RNA-binding protein (also termed HuD) and the IGF2 mRNA binding protein 1 (IGF2BP1) are of immediate interest. ELAVL4 was proposed to antagonize downregulation of MYCN expression by miR-17 (12). Expression of the oncofetal IGF2BP1 is upregulated in MNA neuroblastoma (13, 14), promotes MYCN protein and RNA expression (13), and is considered a potent and conserved inhibitor of miRNA-dependent downregulation of oncogenic factors in cancer (15, 16).

In the presented study, we provide a comprehensive analysis of miRNA expression in 97 neuroblastoma samples and reveal signatures of significantly upregulated as well as decreased miRNAs in MNA neuroblastoma. On the basis of miRNA trapping by RNA affinity purification [miTRAP, (17)], we confirm and report novel MYCN-regulatory miRNAs expressed in MNA neuroblastoma as well as *MYCN*-driven glioblastoma cell models. Finally, we evaluate if trans-acting factors, in particular IGF2BP1 and ELAVL4, or a putative miRNA decoy function of the MYCN-3'UTR uncouple increased expression of MYCN-regulatory miRNAs in neuroblastoma from elevated expression of MYCN protein. Our findings provide strong evidence that enforced expression of MYCN in MNA neuroblastoma essentially relies on IGF2BP1.

MATERIALS AND METHODS

Small RNA Library Construction, High-Throughput Sequencing and Differential Expression Analysis

Total RNA of neuroblastoma tumor samples [provided by Cologne/Essen neuroblastoma tumor bank upon application, as indicated in Bell et al. (13); for tumor information see **Supplementary Table 6**] was extracted from 30 μg of primary tumor tissue using the Qiagen ALLprep tumor protocol with miRNeasy kits (Qiagen). 500 ng of total RNA was used in the small RNA protocol with the TruSeq™ Small RNA sample prepkit v2 (Illumina) according to the instructions of the manufacturer. The barcoded libraries were size restricted between 140 and 165 bp, purified and quantified using the Library Quantification Kit–Illumina/Universal (KAPA Biosystems) according to the instructions of the manufacturer. A pool of 10 libraries was used for cluster generation at a concentration of 10 nM using an Illumina cBot. Sequencing of 51 bp was performed with an IlluminaHighScan-SQ sequencer at the sequencing core facility of the IZKF Leipzig (Faculty of Medicine, University Leipzig) using version 3 chemistry and flowcell according to the instructions of the manufacturer. Demultiplexing of raw reads, adapter trimming and quality filtering were done according to Stokowy et al. (18). Unstranded single-end reads with 51 bp in length were trimmed for adapter and low quality sequences using Cutadapt (v 1.18). Trimmed reads were mapped to the human genome (hg38 UCSC) using Bowtie2 [v 2.2.6, (19)], allowing for one mismatch in the seed region (parameter-N 1). Subsequent, mapped reads were summarized using featureCounts [v 1.6.3, (20)] and miRBase [v 22, (21)] annotations. Differential expression of miRNAs was determined using R package edgeR [v 3.28, (22)] utilizing trimmed mean of M-values [TMM, (23)] normalization of read counts. A false discovery rate (FDR) value below 0.05 was considered as threshold for the determination of differential expression.

Survival Analysis

Survival analyses were performed using differentially expressed miRNAs (*MYCN*-amplified (MNA) *vs.* none *MYCN*-amplified (nMNA)) by use of TMM normalized expression data processed as mentioned in *Small RNA Library Construction, High-Throughput Sequencing and Differential Expression Analysis*. These miRNAs were associated with available clinical data obtained from the analyzed tumor cohort. The log-rank test was implemented in an R-script according to the description in Bewick et al. (24). High and low expression groups were separated by the respective median of normalized miRNA expression values. Hazardous ratios (HR) for differential

expressed miRNAs were determined by Kaplan–Meier plotting using median cut-off. For determining the overall HR of oncogenic and tumor suppressive miRNA signatures respectively, the log_2-transformed expression values of all oncogenic or tumor suppressive miRNAs were first median-centered, subsequently combined and then divided into high and low expression group (median cut-off).

Identification of Putative Oncogenic and Tumor Suppressive miRNAs

We identified miRNAs for a classification of putative oncogenic (upregulated in MNA, poor prognostic value) and tumor suppressive (downregulated in MNA, good prognosis) miRNAs in a MYCN dependent manner. This identification is based on the aforementioned results from differential gene expression (see *Small RNA Library Construction, High-Throughput Sequencing and Differential Expression Analysis*), comparing MNA against nMNA tumors, in combination with the prognostic values from the survival data analysis (see *Survival Analysis*). In more detail, miRNAs were first abundance filtered (average CPM ≥1, counts per million mapped reads) and checked for significant differential expression changes between MNA *vs.* nMNA (FDR <0.05). Subsequent, miRNAs were selected by significant difference in survival by hazard ratios (HR below or above 1) with a log-rank p-value below 0.05. Finally, miRNA duplicates (miRNAs mapped to different chromosomal locations) were removed by selecting miRNAs with most significant FDR from differential expression analysis.

MicroRNA–Target Predictions

Predicted and validated miRNA-MYCN bindings were obtained by utilizing the R-package multiMiR [v1.12.0, database version 2.3.0, (25)]. Eight databases containing predicted and two databases including validated binding information were queried (prediction cutoff 20%) for targeting MYCN mRNA. If a certain miRNA–mRNA pair was obtained by at least two (predicted) and one (validated) database, it was considered as a putative interacting pair (**Supplementary Table 3**).

MiTRAP Experiments

MiTRAP experiments using 3′UTR of MYCN or MS2 control RNA were essentially performed as described recently (17). Purified RNA was sent for short-read RNA sequencing. Single-end sequencing was performed on Illumina HiSeq 1500 platform at Novogene (Hong Kong). Originating sequence reads of 50 bp in length were quality checked [FastQC, v. 0.11.8]. Adapters and low quality read ends were clipped off, resulting in reads with a length of 16–50 bases. Kept reads were further processed as described in *Small RNA Library Construction, High-Throughput Sequencing and Differential Expression Analysis* to determine normalized read counts. Fold enrichment was achieved by comparing miRNAs in the MYCN-3'UTR pulldown to MS2 control pulldown.

Western Blotting

Western blots were analyzed by an Odyssey Infrared Imaging System (LI-COR Biosciences). Antibodies used included anti-AGO2 (clone 11A9, serum was provided by Prof. Dr. Gunther Meister, dilution 1:5 in 5% BSA), anti-VCL (Sigma, V9131, dilution 1:5,000 in 5% BSA), anti-MBP (Cell Signaling, E8032, dilution 1:1,000 in 5% BSA) and IRDye 680/800CW-labeled mouse or rat secondary antibodies (LI-COR Biosciences, dilution 1:10,000 in 5% BSA).

Plasmids and Cloning

Cloning strategies including vectors, oligonucleotides used for PCR and restrictions sites are summarized in **Supplementary Table 5**. All constructs were validated by sequencing.

Cell Culture and Transfection

BE(2)-C cells were cultured in a 1:1 mixture of DMEM/F12 (with HEPES, Gibco) and EMEM (ATCC) supplemented with 10% FBS. KNS42 cells were cultured in DMEM (Gibco) supplemented with 10% FBS. Cells were grown at 37°C and 5% CO_2. 3.5×10^5 BE(2)-C cells were seeded in a 6-well plate and after 6 h transiently transfected with 2.5 µg GFP reporter and 7 µg iRFP vector using 14.5 µl Lipofectamine 3000 reagent (Life Technologies, 19 µl P3000 reagent, 125 µl OPTImem (Gibco)). Medium was changed after 24 h and cells were harvested and analyzed by flow cytometry 48 h post transfection.

Flow Cytometry Analysis

GFP and iRFP fluorescence was measured with a MACSQuant system. Transfected cells were harvested, washed once with PBS and then resuspended in 1% BSA in PBST. To exclude dead cells DAPI was added to the sample by the machine. Cells were gated to analyze a homogenous and single cell population. Mean fluorescence of GFP and iRFP double positive cells was analyzed. For **Figures 4B** and **5C** each GFP reporter (**Figure 3A**) was co-transfected with respective iRFP vectors (**Figures 4A**, **5A**). The mean GFP fluorescence of empty GFP, GFP-MYCN 3′ UTR WT and GFP-MYCN 3′UTR mut transfection was first normalized to respective empty iRFP vector co-transfection and then normalized to empty GFP with respective iRFP vector transfection. For **Figures 5B** the mean iRFP fluorescence was normalized to empty iRFP vector co-transfection.

RESULTS

Deregulated miRNA Expression Distinguishes MNA Neuroblastoma

The miRNA transcriptome was profiled in 97 primary neuroblastoma tumors, including 17 *MYCN*-amplified (MNA) and 80 none *MYCN*-amplified (nMNA) tumors and differential expression of miRNAs between these two groups was investigated (for tumor information see **Supplementary Table 6**). This analysis indicated 52 significantly up- and 66 significantly downregulated miRNAs in MNA when compared to nMNA tumors (FDR <0.05, **Figure 1A**). Among these, we observed seven upregulated miRNAs reported to control MYCN mRNA expression, but only three MYCN-targeting miRNAs downregulated in MNA (**Figure 1A**, red). To generally

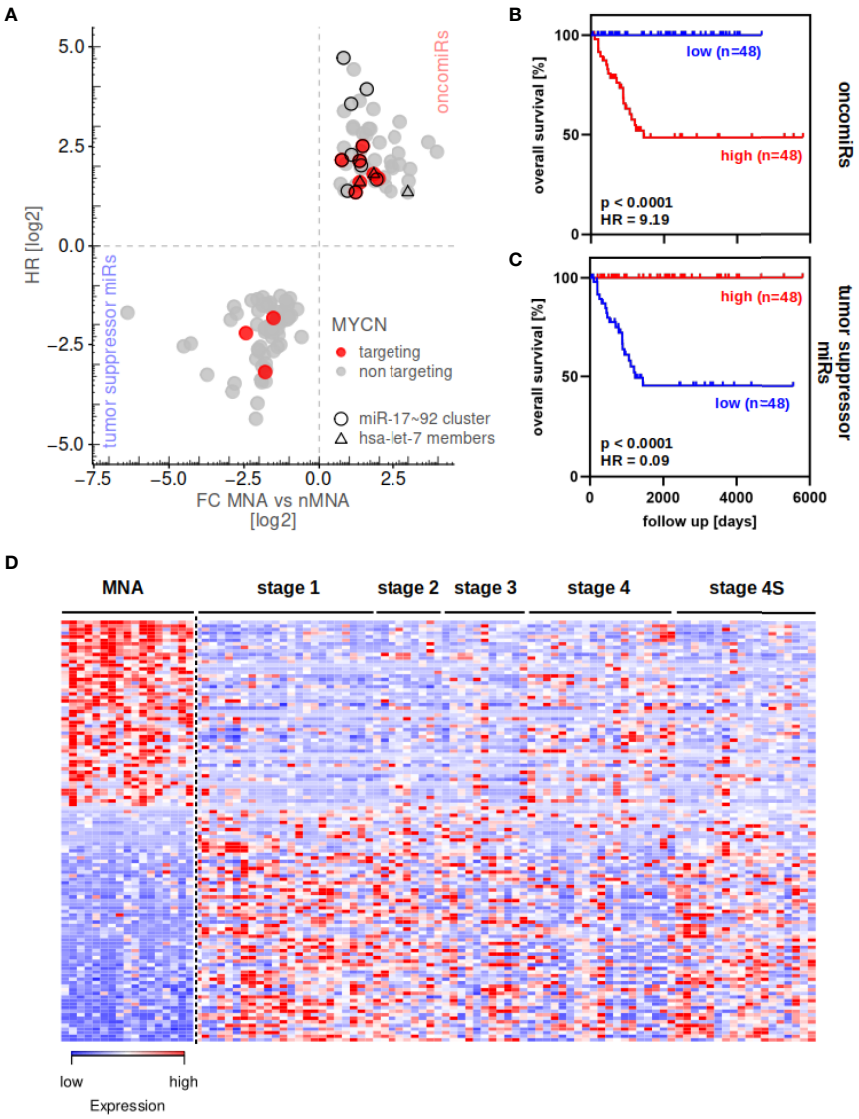

FIGURE 1 | miRNA expression can distinguish between MYCN-amplified and non-amplified tumors. **(A)** Differential miRNA expression analysis in 17 MNA and 80 nMNA neuroblastoma tumors and subsequent determination of hazardous ratio (HR, one sample lack survival data) of these miRNAs revealed 52 oncogenic and 66 tumor suppressive miRNAs (see **Supplementary Table 1** for fold changes and HR). MYCN-targeting miRNAs are indicated by colors, members of the miR-17-92 cluster and let-7 family are indicated by circles and triangles, respectively. Survival analysis of upregulated **(B)** or downregulated **(C)** miRNA signature show strong association of the respective miRNAs to overall patient survival probability. **(D)** The 118 differential expressed miRNAs distinguish MNA and nMNA tumors, as indicated by heatmap. Expression values are scaled for individual miRNAs (rows in heatmap). MYCN-amplified tumors (MNA) as well as clinical staging of nMNA tumors are indicated in the top panel.

investigate to what extent a low or high expression of these miRNAs affects the overall survival in neuroblastoma, we applied Kaplan–Meier survival analysis to these miRNA signatures upregulated and downregulated in MNA neuroblastoma. By dividing the cohort into low and high expressing groups (see *Materials and Methods*), these analysis confirmed that high expression of upregulated miRNAs was associated with substantially reduced overall survival probability, as expected and indicated by a Hazard ratio (HR) of 9.19 (**Figure 1B**). The opposite was observed for miRNAs significantly decreased in MNA tumors, for which low expression was associated with an overall poor prognosis (**Figure 1C**; HR = 0.09). Notably, the investigation of the overall prognosis relevance of each differentially expressed miRNA confirmed a rather oncogenic role, indicated by HR values greater 1, for miRNAs upregulated in MNA. Rather tumor suppressive functions (HR <1) were indicated for miRNAs downregulated in MNA (**Figure 1A**, **Supplementary Table 1**). Accordingly, miRNAs upregulated in MNA were considered to indicate oncogenic (oncomiRs), whereas miRNAs decreased in MNA indicated tumor-suppressive miRNAs, respectively. In agreement with these analyses, the investigation of miRNA expression in individual

tumor samples clearly indicated that MNA tumors are distinguished from nMNA neuroblastoma by a severe upregulation of oncomiRs (red in MNA) and downregulation of tumor suppressive miRNAs (blue in MNA), as depicted by a heat map (**Figure 1D** and **Supplementary Table 2**).

In contrast to previous reports, suggesting downregulation of MYCN-regulatory miRNAs in *MYCN*-driven neuroblastoma (10), we observed a variety of known MYCN-targeting miRNAs among oncomiRs associated with *MYCN* amplification. Most prominently, members of the miR-17-92 cluster, of which miR-17/-18a/-19a/-20a/-25/-92a/-92b and miR-93 were significantly upregulated in MNA neuroblastoma, were among oncomiRs. This is concise with the role of MYC and MYCN protein in promoting expression of this miRNA cluster *via* E-box sequences in the promotor region upstream of the miR-17-92 cluster (26, 27). In support of various previous studies, we furthermore observed upregulation of miR-9 (28), miR-15b-5p (29), miR-16-2-3p (30), and miR-181a/b (27) in MNA tumors. Likewise, we confirmed previously reported downregulation of miRNAs in MNA tumors, including miR-628-5p, miR-137-3p, miR-542-5p and miR-488-5p (29–31). In addition, we identified various previously none reported upregulated and downregulated miRNAs in MNA (see **Supplementary Table 1**). Surprisingly, miR-34c expression was elevated in MNA tumors, although previous studies claimed that the MYCN-targeting miR-34 family is downregulated in high-risk neuroblastoma (32–34). In sum our findings suggested that a variety of miRNAs reported to control MYCN mRNA expression are upregulated in MNA. To corroborate these findings, we re-analyzed the expression of miRNAs predicted to target MYCN mRNA in neuroblastoma. To this end, candidate regulatory miRNAs controlling MYCN expression were identified by investigating eight miRNA prediction databases (**Supplementary Table 3**). In support of the notion that MYCN-regulatory miRNAs are rather downregulated in *MYCN*-driven neuroblastoma (10), the reported miR-542 (35), and the predicted MYCN-regulatory miR-488 were identified among miRNAs downregulated in MNA tumors. In contrast, however, the vast majority of reported MYCN-controlling miRNAs were found to be upregulated in MNA tumors. These included miR-17 (12, 36), miR-19a (5), as well as miR-15b and miR-16 (37). Furthermore miR-20a and miR-93 (same seed sequence as miR-17) and members of the let-7 family, expected or reported to control MYCN mRNA expression, were among miRNAs upregulated in MNA tumors.

MiTRAP Reveals MYCN-Regulatory miRNA Candidates

Our investigation of miRNA expression in MNA neuroblastoma indicated that a substantial number of reported or predicted MYCN-regulatory miRNAs are upregulated in MNA. To evaluate MYCN-targeting directly, we employed miTRAP (miRNA trapping by RNA *in vitro* affinity purification) using the MYCN-3'UTR as bait to identify associating miRNAs in the *MYCN*-amplified BE(2)-C neuroblastoma and *MYCN*-driven KNS42 glioblastoma cell lines [**Figure 2A**, (17)]. KNS42 cells were included to address conserved association of miRNAs. The affinity purification of the MS2-fused MYCN-3´UTR by MS2-binding protein (MS2-BP) resulted in a robust co-purification of the RISC protein AGO2 in both cell lines, whereas neither vinculin (VCL, negative control) nor AGO2 were co-purified with the MS2 bait control (**Figure 2B**). The association of miRNAs was investigated by determining miRNA abundance using small RNA sequencing of MYCN-3'UTR and MS2 control pulldown fractions in three independent analyses. Enrichment of miRNAs was determined by the fold enrichment of miRNAs in the MYCN-3'UTR pulldown compared to MS2 controls. The comparison of miRNA enrichment revealed a striking conservation of miRNA co-purification in both cell lines (**Figure 2C** and **Supplementary Table 4**; $R_P = 0.7784$, $p < 0.0001$). In contrast, miRNA enrichment was largely independent of miRNA abundance (**Supplementary Figure S1**), as indicated by Pearson correlation coefficient of $R_P = -0.001072$ 9BE(2)-C, $p = 0.96880$ and $R_P = -0.002382$ (KNS42, $p = 0.9306$). Among the most severely enriched miRNAs were members of the MYCN-regulatory miR-17-92 cluster (**Figure 2C**, red), e.g. miR-17, as well as other validated MYCN-regulatory miRNAs like miR-29 (38). Notably, among the top 15 enriched miRNAs more than half belong to the miR-17-92 cluster (**Figure 2C**, red and **Supplementary Table 4**). Surprisingly, however, despite substantial abundance (1.15% (BE (2)-C) or 3.12% (KNS42) of all reads in input) and reported regulation of MYCN mRNA (39), let-7 family members were only modestly enriched with the MYCN-3'UTR (**Figure 2C**, cyan). Likewise, although reported to regulate MYCN expression (34), miR-34a was not enriched with the MYCN-3'UTR, presumably due to low abundance. Novel miRNAs potentially controlling MYCN mRNA expression due to substantial and conserved enrichment with the MYCN-3'UTR discovered by miTRAP are miR-193b-3p and the miR-302 family, both predicted as MYCN-regulatory miRNAs, as well as miR-6782-5p and miR-1248 (**Supplementary Table 4**).

The comparison of miRNA enrichment with the MYCN-3'UTR and altered expression of miRNAs in MNA neuroblastoma indicated that the miR-17-92 cluster miRNAs stood out due to substantially increased expression in MNA neuroblastoma and the obviously substantial enrichment by miTRAP in both analyzed cell lines (**Figure 2D**). In sum, the presented analyses provided further evidence that MYCN-regulatory miRNAs, most prominently the miR-17-92 cluster, are enriched in MNA neuroblastoma suggesting mechanisms that limit MYCN downregulation by miRNAs in this diseases subtype.

IGF2BP1 Is a Potent, 3'UTR- and miRNA-Dependent Regulator of MYCN Expression

Our studies imply that elevated *MYCN* expression in MNA neuroblastoma involve mechanisms uncoupling *MYCN*-driven expression of miR-17-92 miRNAs from the inhibition of MYCN mRNA by feed-back regulation. To this end, we addressed the potential involvement of two RNA-binding proteins (RBPs), ELAVL4 and IGF2BP1. ELAVL4 (HuD) was reported to

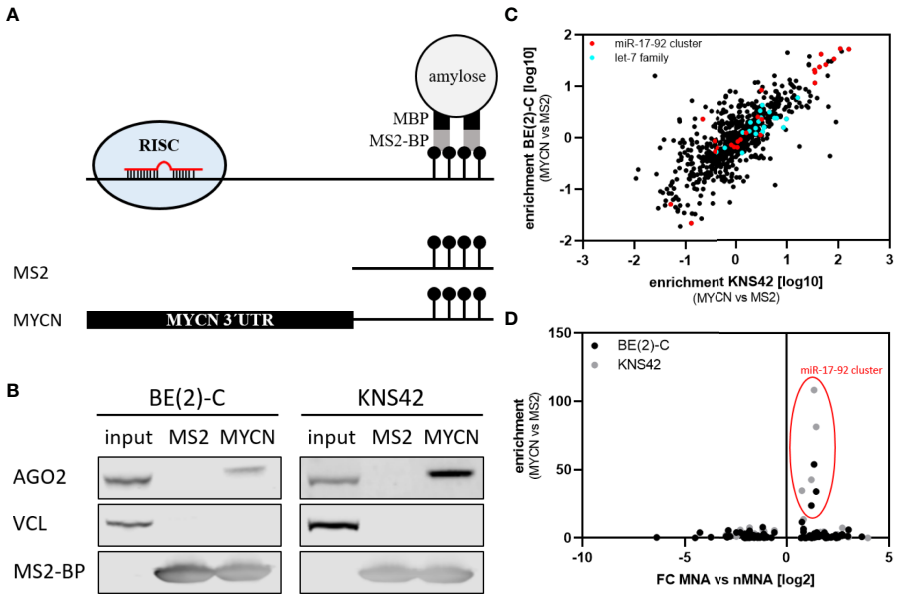

FIGURE 2 | miTRAP identified selective co-purified miRNAs with *in vitro* transcribed bait RNA. **(A)** Scheme of the miTRAP procedure. *In vitro* transcribed bait RNAs comprising two MS2 stem-loops fused to the 3′ end of bait transcripts were immobilized on amylose resin (light gray) *via* recombinant MBP-fused (black) MS2-BP (dark gray) protein (upper panel). Scheme of the used bait RNAs (lower panel). MS2: 120-nt-long control RNA encoded by the template vector, MYCN: wild type 3′ UTR of the MYCN mRNA. **(B)** Western blot analysis of indicated proteins isolated from BE(2)-C and KNS42 cells co-purified with MS2 control transcript (MS2) or the MS2-fused MYCN 3′UTR (MYCN), respectively. Vinculin (VCL) served as negative control for unspecific binding, whereas MS2-BP indicates equal loading of the resin. **(C)** Enrichment of specific miRNAs was calculated as ratio of MYCN 3′UTR compared to MS2 control pulldown. Enrichment from BE(2)-C and KNS42 cells show strong consistency in enriched miRNAs (Pearson correlation: $R_P = 0.7784$, $p < 0.0001$). The miR-17-92 cluster is depicted in red, the let-7 family in cyan. **(D)** The enrichment of miRNAs with the MYCN-3′UTR in BE(2)-C and KNS42 cell lines were compared to the fold change of miRNA expression in MNA versus nMNA tumors. Only members of the miR-17-92 cluster are consistently and substantially enriched at the MYCN 3′UTR and upregulated in MNA tumors.

interfere with miR-17-directed inhibition of MYCN expression by associating with the MYCN-3'UTR (12, 36, 40). However, ELAVL4 mRNA expression is significantly downregulated in MNA neuroblastoma (**Supplementary Figure S2**). IGF2BP1 is an oncofetal RBP upregulated in MNA neuroblastoma and reported to control MYCN expression [(13, 14), **Supplementary Figure S2**]. Moreover, IGF2BP1's main and conserved role in cancer cells is the impairment of miRNA-directed mRNA degradation by recruiting target mRNAs to miRNA/RISC-devoid mRNPs (15, 16).

To investigate MYCN-3'UTR dependent regulation in MNA neuroblastoma BE(2)-C cells, we employed a dual fluorescent reporter assay allowing the rapid assessment of altered protein expression by flow cytometry. In addition to the MYCN wild type 3'UTR fused to GFP (**Figure 3A**), we included a control reporter with a vector encoded 3'UTR (GFP) and a reporter in which targeting seeds of the miR-17-92, let-7 as well as some other MYCN-regulatory, indicated miRNAs were inactivated by mutation. In comparison to the control reporter, the activity of both reporters, either comprising the MYCN wild type 3'UTR or the mutated MYCN-3'UTR showed markedly reduced GFP expression (**Figure 3B**). This clearly indicates a pivotal role of the MYCN-3'UTR in controlling MYCN expression. Notably, the mutation of eight miRNA binding sites led to a significant increase of GFP expression. Thus miRNA-dependent regulation, in particular by the miR-17-92 cluster which summed up to ~63% of MYCN-regulatory miRNAs with inactivated seeds in the mutant reporter (**Figure 3C**), substantially contribute to the 3'UTR-dependent regulation of MYCN expression.

To investigate the potential role of ELAVL4 and IGF2BP1 in the 3'UTR- and miRNA-dependent regulation of MYCN expression, the proteins were co-expressed with GFP reporters as iRFP-fused (near-infrared fluorescent protein) proteins (**Figure 4A**). In addition to wild type IGF2BP1, we also analyzed an RNA-binding deficient mutant protein (I1 mut). This failed to restore RNA-dependent regulation by IGF2BP1 (16, 41–43), but maintains RNA-binding independent regulation of the recently reported protein-directed activation of the SRC kinase (44). Activity of the GFP control reporter remained largely unaffected by the expression of iRFP-fused proteins when comparing mean GFP fluorescent (**Figure 4B**, left panel). On the contrary, expression of the GFP-reporter comprising the wild type MYCN-3'UTR was significantly elevated by co-expression of IGF2BP1 as well as ELAVL4 (**Figure 4B**, middle panel). Importantly, an only modestly increased GFP abundance was observed in cell co-expressing the RNA-binding deficient IGF2BP1. This suggested, that both, IGF2BP1 and ELAVL4, promote MYCN expression, as previously proposed, and that this regulation largely relies on the MYCN-3'UTR. Finally, we analyzed how inactivation of miRNA sites influences regulation by IGF2BP1 and ELAVL4 (**Figure 4B**, right panel). Although only modest, both tested IGF2BP1 proteins led to a slightly

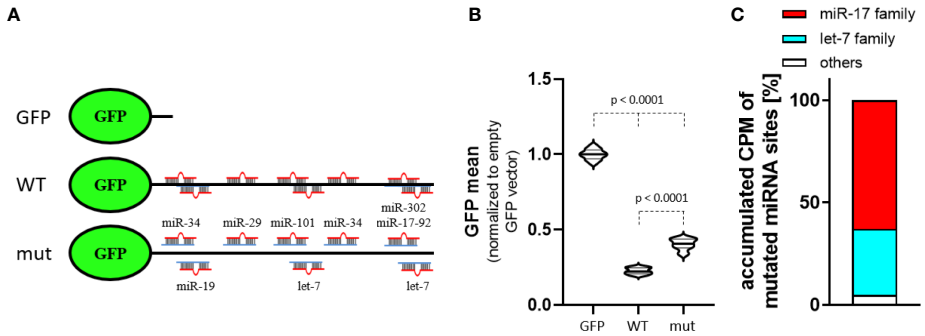

FIGURE 3 | MYCN 3′UTR is a strong miRNA target. **(A)** Scheme of used GFP reporters. Control reporter (GFP) contains only a minimal, vector-encoded 3′UTR. MYCN wildtype (WT) and mutated (mut) 3′UTR were inserted 3′ of the GFP open reading frame. The mutated 3′UTR was generated by conversion of seed sequences in eight indicated miRNA-targeting sites. **(B)** Normalized mean GFP fluorescence in BE(2)-C cells transiently transfected with GFP reporters. The WT MYCN-3′UTR is strongly repressed, indicated by lower GFP fluorescence. Mutation of several miRNA-binding sites increases GFP fluorescence (n = 3). **(C)** Among the accumulated CPM (count per million) of mutated MYCN-regulatory miRNA sites in BE(2)-C the miR-17 seed family (red) and let-7 family (cyan) are the most abundant. Statistical significance was determined by Student's t-test (p-values indicated).

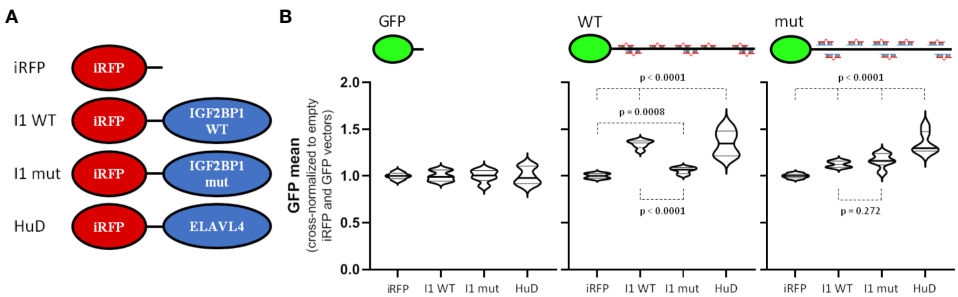

FIGURE 4 | IGF2BP1 and ELAVL4 are potent, 3′UTR-dependent regulators of MYCN expression. **(A)** Scheme of used iRFP vectors. Control vector (iRFP) or vectors with iRFP-fused wildtype IGF2BP1 (I1 WT), RNA-binding deficient mutant IGF2BP1 (I1 mut) or ELAVL4 (HuD) were transfected with GFP reporters (see **Figure 3A**) into BE(2)-C cells. **(B)** Transfected BE(2)-C were analyzed by flow cytometry. GFP and iRFP double positive cells were analyzed to determine the influence of IGF2BP1 (WT and mut) as well as ELAVL4 to the MYCN 3′UTR upon cross-normalization (n = 3). Statistical significance was determined by Student's t-test (p-values indicated).

upregulated expression of the respective GFP-reporter. However, essentially no difference was observed between the wild type IGF2BP1 and RNA-binding deficient protein, suggesting secondary, RNA-binding independent regulation. Surprising was the essentially unaltered activation of the wild type and miRNA-mutated MYCN-3'UTR reporter by ELAVL4. This suggested that either ELAVL4 controls MYCN expression by impairing other miRNAs than miR-17 or secondary, largely miRNA-independent regulation by ELAVL4. In conclusion, these findings suggest IGF2BP1 as a potent, RNA-binding and miRNA-dependent regulator of MYCN expression. Thus, IGF2BP1 likely contributes to the uncoupling of elevated miR-17-92 and MYCN expression.

The miR-17 Seed Family Is the Main Antagonist of MYCN Expression

Our analyses revealed a strong effect of miRNAs of the miR-17 seed family and potential involvement of let-7 family members in controlling MYCN expression in neuroblastoma. Notably, it was proposed that the MYCN-3'UTR serves as a let-7a sponge (11). Aiming to evaluate the postulated potency of the MYCN-3'UTR in sponging main regulatory miRNAs, we explored the activity of iRFP-fused miR-17 and let-7a antisense reporters (**Figure 5A**) when expressing the aforementioned GFP-reporters (**Figure 3A**). The expression of iRFP from both miRNA antisense reporters was markedly reduced in BE(2)-C cells when co-expressed with the GFP control reporter (**Figure 5B**, left panel), indicating substantial activity of miR-17 and let-7a in BE(2)-C cells. Most notably, however, the activity of both antisense reporters remained largely unaffected when expressing either the wild type or the miRNA mutant MYCN-3'UTR fused to GFP (**Figure 5B**, middle and right panel). This strongly argues against a miRNA sponge effect of the MYCN-3'UTR.

Our miTRAP studies revealed a strong enrichment of miR-17-92 cluster miRNAs with the MYCN-3'UTR, whereas let-7 miRNAs, including let-7a, were only modestly enriched (see **Figure 2** and **Supplementary Table 4**). Thus, to evaluate if regulation of the

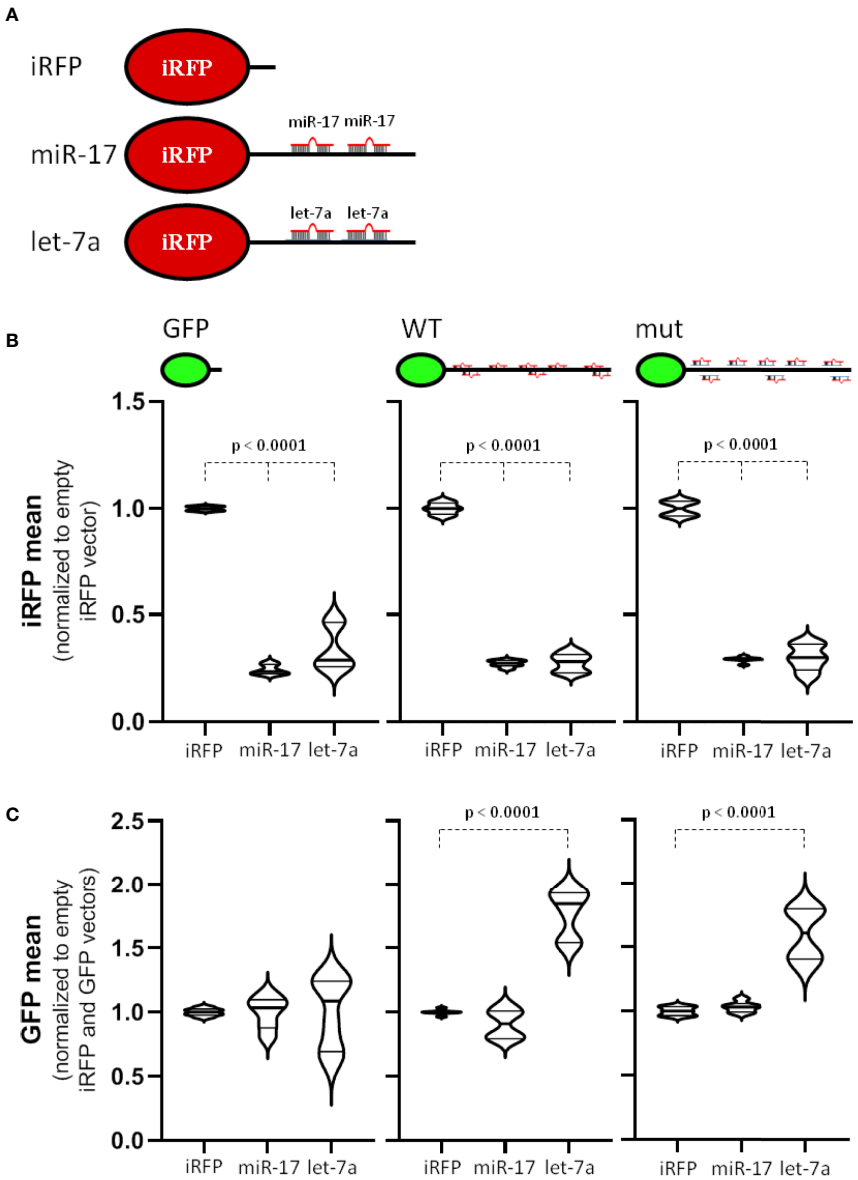

FIGURE 5 | miR-17 is a strong antagonizing miRNA for MYCN 3′UTR. **(A)** Scheme of used iRFP vectors. Control vector (iRFP) contains only a minimal 3′UTR. For miRNA antisense vectors, two perfectly complementary miRNA-targeting sites (miR-17 or let-7a) were cloned behind the iRFP open reading frame. **(B, C)** Transfected BE(2)-C cell were analyzed by flow cytometry. GFP and iRFP double positive cells were analyzed to determine the influence of the MYCN 3′UTR to the antisense reporter **(B)** or the influence of the miRNA antisense reporter to the MYCN 3′UTR **(C)** upon normalization (n = 3). Statistical significance was determined by Student's t-test (p-values indicated).

MYCN-3'UTR by the respective miRNAs is distinct, we evaluated the expression of GFP reporters when expressing the respective iRFP miRNA antisense reporters (**Figure 5C**). Whereas expression of the control GFP reporter remained largely unaffected by the miRNA antisense reporters, the wild type, but also the miRNA mutated (including inactivation of all reported let-7 targeting sites) MYCN-3'UTR reporter showed markedly elevated expression by co-expressing the let-7a antisense reporter. Although requiring further in depth investigation, these findings largely suggest that the let-7-dependent regulation of MYCN expression is largely secondary, but provides no conclusive evidence for a sponging role of the MYCN-3'UTR.

DISCUSSION

We provide a comprehensive analysis of miRNA expression in primary neuroblastoma. These studies reveal that *MYCN*-amplified (MNA) neuroblastoma is sharply distinguished by the upregulated expression of miRNAs associated with adverse diseases outcome

and the downregulation of miRNAs associated with more favorable prognosis. Among sharply upregulated miRNAs are members of the miR-17-92 cluster, which are increased by MYCN at the transcriptional level and impair MYCN expression by feed-back regulation (12, 26, 27). This strongly argues, that elevated MYCN expression in MNA neuroblastoma is not substantially supported by the downregulation of major MYCN-regulatory miRNAs, as previously proposed (10).

In MNA neuroblastoma BE(2)-C cells, expressing both, MYCN protein as well as miR-17-92 at substantial levels, members of the miR-17-92 cluster are the most enriched miRNAs observed in MYCN-3'UTR miTRAP studies. Likewise, we demonstrate striking enrichment of miR-17-92 members with the MYCN-3'UTR also in *MYCN*-driven glioblastoma KNS42 cells. Together with ample evidence for a pivotal role of the miR-17-92 cluster miRNAs in controlling MYCN expression, this indicates that this miRNA family is an essential regulator of MYCN mRNA abundance. However, the co-upregulation of both, MYCN protein and the miR-17-92 cluster miRNAs, in MNA neuroblastoma suggests that miRNA-dependent regulation of MYCN expression is substantially modulated by trans-acting factors controlling MYCN expression *via* the 3'UTR. To this end, we have investigated two RNA-binding proteins (RBPs), previously reported to control MYCN expression in neuroblastoma, ELAVL4 (HuD) and IGF2BP1. Whereas ELAVL4 expression is decreased in MNA neuroblastoma, IGF2BP1 expression is elevated. MNA neuroblastoma is considered an aggressive and de-differentiated disease. In this respect, the downregulation of ELAVL4 is consistent with its proposed role in promoting neural differentiation, as reviewed in (45). On the contrary, IGF2BP1 upregulation in MNA neuroblastoma is supported by previous studies in primary tumors, *MYC/MYCN*-driven transcriptional regulation and conserved oncofetal expression of the protein (13, 14, 46, 47). Notably in this respect, the conserved upregulation or *de novo* synthesis of IGF2BP1 in cancer is primarily observed in progressed, de-differentiated malignancies, as demonstrated for instance in anaplastic thyroid carcinoma (48). MYCN-3'UTR reporter studies provide strong evidence that both proteins modulate MYCN expression in a 3'UTR-dependent manner. This is consistent with the reported role of ELAVL4 in antagonizing downregulation of MYCN expression by miR-17 and recently reported roles in the 3'UTR-dependent enhancement of mRNA translation in neural and neuroblastoma-derived cells (12, 49). However, stimulation of MYCN-3'UTR reporter expression by ELAVL4 remained essentially unaffected by inactivating miR-17 targeting sites. In contrast, the RNA-dependent regulation of MYCN-3'UTR reporters by IGF2BP1 was essentially lost upon inactivation of miR-17 and other miRNA-targeting sites. Together, this provides strong evidence that IGF2BP1 is a potent miRNA antagonist upregulating MYCN mRNA and protein in neuroblastoma. This likely is of pivotal importance in MNA neuroblastoma, where IGF2BP1 probably serves as a *MYCN*-driven antagonist of MYCN-inhibitory miRNAs upregulated in MNA neuroblastoma.

In addition to investigating trans-acting factor promoting MYCN expression in MNA neuroblastoma in a 3'UTR- and miRNA-dependent manner, we also evaluated if the MYCN-3'UTR may serve as a miRNA decoy for MYCN-targeting miRNAs, as previously proposed (11). This was investigated for MYCN-targeting miRNAs upregulated in MNA neuroblastoma, like miR-17-92 cluster miRNAs, or substantially expressed like the let-7 miRNA family. MiTRAP studies indicate that both miRNA families are enriched with the MYCN-3'UTR, although enrichment was substantially pronounced for miR-17-92 cluster miRNAs. MiRNA antisense reporter analyses, however, clearly demonstrate that the MYCN-3'UTR lacks decoy activity, since expression of either reporter remained essentially unchanged when overexpressing the MYCN-3'UTR fused to GFP. Moreover, expression of the miR-17 antisense reporter remained ineffective in changing GFP-MYCN-3'UTR expression providing supportive evidence that neither the antisense nor the native MYCN-3'UTR have miRNA decoy activity. Why the let-7a antisense reporter changed expression of GFP reporters irrespective of let-7 targeting site inactivation remains unclear at present. However, in view of perturbed expression of both reporters, it appears likely that altered GFP reporter expression results from secondary regulation.

In conclusion our studies provide a comprehensive view on the expression of miRNAs in neuroblastoma and provide further insights into the pro-oncogenic role of the RNA-binding protein IGF2BP1 involving positive feed-back regulation with MYCN in neuroblastoma, in particular *MYCN*-amplified (MNA) diseases. These findings reveal new avenues for the treatment of MNA neuroblastoma. In recent studies, we demonstrated that inhibition of IGF2BP1-RNA association by the small molecule BTYNB impairs tumor cell growth *in vitro* and in *xenograft* mouse models (43, 50). Moreover, we recently showed for the first time that circular RNA miRNA decoys directed against the potent oncomiR 21-5p impair tumor cell vitality *in vitro* and tumor growth in *xenograft* models when delivered *via* nanoparticles (51). This highlights new avenues to pursue the targeting of post-transcriptional regulation in cancer, in particular the strongly 3'UTR-dependent regulation of MYCN mRNA in MNA neuroblastoma.

DATA AVAILABILITY STATEMENT

Presented data have been deposited in NCBI's Gene Expression Omnibus and are accessible through GEO Series accession number GSE155945 (https://www.ncbi.nlm.nih.gov/geo/query/acc.cgi?acc=GSE155945). Small RNA-seq normalized count data are also available via the R2: Genomics Analysis and Visualization Platform (http://r2.amc.nl; datasets: "Tumor Neuroblastoma - Bell - 97 - tmm - mirbase22") for interactive use and visualization.

ETHICS STATEMENT

Ethical review and approval was not required for the study on human participants in accordance with the local legislation and

institutional requirements. Written informed consent from the participants' legal guardian/next of kin was not required to participate in this study in accordance with the national legislation and the institutional requirements.

AUTHOR CONTRIBUTIONS

The study was conceptualized by SHü, SHa, JS, and DM. Data analyses were performed by DM and SHa. Experiments were performed by SHa, ML, JB, NB, and BB. The manuscript was written by DM, SHa, JS, and SHü. Figures were prepared by DM and SHa. All authors have read and agreed to the published version of the manuscript. All authors contributed to the article and approved the submitted version.

FUNDING

The work was partially supported by DFG-funding (RTG1591) to SH and intramural Roux-funding and Monika Kutzner Stiftung to JB.

ACKNOWLEDGMENTS

The authors thank the Core Facility Imaging (CFI) of the Martin Luther University, especially Dr. Nadine Bley, for support with all flow cytometry analyses. We thank Prof. Dr. Gunther Meister (University of Regensburg) for providing AGO2 antibody. Special thanks to PD Dr. Knut Krohn (Core Unit DNA-Technology, University Leipzig) for small RNA sequencing. We thank Prof. Dr. Frank Berthold and Dr. Barbara Hero (Children's Hospital, University of Cologne) for providing untreated neuroblastoma tumor samples. Furthermore, we thank Dr. Jacob Haase, Turlapati Raseswari, Marie-Luise Conrad and Annemarie Klatt for help with tumor sample preparation. We acknowledge the financial support of the Open Access Publication Fund of the Martin Luther University Halle-Wittenberg.

SUPPLEMENTARY MATERIAL

The Supplementary Material for this article can be found online at: https://www.frontiersin.org/articles/10.3389/fonc.2021.647737/full#supplementary-material

Supplementary Figure 1 | MiRNA enrichment in miTRAP studies is independent of miRNA abundance. The enrichment of miRNAs with the MYCN-3'UTR (compared to MS2 controls) was plotted over the abundance of respective miRNAs in input samples, as determined by miRNAseq. No correlation of miRNA abundance and enrichment was observed by Pearson correlation in indicated cell lines. BE(2)-C: $R_P = 0.001072$; $p = 0.9688$ and KNS42: $R_P = 0.002382$; $p = 0.9306$.

Supplementary Figure 2 | Expression of IGF2BP1 and ELAVL4 in neuroblastoma. The expression of IGF2BP1 (left panel) and ELAVL4 (right panel) in MNA (92 samples) and nMNA (401 samples) neuroblastoma tumors were analyzed in a public available mRNA-seq data set on R2 database (https://r2.amc.nl; SEQC dataset, GEO ID: GSE49710).

REFERENCES

1. Park JR, Eggert A, Caron H. Neuroblastoma: Biology, Prognosis, and Treatment. *Hematol Oncol Clin North Am* (2010) 24:65–86. doi: 10.1016/j.hoc.2009.11.011
2. Maris JM. Recent Advances in Neuroblastoma. *N Engl J Med* (2010) 362:2202–11. doi: 10.1056/NEJMra0804577
3. Whittle SB, Smith V, Doherty E, Zhao S, McCarty S, Zage PE. Overview and Recent Advances in the Treatment of Neuroblastoma. *Expert Rev Anticancer Ther* (2017) 17:369–86. doi: 10.1080/14737140.2017.1285230
4. Maris JM. The Biologic Basis for Neuroblastoma Heterogeneity and Risk Stratification. *Curr Opin Pediatr* (2005) 17:7–13. doi: 10.1097/01.mop.0000150631.60571.89
5. Buechner J, Einvik C. N-Myc and Noncoding RNAs in Neuroblastoma. *Mol Cancer Res* (2012) 10:1243–53. doi: 10.1158/1541-7786.MCR-12-0244
6. Huang M, Weiss WA. Neuroblastoma and MYCN. *Cold Spring Harb Perspect Med* (2013) 3:a014415. doi: 10.1101/cshperspect.a014415
7. Molenaar JJ, Domingo-Fernandez R, Ebus ME, Lindner S, Koster J, Drabek K, et al. LIN28B Induces Neuroblastoma and Enhances MYCN Levels Via Let-7 Suppression. *Nat Genet* (2012) 44:1199–206. doi: 10.1038/ng.2436
8. Schnepp RW, Khurana P, Attiyeh EF, Raman P, Chodosh SE, Oldridge DA, et al. A LIN28B-RAN-AURKA Signaling Network Promotes Neuroblastoma Tumorigenesis. *Cancer Cell* (2015) 28:599–609. doi: 10.1016/j.ccell.2015.09.012
9. Schnepp RW, Diskin SJ. LIN28B: An Orchestrator of Oncogenic Signaling in Neuroblastoma. *Cell Cycle* (2016) 15:772–4. doi: 10.1080/15384101.2015.1137712
10. Beckers A, Van Peer G, Carter DR, Mets E, Althoff K, Cheung BB, et al. MYCN-Targeting miRNAs are Predominantly Downregulated During MYCNdriven Neuroblastoma Tumor Formation. *Oncotarget* (2015) 6:5204–16. doi: 10.18632/oncotarget.2477
11. Powers JT, Tsanov KM, Pearson DS, Roels F, Spina CS, Ebright R, et al. Multiple Mechanisms Disrupt the Let-7 microRNA Family in Neuroblastoma. *Nature* (2016) 535:246–51. doi: 10.1038/nature18632
12. Samaraweera L, Spengler BA, Ross RA. Reciprocal Antagonistic Regulation of N-myc mRNA by miR17 and the Neuronal-Specific RNA-binding Protein Hud. *Oncol Rep* (2017) 38:545–50. doi: 10.3892/or.2017.5664
13. Bell JL, Turlapati R, Liu T, Schulte JH, Hüttelmaier S. IGF2BP1 Harbors Prognostic Significance by Gene Gain and Diverse Expression in Neuroblastoma. *J Clin Oncol* (2015) 33:1285–93. doi: 10.1200/JCO.2014.55.9880
14. Bell JL, Hagemann S, Holien JK, Liu T, Nagy Z, Schulte JH, et al. Identification of RNA-Binding Proteins as Targetable Putative Oncogenes in Neuroblastoma. *Int J Mol Sci* (2020) 21:5098. doi: 10.3390/ijms21145098
15. Busch B, Bley N, Muller S, Glass M, Misiak D, Lederer M, et al. The Oncogenic Triangle of HMGA2, LIN28B and IGF2BP1 Antagonizes Tumor-Suppressive Actions of the Let-7 Family. *Nucleic Acids Res* (2016) 44:3845–64. doi: 10.1093/nar/gkw099
16. Muller S, Bley N, Glass M, Busch B, Rousseau V, Misiak D, et al. IGF2BP1 Enhances an Aggressive Tumor Cell Phenotype by Impairing miRNA-directed Downregulation of Oncogenic Factors. *Nucleic Acids Res* (2018) 46:6285–303. doi: 10.1093/nar/gky229
17. Braun J, Misiak D, Busch B, Krohn K, Huttelmaier S. Rapid Identification of Regulatory microRNAs by miTRAP (miRNA Trapping by RNA In Vitro Affinity Purification). *Nucleic Acids Res* (2014) 42:e66. doi: 10.1093/nar/gku127
18. Stokowy T, Eszlinger M, Swierniak M, Fujarewicz K, Jarzab B, Paschke R, et al. Analysis Options for High-Throughput Sequencing in miRNA Expression Profiling. *BMC Res Notes* (2014) 7:144. doi: 10.1186/1756-0500-7-144
19. Langmead B, Salzberg SL. Fast Gapped-Read Alignment With Bowtie 2. *Nat Methods* (2012) 9:357–9. doi: 10.1038/nmeth.1923

20. Liao Y, Smyth GK, Shi W. featureCounts: An Efficient General Purpose Program for Assigning Sequence Reads to Genomic Features. *Bioinformatics* (2014) 30:923–30. doi: 10.1093/bioinformatics/btt656
21. Kozomara A, Birgaoanu M, Griffiths-Jones S. miRBase: From microRNA Sequences to Function. *Nucleic Acids Res* (2019) 47:D155–62. doi: 10.1093/nar/gky1141
22. Robinson MD, McCarthy DJ, Smyth GK. edgeR: A Bioconductor Package for Differential Expression Analysis of Digital Gene Expression Data. *Bioinformatics* (2010) 26:139–40. doi: 10.1093/bioinformatics/btp616
23. Robinson MD, Oshlack A. A Scaling Normalization Method for Differential Expression Analysis of RNA-seq Data. *Genome Biol* (2010) 11:R25. doi: 10.1186/gb-2010-11-3-r25
24. Bewick V, Cheek L, Ball J. Statistics Review 12: Survival Analysis. *Crit Care* (2004) 8:389–94. doi: 10.1186/cc2955
25. Ru Y, Kechris KJ, Tabakoff B, Hoffman P, Radcliffe RA, Bowler R, et al. The Multimir R Package and Database: Integration of microRNA-target Interactions Along With Their Disease and Drug Associations. *Nucleic Acids Res* (2014) 42:e133. doi: 10.1093/nar/gku631
26. Fuziwara CS, Kimura ET. Insights Into Regulation of the Mir-17-92 Cluster of miRNAs in Cancer. *Front Med (Lausanne)* (2015) 2:64. doi: 10.3389/fmed.2015.00064
27. Schulte JH, Horn S, Otto T, Samans B, Heukamp LC, Eilers UC, et al. MYCN Regulates Oncogenic MicroRNAs in Neuroblastoma. *Int J Cancer* (2008) 122:699–704. doi: 10.1002/ijc.23153
28. Ma L, Young J, Prabhala H, Pan E, Mestdagh P, Muth D, et al. miR-9, a MYC/MYCN-activated microRNA, Regulates E-cadherin and Cancer Metastasis. *Nat Cell Biol* (2010) 12:247–56. doi: 10.1038/ncb2024
29. Mestdagh P, Fredlund E, Pattyn F, Schulte JH, Muth D, Vermeulen J, et al. Mycn/c-MYC-induced microRNAs Repress Coding Gene Networks Associated With Poor Outcome in MYCN/c-MYC-activated Tumors. *Oncogene* (2010) 29:1394–404. doi: 10.1038/onc.2009.429
30. Megiorni F, Colaiacovo M, Cialfi S, McDowell HP, Guffanti A, Camero, et al. A Sketch of Known and Novel MYCN-associated miRNA Networks in Neuroblastoma. *Oncol Rep* (2017) 38:3–20. doi: 10.3892/or.2017.5701
31. Bray I, Bryan K, Prenter S, Buckley PG, Foley NH, Murphy DM, et al. Widespread Dysregulation of MiRNAs by MYCN Amplification and Chromosomal Imbalances in Neuroblastoma: Association of miRNA Expression With Survival. *PloS One* (2009) 4:e7850. doi: 10.1371/journal.pone.0007850
32. Galardi A, Colletti M, Businaro P, Quintarelli C, Locatelli F, Di Giannatale A. MicroRNAs in Neuroblastoma: Biomarkers With Therapeutic Potential. *Curr Med Chem* (2018) 25:584–600. doi: 10.2174/0929867324666171003120335
33. Mei H, Lin ZY, Tong QS. The Roles of microRNAs in Neuroblastoma. *World J Pediatr* (2014) 10:10–6. doi: 10.1007/s12519-014-0448-2
34. Wei JS, Song YK, Durinck S, Chen QR, Cheuk AT, Tsang P, et al. The MYCN Oncogene is a Direct Target of Mir-34a. *Oncogene* (2008) 27:5204–13. doi: 10.1038/onc.2008.154
35. Schulte JH, Schowe B, Mestdagh P, Kaderali L, Kalaghatgi P, Schlierf S, et al. Accurate Prediction of Neuroblastoma Outcome Based on miRNA Expression Profiles. *Int J Cancer* (2010) 127:2374–85. doi: 10.1002/ijc.25436
36. Lazarova DL, Spengler BA, Biedler JL, Ross RA. HuD, a Neuronal-Specific RNA-binding Protein, is a Putative Regulator of N-myc pre-mRNA Processing/Stability in Malignant Human Neuroblasts. *Oncogene* (1999) 18:2703–10. doi: 10.1038/sj.onc.1202621
37. Chava S, Reynolds CP, Pathania AS, Gorantla S, Poluektova LY, Coulter DW, et al. miR-15a-5p, miR-15b-5p, and miR-16-5p Inhibit Tumor Progression by Directly Targeting MYCN in Neuroblastoma. *Mol Oncol* (2020) 14:180–96. doi: 10.1002/1878-0261.12588
38. Sun G, Lu J, Zhang C, You R, Shi L, Jiang N, et al. MiR-29b Inhibits the Growth of Glioma Via MYCN Dependent Way. *Oncotarget* (2017) 8:45224–33. doi: 10.18632/oncotarget.16780
39. Van Peer G, Mets E, Claeys S, De Punt I, Lefever S, Ongenaert M, et al. A High-Throughput 3' UTR Reporter Screening Identifies microRNA Interactomes of Cancer Genes. *PloS One* (2018) 13:e0194017. doi: 10.1371/journal.pone.0194017
40. Manohar CF, Short ML, Nguyen A, Nguyen NN, Chagnovich D, Yang Q, et al. HuD, a Neuronal-Specific RNA-binding Protein, Increases the In Vivo Stability of MYCN RNA. *J Biol Chem* (2002) 277:1967–73. doi: 10.1074/jbc.M106966200
41. Wachter K, Kohn M, Stohr N, Huttelmaier S. Subcellular Localization and RNP Formation of IGF2BPs (Igf2 mRNA-binding Proteins) is Modulated by Distinct RNA-binding Domains. *Biol Chem* (2013) 394:1077–90. doi: 10.1515/hsz-2013-0111
42. Muller S, Glass M, Singh AK, Haase J, Bley N, Fuchs T, et al. IGF2BP1 Promotes SRF-dependent Transcription in Cancer in a m6A- and miRNA-dependent Manner. *Nucleic Acids Res* (2019) 47:375–90. doi: 10.1093/nar/gky1012
43. Muller S, Bley N, Busch B, Glass M, Lederer M, Misiak C, et al. The Oncofetal RNA-binding Protein IGF2BP1 is a Druggable, Post-Transcriptional Super-Enhancer of E2F-driven Gene Expression in Cancer. *Nucleic Acids Res* (2020) 48:8576–90. doi: 10.1093/nar/gkaa653
44. Bley N, Schott A, Muller S, Misiak D, Lederer M, Fuchs T, et al. IGF2BP1 is a Targetable SRC/MAPK-dependent Driver of Invasive Growth in Ovarian Cancer. *RNA Biol* (2020) 18:391–403. doi: 10.1101/2020.06.19.159905
45. Deschenes-Furry J, Perrone-Bizzozero N, Jasmin BJ. The RNA-Binding Protein HuD: A Regulator of Neuronal Differentiation, Maintenance and Plasticity. *Bioessays* (2006) 28:822–33. doi: 10.1002/bies.20449
46. Bell JL, Wachter K, Muhleck B, Pazaitis N, Kohn M, Lederer M, et al. Insulin-Like Growth Factor 2 mRNA-binding Proteins (IGF2BPs): Post-Transcriptional Drivers of Cancer Progression? *Cell Mol Life Sci* (2013) 70:2657–75. doi: 10.1007/s00018-012-1186-z
47. Noubissi FK, Nikiforov MA, Colburn N, Spiegelman VS. Transcriptional Regulation of CRD-BP by C-Myc: Implications for C-Myc Functions. *Genes Cancer* (2010) 1:1074–82. doi: 10.1177/1947601910395581
48. Haase J, Misiak D, Bauer M, Pazaitis N, Braun J, Potschke R, et al. IGF2BP1 is the First Positive Marker for Anaplastic Thyroid Carcinoma Diagnosis. *Mod Pathol* (2020) 34:32–41. doi: 10.1038/s41379-020-0630-0
49. Tebaldi T, Zuccotti P, Peroni D, Kohn M, Gasperini L, Potrich V, et al. Hud Is a Neural Translation Enhancer Acting on Mtorc1-Responsive Genes and Counteracted by the Y3 Small Non-coding Rna. *Mol Cell* (2018) 71:256–270 e210. doi: 10.1016/j.molcel.2018.06.032
50. Mahapatra L, Andruska N, Mao C, Le J, Shapiro DJ. A Novel Imp1 Inhibitor, BTYNB, Targets c-Myc and Inhibits Melanoma and Ovarian Cancer Cell Proliferation. *Transl Oncol* (2017) 10:818–27. doi: 10.1016/j.tranon.2017.07.008
51. Müller S, Wedler A, Breuer J, Glaß M, Bley N, Lederer M, et al. Synthetic Circular Mir-21 RNA Decoys Enhance Tumor Suppressor Expression and Impair Tumor Growth in Mice. *NAR Cancer* (2020) 2:1–16. doi: 10.1093/narcan/zcaa014

Conflict of Interest: The authors declare that the research was conducted in the absence of any commercial or financial relationships that could be construed as a potential conflict of interest.

frontiers in Oncology

REVIEW
published: 14 June 2021
doi: 10.3389/fonc.2021.694320

Biological Role of MYCN in Medulloblastoma: Novel Therapeutic Opportunities and Challenges Ahead

Sumana Shrestha[1], *Alaide Morcavallo*[1], *Chiara Gorrini*[1*] *and Louis Chesler*[1,2*]

[1] Division of Clinical Studies, Institute of Cancer Research (ICR), London and Royal Marsden NHS Trust, Sutton, United Kingdom, [2] Division of Cancer Therapeutics, The Institute of Cancer Research (ICR), and The Royal Marsden NHS Trust, Sutton, United Kingdom

The constitutive and dysregulated expression of the transcription factor MYCN has a central role in the pathogenesis of the paediatric brain tumour medulloblastoma, with an increased expression of this oncogene correlating with a worse prognosis. Consequently, the genomic and functional alterations of MYCN represent a major therapeutic target to attenuate tumour growth in medulloblastoma. This review will provide a comprehensive synopsis of the biological role of MYCN and its family components, their interaction with distinct signalling pathways, and the implications of this network in medulloblastoma development. We will then summarise the current toolbox for targeting MYCN and highlight novel therapeutic avenues that have the potential to results in better-tailored clinical treatments.

Keywords: MYCN, medulloblastoma, targeted therapy, metabolism, immunotherapy, PROTACs

OPEN ACCESS

Edited by:
Christer Einvik,
Arctic University of Norway, Norway

Reviewed by:
Mariana Maschietto,
Centro Infantil Boldrini, Brazil
Kwok-Ming Yao,
The University of Hong Kong, Hong Kong, SAR China

***Correspondence:**
Chiara Gorrini
chiara.gorrini@icr.ac.uk
Louis Chesler
louis.chesler@icr.ac.uk

Specialty section:
This article was submitted to Molecular and Cellular Oncology, a section of the journal Frontiers in Oncology

Received: *12 April 2021*
Accepted: *19 May 2021*
Published: *14 June 2021*

Citation:
Shrestha S, Morcavallo A, Gorrini C and Chesler L (2021) Biological Role of MYCN in Medulloblastoma: Novel Therapeutic Opportunities and Challenges Ahead. Front. Oncol. 11:694320. doi: 10.3389/fonc.2021.694320

INTRODUCTION

The MYC family of transcription factors, including c-MYC (MYC), MYCL and MYCN are amongst the most commonly altered genes in cancer, including paediatric cancers (1). Tumorigenic activity of the MYC family can result from constitutive activation of associated mitogenic signalling pathways e.g., Wingless (WNT), Hedgehog (SHH), Transforming growth factor beta (TGF-β), or through direct genetic alterations from amplification or chromosomal aberrations. Sequence homology between the two proteins, MYC and MYCN remain relatively high, and similarities remain between organisation of loci, and protein binding sites (2–4). Pioneering developmental studies have been integral in illustrating the interchangeable nature of the MYC proteins, in particular between MYC and MYCN (5). These studies assessing the phenotypic consequences of *Myc* or *Mycn* deficiency in mouse development identified expression divergence during the early developmental stages. Whilst null homozygosity for both *Myc* and *Mycn* resulted in embryonic lethality (approximately E10.5-E11.5), *Myc*-null embryos were associated with marked reduction in size and a general delay in primitive development of the heart (6). *Mycn*-null embryos also exhibited delayed development and stunted growth, as well as diminished cellularity in organs that normally express abundant *Mycn* transcripts, most notably the cranial and spinal ganglia (7–9). Significantly, despite a compensatory *Myc* increase observed in *Mycn* deficient embryos (8), developmental defects occurred that suggested a unique and essential role for *Mycn* during CNS development. Conversely, replacement of endogenous *Myc*-coding sequences with *Mycn*-coding sequences

showed that Mycn is capable of performing most of the essential functions of Myc required for embryonic development and proliferation (5). Whilst the proteins share similarities in structure and binding partner MAX (10), the differences remain in their spatial and temporal expression patterns, with MYCN showing a preference to the early hindbrain development (11–14). Overall, both proteins at the transcriptional level can orchestrate the cell cycle machinery and stimulate cell growth, division, and regulate the differentiation states of cells throughout development.

In this review, we will focus on the role of the MYC family proteins, specifically MYCN, in different subgroups of the childhood brain tumour medulloblastoma (MB). MYC proteins play an important role in MB biology and often are dysregulated in all MB tumours, with *MYC, MYCN* and *MYCL1* each showing commitment to specific subgroup (15). *MYC* and *MYCN* amplifications especially are prominent in MB due to the highly aggressive nature of tumours associated with these aberrations (16). *MYC* and *MYCN* have been considered undruggable for many years as they carry out essential functions in proliferative tissues, suggesting that their inhibition could cause severe side effects. Only recently has there been an improvement in making their protein surfaces amenable to binding small molecules, further accelerating their use in therapeutics (17). We will highlight the potential application of several new therapeutic strategies targeting MYCN and its signalling partners to tackle the overarching obstacles.

MEDULLOBLASTOMA

Clinical and Molecular Diversity of Medulloblastoma

Medulloblastoma is one of the most prevalent malignant paediatric brain tumours (WHO grade IV) (18). MB arises from the posterior fossa and features a heterogeneous tumour landscape. MB accounts for ~63% of childhood intracranial embryonal tumours, and has an incidence of 4.9 per 1 million children, peaking at ~7 years of age (19, 20). The tumour is usually proximal to the fourth ventricle, making metastasis through cerebrospinal fluid (CSF) flow common (21). The current standard of care consists of maximal surgical resection followed by cranio-spinal irradiation (CSI) in patients >3 years, and multi-agent chemotherapy. The overall survival rate ranges from 40-90%, depending on the molecular subtype and other factors such as extent of dissemination and degree of resection. Whilst survival rates have improved overtime due to better understanding and implementation of CSI, ~1/3 of patients still succumb to the disease, and survivors often experience debilitating neurologic, endocrinologic, and cognitive sequelae from treatment (22).

Different Subgroups and Subtypes

Initially, using gene expression analysis techniques, MB was segregated into four distinct molecular subgroups, with differences in genomic drivers, mutational events, methylation patterns and clinical characteristics (23). These groups are known as: wingless (WNT), Sonic hedgehog (SHH), and, group 3 (Grp3), and group 4 (Grp4), also known as non-WNT/non-SHH (24–27). Due to the well-defined developmental pathways of WNT and SHH, many studies have been able to dissect the mechanism of these two groups, whereas Grp3 and Grp4 have recently raised attention owing to next-generation sequencing techniques (15, 28–31). Further gene expression and DNA-methylation analysis of the subgroups by Cavalli et al. introduced additions layers of heterogeneity within the four main subgroups, these are as follows: WNT; WNT-α and WNT-β, SHH; SHH-α, SHH-β, SHH-χ, SHH-δ, Group 3; Grp3-α, Grp3-β, Grp3-χ and Group 4; Grp4-α, Grp4-β, Grp4-χ (32). Adding to this, other variations of subtypes emerged during the same time as several research groups utilised different sample analysis methods (33, 34). Whilst the use of separate analytic techniques provides a more dynamic and richer dataset, it is now essential to compare and combine these differences to produce a single, streamline set of subtypes.

Comparing the clinical features of the subgroups, the WNT subgroup has the most favourable clinical outcomes, with the overall survival standing at >90% (35). However, this is the least common MB subtype, accounting for only 10% of MBs (23). The favourable prognosis associated with activation of the WNT signalling pathway is now being exploited for other subgroups of this cancer (36). The majority of these tumours (86%) harbour activating mutations in β-catenin (*CTNNB1*), a central orchestrator of the canonical WNT pathway (33, 37, 38), or mutations in the tumour suppressor gene *APC (71%)* (39). Further prominent genes identified from whole genome sequencing include *DDX3X (7.6%)*, *SMARCA4 (3.4%)*, *TP53 (~10%)* and *KMT2D (~7%)* (40).

The SHH-subgroup, despite its heterogeneity, is the best clinically and molecularly characterised MB-subgroup. The age of the patient is especially important here as each age group has a distinct transcriptomic profile; adult patients (SHH-δ) show frequent mutation in the TERT promoter, whilst younger patients show enrichment in focal amplifications of *MYCN*, *GLI2*, and *YAP1*, frequent germline or somatic TP53 mutations, and more recently discovery of germline variants in *ELP1* (32, 41–44). *ELP1* encodes the scaffold protein elongator complex protein 1 (ELP1) which is involved in neuronal migration and is responsible for transcriptional elongation (45, 46). Furthermore, *PTCH1* mutation is highly frequent in this subgroup, the only distinction of this within the subtypes is the number of additional aberrations accommodating this mutation; with a higher aberrational load seen in the adult subtype (SHH-δ). More recent research shows a prominent role for *TP53* dysregulation. This frequently arises in conjunction with chromothripsis, a catastrophic genomic rearrangement commonly occurring due to micronucleus formations (29, 42, 47).

In contrast to WNT and SHH, both Grp3, and Grp4 have very few prominent driver genes. Nonetheless, they both show distinct genetic events which define each subgroup as separate entities. Grp3 MB primarily occurs during infancy and childhood and is associated with a high rate of disseminated disease. This subgroup is defined by high levels of *MYC* amplification and a particular genetic signature related to

increased transcription and translation (48). Important genes dysregulated at a somatic level include *SMARCA4*, *KBTBD4*, and *KMT2D*. Furthermore, recent studies have shown increased activation of genes representing the Notch and TGFβ signalling pathways, and a particular inclination for activation of GFI1/GFI1B through enhancer hijacking (49). Grp4 MB is the most prevalent MB subgroup. With a lack of single gene mutations, this subgroup features a higher frequency of disposition to somatic mutations, with notable mutations in histone-modifying genes such as *KDM6A*, *ZMYM3* and *KMT2C*. The recent discovery of ERBB4-SRC signalling in Grp4 tumours has highlighted this pathway as a hallmark of Grp4 MB (50). Both Grp3 and Grp4 groups have recurrent mutations in *KBTBD4*, underpinning the gene as a common candidate tumour driver (33).

Cancer predisposition syndromes remain a risk factors for the development of MB and account for approximately 5-6% of MBs (39). Germline mutations in WNT signalling pathway genes such as *APC* mutations, found in Turcot Syndrome, can lead to the WNT subgroup. SHH MB can be initiated through various germline mutations such as *PTCH1*, occurring in the autosomal dominant condition Gorlin syndrome (known as nevoid basal cell carcinoma syndrome), or aberration in germline *TP53* as seen in Li-Fraumeni syndrome (33). Furthermore, germline mutation in *SMO* from Curry-Jones syndrome is also associated with SHH MB (39). With the advancement in stem cell research and patient-derived iPSC culture systems, this information will inevitably allow for more accurate modelling and prediction of the development of particular subgroups of MB (51).

The innate differences within this highly heterogeneous cancer provides an insight into the putative cells of origin residing in different regions of the cerebellum (32, 52). The embryonic nature of MB makes it difficult to pinpoint the exact cell of origin. Therefore, it is essential to investigate the complete genetic aetiology of these tumours in order to build more accurate and robust models of the disease. The normal development of the cerebellum serves as a healthy control for the development of MB. MB cells are thought to arise from progenitor cell populations from early hindbrain development. This has been investigated for WNT and SHH MB, with WNT tumours thought to arise from the extracerebellar lower rhombic lip, and SHH from cerebellar granule cell precursors (GCPs) (53). More recently, it was postulated that for Grp4, the cellular origin consisted of more differentiated neuronal population, with glutamatergic cells including residues of unipolar brush cells and glutamatergic cerebellar nuclei (30, 54). Whilst for Grp3 origin remains quite vague, with studies referring to a potential origin of undifferentiated progenitor-like lineage with high MYC activity (54).

THE ROLE OF MYCN IN THE ORIGIN OF MEDULLOBLASTOMA

MYCN in Cerebellar Development

When looking at the development of MB, the environment in which the tumour grows should be treated almost as a crime scene, as Bailey and Cushing once wrote "the histogenesis of the brain furnishes the indispensable background for an understanding of its tumours" (55). A defect in the normal expansion of the cerebellar precursor population can lead to uncontrolled proliferation, resulting in the development of MB.

The developing cerebellum is moulded by three distinct pools of progenitor cells; these consist of GCPs from the deep nuclei (emerging from rhombic lip), GABAergic Purkinje cells (arising from multipotent precursors of the primary germinal epithelium in the roof of the 4th ventricle), and CD133/Nestin+ cells (the white matter of the postnatal cerebellum). During postnatal development, GCPs rapidly proliferate and expand in response to SHH secreted by Purkinje cells (56), and mature to become cerebellar granule neurons – the largest neuronal population in the brain (57), as shown in **Figure 1**.

MYCN plays a fundamental role in orchestrating both normal and abnormal development of the cerebellum, with critical functions in precursor growth and maturation **(Figure 1)**. MYCN is present at low levels in many neonatal tissues and expressed at particularly high levels in the hindbrain (8, 58). *MYCN* expression persists during differentiation stages where *MYC* is downregulated (8). *MYCN* expression is predominant in neural stem cells and progenitor cell populations, with its expression diminishing after the cells become committed to more differentiated states. One putative mechanism employed by MYCN to sustain CNS development is the conservation of large domains of chromatin in an euchromatic state (59). This is demonstrated through double knockout animal models of *MYC* and *MYCN*, which showed gene alterations in chromatin structure (60).

MYCN also contributes to cerebellum development downstream of SHH. SHH is an extracellular signalling molecule with a critical role in regulating growth and differentiation in the developing brain (61, 62). SHH signalling upregulates MYCN through activation of PI3K, a corollary of this is glycogen synthase kinase 3 beta (GSK-3β) inhibition, preventing destabilisation of the MYCN protein by GSK-3β and halting skp-cullin-F-box (SCF)-FBXW7 induced proteasomal degradation (63). Several studies have demonstrated SHH as a primary driver of the expansion of GCPs through direct upregulation of MYCN, highlighting the importance of *MYCN* in the proliferation of GCP cells and for their responses to SHH (64, 65). As a mitogen, SHH induces genes involved in cell cycle progression and DNA replication, mainly during the period of post-natal hindbrain expansion. In parallel, the role of *MYCN* is most critical during this phase. Dysfunctional *MYCN* can prime the progenitor cells by altering internal regulatory mechanisms, making them more susceptible to defects in cerebellar development. Studies have shown *MYCN* null neural precursors have high levels of specific cyclin dependent kinase inhibitors (CDKI), $p18I^{nk4c}$ and $p27^{KIP1}$ which induces differentiation programmes in cells, supported by reduced levels of cyclin-D2 (66, 67). More specific to its structure, preventing phosphorylation of the MYCN amino-terminal impedes cell cycle exit of GCPs (68); phosphorylation of the S62 priming site of MYCN by CDK1/

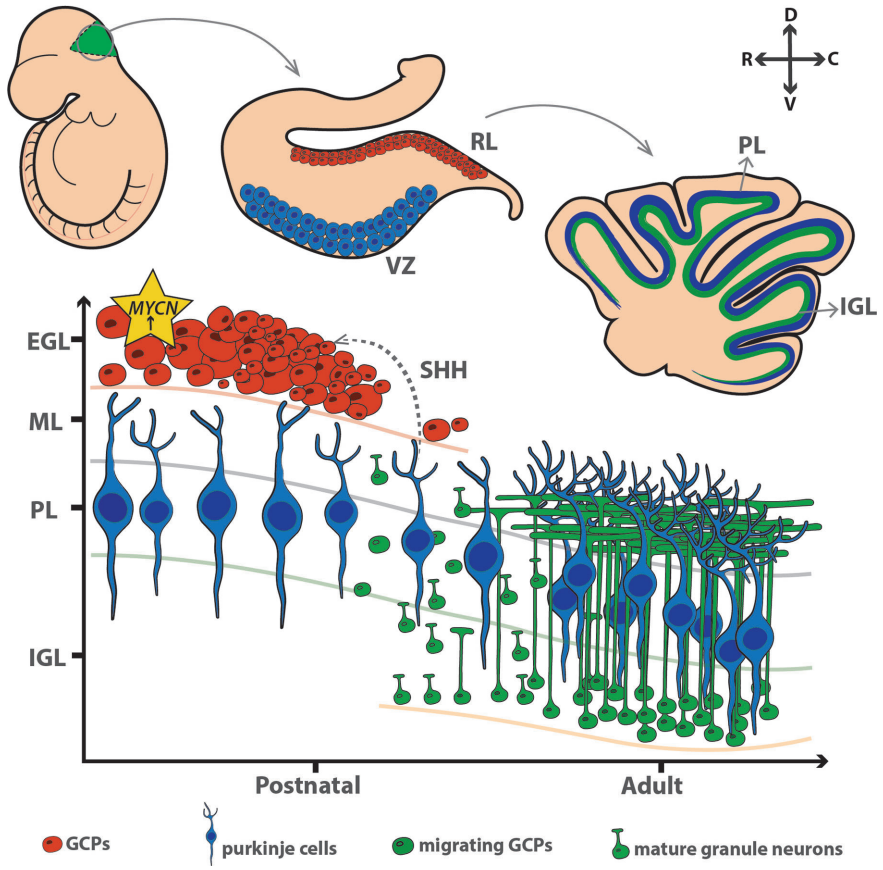

FIGURE 1 | MYCN maintains the proliferation of granule cell progenitors in the external granule layer during early development. VZ, ventricular zone; RL, rhombic lip; PL, purkinje layer; IGL, internal granule layer; EGL, external granule layer; ML, molecular layer; GCP, granule cell precursors. D, dorsal; C, caudal; V, ventral; R, rostral.

cyclin A/B prevents this continuous activation of the cell cycle and allows cell cycle exit (69). MYCN has a vital role in the early cerebellum development. By orchestrating a time-dependent expansion of progenitor cells to form the EGL, it indicates a window of high activity, after which it is downregulates to allow cell cycle arrest and subsequent differentiation and maturation of the cells.

The Role of MYCN in MB Groups

Collectively, this family of oncogene is of particular interest as *MYC* and *MYCN* are each committed to specific subtypes of MB. MYC is often found to be overexpressed in WNT tumours, despite a lack of *MYC* amplification, whereas amplification of MYC is commonly detected in G3 tumours (31). Both *MYCN* amplification and overexpression is observed in SHH MB. *MYCN* amplifications are also present in G4 tumours, however, this is generally at a much lower level compared with the SHH subgroup (31). *MYC* and *MYCN* amplifications in particular have been the main focus in MB due to the highly aggressive nature of tumours associated with these aberrations (16). Alongside genetic abnormalities, dysregulated epigenetic modifiers are also frequently observed in more aggressive medulloblastoma tumours, including those harbouring *MYCN*/MYCN abnormalities (70, 71). The preference of MYC to a distinct subtype suggests potential ideas about MB tumorigenesis.

The WNT Group

Moderately high levels of MYCN and MYCL1 are observed in this subtype compared to Grp3 and Grp4 (72). Furthermore, *MYC* is also highly expressed with comparable levels to those seen in Grp3 (13). This high level *MYC* expression could be explained by *MYC* being a downstream target of WNT signalling (73). Whilst MYC expression usually correlates with poor prognosis in other MB subgroups, the WNT subtype displays the most positive prognosis within the subgroups, regardless of MYC levels (74).

The SHH Group

Gene amplification is a very common event in SHH MB. The most prevalent amplifications include *MYCN* and *MYCL1*, as well as other important genes such as *GLI2*, *MDM4*, *PPM1D* and

YAP1 (15, 75). Patients with SHH subtype MB have a frequent gain of chromosome 2, which harbours *MYCN*, this may also explain the resulting *MYCN* amplification event seen regularly in this subgroup. In subtypes where *MYCN* amplification co-occurs with *TP53*-mutations, there is a worsening of the overall outcome (32, 76). An event linking the two together is chromothripsis. Tumours with high levels of this complex genome arrangement show a positive correlation in the frequency of MYC/MYCN amplifications (77). The chronological order of *TP53* mutation, *MYCN* amplification and chromothripsis is largely unknown and yet to be explored. Pursuing this further will inevitably shed light on novel DNA repair mechanisms which can be utilised for therapeutic targeting.

Studies have shown that MYCN has dual-capacity to produce either SHH-dependent (63) or SHH-independent MB (78). Formation of either is highly dependent on the temporal expression of *MYCN*, either during embryonic or postnatal development (58). This further highlights MYCN's dynamic role in CNS development. Novel pathways fuelling MB growth include the evolutionarily conserved signalling pathway known as the Salvador-Warts-Hippo (Hippo) pathway (79). SHH signalling may have cross talk with the Hippo pathway to regulate important downstream efforts such as the Yes-associated protein (YAP), an oncoprotein shown to promote proliferation of CGPs (80). Indeed, genomic profiling of OLIG2-expressing glial progenitors as transit amplifying cells of SHH-MB revealed that these cells activate oncogenic networks including HIPPO-YAP/TAZ and AURORA-A/MYCN (81).

Group 3

The majority of Grp3 tumours are characterised by high protein levels of MYC, either induced by *MYC* amplifications or by aberrant MYC expression (41). Differential analysis of super-enhancers has identified MYC as a prominent target in Grp3. Thus, MYC is noted as the key driver of Grp3 MB (30). Plasmacytoma Variant Translocation 1 (PVT1) gene fusion in Grp3 is linked to chromothripsis and MYC amplification on chromosome 8q24 (82). New molecular stratification of this subtype into different subgroups, has shown that subgroup II and III harbour amplifications of the *MYC* oncogene and are associated with poor outcomes (83). Interestingly, subgroup V, characterised by amplification of both *MYC* and *MYCN*, is associated with moderate clinical outcomes (83). Moreover, the increased abundance of many proteins involved in mRNA processing, transcription and translation observed in Grp3 MB is associated with high *MYC* expression (48, 50). Interestingly, whilst this subgroup is mainly associated with MYC amplifications, MYCN amplifications is also seen in a minority of patients (5%) (33).

Group 4

The most frequent somatic copy-number alterations (SCNAs) in this group target the gene *SNCAIP* (synuclein, alpha interacting protein) (15). While MYCN amplification also occur in this subtype, they are mutually exclusive with SNCAIP duplications (31).

Current Management of MYCN-Associated MB

Since the identification and isolation of MB as a distinct entity in 1926 by Cushing and Bailey, the prognosis of patients has alleviated from no survival to now, the most positive outcome of 80% 5-year overall survival (OS). This improvement was led through continuous progression in understanding the biological mechanisms behind this cancer and strengthened by emerging technologies and treatments. Although this OS sounds very positive, the reality of the age of these patients, coupled with the harsh quality of life (QOL) observed after the treatments (84, 85) pushes this scientific field to develop more novel and targeted therapies which can ameliorate the dismal QOL.

While our understanding of MB biology and molecular features has greatly improved over the last decade, current treatment regimens for MB have been relatively unchanged. These strategies are principally tailored based on clinico-radiological risk criterion, used to define the standard-risk (SR) or high-risk (HR) group (86). Children who are >3 years with no evidence of metastatic disease (M0), post-surgical residual tumour <1.5 cm^2, and histologically non-anaplastic are categorized as SR, while the remaining are considered HR. Children >3 years who have significant residual disease following surgery, large cell/anaplastic (LC/A) histology and metastatic disease have a worse prognosis with poor survival outcome (87).

Medulloblastomas are typically more radiosensitive than other paediatric brain tumours, including glioblastomas (GBM). Therefore, radiotherapy is an essential element in the multidisciplinary management of children with MB, and postoperative craniospinal axis radiotherapy is considered a curative treatment. Commonly, children >3 years, receive surgery, external beam radiation to the spine and brain, combined with multidrug chemotherapy (cisplatin, vincristine, and cyclophosphamide). While both SR and HR children are treated with radiation, HR patients are given larger boosts of radiation. Children <3 years are treated postoperatively with high-dose chemotherapy as an irradiation-avoiding strategy or with non-high-dose chemotherapy during induction followed by a reduced dose of conformal radiotherapy (CRT) to the tumour bed (88, 89). Radiation is generally avoided in children <3 years due to the adverse effects on the developing brain. Radiation in older children has been linked to reduced IQ and induction of secondary cancers, vasculopathy, hearing loss, and future strokes (90–92). The standardised treatment of MB solely based on histopathology and clinico-radiological risk stratification can lead to unpredictable relapses and therapeutic failures. Disease relapse is the most adverse prognostic factor in MB, occurring in approximately 30% of patients (93). Children with tumour relapse receive various strategies, including continuous administration of low doses of chemotherapeutic, high-dose chemotherapy, intrathecal medication, and re-irradiation, but these approaches are commonly unsuccessful (94, 95).

It is evident from the review that MYCN is a very attractive therapeutic target. Nevertheless, it has proven challenging to target, with current techniques unsuccessful in exploiting the

molecule for therapeutic gain (10). Structurally, MYC proteins lack any enzymatic activity/globular functional domains, which makes it unapproachable for structure-based virtual screening, and undesirable for the long-established enzyme inhibitor design (96). Adding to this, MYCN is also known as an intrinsically disordered (ID) oncoprotein, meaning the protein structure of MYCN in isolation fails to adopt a defined three-dimensional structure (97). This is advantageous for its role as a transcription factor as the ID structure allows MYCN to hold a larger surface area for increased interaction with numerous other proteins – the disordered domains mean it can be "re-used" in multiple pathways (98). However, this makes it challenging to target MYCN directly.

Further to its structure and function, the widespread expression of *MYCN* by all early proliferating cells also poses a concern. The numerous target genes of MYCN makes it difficult to define critical oncogenic effector pathways for precise drugging. Thus, targeting this oncogene may present with unacceptable toxicities (99). However, as most "normal" CNS cells spend the majority of their life in quiescence, the adverse effects may be more negligible than expected (100). Limited direct targeting of MYCN has motivated strategies to look at indirect or MYCN-dependent interactions instead. Due to the high growth-inducing activity of MYCN, its mechanism is controlled at multiple steps.

EMERGING THERAPEUTIC OPPORTUNITIES

Targeting MYCN Stability

The stability of the MYCN protein itself is a critical level of regulation. MYCN is controlled by phosphorylation of specific residues, most of which takes place within Myc box I (MBI). First, phosphorylation mediated by CDK1-CyclinA/B1 complexes occurs at S62, which permits recognition. Second, phosphorylation activity occurs via serine/threonine kinase GSK3β on T58. The phosphorylating activity of GSK3β causes degradation of MYCN. MYCN protein has an ephemeral half-life (20-30 minutes), and is tightly regulated by E3 ubiquitin ligase (E3 ligase) through recruitment and proteasomal degradation (97, 101). Whilst there is also a role played by calpains for the turnover of MYC, the majority of degradation is carried out by the ubiquitin-proteasome system (UPS) (102, 103). The ligases FBXW7 and TRUSS have essential roles in restricting MYCN functions via the UPS. FBXW7 recognises MYCN upon phosphorylation at both S62 and T58, causing MYCN to be specifically degraded during mitosis, providing a mechanism which induces cell cycle exit and differentiation of neural progenitor cells. Thus, increasing the level of FBXW7 would be especially attractive to MB with *MYCN* overexpression. More recently, in a study by Skowron et al. looking at the transcriptome of 250 human SHH MB, they discovered missense mutation within the tryptophan-aspartic acid motif (WD40) of *FBXW7* in SHH MBs (42). This supports the idea of targeting this important ligase to alter MYCN activity. Another ligase responsible for restricting MYCN function is the HECT (Homologous to the E6-AP Carboxy Terminus)-domain ubiquitin ligase, HUWE1. This degradation system acts by priming the protein through addition of Lys 48-mediated linkages. HUWE1 carries this out for both MYC and MYCN, but shows a greater efficiency for the latter (104). Interfering with this mechanism, at the MYCN protein level, remains a potential strategy of intervention.

The degradation of MYCN can be further inhibited by the activation of PI3K/AKT/mTOR axis, as active AKT can phosphorylate and inactivate GSK-3β, leading to MYCN stabilisation. Targeting PI3K may therefore be valuable to control the level of *MYCN* (105) (**Figure 2**). This has been attempted through various candidate inhibitors such as taselisib, copanlisib, pictilisib, buparlisib, dacotilisib and idelasib, only to find the emergence of resistance to be common, and usually associated with upregulation of *MYCN*. To overcome this, studies have tried to utilise a combination therapy method with compounds such as SF2523 (106). This compound was investigated in a study by Andrews et al. in which it was able to inhibit both the MYC transcriptional co-factor, BRD4 and PI3K with increased efficacy and reduced toxicity to animals (106). More recent compounds targeting this pathway, and are ongoing clinical trials include LY3023414 [NCT03155620] and AZD2014 [NCT02813135]. In addition to the PI3K/AKT/mTOR pathway, WNT and SHH also play a role in inactivating GSK-3β, leading to upregulation and stabilisation of MYCN. Both pathways hold potential targets to regulate this stabilisation.

Recently, Aurora kinase A (AURKA), a member of the Aurora family of mitotic regulators, has been shown to form a complex with MYCN, to prevent its degradation by FBXW7. AURKA stabilises MYCN via a direct interaction with a protein binding site flanking MYCN's MBI sequence (107), this stabilisation of MYCN exacerbates its oncogenic functions, and prevents differentiation of neuroblasts in MYCN-driven neuroblastoma (NB) cell lines, leading to aberrant proliferation (108). It is likely that AURKA exerts similarly deleterious effects in MYCN-driven MB, with evidence for this provided by significantly decreased tumour volumes, and a tendency towards increased survival in *Ptch1*$^{+/-}$;*p53*$^{-/-}$ mice treated with the AURKA inhibitor CD535 (109). Other inhibitors which target the AURKA complex with MYCN include MLN8054 and MLN8237. Upon destabilisation of the complex by these small molecule inhibitors, AURKA is no longer able to protect MYCN from proteasomal degradation. Using MLN8237, which blocks the interaction between AURKA and MYCN, our group was able to demonstrate that AURKA inhibition is effective against NB in a MYCN-driven transgenic mouse model (TH-MYCN), in which high-level expression of MYCN is driven in neural crest by a tyrosine hydroxylase (TH) promoter (110). Correlating with this finding, MLN8237 also significantly impaired the growth of MB allografts derived from GTML (Glt1-tTA/TRE-MYCN-Luc) tumour-derived neurosphere cell lines (111, 112). Additionally, MLN8237's *in vivo* activity was positively confirmed using a panel of human NB xenografts

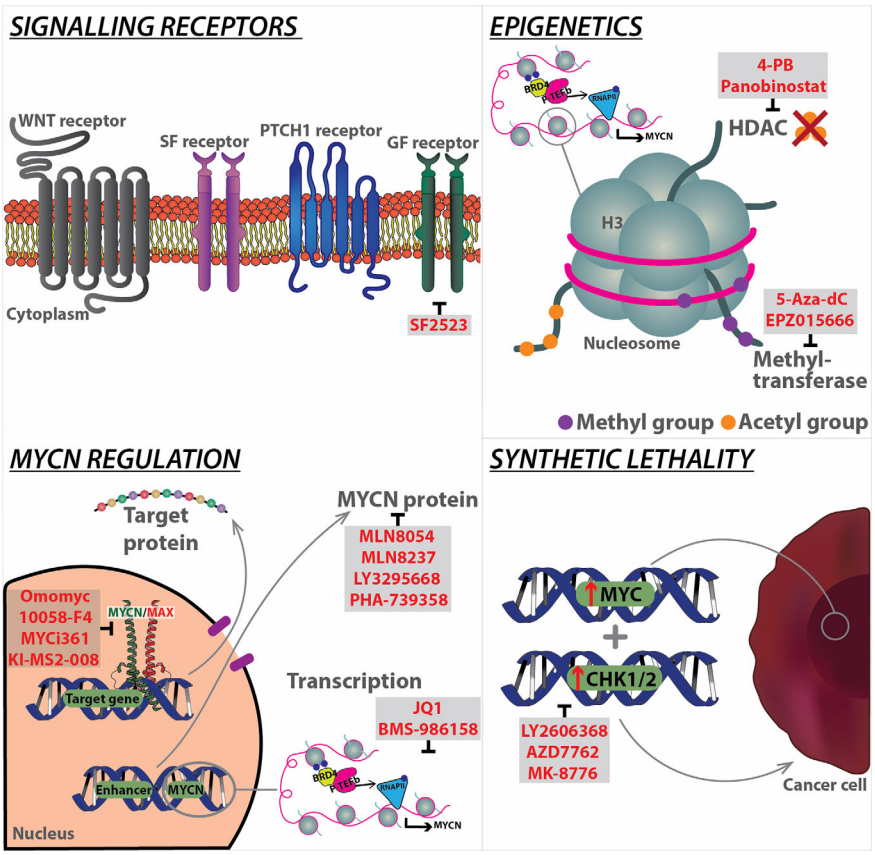

FIGURE 2 | Overview of current strategies targeting MYCN at different levels, from signalling receptors to downstream regulation, as well as epigenetics, and synthetic lethality. Specific modalities (highlighted in red) have been developed to target the mechanistic components of each pathway. BRD4, Bromodomain-containing protein 4; GF, Growth Factor; HDAC, Histone deacetylases; MAX, MYC-associated factor X; P-TEFb, Positive transcription elongation factor b; PTCH1, Patched 1; RNA pol II, RNA polymerase II; SF, Survival factor; WNT, Wingless.

(113). Another AURKA inhibitor, namely PHA-739358, suppress proliferation of human SHH MB models, including allografts of *Patched* mutant tumour cells and patient-derived xenografts (114) (**Figure 2**).

These findings have led to the investigation of AURKA inhibitors for the treatment of MYCN-dependent paediatric cancers. However, despite the encouraging results in pre-clinical studies, clinical trials with different Aurora Kinase inhibitors showed a limited efficacy against solid tumours (115). This has been attributed to mechanisms of resistance triggered by strong upregulation of ATP-binding cassette transporters, such as ABCB1, ABCG2 and ABCC2, and the emergence of AURKA mutations, impairing the efficient binding of the inhibitor in the ATP pocket of the enzyme and functional single nucleotide polymorphisms (SNP) (116, 117). In an analysis of a highly specific AURKA inhibitor LY3295668 in 560 cancer cell lines, NB was among the most sensitive tumour type tested, with *MYC/MYCN* amplification identified as among the strongest predictors of sensitivity to this agent (**Figure 2**). Phase I trial of alisertib with irinotecan and temozolomide showed promising results prompting to a phase 2 study in children with relapsed/refractory NB. While these clinical studies supported a potential role for AURKA inhibition in the management of patients with advanced NB, patients with MYCN/MYC-driven tumours still showed poor outcomes despite treatment with this regimen (118). Inhibition of another component of AURK family, AURKB, has been found to sensitize MYC overexpressed Grp3 MB cells to cell death both *in vitro* and *in vivo* (119).

Targeting MYCN Transcriptional Activity

Another therapeutic opportunity against MYCN-dependent MB is the use of drugs that effect the transcriptional activity of MYCN. For instance, MYC family gene expression depends on the activity of the co-factor bromodomain and extra-terminal (BET) family member BRD4. The bromodomain and extra-terminal (BET) family contain bromodomains (BRD), acetyl-lysine-specific protein interaction modules that play a key role in regulating gene transcription and are evolutionarily conserved and present in diverse nuclear proteins (120).

The BET family member BRD4 is of particular relevance to MYC-driven MB (**Figure 2**). *MYC* gene expression is dependent

on the activity of the BET family members (121). BRD4 preferentially binds to acetylated lysine residues K9/14 of histone H3, and deacetylated lysine residues K5/K12 of histone H4 (122, 123), following this BRD4 interacts with the positive transcription elongation factor b (P-TEFb) complex, leading to RNA polymerase II transcriptional activity (124). BRD4 is recruited to a wide range of promoter regions, including those for G1 cell cycle regulators (125, 126), and MYC (121, 127, 128), following this BRD4 co-recruits P-TEFb leading to gene transcription, which in the case of MYC is essential for MYC-dependent stimulation of its target genes (129). Taken together this highlights the potential of BET proteins, in particular BRD4, in driving cell cycle and MYC dysregulation, a corollary of which may be aberrant proliferation and tumorigenesis. By using a cell permeable BET inhibitor (BETi) called JQ1, a thieno-triazolo-1,4-diazepine, which displaces BET bromodomains from chromatin by competitively binding to the acetyl lysine recognition pocket, different research teams have demonstrated that tumours with deregulated MYC are susceptible to JQ1 inhibition both *in vitro* and *in vivo* (121, 127, 130, 131). In an unbiased screen of a collection of 673 genetically characterized tumour-derived cellular models, NB cell lines were identified as among the most JQ1 sensitive and MYCN amplification as the most predictive marker of sensitivity (132). Additional studies have demonstrated that JQ1 also suppresses MYC/MYCN expression and MYC/MYCN-associated transcriptional activity in MB, resulting in an overall decrease in MB cell viability (132–134). JQ1 treatment has been shown to be effective in MYC- and MYCN-driven MB by targeting cancer dependency genes driven by super-enhancers. More recently, the pan-BETi clinical compound Molibresib (GSK525762) shows positive outcome in Phase I and awaits further clinical trial result (135) (**Figure 2**).

Cyclin-dependent kinases, especially CDK1 and CDK2, are key players in stabilizing phosphorylation of MYC proteins at S62 upon activation (69, 136, 137). Mechanistically, the response to BET inhibitors in MB is regulated by the suppression of genes involved in neuronal differentiation and progression through the cell cycle. In particular, the upregulation of the cell-cycle regulator CCND2 is a key mediator of sensitivity or resistance to BET inhibitors. Indeed, cells that tolerate BET inhibition do not terminally differentiate, maintain high expression of CCND2, that allows them to cycle through the S-phase. More recently it has been shown that JQ1 combined with Milciclib, an inhibitor of the MYC-stabilising enzyme CDK2, results in synergistic anti-tumoral effects. Mice xenograft of the human MB MB002 cell line showed prolonged survival when treated with JQ1 and Milciclib compared to vehicle and individual JQ1 or Milciclib treatment (138). This provides a strategy by which MYC, an 'undruggable' protein, may be indirectly targeted for therapeutic gain. Several small molecule BET inhibitors, structurally related to JQ1, are in clinical development and have shown preliminary clinical activity in solid tumours and blood cancers (139, 140). A phase I clinical trial with the BET inhibitor, BMS-986158, is currently ongoing in patients with paediatric cancers [NCT03936465].

Cyclin dependent kinases such as CDK7 and CDK9 play a key role in regulating transcriptional activity of MYCN (141–143). We have identified strong enrichment for CDK9 at both the MYCN promoter and the distal super enhancer and shown that pharmacologic blockade of CDK9 using Fadraciclib targeted MYCN-dependent transcriptional landscape (143). Several small molecule inhibitors targeting CDK7 and CDK9 (such as fadraciclib, dinaciclib and BAY1143572) have been shown to inhibit MYCN transcription and selectively kill MYCN amplified or expressing neuroblastoma, medulloblastoma and other cancer cells and are currently in early phase clinical trial.

Targeting MYCN-Associated Epigenetic Molecules

MYC family genes also regulate transcription via epigenetic modifications, suggesting that epigenetic drugs could be used in the clinic to successfully treat MYC/MYCN-amplified tumours. Epigenetic alterations and aberrant expression of genes controlling epigenetic mechanisms have been identified in several cancers, including NB and MB. In this regard, numerous *in vitro* and *in vivo* evidence indicate that histone deacetylase inhibitors (HDACi) suppress MYCN expression and are promising candidates for novel treatment strategies of paediatric cancers (144–146). Selective inhibition of HDAC8 by small-molecule inhibitors kills tumour growth in xenograft mouse models of MYCN-amplified NB (147). The combination of the HDAC inhibitor, 4-phenylbutyrate (4-PB) and the demethylation agent, 5-Aza-2'deoxycytidine (5-Aza-dC) reduces DNA methyltransferase activity, global methylation and induces apoptosis in MB cell lines (148). Ecker and colleagues found HDAC2 to be overexpressed in MB subgroups with poor prognosis (SHH, Grp3 and Grp4) harbouring a MYC amplification compared to normal brain and the WNT subgroup. Indeed, increased sensitivity to HDACi is specifically observed in MYC amplified cells (149). HDACi further enhances the anticancer efficacy of other therapeutic regimens, such as ionizing radiation (IR) and can synergize with PI3K or MAPK/ERK inhibitors to impair tumour growth in vivo (150–152). Mechanistically, HDACi have been associated with different biological activities in MB, including the dissipation of mitochondrial membrane potential, changes in cell stemness, increased expression of the FOXO1 tumour suppressor gene, enhancing mitochondrial apoptosis in a p53-dependent manner and inhibition of the Hedgehog signalling (150, 152–154). Taken together, these data provide strong support for clinical testing of HDACi in the treatment of paediatric brain cancer patients, particularly those with MB. Further studies supporting this include a phase I trial and pharmacokinetic study of SAHA in children with solid tumours found to be well-tolerated (155), and a phase-I consortium clinical study recommending vorinostat in combination with the proteasome inhibitor bortezomib for future phase 2 studies in children with recurrent or refractory solid tumours (156).

HDACs represent an important epigenetic mechanism by which MYCN exerts its transcriptional effects. Treatment of murine and human PDX medulloblastoma cell lines with the pan-HDAC inhibitor Panobinostat lead to significant decreases in cell viability, with the lowest IC50 (14.4nM) seen in Grp3

MYC-driven PDX cells, and a marginally higher IC50 (25.27nM) in Grp4 MYCN-driven PDX (152). Exploration of the mechanism of HDAC inhibition using mouse MYC-driven medulloblastoma cell lines and Grp3 MYC-driven PDX cells revealed that HDAC inhibition significantly alters gene expression in treated MB cells. Having particularly notable effects on BRD4 target genes, MYC target genes, and stem cell proliferation genes, which were all downregulated following Panobinostat treatment. Further analysis of differential gene expression changes in these cells identified increased FOXO1 expression, and its subsequent interactions, as a key driver of the efficacy of HDAC inhibitors in MYC-driven medulloblastoma cells. This increase in FOXO1 expression may also be synergistically increased via combination therapy of Panobinostat with the PI3K inhibitor buparlisib (BKM-120) (152). Whilst the potential efficacy of HDAC inhibitors such as Panobinostat has been relatively neglected in MYCN-driven Grp4 and SHH MB, data from studies of MYCN-driven NB may provide evidence for HDAC inhibitors having similar effects on MYCN activity to those seen in MYC-driven cell lines. In one study of particular note, Panobinostat and the BRD4 inhibitor JQ1 acted synergistically to increase apoptosis and inhibit growth in human Kelly and SK-N-BE (2) MYCN-driven NB cells, whilst also synergistically reducing MYCN protein levels, but not mRNA levels (157). Together these studies in Grp3 MB and NB suggest that inhibition of HDACs may also be efficacious in MYCN-driven medulloblastoma. Future studies utilising Grp4 MB PDX cells will be required to confirm this hypothesis (**Figure 2**).

MYC-driven primary medulloblastoma tumours have high expression of the arginine methyltransferase PRMT5 compared to non-MYC medulloblastoma tumours and adjacent normal tissues (158). PRMT5 is the major symmetric arginine methylase of histone tails and this histone modification is associated to both transcription activation and repression (159). PRMT5-mediated arginine methylation modulates a variety of cellular processes including cell growth, metastasis, ribosome biogenesis, cellular differentiation, gene transcription, germ cell specification, alternative splicing, and Golgi apparatus formation. Interestingly, the PRMT5 inhibitor EPZ015666 significantly suppressed cell growth and induced apoptosis in MYC-driven medulloblastoma cells (159) (**Figure 2**). A variety of PRMT5 enzymatic inhibitors are currently applied in clinical trials of myelodysplastic syndrome, acute myeloid leukaemia, breast cancer and B cell non-Hodgkin lymphoma, prompting for further investigation in medulloblastoma [NCT03614728, NCT03573310, NCT02783300] (160).

Targeting MYC-MAX Complexes

The bHLH-LZ structure of MYCN allows it to dimerise with various proteins, this is particularly relevant for its obligate partner MAX, with this interaction forming a stable four-helix bundle. MYCN/MAX heterodimers are required for non-consensus binding, as well as binding to the E-box sequences (161). Once bound to promoters of target genes, the complex can recruit transcriptional coactivators, elongation factors, and histone modifying enzymes to initiate gene transcription. Antagonists of this heterodimer complex represent strong candidates for MYCN-specific inhibitors. MAX forms homodimers, and heterodimers with other partners such as MNT and the MAD family members MAD1-4; these compete with MYCN for MAX. Complexes with MAD predominantly occur in resting or differentiated cells, whilst MYCN/MAX complexes are common in proliferating cells (162, 163). A potent inhibitor of the complex is Omomyc. This is a dominant-negative Myc peptide which facilitates the binding with the MYC protein through four specifically designed amino acid substitutions, thus disrupting the binding between MYC/MAX. This molecule has shown to promote apoptosis is many cancers retaining high MYC activity (133, 164), in particular with a preference for MB tumours (165). Other notable small-molecule MYCN/MAX inhibitors include 10058-F4, MYCi361, MYCi975 and KI-MS2-008 (17, 166, 167) (**Figure 2**).

Synthetic Lethal Targets of MYCN

A revolutionary method of indirectly targeting MYCN is to use the approach of synthetic lethal interactions. This term is defined as the extreme form of negative genetic interaction wherein the combination of two genes leads to cell death, whilst the two genes alone have no effect on viability of the cell. Synthetic lethal screens for MYCN amplification/overexpression have been more extensively investigated in NB, and more recently in MB due to identification of specific cell cycle checkpoint kinases (Chk1/2). In particular for Grp3 MB, Endersby et al. showed increased sensitivity of MYC amplified Grp3 MB cells to these check inhibitors (Chki) Prexasertib (LY2606368, (Chk1/2i), AZD7762 (Chk1/2i), and MK-8776 (Chk1i), with LY2606368 showing superior activity over the other compounds (**Figure 2**). Ongoing basket trial for this compound is further investigating its anti-tumour activity [NCT02873975]. Furthermore, when used in combination with typical cancer drugs, LY2606368/gemcitabine combination showed specific activity for Grp3 MB subgroup alone. Whilst SHH MB showed reduced sensitivity to the LY2606368 compound alone, better outcome was seen when used in combination as LY2606368/cyclophosphamide (168). Current ongoing trial for these combinations include SHH and Grp3/4 patients [NCT04023669].

FUTURE AREAS OF RESEARCH FOR INNOVATIVE THERAPIES

MYCN-Driven Cancer Metabolism

Being a high-grade tumour, MB must balance energy metabolism with the need to synthesize the macromolecules essential for its rapid proliferation. This contrasts with lower grade tumours that do not require constant accumulation of biomass and can therefore prioritize ATP production. Likewise, the neural progenitors from which it derives, MB cellular metabolism is characterized by increased lipogenesis and aerobic glycolysis. Indeed, both normal and malignant neuronal cells face similar challenges: they need the largest amount of ATP to support electrical activity and intercellular communication, but this

requirement must be in balance with the additional metabolic requirements of rapid proliferation (169).

During the early stage of development, the rapid expansion of cerebellar GCPs (CGCP), fuelled by SHH signalling, compete for intermediates for the synthesis of lipids, nucleic acids and proteins with the downstream generation of ATP. SHH induces lipogenesis in CGCPs through a mechanism dependent on E2F1 transcriptional activity, involving the up-regulation of fatty acid synthase (FASN) and acetyl-CoA carboxylase 1 (ACC1). In parallel, it down-regulates fatty acid catabolism enzymes, including acyl-CoA oxidase 1 (ACOX1) and medium chain acyl-CoA dehydrogenase (MCAD) (170–172). SHH signalling also induces aerobic glycolysis in CGCPs and tumour cells to support biosynthesis (173). Hexokinase-2 (Hk2) is a key metabolic regulator induced by SHH, its importance is highlighted upon deletion, which leads to impairment in CGCP development and reduced tumorigenesis in the MB-prone SmoM2 mouse model (174). The nutrient sensor peroxisome proliferator-activated receptor γ (PPARγ) is also involved in SHH-mediated regulation of glycolysis; pharmacological blockade of PPARγ inhibits CGCP proliferation and extends animal survival in the NeuroD2-SmoA1 mouse model of MB by inducing cell death (170).

The activation of *MYC* family is a key point of convergence of the metabolic features of many different cancer types. Similar to its family members, MYCN is a potent regulator of cellular metabolism, through controlled expression of amino acid transporters and other proteins involved in aerobic glycolysis, oxidative phosphorylation, detoxification of reactive oxygen species (ROS), and fatty acid oxidation (175). While numerous studies have demonstrated a key role of MYCN in NB and GBM metabolism (176–180), its metabolic function in medulloblastoma still remains elusive. It is likely that in these tumours, as in other cancers, MYCN reconfigures metabolism to favour aerobic glycolysis and a dependency on the serine-glycine-one-carbon (SGOC) to generate metabolic products starting from serine and glycine amino acids (181).

Selective targeting of tumour glucose metabolism has long been considered as an attractive therapeutic strategy. MYC invariably promotes expression of critical enzymes involved in aerobic glycolysis, such as HK2 and LDHA, making cancer cells more vulnerable to glycolysis inhibition. 2-Deoxyglucose, an analogue of glucose that binds and inhibits HK2, has yielded promising antitumour activity *in vitro* and *in vivo*. Aerobic glycolysis produces excessive lactate that is toxic to tumour cells. MYC modulates lactate export by inducing MCT1/MCT2 expression to shift toxic levels of lactate within tumour cells. Therefore, a potential, effective strategy is to block MYC-driven lactate export by MCT1/MCT2 inhibitors. Of note, clinical trials of the MCT1 inhibitor AZD3965 in diffuse large B cell lymphoma and Burkitt's lymphoma, two typical MYC-driven cancer types, are currently ongoing [NCT01791595] (**Figure 3**).

Inhibitors of glutaminase or transaminase have shown the therapeutic efficacy in multiple MYC-driven tumour models, and a representative glutaminase inhibitor, CB-839, is currently under clinical trials for patient treatment. MYC and SLC7A5 constitute a feedback loop to amplify MYC transcriptional program, and sustain essential amino acid (EAA) metabolism in tumour cells (182). In principle, therapeutic targeting of SLC7A5 would offer an opportunity to unleash the functional association between MYC and SLC7A5, leading to tumour suppression. JPH203 (also known as KYT-0353), a specific SLC7A5 inhibitor (183) can be evaluated as a MYC-selective cancer therapeutics in the future clinical trials (**Figure 3**). MYC is a key player in regulation of lipid metabolic reprogramming. ACC, FASN, and 3-Hydroxy-3-Methylglutaryl-CoA reductase (HMGCR), three key enzymes for lipid metabolism, are significantly activated by MYC. ND-646, an allosteric inhibitor of ACC that prevents ACC dimerization and subsequently suppresses fatty acid synthesis, has shown efficacy in mouse models of lung cancer (184). TVB-2640 is a highly potent, selective, and reversible first-in-class inhibitor of FASN. Its monotherapy and in combination with paclitaxel have entered the clinical trial stage [NCT03179904]. Lovastatin, simvastatin, and atorvastatin are specific HMGCR inhibitors that have been FDA approved to lower cholesterol (185). Targeting these enzymes may be a therapeutic alternative for MYC-driven cancers (**Figure 3**). However, caution should also be taken because it remains unclear as to which aspects of cell metabolism could represent a realistic, targetable vulnerability of tumour cells in comparison with normal counterparts. It should be noted that cancer cells acquire metabolic adaptations in response to a variety of cell-extrinsic and cell-intrinsic cues, thus, MYC effects on cellular metabolism depend both on the tissue of tumour origin and on interaction with tumour microenvironment. A better understanding of these metabolic diversities will improve our ability to define their contribution to aggressive tumour progression.

Immunotherapy in Medulloblastoma

The last decade has seen a tremendous progress in our understanding of how cancer cell evade the immune system and how to harness these mechanisms to develop new therapies. Cancer immunotherapy has proven successful in the so-called "hot" tumours, such as lung cancer and melanoma, characterized by high infiltrating immune cells, while "cold" tumour with low infiltrates still represents a therapeutic challenge for immunotherapy.

The MB microenvironment inhabits reduced numbers of infiltrating immune cells and have been generally considered as immunologically "cold". This is largely backed by a limited amount of information existing on the immune microenvironment. Whilst this is the current understanding, the paracrine signalling between the tumour microenvironment suggests the existence of a more intricate interaction (186). More recently, an increasing number of studies have shed light on the immune profiling of MB, in an attempt to use these data as diagnostic and prognostic tools. Grabovska and colleagues have mapped the tumour immune microenvironment of >6000 primarily paediatric tumour of the CNS, by using methylCIBERSORT, an algorithm derived from CIBERSORT and based on genome-wide DNA methylation data (187, 188).

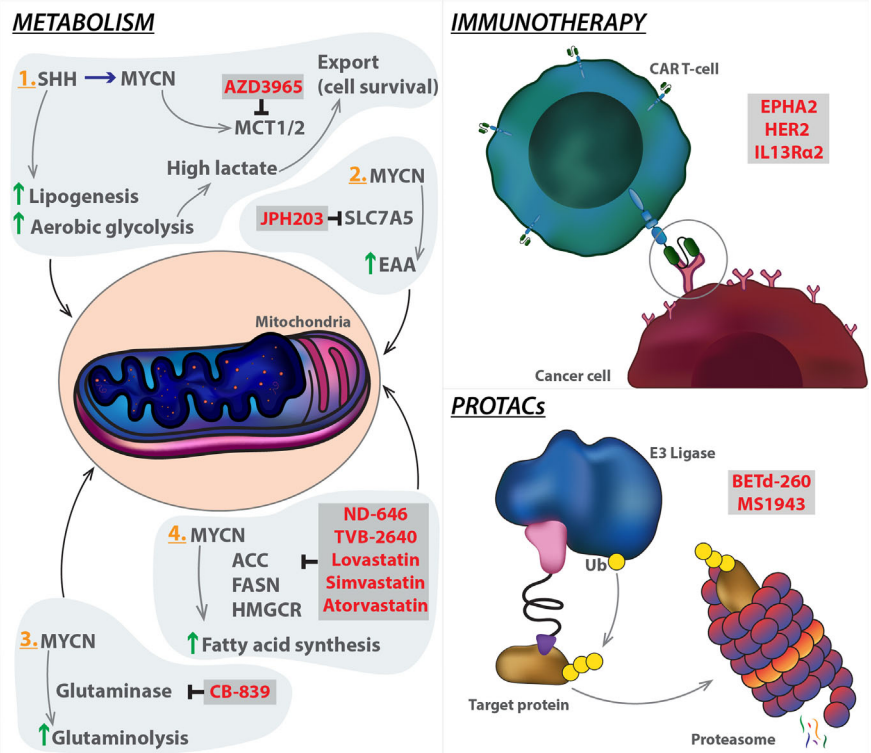

FIGURE 3 | Emerging strategies targeting MYCN. Innate systems regulating metabolism and immune response can be manipulated in cancer models to hijack the tumorigenic mechanism. PROTAC technology can be used to target MYCN (the target protein) by enhancing protein degradation through coupling with E3 ligase, which ubiquitinates the protein leading to degradation via the proteasome. Specific modalities (highlighted in red) have been developed to target the mechanistic components of each pathway. SHH, Sonic hedgehog; MCT1/2, Monocarboxylate transporter 1; SLC7A5, Solute carrier family 7 member 5; EAA, Essential amino acid; CAR T-cell, Chimeric antigen receptor T cells; ACC, Acetyl-CoA carboxylase; FASN, Fatty acid synthase; HMGCR, 3-hydroxy-3-methylglutaryl-CoA reductase; PROTACs, proteolysis targeting chimeras.

By combining methyCIBERSORT data with pre-existing clinico-pathological and parallel multi-omics, the study exhibited varying proportions of infiltrates within the four classic subgroups of MB. CD8+ T cells (27% of all non-cancer cells), B cells (16%), and eosinophils (15%) (187) were the most abundantly estimated non-cancer cell infiltrates within all MB tumours. The distribution of cell types within the subgroups showed Grp3 MB holding the highest proportion of CD8+ T cells, Grp4 MB homing the natural killer (NK) cells, and SHH MB, the B cells. MYC amplification in Grp3 MB is associated with a significantly higher frequency of tumour infiltrating lymphocytes, CD8+ T cells, and B cells and a lower infiltration of regulatory T cells (Treg). Interestingly, this immune infiltrate analysis further supports the recent refinement of the Grp3/Grp4 MB subgroups into eight subtypes I–VIII (83).

In all cases, the methyCIBERSORT estimates of TILs aligns with the "Cytolytic score", derived from the expression of granzyme A (GZMA) and perforin 1 (PRF1), secreted by effector cytotoxic T cells and NK cells. In another gene expression study, a smaller cohort of SHH MB tumours show high content of fibroblasts, T cells and macrophages, whilst Grp4 MB expresses markers of cytotoxic lymphocytes. SHH MB subgroup has increased expression of inflammation-related genes (CD14, PTX3, CD4, CD163, CSF1R, and TGFB2) and significantly higher infiltration of tumour-associated fibroblasts than Grp3 MB and Grp4 MB (189). In another cohort, cytotoxic T-cells, with variable activation status, showed no correlation with overall survival of the patients (190). While these studies prove that immune profiles are specific to the different molecular subgroups of MB, their applicability in the clinical settings is still unclear. Moreover, data on the immune checkpoint proteins, PD-1 and PD-L1 are limited and controversial, due both to technical challenges to detect these markers or discrepancy between *in vitro* and *in vivo* results (191–193).

Another reason why MB are considered "cold" is the relatively low expression of cancer-specific antigens on their cell surface. Orlando and colleagues have recently reported expression of the tumour-associated antigen PRAME in 82% of MB tumour tissues. However, its levels only showed correlation with the worst overall survival groups. Moreover, MB cells targeted using genetically modified T cells carrying a PRAME-specific TCR controlled tumour growth in an orthotopic mouse model of MB (194). Intrathecal delivery of T cells engineered to express EPHA2, HER2 and interleukin 13 receptor α2 (IL13Rα2)

chimeric antigen receptors showed efficacy in the treatment for primary, metastatic, and recurrent Grp3-MB xenografts in mouse models. Administration of these chimeric antigen receptor T (CAR-T) cells into the CSF, alone or in combination with the epigenetic modifier azacytidine, was highly effective against different metastatic mouse models of Grp3 MB, thereby providing a rationale for CAR-T approaches in the clinic (195) **(Figure 3)**.

While computational analyses are advancing our general knowledge of MB-tumour microenvironment (TME), the direct link between MYCN expression and TME profiling is still under investigation. What has emerged in neuroblastoma and other malignancies (small cell lung cancer, rhabdomyosarcoma, Wilms' tumour, retinoblastoma, acute myeloid leukaemia, and T-acute lymphoid leukaemia) is that MYCN has a great role in dysregulating the immune network. In neuroblastoma patients for instance, gene set enrichment analysis has shown that *MYCN* levels negatively correlate with genes involved in different immune system pathways, especially those associated to interferon gamma and phagocytosis (196). Overall, MYCN suppresses the immune landscape, through dysregulation of immune checkpoints, CD4+ helper T (Th) cytokines, major histocompatibility complex (MHC) genes, and Toll-like receptors (TLRs) (197). Apart from tumour cases with MYCN gene amplification, the immune system dysregulation can occur as a consequence of other events leading to increased MYCN activity (mRNA and protein stabilization, mi-RNA alteration). Based on these considerations, it is imperative to have a better understanding of the mechanistic components linking MYCN to MB-TME functions. The blockage of MYCN or specific MYCN dependencies could ameliorate the immune suppression by restoring the responsiveness of the immune system, opening the way to combinatorial treatments with immunotherapies. In this context, the link between MYCN and polycomb repressive complex 2 (PRC2) may offer a promising therapeutic opportunity via a mechanism that alters TME immunogenicity (198, 199).

Use of PROTACs

Proteolysis targeting chimeras (PROTAC) and hydrophobic tagging are successful technologies/strategies for selective degradation of the target protein (200, 201). Although PROTAC technology has been rapidly gaining momentum in the drug discovery field, the hydrophobic tagging approach has received considerably less attention from the biomedical community. This approach utilizes a bulky and hydrophobic group attaching to a small-molecule binder of the target protein. The binding of this bivalent compound to the target protein leads to misfolding of the target protein and its subsequent degradation by the proteasome (202). Targeting oncogenic proteins for degradation using PROTACs recently gained an increased momentum in the field of cancer research. Compared with BET inhibitors HJB-97 and JQ1, the activity of the PROTAC BET degrader BETd-260 increased over 1000 times (203). The degrader complex showed stability through cooperative binding between AURKA and CEREBLON (204). The enhancer of zeste homolog 2 (EZH2) is the main enzymatic subunit of the polycomb repressive complex 2, which catalyses tri-methylation of lysine 27 on histone H3 (H3K27me3) to promote transcriptional silencing. PRC2 complex has important roles in tissue development, primarily to maintain cell identity (205). EZH2 is overexpressed in multiple types of cancer including triple-negative breast cancer (TNBC), and high expression levels correlate with poor prognosis. In MB, studies have shown increased expression of EZH2 in all subgroups, with particularly high levels in G3 and G4 (206, 207). The link between this enzyme and MYC or MYCN remains largely unexplored. Whilst studies have shown correlation between levels of the enzyme and MYC activity (208), the causation behind this is yet to be mapped. Nonetheless, Chen et al. showed in MYCN amplified neuroblastoma, a strong dependency between tumour cells and the PRC2 complex. MYCN was shown to directly activate EZH2 by binding to its promoter, leading to inhibition of neuronal differentiation networks in *MYCN*-amplified (209). This approach should also be applied to MB to elucidate the underlying mechanism. Several EZH2 inhibitors, which inhibit the methyltransferase activity of EZH2, have shown promising results in treating sarcoma and follicular lymphoma in clinics. However, EZH2 inhibitors are ineffective at blocking proliferation of TNBC cells, even though they effectively reduce the H3K27me3 mark. Using a hydrophobic tagging approach, generation of MS1943, a first-in-class EZH2 selective degrader that effectively reduces EZH2 levels in cells (210) **(Figure 3)**.

CONCLUSION AND FUTURE OUTLOOK

In this review, we have highlighted the relationship between *MYCN* and the paediatric brain tumour medulloblastoma, with an emphasis on the emerging therapeutic avenues to target this. The ever-increasing advancements in sequencing technologies, coupled with global efforts to improve the disease models through strong collaborations, and the use of more humanised systems, is rapidly dissecting the precise role of MYCN in all MB subgroups. Model systems such as patient-derived iPSCs (51, 211, 212), and human hindbrain-derived neuroepithelial stem cells (213) align with the developmental trajectory of the CNS, therefore are likely to reflect a more authentic evolution of the tumour through targeting of relevant oncogenes such as MYCN. Novel MB targeting strategies using PROTACs, and CAR T-cell therapy offer a selective advantage over the more generic inhibitors. Additional focus on the metabolic dependencies of MB tumours can shed light on the most vulnerable target for tumour growth. Whilst the supporting evidence indicate a practical use for these technologies in MB, these mechanisms remain largely unexplored. Recently, liquid biopsies using CSF to assess circulating tumour DNA have been used to genetically characterise MB (214). This is an important development in the management of MB, one particularly relevant to the potential MYCN-focussed therapeutic approaches discussed here, as liquid biopsies detect the majority of MYCN-effecting

mutations such as *MYCN* and *Gli2* amplification, and *SUFU* loss (214). As CSF may be obtained during hydrocephalus surgery, a common procedure for MB patients, this will open the possibility to personalised medicine approaches for the treatment of this devastating disease. Furthermore, MB is a brain tumour protected from the systematic delivery of cancer drugs by the blood brain barrier (BBB). This defence system is a unique problem which prevents majority of the current therapies from succeeding. Utilising lipid-soluble cargoes such as nanoparticles which disintegrate at the target site (215, 216), or focused ultrasound techniques e.g., pulsed ultrasound (217), can greatly improve the delivery of targeted drugs.

It is certainly evident that MYCN is a phenomenally complex molecule. As illustrated in this review, the multiple downstream signalling pathways directly or indirectly regulated by Myc highlights that targeting this oncogene is a compelling, yet challenging strategy for MB. Our ultimate goal is to increase the proportion of surviving patients, more specifically by reverting the adverse effects of disseminated disease and treatment sequelae. Thus, our expanding knowledge of the mechanisms in this cancer offers the promise to formulate more targeted therapies and translate this to the clinic in the best form.

AUTHOR CONTRIBUTIONS

SS and CG wrote the review with advice and contribution from AM and LC. SS made the figures with input from AM and CG. All authors contributed to the article and approved the submitted version.

FUNDING

This review article was financially supported by The Institute of Cancer Research PhD studentship (SS), Higher Education Funding Council of England (LC) and The Institute of Cancer Research funding scheme (CG).

ACKNOWLEDGMENTS

We would like to thank Evon Poon and Colin Kwok for their invaluable advice and support. Many apologies to our colleagues who were unable to be cited due to space constraints. The insightful discussions within the team were instrumental in the planning of this review.

REFERENCES

1. Dang CV. MYC on the Path to Cancer. *Cell Cell Press;* (2012) 149p:22–35. doi: 10.1016/j.cell.2012.03.003
2. Westermann F, Muth D, Benner A, Bauer T, Henrich KO, Oberthuer A, et al. Distinct Transcriptional MYCN/C-MYC Activities Are Associated With Spontaneous Regression or Malignant Progression in Neuroblastomas. *Genome Biol* (2008) 9(10):R150. doi: 10.1186/gb-2008-9-10-r150
3. Beltran H. The N-myc Oncogene: Maximizing its Targets, Regulation, and Therapeutic Potential. *Mol Cancer Res* (2014) 12(6):815–22. doi: 10.1158/1541-7786.MCR-13-0536
4. Kohl NE, Legouy E, Depinho RA, Nisen PD, Smith RK, Gee CE, et al. Human N-myc is Closely Related in Organization and Nucleotide Sequence to C-Myc. *Nature* (1986) 319(6048):73–7. doi: 10.1038/319073a0
5. Malynn BA, De Alboran IM, O'Hagan RC, Bronson R, Davidson L , DePinho RA, et al. N-Myc can Functionally Replace C-Myc in Murine Development, Cellular Growth, and Differentiation. *Genes Dev [Internet]* (2000) 14(11):1390–9. doi: 10.1101/gad.14.11.1390
6. Davis AC, Wims M, Spotts GD, Hann SR, Bradley A. A Null C-Myc Mutation Causes Lethality Before 10.5 Days of Gestation in Homozygotes and Reduced Fertility in Heterozygous Female Mice. *Genes Dev [Internet]* (1993) 7(4):671–82. doi: 10.1101/gad.7.4.671
7. Charron J, Malynn B, Fisher P, Stewart V, Jeannotte L, Goff S, et al. Embryonic Lethality in Mice Homozygous for a Targeted Disruption of the N-myc Gene. *Genes Dev* (1992) 6(12A):2248–57. doi: 10.1101/GAD.6.12A.2248
8. Stanton BR, Perkins AS, Tessarollo L, Sassoon DA, Parada LF. Loss of N-myc Function Results in Embryonic Lethality and Failure of the Epithelial Component of the Embryo to Develop. *Genes Dev [Internet]* (1992) 6 (12):2235–47. doi: 10.1101/gad.6.12a.2235
9. Sawai S, Shimono A, Wakamatsu Y, Palmes C, Hanaoka K, Kondoh H. Defects of Embryonic Organogenesis Resulting From Targeted Disruption of the N-myc Gene in the Mouse. *Development* (1993) 117(4):1445–55. doi: 10.1242/dev.117.4.1445
10. Meyer N, Penn LZ. Reflecting on 25 Years With MYC [Internet. *Nat Rev Cancer* (2008) 8:976–90. doi: 10.1038/nrc2231
11. Zimmerman KA, Yancopoulos GD, Collum RG, Smith RK, Kohl NE, Denis KA, et al. Differential Expression of Myc Family Genes During Murine Development. *Nature* (1986) 319(6056):780–3. doi: 10.1038/319780a0
12. Hatton BA, Knoepfler PS, Kenney AM, Rowitch DH, Moreno De Alborán I, Olson JM, et al. N-Myc is an Essential Downstream Effector of Shh Signaling During Both Normal and Neoplastic Cerebellar Growth. *Cancer Res [Internet]* (2006) 66(17):8655–61. doi: 10.1158/0008-5472.CAN-06-1621
13. Roussel MF, Robinson GW. Role of MYC in Medulloblastoma. *Cold Spring Harb Perspect Med* (2013) 3(11):a014308. doi: 10.1101/cshperspect.a014308
14. Huang M, Weiss WA. Neuroblastoma and MYCN. *Cold Spring Harb Perspect Med* (2013) 3(10):a014415. doi: 10.1101/cshperspect.a014415
15. Northcott PA, Shih DJH, Peacock J, Garzia L, Sorana Morrissy A, Zichner T, et al. Subgroup-Specific Structural Variation Across 1,000 Medulloblastoma Genomes. *Nature* (2012) 487(7409):49–56. doi: 10.1038/nature11327
16. Pfister S, Remke M, Benner A, Mendrzyk F, Toedt G, Felsberg J, et al. Outcome Prediction in Pediatric Medulloblastoma Based on DNA Copy-Number Aberrations of Chromosomes 6q and 17q and the MYC and MYCN Loci. *J Clin Oncol [Internet]* (2009) 27(10):1627–36. doi: 10.1200/JCO.2008.17.9432
17. Han H, Jain AD, Truica MI, Izquierdo-Ferrer J, Anker JF, Lysy B, et al. Small-Molecule MYC Inhibitors Suppress Tumor Growth and Enhance Immunotherapy. *Cancer Cell [Internet]* (2019) 36(5):483–97.e15. doi: 10.1016/j.ccell.2019.10.001
18. Louis DN, Perry A, Reifenberger G, von Deimling A, Figarella-Branger D, Cavenee WK, et al. The 2016 World Health Organization Classification of Tumors of the Central Nervous System: A Summary. *Acta Neuropathol* (2016) 131(6):803–20. doi: 10.1007/s00401-016-1545-1
19. Louis DN, Ohgaki H, Wiestler OD, Cavenee WK, Burger PC, Jouvet A, et al. The 2007 WHO Classification of Tumours of the Central Nervous System. *Acta Neuropathol* (2007) 114(2):97–109. doi: 10.1007/s00401-007-0243-4
20. Tsui K, Gajjar A, Li C, Srivastava D, Broniscer A, Wetmore C, et al. Subsequent Neoplasms in Survivors of Childhood Central Nervous System Tumors: Risk After Modern Multimodal Therapy. *Neuro Oncol [Internet]* (2015) 17(3):448–56. doi: 10.1093/neuonc/nou279
21. Sonabend AM, Ogden AT, Maier LM, Anderson DE, Canoll P, Bruce JN, et al. Medulloblasoma: Challenges for Effective Immunotherapy. *J Neuro-Oncol J Neurooncol* (2012) 108:1–10. doi: 10.1007/s11060-011-0776-1
22. Polkinghorn WR, Tarbell NJ. Medulloblastoma: Tumorigenesis, Current Clinical Paradigm, and Efforts to Improve Risk Stratification. *Nat Clin Pract Oncol* (2007) 4:295–304. doi: 10.1038/ncponc0794
23. Taylor MD, Northcott PA, Korshunov A, Remke M, Cho YJ, Clifford SC, et al. Molecular Subgroups of Medulloblastoma: The Current Consensus. *Acta Neuropathol* (2012) 123(4):465–72. doi: 10.1007/s00401-011-0922-z

24. Thompson MC, Fuller C, Hogg TL, Dalton J, Finkelstein D, Lau CC, et al. Genomics Identifies Medulloblastoma Subgroups That are Enriched for Specific Genetic Alterations. *J Clin Oncol [Internet]* (2006) 24(12):1924–31. doi: 10.1200/JCO.2005.04.4974
25. Kool M, Koster J, Bunt J, Hasselt NE, Lakeman A, Van Sluis P, et al. Integrated Genomics Identifies Five Medulloblastoma Subtypes With Distinct Genetic Profiles, Pathway Signatures and Clinicopathological Features. *PloS One [Internet]* (2008). doi: 10.1371/journal.pone.0003088
26. Cho YJ, Tsherniak A, Tamayo P, Santagata S, Ligon A, Greulich H, et al. Integrative Genomic Analysis of Medulloblastoma Identifies a Molecular Subgroup That Drives Poor Clinical Outcome. *J Clin Oncol [Internet]* (2011) 29(11):1424–30. doi: 10.1200/JCO.2010.28.5148
27. Northcott PA, Korshunov A, Witt H, Hielscher T, Eberhart CG, Mack S, et al. Medulloblastoma Comprises Four Distinct Molecular Variants. *J Clin Oncol* (2011) 29(11):1408–14. doi: 10.1200/JCO.2009.27.4324
28. Pugh TJ, Weeraratne SD, Archer TC, Pomeranz Krummel DA, Auclair D, Bochicchio J, et al. Medulloblastoma Exome Sequencing Uncovers Subtype-Specific Somatic Mutations. *Nature. Nat Publishing Group* (2012) 488p:106–10. doi: 10.1038/nature11329
29. Rausch T, Jones DTW, Zapatka M, Stütz AM, Zichner T, Weischenfeldt J, et al. Genome Sequencing of Pediatric Medulloblastoma Links Catastrophic DNA Rearrangements With Tp53 Mutations. *Cell* (2012) 148(1–2):59–71. doi: 10.1016/j.cell.2011.12.013
30. Lin CY, Erkek S, Tong Y, Yin L, Federation AJ, Zapatka M, et al. Active Medulloblastoma Enhancers Reveal Subgroup-Specific Cellular Origins. *Nat [Internet]* (2016) 530(7588):57–62. doi: 10.1038/nature16546
31. Northcott PA, Jones DTW, Kool M, Robinson GW, Gilbertson RJ, Cho YJ, et al. Medulloblastomics: The End of the Beginning [Internet. *Nat Rev Cancer. NIH Public Access* (2012) 12:818–34. doi: 10.1038/nrc3410
32. Cavalli FMG, Remke M, Rampasek L, Peacock J, Shih DJH, Luu B, et al. Intertumoral Heterogeneity Within Medulloblastoma Subgroups. *Cancer Cell [Internet]* (2017) 31(6):737–54.e6. doi: 10.1016/j.ccell.2017.05.005
33. Northcott PA, Buchhalter I, Morrissy AS, Hovestadt V, Weischenfeldt J, Ehrenberger T, et al. The Whole-Genome Landscape of Medulloblastoma Subtypes. *Nature* (2017) 547(7663):311–7. doi: 10.1038/nature22973
34. Schwalbe EC, Lindsey JC, Nakjang S, Crosier S, Smith AJ, Hicks D, et al. Novel Molecular Subgroups for Clinical Classification and Outcome Prediction in Childhood Medulloblastoma: A Cohort Study. *Lancet Oncol* (2017) 18(7):958–71. doi: 10.1016/S1470-2045(17)30243-7
35. Ellison DW, Onilude OE, Lindsey JC, Lusher ME, Weston CL, Taylor RE, et al. β-Catenin Status Predicts a Favorable Outcome in Childhood Medulloblastoma: The United Kingdom Children's Cancer Study Group Brain Tumour Committee. *J Clin Oncol* (2005) 23(31):7951–7. doi: 10.1200/JCO.2005.01.5479
36. Manoranjan B, Venugopal C, Bakhshinyan D, Adile AA, Richards L, Kameda-Smith MM, et al. Wnt Activation as a Therapeutic Strategy in Medulloblastoma. *Nat Commun* (2020) 11(1):1–12. doi: 10.1038/s41467-020-17953-4
37. Eberhart CG, Tihan T, Burger PC. Nuclear Localization and Mutation of β-Catenin in Medulloblastomas. *J Neuropathol Exp Neurol [Internet]* (2000) 59 (4):333–7. doi: 10.1093/jnen/59.4.333
38. Polakis P. The Oncogenic Activation of β-Catenin. *Curr Opin Genet Dev [Internet]* (1999) 9(1):15–21. doi: 10.1016/S0959-437X(99)80003-3
39. Waszak SM, Northcott PA, Buchhalter I, Robinson GW, Sutter C, Groebner S, et al. Spectrum and Prevalence of Genetic Predisposition in Medulloblastoma: A Retrospective Genetic Study and Prospective Validation in a Clinical Trial Cohort. *Lancet Oncol [Internet]* (2018) 19 (6):785–98. doi: 10.1016/S1470-2045(18)30242-0
40. Northcott PA, Dubuc AM, Pfister S, Taylor MD. Molecular Subgroups of Medulloblastoma. *Expert Rev Neurother* (2012) 12(7):871–84. doi: 10.1586/ern.12.66
41. Northcott PA, Hielscher T, Dubuc A, Mack S, Shih D, Remke M, et al. Pediatric and Adult Sonic Hedgehog Medulloblastomas are Clinically and Molecularly Distinct. *Acta Neuropathol [Internet]* (2011) 122(2):231–40. doi: 10.1007/s00401-011-0846-7
42. Skowron P, Farooq H, Cavalli FMG, Morrissy AS, Ly M, Hendrikse LD, et al. The Transcriptional Landscape of Shh Medulloblastoma. *Nat Commun* (2021) 12(1):1749. doi: 10.1038/s41467-021-21883-0
43. Tikhonov DB, Mellor IR, Usherwood PNR. Modeling Noncompetitive Antagonism of a Nicotinic Acetylcholine Receptor. *Biophys J* (2004) 87 (1):159–70. doi: 10.1529/biophysj.103.037457
44. Waszak SM, Robinson GW, Gudenas BL, Smith KS, Forget A, Kojic M, et al. Germline Elongator Mutations in Sonic Hedgehog Medulloblastoma. *Nature* (2020) 580(7803):396–401. doi: 10.1038/s41586-020-2164-5
45. Otero G, Fellows J, Yang L, De Bizemont T, Dirac AMG, Gustafsson CM, et al. Elongator, a Multisubunit Component of a Novel RNA Polymerase Ii Holoenzyme for Transcriptional Elongation. *Mol Cell* (1999) 3(1):109–18. doi: 10.1016/S1097-2765(00)80179-3
46. Hunnicutt BJ, Chaverra M, George L, Lefcort F. Ikap/Elp1 is Required in Vivo for Neurogenesis and Neuronal Survival, But Not for Neural Crest Migration. *PloS One* (2012) 7(2):e32050. doi: 10.1371/journal.pone.0032050
47. Zhukova N, Ramaswamy V, Remke M, Pfaff E, Shih DJH, Martin DC, et al. Subgroup-Specific Prognostic Implications of TP53 Mutation in Medulloblastoma. *J Clin Oncol* (2013) 31(23):2927–35. doi: 10.1200/JCO.2012.48.5052
48. Archer TC, Ehrenberger T, Mundt F, Gold MP, Krug K , Mah CK, et al. Proteomics, Post-translational Modifications, and Integrative Analyses Reveal Molecular Heterogeneity Within Medulloblastoma Subgroups. *Cancer Cell* (2018) 34(3):396–410.e8. doi: 10.1016/j.ccell.2018.08.004
49. Northcott PA, Lee C, Zichner T, Stütz AM, Erkek S, Kawauchi D, et al. Enhancer Hijacking Activates GFI1 Family Oncogenes in Medulloblastoma. *Nature* (2014) 511(7510):428–34. doi: 10.1038/nature13379
50. Forget A, Martignetti L, Puget S, Calzone L, Brabetz S, Picard D, et al. Aberrant ERBB4-SRC Signaling as a Hallmark of Group 4 Medulloblastoma Revealed by Integrative Phosphoproteomic Profiling. *Cancer Cell [Internet]* (2018) 34(3):379–95.e7. doi: 10.1016/j.ccell.2018.08.002
51. Huang M, Tailor J, Zhen Q, Gillmor AH, Miller ML, Weishaupt H, et al. Engineering Genetic Predisposition in Human Neuroepithelial Stem Cells Recapitulates Medulloblastoma Tumorigenesis. *Cell Stem Cell* (2019) 25 (3):433–46.e7. doi: 10.1016/j.stem.2019.05.013
52. Bihannic L, Ayrault O. Insights Into Cerebellar Development and Medulloblastoma. *Bull Cancer* (2016) 103(1):30–40. doi: 10.1016/j.bulcan.2015.11.002
53. Gibson P, Tong Y, Robinson G, Thompson MC, Currle DS, Eden C, et al. Subtypes of Medulloblastoma Have Distinct Developmental Origins. *Nature* (2010) 468(7327):1095–9. doi: 10.1038/nature09587
54. Hovestadt V, Smith KS, Bihannic L, Filbin MG, Shaw MKL, Baumgartner A, et al. Resolving Medulloblastoma Cellular Architecture by Single-Cell Genomics. *Nat [Internet]* (2019) 572(7767):74–9. doi: 10.1038/s41586-019-1434-6
55. Bailey P, Cushing H. A Classification of the Tumours of the Glioma Group on a Histogenetic Basis, With a Correlated Study of Prognosis. *Lippincott [Internet]* (1926) 14(55):554–5. doi: 10.1002/bjs.1800145540
56. Wallace VA. Purkinje-Cell-Derived Sonic Hedgehog Regulates Granule Neuron Precursor Cell Proliferation in the Developing Mouse Cerebellum. *Curr Biol [Internet]* (1999) 9(8):445–8. doi: 10.1016/S0960-9822(99)80195-X
57. Azevedo FAC, Carvalho LRB, Grinberg LT, Farfel JM, Ferretti REL, Leite REP, et al. Equal Numbers of Neuronal and Nonneuronal Cells Make the Human Brain an Isometrically Scaled-Up Primate Brain. *J Comp Neurol [Internet]* (2009) 513(5):532–41. doi: 10.1002/cne.21974
58. Swartling FJ, Grimmer MR, Hackett CS, Northcott PA, Fan QW, Goldenberg DD, et al. Pleiotropic Role for MYCN in Medulloblastoma. *Genes Dev [Internet]* (2010) 24(10):1059–72. doi: 10.1101/gad.1907510
59. Knoepfler PS, Zhang XY, Cheng PF, Gafken PR, McMahon SB, Eisenman RN. Myc Influences Global Chromatin Structure. *EMBO J [Internet]* (2006) 25(12):2723–34. doi: 10.1038/sj.emboj.7601152
60. Wey A, Knoepfler PS. C-Myc and N-myc Promote Active Stem Cell Metabolism and Cycling as Architects of the Developing Brain. *Oncotarget [Internet]* (2010) 1(2):120–30. doi: 10.18632/oncotarget.116
61. Dahmane N, Ruiz-i-Altaba A. Sonic Hedgehog Regulates the Growth and Patterning of the Cerebellum. *Development* (1999) 15126(14):3089–100. doi: 10.1242/dev.126.14.3089
62. Dahmane N, Sánchez P, Gitton Y, Palma V, Sun T, Beyna M, et al. The Sonic Hedgehog-Gli Pathway Regulates Dorsal Brain Growth and Tumorigenesis - Pubmed. *Development* (2001) p:5201–12. doi: 10.1242/dev.128.24.5201
63. Oliver TG, Grasfeder LL, Carroll AL, Kaiser C, Gillingham CL, Lin SM, et al. Transcriptional Profiling of the Sonic Hedgehog Response: A Critical Role for N-myc in Proliferation of Neuronal Precursors. *Proc Natl Acad Sci U.S.A. [Internet]* (2003) 100(12):7331–6. doi: 10.1073/pnas.0832317100
64. Pomeroy SL, Tamayo P, Gaasenbeek M, Sturla LM, Angelo M, McLaughlin ME, et al. Prediction of Central Nervous System Embryonal Tumour

Outcome Based on Gene Expression. *Nat [Internet]* (2002) 415(6870):436–42. doi: 10.1038/415436a
65. Kenney AM, Cole MD, Rowitch DH. Nmyc Upregulation by Sonic Hedgehog Signaling Promotes Proliferation in Developing Cerebellar Granule Neuron Precursors. *Development* (2003) 130p:15–28. doi: 10.1242/dev.00182
66. Miyazawa K, Himi T, Garcia V, Yamagishi H, Sato S, Ishizaki Y. A Role for p27/Kip1 in the Control of Cerebellar Granule Cell Precursor Proliferation. *J Neurosci [Internet]* (2000) 20(15):5756–63. doi: 10.1523/jneurosci.20-15-05756.2000
67. Gartel AL, Shchors K. Mechanisms of C-Myc-Mediated Transcriptional Repression of Growth Arrest Genes. *Exp Cell Res Acad Press Inc* (2003) 283:17–21. doi: 10.1016/S0014-4827(02)00020-4
68. Kenney AM, Widlund HR, Rowitch DH. Hedgehog and PI-3 Kinase Signaling Converge on Nmyc1 to Promote Cell Cycle Progression in Cerebellar Neuronal Precursors. *Dev Company Biologists Ltd* (2004) 131:217–28. doi: 10.1242/dev.00891
69. Sjostrom SK, Finn G, Hahn WC, Rowitch DH, Kenney AM. The Cdk1 Complex Plays a Prime Role in Regulating N-Myc Phosphorylation and Turnover in Neural Precursors. *Dev Cell* (2005) Sep 19(3):327–38. doi: 10.1016/j.devcel.2005.07.014
70. Roussel MF, Stripay JL. Epigenetic Drivers in Pediatric Medulloblastoma. *Cerebellum* (2018) 17(1):28re2–36. doi: 10.1007/s12311-017-0899-9
71. Yi J, Wu J. Epigenetic regulation in medulloblastoma. *Mol Cell Neurosci* (2018) 87:65re2–76. doi: 10.1016/j.mcn.2017.09.003
72. Robinson G, Parker M, Kranenburg TA, Lu C, Chen X, Ding L, et al. Novel Mutations Target Distinct Subgroups of Medulloblastoma. *Nat [Internet]* (2012) 488(7409):43–8. doi: 10.1038/nature11213
73. He TC, Sparks AB, Rago C, Hermeking H, Zawel L, Da Costa LT, et al. Identification of c-MYC as a Target of the APC Pathway. *Sci (80-) [Internet]* (1998) 281(5382):1509–12. doi: 10.1126/science.281.5382.1509
74. Park AK, Lee SJ, Phi JH, Wang KC, Kim DG, Cho BK, et al. Prognostic Classification of Pediatric Medulloblastoma Based on Chromosome 17p Loss, Expression of MYCC and MYCN, and Wnt Pathway Activation. *Neuro Oncol* (2012) 14(2):203–14. doi: 10.1093/neuonc/nor196
75. Roussel MF, Hatten ME. Cerebellum: Development and Medulloblastoma. *Curr Topics Dev Biol NIH Public Access* (2011) 94:235–82. doi: 10.1016/B978-0-12-380916-2.00008-5
76. Ramaswamy V, Remke M, Bouffet E, Bailey S, Clifford SC, Doz F, et al. Risk Stratification of Childhood Medulloblastoma in the Molecular Era: The Current Consensus. *Acta Neuropathol [Internet]* (2016) 131(6):821–31. doi: 10.1007/s00401-016-1569-6
77. Ratnaparkhe M, Wong JKL, Wei PC, Hlevnjak M, Kolb T, Simovic M, et al. Defective DNA Damage Repair Leads to Frequent Catastrophic Genomic Events in Murine and Human Tumors. *Nat Commun* (2018) Dec 19(1):1–13. doi: 10.1038/s41467-018-06925-4
78. Swartling FJ, Savov V, Persson AI, Chen J, Hackett CS, Northcott PA, et al. Distinct Neural Stem Cell Populations Give Rise to Disparate Brain Tumors in Response to N-MYC. *Cancer Cell [Internet]* (2012) 21(5):601–13. doi: 10.1016/j.ccr.2012.04.012
79. Fernandez LA, Squatrito M, Northcott P, Awan A, Holland EC, Taylor MD, et al. Oncogenic YAP Promotes Radioresistance and Genomic Instability in Medulloblastoma Through IGF2-mediated Akt Activation. *Oncogene [Internet]* (2012) 31(15):1923–37. doi: 10.1038/onc.2011.379
80. Fernandez LA, Northcott PA, Dalton J, Fraga C, Ellison D, Angers S, et al. YAP1 is Amplified and Up-Regulated in Hedgehog-Associated Medulloblastomas and Mediates Sonic Hedgehog-Driven Neural Precursor Proliferation. *Genes Dev [Internet]* (2009) 23(23):2729–41. doi: 10.1101/gad.1824509
81. Zhang L, He X, Liu X, Zhang F, Huang LF, Potter AS, et al. Single-Cell Transcriptomics in Medulloblastoma Reveals Tumor-Initiating Progenitors and Oncogenic Cascades During Tumorigenesis and Relapse. *Cancer Cell* (2019) 1636(3):302–18. doi: 10.1016/j.ccell.2019.07.009
82. Onagoruwa OT, Pal G, Ochu C, Ogunwobi OO. Oncogenic Role of PVT1 and Therapeutic Implications [Internet] *Front Oncol Front Media SA* (2020) 10:17. doi: 10.3389/fonc.2020.00017
83. Sharma T, Schwalbe EC, Williamson D, Sill M, Hovestadt V, Mynarek M, et al. Second-Generation Molecular Subgrouping of Medulloblastoma: An International Meta-Analysis of Group 3 and Group 4 Subtypes. *Acta Neuropathol [Internet]* (2019) 138(2):309–26. doi: 10.1007/s00401-019-02020-0
84. Medeiros CB, Moxon-Emre I, Scantlebury N, Malkin D, Ramaswamy V, Decker A, et al. Medulloblastoma has a Global Impact on Health Related Quality of Life: Findings From an International Cohort. *Cancer Med* (2020) 219(2):447–59. doi: 10.1002/cam4.2701
85. Northcott PA, Robinson GW, Kratz CP, Mabbott DJ, Pomeroy SL, Clifford SC, et al. Medulloblastoma [Internet]. *Nat Rev Dis Primers Nat Publishing Group* (2019) 5p:1–20. doi: 10.1038/s41572-019-0063-6
86. Gajjar A, Chintagumpala M, Ashley D, Kellie S, Kun LE, Merchant TE, et al. Risk-Adapted Craniospinal Radiotherapy Followed by High-Dose Chemotherapy and Stem-Cell Rescue in Children With Newly Diagnosed Medulloblastoma (St Jude Medulloblastoma-96): Long-Term Results From a Prospective, Multicentre Trial. *Lancet Oncol* (2006) 7(10):813–20. doi: 10.1016/S1470-2045(06)70867-1
87. Von Bueren AO, Von Hoff K, Pietsch T, Gerber NU, Warmuth-Metz M, Deinlein F, et al. Treatment of Young Children With Localized Medulloblastoma by Chemotherapy Alone: Results of the Prospective, Multicenter Trial Hit 2000 Confirming the Prognostic Impact of Histology. *Neuro Oncol* (2011) 13(6):669–79. doi: 10.1093/neuonc/nor025
88. Rutkowski S, Gerber NU, Von Hoff K, Gnekow A, Bode U, Graf N, et al. Treatment of Early Childhood Medulloblastoma by Postoperative Chemotherapy and Deferred Radiotherapy. *Neuro Oncol* (2009) 11 (2):201–10. doi: 10.1215/15228517-2008-084
89. Ashley DM, Merchant TE, Strother D, Zhou T, Duffner P, Burger PC, et al. Induction Chemotherapy and Conformal Radiation Therapy for Very Young Children With Nonmetastatic Medulloblastoma: Children's Oncology Group Study P9934. *J Clin Oncol* (2012) 30(26):3181–6. doi: 10.1200/JCO.2010.34.4341
90. Nanney AD, El Tecle NE, El Ahmadieh TY, Daou MR, Bit Ivan EN, Marymont MH, et al. Intracranial Aneurysms in Previously Irradiated Fields: Literature Review and Case Report [Internet]. *World Neurosurgery Elsevier Inc* (2014) 81:511–9. doi: 10.1016/j.wneu.2013.10.044
91. Merchant TE, Kiehna EN, Li C, Shukla H, Sengupta S, Xiong X, et al. Modeling Radiation Dosimetry to Predict Cognitive Outcomes in Pediatric Patients With Cns Embryonal Tumors Including Medulloblastoma. *Int J Radiat Oncol Biol Phys* (2006) 65(1):210–21. doi: 10.1016/j.ijrobp.2005.10.038
92. Tanyildizi Y, Keweloh S, Neu MA, Russo A, Wingerter A, Weyer-Elberich V, et al. Radiation-Induced Vascular Changes in the Intracranial Irradiation Field in Medulloblastoma Survivors: An Mri Study. *Radiother Oncol* (2019) 136:50–5. doi: 10.1016/j.radonc.2019.03.017
93. Ramaswamy V, Remke M, Bouffet E, Faria CC, Perreault S, Cho YJ, et al. Recurrence Patterns Across Medulloblastoma Subgroups: An Integrated Clinical and Molecular Analysis. *Lancet Oncol* (2013) 14(12):1200–7. doi: 10.1016/S1470-2045(13)70449-2
94. Sabel M, Fleischhack G, Tippelt S, Gustafsson G, Doz F, Kortmann R, et al. Relapse Patterns and Outcome After Relapse in Standard Risk Medulloblastoma: A Report From the HIT-SIOP-PNET4 Study. *J Neurooncol* (2016) 129(3):515–24. doi: 10.1007/s11060-016-2202-1
95. Aguilera D, Mazewski C, Fangusaro J, MacDonald TJ, McNall-Knapp RY, Hayes LL, et al. Response to Bevacizumab, Irinotecan, and Temozolomide in Children With Relapsed Medulloblastoma: A Multi-Institutional Experience. *Child's Nerv Syst* (2013) 29(4):589–96. doi: 10.1007/s00381-012-2013-4
96. Thaimattam R, Banerjee R, Miglani R, Iqbal J. Protein Kinase Inhibitors: Structural Insights Into Selectivity. *Curr Pharm Des [Internet]* (2007) 13 (27):2751–65. doi: 10.2174/138161207781757042
97. Andresen C, Helander S, Lemak A, Farès C, Csizmok V, Carlsson J, et al. Transient Structure and Dynamics in the Disordered C-Myc Transactivation Domain Affect Bin1 Binding. *Nucleic Acids Res* (2012) 40(13):6353–66. doi: 10.1093/nar/gks263
98. Madan Babu M, van der Lee R, Sanchez De Groot N, Rg Gsponer J, Gough J, Dunker K. Intrinsically Disordered Proteins: Regulation and Disease This Review Comes From a Themed Issue on Sequences and Topology Edited. *Curr Opin Struct Biol [Internet]* (2011) 21:1–9. doi: 10.1016/j.sbi.2011.03.011
99. Clausen DM, Guo J, Parise RA, Beumer JH, Egorin MJ, Lazo JS, et al. In Vitro Cytotoxicity and In Vivo Efficacy, Pharmacokinetics, and Metabolism of 10074-G5, a Novel Small-Molecule Inhibitor of c-Myc/Max Dimerization.

J Pharmacol Exp Ther [Internet] (2010) 335(3):715–27. doi: 10.1124/jpet.110.170555
100. Wang YAZ, Plane JM, Jiang P, Zhou CJ, Deng W. Concise Review: Quiescent and Active States of Endogenous Adult Neural Stem Cells: Identification and Characterization [Internet]. *Stem Cells NIH Public Access;* (2011) 29:907–12. doi: 10.1002/stem.644
101. Dani C, Blanchard JM, Piechaczyk M, El Sabouty S, Marty L, Jeanteur P. Extreme Instability of Myc mRNA in Normal and Transformed Human Cells. *Proc Natl Acad Sci USA [Internet]* (1984) 81(22 I):7046–50. doi: 10.1073/pnas.81.22.7046
102. Small GW, Chou TY, Dang CV, Orlowski RZ. Evidence for Involvement of Calpain in C-Myc Proteolysis In Vivo. *Arch Biochem Biophys [Internet]* (2002) 400(2):151–61. doi: 10.1016/S0003-9861(02)00005-X
103. Thomas LR, Tansey WP. Proteolytic Control of the Oncoprotein Transcription Factor Myc. *In: Adv Cancer Res [Internet] Acad Press Inc* (2011) 77–106. doi: 10.1016/B978-0-12-386469-7.00004-9
104. Zhao X, Heng JIT, Guardavaccaro D, Jiang R, Pagano M, Guillemot F, et al. The HECT-domain Ubiquitin Ligase Huwe1 Controls Neural Differentiation and Proliferation by Destabilizing the N-Myc Oncoprotein. *Nat Cell Biol [Internet]* (2008) 10(6):643–53. doi: 10.1038/ncb1727
105. Chesler L, Schlieve C, Goldenberg DD, Kenney A, Kim G, McMillan A, et al. Inhibition of Phosphatidylinositol 3-Kinase Destabilizes Mycn Protein and Blocks Malignant Progression in Neuroblastoma. *Cancer Res [Internet]* (2006) 66(16):8139–46. doi: 10.1158/0008-5472.CAN-05-2769
106. Andrews FH, Singh AR, Joshi S, Smith CA, Morales GA, Garlich JR, et al. Dual-Activity PI3K-BRD4 Inhibitor for the Orthogonal Inhibition of MYC to Block Tumor Growth and Metastasis. *Proc Natl Acad Sci USA [Internet]* (2017) 114(7):E1072–80. doi: 10.1073/pnas.1613091114
107. Richards MW, Burgess SG, Poon E, Carstensen A, Eilers M, Chesler L, et al. Structural Basis of N-Myc Binding by Aurora-A and its Destabilization by Kinase Inhibitors. *Proc Natl Acad Sci USA [Internet]* (2016) 113(48):13726–31. doi: 10.1073/pnas.1610626113
108. Otto T, Horn S, Brockmann M, Eilers U, Schüttrumpf L, Popov N, et al. Stabilization of N-Myc is a Critical Function of Aurora A in Human Neuroblastoma. *Cancer Cell [Internet]* (2009) 15(1):67–78. doi: 10.1016/j.ccr.2008.12.005
109. Gustafson WC, Meyerowitz JG, Nekritz EA, Chen J, Benes C, Charron E, et al. Drugging MYCN Through an Allosteric Transition in Aurora Kinase a. *Cancer Cell [Internet]* (2014) 26(3):414–27. doi: 10.1016/j.ccr.2014.07.015
110. Brockmann M, Poon E, Berry T, Carstensen A, Deubzer HE, Rycak L, et al. Small Molecule Inhibitors of Aurora-A Induce Proteasomal Degradation of N-Myc in Childhood Neuroblastoma. *Cancer Cell [Internet]* (2013) 24 (1):75–89. doi: 10.1016/j.ccr.2013.05.005
111. Ahmad Z, Jasnos L, Gil V, Howell L, Hallsworth A, Petrie K, et al. Molecular and in Vivo Characterization of Cancer-Propagating Cells Derived From MYCN-dependent Medulloblastoma. *PloS One* (2015) 10(3):e0119834. doi: 10.1371/journal.pone.0119834
112. Hill RM, Kuijper S, Lindsey JC, Petrie K, Schwalbe EC, Barker K, et al. Combined MYC and P53 Defects Emerge at Medulloblastoma Relapse and Define Rapidly Progressive, Therapeutically Targetable Disease. *Cancer Cell* (2015) 27(1):72–84. doi: 10.1016/j.ccell.2014.11.002
113. Maris JM, Morton CL, Gorlick R, Kolb EA, Lock R, Carol H, et al. Initial Testing of the Aurora Kinase a Inhibitor MLN8237 by the Pediatric Preclinical Testing Program (Pptp). *Pediatr Blood Cancer* (2010) 55(1):26–34. doi: 10.1002/pbc.22430
114. Markant SL, Esparza LA, Sun J, Barton KL, McCoig LM, Grant GA, et al. Targeting Sonic Hedgehog-Associated Medulloblastoma Through Inhibition of Aurora and Polo-Like Kinases. *Cancer Res* (2013) 73(20):6310–22. doi: 10.1158/0008-5472.CAN-12-4258
115. Bavetsias V, Linardopoulos S. Aurora Kinase Inhibitors: Current Status and Outlook [Internet]. *Front Oncol* (2015) 5:278. doi: 10.3389/fonc.2015.00278
116. Kollareddy M, Zheleva D, Dzubak P, Brahmkshatriya PS, Lepsik M, Hajduch M. Aurora Kinase Inhibitors: Progress Towards the Clinic [Internet]. *Investigational New Drugs Invest New Drugs* (2012) 30:2411–32. doi: 10.1007/s10637-012-9798-6
117. Niu H, Shin H, Gao F, Zhang J, Bahamon B, Danaee H, et al. Aurora A Functional Single Nucleotide Polymorphism (Snp) Correlates With Clinical Outcome in Patients With Advanced Solid Tumors Treated With Alisertib, an Investigational Aurora A Kinase Inhibitor. *EBioMedicine* (2017) 25:50–7. doi: 10.1016/j.ebiom.2017.10.015
118. DuBois SG, Mosse YP, Fox E, Kudgus RA, Reid JM, McGovern R, et al. Phase II Trial of Alisertib in Combination With Irinotecan and Temozolomide for Patients With Relapsed or Refractory Neuroblastoma. *Clin Cancer Res* (2018) 24(24):6142–9. doi: 10.1158/1078-0432.CCR-18-1381
119. Diaz RJ, Golbourn B, Faria C, Picard D, Shih D, Raynaud D, et al. Mechanism of Action and Therapeutic Efficacy of Aurora Kinase B Inhibition in MYC Overexpressing Medulloblastoma. *Oncotarget* (2015) 6 (5):3359–74. doi: 10.18632/oncotarget.3245
120. Filippakopoulos P, Picaud S, Mangos M, Keates T, Lambert JP, Barsyte-Lovejoy D, et al. Histone Recognition and Large-Scale Structural Analysis of the Human Bromodomain Family. *Cell [Internet]* (2012) 149(1):214–31. doi: 10.1016/j.cell.2012.02.013
121. Delmore JE, Issa GC, Lemieux ME, Rahl PB, Shi J, Jacobs HM, et al. Bet Bromodomain Inhibition as a Therapeutic Strategy to Target C-Myc. *Cell [Internet]* (2011) 146(6):904–17. doi: 10.1016/j.cell.2011.08.017
122. Dey A, Chitsaz F, Abbasi A, Misteli T, Ozato K. The Double Bromodomain Protein Brd4 Binds to Acetylated Chromatin During Interphase and Mitosis. *Proc Natl Acad Sci USA [Internet]* (2003) 100(15):8758–63. doi: 10.1073/pnas.1433065100
123. Nishiyama A, Mochizuki K, Mueller F, Karpova T, McNally JG, Ozato K. Intracellular Delivery of Acetyl-Histone Peptides Inhibits Native Bromodomain-Chromatin Interactions and Impairs Mitotic Progression. *FEBS Lett [Internet]* (2008) 582(10):1501–7. doi: 10.1016/j.febslet.2008.03.044
124. Sims RJ, Belotserkovskaya R, Reinberg D. Elongation by RNA Polymerase II: The Short and Long of it. *Genes Dev Genes Dev* (2004) 18p:2437–68. doi: 10.1101/gad.1235904
125. Mochizuki K, Nishiyama A, Moon KJ, Dey A, Ghosh A, Tamura T, et al. The Bromodomain Protein Brd4 Stimulates G1 Gene Transcription and Promotes Progression to S Phase. *J Biol Chem [Internet]* (2008) 283 (14):9040–8. doi: 10.1074/jbc.M707603200
126. Dey A, Nishiyama A, Karpova T, McNally J, Ozato K. Brd4 Marks Select Genes on Mitotic Chromatin and Directs Postmitotic Transcription. *Mol Biol Cell [Internet]* (2009) 20(23):4899–909. doi: 10.1091/mbc.E09-05-0380
127. Mertz JA, Conery AR, Bryant BM, Sandy P, Balasubramanian S, Mele DA, et al. Targeting MYC Dependence in Cancer by Inhibiting Bet Bromodomains. *Proc Natl Acad Sci USA [Internet]* (2011) 108(40):16669–74. doi: 10.1073/pnas.1108190108
128. Ba M, Long H, Yan Z, Wang S, Wu Y, Tu Y, et al. Brd4 Promotes Gastric Cancer Progression Through the Transcriptional and Epigenetic Regulation of C-MYC. *J Cell Biochem [Internet]* (2018) 119(1):973–82. doi: 10.1002/jcb.26264
129. Gargano B, Amente S, Majello B, Lania L. P-TEFb is a Crucial Co-Factor for Myc Transactivation. *Cell Cycle [Internet]* (2007) 6(16):2031–7. doi: 10.4161/cc.6.16.4554
130. Jake Slavish P, Chi L, Yun MK, Tsurkan L, Martinez NE, Jonchere B, et al. Bromodomain-Selective BET Inhibitors are Potent Antitumor Agents Against MYC-driven Pediatric Cancer. *Cancer Res* (2020) 80(17):3507–18. doi: 10.1158/0008-5472.CAN-19-3934
131. Henssen A, Thor T, Odersky A, Heukamp L, El-Hindy N, Beckers A, et al. Bet Bromodomain Protein Inhibition is a Therapeutic Option for Medulloblastoma. *Oncotarget [Internet]* (2013) 4(11):2080–95. doi: 10.18632/oncotarget.1534
132. Puissant A, Frumm SM, Alexe G, Bassil CF, Qi J, Chanthery YH, et al. Targeting MYCN in Neuroblastoma by BET Bromodomain Inhibition. *Cancer Discovery* (2013) 3(3):309–23. doi: 10.1158/2159-8290.CD-12-0418
133. Alimova I, Pierce A, Danis E, Donson A, Birks DK, Griesinger A, et al. Inhibition of MYC Attenuates Tumor Cell Self-Renewal and Promotes Senescence in SMARCB1-deficient Group 2 Atypical Teratoid Rhabdoid Tumors to Suppress Tumor Growth *In Vivo*. *Int J Cancer [Internet]* (2019) 144(8):1983–95. doi: 10.1002/ijc.31873
134. Bandopadhayay P, Bergthold G, Nguyen B, Schubert S, Gholamin S, Tang Y, et al. Bet Bromodomain Inhibition of MYC-amplified Medulloblastoma. *Clin Cancer Res [Internet]* (2014) 20(4):912–25. doi: 10.1158/1078-0432.CCR-13-2281
135. Piha-Paul SA, Hann CL, French CA, Cousin S, Braña I, Cassier PA, et al. Phase 1 Study of Molibresib (GSK525762), a Bromodomain and Extra-Terminal Domain Protein Inhibitor, in NUT Carcinoma and Other Solid Tumors. *JNCI Cancer Spectr* (2020) 4(2):pkz093. doi: 10.1093/jncics/pkz093

136. Hydbring P, Bahram F, Su Y, Tronnersjö S, Högstrand K, Von Der Lehr N, et al. Phosphorylation by Cdk2 is Required for Myc to Repress Ras-Induced Senescence in Cotransformation. *Proc Natl Acad Sci USA* (2010) 107(1):58–63. doi: 10.1073/pnas.0900121106
137. Sears R, Nuckolls F, Haura E, Taya Y, Tamai K, Nevins JR. Multiple Ras-dependent Phosphorylation Pathways Regulate Myc Protein Stability. *Genes Dev [Internet]* (2000) 14(19):2501–14. doi: 10.1101/gad.836800
138. Bolin S, Borgenvik A, Persson CU, Sundström A, Qi J, Bradner JE, et al. Combined BET Bromodomain and CDK2 Inhibition in MYC-driven Medulloblastoma. *Oncogene [Internet]* (2018) 37(21):2850–62. doi: 10.1038/s41388-018-0135-1
139. Lewin J, Soria JC, Stathis A, Delord JP, Peters S, Awada A, et al. Phase Ib Trial With Birabresib, a Small-Molecule Inhibitor of Bromodomain and Extraterminal Proteins, in Patients With Selected Advanced Solid Tumors. In: Journal of Clinical Oncology. *Am Soc Clin Oncol* (2018) p:3007–14. doi: 10.1200/JCO.2018.78.2292
140. Ameratunga M, Braña I, Bono P, Postel-Vinay S, Plummer R, Aspegren J, et al. First-in-Human Phase 1 Open Label Study of the BET Inhibitor ODM-207 in Patients With Selected Solid Tumours. *Br J Cancer* (2020) 123 (12):1730–6. doi: 10.1038/s41416-020-01077-z
141. Buzzetti M, Morlando S, Solomos D, Mehmood A, Cox AWI, Chiesa M, et al. Pre-Therapeutic Efficacy of the CDK Inhibitor Dinaciclib in Medulloblastoma Cells. *Sci Rep* (2021) 11(1):5374. doi: 10.1038/s41598-021-84082-3
142. Chipumuro E, Marco E, Christensen CL, Kwiatkowski N, Zhang T, Hatheway CM, et al. Cdk7 Inhibition Suppresses Super-Enhancer-Linked Oncogenic Transcription in MYCN-driven Cancer. *Cell* (2014) 159(5):1126–39. doi: 10.1016/j.cell.2014.10.024
143. Poon E, Liang T, Jamin Y, Walz S, Kwok C, Hakkert A, et al. Orally Bioavailable Cdk9/2 Inhibitor Shows Mechanism-Based Therapeutic Potential in MYCN-driven Neuroblastoma. *J Clin Invest* (2020) 130 (11):5875–92. doi: 10.1172/JCI134132
144. Pak E, Mackenzie EL, Zhao X, Pazyra-Murphy MF, Park PMC, Wu L, et al. A Large-Scale Drug Screen Identifies Selective Inhibitors of Class I Hdacs as a Potential Therapeutic Option for SHH Medulloblastoma. *Neuro Oncol* (2019) 21(9):1150–63. doi: 10.1093/neuonc/noz089
145. Perla A, Fratini L, Cardoso PS, Nör C, Brunetto AT, Brunetto AL, et al. Histone Deacetylase Inhibitors in Pediatric Brain Cancers: Biological Activities and Therapeutic Potential [Internet]. Vol. 8, Frontiers in Cell and Developmental Biology. *Front Media SA* (2020). doi: 10.3389/fcell.2020.00546
146. de Andrade P F, Andrade A, de Paula Queiroz R, Trevisan F, Tone L, Valera E. Novel Histone Deacetylase Inhibitors for the Treatment of Pediatric Brain Tumors. *Cent Nerv Syst Agents Med Chem* (2014) 14(2):90–5. doi: 10.2174/1871524914666141112093541
147. Rettig I, Koeneke E, Trippel F, Mueller WC, Burhenne J, Kopp-Schneider A, et al. Selective Inhibition of HDAC8 Decreases Neuroblastoma Growth In Vitro and In Vivo and Enhances Retinoic Acid-Mediated Differentiation. *Cell Death Dis* (2015) 6(2):e1657. doi: 10.1038/cddis.2015.24
148. Marino AM, Frijhoff J, Calero R, Baryawno N, Östman A, Johnsen JI. Effects of Epigenetic Modificators in Combination With Small Molecule Inhibitors of Receptor Tyrosine Kinases on Medulloblastoma Growth. *Biochem Biophys Res Commun* (2014) 450(4):1600–5. doi: 10.1016/j.bbrc.2014.07.042
149. Ecker J, Oehme I, Mazitschek R, Korshunov A, Kool M, Hielscher T, et al. Targeting Class I Histone Deacetylase 2 in MYC Amplified Group 3 Medulloblastoma. *Acta Neuropathol Commun* (2015) 3:22. doi: 10.1186/s40478-015-0201-7
150. Sonnemann J, Kumar KS, Heesch S, Müller C, Hartwig C, Maass M, et al. Histone Deacetylase Inhibitors Induce Cell Death and Enhance the Susceptibility to Ionizing Radiation, Etoposide, and TRAIL in Medulloblastoma Cells. *Int J Oncol* (2006) 28(3):755–66. doi: 10.3892/ijo.28.3.755
151. da Cunha Jaeger M, Ghisleni EC, Cardoso PS, Siniglaglia M, Falcon T, Brunetto AT, et al. HDAC and MAPK/ERK Inhibitors Cooperate to Reduce Viability and Stemness in Medulloblastoma. *J Mol Neurosci* (2020) 70 (6):981–92. doi: 10.1007/s12031-020-01505-y
152. Pei Y, Liu KW, Wang J, Garancher A, Tao R, Esparza LA, et al. HDAC and PI3K Antagonists Cooperate to Inhibit Growth of MYC-Driven Medulloblastoma. *Cancer Cell [Internet]* (2016) 29(3):311–23. doi: 10.1016/j.ccell.2016.02.011
153. Häcker S, Karl S, Mader I, Cristofanon S, Schweitzer T, Krauss J, et al. Histone Deacetylase Inhibitors Prime Medulloblastoma Cells for Chemotherapy-Induced Apoptosis by Enhancing P53-Dependent Bax Activation. *Oncogene* (2011) 30(19):2275–81. doi: 10.1038/onc.2010.599
154. Coni S, Mancuso AB, Di Magno L, Sdruscia G, Manni S, Serrao SM, et al. Corrigendum: Selective Targeting of HDAC1/2 Elicits Anticancer Effects Through Gli1 Acetylation in Preclinical Models of SHH Medulloblastoma [Internet]. *Sci Rep NLM (Medline)* (2017) 7:46645. doi: 10.1038/srep46645
155. Fouladi M, Park JR, Stewart CF, Gilbertson RJ, Schaiquevich P, Sun J, et al. Pediatric Phase I Trial and Pharmacokinetic Study of Vorinostat: A Children's Oncology Group Phase I Consortium Report. *J Clin Oncol* (2010) 28(22):3623–9. doi: 10.1200/JCO.2009.25.9119
156. Muscal JA, Thompson PA, Horton TM, Ingle AM, Ahern CH, McGovern RM, et al. A Phase I Trial of Vorinostat and Bortezomib in Children With Refractory or Recurrent Solid Tumors: A Children's Oncology Group Phase I Consortium Study (Advl0916). *Pediatr Blood Cancer* (2013) 60(3):390–5. doi: 10.1002/pbc.24271
157. Shahbazi J, Liu PY, Atmadibrata B, Bradner JE, Marshall GM, Lock RB, et al. The Bromodomain Inhibitor Jq1 and the Histone Deacetylase Inhibitor Panobinostat Synergistically Reduce N-Myc Expression and Induce Anticancer Effects. *Clin Cancer Res [Internet]* (2016) 22(10):2534–44. doi: 10.1158/1078-0432.CCR-15-1666
158. Chaturvedi NK, Mahapatra S, Kesherwani V, Kling MJ, Shukla M, Ray S, et al. Role of Protein Arginine Methyltransferase 5 in Group 3 (Myc-Driven) Medulloblastoma. *BMC Cancer* (2019) 19(1):1056. doi: 10.1186/s12885-019-6291-z
159. Migliori V, Phalke S, Bezzi M, Guccione E. Arginine/Lysine-Methyl/Methyl Switches: Biochemical Role of Histone Arginine Methylation in Transcriptional Regulation [Internet]. *Epigenomics Epigenomics* (2010) 2p:119–37. doi: 10.2217/epi.09.39
160. Bonday ZQ, Cortez GS, Grogan MJ, Antonysamy S, Weichert K, Bocchinfuso WP, et al. Lly-283, a Potent and Selective Inhibitor of Arginine Methyltransferase 5, PRMT5, With Antitumor Activity. *ACS Med Chem Lett* (2018) 9(7):612–7. doi: 10.1021/acsmedchemlett.8b00014
161. Blackwell TK, Huang J, Ma A, Kretzner L, Alt FW, Eisenman RN, et al. Binding of Myc Proteins to Canonical and Noncanonical Dna Sequences. *Mol Cell Biol [Internet]* (1993) 13(9):5216–24. doi: 10.1128/mcb.13.9.5216
162. Ayer DE, Eisenman RN. A Switch From Myc:Max to Mad:Max Heterocomplexes Accompanies Monocyte/Macrophage Differentiation. *Genes Dev [Internet]* (1993) 7(11):2110–9. doi: 10.1101/gad.7.11.2110
163. Adhikary S, Eilers M. Transcriptional Regulation and Transformation by Myc Proteins. *Nat Rev Mol Cell Biol Nat Publishing Group* (2005) 6p:635–45. doi: 10.1038/nrm1703
164. Beaulieu ME, Jauset T, Massó-Vallés D, Martínez-Martín S, Rahl P, Maltais L, et al. Intrinsic Cell-Penetrating Activity Propels Omomyc From Proof of Concept to Viable Anti-Myc Therapy. *Sci Transl Med [Internet]* (2019) 11 (484):5012. doi: 10.1126/scitranslmed.aar5012
165. Jung LA, Gebhardt A, Koelmel W, Ade CP, Walz S, Kuper J, et al. Omomyc Blunts Promoter Invasion by Oncogenic MYC to Inhibit Gene Expression Characteristic of MYC-dependent Tumors. *Oncogene [Internet]* (2017) 36 (14):1911–24. doi: 10.1038/onc.2016.354
166. Struntz NB, Chen A, Deutzmann A, Wilson RM, Stefan E, Evans HL, et al. Stabilization of the Max Homodimer With a Small Molecule Attenuates Myc-Driven Transcription. *Cell Chem Biol [Internet]* (2019) 26(5):711–723.e14. doi: 10.1016/j.chembiol.2019.02.009
167. Müller I, Larsson K, Frenzel A, Oliynyk G, Zirath H, Prochownik EV, et al. Targeting of the MYCN Protein With Small Molecule c-MYC Inhibitors. *PloS One* (2014) 9(5):e97285. doi: 10.1371/journal.pone.0097285
168. Endersby R, Whitehouse J, Pribnow A, Kuchibhotla M, Hii H, Carline B, et al. Small-Molecule Screen Reveals Synergy of Cell Cycle Checkpoint Kinase Inhibitors With DNA-damaging Chemotherapies in Medulloblastoma. *Sci Transl Med* (2021) 13(577):7401. doi: 10.1126/scitranslmed.aba7401
169. Bélanger M, Allaman I, Magistretti PJ. Brain Energy Metabolism: Focus on Astrocyte-neuron Metabolic Cooperation [Internet]. *Cell Metab Cell Metab;* (2011) 14:724–38. doi: 10.1016/j.cmet.2011.08.016
170. Bhatia B, Potts CR, Guldal C, Choi SP, Korshunov A, Pfister S, et al. Hedgehog-Mediated Regulation of PPARc Controls Metabolic Patterns in

Neural Precursors and Shh-Driven Medulloblastoma. *Acta Neuropathol* (2012) 123(4):587–600. doi: 10.1007/s00401-012-0968-6
171. Bhatia B, Hsieh M, Kenney AM, Nahlé Z. Mitogenic Sonic Hedgehog Signaling Drives E2F1-dependent Lipogenesis in Progenitor Cells and Medulloblastoma. *Oncogene* (2011) 30(4):410–22. doi: 10.1038/onc.2010.454
172. Tech K, Deshmukh M, Gershon TR. Adaptations of Energy Metabolism During Cerebellar Neurogenesis are Co-Opted in Medulloblastoma [Internet]. *Cancer Letters Elsevier Ireland Ltd* (2015) 356:268–72. doi: 10.1016/j.canlet.2014.02.017
173. Di Magno L, Manzi D, D'Amico D, Coni S, Macone A, Infante P, et al. Druggable Glycolytic Requirement for Hedgehog-dependent Neuronal and Medulloblastoma Growth. *Cell Cycle* (2014) 13(21):3404–13. doi: 10.4161/15384101.2014.952973
174. Gershon TR, Crowther AJ, Tikunov A, Garcia I, Annis R, Yuan H, et al. Hexokinase-2-Mediated Aerobic Glycolysis is Integral to Cerebellar Neurogenesis and Pathogenesis of Medulloblastoma. *Cancer Metab* (2013) 1(1):2. doi: 10.1186/2049-3002-1-2
175. Yoshida GJ. Beyond the Warburg Effect: N-Myc Contributes to Metabolic Reprogramming in Cancer Cells [Internet]. *Front Oncol* (2020) 10:791. doi: 10.3389/fonc.2020.00791
176. Oliynyk G, Ruiz-Pérez MV, Sainero-Alcolado L, Dzieran J, Zirath H, Gallart-Ayala H, et al. Mycn-Enhanced Oxidative and Glycolytic Metabolism Reveals Vulnerabilities for Targeting Neuroblastoma. *iScience* (2019) Nov 2221:188–204. doi: 10.1016/j.isci.2019.10.020
177. Rellinger EJ, Craig BT, Alvarez AL, Dusek HL, Kim KW, Qiao J, et al. Fx11 Inhibits Aerobic Glycolysis and Growth of Neuroblastoma Cells. *In: Surg (United States) Mosby Inc* (2017) p:747–52. doi: 10.1016/j.surg.2016.09.009
178. Dorneburg C, Fischer M, Barth TFE, Mueller-Klieser W, Hero B, Gecht J, et al. LDHA in Neuroblastoma is Associated With Poor Outcome and its Depletion Decreases Neuroblastoma Growth Independent of Aerobic Glycolysis. *Clin Cancer Res* (2018) 24(22):5772–83. doi: 10.1158/1078-0432.CCR-17-2578
179. Zhao E, Hou J, Cui H. Serine–Glycine-One-Carbon Metabolism: Vulnerabilities in MYCN-amplified Neuroblastoma. *Oncogenesis* (2020) 9:14. doi: 10.1038/s41389-020-0200-9
180. Tjaden B, Baum K, Marquardt V, Simon M, Trajkovic-Arsic M, Kouril T, et al. N-Myc-Induced Metabolic Rewiring Creates Novel Therapeutic Vulnerabilities in Neuroblastoma. *Sci Rep* (2020) 10:7157. doi: 10.1038/s41598-020-64040-1
181. Garcia AR, Arsenian-Henriksson M. Serine-Glycine-One-Carbon Metabolism: The Hidden Achilles Heel of MYCN-amplified Neuroblastoma? *Cancer Res* (2019) 79(15):3818–9. doi: 10.1158/0008-5472.CAN-19-1816
182. Yue M, Jiang J, Gao P, Liu H, Qing G. Oncogenic MYC Activates a Feedforward Regulatory Loop Promoting Essential Amino Acid Metabolism and Tumorigenesis. *Cell Rep* (2017) 21(13):3819–32. doi: 10.1016/j.celrep.2017.12.002
183. Oda K, Hosoda N, Endo H, Saito K, Tsujihara K, Yamamura M, et al. L-Type Amino Acid Transporter 1 Inhibitors Inhibit Tumor Cell Growth. *Cancer Sci* (2010) 101(1):173–9. doi: 10.1111/j.1349-7006.2009.01386.x
184. Svensson RU, Parker SJ, Eichner LJ, Kolar MJ, Wallace M, Brun SN, et al. Inhibition of Acetyl-Coa Carboxylase Suppresses Fatty Acid Synthesis and Tumor Growth of non-Small-Cell Lung Cancer in Preclinical Models. *Nat Med* (2016) 22(10):1108–19. doi: 10.1038/nm.4181
185. Longo J, van Leeuwen JE, Elbaz M, Branchard E, Penn LZ. Statins as Anticancer Agents in the Era of Precision Medicine. *Clin Cancer Res* (2020) 26(22):5791–800. doi: 10.1158/1078-0432.ccr-20-1967
186. Yauch RL, Gould SE, Scales SJ, Tang T, Tian H, Ahn CP, et al. A Paracrine Requirement for Hedgehog Signalling in Cancer. *Nature* (2008) 455 (7211):406–10. doi: 10.1038/nature07275
187. Grabovska Y, Mackay A, O'Hare P, Crosier S, Finetti M, Schwalbe EC, et al. Pediatric Pan-Central Nervous System Tumor Analysis of Immune-Cell Infiltration Identifies Correlates of Antitumor Immunity. *Nat Commun* (2020) 11:4324. doi: 10.1038/s41467-020-18070-y
188. Chakravarthy A, Furness A, Joshi K, Ghorani E, Ford K, Ward MJ, et al. Pan-Cancer Deconvolution of Tumour Composition Using DNA Methylation. *Nat Commun* (2018) 9:3220. doi: 10.1038/s41467-018-05570-1
189. Margol AS, Robison NJ, Gnanachandran J, Hung LT, Kennedy RJ, Vali M, et al. Tumor-Associated Macrophages in SHH Subgroup of Medulloblastomas. *Clin Cancer Res* (2015) 21(6):1457–65. doi: 10.1158/1078-0432.CCR-14-1144
190. Vermeulen JF, Van Hecke W, Adriaansen EJM, Jansen MK, Bouma RG, Villacorta Hidalgo J, et al. Prognostic Relevance of Tumor-Infiltrating Lymphocytes and Immune Checkpoints in Pediatric Medulloblastoma. *Oncoimmunology* (2017) 7(3):e1398877. doi: 10.1080/2162402X.2017.1398877
191. Diao S, Gu C, Zhang H, Yu C. Immune Cell Infiltration and Cytokine Secretion Analysis Reveal a non-Inflammatory Microenvironment of Medulloblastoma. *Oncol Lett* (2020) 20(6):397. doi: 10.3892/ol.2020.12260
192. Martin AM, Nirschl CJ, Polanczyk MJ, Bell WR, Nirschl TR, Harris-Bookman S, et al. Pd-L1 Expression in Medulloblastoma: An Evaluation by Subgroup. *Oncotarget* (2018) 9(27):19177–91. doi: 10.18632/oncotarget.24951
193. Aoki T, Hino M, Koh K, Kyushiki M, Kishimoto H, Arakawa Y, et al. Low Frequency of Programmed Death Ligand 1 Expression in Pediatric Cancers. *Pediatr Blood Cancer* (2016) 63(8):1461–4. doi: 10.1002/pbc.26018
194. Orlando D, Miele E, De Angelis B, Guercio M, Boffa I, Sinibaldi M, et al. Adoptive Immunotherapy Using Prame-Specific T Cells in Medulloblastoma. *Cancer Res* (2018) 78(12):3337–49. doi: 10.1158/0008-5472.CAN-17-3140
195. Donovan LK, Delaidelli A, Joseph SK, Bielamowicz K, Fousek K, Holgado BL, et al. Locoregional Delivery of CAR T Cells to the Cerebrospinal Fluid for Treatment of Metastatic Medulloblastoma and Ependymoma. *Nat Med* (2020) 26(5):720–31. doi: 10.1038/s41591-020-0827-2
196. Raieli S, Di Renzo D, Lampis S, Amadesi C, Montemurro L, Pession A, et al. Mycn Drives a Tumor Immunosuppressive Environment Which Impacts Survival in Neuroblastoma. *Front Oncol* (2021) 11:625207. doi: 10.3389/fonc.2021.625207
197. Casey SC, Baylot V, Felsher DW. The MYC Oncogene is a Global Regulator of the Immune Response [Internet]. *Blood. Am Soc Hematol* (2018) 131:2007–15. doi: 10.1182/blood-2017-11-742577
198. Christofides A, Karantanos T, Bardhan K, Boussiotis VA. Epigenetic Regulation of Cancer Biology and Anti-Tumor Immunity by EZH2 [Internet]. *Oncotarget Impact Journals LLC;* (2016) 7:85624–40. doi: 10.18632/oncotarget.12928
199. Dai X, Bu X, Gao Y, Guo J, Hu J, Jiang C, et al. Energy Status Dictates PD-L1 Protein Abundance and Anti-Tumor Immunity to Enable Checkpoint Blockade. *Mol Cell* (2021). doi: 10.1016/j.molcel.2021.03.037
200. Sakamoto KM, Kim KB, Kumagai A, Mercurio F, Crews CM, Deshaies RJ. Protacs: Chimeric Molecules That Target Proteins to the Skp1-Cullin-F Box Complex for Ubiquitination and Degradation [Internet]. *Natl Acad Sci* (2001). doi: 10.1073/pnas.141230798
201. Ding Y, Fei Y, Lu B. Emerging New Concepts of Degrader Technologies [Internet. *Trends Pharmacol Sci Elsevier Ltd* (2020) 41p:464–74. doi: 10.1016/j.tips.2020.04.005
202. Ravid T, Hochstrasser M. Diversity of Degradation Signals in the Ubiquitin-Proteasome System [Internet]. *Nat Rev Mol Cell Biol Nat Publishing Group* (2008) 9:679–89. doi: 10.1038/nrm2468
203. Shi C, Zhang H, Wang P, Wang K, Xu D, Wang H, et al. Protac Induced-BET Protein Degradation Exhibits Potent Anti-Osteosarcoma Activity by Triggering Apoptosis. *Cell Death Dis* (2019) 10:815. doi: 10.1038/s41419-019-2022-2
204. Adhikari B, Bozilovic J, Diebold M, Schwarz JD, Hofstetter J, Schröder M, et al. Protac-Mediated Degradation Reveals a non-Catalytic Function of AURORA-A Kinase. *Nat Chem Biol* (2020) 16(11):1179–88. doi: 10.1038/s41589-020-00652-y
205. Margueron R, Reinberg D. The Polycomb Complex PRC2 and its Mark in Life [Internet]. *Nature* (2011) 469:343–9. doi: 10.1038/nature09784
206. Zhang H, Zhu D, Zhang Z, Kaluz S, Yu B, Devi NS, et al. Ezh2 Targeting Reduces Medulloblastoma Growth Through Epigenetic Reactivation of the BAI1/p53 Tumor Suppressor Pathway. *Oncogene* (2020) 39(5):1041–8. doi: 10.1038/s41388-019-1036-7
207. Vo BHT, Li C, Morgan MA, Theurillat I, Finkelstein D, Wright S, et al. Inactivation of Ezh2 Upregulates Gfi1 and Drives Aggressive Myc-Driven Group 3 Medulloblastoma. *Cell Rep [Internet]* (2017) 18(12):2907–17. doi: 10.1016/j.celrep.2017.02.073
208. Alimova I, Venkataraman S, Harris P, Marquez VE, Northcott PA, Dubuc A, et al. Targeting the Enhancer of Zeste Homologue 2 in Medulloblastoma. *Int J Cancer* (2012) 131(8):1800–9. doi: 10.1002/ijc.27455
209. Chen L, Alexe G, Dharia NV, Ross L, Iniguez AB, Conway AS, et al. Crispr-Cas9 Screen Reveals a MYCN-amplified Neuroblastoma Dependency on EZH2. *J Clin Invest* (2018) 128(1):446–62. doi: 10.1172/JCI90793

210. Ma A, Stratikopoulos E, Park KS, Wei J, Martin TC, Yang X, et al. Discovery of a First-in-Class Ezh2 Selective Degrader. *Nat Chem Biol* (2020) 16(2):214–22. doi: 10.1038/s41589-019-0421-4
211. Čančer M, Hutter S, Holmberg KO, Rosén G, Sundström A, Tailor J, et al. Humanized Stem Cell Models of Pediatric Medulloblastoma Reveal an Oct4/mTOR Axis That Promotes Malignancy. *Cell Stem Cell* (2019) 25(6):855–70.e11. doi: 10.1016/j.stem.2019.10.005
212. Susanto E, Navarro AM, Zhou L, Sundström A, van Bree N, Stantic M, et al. Modeling SHH-driven Medulloblastoma With Patient Ips Cell-Derived Neural Stem Cells. *Proc Natl Acad Sci USA* (2020) 117(33):20127–38. doi: 10.1073/PNAS.1920521117
213. Tailor J, Kittappa R, Leto K, Gates M, Borel M, Paulsen O, et al. Stem Cells Expanded From the Human Embryonic Hindbrain Stably Retain Regional Specification and High Neurogenic Potency. *J Neurosci* (2013) 33(30):12407–22. doi: 10.1523/JNEUROSCI.0130-13.2013
214. Escudero L, Llort A, Arias A, Diaz-Navarro A, Martínez-Ricarte F, Rubio-Perez C, et al. Circulating Tumour Dna From the Cerebrospinal Fluid Allows the Characterisation and Monitoring of Medulloblastoma. *Nat Commun* (2020) 11(1):1–11. doi: 10.1038/s41467-020-19175-0
215. Wyatt EA, Davis ME. Nanoparticles Containing a Combination of a Drug and an Antibody for the Treatment of Breast Cancer Brain Metastases. *Mol Pharm* (2020) 17(2):717–21. doi: 10.1021/acs.molpharmaceut.9b01167
216. Kim J, Dey A, Malhotra A, Liu J, Ahn SI, Sei YJ, et al. Engineered Biomimetic Nanoparticle for Dual Targeting of the Cancer Stem-Like Cell Population in Sonic Hedgehog Medulloblastoma. *Proc Natl Acad Sci USA* (2020) 117 (39):24205–12. doi: 10.1073/pnas.1911229117
217. Carpentier A, Canney M, Vignot A, Reina V, Beccaria K, Horodyckid C, et al. Clinical Trial of Blood-Brain Barrier Disruption by Pulsed Ultrasound. *Sci Transl Med* (2016) 8(343):343re2–2. doi: 10.1126/scitranslmed.aaf6086

Conflict of Interest: The authors declare that the research was conducted in the absence of any commercial or financial relationships that could be construed as a potential conflict of interest.

frontiers in Oncology

ORIGINAL RESEARCH
published: 25 June 2021
doi: 10.3389/fonc.2021.669667

NLRR1 Is a Potential Therapeutic Target in Neuroblastoma and MYCN-Driven Malignant Cancers

Atsushi Takatori[*], *MD. Shamim Hossain*[†], *Atsushi Ogura*, *Jesmin Akter*[†], *Yohko Nakamura and Akira Nakagawara*[*†]

Division of Innovative Cancer Therapeutics, Chiba Cancer Center Research Institute, Chiba, Japan

Receptor tyrosine kinases (RTKs) receive different modulation before transmitting proliferative signals. We previously identified neuronal leucine-rich repeat 1 (NLRR1) as a positive regulator of EGF and IGF-1 signals in high-risk neuroblastoma cells. Here, we show that NLRR1 is up-regulated in various adult cancers and acts as a key regulator of tumor cell proliferation. In the extracellular domains of NLRR1, fibronectin type III (FNIII) domain is responsible for its function to promote cell proliferation. We generated monoclonal antibodies against the extracellular domains of NLRR1 (N1mAb) and screened the positive N1mAbs for growth inhibitory effect. The treatment of N1mAbs reduces tumor cell proliferation *in vitro* and *in vivo*, and sensitizes the cells to EGFR inhibitor, suggesting that NLRR1 is a novel regulatory molecule of RTK function. Importantly, epitope mapping analysis has revealed that N1mAbs with growth inhibitory effect recognize immunoglobulin-like and FNIII domains of NLRR1, which also indicates the importance of FNIII domain in the function of NLRR1. Thus, the present study provides a new insight into the development of a cancer therapy by targeting NLRR1 as a modulator of proliferative signals on cellular membrane of tumor cells.

Keywords: neuronal leucine-rich repeat 1, neuroblastoma, epidermal growth factor receptor, monoclonal antibody, epitope mapping

OPEN ACCESS

Edited by:
Elena Adinolfi,
University of Ferrara, Italy

Reviewed by:
Letizia Lanzetti,
University of Torino, Italy
Valentina Vultaggio Poma,
University of Ferrara, Italy

****Correspondence:***
Atsushi Takatori
atakatori@chiba-cc.jp
Akira Nakagawara
nakagawara-akira@saga-himat.jp

†Present address:
MD. Shamim Hossain, Department of Neuroinflammation and Brain Fatigue Science, Kyushu University Graduate School of Medical Sciences, Fukuoka, Japan
Jesmin Akter, Department of Clinical Oncology, Saitama Cancer Center, Saitama, Japan
Akira Nakagawara, Saga International Carbon Particle Beam Radiation Cancer Therapy Center, Tosu, Japan

Specialty section:
This article was submitted to Molecular and Cellular Oncology, a section of the journal Frontiers in Oncology

Received: *19 February 2021*
Accepted: *07 June 2021*
Published: *25 June 2021*

Citation:
Takatori A, Hossain MS, Ogura A, Akter J, Nakamura Y and Nakagawara A (2021) NLRR1 Is a Potential Therapeutic Target in Neuroblastoma and MYCN-Driven Malignant Cancers. Front. Oncol. 11:669667. doi: 10.3389/fonc.2021.669667

INTRODUCTION

Neuroblastoma (NB), originally arising from the sympathoadrenal lineage of the neural crest, is one of the most common extracranial solid tumors in childhood. NBs in patients less than 1 year of age often regress spontaneously, resulting in a favorable prognosis (1). In contrast, tumors found over 1 year of age are usually aggressive leading to poor prognosis. A subset of NB with

Abbreviations: ALK, anaplastic lymphoma kinase; DMEM, Dulbecco's Modified Eagle Medium; BrdU, 5-bromo-2-deoxyuridine; DTSSP 3,3′-Dithiobis(sulfosuccinimidylpropionate); EGF, epidermal growth factor; EGFR, epidermal growth factor receptor; FBS, fetal bovine serum; FCM, flow cytometric analysis; FNIII, fibronectin type II; IHA, hemagglutinin; Hpfs, high power fields; Ig, immunoglobulin-like; IGF, insulin-like growth factor; LRR, leucine-rich repeats; N1mAb, monoclonal antibodies against the extracellular domains of NLRR1; NB, neuroblastoma; NLRR, neuronal leucine-rich repeat; mAbs, monoclonal antibodies; PBS, phosphate-buffered saline; qRT-PCR, quantitative real-time RT-PCR; RTK, Receptor tyrosine kinases.

poor prognosis is characterized by the presence of genetic aberrations, such as gain of chromosome 17q, loss of chromosome 11q, and amplification of *MYCN* oncogene (2, 3). MYCN is a nuclear transcription factor and one of the most important prognostic indicators of poor clinical outcome (4). In general, MYCN regulates cell proliferation through transcriptional regulation of its target genes in both positive and negative manners (5, 6). However, genes contributing to tumor growth and aggressiveness of NB under MYCN regulation still remain elusive.

Tumor growth is mediated by the activity of receptor tyrosine kinases (RTKs) functionally regulated by different mechanisms including gene expression, endocytosis, dephosphorylation, and crosstalk with other membrane proteins (7–9). Our previous studies have revealed that neuronal leucine-rich repeat 1 (NLRR1), a type I transmembrane protein, is associated with tumorigenesis by promoting cell proliferation through the activation of ERK mediated by EGF and IGF-1 (10) and negatively regulating anaplastic lymphoma kinase (ALK) (11) in NB, although the contribution of NLRR1 to other types of cancers is not understood. NLRR1 was originally identified in a cDNA project to seek new therapeutic target genes differentially expressed between favorable and unfavorable NBs (12, 13). The human NLRR family consists of three members, NLRR1, NLRR2, and NLRR3. NLRR1 expression is significantly high in advanced stages of NB with poor prognosis, whereas that of NLRR3 is significantly high in early stages of NB with good prognosis (14, 15). Interestingly, transcription of *NLRR1* and *NLRR3* is oppositely regulated by MYCN, a member of MYC family of oncogenes frequently amplified in aggressive NB. These previous findings suggested NLRR1 as an executer protein for aggressiveness of NB under MYCN regulation and a possible therapeutic target to control tumor growth.

In high-risk NB, despite a great improvement of its combinatorial therapy with surgical resection, intensive chemotherapy, radiotherapy, and immunotherapy, only 40 to 50% of patients survive long term (3, 16). Therefore, new and efficient therapeutic strategies are required to improve overall survival of the high-risk group. To date, clinical trials of molecular targeted therapy (e.g. EGFR, IGF-IR, or ALK) have been performed in pediatric solid tumors (17–19). However, more preclinical and clinical trials are needed to identify key targets that can be efficiently exploited therapeutically and help develop a patient-tailored therapy because NB is a heterogeneous tumor (3).

In the present study, we found the up-regulation of NLRR1 expression in various adult cancers and non-NB cell lines. Hybridomas producing monoclonal antibodies (mAbs) to extracellular part of NLRR1 were developed and subjected to screening assays. Monoclonal antibody against NLRR1 (N1mAb) with growth inhibitory effect was found to target the domains of NLRR1 responsible for its function to regulate cell proliferation. Furthermore, the treatment of N1mAb suppressed EGF signals, potentiated the effect of EGFR inhibitor, and decreased the tumor growth in mouse xenograft models.

MATERIALS AND METHODS

Reagents and Antibodies

EGF and IGF-I were from Sigma (St. Louis, MO, USA). Complete protease inhibitor cocktail and phosphatase inhibitor cocktail were from Roche (Indianapolis, IN, USA); 5-bromo-2-deoxyuridine (BrdU) was from Sigma; 3,3′-Dithiobis (sulfosuccinimidylpropionate) (DTSSP) was from Thermo Fisher Scientific (Rockford, IL, USA). Antibodies against phospho-EGFR (#2236), phospho-ERK (#9101), phospho-Akt (#9271), EGFR (#4267), ERK (#9102), Akt (#9272), and myc tag (#2276) were from Cell Signaling Technology (Danvers, MA, USA); anti-β-III tubulin (Tuj1) antibody (#MMS-435P) was from Covance (Princeton, NJ, USA); anti-HA tag antibody (#11867423001) was from Roche; anti-BrdU antibody (#M0744) was from DakoCytomation (Glostrup, Denmark); anti-actin (#A5060) was from Sigma; and the sheep polyclonal anti-NLRR1 antibody (#AF4990) was from R&D Systems (Minneapolis, MN, USA). AG1478 was from Calbiochem (Darmstadt, Germany). Lung and prostate tissue lysate arrays (Tissue Lysate Dipstick Array) were from Protein Biotechnologies (Ramona, CA, USA).

Quantitative Real-Time PCR

Total RNA was extracted from 12 lung adenocarcinoma or nine squamous cell carcinoma and adjacent non-cancerous tissues as well as NB and non-NB cell lines using TRIzol reagent (Invitrogen) according to the manufacturer's instructions, and reverse transcription was performed with SuperScript II reverse transcriptase (Invitrogen). qRT-PCR was carried out using 7500 Real-Time PCR System (Applied Biosystems), according to the manufacturer's protocol. TaqMan probe for *NLRR1* (Assay ID: Hs00979743_m1) and *β-actin* control reagent kit were purchased from Applied Biosystems. The mRNA levels of each gene were standardized by *β-actin*. All human neuroblastoma specimens used in the present study were obtained at various institutions and hospitals in Japan and provided to the Chiba Cancer Center Neuroblastoma Tissue Bank with appropriate informed consent. The procedure of this study was reviewed and approved by the internal review board of Chiba Cancer Center.

Cell Culture

HEK293 and MCF7 cells were cultured in Dulbecco's Modified Eagle Medium (DMEM; Sigma) supplemented with 10% fetal bovine serum (FBS; Invitrogen, Carlsbad, CA, USA). Human neuroblastoma SH-SY5Y and SK-N-BE(2) cells were maintained in RPMI 1640 (Sigma) supplemented with 10% FBS. HEK293 cells were obtained from the JCRB Cell Bank and MCF7 and SH-SY5Y cells were from ATCC, while SK-N-BE(2) cells were purchased from the European Collection of Authenticated Cell Cultures. Mycoplasma contamination was tested by Mycoplasma Detection Set (Takara), and short tandem repeat analysis was performed for cell authentication (Promega). Transient transfection with C-terminal hemagglutinin (HA) or myc-tagged human NLRR1 plasmids was performed using Fugene HD (Roche) or Lipofectamine2000 (Invitrogen) according to the

manufacturer's instructions. Seventy to eighty percent confluent monolayers of transfected cells were treated with growth factors for the indicated times after 16 h serum starvation, and cell lysates were subjected to western blot analyses. Cell proliferation was determined using a Cell Counting Kit-8 (Dojindo, Japan).

Generation of NLRR1 Stable Knockdown Cell Lines Using shRNA Lentiviruses

SK-N-BE cells were infected with four different MISSION lentiviral particles encoding NLRR1 shRNAs (Sigma). NLRR1 shRNA target sequences were as follows: #1, CCGGCCACAACTTTGCGTAT GTGAACTCGAGTTCACATACGCAAAGTTGTGGTTTTTTG; #2, CCGGCCACCTGAACTCCAACAAATTCTCGAG AATTTGTTGGAGTTCAGGTGGTTTTTTG; #3, CCGGG CTGAACAACAATGCCTTGAACTCGAGTTCAAGG CATTGTTGTTCAGCTTTTTTG; and #4, CCGGGCTAGACTT GTTACCTTCGTTCTCGAGAACGAAGGTAACAAGTCTAG CTTTTTTG. Stable cell lines were generated by selection with puromycin (0.8 μg/ml). To exclude the possibility of off-target effects of NLRR1 shRNAs, 3′UTR-targeted #4 shRNA stably expressing SK-N-BE cells were transiently introduced with pcDNA3-NLRR1-HA expression plasmid and subjected to cell proliferation assays, as above.

Histology and Immunostaining

Human tissue array slides were obtained from Super Bio Chips (Seoul, Korea) and subjected to immunostaining using polyclonal anti-NLRR1 antibody (1:25). BrdU was injected intraperitoneally into mice bearing tumors at a dose of 100 μg/g body weight 24 h before autopsy. Tumor tissues were fixed in 4% paraformaldehyde, dehydrated with a graded ethanol series, and embedded in paraffin. Sections (4 μm) were deparaffinized by immersion in xylene and rehydrated, followed by immunostaining for BrdU. Number of BrdU-positive cells was counted in four high power fields (hpfs) of each tumor at ×400 magnification.

Immunoprecipitation and Western Blot Analyses

HEK293 cells expressing HA-tagged and myc-tagged NLRR1 were treated with cross-linker (DTSSP) for 2 h at 4°C. The cell lysates (500–750 μg) were incubated with appropriate antibodies for 1 h at 4°C, followed by incubation with protein G-agarose at 4°C overnight. After extensive washing of the beads with lysis buffer, the immunoprecipitates were detected by western blot analyses. Total cell lysates were resolved by SDS-PAGE followed by western blot detection using the indicated antibodies (1:1,000).

Biotin Labeling on Cell Surface

HEK293 cells were transiently transfected with C-terminal tagged human NLRR1, NLRR2, or NLRR3 plasmids and treated with EZ-Link Sulfo-NHS-LC-LC-Biotin (Thermo Fisher Scientific) or vehicle alone for 30 min at room temperature. Cell lysates (500 μg) were incubated with NeutrAvidin Agarose Resin (Thermo Fisher Scientific). The precipitated proteins were resolved by SDS-PAGE followed by western blot detection using appropriate antibodies.

Generation of Anti-Human NLRR1 Monoclonal Antibodies

The monoclonal antibodies were generated against extracellular domain of NLRR1 (MBL, Nagoya, Japan). The purified proteins of NLRR1 extracellular domain and complete Freund's adjuvant (1:1) were injected into mice. Three days after the final injection, lymph-node cells were removed from immunized mice and were fused with P3U1 myeloma cells at a ratio of 5:1 by the polyethyleneglycol-400 procedure. Cultured supernatants of the hybridomas were screened in transfectants expressing NLRR1 by flow cytometric analysis (FCM) and the binding assay in 96-well plate coated with NLRR1 proteins. After cloning of the hybridomas which showed the positive results in FCM and/or the binding assay, the culture supernatants from wells were tested for growth inhibitory effect by culturing CHP134 cells at 1×10^5/ml in the medium containing 50% of the conditioned medium from the hybridomas. For the positive hybridomas, the monoclonal antibodies were purified by protein A Sepharose column chromatography by MBL.

Characterization of NLRR1 mAb

The isotype of each of the N1mAbs was determined by MBL. The plasmids for NLRR1 lacking the extracellular domains (ΔLRR, ΔIg, and ΔFNIII) were prepared using Infusion (Clontech, Mountain View, CA, USA). Peptide microarray was generated by JPT Peptide Technologies GmbH (Berlin, Germany) and analyzed by SureScan Microarray Scanner (Agilent Technology, Santa Clara, CA, USA). For flow cytometry, HEK293 cells were transiently transfected with the plasmids of NLRR1 lacking the extracellular domains and resuspended in phosphate-buffered saline (PBS). The cells were incubated with N1mAbs for 1 h at 4°C followed by the incubation with Alexa Fluor 488-labeled anti-mouse IgG (Thermo Fisher Scientific). The cells were analyzed using FACSCalibur (BD, San Diego, CA, USA).

Tumor Growth Inhibition Study

SH-SY5Y cells stably expressing NLRR1 were established by transfection followed by selection with G418 at concentration of 600 μg/ml for about 4–6 weeks (10). Seven-week-old SCID mice (Charles River Laboratories) were subcutaneously inoculated with 5 x 10^6 SH-SY5Y cells stably expressing NLRR1 and CHP134 cells in 0.1 ml of PBS/Matrigel. After implantation, tumor sizes were measured using the following formula: $[(\text{width})^2 \times \text{length}]/2$. After tumors became >75 mm^3, mice were randomized into two groups and intraperitoneally administered with vehicle or NLRR1 monoclonal antibody #281 twice a week for 3 weeks. For *in vivo* imaging, N1mAb 281 was labeled with HiLyte Fluor 750 using AnaTag Protein Labeling Kit (AnaSpec, Fremont, CA, USA) and visualized using a Lumazone imaging system (Roper Scientific, Tucson, AZ, USA) after injection into the tail vein. All mice were maintained in a specific pathogen-free animal facility. All animal experiments were approved by the Animal Care and Use Committee of Chiba Cancer Center Research Institute.

Statistical Analysis

Student's *t*-tests (two-tailed) and ANOVA tests were employed to examine the differences between two groups and that of differences between more than two groups, respectively. In xenograft study, the difference between groups was evaluated by two-way repeated measures ANOVA followed by Bonferroni posttest. *, $P < 0.05$; **, $P < 0.01$; and ***, $P < 0.001$ *versus* saline at each time; ##, $P < 0.01$ *versus* saline group.

RESULTS

NLRR1 Expression Is Up-Regulated in Many Cancers

NLRR1 expression is significantly high in advanced stages of NBs with poor clinical outcome (20). High expression of *NLRR1* was also detected in NB cell lines and non-NB cell lines (**Figure S1A**). Here, we further examined NLRR1 expression in various cancer tissues. Immunohistochemistry revealed strong staining in cancer tissues from skin, lung, and breast as compared with the corresponding normal tissues (**Figures 1A** and **S1B**). Higher expression of NLRR1 in adult cancer tissues (lung and prostate) compared to normal tissue was also indicated by tissue lysate arrays (**Figure S1C**). To confirm the elevated expression of *NLRR1*, we measured mRNA expression in primary lung cancers by quantitative real-time RT-PCR (qRT-PCR). High expression of *NLRR1* was observed in tumorous tissues; eight out of twelve adenocarcinomas and three out of nine squamous cell carcinomas showed more than two-fold higher expression of *NLRR1* than normal tissues (**Figure 1B**). These data suggest that NLRR1 may contribute to the malignant status and serve as a biomarker not only in NB, but also in adult cancers.

NLRR1 Increases Cell Proliferation by Enhancing the Cellular Signals of EGF and IGF

Similar to our previous observation in NB cells (10), overexpression of NLRR1 increased the cell growth in NLRR1-low-expressing MCF7 breast cancer cells (**Figure 1C**) and the activation of ERK in the cells was enhanced when treated with EGF and IGF in dose-dependent manner (**Figures 1D, E**) and time-dependent manner (**Figure S2**). To confirm the requirement of NLRR1 for cell proliferation, we performed NLRR1 depletion using lentiviral shRNAs in SK-N-BE NB cells with a moderate level of NLRR1 expression (10). Four different lentiviruses were prepared for stable cell lines and NLRR1 knockdown dramatically diminished cell proliferation (**Figure S3A**). The reduced proliferation with shRNA targeting 3′-UTR region of *NLRR1* was recovered by exogenous NLRR1 expression in a dose-dependent manner (**Figure S3B**), suggesting that NLRR1 expression is crucial to maintain normal cell proliferation.

FNIII Domain Is the Functional Region of NLRR1 Required for Enhancing Growth Signaling

NLRR1 is a glycosylated transmembrane protein with external leucine-rich repeats (LRRs), immunoglobulin-like (Ig), fibronectin type III (FNIII) domains and a short intracellular tail. To identify the functional domains of NLRR1, we constructed the expression vectors of NLRR1 with the deletions in extracellular domains (ΔLRR, ΔIg, and ΔFNIII). Cell growth assay in MCF7 cells expressing the deletion mutant NLRR1 revealed that the deletion of FNIII domain significantly reduced the cell growth compared to wild-type NLRR1 (**Figure 1F**). In addition, the phosphorylation of ERK upon EGF treatment was diminished in ΔFNIII-expressing cells, while NLRR1 lacking ΔLRR had a comparable phospho-ERK. Of note, the deletion of Ig domain resulted in the reduced activation of ERK upon EGF treatment (**Figure 1G**). These data suggest that FNIII domain is a responsible domain of NLRR1 to enhance EGF signaling and increase cell proliferation and that Ig domain has an auxiliary function to support FNIII domain.

N1mAb Suppresses Cell Proliferation

To produce mAbs against NLRR1, the purified proteins of NLRR1 extracellular domain were used to immunize mice. To obtain a mAb that blocks the function of NLRR1, we tested cultured supernatants from candidate hybridomas sequentially by FCM and ELISA (**Figure S4A**). The positive cultured supernatants were further examined in growth inhibition assays using NLRR1-expressing cells. The cell growth treated with NLRR1 IgG mAbs of No. 240, 281, and 300, was suppressed, while little effect was observed by FCM-negative NLRR1 mAb No. 23 (**Figure S4B**). After purification of the positive IgG mAbs, CHP134 NB cells were cultured in the medium containing varying amounts of the purified candidate mAbs. Four days after treatment, the proliferation of cells was greatly inhibited by NLRR1 mAbs, especially by N1mAb 281 and 300, in a dose-dependent manner (**Figure 2A**). Among the mAbs, N1mAb281 was more effective in suppressing cell proliferation compared to other mAbs, and it was selected for further investigation. The growth inhibition assay using N1mAb281 was performed in NB cells (SK-N-DZ, NLF, SK-N-BE), breast cancer cells (MCF7), and lung cancer cells (A549). The treatment with high dose of N1mAb281 (100 μg/ml) significantly suppressed cell growth in NLF and SK-N-BE cells, while the marginal inhibitory effect was observed in SK-N-DZ, MCF7 and A549 cells (**Figure 2B**).

The Treatment of N1mAb Inhibits Tumor Growth

We next checked the efficacy of N1mAb treatment in xenograft model using SCID mice bearing NLRR1-stably expressing SH-SY5Y (SH-SY5Y/NLRR1) tumors. Even at relatively low dose (100 μg, twice a week), treatment of N1mAb led to significant suppression of tumor growth of SH-SY5Y/NLRR1 cells, strongly supporting the growth inhibitory effect of N1mAb (**Figure 3A**). The localization of N1mAb in the tumor was confirmed using near-infrared fluorescent-labeled N1mAb 281 systemically administered by tail vein injection (**Figure S5**). We further determined the antitumor effect of N1mAb on endogenously expressed NLRR1 in CHP134 tumor xenograft. As shown in **Figure 3B**, N1mAb treatment (200 μg, twice a week) significantly reduced the tumor growth with 51% tumor regression without a

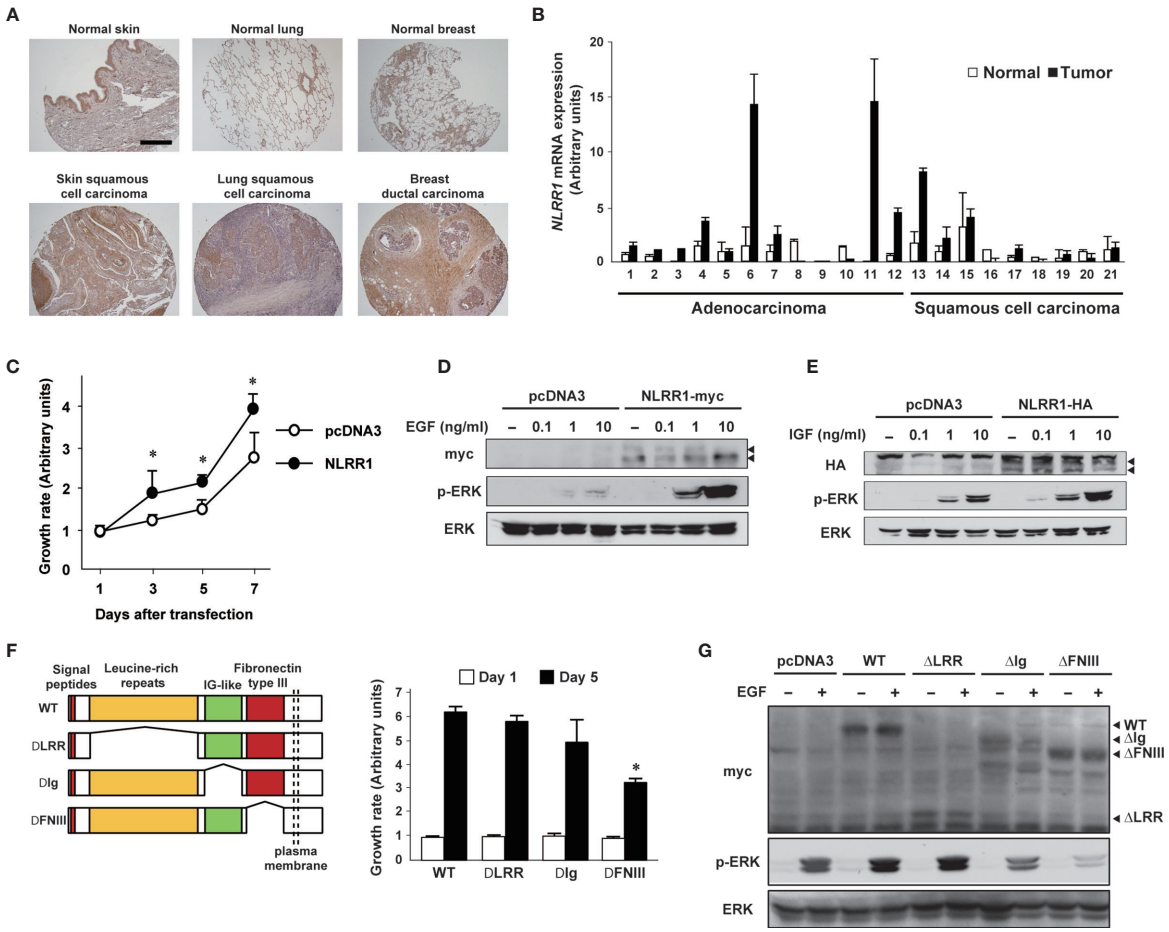

FIGURE 1 | NLRR1 is up-regulated in various cancers and the Ig and FNIII domains are responsible for its function. **(A)** Immunohistochemistry using anti-N-terminal NLRR1 antibody in human normal and cancerous skin, lung, and breast tissue. The scale bar represents 500 μm. **(B)** Relative expression levels of NLRR1 mRNA in normal and lung carcinoma tissues (twelve adenocarcinoma and nine squamous cell carcinoma). Relative expression levels of *NLRR1* mRNA were determined by calculating the ratio between *β-actin* and *NLRR1*. **(C)** Overexpression of NLRR1 tagged with myc in NLRR1 low-expressing MCF7 cells promotes cell proliferation. Quantification of cell proliferation was performed by WST-8 assays. Results are given as mean ± SD. *$P < 0.05$, compared to pcDNA3. **(D, E)** NLRR1-expressing cells show ERK activation upon EGF and IGF treatment at low concentrations. MCF7 cells were transfected with pcDNA3-NLRR1 and treated with different concentrations of EGF **(D)** or IGF **(E)**. Ten minutes after treatment, the cell lysates were collected. Arrowheads, glycosylated NLRR1. **(F)** Deletion of FNIII domain resulted in a marked suppression of cell growth in MCF7 cells. Wild-type (WT) of NLRR1 or deletion mutants lacking leucine-rich repeats (LRR), immunoglobulin-like (Ig) or fibronectin type III (FNIII) were transiently expressed in MCF7 cells and subjected to WST-8 assays. Data were normalized to the results at Day 1 and indicated as mean ± SD. *$P < 0.05$, compared to WT. **(G)** FNIII domain is responsible for enhancing ERK phosphorylation upon EGF treatment. MCF7 cells expressing NLRR1 deletion mutants were treated with EGF (10 ng/ml) for 10 min, and the cell lysates were subjected to western blot analyses.

loss of body weight (data not shown). To examine the effect of N1mAb in cell proliferation *in vivo*, we performed immunohistochemistry for BrdU-labeled cells and found that the number of BrdU positive cells was significantly decreased in N1mAb-treated CHP134 xenograft tumors (**Figures 3C, D**). Hence, we concluded that the treatment of N1mAb induces growth inhibitory effect *in vitro* and *in vivo*.

N1mAb 281 Binds to Ig and FNIII Domains of NLRR1

To elucidate the mechanism of growth inhibition by N1mAb, the binding property of N1mAb 281 was examined by immunoprecipitation and indirect flow cytometry. HEK293 cells overexpressing HA-tagged NLRR1 were subjected to immunoprecipitation assay. As shown in **Figure 4A**, HA-tagged NLRR1 was immunoprecipitated with N1mAb 281. To further examine a responsible region of NLRR1 protein for the binding of N1mAb 281, HEK293 cells transfected with expression vectors of NLRR1 wild-type, ΔLRR, ΔIg, or ΔFNIII were immunostained with N1mAb 281 followed by Alexa Fluor 488 conjugated anti-mouse IgG. The population of NLRR1-expressed cells detected by N1mAb 281 was decreased by deletion of Ig and FNIII domains, while NLRR1 lacking LRR domain exhibited little change compared to NLRR1 wild-type (**Figure 4B**). According to these results, we postulated that N1mAb 281 binds to Ig and/or FNIII domains of NLRR1. To identify the epitope sites recognized by N1mAb 281, we

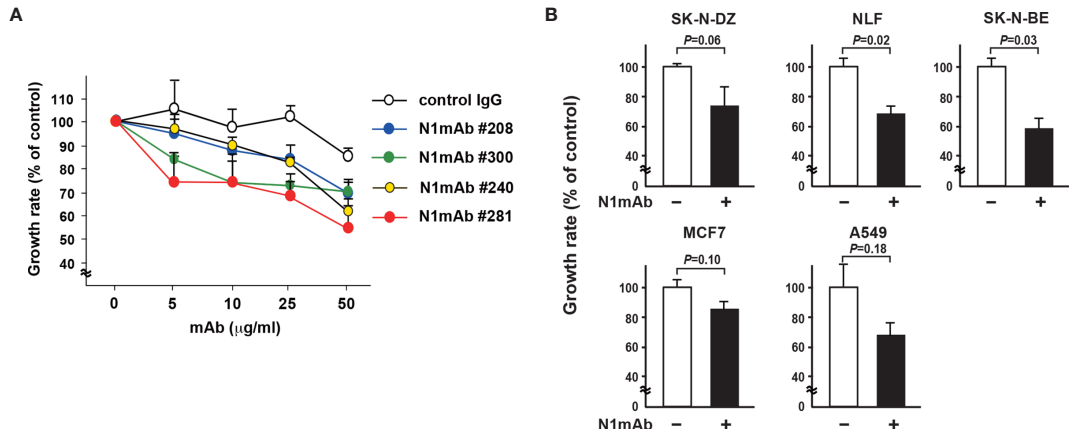

FIGURE 2 | Generation of monoclonal antibodies against the extracellular domain of NLRR1 with growth inhibitory effect. **(A)** CHP134 NB cells were cultured in the medium containing varying amounts of the purified candidate mAbs. Four days after treatment, the proliferation of cells was subjected to WST-8 assays. Data were normalized to the results for untreated cells and represented as percentage of control (mean ± SD). **(B)** NB cells (SK-N-DZ, NLF, SK-N-BE), breast cancer cells (MCF7), and lung cancer cells (A549) were treated with N1mAb 281 at 100 μg/ml for 5 days. Quantification of cell proliferation was performed by WST-8 assays. Data are presented as the mean ± SD. The *P*-value was determined by the unpaired *t*-test.

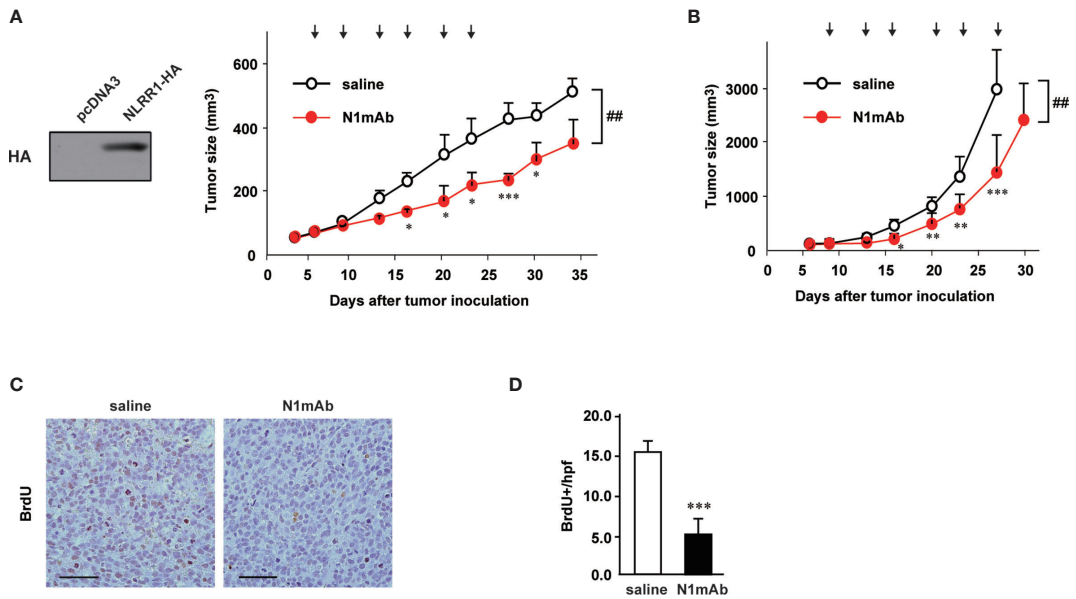

FIGURE 3 | NLRR1 monoclonal antibody inhibits NB tumor growth *in vivo*. **(A)** Female SCID mice were subcutaneously inoculated with SH-SY5Y cells stably expressing NLRR1 and randomized into two groups (seven mice per group). Mice were i.p. injected with saline or N1mAb 281 (100 μg) twice a week for 3 weeks (arrows). Data are shown as mean tumor volume ± SD. **(B)** SCID mice (seven mice per group) bearing CHP134 xenografts were injected i.p. with saline or N1mAb 281 (200 μg) twice a week for 3 weeks (arrows). The difference between groups was evaluated by two-way repeated measures ANOVA followed by Bonferroni posttest. $^{*}P < 0.05$; $^{**}P < 0.01$; and $^{***}P < 0.001$ *versus* saline at each time; $^{\#\#}P < 0.01$ *versus* saline group. **(C)** Twenty-four hours after BrdU administration (100 μg/g of body weight), all mice bearing CHP134 tumors in **(B)** were sacrificed and the paraffin sections of tumor tissues were subjected to BrdU immunohistochemistry to quantify cell proliferation. **(D)** The number of BrdU-positive cells in tumor tissues was counted per high power field (hpf). Data are mean ± SD obtained from seven mice for each group.

next generated 12-amino acid peptide microarray against Ig and FNIII domains from Pro 424 to Thr 614 (**Figure 4C**). As shown in **Figure 4D**, positive signals on microarrays in three independent experiments of immunostaining with N1mAb 281 were obtained mainly with the two regions of spots in Ig domain and three regions in FNIII domain (**Figure 4E**). These data suggest that the N1mAb 281 can recognize the discontinuous epitopes of Ig and FNIII domains in the extracellular part of NLRR1. We failed to detect

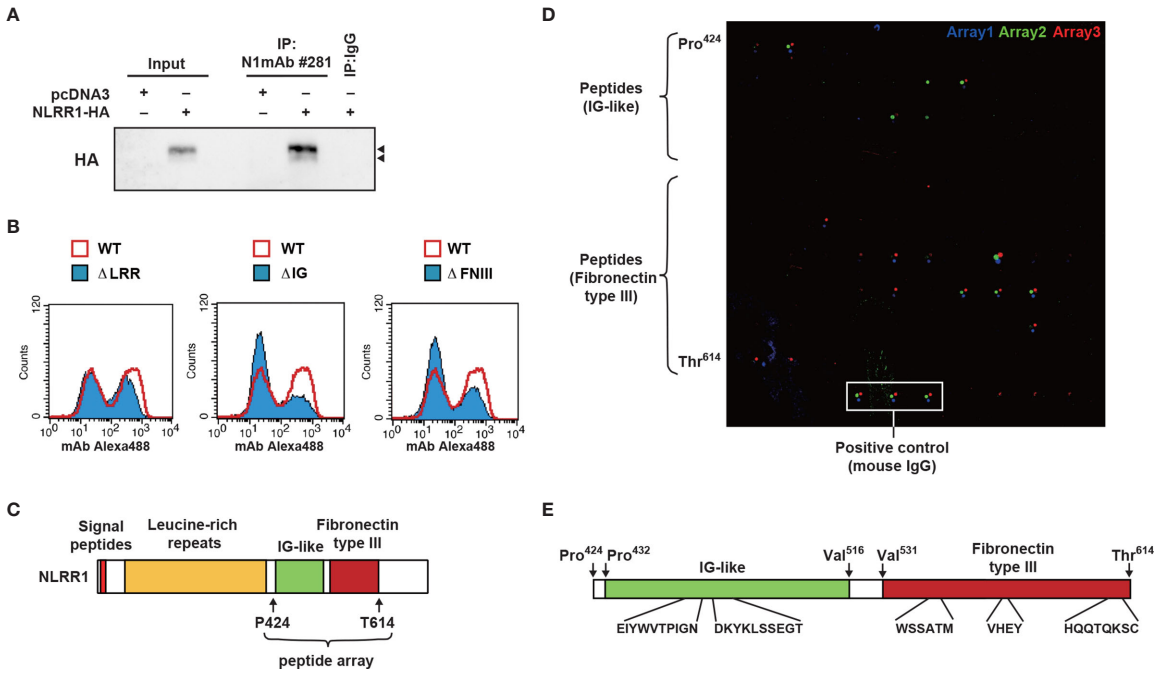

FIGURE 4 | Epitope mapping of N1mAb 281 using a peptide microarray. **(A)** HA-tagged NLRR1 was expressed in HEK293 cells, and the cell lysates were subjected to immunoprecipitation using N1mAb 281. Normal mouse IgG was used as a negative control. NLRR1 protein was detected by anti-HA antibody. Input represents 2% of the total lysates used for immunoprecipitation. Arrowheads, glycosylated NLRR1. **(B)** HEK293 cells were transfected with plasmids encoding wild-type (WT) of NLRR1 or deletion mutants lacking leucine-rich repeats (LRRs), immunoglobulin-like (Ig), or fibronectin type III (FNIII). The binding of N1mAb 281 was assessed by flow cytometry to find the domains recognized by the antibody. **(C)** Schematic representation of NLRR1. Peptide microarray was prepared for Ig and FNIII domains by spotting 91 overlapping 12-mer peptides and immunostained with N1mAb 281. **(D)** Bound antibodies were detected with Alexa 546-labeled anti-mouse IgG. The scanned arrays obtained from three independent experiments were indicated. **(E)** Sequence of the peptides positive for all three independent experiments are indicated.

the bands of NLRR1 by western blot analysis using N1mAb 281 (data not shown), indicating that the antibody binds to the two domains of NLRR1 in a conformation-dependent manner. We further examined the epitope sites recognized by the other N1mAbs, 300 and 240 (growth inhibitory effect positive and negative, respectively). N1mAb 300, which showed a comparable growth inhibitory effect to N1mAb 281 (**Figure 2A**), detected the peptides from both Ig and FNIII domains, whereas N1mAb 240 with a weak growth inhibitory effect showed no signals in the peptide microarray (**Figure S6**). These results suggest that the growth inhibitory effect of N1mAb 281 is exerted through binding to Ig and FNIII domains of NLRR1.

Combinatory Use of N1mAb With EGFR Inhibitor Is Effective in the Resistant Cancer Cells

Next, we tested N1mAbs for the combinatorial effect with EGFR inhibitor because previous reports showed that EGFR is expressed in NB and adult cancers and could be a therapeutic target for these tumors (21, 22). The results in **Figure 5A** demonstrate that the additional treatment with N1mAb 281 resulted in the reduced cell proliferation at low concentration of AG1478 EGFR inhibitor. Compared with AG1478 alone, treatment with N1mAb 281 reduced 40% of viable cells co-treated with AG1478. In AG1478-resistant lung cancer A549 cells, N1mAb #281 treatment increased the sensitivity to AG1478 treatment (**Figure 5B**). A similar result was obtained by N1mAb 300 (**Figure S7**). In addition, the activation of EGF signals was examined in N1mAb pre-treated SH-SY5Y/NLRR1 cells. The phosphorylation of EGFR, HER2, and the downstream molecules, Akt and ERK, was greatly decreased by N1mAb 281 treatment (**Figure 5C**). The reduced downstream signals upon EGF treatment were also observed in NLRR1-stably expressing MCF7 cells (**Figure 5D**). Because NLRR1 knockdown in SK-N-BE cells resulted in the impaired cell proliferation (**Figure S3**), we treated the cells with N1mAb for 7 days to check the influence on EGF signaling molecules. As shown in **Figure 5E**, N1mAb treatment down-regulated ERK activation, although the reduced expression of EGFR and phosphorylation of Akt was observed only in N1mAb 281-treated cells. Of note, N1mAb treatment increased the expression of HER2 and NLRR1, implying a mechanism of feedback up-regulation of the expression against NLRR1 inhibition. Thus, N1mAb treatment suppresses EGF signals and sensitizes the cells to the growth suppression induced by EGFR inhibitor treatment.

To understand the mechanism how N1mAb inhibits the function of NLRR1, we first performed immunoprecipitation assay using vectors for two different tagged NLRR1 and found

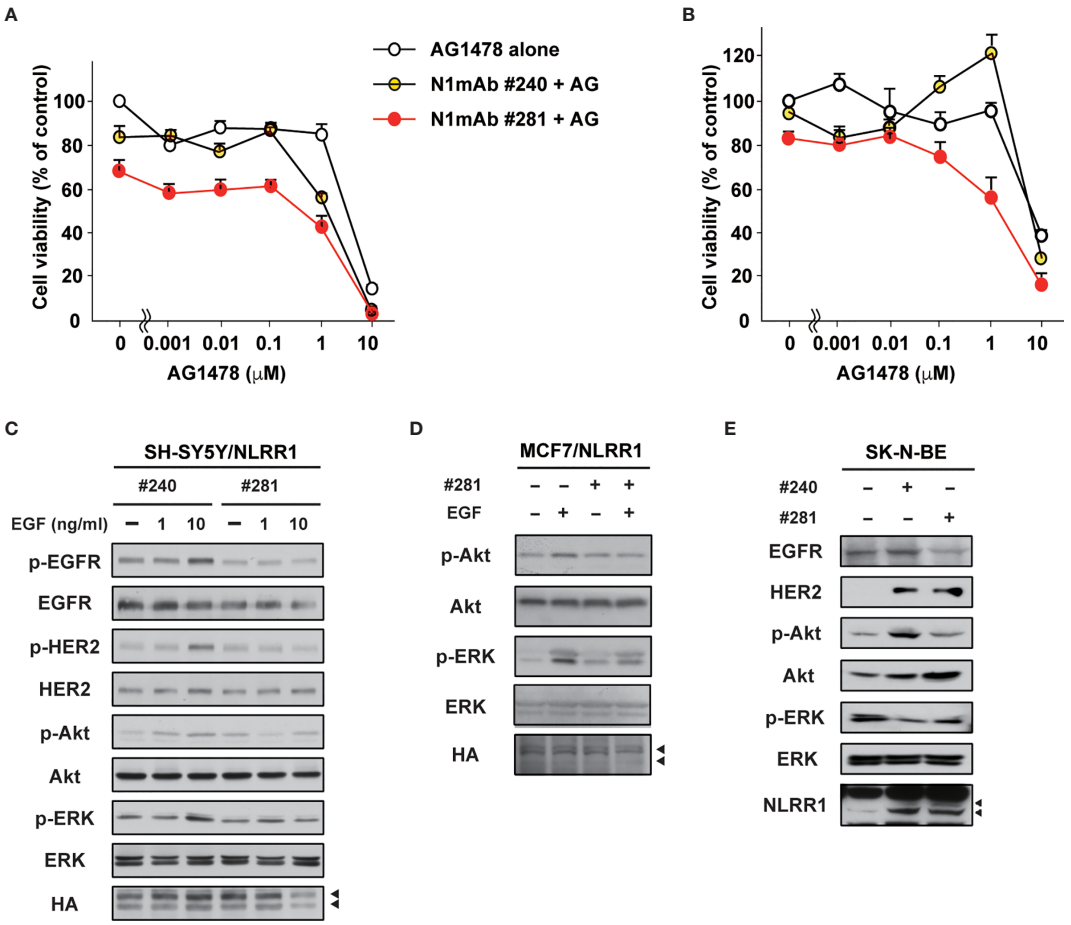

FIGURE 5 | N1mAbs potentiates EGFR inhibitor-induced growth suppression. **(A)** NLRR1-stably expressing SH-SY5Y cells were treated with N1mAb 281 (25 μg/ml) and different concentrations of AG1478 (AG) for 72 h Data are represented as mean ± SD. Quantification of cell proliferation was performed by WST-8 assays. Data were normalized to the results for untreated cells and represented as percentage of control (mean ± SD). **(B)** AG1478-resistant A549 cells were treated with N1mAb 281 and different concentrations of AG1478 for 72 h **(C)** NLRR1-stably expressing SH-SY5Y cells were starved and treated with N1mAb 240 or 281 at 25 μg/ml for 3 h, followed by EGF treatment at the indicated concentration for 10 min. Cell lysates were subjected to western blot analyses. Arrowheads, glycosylated NLRR1. **(D)** MCF7 cells overexpressing NLRR1 were starved and treated with N1mAb 281 at 25 μg/ml for 3 h, followed by EGF treatment (1 ng/ml) for 10 min. The cell lysates were subjected to western blot analyses. **(E)** To check the effect of the long-term treatment of N1mAbs, SK-N-BE cells were incubated with N1mAbs (30 μg/ml) for 7 days with medium change every 2 days, and the cell lysates were subjected to western blot analyses.

that NLRR1 proteins form self-multimers (**Figures 6A** and **S8A**). Because cell surface biotinylation confirmed the localization of NLRR1 to the cell surface (**Figure S8B**), we postulated that NLRR1 might be present on the cell surface as self-multimer. Therefore, we pre-treated the cells expressing the two different tagged NLRR1 with N1mAbs and found that N1mAb 281 blocked the self-multimerization of NLRR1, whereas N1mAb 23, a negative control antibody, showed little or no effect (**Figures 6B** and **S8C**). To further examine the importance of NLRR1 self-interaction on its function, we prepared conditioned medium from HEK293 cells expressing extracellular domain of NLRR1 (**Figure 6C**). Treatment of the conditioned medium containing 10% FBS induced phosphorylation of ERK in control MCF7 cells, whereas NLRR1-expressing cells had no phosphorylation of ERK at 15 min after treatment (**Figure 6D**). These data suggest that the inhibition of self-multimerization by the antibody or free extracellular protein of NLRR1 blocks the function of NLRR1 and represses growth-promoting intracellular signals.

DISCUSSION

We demonstrate that NLRR1 expression is up-regulated in adult cancer tissues including lung and breast in addition to unfavorable NBs. NLRR1 is involved in determining the malignant status of cancer cells by enhancing the proliferative signaling of EGFR and IGF-IR. This is unique to NLRR1 among NLRR family members despite their close similarity in protein structures with high evolutional conservation (15). EGFR family receptors and IGF-IR, expressed in a wide variety of human cancers including NB, contribute to cell proliferation and tumor

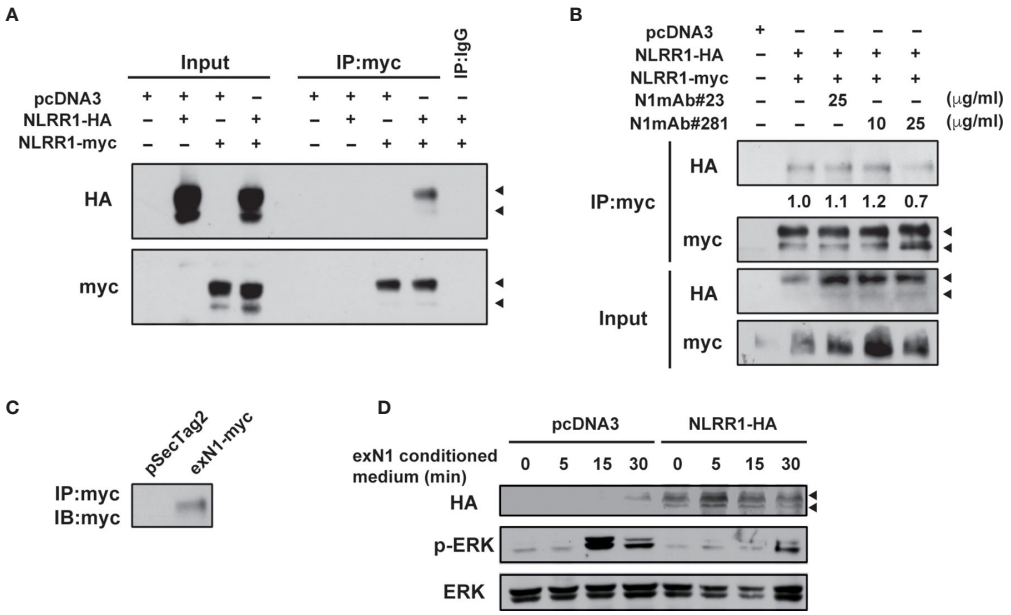

FIGURE 6 | N1mAb 281 blocks the self-interaction of NLRR1 on cell surface. **(A)** HA-tagged and myc-tagged NLRR1 were expressed in HEK293 cells and the cell lysates were collected after crosslinking with membrane-impermeable DTSSP. Immunoprecipitation was performed using anti-myc antibody, and the immunoprecipitates were subjected to western blot analyses. Arrowheads, glycosylated NLRR1. **(B)** HA-tagged NLRR1 co-immunoprecipitated with myc-tagged NLRR1 was reduced by N1mAb 281 treatment. HEK293 cells expressing HA-tagged and myc-tagged NLRR1 were treated with N1mAb 23 or 281 at the indicated concentration for 3 h The cell lysates were collected after DTSSP treatment and subjected to immunoprecipitation using anti-myc antibody. **(C)** HEK293 cells were transfected with pSecTag2 vector (Invitrogen) containing the extracellular domain of NLRR1 tagged with myc (exN1). The secreted exN1 protein in the conditioned medium supplemented with 10% FBS was confirmed by immunoprecipitation using anti-myc antibody. **(D)** MCF7 cells were transfected with empty or pcDNA3-NLRR1-HA vectors and treated with the conditioned medium containing exN1 **(C)** for the indicated time. The cell lysates were collected and subjected to western blot analyses.

progression (23, 24). However, their expression levels in NB show no apparent correlation with the tumor stages (21, 25). On the other hand, high levels of NLRR1 expression are significantly associated with poor prognosis of NB (14, 20). Therefore, it is likely that the clinical significance of EGFR and IGF-IR in the pathogenesis of NB is at least in part inferred from their co-expression with NLRR1.

Transmembrane proteins that function to regulate cell proliferation have been the most popular candidates for therapeutic targets to develop a novel remedy against cancers. In particular, kinase inhibitors and neutralizing antibodies have been developed against RTKs of which the knockdown expression shows a great repression of cell growth and survival. Given that NLRR1 knockdown repressed NB cell proliferation, these lines of evidence regarding NLRR1 function in the present study may provide us an attractive scientific basis for targeting NLRR1. Three possible mechanisms of the inhibitory effect by single usage of NLRR1 antibody are hypothesized: [1] inhibition of NLRR1 self-dimerization which is shown in **Figure 6B**, although it is not clear yet whether N1mAb can recognize the dimeric conformation of NLRR1 Ig and FNIII domains, [2] induction of NLRR1 internalization, and [3] competitive inhibition of an endogenous unknown ligand for NLRR1. Further experiments may answer these remaining questions partly by investigating NLRR1 trafficking upon antibody treatment.

Our present characterization of epitopes recognized by N1mAbs revealed that N1mAbs with growth inhibitory activity bind to Ig and FNIII domains of NLRR1 (**Figure 4**). It is noteworthy to mention that, by the deletion mutant experiments, the same domains of NLRR1 were demonstrated to be required for its function in the regulation of cell proliferation (**Figure 1**). These data suggest that the Ig and FNIII domains are ideal antigen to raise a therapeutic antibody with potent growth inhibitory activity for malignant tumors with NLRR1 expression. The epitope sites of human NLRR1 recognized by N1mAbs have 100% identity to the sequence corresponding to mouse Nlrr1. The treatment of N1mAb in mice showed no influence on the gain of body weight and health condition, suggesting that the possible adverse effects by anti-NLRR1 therapy might be small.

We also tested combinatorial use of N1mAb with EGFR kinase inhibitor. At present, it has been proposed that partial inhibition of multiple targets could be more effective than full inhibition of a single molecule in NB therapy (3, 26). Indeed, N1mAb has more intensive inhibitory effect in combination with EGFR inhibitor, which may offer a novel therapeutic option to address some issues including acquired resistance and adverse effects arising from molecular targeting treatments (27).

Thus, we propose here that NLRR1 is a novel molecular target for treating particular cancers including NB and that its function to regulate growth signals is dependent on its extracellular domain which can be a target for antibody-based therapy of NLRR1-expressing cancers.

DATA AVAILABILITY STATEMENT

The raw data supporting the conclusions of this article will be made available by the authors, without undue reservation.

ETHICAL STATEMENT

Ethical review and approval was not required for the study on human participants in accordance with the local legislation and institutional requirements. Written informed consent for participation was not required for this study in accordance with the national legislation and the institutional requirements. The animal study was reviewed and approved by Animal Care and Use Committee of Chiba Cancer Center Research Institute.

AUTHOR CONTRIBUTIONS

AT and AN conceived and designed the experiments. AT, SH, AO, JA, and YN performed the experiments. AT, SH, and AN analyzed the data. YN contributed reagents/materials/analysis tools. AT and AN wrote the paper. All authors contributed to the article and approved the submitted version.

FUNDING

This work was supported by a Grant-in-Aid from the Japan Ministry of Health, Labour and Welfare for Third Term Comprehensive Control Research for Cancer to AN, JSPS KAKENHI Grant Number JP21390317, JP24249061 to AN, JP19890276 to AT, MEXT KAKENHI Grant Number JP22791016 to AT, and a grant from the Takeda Science Foundation to AN.

ACKNOWLEDGMENTS

We thank. M. Ohira, Yuki Nakamura and M. Fukuda (Chiba Cancer Center Research Institute, Chiba, Japan) for their technical advice and excellent assistance.

SUPPLEMENTARY MATERIAL

The Supplementary Material for this article can be found online at: https://www.frontiersin.org/articles/10.3389/fonc.2021.669667/full#supplementary-material

REFERENCES

1. Brodeur GM. Neuroblastoma: Biological Insights Into a Clinical Enigma. *Nat Rev Cancer* (2003) 3(3):203–16. doi: 10.1038/nrc1014
2. Kohl NE, Gee CE, Alt FW. Activated Expression of the N-Myc Gene in Human Neuroblastomas and Related Tumors. *Science* (1984) 226 (4680):1335–7. doi: 10.1126/science.6505694
3. Park JR, Eggert A, Caron H. Neuroblastoma: Biology, Prognosis, and Treatment. *Hematol Oncol Clin North Am* (2010) 24(1):65–86. doi: 10.1016/j.hoc.2009.11.011
4. Cohn SL, Tweddle DA. MYCN Amplification Remains Prognostically Strong 20 Years After Its "Clinical Debut". *Eur J Cancer* (2004) 40(18):2639–42. doi: 10.1016/j.ejca.2004.07.025
5. Blackwood EM, Kretzner L, Eisenman RN. Myc and Max Function as a Nucleoprotein Complex. *Curr Opin Genet Dev* (1992) 2(2):227–35. doi: 10.1016/S0959-437X(05)80278-3
6. Staller P, Peukert K, Kiermaier A, Seoane J, Lukas J, Karsunky H, et al. Repression of P15ink4b Expression by Myc Through Association With Miz-1. *Nat Cell Biol* (2001) 3(4):392–9. doi: 10.1038/35070076
7. Sorkin A, Goh LK. Endocytosis and Intracellular Trafficking of ErbB. *Exp Cell Res* (2009) 315(4):683–96. doi: 10.1016/j.yexcr.2008.07.029
8. Ivaska J, Heino J. Cooperation Between Integrins and Growth Factor Receptors in Signaling and Endocytosis. *Annu Rev Cell Dev Biol* (2011) 27:291–320. doi: 10.1146/annurev-cellbio-092910-154017
9. Jin W, Chen BB, Li JY, Zhu H, Huang M, Gu SM, et al. TIEG1 Inhibits Breast Cancer Invasion and Metastasis by Inhibition of Epidermal Growth Factor Receptor (EGFR) Transcription and the EGFR Signaling Pathway. *Mol Cell Biol* (2012) 32(1):50–63. doi: 10.1128/MCB.06152-11
10. Hossain S, Takatori A, Nakamura Y, Suenaga Y, Kamijo T, Nakagawara A. NLRR1 Enhances EGF-Mediated MYCN Induction in Neuroblastoma and Accelerates Tumor Growth *In Vivo*. *Cancer Res* (2012) 72(17):4587–96. doi: 10.1158/0008-5472.CAN-12-0943
11. Satoh S, Takatori A, Ogura A, Kohashi K, Souzaki R, Kinoshita Y, et al. Neuronal Leucine-Rich Repeat 1 Negatively Regulates Anaplastic Lymphoma Kinase in Neuroblastoma. *Sci Rep* (2016) 6:32682. doi: 10.1038/srep32682
12. Ohira M, Morohashi A, Inuzuka H, Shishikura T, Kawamoto T, Kageyama H, et al. Expression Profiling and Characterization of 4200 Genes Cloned From Primary Neuroblastomas: Identification of 305 Genes Differentially Expressed Between Favorable and Unfavorable Subsets. *Oncogene* (2003) 22(35):5525–36. doi: 10.1038/sj.onc.1206853
13. Ohira M, Oba S, Nakamura Y, Isogai E, Kaneko S, Nakagawa A, et al. Expression Profiling Using a Tumor-Specific cDNA Microarray Predicts the Prognosis of Intermediate Risk Neuroblastomas. *Cancer Cell* (2005) 7(4):337–50. doi: 10.1016/j.ccr.2005.03.019
14. Hossain MS, Ozaki T, Wang H, Nakagawa A, Takenobu H, Ohira M, et al. N-MYC Promotes Cell Proliferation Through a Direct Transactivation of Neuronal Leucine-Rich Repeat Protein-1 (NLRR1) Gene in Neuroblastoma. *Oncogene* (2008) 27(46):6075–82. doi: 10.1038/onc.2008.200
15. Akter J, Takatori A, Hossain MS, Ozaki T, Nakazawa A, Ohira M, et al. Expression of NLRR3 Orphan Receptor Gene Is Negatively Regulated by MYCN and Miz-1, and Its Downregulation Is Associated With Unfavorable Outcome in Neuroblastoma. *Clin Cancer Res* (2011) 17(21):6681–92. doi: 10.1158/1078-0432.CCR-11-0313
16. Pinto NR, Applebaum MA, Volchenboum SL, Matthay KK, London WB, Ambros PF, et al. Advances in Risk Classification and Treatment Strategies for Neuroblastom. *J Clin Oncol* (2015) 33(27):3008–17. doi: 10.1200/JCO.2014.59.4648
17. Mellinghoff IK, Wang MY, Vivanco I, Haas-Kogan DA, Zhu S, Dia EQ, et al. Molecular Determinants of the Response of Glioblastomas to EGFR Kinase Inhibitors. *N Engl J Med* (2005) 353(19):2012–24. doi: 10.1056/NEJMoa051918

18. Kolb EA, Gorlick R, Lock R, Carol H, Morton CL, Keir ST, et al. Initial Testing (Stage 1) of the IGF-1 Receptor Inhibitor BMS-754807 by the Pediatric Preclinical Testing Program. *Pediatr Blood Cancer* (2011) 56(4):595–603. doi: 10.1002/pbc.22741
19. Mosse YP, Lim MS, Voss SD, Wilner K, Ruffner K, Laliberte J, et al. Safety and Activity of Crizotinib for Paediatric Patients With Refractory Solid Tumours or Anaplastic Large-Cell Lymphoma: A Children's Oncology Group Phase 1 Consortium Study. *Lancet Oncol* (2013) 14(6):472–80. doi: 10.1016/S1470-2045(13)70095-0
20. Hamano S, Ohira M, Isogai E, Nakada K, Nakagawara A. Identification of Novel Human Neuronal Leucine-Rich Repeat (hNLRR) Family Genes and Inverse Association of Expression of Nbla10449/hNLRR-1 and Nbla10677/hNLRR-3 With the Prognosis of Primary Neuroblastomas. *Int J Oncol* (2004) 24(6):1457–66. doi: 10.3892/ijo.24.6.1457
21. Ho R, Minturn JE, Hishiki T, Zhao H, Wang Q, Cnaan A, et al. Proliferation of Human Neuroblastomas Mediated by the Epidermal Growth Factor Receptor. *Cancer Res* (2005) 65(21):9868–75. doi: 10.1158/0008-5472.CAN-04-2426
22. Michaelis M, Bliss J, Arnold SC, Hinsch N, Rothweiler F, Deubzer HE, et al. Cisplatin-Resistant Neuroblastoma Cells Express Enhanced Levels of Epidermal Growth Factor Receptor (EGFR) and Are Sensitive to Treatment With EGFR-Specific Toxins. *Clin Cancer Res* (2008) 14(20):6531–7. doi: 10.1158/1078-0432.CCR-08-0821
23. Janet T, Ludecke G, Otten U, Unsicker K. Heterogeneity of Human Neuroblastoma Cell Lines in Their Proliferative Responses to Basic FGF, NGF, and EGF: Correlation With Expression of Growth Factors and Growth Factor Receptors. *J Neurosci Res* (1995) 40(6):707–15. doi: 10.1002/jnr.490400602
24. Kurihara S, Hakuno F, Takahashi S. Insulin-Like Growth Factor-I-Dependent Signal Transduction Pathways Leading to the Induction of Cell Growth and Differentiation of Human Neuroblastoma Cell Line SH-SY5Y: The Roles of MAP Kinase Pathway and PI 3-Kinase Pathway. *Endocr J* (2000) 47(6):739–51. doi: 10.1507/endocrj.47.739
25. Opel D, Poremba C, Simon T, Debatin KM, Fulda S. Activation of Akt Predicts Poor Outcome in Neuroblastoma. *Cancer Res* (2007) 67(2):735–45. doi: 10.1158/0008-5472.CAN-06-2201
26. Verissimo CS, Molenaar JJ, Fitzsimons CP, Vreugdenhil E. Neuroblastoma Therapy: What Is in the Pipeline? *Endocr Relat Cancer* (2011) 18(6):R213–231. doi: 10.1530/ERC-11-0251
27. Herbst RS, Shin DM. Monoclonal Antibodies to Target Epidermal Growth Factor Receptor-Positive Tumors: A New Paradigm for Cancer Therapy. *Cancer* (2002) 94(5):1593–611. doi: 10.1002/cncr.10372

Conflict of Interest: The authors declare that the research was conducted in the absence of any commercial or financial relationships that could be construed as a potential conflict of interest.

frontiers in Oncology

ORIGINAL RESEARCH
published: 23 August 2021
doi: 10.3389/fonc.2021.688852

Secondary Structure of Human *De Novo* Evolved Gene Product NCYM Analyzed by Vacuum-Ultraviolet Circular Dichroism

Tatsuhito Matsuo[1†‡], *Kazuma Nakatani*[2,3,4‡], *Taiki Setoguchi*[2,5], *Koichi Matsuo*[6], *Taro Tamada*[1*] and *Yusuke Suenaga*[2*]

[1] Institute for Quantum Life Science, National Institutes for Quantum and Radiological Science and Technology, Ibaraki, Japan, [2] Department of Molecular Carcinogenesis, Chiba Cancer Center Research Institute, Chiba, Japan, [3] Graduate School of Medical and Pharmaceutical Sciences, Chiba University, Chiba, Japan, [4] Innovative Medicine CHIBA Doctoral World-leading Innovative & Smart Education (WISE) Program, Chiba University, Chiba, Japan, [5] Department of Neurosurgery, Chiba Cancer Center, Chiba, Japan, [6] Hiroshima Synchrotron Radiation Center, Hiroshima University, Hiroshima, Japan

NCYM, a *cis*-antisense gene of *MYCN*, encodes a Hominidae-specific protein that promotes the aggressiveness of human tumors. Newly evolved genes from non-genic regions are known as *de novo* genes, and *NCYM* was the first *de novo* gene whose oncogenic functions were validated *in vivo*. Targeting NCYM using drugs is a potential strategy for cancer therapy; however, the NCYM structure must be determined before drug design. In this study, we employed vacuum-ultraviolet circular dichroism to evaluate the secondary structure of NCYM. The SUMO-tagged NCYM and the isolated SUMO tag in both hydrogenated and perdeuterated forms were synthesized and purified in a cell-free *in vitro* system, and vacuum-ultraviolet circular dichroism spectra were measured. Significant differences between the tagged NCYM and the isolated tag were evident in the wavelength range of 190–240 nm. The circular dichroism spectral data combined with a neural network system enabled to predict the secondary structure of NCYM at the amino acid level. The 129-residue tag consists of α-helices (approximately 14%) and β-strands (approximately 29%), which corresponded to the values calculated from the atomic structure of the tag. The 238-residue tagged NCYM contained approximately 17% α-helices and 27% β-strands. The location of the secondary structure predicted using the neural network revealed that these secondary structures were enriched in the Hominidae-specific region of NCYM. Deuteration of NCYM altered the secondary structure at D90 from an α-helix to another structure other than α-helix and β-strand although this change was within the experimental error range. All four nonsynonymous single-nucleotide polymorphisms (SNPs) in human populations were in this region, and the amino acid alteration in SNP N52S enhanced Myc-nick production. The D90N mutation in NCYM promoted NCYM-mediated MYCN stabilization. Our results reveal the secondary

OPEN ACCESS

Edited by:
Tao Liu,
University of New South Wales, Australia

Reviewed by:
Elizabeth A. Proctor,
The Pennsylvania State University, United States
Masahito Tanaka,
National Institute of Advanced Industrial Science and Technology (AIST), Japan

***Correspondence:**
Yusuke Suenaga
ysuenaga@chiba-cc.jp
Taro Tamada
tamada.taro@qst.go.jp

†Present address:
Tatsuhito Matsuo, Laboratoire Interdisciplinaire de Physique (LiPhy), Grenoble-Alpes University, Saint Martin d'Hères, France and Institut Laue-Langevin, Grenoble, France

‡*These authors have contributed equally to this work*

Specialty section:
This article was submitted to Molecular and Cellular Oncology, a section of the journal Frontiers in Oncology

Received: *31 March 2021*
Accepted: *31 July 2021*
Published: *23 August 2021*

Citation:
Matsuo T, Nakatani K, Setoguchi T, Matsuo K, Tamada T and Suenaga Y (2021) Secondary Structure of Human De Novo Evolved Gene Product NCYM Analyzed by Vacuum-Ultraviolet Circular Dichroism. Front. Oncol. 11:688852. doi: 10.3389/fonc.2021.688852

structure of NCYM and demonstrated that the Homininae-specific domain of NCYM is responsible for MYCN stabilization.

Keywords: NCYM, MYCN, de novo evolved protein, secondary structure, VUVCD, perdeuterated protein, SNP, Myc-nick

INTRODUCTION

NCYM is a *cis*-antisense gene of *MYCN* (1) and encodes an oncogenic protein that promotes the aggressiveness of neuroblastomas (1–5). NCYM regulates the proliferation, invasion, migration, stemness, and apoptosis of cancer cells by stabilizing MYCN (1–5) and/or β-catenin (1, 6) by inhibiting GSK3β. The open reading frame (ORF) is located in the *MYCN* promoter, and mutations introduced during the evolution of Homininae resulted in the generation of the coding transcript of *NCYM* from the non-genic region (1, 5). New genes originating from non-genic regions are known as *de novo* genes (7–10), and NCYM is the first human *de novo* gene product whose oncogenic functions have been validated *in vivo* (5, 9). Because of its *de novo* emergence, NCYM does not shows homology to other known proteins, and its functional domain structure remains unclear.

Newly evolved proteins, including *de novo* gene products (hereinafter *de novo* evolved proteins), are predicted to be small and disordered proteins (11); generally, these high-dimensional structures are difficult to analyze by crystallization/cryo-electron microscopy. Bungard et al. (12) showed that the yeast *de novo* evolved protein Bsc4 folds to a partially ordered three-dimensional structure, forming compact oligomers with high β-sheet content and a hydrophobic core using near-UV circular dichroism as well as nuclear magnetic resonance. They revealed that *de novo* evolved proteins could have some structural order as well as native-like properties; however, the precise locations of the ordered secondary structure in Bsc4 remain unclear.

In this study, we investigated the secondary structure of NCYM by synchrotron radiation vacuum-ultraviolet circular dichroism technology (VUVCD) combined with a neural network. Synchrotron radiation VUVCD enables the analysis of the content and number of segments in the secondary structure of proteins at a wider range of wavelengths compared to near-UV circular dichroism (13, 14). Furthermore, the analysis of results combined with a neural network can predict the locations of the secondary structure of proteins at the amino acid sequence level (15). We carried out VUVCD measurements on both hydrogenated NCYM and perdeuterated NCYM, because some perdeuterated proteins have been reported to change their local structure and to have decreased protein stability compared with their hydrogenated counterparts, affecting their function/activity (16–18). A comparison of the possible differences in the secondary structures between these molecules may provide insights into regions that contribute to molecular stability and function. In addition, we determined whether perdeuterated proteins are helpful for gaining insights into the *de novo* evolved protein structure-function relationship.

METHODS

Purification of the NCYM Protein by *In Vitro* Cell-Free System

We purchased the following proteins in solution produced by an *in vitro* cell-free system from Taiyo Nippon Sanso Corporation (Tokyo, Japan)

-SUMO-tagged NCYM protein in hydrogenated form at 1.1 mg/mL
-SUMO-tag in hydrogenated form at 0.6 mg/mL
-SUMO-tagged NCYM protein in perdeuterated form at 1.4 mg/mL
-SUMO-tag in perdeuterated form at 1.4 mg/mL

The protein concentration was determined spectrophotometrically using the extinction coefficient $E_{280}^{1\%}$ of 3.74 and 1.99 for SUMO-tagged NCYM and the isolated SUMO-tag, respectively. The buffer composition was 20 mM phosphate buffer (pH or pD 8.0), 3 mM DTT. The isolated SUMO tag was separately synthesized and purified from the SUMO-tagged NCYM (**Figures 1A, B**).

Measurements of VUVCD Spectra

A VUVCD spectrophotometer (Hiroshima Synchrotron Radiation Center, Hiroshima University, Japan) and an assembled-type optical cell with CaF_2 windows were used to measure the VUVCD spectra of the four samples described above from 260 to 175 nm at 25°C. The isolated SUMO tags were measured for comparison. The details of the optical systems of the spectrophotometer and design of the sample cell have been described previously (19). The path length in the optical cell was adjusted to 50 μm using a Teflon spacer. All spectra were measured under the following conditions: slit, 1.0 mm; time constant, 4 s; scan speed, 20 nm/min; and accumulations, 4–8. The molar circular dichroism, $\Delta\varepsilon$, which is in normalized units of CD, was obtained from the path length of the optical cell and solute concentrations. The values of error in the CD spectrum were within 5%, which was mainly attributable to noise and inaccuracy in the optical path length.

Analysis of the Secondary-Structure Content and Segments of NCYM Using VUVCD and SELCON 3

The contents of α-helices, β-strands, turns, and unordered structures of proteins were estimated from the corresponding VUVCD spectra using the SELCON3 program and a database of VUVCD spectra and secondary-structure contents for 31

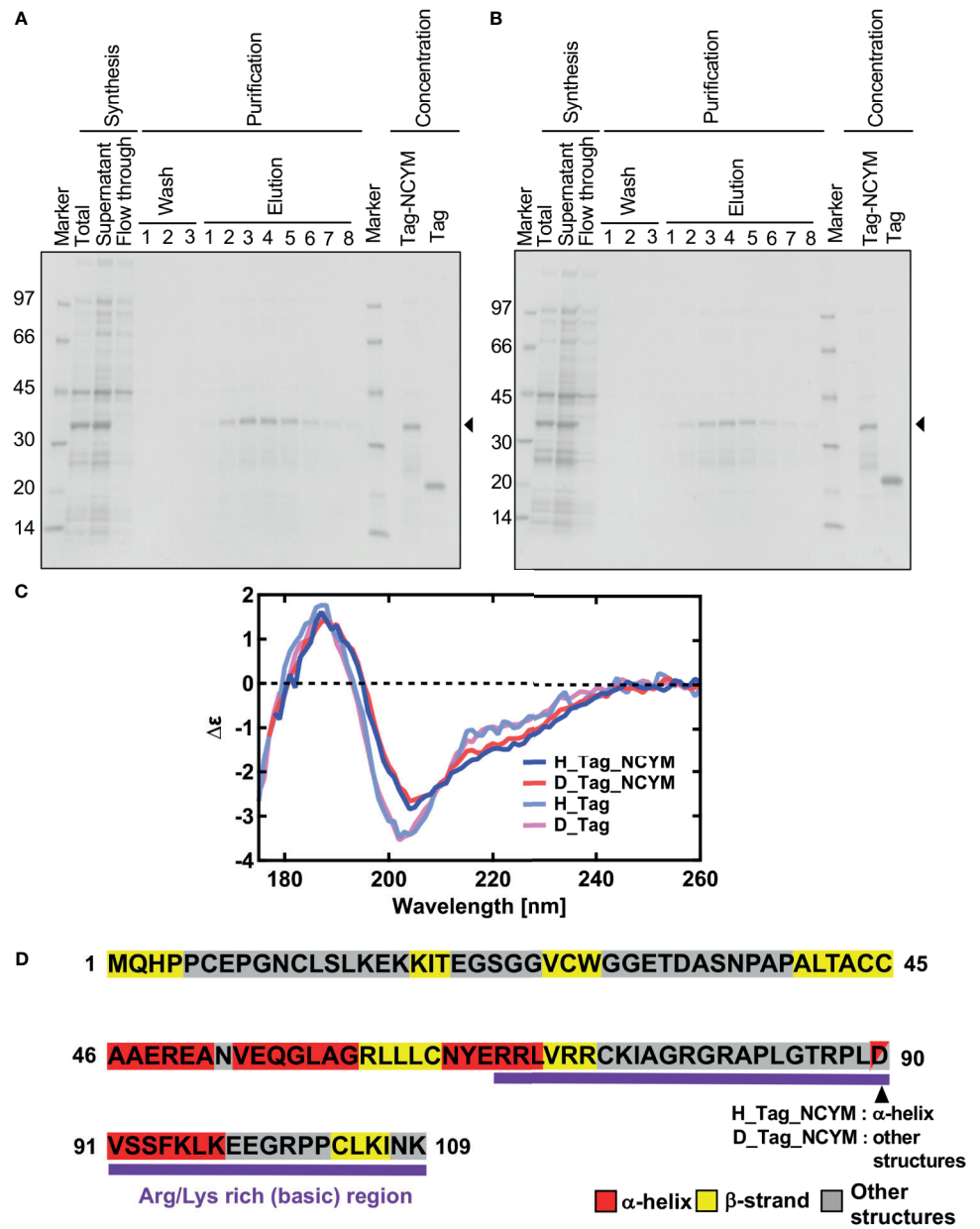

FIGURE 1 | Vacuum-ultraviolet circular dichroism (VUVCD) analyses revealed the secondary structure of NCYM. **(A)** NCYM with SUMO tag (arrow) and the isolated SUMO tag were synthesized and purified using an *in vitro* cell-free system. **(B)** Perdeuterated NCYM with SUMO tag (arrow) and the isolated SUMO tag were synthesized and purified using an *in vitro* cell-free system. **(C)** VUVCD spectra for hydrogenated SUMO-tagged NCYM (H_Tag_NCYM), perdeuterated SUMO-tagged NCYM (D_Tag_NCYM), hydrogenated SUMO tag (H_Tag), and perdeuterated SUMO tag (D_Tag). **(D)** Secondary structure of NCYM predicted using the neural network. Secondary structures are highlighted in red, yellow, and gray for α-helix, β-strand, and other structures, respectively. Arg/Lys-rich (basic) region is highlighted in purple.

reference proteins (13–15, 19). The number of α-helix and β-strand segments was calculated from the distorted α-helix and distorted β-strand contents, respectively (19). The root-mean-square deviation (δ) and the Pearson correlation coefficient (r) between the X-ray and VUVCD estimates of the secondary-structure contents of the reference proteins were 0.058 and 0.85, respectively (13, 15).

Analysis of the Positions of the Secondary Structures of NCYM Using VUVCD and Neural-Network Method

The positions of α-helix and β-strand segments in the amino-acid sequence were predicted using a neural-network (NN) method based on the secondary-structure contents and the number of segments obtained in the VUVCD analysis

(VUVCD-NN method). The computational protocol is described in detail elsewhere (14). Briefly, we utilized an NN algorithm (20) that predicts the position of secondary structures using the evolutionary sequence information based on the position-specific scoring matrices generated using the PSI-BLAST tool. A training dataset of 607 proteins used in the NN algorithm was obtained from the X-ray structures in the PDB and the weights and biases of 20 amino acids for α-helices and β-strands were calculated from the secondary structures and amino-acid sequences of these 607 proteins. The positions of α-helices and β-strands in the amino acid sequence were assigned in a descending order of the α-helix and β-strand weights of the 20 amino acids until the determined numbers of α-helix and β-strand residues converged to those estimated from the VUVCD analysis. Next, the numbers of α-helix and β-strand segments estimated from the VUVCD analysis were introduced in NN calculation until the predicted numbers of segments converged to those obtained from VUVCD estimation. If the predicted numbers of residues and segments for α-helices and β-strands did not converge to the VUVCD estimates, the sequence alignment that minimized the difference between the two estimates was taken as the final value. The turns and unordered structures estimated using SELCON3 were classified as "other structures" in the VUVCD-NN method. The predictive accuracy of this method for the positions of α-helix and β-strand segments was 74.9% for the 30 reference soluble proteins (14).

The predictive accuracy obtained from the randomization protocol is around 36.8% (21). Further, when we use only NN method, the accuracy was 70.9% and this accuracy finally improved to 74.9% when the method was combined with the experimental data (14).

The method has been used for the structural analysis of unknown proteins in the native and other states so far (22, 23).

Purification of GST-Fused NCYM Protein in Bacteria

The open reading frame of NCYM was inserted into the pGEX-6p-1 plasmid so that the GST tag was attached to the N-terminus of NCYM. The plasmid was transformed to BL21 (DE3) cells, which were then grown at 30°C in Luria broth medium supplemented with ampicillin at a concentration of 0.1 mg/mL. At OD = 1.0, protein expression was induced by adding isopropyl-β-D-thiogalactopyranoside at a concentration of 1 mM, followed by 3 h of incubation.

After harvest, the cell pellets were lysed by sonication in phosphate-buffered saline supplement with a protease inhibitor cocktail cOmplete (Roche, Mannheim, Germany). The lysate was subjected to ultracentrifugation and its supernatant was applied to a GSTrap FF column (GE Healthcare, Little Chalfont, UK), which was equilibrated with phosphate-buffered saline. NCYM attached to the GST-tag was purified using elution buffer containing 50 mM Tris-HCl (pH 8.0) and 10 mM reduced glutathione, and the eluate was stored at 4°C. When NCYM was purified without the GST-tag, the column described above was detached from the system and PreScission Protease (GE Healthcare) was added, followed by incubation for 17–18 h at 4°C. After reattaching the column to the system, buffer containing 50 mM Tris-HCl (pH 8.0), 100 mM NaCl, 1 mM EDTA, and 1 mM DTT was used to elute NCYM. Finally, GST-tagged molecules attached to the column were eluted with elution buffer. Using the Bradford method (bovine serum albumin was used as a standard), the yields were determined to be 17.5 and 3.8 mg/L culture for NCYM with and without the GST-tag, respectively.

Analyses of Single-Nucleotide Polymorphisms in the NCYM Gene

We analyzed single-nucleotide polymorphisms (SNPs) in *NCYM* using the Japanese Multi Omics Reference Panel (jMorp, https://jmorp.megabank.tohoku.ac.jp/202102/variants).

Cell Culture and Transfection

The human neuroblastoma cell line SH-SY5Y was maintained in DMEM supplemented with 10% fetal bovine serum, 50 U/mL penicillin, and 50 μg/mL streptomycin. The human neuroblastoma cell line IMR32 was maintained in RPMI-1640 medium supplemented with 10% fetal bovine serum, 50 U/mL penicillin, and 50 μg/mL streptomycin.

Plasmid transfections were performed using Lipofectamine 3000 transfection reagent (Invitrogen, Carlsbad, CA, USA) according to the manufacturer's instructions. At 24 h after transfection, we prepared total RNA for quantitative real-time RT-PCR. At 24 or 72 h after transfection, we prepared cell lysates for western blotting.

Subcellular Fractionation

To prepare nuclear and cytoplasmic extracts, the cells were lysed in 10 mM Tris-HCl (pH 8.0), 1 mM EDTA, 0.5% Nonidet P-40 (Nacalai Tesque, Kyoto, Japan), and cOmplete™ Protease Inhibitor Cocktail Tablets and centrifuged at 17,800 ×*g* for 10 min to collect the soluble fractions, which were referred to as cytosolic extracts. Insoluble materials were washed with lysis buffer and further dissolved in RIPA buffer to collect the nuclear extracts.

Western Blotting

Cells were lysed with RIPA buffer, Benzonase (Millipore, Billerica, MA, USA), and $MgCl_2$ at final concentrations of 25 U/μL and 2 mM, respectively, incubated at 37°C for 1 h, and centrifuged at 10,000 × *g* for 10 min at 4°C, after which the supernatant was collected. The supernatant was denatured in SDS sample buffer with or without 2-mercaptoethanol (reducing or non-reducing, respectively). Cell proteins were resolved by SDS-PAGE before being electroblotted onto polyvinylidene fluoride membranes. We incubated the membranes with the following primary antibodies for 60 min: anti-NCYM [1:1000 dilution (1)], anti-MYCN antibody (1:1000 dilution; Cell Signaling Technology, Danvers, MA, USA), anti-Lamin B (1:1000 dilution; Millipore), anti-α-tubulin (1:1000 dilution; Cell Signaling Technology), anti-HA (1:1000 dilution; Cell Signaling Technology), and anti-actin (1:1000 dilution; Wako, Osaka, Japan). The membranes were then incubated with horseradish peroxidase-conjugated secondary antibody (anti-rabbit IgG at 1:5000 dilution or anti-mouse IgG at 1:5000 dilution; both from Cell Signaling Technology), and the bound

proteins were visualized using a chemiluminescence-based detection kit (ImmunoStar Zeta, Wako; ImmunoStar LD, Wako).

RNA Isolation and Quantitative Real-Time RT-PCR

The total RNA from plasmid-transfected SH-SY5Y cells was prepared using an RNeasy Mini kit (Qiagen, Hilden, Germany) following the manufacturer's instructions. cDNA was synthesized using SuperScript II with random primers (Invitrogen). Quantitative real-time RT-PCR (qRT-PCR) using a StepOnePlus™ Real-Time PCR System (Thermo Fisher Scientific, Waltham, MA, USA) was performed with SYBR green PCR. The following primer sets were used: *MYCN*, 5′-TCCATGACAGCGCTAAACGTT-3′, and 5′-GGAACACAC ACAAGGTGACTTCAAC-3′. *β-actin* expression was quantified using the TaqMan real-time PCR assay. The mRNA levels of *MYCN* gene were standardized using that of *β-actin*.

Vector Construction

Plasmid vectors were synthesized by GenScript Japan (Tokyo, Japan) as follows. Plasmid vectors encoding the HA-NCYM ORF (WT) and amino acid mutants of HA-NCYM ORF (E7G(A20G), N52S(A155G), G59R(G175A), L63P(T188C), Y66S(A197C), L70V (C208G), V71D(T 212A), G78E(G233A), D90N(G268A), and E98G(A293G)) were synthesized using the restriction enzymes KpnI and BamHI with pcDNA3. 1-N-HA is a vector with a CMV promoter for expressing proteins with an HA tag at the N-terminus. The start codon of the ORF of NCYM was deleted.

RESULTS

VUVCD Analyses Revealed the Secondary Structure of the NCYM Protein

Significant differences in the spectra were observed in the wavelength range of 190–240 nm between the tagged proteins and tag only solution (**Figure 1C**). These differences arise from the spectra of NCYM. The secondary structure contents and segments of the isolated SUMO tag were analyzed using the VUVCD spectra and SELCON3 program (15, 19). The isolated SUMO tag (129 residues) contained 14.2% α-helices and 29.2% β-strands in the hydrogenated state and 13.9% α-helices and 28.7% β-strands in the perdeuterated state (**Table 1**). The atomic structure (PDB ID: 3PGE) of tag fragment (80 residues) from X-ray crystallography showed that this fragment contains 14% helices and 32% sheets. The lengths of the tags in the X-ray and VUVCD methods differed but the secondary structure contents estimated by VUVCD agreed well with those of the crystal structure. The SUMO-tagged NCYM (238 residues) in the hydrogenated state was found to contain 17.1% α-helices and 27.2% β-strands (**Table 1**), indicating that NCYM forms the characteristic secondary structures when tagged with SUMO. To investigate the disordered nature of *de novo* evolved proteins, we synthesized perdeuterated NCYM with a SUMO tag and the isolated SUMO tag using an *in vitro* cell-free system (**Figure 1B**). Small differences in the spectra were observed in the wavelength range of 210–220 nm between perdeuterated and hydrogenated NCYM (**Figure 1C**). The secondary structure analysis showed that perdeuterated SUMO-tagged NCYM contains 16.3% α-helices and 27.0% β-strands (**Table 1**). The secondary structure contents between perdeuterated and hydrogenated NCYM were identified within the calculation error range of SELCON 3 program, but the differences between both spectra around 220 nm affect the helical contents because the CD intensity at 222 nm is highly sensitive to the amount of helical structure (13).

Prediction of the Secondary Structure of NCYM at the Single Amino-Acid Level

To predict the secondary structure of NCYM at the amino-acid sequence level, we used the sequence-based prediction method (PSIPRED, JPred4, trRosetta, and RaptorX), which can estimate the secondary structure only from the amino-acid sequence of the target protein (24–27). The predicted results and the estimated secondary structure contents are shown in **Figure S1**. Evidently, these results had large variations in the region of the NCYM. Furthermore, the secondary structure contents from the VUVCD results (**Table 1**) are different to those obtained from these sequence-based prediction methods. This indicates that the prediction of the secondary structure of NCYM would not be adequate for the current algorithms, probably due to specificities of amino-acid sequence of *de novo* evolved protein. Hence, from the perspective of the secondary structure contents, we used the experimental data obtained from the VUVCD analysis to predict the secondary structures of NCYM at the amino-acid sequence level.

We predicted the positions of the secondary structures in SUMO-tagged NCYM and the isolated SUMO tag at the amino acid sequence level (**Figures 1D** and **S2**) using the neural network system combined with the contents and segments of secondary structures obtained using the VUVCD analysis (**Table 1**) (14). The predicted sequence of the secondary

TABLE 1 | Secondary structure content of the NCYM samples used for the VUVCD measurements.

	N_{res}	H(r)	H(d)	S(r)	S(d)	N_{helix}	N_{strand}
H_Tag_NCYM	238	6.7	10.4	15.9	11.3	6	13
D_Tag_NCYM	238	6.5	9.8	15.9	11.1	6	13
H_Tag	129	5.4	8.8	16.6	12.6	3	8
D_Tag	129	4.9	9.0	16.3	12.4	3	8

N_{res} denotes the number of residues contained in the samples. H(r), H(d), S(r), and S(d) are the fraction (%) of ordered α-helix, disordered α-helix, ordered β-strand, and disordered β-strand, respectively. N_{helix} and N_{strand} show the number of α-helix and β-strand (sum of the ordered and disordered structures) contained in the corresponding samples, respectively.

structure of the tag was consistent with that of X-ray crystallography with 75% accuracy (data not shown), which is the same as the average performance for the 30 reference proteins (15). Comparisons between the secondary structure sequences of SUMO-tagged NCYM and the isolated SUMO tag revealed that NCYM contains seven β-strands and four α-helices (**Figure 1D**). Three of the four α-helices were localized in the central region of NCYM. In addition, the protein database UniProt revealed the presence of compositional bias to Arg/Lys-rich (basic) at the C-terminal (68–109 aa) of NCYM (UniProt KB-P40205 NCYM Human, **Figure 1D**). According to the amino acid sequence only, NCYM was previously predicted to be a basic helix-loop-helix protein (28) (**Figure S3**), but the predicted regions of the helix in the present study differed from those in the previous report. This is likely because we considered the secondary structure contents experimentally obtained from the VUVCD method (**Table 1**). The sequences of secondary structures of hydrogenated and perdeuterated NCYM proteins were identical to each other but showed slight differences in aspartic acid (D90) (other structure in the perdeuterated protein and α-helical structure in the hydrogenated structure), as shown in **Figure 1D**. This indicates that D90 might perturb the conformation of the NCYM. Note that "other structure" comprises all secondary structures other than α-helix and β-strand. Considering the experimental and analytical errors, the differences in the secondary structures of SUMO-tagged NCYM between hydrogenated and perdeuterated forms including D90 assignment are expected to be within the error range. Nevertheless, as aspartate often plays a major role in protein function, as in the catalytic triad, the secondary structural change at D90 from α-helix (hydrogenated state) to other structures (perdeuterated state) suggests that this residue is more prone to differences in local physicochemical environments (hydrogenated *vs*. perdeuterated) and is thus involved in the molecular stability of NCYM and its function. Therefore, it is worth investigating the possible role of D90 in the interaction with MYCN or GSK3β, especially focusing on the negative charge of D90. We chose asparagine for generating NCYM D90 mutant because it resembles aspartic acid the most, with a difference only in one chemical group change which made the residue polar instead of charged. For this purpose, the D90N mutant was generated and its effect on NCYM function was studied, although D90N is yet to be detected as a naturally occurring mutation in humans.

NCYM Forms Oligomers

Because the structurally characterized *de novo* evolved protein Bsc4 forms oligomers (12), we examined the oligomer structure formation ability of NCYM. The NCYM protein was synthesized and purified from bacterial cells (**Figure S4A**). The bands of purified NCYM were detected at the predicted sizes of monomers, dimers, trimers, and tetramers *via* non-reducing SDS-PAGE (**Figure S4B**). Next, whole cell extracts of *MYCN*-amplified neuroblastoma cells IMR32 were prepared to detect oligomers of endogenous NCYM (**Figure S4C**). To prevent the oligomers of NCYM from degrading, the samples were prepared without sonication. The addition of benzonase increased the concentration of soluble NCYM protein, and the bands of endogenous NCYM were detected at the predicted sizes of monomers, dimers, trimers, tetramers, and pentamers in a western blot under reducing conditions (**Figure S4C**). To study the subcellular localization of NCYM oligomers, western blotting of the nuclear fraction was performed. Monomeric bands of NCYM were detected in the nucleus, and bands predicted to be dimers, trimers, and tetramers were detected in the cytoplasm (**Figure S4D**).

Non-Synonymous SNPs in NCYM Are Enriched in the Domain Structure

Next, we conducted a search for SNPs of NCYM in the human population using the Japanese Multi Omics Reference Panel (jMorp, **Supplementary Table 1**). All four non-synonymous SNPs (N52S, L63P, L70V, and V71D) in humans and two of five non-synonymous substitutions in chimpanzee (G59R and Y66S) were found to be accumulated in the central domain structure of the NCYM (**Figure 2A**). The frequencies of these SNPs differed among people of different ethnicities, with the highest proportion observed for L70V. Substitution of the 35th serine, a phosphorylation site (Japan Proteome Standard Repository/Database, ID: PSM204_1_28892), of NCYM to cysteine (S35C) was detected at a frequency of 0.0001 in African people. A frameshift mutation causing a deletion in the NCYM (I19N*17) was found in Japanese, African, and Non-Finnish European people, and it causes the protein to have similar amino acid sequences as the ancestral form of NCYM (**Table 2**). A previous study reported that NCYM stabilizes the MYCN protein (1) and promotes Myc-nick production (3). To investigate the effect of amino acid substitutions on the function of NCYM, variants of NCYM including the D90N mutant were overexpressed in the neuroblastoma cell line SH-SY5Y. Western blotting revealed that the expression of MYCN increased upon overexpression of the NCYM variant of D90N (**Figure 2B**). The real-time RT-PCR showed no change in the mRNA expression level of *MYCN* (**Figure 2C**). We detected Myc-nick production at 72 h (**Figure 2D**), and N52S mutation of NCYM significantly increased Myc-nick production (**Figure 2E**).

DISCUSSION

In this study, we revealed the secondary structure of NCYM and showed that α-helices and β-strands were enriched in the central region (amino acids 40–73) of NCYM, which emerged in Homininae by two frameshifts in the ORF (1, 5). Furthermore, it was found that the D90N mutation activated NCYM-mediated MYCN stabilization. Within the ORF of NCYM, all four nonsynonymous SNPs were in the central region, three of which showed high frequency in East Asians and N52S promoted the NCYM function to produce Myc-nick. Therefore, the central region of NCYM appears to be a functional domain responsible for NCYM-mediated Myc-nick production.

Although the D90N mutation is not one of the naturally occurring mutations, we found that D90N increases MYCN

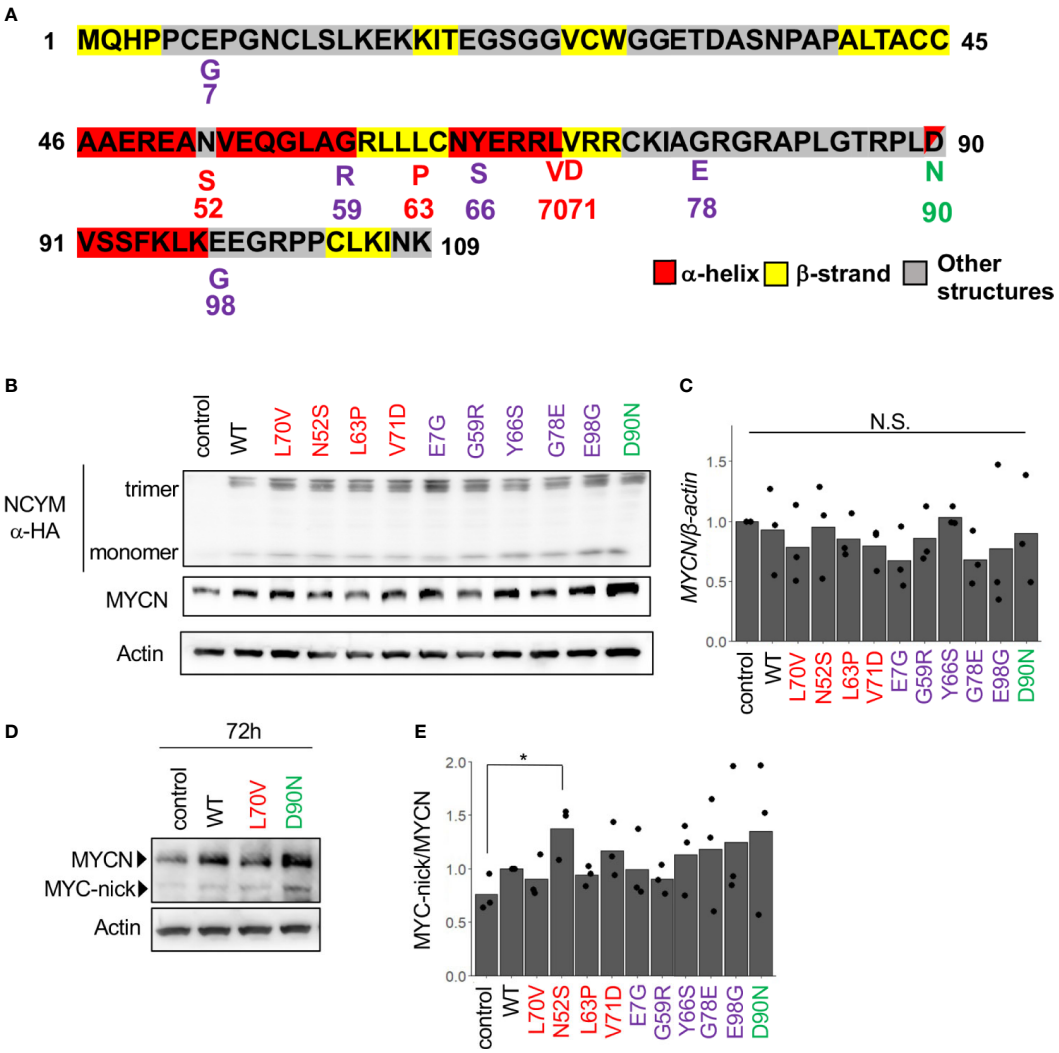

FIGURE 2 | MYCN stabilization and Myc-nick production by each NCYM variant. **(A)** NCYM amino acid sequences. Purple, variants found in chimpanzees; red, variants found in humans; green, D90N, a mutant of NCYM in which the 90th aspartic acid is substituted with asparagine. **(B)** Western blotting of HA-NCYM, MYCN proteins in NCYM SNP plasmid-transfected SH-SY5Y cells. At 24 h after transfection, the cells were subjected to western blotting. Actin was used as a loading control. Control: empty vector. **(C)** Quantitative real-time RT-PCR analyses of *MYCN* in NCYM SNP plasmid-transfected SH-SY5Y cells. At 24 h after transfection, mRNA expression levels were measured by real-time RT-PCR with *β-actin* as an internal control. N.S., not significant. Data were analyzed using Student's *t* test (comparison with control). **(D)** Western blotting of MYCN and Myc-nick proteins in NCYM SNP plasmid-transfected SH-SY5Y cells. At 72 h after transfection, cells were subjected to western blotting. Actin was used as a loading control. **(E)** Quantification of western blotting analysis of NCYM SNP plasmid-transfected SH-SY5Y cells. At 72 h after transfection, the cells were subjected to western blotting. Myc-nick level was normalized to MYCN level. Data are shown as plots and means of three independent experiments. *p < 0.05. Data were analyzed using Student's *t* test (comparison with control).

TABLE 2 | Frequency of NCYM SNPs.

ref SNP	Variant	Frequency						Remark
		AFR	NFE	AMR	ASJ	EAS	JPN	
rs181162426	N52S	0.0002	–	–	–	0.0263	0.0022	High frequency (>0.01)
rs190044705	L63P	–	–	–	–	0.0006	0.0237	High frequency (>0.01)
rs11886063	L70V	0.9986	0.9958	1	1	1	1	High frequency (>0.01)
rs75731159	V71D	–	0.0007	–	–	0.0148	0.0383	High frequency (>0.01)
rs919133132	I19N*17	0.0002	0.0004	–	–	–	0.0001	Ancestral variant
Rs973265238	S35C	0.0001	–	–	–	–	–	Phosphorylation site

JPN, Japanese; AFR, African; AMR, American; ASJ, Ashkenazi Jewish; EAS, East Asia; NFE, Non-Finnish European. - indicates not detected.

stabilization, suggesting that the negative charge in D90 has an inhibitory effect on the binding of NCYM to MYCN or GSK3β. Thus, the use of both hydrogenated and perdeuterated NCYM proteins enabled to identify a residue that significantly modulates NCYM function, raising a possibility that protein deuteration might be useful for studying the molecular mechanism of protein activity. Moreover, further systematic biochemical studies using different mutations at D90 would be beneficial to decipher the effects of volume, polarity, and hydrophobicity of the residue at this site on NCYM function.

In this study, the secondary structure of SUMO-tagged NCYM was analyzed. In the intrinsically disordered regions in proteins, their transiently folded and disordered states are typically in equilibrium with each other, and the interaction with other molecules shifts this equilibrium toward the former (29). Although the effect of non-covalent interactions with other proteins on protein structure may be different from that of the covalent binding of the tag, it is possible that the SUMO tag stabilizes NCYM conformation, thus facilitating the folding of some regions in NCYM that would otherwise be disordered when isolated. In this case, it indicates that the regions of NCYM where the folded secondary structure was assigned are susceptible to a slight change in local physicochemical environments caused by binding of the SUMO tag, suggesting that these regions contribute to the molecular stability of NCYM. Therefore, in order to better understand the structural properties of NCYM, the folded state of NCYM with SUMO tag should be compared with the structure of the isolated NCYM in the near future.

The western blotting analysis revealed that NCYM exists as oligomers in addition to monomers, and NCYM oligomers were detected even under reducing conditions. This suggests that the interaction between monomers in the NCYM oligomers is strong enough not to be disrupted easily by the thermal energy. Therefore, it is possible that the secondary structure of NCYM changes as it forms oligomers, especially in the binding interface between monomers. The fact that NCYM oligomers are detected in the fraction of the cytoplasm while NCYM monomers are detected in the fraction of the nucleus implies that subcellular localization of these molecular species might be an important factor for NCYM function, which requires structural characterization of NCYM oligomers and monomers.

The present study also revealed the first function-structure relationships of *de novo* evolved proteins. *De novo* evolved proteins, by definition, lack homology to known proteins or known functional domains and show high flexibility, as observed in intrinsically disordered proteins (11). These features have impeded the functional and structural characterization of *de novo* evolved proteins. The present study suggests that synchrotron-radiation VUVCD with perdeuterated proteins is a promising strategy for identifying functional domain structures of *de novo* evolved proteins. SNPs in populations are also useful for functional characterization of *de novo* evolved proteins because they occasionally include amino acids that are essential for protein functions.

The existence of nonsynonymous SNP that affects NCYM-mediated Myc-nick production supports that *NCYM* is a bona fide protein-coding gene (1, 5), rather than a long noncoding RNA. Nonsynonymous SNPs at the phosphorylation site of NCYM (S35C) further support that *NCYM* encodes proteins. In addition to noncoding variants of *NCYM*/*MYCNOS* (NR_110230, transcript variant 1 in the National Center for Biotechnology Information database) (30, 31), the transcript variants of coding *NCYM* (NR_161162 and NR_161163, transcript variants 2 and 3) have been proposed to function as long noncoding RNAs that enhance MYCN expression (32, 33) and promote metastasis (32), as reported for protein function (1). Two contradictory molecular mechanisms have been proposed for MYCN induction as mediated by noncoding *NCYM* transcripts (32, 33). One study reported that *NCYM* noncoding RNA stimulates the upstream promoter of *MYCN via* the recruitment of CTCF (32), and the other showed that *NCYM* noncoding RNA suppressed the upstream promoter and stimulated the internal promoter activity of *MYCN*, resulting in efficient translation of MYCN (33). Under our experimental conditions, we did not detect *MYCN* mRNA induction after transduction of wild-type NCYM, and no significant difference in *MYCN* mRNA levels was observed in cells that overexpressed NCYM variants. Further studies are required to examine whether these variants affect the noncoding functions of NCYM.

Orthologous transcripts of *NCYM* are widely detected in mammals (5), but the ORF emerged in Homininae during evolution (1, 5). Similar to other *de novo* genes (34), we detected ORF-disrupting SNPs which caused the *NCYM* gene resemble the ancestral-type sequence. Furthermore, one NCYM SNP mutant found in East Asians promoted Myc-nick production. In addition to neuroblastomas, high expression of *MYCN* or *NCYM* is associated with poor outcomes in hepatocellular carcinomas (35) or cholangiocarcinomas (5), respectively. Therefore, the roles of NCYM SNPs in the development of these tumors, frequently found in East Asians, should be further studied.

DATA AVAILABILITY STATEMENT

The original contributions presented in the study are included in the article/**Supplementary Material**. Further inquiries can be directed to the corresponding authors.

AUTHOR CONTRIBUTIONS

TM, KN, KM, TT, and YS performed the experiments, acquired, and analyzed the data. TM, KN, KM, TS, TT, and YS wrote the manuscript. KN, TS, TT, and YS acquired funds. TT and YS designed and supervised the study. All authors contributed to the article and approved the submitted version.

FUNDING

This work was partially supported by the Interstellar Initiative (grant number 18jm0610006h0001 to YS) from the Japan Agency for Medical Research and Development, Grant-in-Aid

for Scientific Research (C) (JSPS Kakenhi Grant No. 18K08162 and No. 21K08610 to YS), Grant-in-Aid for Scientific Research (C) (JSPS Kakenhi Grant 20K09338 to TS) from the Japan Society for the Promotion of Science, Innovative Medicine CHIBA Doctoral WISE Program (to KN) from Chiba University, Kawano Masanori Memorial Public Interest Incorporated Foundation for Promotion of Pediatrics (to YS).

ACKNOWLEDGMENTS

We thank Atsushi Takatori, Yoshitaka Hippo, and Yohko Yamaguchi for their helpful comments.

SUPPLEMENTARY MATERIAL

The Supplementary Material for this article can be found online at: https://www.frontiersin.org/articles/10.3389/fonc.2021.688852/full#supplementary-material

Supplementary Figure 1 | Secondary structures of SUMO-tagged NCYM using the sequence-based prediction methods. **(A)** From top to bottom, positions of the SUMO-tagged NCYM predicted using PSIPRED, JPred4, trRosetta, and RaptorX are shown. α-Helix, β-strand, and other structures are shown in red, yellow, and gray, respectively. **(B)** Contents of α-helix, β-strand, and other structures estimated using the prediction methods used in **(A)**. N_{helix} and N_{strand} denote the number of α-helix and β-strand, respectively.

Supplementary Figure 2 | Secondary structure of hydrogenated SUMO-tagged NCYM (H_Tag_NCYM), perdeuterated SUMO-tagged NCYM (D_Tag_NCYM), hydrogenated SUMO tag (H_Tag), and perdeuterated SUMO tag (D_Tag) predicted by the neural network. Note that in the region I119–P133 of H_Tag_NCYM, there are two β-strands, that is, I119–G128 and G129–P133. The residues belonging to the disordered β-strand, which are assigned by the neural network, correspond to the edges of the β-strands (I119, G128, G129, and P133 in this case). The fraction of the ordered and disordered β-strand is listed in **Table 1**.

Supplementary Figure 3 | Comparison of the structure of NCYM between the present study and previous report.

Supplementary Figure 4 | NCYM forms oligomers. **(A)** Purification of NCYM. **(B)** Western blotting showing the monomer, dimer, trimer, and tetramer structures of purified NCYM in non-reducing conditions, but the protein did not form an oligomer under reducing conditions. **(C)** Western blots showing monomer, dimer, trimer, tetramer, and pentamer structures of NCYM from IMR32 cells. **(D)** Western blotting of nuclear and cytoplasmic fractions from IMR32 cells. Monomers and oligomers of NCYM were found in the nucleus cytoplasm, respectively.

Supplementary Table 1 | Single-nucleotide polymorphisms (SNPs) in *NCYM*.

REFERENCES

1. Suenaga Y, Islam SR, Alagu J, Kaneko Y, Kato M, Tanaka Y, et al. NCYM, a Cis-Antisense Gene of MYCN, Encodes a *De Novo* Evolved Protein That Inhibits GSK3β Resulting in the Stabilization of MYCN in Human Neuroblastomas. *PLoS Genet* (2014) 10:e1003996. doi: 10.1371/journal.pgen.1003996
2. Kaneko Y, Suenaga Y, Islam SM, Matsumoto D, Nakamura Y, Ohira M, et al. Functional Interplay Between MYCN, NCYM, and OCT4 Promotes Aggressiveness of Human Neuroblastomas. *Cancer Sci* (2015) 106:840–7. doi: 10.1111/cas.12677
3. Shoji W, Suenaga Y, Kaneko Y, Islam SR, Alagu J, Yokoi S, et al. NCYM Promotes Calpain-Mediated Myc-Nick Production in Human MYCN-Amplified Neuroblastoma Cells. *Biochem Biophys Res Commun* (2015) 461:501–6. doi: 10.1016/j.bbrc.2015.04.050
4. Suenaga Y, Yamamoto M, Sakuma T, Sasada M, Fukai F, Ohira M, et al. TAp63 Represses Transcription of MYCN/NCYM Gene and Its High Levels of Expression Are Associated With Favorable Outcome in Neuroblastoma. *Biochem Biophys Res Commun* (2019) 518:311–8. doi: 10.1016/j.bbrc.2019.08.052
5. Suenaga Y, Nakatani K, Nakagawara A. De Novo Evolved Gene Product NCYM in the Pathogenesis and Clinical Outcome of Human Neuroblastomas and Other Cancers. *Jpn J Clin Oncol* (2020) 50:839–46. doi: 10.1093/jjco/hyaa097
6. Zhu X, Li Y, Zhao S, Zhao S. LSINCT5 Activates Wnt/β-Catenin Signaling by Interacting With NCYM to Promote Bladder Cancer Progression. *Biochem Biophys Res Commun* (2018) 502:299–306. doi: 10.1016/j.bbrc.2018.05.076
7. Van Oss SB, Carvunis AR. De Novo Gene Birth. *PLoS Genet* (2019) 15: e1008160. doi: 10.1371/journal.pgen.1008160
8. McLysaght A, Hurst LD. Open Questions in the Study of *De Novo* Genes: What, How and Why. *Nat Rev Genet* (2016) 17:567–78. doi: 10.1038/nrg.2016.78
9. McLysaght A, Guerzoni D. New Genes From Non-Coding Sequence: The Role of *De Novo* Protein-Coding Genes in Eukaryotic Evolutionary Innovation. *Philos Trans R Soc Lond B* (2015) 370:20140332. doi: 10.1098/rstb.2014.0332
10. Zhang YE, Long M. New Genes Contribute to Genetic and Phenotypic Novelties in Human Evolution. *Curr Opin Genet Dev* (2014) 29:90–6. doi: 10.1016/j.gde.2014.08.013
11. Wilson BA, Foy SG, Neme R, Masel J. Young Genes Are Highly Disordered as Predicted by the Preadaptation Hypothesis of *De Novo* Gene Birth. *Nat Ecol Evol* (2017) 1:146. doi: 10.1038/s41559-017-0146
12. Bungard D, Copple JS, Yan J, Chhun JJ, Kumirov VK, Foy SG, et al. Foldability of a Natural *De Novo* Evolved Protein. *Structure* (2017) 25:1687–96.e4. doi: 10.1016/j.str.2017.09.006
13. Matsuo K, Yonehara R, Gekko K. Secondary-Structure Analysis of Proteins by Vacuum-Ultraviolet Circular Dichroism Spectroscopy. *J Biochem* (2004) 135:405–11. doi: 10.1093/jb/mvh048
14. Matsuo K, Watanabe H, Gekko K. Improved Sequence-Based Prediction of Protein Secondary Structures by Combining Vacuum-Ultraviolet Circular Dichroism Spectroscopy With Neural Network. *Proteins* (2008) 73:104–12. doi: 10.1002/prot.22055
15. Matsuo K, Yonehara R, Gekko K. Improved Estimation of the Secondary Structures of Proteins by Vacuum-Ultraviolet Circular Dichroism Spectroscopy. *J Biochem* (2005) 138:79–88. doi: 10.1093/jb/mvi101
16. Meilleur F, Contzen J, Myles DAA, Jung C. Structural Stability and Dynamics of Hydrogenated and Perdeuterated Cytochrome P450cam (Cyp101). *Biochemistry* (2004) 43:8744–53. doi: 10.1021/bi049418q
17. Ramos J, Laux V, Haertlein M, Boeri Erba E, McAuley KE, Forsyth VT, et al. Structural Insights Into Protein Folding, Stability and Activity Using *In Vivo* Perdeuteration of Hen Egg-White Lysozyme. *IUCrJ* (2021) 8:372–83. doi: 10.1107/S2052252521001299
18. Liu X, Hanson BL, Langan P, Viola RE. The Effect of Deuteration on Protein Structure: A High-Resolution Comparison of Hydrogenous and Perdeuterated Haloalkane Dehalogenase. *Acta Crystallogr D* (2007) 63:1000–8. doi: 10.1107/S0907444907037705
19. Sreerama N, Woody RW. Estimation of Protein Secondary Structure From Circular Dichroism Spectra: Comparison of CONTIN, SELCON, and CDSSTR Methods With an Expanded Reference Set. *Anal Biochem* (2000) 287:252–60. doi: 10.1006/abio.2000.4880
20. Jones JT. Protein Secondary Structure Prediction Based on Position-Specific Scoring Matrices. *J Mol Biol* (1999) 292:195–202. doi: 10.1006/jmbi.1999.3091
21. Rost B, Sander C. Prediction of Protein Secondary Structure at Better Than 70% Accuracy. *J Mol Biol* (1993) 232:584–99. doi: 10.1006/jmbi.1993.1413
22. Matsuo K, Kumashiro M, Gekko K. Characterization of the Mechanism of Interaction Between A1-Acid Glycoprotein and Lipid Membranes by Vacuum-Ultraviolet Circular-Dichroism Spectroscopy. *Chirality* (2020) 32:594–604. doi: 10.1002/chir.23208

23. Matsusaki M, Okuda A, Matsuo K, Gekko K, Masuda T, Naruo Y, et al. Regulation of Plant ER Oxidoreductin 1 (ERO1) Activity for Efficient Oxidative Protein Folding. *J Biol Chem* (2019) 294:18820–35. doi: 10.1074/jbc.RA119.010917
24. Buchan DWA, Jones DT. The PSIPRED Protein Analysis Workbench: 20 Years on. *Nucleic Acids Res* (2019) 47:W402–7. doi: 10.1093/nar/gkz297
25. Drozdetskiy A, Cole C, Procter J, Barton GJ. JPred4: A Protein Secondary Structure Prediction Server. *Nucleic Acids Res* (2015) 43:W389–94. doi: 10.1093/nar/gkv332
26. Yang J, Anishchenko I, Park H, Peng Z, Ovchinnikov S, Baker D. Improved Protein Structure Prediction Using Predicted Interresidue Orientations. *Proc Natl Acad Sci U S A* (2020) 117:1496–503. doi: 10.1073/pnas.1914677117
27. Kallberg M, Wang H, Wang S, Peng J, Wang Z, Lu H, et al. Template-Based Protein Structure Modeling Using the RaptorX Web Server. *Nat Protoc* (2012) 7:1511–22. doi: 10.1038/nprot.2012.085
28. Armstrong BC, Krystal GW. Isolation and Characterization of Complementary DNA for N-Cym, a Gene Encoded by the DNA Strand Opposite to N-Myc. *Cell Growth Differ* (1992) 3:385–90.
29. Kim D-H, Han K-H. Transient Secondary Structures as General Target-Binding Motifs in Intrinsically Disordered Proteins. *Int J Mol Sci* (2018) 19:3614. doi: 10.3390/ijms19113614
30. O'Brien EM, Selfe JL, Martins AS, Walters ZS, Shipley JM. The Long Non-Coding RNA MYCNOS-01 Regulates MYCN Protein Levels and Affects Growth of MYCN-Amplified Rhabdomyosarcoma and Neuroblastoma Cells. *BMC Cancer* (2018) 18:217. doi: 10.1186/s12885-018-4129-8
31. Yu J, Ou Z, Lei Y, Chen L, Su Q, Zhang K. LncRNA MYCNOS Facilitates Proliferation and Invasion in Hepatocellular Carcinoma by Regulating miR-340. *Hum Cell* (2020) 33:148–58. doi: 10.1007/s13577-019-00303-y
32. Zhao X, Li D, Pu J, Mei H, Yang D, Xiang X, et al. CTCF Cooperates With Noncoding RNA MYCNOS to Promote Neuroblastoma Progression Through Facilitating MYCN Expression. *Oncogene* (2016) 35:3565–76. doi: 10.1038/onc.2015.422
33. Vadie N, Saayman S, Lenox A, Ackley A, Clemson M, Burdach J, et al. MYCNOS Functions as an Antisense RNA Regulating MYCN. *RNA Biol* (2015) 12:893–9. doi: 10.1080/15476286.2015.1063773
34. Guerzoni D, McLysaght A. De Novo Genes Arise at a Slow But Steady Rate Along the Primate Lineage and Have Been Subject to Incomplete Lineage Sorting. *Genome Biol Evol* (2016) 8:1222–32. doi: 10.1093/gbe/evw074
35. Qin XY, Suzuki H, Honda M, Okada H, Kaneko S, Inoue I, et al. Prevention of Hepatocellular Carcinoma by Targeting MYCN-Positive Liver Cancer Stem Cells With Acyclic Retinoid. *Proc Natl Acad Sci U S A* (2018) 115:4969–74. doi: 10.1073/pnas.1802279115

Conflict of Interest: The authors declare that the research was conducted in the absence of any commercial or financial relationships that could be construed as a potential conflict of interest.

Advantages of publishing in Frontiers

OPEN ACCESS
Articles are free to read for greatest visibility and readership

FAST PUBLICATION
Around 90 days from submission to decision

HIGH QUALITY PEER-REVIEW
Rigorous, collaborative, and constructive peer-review

TRANSPARENT PEER-REVIEW
Editors and reviewers acknowledged by name on published articles

Frontiers
Avenue du Tribunal-Fédéral 34
1005 Lausanne | Switzerland

Visit us: www.frontiersin.org
Contact us: frontiersin.org/about/contact

REPRODUCIBILITY OF RESEARCH
Support open data and methods to enhance research reproducibility

DIGITAL PUBLISHING
Articles designed for optimal readership across devices

FOLLOW US
@frontiersin

IMPACT METRICS
Advanced article metrics track visibility across digital media

EXTENSIVE PROMOTION
Marketing and promotion of impactful research

LOOP RESEARCH NETWORK
Our network increases your article's readership